studies in surface science and catalysis

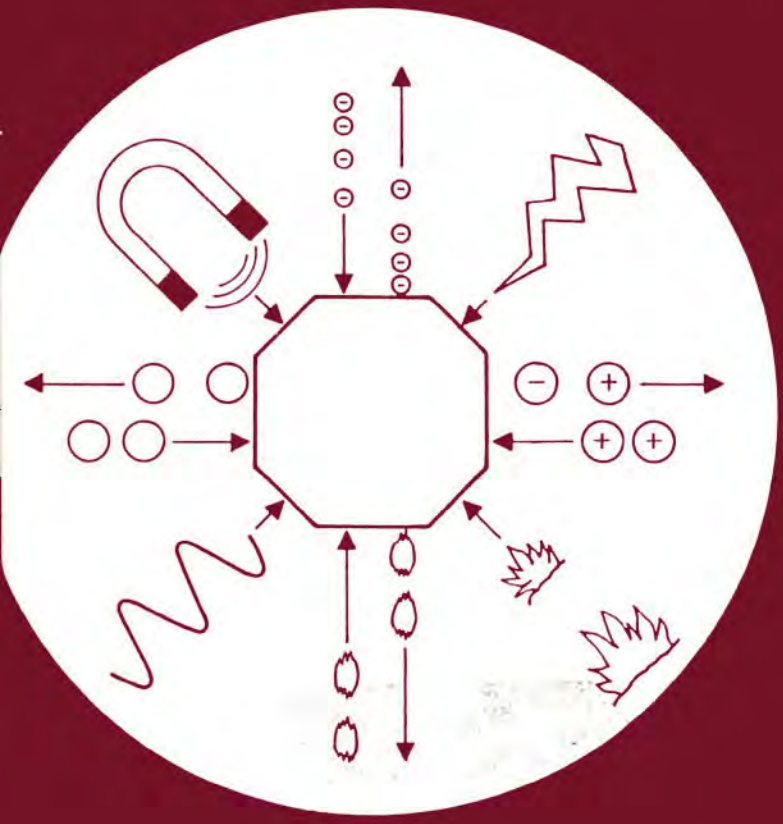

25

CATALYTIC POLYMERIZATION OF OLEFINS

T. Keii
K. Soga
(editors)

elsevier

Studies in Surface Science and Catalysis 25

CATALYTIC POLYMERIZATION OF OLEFINS

This page intentionally left blank

Studies in Surface Science and Catalysis 25

CATALYTIC POLYMERIZATION OF OLEFINS

Proceedings of the International Symposium on Future Aspects of Olefin Polymerization, Tokyo Japan, 4–6 July 1985

Edited by

Tominaga Keii
Numazu College of Technology, OoKa 3600, Numazu 410, Japan
Kazuo Soga
Research Laboratory of Resources Utilization, Tokyo Institute of Technology, Midori-ku, Yokohama 227, Japan

1986

KODANSHA
Tokyo

ELSEVIER
Amsterdam–Oxford–New York–Tokyo

Copublished by
KODANSHA LTD., Tokyo

and
ELSEVIER SCIENCE PUBLISHERS B. V., Amsterdam

exclusive sales rights in Japan
KODANSHA LTD.
12-21, Otowa 2-chome, Bunkyo-ku, Tokyo 112, Japan

for the U.S.A. and Canada
ELSEVIER SCIENCE PUBLISHING COMPANY, INC.
52 Vanderbilt Avenue, New York, NY 10017

for the rest of the world
ELSEVIER SCIENCE PUBLISHERS B. V.
25 Sara Burgerhartstraat, P.O. Box 211, 1000 AE Amsterdam, The Netherlands

Library of Congress Cataloging-in-Publication Data

International Symposium of Future Aspects of Olefin Polymerization (1985 : Tokyo, Japan)
Catalytic polymerization of olefins.

(Studies in surface science and catalysis ; 25)
Bibliography: p.
Includes index.
1. Olefins--Congresses. 2. Polymers and polymerization--Congresses. I. Soga, Kazuo, 1939- . II. Keii, Tominaga, 1920- . III. Title. IV. Series.
QD305.H7I55 1985 547'.41204593 85-31700
ISBN 0-444-99518-8 (U.S.)

ISBN 0-444-99518-8 (Vol. 25)
ISBN 0-444-41801-6 (Series)

ISBN 4-06-202265-6 (Japan)

PRINTED IN JAPAN

List of Contributors

Numbers in parentheses refer to the pages on which a contributor's paper begins.

AMMENDOLA, PAOLO (241) University of Salerno, 84100 - Salerno, Italy.

BEACH, DAVID L. (443) Gulf Research and Development Company, P.O. Drawer 2038, Pittsburgh, Pennsylvania 15230, U.S.A.

BERTHOLD, J. (29) Kunststoff-Forschung, Hoechst AG, 6230 Frankfurt (M) 80, Federal Republic of Germany

BÖHM, L.L. (29) Kunststoff-Forschung, Hoechst AG, 6230 Frankfurt (M) 80, Federal Republic of Germany

BUKATOV, G.D. (71) Institute of Catalysis, Novosibirsk 630090, U.S.S.R.

BURFIELD, DAVID R. (387) Department of Chemistry, University of Malaya, Kuala Lumpur 22-11, Malaysia

CAI, SHIMIAN (431) Institute of Chemistry Academia Sinica, Beijing, the People's Republic of China

CHEN, ZANPO (431) Institute of Chemistry Academia Sinica, Beijing, the People's Republic of China

DOI, Y. (109, 257) Research Laboratory of Resources Utilization, Tokyo Institute of Technology, Midori-ku, Yokohama 227, Japan

DURANEL, L. (147) CRNS - Laboratoire des Matériaux Organiques BP 34 LACQ - 64170 Artix, France

EWEN, JOHN A. (271) Fina Oil and Chemical Company, Box 1200, Deer Park, Texas 77536, U.S.A.

FENZL, W. (215) Max-Planck-Institut für Kohlenforschung, D-4330 Mülheim a. d. Ruhr, Federal Republic of Germany

FINK, G. (215, 231) Max-Planck-Institut für Kohlenforschung, D-4330 Mülheim a. d. Ruhr, Federal Republic of Germany

FLOYD, S. (339) Department of Chemical Engineering, University of Wisconsin, Madison, WI 53706, U.S.A.

FRANKE, R. (29) Kunststoff-Forschung, Hoechst AG, 6230 Frankfurt (M) 80, Federal Republic of Germany

GALLARDO, J.A. (123) Laboratorio de Polimeros, Centro de Química, IVIC. Apartado 1872, Caracas 1010A, Venezuela

GUYOT, A. (147) CNRS - Laboratoire des Matériaux Organiques BP 24 - 69390 LYON VERNAISON, France

HERNANDEZ, J.G. (123) Laboratorio de Polimeros, Centro de Química, IVIC. Apartado 1872, Caracas 1010A, Venezuela

ISHII, K. (109) Research Laboratory of Resources Utilization, Tokyo Institute of Technology, Midori-ku, Yokohama 227, Japan

JACOBSON, FELIX I. (323) Union Carbide Corporation, UNIPOL Systems Department, P.O. Box 670, Bound Brook, NJ 08805, U.S.A.

KAMINSKY, W. (293) Institut für Technische und Makromolekulare Chemie, Universität Hamburg, Bundesstr. 45, D-2000 Hamburg 13, Federal Republic of Germany

KAROL, FREDERICK J. (323) Union Carbide Corporation, UNIPOL Systems Department, P.O. Box 670, Bound Brook, NJ 08805, U.S.A.

KASHIWA, N. (43) Research Center, Mitsui Petrochemical Industries, Ltd., Kuga-gun, Yamaguchi-ken 740, Japan
KATAOKA, T. (407) Numazu College of Technology, Numazu-shi 410, Japan
KAWASAKI, M. (43) Research Center, Mitsui Petrochemical Industries, Ltd., Kuga-gun, Yamaguchi-ken 740, Japan
KAWATA, T. (109) Research Laboratory of Resources Utilization, Tokyo Institute of Technology, Midori-ku, Yokohama 227, Japan
KEII, TOMINAGA (1, 257) Numazu College of Technology, Ooka 3600, Numazu 410, Japan
KEIM, W. (201) Institut für Technische Chemie und Petrolchemie der Rheinisch-Westfälischen Technischen Hochschule Aachen, Worringer Weg 1, D5100 Aachen, Federal Republic of Germany
KISSIN, YURY V. (443) Gulf Research and Development Company, P.O. Drawer 2038, Pittsburgh, Pennsylvania 15230, U.S.A.
LACOMBE, J.L. (147) ATO CHEM-SNEA(P)-BP 34 LACQ - 64170 Artix, France
LIN, SHANGAN (91) Institute of Polymer Science, Zhongshan University, Guangzhou, the People's Republic of China
Liu, HUANQIN (431) Institute of Chemistry Academia Sinica, Beijing, the People's Republic of China
LOI, PATRICK S.T. (387) Department of Chemistry, University of Malaya, Kuala Lumpur 22-11, Malaysia
LU, YUN (91) Institute of Polymer Science, Zhongshan University, Guangzhou, The People's Republic of China
LU, ZEJIAN (91) Institute of Polymer Science, Zhongshan University, Guangzhou, the People's Republic of China
MAKHTARULIN, S.I. (71) Institute of Catalysis, Novosibirsk 630090, U.S.S.R.
MANN, G.E. (339) Department of Chemical Engineering, University of Wisconsin, Madison, WI 53706, U.S.A.
MEYER, H. (369) Institut fuer Technische Chemie, Technische Universitaet Berlin, Straße des 17. Juni 135, D - 1000 Berlin 12, Federal Republic of Germany
MICHAEL, R. (369) Institut fuer Technische Chemie, Technische Universitaet Berlin, Straße des 17. Juni 135, D - 1000 Berlin 12, Federal Republic of Germany
MIKENAS, T.B. (71) Institute of Catalysis, Novosibirsk 630090, U.S.S.R.
MÖHRING, V. (231) Max-Planck-Institut für Kohlenforschung, D-4330 Mülheim a. d. Ruhr, Federal Republic of Germany
MOROZ, E.M. (71) Institute of Catalysis, Novosibirsk 630090, U.S.S.R.
MUÑOZ-ESCALONA A. (123) Laboratorio de Polimeros. Centro de Quimica. IVIC. Apartado 1872, Caracas 1010A. Venezuela
MYNOTT, R. (215) Max-Planck-Institut für Kohlenforschung, D-4330 Mülheim a. d. Ruhr, Federal Republic of Germany
NESTEROV, G.A. (181) Institute of Catalysis, Novosibirsk 630090, U.S.S.R.
NOZAWA, F. (257) Research Laboratory of Resources Utilization, Tokyo Institute of Technology, Midori-ku, Yokohama 227, Japan
OHNISHI, R. (109) Research Laboratory of Resources Utilization, Tokyo Institute of Technology, Midori-ku, Yokohama 227, Japan
PERKOVETS, D.V. (71) Institute of Catalysis, Novosibirsk 630090, U.S.S.R.
PINO, P. (461) Swiss Federal Institut of Technology, Institut fuer Polymere, Universitätsstrasse 6, 8092 Zuerich, Switzerland
QUIJADA, RAUL (419) Centro de Pesquisas e Desenvolvimento da PETROBRÁS Universidade Federal do Rio de Janeiro, the Republic of Brazil

RAY, W.H. (339) Department of Chemical Engineering, University of Wisconsin, Madison, WI 53706, U.S.A.

REICHERT, K.H. (369) Institut fuer Technische Chemie, Technische Universitaet Berlin, Straße des 17, Juni 135, D - 1000 Berlin 12, the Federal Republic of Germany

ROTZINGER, B. (461) Swiss Federal Institut of Technology, Institut fuer Polymere, Universitätsstrasse 6, 8092 Zuerich, Switzerland

SANO, T. (109) Research Laboratory of Resources Utilization, Tokyo Institute of Technology, Midori-ku, Yokohama 227, Japan

SHIONO, T. (109) Research Laboratory of Resources Utilization, Tokyo Institute of Technology, Midori-ku, Yokohama 227, Japan

SPITZ, R. (147) CNRS - Laboratoire des Matériaux Organiques BP 24 - 69390 LYON VERNAISON, France

STROBEL, W. (29) Kunststoff-Forschung, Hoechst AG, 6230 Frankfurt (M) 80, Federal Republic of Germany

SOGA, K. (257) Research Laboratory of Resources Utilization, Tokyo Institute of Technology, Midori-ku, Yokohama 227, Japan

SUZUKI, S. (257) Research Laboratory of Resources Utilization, Tokyo Institute of Technology, Midori-ku, Yokohama 227, Japan

TAIT, P.J.T. (305) Department of Chemistry, UMIST, Manchester M60, 1QD, England

TANG, SHIPEI (165) Beijing Research Institute of Chemical Industry, He Ping Li, Beijing, The People's Republic of China

TERANO, M. (407) Toho Titanium Co., Chigasaki-shi 253, Japan

von ACHENBACH, E. (461) Swiss Federal Institut of Technology, Institut fuer Polymere, Universitätsstrasse 6, 8092 Zuerich, Switzerland

WANDERLEY, ANA MARIA RAMOS (419) PETROQUISA - PETROBRÁS QUÍMICA S.A. e Instituto de Macromoléc Universidade Federal do Rio de Janeiro, the Republic of Brazil

WANG, HAIHUA (91) Institute of Polymer Science, Zhongshan University, Guangzhou, the People's Republic of China

WOLFMEIER, U. (29) Kunstostoff-Forschung, Hoechst AG, 6230 Frankfurt (M) 80, the Federal Republic of Germany

XIAO, SHIJING (431) Institute of Chemistry Academia Sinica, Beijing, the People's Republic of China

YERMAKOV, Yu.I. (181) Institute of Catalysis, Novosibirsk 630090, U.S.S.R.

YOSHITAKE, J. (43) Research Center, Mitsui Petrochemical Industries, Ltd., Kuga-gun, Yamaguchi-ken 740, Japan

ZAMBELLI, ADOLFO (241) University of Salerno, 84100 - Salerno, Italy.

ZAKHAROV, V.A. (71, 181) Institute of Catalysis, Novosibirsk 630090, U.S.S.R.

ZHANG, QIXING (91) Institute of Polymer Science, Zhongshan University, Guangzhou, the People's Republic of China

This page intentionally left blank

Preface

Over two decades have elapsed since the discovery of the Ziegler-Natta catalyst. Tremendous research effort has been aimed at improving this marvelous catalyst. In twenty-five years since the first publication more than 15,000 papers and patents have appeared concerning it and related subjects. This effort has yielded new generations of Ziegler-Natta catalysts with superior activity and stereospecificity. The complexities arising from the heterogeneity of the catalyst, however, have hindered understanding of the catalytic processes which take place on the catalyst surface. Nevertheless, many fundamental features of the catalyst system have now been clarified reasonably well. Recently, a highly active homogeneous catalytic system has been developed, which is capable of catalyzing even isotactic polymerization of propene. There is no doubt that this finding will not only contribute to our understanding of the detailed mechanism of polymerization, but also stimulate the development of various kinds of tailored polymers. Thus this subject will remain of paramount importance in the development of chemistry and polymer science for a long time to come.

A timely symposium on "Future Aspects on Olefin Polymerization" was held in Tokyo in July 1985. Many active researchers reported recent advances in the field. The proceedings of the symposium are presented in this volume. The editors are pleased to include herein the paper by Dr. Y. V. Kissin, which was scheduled in the program but could not be presented at the symposium.

We wish to take this opportunity to express our gratitude to all the authors who contributed to these proceedings.

November 15, 1985

Tominaga Keii
Numazu College of Technology
and
Kazuo Soga
Research Laboratory of Resources Utilization
Tokyo Institute of Technology

Contents

Studies in Surface Science and Catalysis

Volume 1 **Preparation of Catalysts I.** Scientific Bases for the Preparation of Heterogeneous Catalysts. Proceedings of the First International Symposium held at the Solvay Research Centre, Brussels, October 14—17, 1975
edited by **B. Delmon, P.A. Jacobs and G. Poncelet**

Volume 2 **The Control of the Reactivity of Solids.** A Critical Survey of the Factors that Influence the Reactivity of Solids, with Special Emphasis on the Control of the Chemical Processes in Relation to Practical Applications
by **V.V. Boldyrev, M. Bulens and B. Delmon**

Volume 3 **Preparation of Catalysts II.** Scientific Bases for the Preparation of Heterogeneous Catalysts. Proceedings of the Second International Symposium, Louvain-la-Neuve, September 4 -7, 1978
edited by **B. Delmon, P. Grange, P. Jacobs and G. Poncelet**

Volume 4 **Growth and Properties of Metal Clusters.** Applications to Catalysis and the Photographic Process. Proceedings of the 32nd International Meeting of the Société de Chimie physique, Villeurbanne, September 24—28, 1979
edited by **J. Bourdon**

Volume 5 **Catalysis by Zeolites.** Proceedings of an International Symposium organized by the Institut de Recherches sur la Catalyse—CNRS—Villeurbanne and sponsored by the Centre National de la Recherche Scientifique, Ecully (Lyon), September 9—11, 1980
edited by **B. Imelik, C. Naccache, Y. Ben Taarit, J.C. Vedrine, G. Coudurier and H. Praliaud**

Volume 6 **Catalyst Deactivation.** Proceedings of the International Symposium, Antwerp, October 13—15, 1980
edited by **B. Delmon and G.F. Froment**

Volume 7 **New Horizons in Catalysis.** Proceedings of the 7th International Congress on Catalysis, Tokyo, 30 June—4 July 1980
edited by **T. Seiyama and K. Tanabe**

Volume 8 **Catalysis by Supported Complexes**
by **Yu.I. Yermakov, B.N. Kuznetsov and V.A. Zakharov**

Volume 9 **Physics of Solid Surfaces.** Proceedings of the Symposium held in Bechyňe, Czechoslovakia, September 29—October 3, 1980
edited by **M. Láznička**

Volume 10 **Adsorption at the Gas—Solid and Liquid—Solid Interface.** Proceedings of an International Symposium held in Aix-en-Provence, September 21—23, 1981
edited by **J. Rouquerol and K.S.W. Sing**

Volume 11 **Metal-Support and Metal-Additive Effects in Catalysis.** Proceedings of an International Symposium organized by the Institut de Recherches sur la Catalyse—CNRS—Villeurbanne and sponsored by the Centre National de la Recherche Scientifique, Ecully (Lyon), September 14—16, 1982
edited by **B. Imelik, C. Naccache, G. Coudurier, H. Praliaud, P. Meriaudeau, P. Gallezot, G.A. Martin and J.C. Vedrine**

Volume 12 **Metal Microstructures in Zeolites.** Preparation—Properties—Applications. Proceedings of a Workshop, Bremen, September 22—24, 1982
edited by **P.A. Jacobs, N.I. Jaeger, P. Jirů and G. Schulz-Ekloff**

Volume 13 **Adsorption on Metal Surfaces.** An Integrated Approach
edited by **J. Bénard**

Volume 14 **Vibrations at Surfaces.** Proceedings of the Third International Conference, Asilomar, California, U.S.A., 1—4 September 1982
edited by **C.R. Brundle and H. Morawitz**

Volume 15 **Heterogeneous Catalytic Reactions Involving Molecular Oxygen**
by **G.I. Golodets**

Volume 16 **Preparation of Catalysts III.** Scientific Bases for the Preparation of Heterogeneous Catalysts. Proceedings of the Third International Symposium, Louvain-la-Neuve, September 6—9, 1982
edited by **G. Poncelet, P. Grange and P.A. Jacobs**

Volume 17 **Spillover of Adsorbed Species.** Proceedings of the International Symposium, Lyon-Villeurbanne, September 12—16, 1983
edited by **G.M. Pajonk, S.J. Teichner and J.E. Germain**

Volume 18 **Structure and Reactivity of Modified Zeolites.** Proceedings of an International Conference, Prague, July 9—13, 1984
edited by **P.A. Jacobs, N.I. Jaeger, P. Jírů, V.B. Kazansky and G. Schulz-Ekloff**

Volume 19 **Catalysis on the Energy Scene.** Proceedings of the 9th Canadian Symposium on Catalysis, Québec, P.Q., September 30—October 3, 1984
edited by **S. Kaliaguine and A. Mahay**

Volume 20 **Catalysis by Acids and Bases.** Proceedings of an International Symposium organized by the Institut de Recherches sur la Catalyse—CNRS—Villeurbanne and sponsored by the Centre National de la Recherche Scientifique, Villeurbanne (Lyon), September 25—27, 1984
edited by **B. Imelik, C. Naccache, G. Coudurier, Y. Ben Taarit and J.C. Vedrine**

Volume 21 **Adsorption and Catalysis on Oxide Surfaces.** Proceedings of a Symposium, Brunel University, Uxbridge, June 28—29, 1984
edited by **M. Che and G.C. Bond**

Volume 22 **Unsteady Processes in Catalytic Reactors**
by **Yu.Sh. Matros**

Volume 23 **Physics of Solid Surfaces 1984**
edited by **J. Koukal**

Volume 24 ***Zeolites*: Synthesis, Structure, Technology and Application.** Proceedings of the International Symposium, Portorož-Portorose, September 3—8, 1984
B. Drzaj, S. Hocevar and S. Pejovnik
edited by **B. Držaj, S. Hočevar and S. Pejovnik**

MECHANISTIC STUDIES ON ZIEGLER-NATTA CATALYSIS
-A Methodological Reconsideration-

TOMINAGA KEII
Numazu College of Technology, Ooka 3600, Numazu 410, Japan

SUMMARY

Although our present fundamental understanding of Ziegler-Natta catalysis is one of the most advanced among the commercial catalysts, it is still far from perfect. Here, the kinetic approaches are critically summarized on the basis of a three-stage methodological classification system: characterization, phenomenological formalism and mechanistic approach. Under characterization the present conception of stereoregularity is criticized. In the second stage the proposed rate equations are discussed in light of experimental precision and kinetic models. The contradictions of our models with the experimental data found in studies on the effect of hydrogen on polymerization are pointed out, and the theories proposed for molecular weight distributions are discussed. Under mechanistic approach, the confusion in defining polymerization centers are pointed out. The definition suffers from both the definition in radical polymerizations and experimental operations. Reconsideration reveals some problems which remain unsolved and these are listed herein. Finally, an attempt is made to explain the effect of hydrogen on both polymerization rate and molecular weight.

INTRODUCTION

What is the present status of our understanding of Ziegler-Natta polymerization ?

Since the findings of Ziegler and Natta first made their impact felt on the world plastic industry, much fundamental research has been conducted on the nature of Ziegler-Natta catalysts. Undoubtedly, our fundamental understanding of these catalysts is the most advanced of the many commercial catalysts. Of course, there are some widely investigated catalytic reactions such as the transition metal-cata-

lyzed hydrogenation of olefin and ammonia synthesis. The understanding of such reactions, however, still remains in the phenomenological stages because of the lack of methods to determine the number of active centers. On this point, our working methods for determining the concentration of polymerization centers are so remarkably advantageous in the fundamental research of Ziegler-Natta catalysts that we can discuss them in terms of respective sets of rate constants of elementary reactions such as propagation and transfers.

The success of the ongoing fundamental research has, more or less, built some solid bases for future technical developments. Nevertheless, our present understanding is far from a complete understanding of the nature of Ziegler-Natta catalysts. Indeed it is uncertain whether complete understanding is possible.

In this article, the author will reconsider mainly the present kinetic approaches on the mechanism of Ziegler-Natta polymerization and point out some problems which remain unsolved, classifying them according to a three-stage methodological rating system.

The three stages taken up here are characterization, phenomenological formalism and mechanistic approach. The first stage is description of phenomena. In the research on commercial catalysts descriptive efforts usually suffer from application. The second stage is a middle stage between the others, generally regarded as a stage of explanation in understanding. However, the author deals with this as an independent stage useful in the course of scientific discovery. The last stage is the explanation of phenomena. Many separate studies on various researches using numerous methods are classified into these three stages and reconsidered. The purpose of this reconsideration is to improve the tools of research and to clarify the problems which exist in order to further advance our understanding of Ziegler-Natta catalysis.

METHODOLOGICAL SUMMARY OF ONGOING STUDIES

The research efforts which have been devoted to the fundamental understanding of Ziegler-Natta catalysis may be summarized as follows on the basis of the above classification method.

(1) Characterization

Catalyst yield for a prescribed time.
Polymerization rate-time curve.
Stereoregularity of produced polymers.
Molecular weight of produced polymers.
Molecular weight distribution of produced polymers.
Specific surface area, pore structure and particle shape of catalysts.

(2) Phenomenological Formalism

Kinetic studies to construct rate equations.
Kinetic analysis of rate-time curves.
Kinetic studies of molecular weights.
Kinetic studies of effects of additives.
Construction of MWD equation.

(3) Mechanistic Approach

Kinetic analysis of molecular weight-time curves.
Measurement of active center concentration:
radioactive tracer tagging,
poisoning of catalyst activity.
ESR measurement during polymerization.
Chemical analysis of catalyst.
Electron microscopy of the surface of catalyst.
Microscopy of polymer particles and catalyst particles.

Reconsideration of Characterization Studies (1)

The above methodological classification of ongoing research may be useful for re-evaluating our present line of approach. As to the characterization methods the following should be pointed out. In a purely fundamental point of view, the characterization of a catalyst must be done by factors which are directly connected to the nature of the catalyst, i.e. the activity and selectivity of the catalyst. Furthermore, catalyst yield cannot be used as representative of activity, except in the case of "kinetic analysis of molecular weight-time curve." What we must discuss here mainly is "stereoregulation (tacticity)" of produced polymers as a characterization factor of the stereospecificity of a catalyst. Usually we use the weight fraction of heptane-insoluble polymers as the stereoregularity. This is the most convenient characterization of produced polymers for

practical use, and this may also be useful for the characterization of stereospecificity of the catalyst. As is well-known, total polymers can be fractionized by the use of a set of solvents. The extraction of polymers by boiling heptane is only one of many ways of separating polymers into two groups, crystalline and amorphous. Furthermore, the recent development of ^{13}C-NMR spectroscopy has revealed that the microtacticities of polymer fractions by heptane extraction are not so different, i.e. 90% < (insoluble polymers) and 30% > (soluble polymers) in percent meso-diads. Therefore, the weight fraction of heptane-insoluble polymers cannot be used as being representative of the stereospecificity of a catalyst, in the sense of catalyst selectivity to yield a polymer of isotactic structure. Of course, the weight fraction can be used as can selectivity to yield the polymer insoluble for boiling heptane. The relationship between the solubility of a polymer solid for a solvent and the microstructure of the polymer chain is a problem of polymer physics. The stereoregularity of produced polymers in the fundamental characterization should be represented by a micro-tacticity distribution, e.g. a spectrum of differential weight of polymer versus percent meso-diads. It should be noted that the use of solubility as a measure of catalyst stereospecificity is not effective in fundamental research, although it is convenient for practical purposes. There is no problem concerning the average molecular weight of produced polymers, since the development of GPC gave us number average and weight average molecular weights. The use of viscosity average molecular weight as a substitute for number average molecular weight must be avoided, even though viscosity average molecular weight is closely connected to "melt flow index."

The BET method for measuring specific surface areas and pore structures of solid catalysts is not useful for the Ziegler-Natta catalysts because of its applicability to ensembles of secondary particles. The working state of the catalyst particles may be that of the primary particles as a result of deaggregation of secondary particles. In addition, the deaggregation in the case of $MgCl_2$-supported catalysts may be more complicated. Thus it is necessary to develop some methods useful for catalysts. However, the BET method is effective qualitatively for traditional $TiCl_3$ and Solvey catalysts, the BET-surface areas of which may be those of primary particles.

Reconsideration of Phenomenological Formalism (2)

(a) The experimental equations proposed for stationary rates are those of adsorption kinetics, as follows.

$$R_p = \frac{k[M]K[A]}{1 + K[A]} \tag{1}$$

$$R_p = \frac{k[M]K[A]}{(1 + K[A])^2} \tag{2}$$

$$R_p = \frac{kK_M[M]K_A[A]}{(1 + K_M[M])(1 + K_A[A])} \tag{3}$$

$$R_p = \frac{kK_M[M]K_A[A]}{(1 + K_M[M] + K_A[A])^2} \tag{4}$$

$$R_p = \frac{k[M]K[A]^2}{(1 + K[A]^2)} \tag{5}$$

$$R_p = \frac{k[M]K[A']^{1/2}}{1 + K[A']^{1/2}}$$

$$\text{with } [A'] = [A] - \text{const.} \tag{6}$$

Equations (5) and (6) are emphasize the dependence of the rate on the concentration of alkylaluminum [A] in the region of low concentration. Indeed, the dependency seems to be of a second order with respect to [A] in the region of low concentration. However, the molar ratios, [A]/[Ti], in such region are less than unity, which strongly suggests that the true concentrations of alkylaluminum are lower than those expected from its dosed amount, because of the consumption by the alkylation of titanium chlorides. In addition, the second order dependence of the polymerization rate on alkylaluminium may not be realistic in conventional heterogenous kinetics. In the latter sense, equation (6) was proposed[1] as being compatible

with a kinetic model in which alkylaluminum participates in its monomer form. However, the applicability of (6) has not been supported by experiments. The first four types of rate equations, (1)-(4), may be useful for the phenomenological formulation of the polymerization rate. The four equations are discussed below. Equation (3) has been obtained from propylene polymerization with some soluble Ziegler catalysts at low temperatures (around -78°C),[2] while equations (1) and (2) have been obtained from polymerization with heterogeneous catalysts in a slurry system at medium temperatures (30-100°C).[3] Because of the constant K_M of small value, the Langmuir dependence of rate on monomer concentration [M] appears only in low temperature polymerization where higher concentrations of monomers (about 10 mol/l) can be used. On the other hand, the monomer concentrations in slurry polymerizations under several atmospheric pressures are lower (0.4 mol/l at 40°C and 1 atm) and the simple first order kinetics with respect to [M] in equation (1), as an approximate form, appears. Similarly, equation (2) may be regarded as an approximate form of equation (4) which was proposed by Vessely[4] for propylene polymerization with $TiCl_3/AlEt_3$ at 50°C and [M] = 0.58 and 2.3 mol/l. The applicability of equation (4), however, has not been confirmed for propylene polymerizations under similar conditions, though the equation is useful for further kinetic consideration of the polymerization. It is worthwhile to examine the effect of the monomer concentration on polymerization rate for a wider range of propylene pressure. The observed rates of propylene polymerization in liquid pool (vapor pressure is about 30 atm) roughly correspond to those expected from slurry polymerization under about 20 atm. This cannot be taken simply as evidence of the role of $K_M[M]$ in the denominator of rate equation, because of the fugacity effect of propylene appears in such a high-pressure region.

According to adsorption kinetics, the above rate equations may be understood as follows. Assuming that the rate of polymerization corresponds to the rate of the rate-determining step of propagation (chain growing), the rate equations (3) and (4), Langmuir-Hinshelwood type, are considered to represent the surface reaction between an adsorbed monomer and an adsorbed alkylaluminum-dimer. The difference between (3) and (4) is that the adsorption sites of both molecules are the same in (4) while they are not the same but specific for each

molecule in (3). A problem arises from the kinetic interpretation of another equeation. For equation (1) , Rideal type, there are three possibilities: one is that equation (1) corresponds to the reaction between a solute monomer and an adsorbed alkylaluminum-dimer (Rideal mechanism[5]), the second is that (1) is an approximate form of (3) when $K_M[M]$ is negligibly smaller than unity, and the third possibility is that (1) is an approximate form of (4) when $K_M[M]$ is negligible and $K_A[A]$ is comparable to unity. The last interpretation also corresponds to the possibility that (1) is an approximate form of (2). As for (2) a similar formalism may be applied. That is, it may be considered as representing the reaction of a solute monomer with a pair of adsorbed alkylaluminum-dimer molecules and a vacant site, or it may be an approximate form of (4). The problem to decide whether an equation is an approximate form or not is one of experimental level, mentioned above. However, the decision is also connected with the problem that we prefer to take a plausible kinetic model. The possibility that (2) represents a special three-body reaction which involves a vacancy may be eliminated. Then (2) must be an approximate form of (4), which corresponds to the surface reaction between an adsorbed monomer and an adsorbed alkylaluminum-dimer.

From these considerations we must recognize the three rate equations, (1), (3) and (4), as being confirmed on the phenomonological level, taking into account that (1) is perhaps an approximate form of (3) or (4).

Based upon conventional kinetics, we can take these three rate equations thus obtained as representing possible kinetic models (phenomenological forms or reaction types of the mechanism of the rate-determining step of chain-growing reaction). That is, we can suppose that the molecularity of the rate-determining step is (2), i.e. the step is the reaction of an adsorbed alkylaluminum-dimer with a solute monomer in the case of (1), or an adsorbed monomer in the cases of (3) and (4). In Ziegler-Natta catalysis, however, the above kinetic conclusion has not been accepted because of its contradiction with the Cossee Mechanism[6] in which alkylaluminum does not participate as the dimer but as the monomer. Can we find a plausible explanation for this contradiction between the kinetic conclusion and the chemical model ? In this connection, it may be necessary to check other

possibilities that these rate equations do not represent the usual models of adsorption kinetics but other kinetic models, e.g. those based on some stationary states which are different from adsorption (coordination) equilibrium. For this a key may be to clear the temperature coefficient of K_A, which has not been well established.

(b) The dependence of rate on polymerization time

As is well-known, except for the living polymerization systems found by Doi et al.,[2] the rates of all polymerization systems change with time.[3] The rate of propylene polymerization with $TiCl_3$ /AlR_3 increases to its maximum and then gradually decreases to stationary value. With AlR_2X, the rate increases to its stationary value followed by a slight decrease. In the cases of ethylene polymerization with $TiCl_3/AlEt_3$ or $AlEt_2Cl$ and of propylene polymerizations with $TiCl_3/ZnEt_2$ or $MgCl_2$-supported $TiCl_4/AlEt_3$, the rates of polymerization monotonically decrease to stationary values. In addition to the above types of rate changes, the details of the changes depend on the kinds of monomer, catalyst and cocatalyst as well as on temperature.[3]

The initial increase of polymerization rate depends on the order of addition of monomer and alkylaluminum to $TiCl_3$ as

$$(dR_{p,t}/dt)_o = \frac{k[M]^2K_A[A]}{1 + K_A[A]} \tag{7}$$

in the case of polymerization started by the final addition of monomer, and

$$(dR_{p,t}/dt)_o = k[M][A] \tag{8}$$

in the case of polymerization started by the final addition of alkylaluminum. The case of polymerization started by the final addition of $TiCl_3$ has not been examined. The above two kinetic equations for

the initial increase of polymerization rate can be understood on the basis of a kinetic model which does not contradicted all models corresponding to (1), (3) and (4). That is, the rate increase is due to the increase of polymerization center concentration. Assuming the rate equation for the polymerizations to be

$$R_p = k_p[M]C^* \tag{9}$$

we have

$$(dC^*/dt)_o = \frac{k''[M]K_A[A]}{1 + K_A[A]} \tag{10}$$

and

$$(dC^*/dt)_o = k''[A] \tag{11}$$

These two equations can be considered as those which express that the polymerization centers are formed by the reaction of a solute monomer and an adsorbed alkylaluminum-dimer equilibrated with solution in the case of (10) and by the adsorption of an alkylaluminum-dimer from solution in the case of (11). These are compatible with the usual initiation model that Ti-R changes into polymerization center C^* by the insertion of one monomer, $R^* + M \longrightarrow M_1^*$ in conventional radical polymerizations.

Some studies have been conducted on rate decreases. The gradual decrease of the polymerization rate after reaching maximum in propylene polymerization with $TiCl_3/AlEt_3$ could be expressed by a first order decay with respect to the rate itself and the decay constant was mostly independent of both [A] and [M].[3] The rapid decay of the rate just after the beginning of propylene polymerization with $MgCl_2$-supported catalyst is rather complicated. We can express it by a

second order decay, except for the initial region of more rapid decay.[7] Galli et al., however, proposed a first order decay.[8] Thus, the rate decay in the case of the highly active supported catalysts should be examined more closely, which may be important also in a technical sense for enhancing the catalyst yield. However, some useful results may be noted here. According to the results obtained by Suzuki and the author,[7] the form of the rate equation is independent of the polymerization time at which the rate equation is determined, excepting only the values of the apparent rate constant, k, as

$$R_{p,t} = \frac{k(t)[M]K_A[A]}{(1 + K_A[A])^2} \qquad (12)$$

This suggests that the rate decay is independent of monomer and alkylaluminum. Furthermore, the decay does not stop but continues during intermission of polymerization after the monomer is removed, indicating that the produced polymer is not responsible for the rate decay and suggesting that the diffusion of monomer through polymer is not responsible for the rate-determining step of chain growing. In connection with the mechanism of the rate decay, Ambroz showed that alkylation of $TiCl_3$ corresponded to the rate decay,[9] and Kashiwa showed that reoxidation of deactivated catalyst recovered its catalytic activity.[10]

(c) Kinetic studies on average molecular weights

In the case of living polymerization of propylene with $V(acac)_3/AlEt_2Cl$[7] the molecular weight was expressed by

$$\bar{M}_t = \frac{kK_M[M]t}{1 + K_M[M]} \qquad (13)$$

and the yield at the same time by

$$Y_t = \frac{kK_M[M]K_A[A]t}{(1 + K_M[M])(1 + K_A[A])} \qquad (14)$$

From these two equations we have the number of growing chains, i.e. the concentration of polymerization centers as

$$[N] = C^* = Y_t/\bar{M}_t = \frac{\alpha[V]K_A[A]}{1 + K_A[A]} \qquad (15)$$

where [V] is the concentration of $V(acac)_3$ and α is a constant less than unity. This system is a trivial case of polymerization without transfer reaction but it is important as a controlled system for the discussion of transfer reactions. Non-living polymerization with $V(acac)_3/Al_2Et_3Cl_3$[26] can be understood as polymerization where only a transfer by adsorbed monomer occurs in addition to the situation of the case with $AlEt_2Cl$. The effect of molecular hydrogen on the transfer reaction is clearly understandable with the living polymerization system. The concentration of total chains in the presence of hydrogen can be represented by

$$[N]_t = C^*(1 + k_h[H_2]t) \qquad (16)$$

This form is compatible with the idea that the transfer reaction by hydrogen occurs as

$$\text{cat-P} + H_2 \xrightarrow{k_h} \text{cat-H} + \text{PH} \qquad (17)$$

with rapid reinitiation

$$\text{cat-H} + \text{M} \longrightarrow \text{cat-P} \qquad (18)$$

In heterogeneous catalysis the corresponding situation is one of confusion, because many observed dependencies of the transfer reaction on hydrogen pressure are not of first but half order. Natta[11] was aware of this discrepancy between the above idea and his own experimental result. He suggested the role of atomic hydrogen, which was compatible with the fact that a rapid equilibriation reaction between H_2 and D_2 occurs in the gas phase of propylene polymerization system with $TiCl_3/AlEt_3$.[12] At the phenomenological level, however, experimental confirmation of the kinetic order is necessary to determine whether it is of half order or Langmuir type, as in the case of the dependence of polymerization rate on concentrations of alkylaluminum. More strictly, the effect of hydrogen must be reconsidered in connection with the other effect of hydrogen on the catalysis, e.g. the effect on polymerization rate. Essentially, the effects of hydrogen on the catalysis can be summarized as being additives on polymerization systems.

(d) Effects of additives

The effect of hydrogen on polymerization rate has not been established experimentally. For a long time it has been generally accepted that the polymerization rate decreases upon the addition of hydrogen. The rates of propylene polymerization in the presence of hydrogen were represented by

$$R_p^H = R_p - a[H_2]^{1/2} \qquad (19)$$

or

$$R_p^H = \frac{R_p}{1 + b[H_2]^{1/2}} \qquad (20)$$

where a and b are constant. These were obtained with stationary polymerizations with $TiCl_3/AlEt_3$. Equation (19) was reported by Natta[11] who supposed (17) to be rapid and (18) to be slow, while equation (20) was reported by the present author and his co-workers.[12] Our report was based on the assumption that hydrogen atoms adsorbed dissociatively are inactive for polymerization but active for transfer. This assumption, however, is faulty, because the half order dependence on hydrogen refutes the first half of the supposition and coordination chemistry refutes the latter half. Thus, we have no plausible explanation for the rate lowering by hydrogen as represented above. In addition, it has been recognized that this effect of hydrogen on polymerization rate is not simple but complicated. The effect of hydrogen in polymerization with $TiCl_3/AlEt_2Cl$ is usually one of rate-lowering but sometimes it has no effect on the rate or an effect of slight rate-enhancement.[13] Also, marked enhancement by hydrogen has been noted by Mason et al.,[14] who examined butene-1 polymerization, and by Pijpers et al.,[15] who examined 4-methyl-1-pentene polymerization; both used $TiCl_3$ activated by $Al(i\text{-}Bu)_3$, $AlEt_3$ or $AlEt_2Cl$. These notes on rate-enhancement have not been generally accepted because of the use of $TiCl_3$(AA), $AlCl_3$ of which might be responsible for the effect. However, the enhancement of polymerization rate by hydrogen is now well established by many authors[16-18] who examined propylene polymerizations with $MgCl_2$-supported $TiCl_4/AlEt_3$. The rate enhancement by hydrogen refutes decisively the idea based on the combination of (17) and (18). It is necessary to come up with a new idea which can cover both types of effects of hydrogen: lowering molecular weight and complicated effects on polymerization rate. The latter effect should particularly be examined in connection with polymerization conditions, which means that the fundamental understanding of the effect of hydrogen is still in the stage of "characterization," as Natta[11] found the effect of hydrogen to be reversible and we found that in the absence of solute alkylaluminum the effect is irreversible, in spite of the presence of a monomer.[3] That is to say, the description of the effect of hydrogen is still not complete.

The most important effect of additives is undoubtedly that as electron donors. The effect of an electron donor substance has many aspects, i.e. on the stereoregularity and molecular weight of pro-

duced polymers and also on the polymerization rate. Although many studies have been conducted on the effect of electron donor substances, our understanding remains in the phenomenological stage. A reciprocal relationship between "isotacticity" and polymerization rate was pointed out by the author[3] in polymerization with $TiCl_3$-/$AlEt_3$. The relation can be understood on the basis that the polymerization centers constitute two kinds: one that is highly stereospecific and the other less so; and the addition of a substance which acts as poison to centers of the latter kind causes such a relation. In the case of electron donor substances which react not only with transition metals but also with alkylaluminum their effect may appear in a complex way. Indeed, their complexations with alkylaluminum results in lowering the effective concentration of the latter, changing the polymerization rate. Here, both the complexes and their decomposed compounds may cause further complicated effects on the polymerization, as pointed out by Guyot[19] and Soga.[20] However, the foregoing studies on the effect of additives on the stereospecificities of $TiCl_3$ were limited by rather narrow allowances of "stereoregularity" such as those from 80% to 95% in wt% of heptane-insoluble fraction, because of the industry oriented character of the studies. In a purely fundamental viewpoint some substances which widely depress "stereoregularity" should be used, even if such substances are not useful for industry. In this connection the effect of ethylbenzoate (EB) on $MgCl_2$-supported $TiCl_4$ catalyst is a good target of our studies. The author proposed an explanation for the effect of EB on the basis of the above-mentioned idea of poisoning of "atactic" centers and lowering of effective concentration of $AlEt_3$.[21] On the other hand, Kashiwa prefers a different idea, i.e. that EB produces new highly "isotactic" centers and kills "atactic" centers.[22] The formation of new "isotactic" centers should be followed by rate increases in any rate. The observed small increase of the rate in the region of small amounts of EB added is now the target of the two different explanations. Of course, some remarkable increases in polymerization rates upon the addition of electron donor substances such as amines have been confirmed with the traditional catalyst system.[23] In the case of living polymerization with $V(acac)_3$/$AlEt_2Cl$ an increase in the number of living polymers (polymerization centers) upon the addition of anisol was confirmed by Ueki et al.[24]

The rate-increase with a maximum in the same catalyst system was observed earlier by Zambelli et al.[25] It is questionable whether the fundamental understanding of the effect of electron donor substances can be improved using our present research methods which are in the phenomenological stage.

(e) Construction of molecular weight distribution

The molecular weight distributions (MWD) of polymers produced with $V(acac)_3$ are well represented by a Poisson distribution (in the case of living polymerization with $AlEt_2X$) or Flory's most probable distribution (in the case of polymerization with transfer with $Al_2Et_3Cl_3$).[26] These formulations are compatible with our kinetic models.

Those of polymers obtained with heterogeneous catalysts have been expressed empirically by Wesslau with log-normal distribution[27] and by Tung with exponential distribution.[28] The "isotactic" polymers obtained with $TiCl_3/AlEt_3$ were expressed by Tung's distribution while the "atactic" polymers express irregular ones.[29] On the other hand, both polymers obtained with $MgCl_2$-supported catalyst have been well represented by Wesslau and the only difference between them is a constant deviation in the logarithm of molecular weight, i.e. $M_{iso} = 7\ M_{ata}$.[30] These results suggest that the polymers obtained with the traditional catalyst are mixtures of polymers of two different kinds in distribution and the latter are not mixtures but polymers of single distribution. The phenomenological explanation of these empirical equations of MWD has been not yet fixed. However, the remarkable character of these MWDs is that they are all broad. That is, the polydispersity of these MWDs is larger than 2. This character has been recognized and discussed. At present, three approaches are in controversy. Gordon and Roe supposed that physical adsorption of a long chain retards the transfer reaction in accordance with the length of chain and derived a theoretical MWD which is similar to Wesslau's.[31] Clark and Bailey tried to explain on the basis of non-uniformity of polymerization centers for transfer rate.[32] The present author pointed out that a surface heterogeneity for propagation rate constant, $f(k_p) = ak_p^{-b}$, results in MWD curves similar to experimental ones.[30,33] The third group is based on the monomer diffusion control model of polymerization.[34-

36) The last model may be correlated with the physical change occurring in heterogeneous polymerization, i.e. the catalyst particles continue to disintegrate (deaggregate) in the matrix of growing polymers during polymerization. It is not easy to determine which is predominant among these three theories of chain length, non-uniformity of polymerization centers and of diffusion control. One criterion has been proposed by Roe, who pointed out the importance of the effect of hydrogen on the polydispersity of polymer produced.[37] Many experiments showed no effect of hydrogen on polydispersity, which is good evidence for the theory of non-uniform centers, according to Roe. However, sometimes a slight decrease of the polydispersity in the region of low concentrations of hydrogen added was found, supporting the other two theories.

The above three theories are essentially based upon the same idea that the broadening of MWD might be explained by revising Flory's distribution with the use of its parameter averaged by some procedure related to the surface of the catalyst. Flory's most probable distribution for high polymers may be represented by the normalized frequency function,

$$N_n / \sum N_n = \rho \exp(-n\rho) \tag{21}$$

with

$$\rho = \frac{k_{tr}}{k_p[M]} \ll 1 \tag{22}$$

This distribution gives $1/\rho$ and $2/\rho^2$ for the first moment and the second moment, respectively. The polydispersity, $\overline{M}_w/\overline{M}_n$, can be represented by $(2/\rho^2)/(1/\rho)^2 = 2$. Therefore, if the parameter ρ could be replaced by an averaged one, $\langle\rho\rangle$, the polydispersity must be represented by $(2/\langle\rho^2\rangle)/(1/\langle\rho\rangle)^2 > 2$. The targets of averaging procedure were k_{tr}, k_p and [M] in the above three theories. Apart from the physics, this may be treated as a mathematical problem to find the

function $f(\rho)$ from the following equation.

$$\text{Empirical frequency function} = \langle \rho\exp(-n\rho) \rangle = \rho\exp(-n\rho)f(\rho)d\rho \quad (23)$$

This mathematical procedure applied to both empirical distributions numerically gave us an approximate form

$$f(\rho) = a\rho^{-b} \quad (24)$$

It is important in physics to attribute a model to the last function. We attribute the surface heterogeneity of k_p[30),(33)] on the basis of the experimental result obtained with CO poisoning (inhibition) method. At any rate, other experiments of higher methodology must be conducted to solve the problem.

Reconsideration of the Mechanistic Approach (3)

(a) Kinetic analysis of molecular weight-time curve

In heterogeneous polymerizations the most useful equation is

$$\bar{P}_{n,t} = \frac{Y_t}{C^* + Y_t/\bar{P}_{n,\infty}} \quad (25)$$

where Y is the yield, P_n the number average degree of polymerization and the subscript t the value at time t. Applying this equation to the experimental data, we have the value of polymerization center concentration, C^*. However, this method must be used with great care. The use of the equation in its linear form,

$$Y_t/\bar{P}_{n,t} = C^* + Y_t/\bar{P}_{n,\infty} \quad (26)$$

is erroneous for data of higher yields where the linearity of the values of the left hand side against the yields is well guaranteed. The linearity guaranteed by higher yields may lead to a smaller value of C^*. It should be noted that the method is effective only for data in which $\bar{P}_{n,t}$ changes largely with time, i.e. for the cases where the values of $Y_t/\bar{P}_{n,\infty}$ are comparable to the value of C^*. In addition, the above method cannot be used for cases where the polymerization rate increases with time and the rate constant of propagation or transfer changes with chain length or C^*. In such cases, this method must be further refined.

(b) Measurements of active center concentration

In principle, the radio active tracer tagging method[38,39] may be better than the poisoning (inhibition) method[40-42] which is based on the assumption that all adsorptions occur only on the active centers. However, the former method itself may also be narrow because of the uncertainty of the mechanism of the insertion of the tracer into growing chains. Besides these discussion on techniques, the author calls attention to the definition of "active centers" or "polymerization centers." In traditional heterogeneous catalysis "Active Centers (Sites)" means the surface sites on which a reaction can occur. In polymerization we use the term "polymerization centers". "Polymerization center" is usually defined by C^* of the "rate equation,"

$$R_p = k_p[M]C^* \tag{9}$$

which has been well established with the radical polymerizations in homogeneous systems. Therefore, this definition is undoubtedly an empirical one and lower in dimension than the present status of our understanding of "polymerization centers" in coordination polymerizations. In our understanding, even in the phenomenological rank, the rate-determining step is the insertion of a coordinated monomer into a growing chain, expressed by

$$R_p = k_{ins} C_o \Theta(M) \Theta(P^*) \tag{27}$$

where k_{ins} is the rate constant of the insertion, C_o the total number of active sites (two sites per an active metal site in the polymerization expressed by (4) or (2)), $\theta(M)$ or $\theta(P^*)$ the occupation probability of the coordinated monomer or growing chain on the site. If we take the phenomenological model in traditional adsorption kinetics for these two probabilities as

$$\Theta(M) = \frac{K_M[M]}{1 + K_M[M] + K_A[A]} \tag{28}$$

and

$$\Theta(P^*) = \frac{K_A[A]}{1 + K_M[M] + K_A[A]} \tag{29}$$

we have the following expression for C^* defined by (9).

$$C^* = C_o \Theta(P^*)(1-\Theta(P^*)-\Theta(M)) = C_o \frac{K_A[A]}{(1 + K_M[M] + K_A[A])^2} \tag{30}$$

The right hand side indicates the number of sites on which a P^* and a vacancy exist. On the other hand, the total number of growing polymers may be expressed by

$$C_o \Theta(P^*) = C_o \frac{K_A[A]}{(1 + K_M[M] + K_A[A])} \tag{31}$$

which may be the subject of a tagging method using labeled water and alcohols. The method using radioactive CO may give the total number of growing chains combined with vacancies, in which case the two methods will not give the same but different values with the latter always giving a small value.[43] The chemisorption of CO or allene can occur on all vacant sites, not only on active but also on inactive sites. Thus, the definition of working sites of the catalysts should be reconsidered taking into account present methods and the theory of coordination polymerization.

Here, a new kind of experimental results is described and discussed. Giannini found that the observed value of polymerization rate constant defined by (9) increased by increasing the observed value of C^* obtained using radioactive CO.[44] Murata et al. found that the decrease of polymerization rate on the addition of CO was not constant but gradually lowered with increasing CO added in the gas phase polymerizations with traditional and $MgCl_2$-supported catalysts.[45] A similar result has been obtained by Tait who examined the inhibition effect of CO and allene on polymerization with traditional catalysts.[42] As shown by the author,[30,33] the latter results may be explained by polymerization centers non-uniform in k_p value (of so-called surface heterogeneity for k_p). Of course, this discussion is based on the assumption that all adsorbates occupy only the active sites.

(c) Other methods used for mechanistic research

The spectroscopic methods which have been used are ESR and IR. The use of ESR method combined with polymerization gave some correlations between ESR active species and polymerization activities during polymerization.[46] Okura et al. pointed out the close correlations between ESR intensity and rate of propylene polymerization during polymerization with $TiCl_3/AlEt_3$ or $AlEt_2Cl$.[47] The intensity was proportional to the surface area of $TiCl_3$ during milling, suggesting that the surface Ti^{+3} ions are responsible for the ESR signal. Recently, Chien discussed this point.[48] The complexities arising from the surface generally make spectroscopic analyses less powerful. However, at present the field of heterogeneous catalysts such as metals and zeolites is in a more advanced stage than is ours. On the other hand, the microscopies applied to the surface or particles

of catalysts gave us some important information. Rodorigues et al. obtained beautiful photographs of the surface of a single $TiCl_3$ crystal activated by $AlMe_3$ just after ethylene polymerization for a short time.[49] The photographs showed that polymerization occurred on dislocation of the crystal. Okura obtained a similar photograph from the surface of an active $TiCl_3$ polycrystal, showing that polymerization occurred on the defective structures on the surface.[50] Clearly, this kind of experiment using single crystals is very important and fruitful, because that we can see directly the reaction loci by the spots of produced polymers. This approach should be further investigated. It is also believed that comparison of particle shapes of catalysts and polymers may lead to establishing the concept of replication effect of the catalyst.

The thermogravitational method, which is described by Terano et al.[51] in this monograph, and elementary analysis may be effective for cases where substances such as $TiCl_4$ or EB do not correspond to inactive sites but to active sites. In this connection, precise measurements of the concentration of the active fraction in the total concentration of Ti, for example, are very important.

PROBLEMS WHICH REMAIN UNSOLVED

(a) How we can correlate the rate equations to our present models of the initiation reaction such as the Cossee model ?
(b) Are the active sites uniform or non-uniform ?
(c) Does alkylaluminum participate in the active sites ?
(d) Does EB participate in the active sites ?
(e) What is the mechanism of the effects of hydrogen ?
(f) Are there some uselful phenomenological relations, such as "Linear Free Energy - Energy Relation", in our field ?
(g)Are the present kinetics of copolymerization effective for heterogeneous polymerization ?

AN ATTEMPT TO EXPLAIN THE EFFECTS OF HYDROGEN

As mentioned above, the effects of hydrogen on polymerization are not yet established. The author's supposition is described herein. The following kinetic model seems to be applicable to the effect of hydrogen on the rate of polymerization in some polymerization systems.

The basic idea of the model is that hydrogen adsorbs dissociatively on the active sites and forms active hydrides, e.g. Ti-H, for the insertion of monomer and transfer of growing chain. The adsorption of hydrogen occurs not only on the site which is available for the growing chain but also on the site which is available only for the monomer in the case of (3). This is plausible because of the molecular size of hydrogen, and the rate equation in the presence of hydrogen may be represented as follows.

$$R_p^H = k_{ins} C_o \theta(M)(\theta(P^*) + \theta(H_2)) \tag{32}$$

with

$$\theta(M) = \frac{K_M[M]}{1 + K_M[M] + K_H[H_2]} \tag{33}$$

or

$$\theta(M) = \frac{K_M[M]}{1 + K_M[M] + K_A[A] + K_H[H_2]} \tag{34}$$

and

$$\theta(P^*) + \theta(H) = \frac{K_A[A] + K_H[H_2]}{1 + K_A[A] + K_H[H_2]} \tag{35}$$

or

$$\theta(P^*) + \theta(H) = \frac{K_A[A] + K_H[H_2]}{1 + K_M[M] + K_A[A] + K_H[H_2]} \tag{36}$$

The set, (33) and (35), is applied to the polymerization, the rate of which is expressed by (3), and the set, (34) and (36), to the polymerization expressed by (4). Accordingly, these two sets can be applied to the polymerizations expressed by (1) and (2) respectively, providing that $K_M[M] < 1$.

The above rate equation corresponding to that of the initiation reaction, Ti-H + M $\longrightarrow$ Ti-P, is rapid and the following insertion of monomer is then the same as that of usual polymerization center (k_{ins} is the same). The rate equations with the two sets of probability expressions result in rate-increase or rate-decrease upon addition of hydrogen, according to the nature of the catalyst and the experimental conditions of the original polymerization system. For covenience, this will be shown in an approximate form of rate equations in the case of negligibly small $K_M[M]$.

$$R_p^H = \frac{k(K_A[A] + K_H[H_2]}{(1 + K_A[A] + K_H[H_2])^2} \tag{37}$$

This equation can be changed into the following form,

$$R_p^H = R_p \frac{1 + a[H_2]}{(1 + \theta^o(P^*)a[H_2])^2} \tag{38}$$

where R_p is the rate of the polymerization in the absence of hydrogen and a and $\theta^o(P^*)$ are

$$a = K_H/K_A[A] \tag{39}$$

and

$$\theta^o(P^*) = \frac{K_A[A]}{1 + K_A[A]} \tag{40}$$

From these we have the following relations for the polymerizations in the presence of hydrogen

$$R_p^H/R_p \leq 1 \text{ when } \theta^o(P^*) \geq 1/2 \text{ or } K_A[A] \geq 1 \quad (41)$$

$$R_p^H/R_p > 1 \text{ when } \theta^o(P^*) < 1/2 \text{ or } K_A[A] < 1 \quad (42)$$

and

$$(R_p^H/R_p)_{max} = 1/4\theta^o(P^*)(1 - \theta^o(A)) > 1 \text{ when } K_A[A] < 1 \quad (43)$$

These relations show us that the polymerizations, the value of $K_A[A]$ of which is not less than unity, show rate-decreases upon addition of hydrogen whereas the polymerizations with $K_A[A]$ of values smaller than unity show rate-increase to maximum increase, which is determined by (43), followed by gradual decrease to zero. This conclusion may qualitatively be compatible with the foregoing experiments. Almost all cases where rate-lowerings were observed were under conditions in which the value of $K_A[A]$ was close to unity or larger than unity (in the case of (1)), i.e. high concentrations of alkylaluminum and lower temperatures. This assumption regarding the conditions can be deduced from the fact that the polymerizations were in their optimum rates corresponding to the above values of $K_A[A]$. In cases of $MgCl_2$-supported catalysts the polymerizations are carried out under the conditions of low value of [A] and rather higher temperatures, which favor rate-increases up on the addition of hydrogen. Indeed, the marked effect of hydrogen on polymerization rate observed by Guastella and Giannini[16] in polymerizations with $MgCl_2$-supported $TiCl_4/AlEt_3$ and the slight effect observed by Ueki et al.[52] may be explained quantitatively by (38), and (32) combined with the set, (33) and (35), respectively.

The above model of the effect of hydrogen leads to the explanation of the transfer reaction by hydrogen in which that adsorbed

hydrogen reacts with a growing chain to form a dead polymer. Thus, the transfer reaction must be proportional to the concentration of adsorbed hydrogen, which may be expressed by a Langmuir equation that appears as half order respect to hydrogen pressure. This point must be discussed. In addition, the dissociative adsorption of hydrogen is essentially an oxidative adsorption and the adsorption may activate some inactive sites of highly reduced Ti^{+2} or Ti^{+1}. This effect must also be considered. A detailed study will be published in the near future.

REFERENCES

1. A.K.Ingberman, I.I.Levine, and R.J.Turbett, J. Polym. Sci. A1-4, 2781 (1966).
2. Y.Doi, S.Ueki, and T.Keii, Macromolecules, 12, 814 (1979).
3. T.Keii, "Kinetics of Ziegler-Natta Polymerization," Kodansha-Chapman-Hall co-pub. London-Tokyo, (1972).
4. K.Vesely, Pure Appl. Chem., 4, 407 (1962).
5. J.Boor, Makromol. Rev., 2, 115 (1967).
6. P.Cossee, J. Catal., 3, 80 (1964).
7. T.Keii, E.Suzuki, M.Tamura, M.Murata, and Y.Doi, Makromol. Chem., 183, 2285 (1982).
8. P.Galli, L.Luciani, and G.Cecchin, Angew. Makromol. Chem., 94, 63 (1981).
9. J.Ambroz, P.Osecky, J.Mejzlik, and O.Hamerik, J. Polym. Sci., C-16, 423 (1967).
10. N.Kashiwa and J.Yoshitake, Makromol. Chem., 185, 1133 (1984).
11. G.Natta, Chimie Ind. (Milano) 41, 519 (1959).
12. T.Keii, A.Kojima, I.Okura, and A.Takahashi, J. Chem. Soc. Jpn., 1143 (1975).
13. I.Okura, K.Soga, A.Kojima, and T. Keii, J. Polym. Sci., A1-8, 2717 (1970).
14. C.D.Mason and R.J.Schaffhauser, Polymer Lett., 9, 661 (1971).
15. E.M.J.Pijpers and B.C.Roest, Eur. Polym. J., 8, 1151 (1972).
16. G.Guastalla and G.Giannini, Makromol. Chem., Rapid Comm., 4, 519 (1983).
17. M.Kioka and N.Kashiwa, Japan Kokai 58-83006 (May 18, 1983).
18. E.Suzuki, Dr. Thesis, Tokyo Institute of Technology,(1982).
19. R.Spitz, J.L.Lacombe, M.Primet, and A.Guyot, Proc. MMI-symposium,

(1983) p.389.
20. K.Soga, M.Terano, and S.Ikeda, Polymer Bull., 3, 179 (1980).
21. T.Keii, E.Suzuki, M.Tamura, and Y.Doi, Proc. MMI-symposium (1983) p.97.
22. N.Kashiwa, ibid., p.379.
23. J.Boor, "Ziegler-Natta Catalysts and Polymerizations," Academic Press (1979) p.224.
24. Y.Doi, S.Ueki, and T.Keii, Makromol. Chem., Rapid Comm., 3, 225 (1982).
25. A.Zambelli, I.Pasquon, R.Signorini, and G.Natta, Makromol. Chem., 112, 160 (1968).
26. S.Ueki, Dr. Thesis, Tokyo Institute of Technology, (1982).
27. H.Wesslau, Makromol. Chem., 20, 111 (1956).
28. L.H.Tung, J. Polym. Sci., 20, 495 (1956), 24, 333 (1957).
29. A.Morinaga, M. Eng. Thesis, Tokyo Institute of Technology, (1976).
30. T.Keii, Y.Doi, E.Suzuki, M.Tamura, M.Murata, and K.Soga, Makromol. Chem., 185, 1537 (1984).
31. M.Gordon and R.-J.Roe, Polymer, 2, 41 (1961).
32. A.Clark and G.C.Bailey, J. Catal., 2, 230 (1963).
33. T.Keii, Memoire Numazu College of Technology (1985) p.1.
34. W.R.Schmeal and J.R.Street, AIChE J., 17, 1188 (1972).
35. D.Singh and R.P.Merrill, Macromolecules, 4, 599 (1971).
36. T.W.Taylor, K.Y.Choi, H.Yuan, and W.H.Ray, Proc. MMI-Symposium,(1983) p.191.
37. R.-J.Roe, Polymer, 2, 60 (1961).
38. Yu.I.Yermakov, V.A.Zakharov, G.D.Bukatov, Proc. 5-th Intern. Congress on Catal., (1973) vol.1, p.399.
39. V.A.Zakharov, G.D.Bukatov, N.B.Chumaevski, Yu.I.Yermakov, React. Kinet. Catal. Lett., 1, 247 (1974).
40. A.Caunt, Moretonhampstead Conference, 1975.
41. A.Caunt, Br. Polymer J., 13, 22 (1981).
42. P.J.T.Tait, Proc. MMI-symposium, (1983) p.115.
43. T.Keii, J. Res. Inst., Hokkaido Univ., 28, 3 (1980).
44. G.Giannini, Makromol. Chem. Suppl., 5, 216 (1981).
45. Y.Doi, M.Murata, K.Yano, and T.Keii, I & EC Product Res. & Develop., 21, 580 (1982).
46. G.Henrici-Olive and S.Olive, Angew. Chem., 79, 764 (1967).

47. I.Okura and T.Keii, US-Japan Seminar on Catal., Honolulu (1971), see ref(3).
48. J.C.W.Chien, Catal. Rev.-Sci. Eng., 26, 613 (1984).
49. L.Rodriquez and G.Gabant, J. Polym. Sci., C-4, 125 (1964).
50. I.Okura see ref.(3) p.238.
51. M.Terano, T.Kataoka, and T.Keii, this volume
52. Y.Doi, S.Ueki, and T.Keii, Polymer, 21, 1352 (1980).

This page intentionally left blank

ZIEGLER POLYMERIZATION OF ETHYLENE: CATALYST DESIGN AND MOLECULAR MASS DISTRIBUTION

L.L. BÖHM, J. BERTHOLD, R. FRANKE, W. STROBEL, U. WOLFMEIER
Kunststoff-Forschung, Hoechst AG, 6230 Frankfurt (M) 80, Germany

ABSTRACT

For high density polyethylene the molecular mass distribution is one of the most important basic parameter. As the processability strongly depends on both molecular mass and molecular mass distribution, great efforts have been made to determine the origins of molecular mass distribution and, consequently, to control molecular mass distribution in technical processes. While the regulation of the molecular mass in polymerization processes is well understood today, there is no commonly accepted theory which could explain the dependence of molecular mass distribution on catalyst structure and polymerization parameters.

From experimental results we conclude that the molecular mass distribution of polyethylene prepared with heterogeneous Ziegler systems is mainly determined by chemical properties of the catalyst. Therefore we conclude that broad molecular mass distributions originate from number and properties of the different types or states of active sites.

Starting from this hypothesis, we successfully developed a catalytic system which enables us to control molecular mass distribution by specific manipulations of the catalyst as well as by changing the conditions of the polymerization process.

INTRODUCTION

Highly active Ziegler catalytic systems for the polymerization of ethylene, consisting of a heterogeneous transition metal catalyst and an aluminium-organic compound as a cocatalyst, are available since about

1966. These catalysts are at least by a facter of 20 more active than conventional Ziegler systems[1,2]. In a comprehensive paper, Diedrich described all types of highly active catalytic systems known until 1975[3]. For more than 10 years, these modern catalysts have been applied to technical processes often called "second generation processes". They are simpler and more economic than comparable "first generation processes"[3].

Todays research in industrial laboratories is concentrated upon improvements of these "second generation processes". New highly active catalytic systems have to be developed to produce "tailor made" polymers in easily controllable polymerization plants[4].

One important field is the search for catalytic systems which allow to regulate the molecular mass distributions, either by variation of the catalyst composition, or by manipulation of the process.

In this paper, our knowledge of the origins of molecular mass distribution will be summarized, and we will indicate how to regulate molecular mass distribution by catalyst design or process control.

MOLECULAR MASS DISTRIBUTIONS OF ZIEGLER POLYETHYLENES

In previous papers[5-8] it was reported that the Ziegler polymerization process comprises a propagation process and different chain transfer reactions for example with hydrogen and the cocatalyst.

Under usual polymerization conditions as in polymerization plants, high molecular mass polyethylene compounds with Schulz-Flory[9,10] most probable molecular mass distributions should be formed[11]. For polymerization in a slurry process with formation of semicrystalline polyethylene particles, insoluble in the hydrocarbon dispergent medium, these conditions imply constant monomer, hydrogen, and cocatalyst concentrations, plus constant temperature between 20 and 90 °C, ethylene partial pressures up to 10 bar and constant space time yield.

Kaminsky, Sinn and coworkers[12-14] reported a system consisting of dicyclopentadienyl zirconium dichloride and an oligomeric methylaluminoxane compound. Within experimental error, this system produces high mole-

cular mass polyethylene with a Schulz-Flory most probable molecular mass distribution when operating under technical conditions. The experimental result is shown in Figure 1. The polymer sample was prepared in the laboratory of Kaminsky, the g.p.c. measurements were carried out in Hoechst AG laboratories.

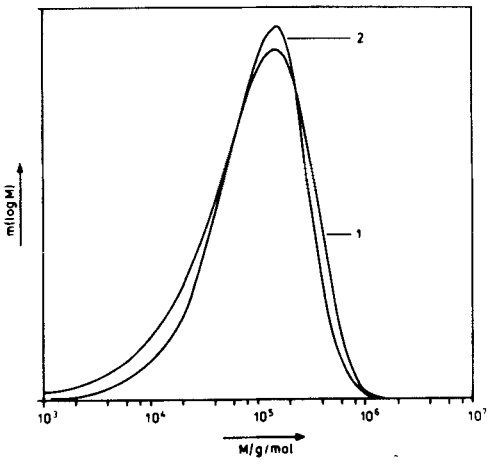

Figure 1. **1:** Schulz-Flory most probable molecular mass distribution with $M_n = 1.45 \cdot 10^5$ g/mol
2: Polyethylene sample prepared by Kaminsky et al.

These experiments confirm that, in principle, polymers with the Schulz-Flory most probable molecular mass distribution can be synthesized with Ziegler systems. In a paper, Clark and Bailey[15] demonstrated that polymers with polydispersity indices of 2 can be formed by means of heterogeneous catalytic systems, irrespective of the reaction mechanism. This holds true for the Rideal[16] as well as for the Langmuir-Hinshelwood[17,18] mechanism, provided that there is only one type of active sites.

The formation of polyethylenes with much broader molecular mass distributions which may be fitted to logarithmic normal or exponential functions (Wesslau[19], Tung[20]) has been explained by certain models: In these models, special reaction effects are assigned to the heterogenity of the catalytic system. Gordon and Roe[21] proposed the chain transfer reac-

tion to be determined by the degree of polymerization, because the polymer chain is adsorbed on the surface of the catalyst. Based on this assumption, the molecular mass distributions of polyethylene samples were calculated in accordance with experimental results. From this model it has been concluded that the molecular mass distribution is to change with average molecular mass. *High molecular compounds should have broad distributions*, low molecular compounds narrow ones[22]. But this does not agree with experimental results for samples prepared with a highly active Mg,Ti-catalyst[8] and $Al(C_2H_5)_3$ as cocatalyst. The molecular mass distributions are shown as integral plots for logarithmic normal functions on Figure 2.

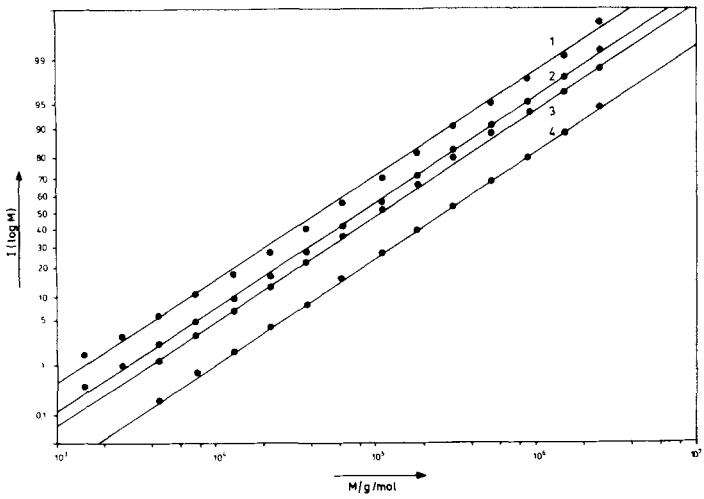

Figures 2. Integral mass distribution functions:
1: $M_n = 1{,}7 \cdot 10^4$; 2: $M_n = 3{,}1 \cdot 10^4$; 3: $M_n = 4{,}2 \cdot 10^4$;
4: $M_n = 1{,}05 \cdot 10^5$; $M_w/M_n = 7{,}5 \pm 2$

The integral plot is used because this plot indicates the same molecular mass distribution by parallel straight lines. The average molecular mass was changed by varying the hydrogen partial pressure. This result has also been confirmed by rheological measurements of Fleißner[23]; he showed the shear viscosity curves to have the same shape irrespective of the viscosity value. It has also been found that the elastic behavior of all samples was the same. These results demonstrate that at least for the highly active Mg,Ti/$Al(C_2H_5)_3$ system under investigation, the Gordon- Roe model cannot be valid.

In many papers[24-29] it has been pointed out that the insoluble polymer formed under slurry or gas phase polymerization conditions is coating the catalyst particles and building up a diffusion barrier for the incoming monomer. As a consequence the polydispersity M_w/M_n reaches high values at the beginning of polymerization and decreases with time. Experimental results show the slightly modified "polymeric flow model" of Ray and coworkers[29] to be the best model to describe the particle forming process during ethylene polymerization with the Mg,Ti/Al$(C_2H_5)_3$ system[8]. The experiments do not show the polymerization process to be diffusion controlled. This is demonstrated in Figure 3.

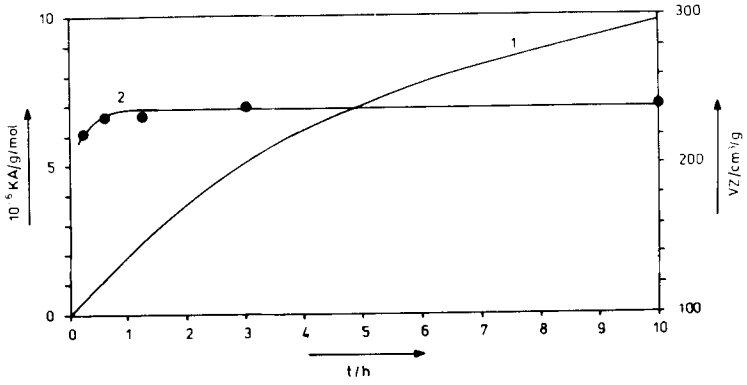

Figure 3. Catalyst yield KA (g/mM Ti) (curve 1) and viscosity number VZ (curve 2) versus time; Mg,Ti/Al$(C_2H_5)_3$ system, 85 °C, with hydrogen

The linear increase of catalyst yield and the nearly constant viscosity numbers as functions of time show that at least for this system diffusion limitation of ethylene under slurry polymerization conditions cannot be detected. The molecular mass distribution also does not change. In all cases it was logarithmic normal with M_w/M_n values of 7,5 $\pm$ 2 as shown in Figure 2.

The formation of polyethylene with molecular mass distributions much broader than the Schulz-Flory distribution can be explained by the existence of different types or states of active sites at the surface of the heterogeneous catalyst particle polymerizing simultaneously. This

model was proposed by different authors[39,15,22]. There are experimental results supporting this model[7,31]. It has been shown by investigation of polymerization kinetics that the propagation rate constant for the Mg,Ti/$Al(C_2H_5)_3$ system is 80 $dm^3/mol \cdot s$ at 85 °C. On the other hand it is also known for this system that the molecular mass increases very rapidly with time. If a polymer sample is withdrawn from the reactor 15 seconds after ethylene addition, the molecular mass distribution shows high molecular mass compounds just like the major amounts of a sample taken after 2 hours polymerization time[7]. This is shown in Figure 4.

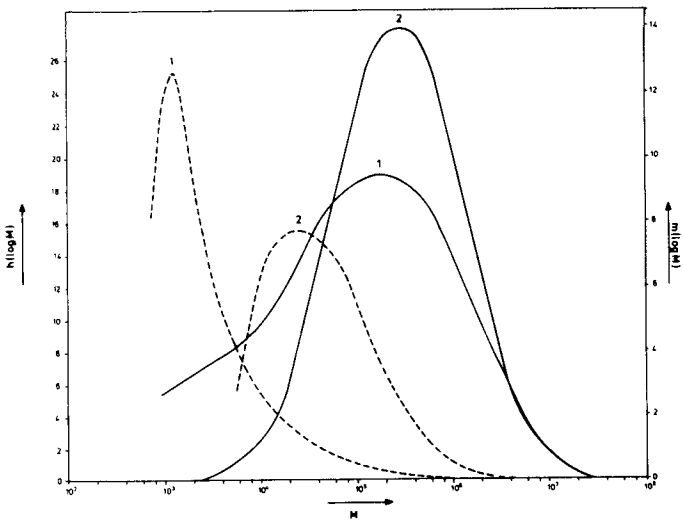

Figure 4. Molecular mass distribution (---frenquency and ——mass distribution): Mg,Ti/$Al(C_2H_5)_3$ system, 85 °C, without hydrogen; polymerization time: 1 : 15 sec; 2 : 2 h

From the degree of polymerization of the high molecular fraction of the 15 seconds sample it may be assumed that there must be active sites with propagation rate constants of at least 2,9 10^3 $dm^3/mol \cdot s$. In comparison to the average value of 80 $dm^3/mol \cdot s$ determined from kinetic measurements, this shows the propagation rate constants to be quite different for the different types or states of active sites at least for this system. Similar results were published by Meyer and Reichert[31].

From all these experimental results it must be concluded that the molecular mass distribution of polyethylene prepared with heterogeneous systems is mainly influenced and determined by the number and properties of the different types or states of active sites. Starting from this hypothesis "tailor made" catalysts for the preparation of polyethylene samples with different molecular mass distributions have been developed.

MANIPULATION OF MOLECULAR MASS DISTRIBUTION IN BATCH PROCESSES

The basic idea was to prepare a catalyst composed of several or at least two components which produce polyethylene with different average values of molecular mass under the same polymerization conditions. The Mg,Ti-catalyst described elsewhere[5-8] was coated with a further transition metal component. How the morphology of the Mg,Ti catalyst is changed can be visibilized by Scanning Electron Microscopy as shown in Figure 5.

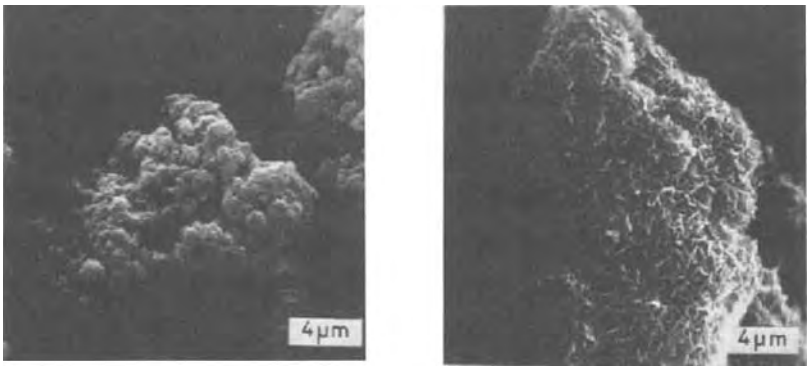

Figure 5. Scanning Electron Micrographs of the catalyst surfaces; magnification: 6.000; Mg,Ti-catalyst (left side); Coated Mg,Ti-catalyst (right side).

This catalyst was used for ethylene polymerization under the following experimental conditions: A reactor was filled with diesel oil at 85 °C (100 dm^3), the cocatalyst (in this case isoprenyl-aluminium[32]; 360 mmol) was added, then the catalyst (10 mmol Ti-compound) was introduced. Before pressurizing the reactor first with hydrogen (5,3 bar) and then with ethylene (3,0 bar). Both components (catalyst, cocatalyst) had time

to react with each other for 10 minutes or longer. The polymerization was observed by measuring catalyst yield KA, viscosity number VZ and molecular mass distribution versus time. The results are shown in Figures 6, 7.

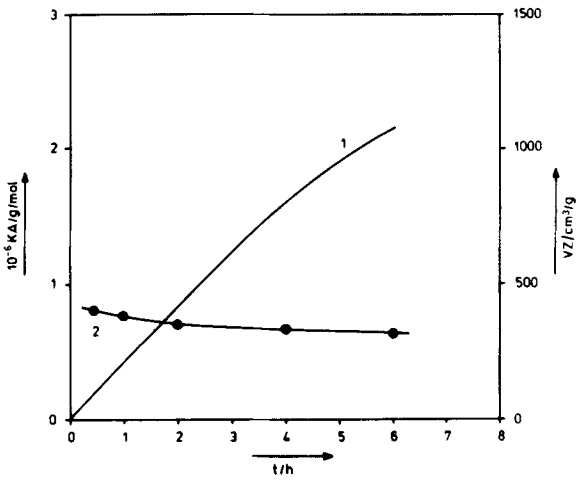

Figure 6. Catalyst yield KA (curve 1) and viscosity number VZ (curve 2) versus time t; catalyst and cocatalyst react for 10 minutes before ethylene introduction

There is no surprizing effect discovered in this experiment. Catalyst yield increases with time, first rapidly, then slowly. The viscosity number VZ as a measure of average molecular mass is nearly constant with time, and the molecular mass distribution does not depend on time, but shows a high molecular mass portion. This demonstrates that 2 catalytic systems are polymerizing simultaneously, in accordance with catalyst preparation.

The reactor was filled again with diesel oil at 85 °C (100 dm^3), then the cocatalyst was added (100 mmol). The reactor was pressurized with hydrogen (5,3 bar) and ethylene (3,0 bar). The polymerization was started by injection of the catalyst (10 mmol Ti-compound) into the pressurized reactor. Again catalyst yield KA, viscosity number VZ, and molecular mass distribution were recorded as functions of time. These data are plotted in Figure 8, 9.

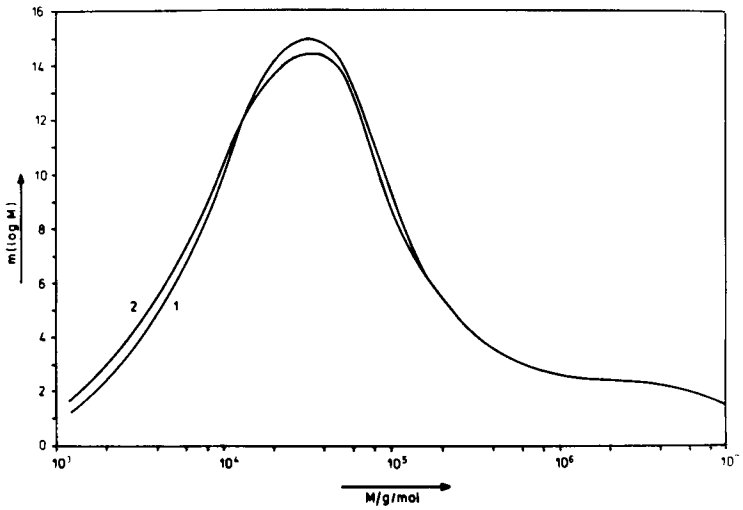

Figure 7. Molecular mass distribution as a function of reaction time: 1 : 35 min; 2 : 6 h; values $>10^8$ g/mol are not given, because these compounds cannot be completely separated. For reaction conditions see Figure 6.

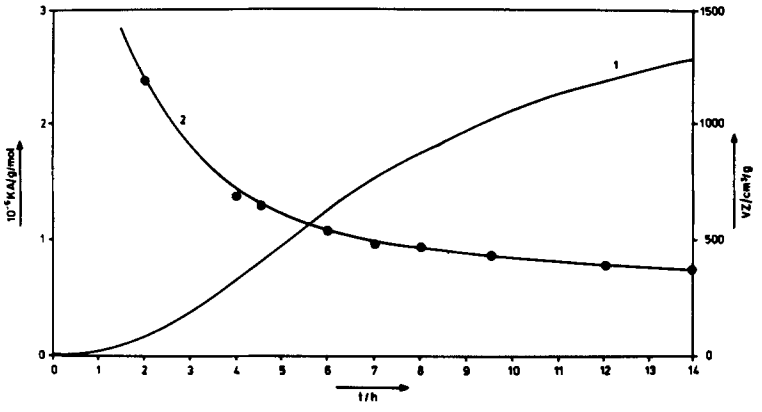

Figure 8. Catalyst yield KA (curve 1) and viscosity number VZ (curve 2) versus time t; catalyst and cocatalyst did not react before ethylene introduction.

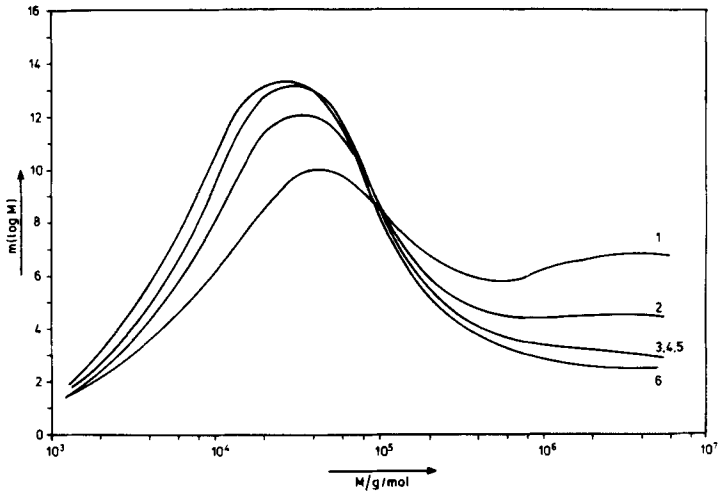

Figure 9. Molecular mass distribution as function of reaction time: 1 : 2 h; 2 : 4,5 h; 3 : 7 h; 4 : 9,5 h; 5 : 12 h; 6 : 14 h. For reaction conditions see Figure 8.

The experimental results presented in Figure 8 and 9 show the catalyst yield to be very low over a long time (2,5 h), then increases until the rate maximum is reached at 5 h, and finally increases slowly to reach a nearly constant value after 14 h. This behaviour is completely different in relation to the behaviour shown in Figure 6. The viscosity number versus time curve is again quite different in comparison to the curve in Figure 6 demonstrating this curve to be extremely time dependent. At short reaction times the viscosity numbers are high and decrease with time until they reach approximately the same value as plotted in Figure 6.

Figure 9 clearly points out the different behaviour, because this picture shows different bimodal molecular mass distributions depending on reaction time. As all curves intersect at one point it must be concluded that there are two catalytic systems operating independently. The main point is - and this is of great importance - that these molecular mass distributions can be varied by changing the polymerization time. The bimodal distributions obtained are very favorable in regard to properties and application of those polymers.

DISCUSSION

The basic catalyst consists of a highly active Mg,Ti-catalyst which forms polyethylene with molecular mass distributions not depending on average molecular mass or viscosity number and time as pointed out in Figures 2, 3 (cocatalyst $Al(C_2H_5)_3$). There are no possibilities to influence the molecular mass distribution by changing the formation of the catalytic system.

If this catalyst is coated with another transition metal compound, a new catalyst is formed, the behaviour of which is extremely different from the basic catalyst. By changing conditions during catalytic system formation, time independent or time dependent molecular mass distributions can be observed under the same process parameters in a batch process. An explanation for this behaviour which is in accordance with all experimental results so far observed, is shown in Figure 10.

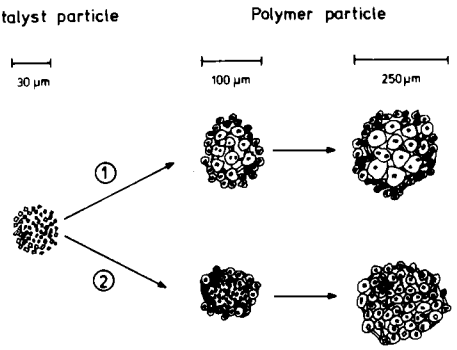

Figure 10. Catalyst design and particle forming process: **1** Before ethylene addition, catalyst and cocatalyst have reacted for at least 10 minutes; **2** Before ethylene addition both components have not interacted.

Figure 10 represents the catalyst particle to consist of smaller primary particles of two different types (filled and open particles). The

filled particles are located in the center and they are coated with open particles. This picture is consistent with catalyst preparation. Path 1 shows that all primary particles start polymerization if catalyst and cocatalyst have had time to interact before ethylene addition. In this case catalyst yield KA increases rapidly with time t; viscosity number VZ and molecular mass distribution are nearly independent of time t. Molecular mass distribution is catalyst dependent, but time independent.

Path 2 is an alternative way to prepare polyethylene with the same catalytic system. If there is no time for catalyst/cocatalyst interaction before ethylene addition, only the primary particles at the surface start polymerization because they are activated by the cocatalyst. In this case catalyst yield KA increases very slowly with time t, and the viscosity number VZ is extremely high, because the open catalyst particles are less active but produce high molecular polyethylene even at high hydrogen content ($\sim$64 Vol.-%). During polymerization the cocatalyst penetrates into the polymerizing particle by diffusion to activate the primary particles in the center. The polymerization rate increases and the viscosity number decreases with time, because the filled primary particles are more active and average molecular mass is regulated effectively by hydrogen. As a consequence the molecular mass distribution changes with time. So in this case molecular mass distribution is catalyst and time dependent.

The concept that cocatalyst diffusion into the polymerizing particle is basically the regulating process for molecular mass distribution can be supported by experiments demonstrating that polymerization behaviour and molecular mass distribution via path 2 can be influenced by cocatalyst concentration and the type of cocatalyst. If in path 2 cocatalyst concentration is increased and/or molecular mass of cocatalyst decreases the behaviour is shifted in the direction of the path 1 behaviour. Consequently this catalytic system can be influenced easily by different parameters to change the bimodal molecular mass distribution.

Evidently the highly flexible catalytic system developed is capable of producing "tailor made" high molecular polyethylenes in batch as well as continuous processes.

REFERENCES

1. K. Ziegler, E. Holzkamp, E. Breil, H. Martin, Angew. Chem. 67, 426, 541 (1955)
2. DE 973 626 (1953), Inv. K. Ziegler, H. Breil, E. Holzkamp, H. Martin; C.A. 68, 105 657 (1968)
3. B. Diedrich, Appl. Polym. Symp. 26, 1 (1975)
4. K. Weissermel, H. Cherdron, J. Berthold, B. Diedrich, K.D. Keil, K. Rust, H. Strametz, T. Toth, J. Polym. Sci., Symp. 51, 187 (1975)
5. L.L. Böhm, Polymer 19, 545 (1978)
6. L.L. Böhm, Polymer 19, 553 (1978)
7. L.L. Böhm, Polymer 19, 561 (1978)
8. L.L. Böhm, Chem. Ing. Techn. 56, 674 (1984)
9. G.V. Schulz, Z. Phys. Chem. B 30, 379 (1935)
10. P.J. Flory, J. Amer. Chem. Soc. 58, 1877 (1936)
11. L.L. Böhm, H. Passing, Makromol. Chem. 177, 1097 (1976)
12. H. Sinn, W. Kaminsky, Adv. Organomet. Chem. 18, 99 (1980)
13. W. Kaminsky, Polymerization and Copolymerization with a Highly Active, Soluble Ziegler-Natta-Catalyst in Transition Metal Catalyzed Polymerizations, Ed. R.P. Quirk, Harword Academic Publ., Chur, London, New York, 1983, p. 225
14. W. Kaminsky, M. Miri, H. Sinn, R. Woldt, Makromol. Chem., Rapid Comm. 4, 417 (1983)
15. A. Clark, G.C. Bailey, J. Catal. 2, 230 (1963)
16. E.K. Rideal, Proc. Cambridge Phil. Soc. 35, 130 (1939)
17. I. Langmuir, Trans. Faraday Soc. 17, 621 (1921)
18. C.N. Hinshelwood, Kinetics of Chemical Change, Oxford University Press, New York, 1940
19. H. Wesslau, Makromol. Chem. 20, 111 (1956)
20. L.H. Tung, J. Polym. Sci. 20, 495 (1956)
21. M. Gordon, R.-J. Roe, Polymer 2, 41 (1961)
22. R.-J. Roe, Polymer 2, 60 (1961)
23. M. Fleissner, Angew. Makromol. Chem. 94, 197 (1981)
24. V.W. Buls, T.L. Higgins, J. Polym. Sci., A-1, 8, 1037 (1970)
25. D. Singh, R.P. Merrill, Macromolecules 4, 599 (1971)
26. W.R. Schmeal, J.R. Street, AICHEJ. 17, 1188 (1971)
27. J.R. Crabtree, F.N. Grimsby, A.J. Nummelin, J.M. Sketchley, J. Appl. Polym. Sci., 17, 959 (1973)

28. E.J. Nagel, V.A. Kirillov, W.H. Ray, Ind. Eng. Chem., Prod. Res. Dev. 19, 372 (1980)
29. T.W. Taylor, K.Y. Choi, H. Yuan, W.H. Ray, Physicochemical Kinetics of Liquid Phase Propylene Polymerization in Transition Metal Catalyzed Polymerizations, Ed. R.P. Quirk, Harword Academic Publ., Chur, London, New York, 1981, p. 191
30. G. Natta, J. Polymer. Sci. 34, 21 (1959)
31. H. Meyer, K.H. Reichert, Angew. Makromol. Chem. 57, 211 (1977)
32. H. Hoberg, H. Martin, R. Rienäcker, K. Zosel, K. Ziegler, Brennstoff-Chemie 50, 217 (1969)

THE ROLE OF ETHYL BENZOATE IN HIGH-ACTIVITY AND HIGH-STEREOSPECIFICITY $MgCl_2$-SUPPORTED $TiCl_4$ CATALYST SYSTEM

N.KASHIWA, M.KAWASAKI and J.YOSHITAKE
Research Center, Mitsui Petrochemical Industries, Ltd., Waki-cho, Kuga-gun, Yamaguchi-ken, 740, Japan

ABSTRACT

The role of ethyl benzoate (EB) in a highly active and highly stereospecific $MgCl_2/TiCl_4$-$AlEt_3$/EB catalyst system for propylene polymerization was investigated. It was found that suitable amounts of EB increased the yield of isotactic polymers, at the same time decreasing very sharply the yield of atactic polymers and consequently enhancing stereospecificity. From the results of a kinetic study of short-time polymerization, the said increase in yield of isotactic polymers and decrease in yield of atactic polymers may be attributed to increase in the value of the propagation rate constant at isotactic active centers and decrease of the concentration of atactic active centers.

INTRODUCTION

For propylene polymerization, Mitsui Petrochemical Industries Ltd., in collaboration with Montedison S.P.A., was the first in the world to succeed in the research and development of activity-high stereospecific $MgCl_2$-supported $TiCl_4$ catalyst systems,[1] and subsequently in their manufacture on an industrial scale in conjunction with resource and energy coservation. In these catalyst systems, an electron donor (Lewis base) such as an ester is used as an important catalyst component for outstanding effectiveness. It is the purpose of this paper to discuss the role of ethyl benzoate known as a typical example of an effective electron donor by comparing the catalyst systems of $MgCl_2/TiCl_4$-$AlEt_3$ and $MgCl_2/TiCl_4$-$AlEt_3$/ethyl benzoate.

EXPERIMENTAL

Preparation of the catalysts:

$MgCl_2/TiCl_4$: 2.8 Kg of stainless steel balls (15mm in diameter) was put into a pot of internal volume 800 ml. The inside of the pot was purged efficiently with N_2, then $MgCl_2$(20g) was added and the pot was placed on a roller-type milling machine for 60 h at room temperature. Ten grams of the solid thus obtained was transferred into a flask, reacted for 2 h at 80°C with 100 ml of $TiCl_4$; the solid portion was then separated by filtration and washed with n-decane. Eight milligrams of Ti atoms was contained in 1 g of the supported Ti catalyst.

$TiCl_3$(AA): The product used was TAC-131 made by Toho Titanium Co., Ltd.

Polymerization:

Chapter 1: (a) Propylene polymerization was conducted by adding 500 ml of n-decane solvent to a 1000 ml glass flask. After saturating the solvent with propylene, $AlEt_3$(0.5 mmol) and $MgCl_2/TiCl_4$(or $TiCl_3$(AA), 0.05 mmol) were added and polymerization was performed for 1 h at 60°C under atmospheric pressure. After completion of polymerization, a slight amount of ethanol was first added to the system to stop the polymerization and followed by a large quantity of methanol. The resulting solid polymer was collected and dried under decreased pressure.

(b) Propylene polymerization was done by adding 250 ml of n-decane solvent to a 500 ml glass flask. After saturating the solvent with propylene, $AlEt_3$(0.725, 1.45, 2.175, 2.90 or 3.625 mmol) and $MgCl_2/TiCl_4$ catalyst (0.145 mmol of Ti) were added ([Al]/[Ti]=5, 10, 15, 20 or 25) and polymerization was performed for 30 min at 50°C under atmospheric pressure. The rest of the polymerization procedure was the same as (a).

Chapter 2: After saturating the solvent with propylene, $AlEt_3$(3 mmol), EB(0, 0.3625, 0.725, 1.015, 1.450 or 2.175 mmol) and $MgCl_2/TiCl_4$ catalyst (0.145 mmol of Ti) were added in the said order ([Al]/[Ti]=25, [EB]/[Ti]=0, 2.5, 5.0, 10.0 or 15.0). The rest of the polymerization procedure was the same as described in chapter 1.

Chapter 3: (a) Propylene polymerization was performed for 5 min, 10 min, 20 min and 30 min with $MgCl_2/TiCl_4$-$AlEt_3$ or $MgCl_2/TiCl_4$-$AlEt_3$/EB at the condition of [Al]=14.5 mmol/l, [Ti]=0.58 mmol/l, [EB]=0 or 4.06 mmol/l. The rest of the polymerization procedure was the same as

described in chapter 2.

(b) EB (1.015 mmol) was added into the polymerization system with $MgCl_2/TiCl_4$-$AlEt_3$ 5 min after start of polymerization. The rest of the polymerization procedure was the same as described in chapter 1.

Chapter 4: (a) Catalyst system $MgCl_2/TiCl_4$-$AlEt_3$/EB: Propylene polymerization was carried out in 500 ml of n-decane, which was first filled with propylene. $AlEt_3$ (5.0 mmol), EB (1.25 mmol) and $MgCl_2/TiCl_4$ catalyst (0.2 mmol of Ti) were added in the said order, and polymerization was performed at 60°C for a short time (7-60 sec). The rest of the polymerization procedure was the same as described in chapter 1.

(b) Catalyst system $MgCl_2/TiCl_4$-$AlEt_3$: Polymerization conditions were the same as those in (a) of this chapter except that EB was not used.

Characterization of the produced polymer

Isotactic Index (I.I.) of the polymer produced was measured as the weight fraction of polymer insoluble in boiling heptane. The ^{13}C-NMR isotactic value was determined from the triad peaks of the primary carbon resonances. The polydispersity and $\bar{M}n$ of the polymers were measured by gel permeation chromatography (GPC) (Waters Associates, Model ALC/GPC 150C) using mix polystyrene gel column (10^7, 10^6, 10^5, 10^4 and 10^3 Å pore sizes) and at 135°C with o-dichlorobenzene as solvent.

RESULTS AND DISCUSSION

1. Propylene polymerization with the $MgCl_2/TiCl_4$-$AlEt_3$ catalyst system:

- Comparison with the $TiCl_3$(AA)-$AlEt_3$ catalyst system
- Effect of the concentration of $AlEt_3$

The $MgCl_2$-supported $TiCl_4$ catalyst system is well known to exhibit very high activity in olefin polymerization. Fig. 1 shows the kinetic curve obtained for propylene polymerization with $MgCl_2$-supported $TiCl_4$ (represented as $MgCl_2/TiCl_4$) catalyst in conjunction with $AlEt_3$. $MgCl_2/TiCl_4$ catalyst was obtained by ball-milling of $MgCl_2$ followed by reacting with $TiCl_4$ and separating the solid product. For comparison, the kinetic curve under identical conditions is shown in Fig. 1 for $TiCl_3$(AA)-$AlEt_3$. Table 1 shows propylene polymerization activity and the analytical results of polypropylene with each catalyst system.

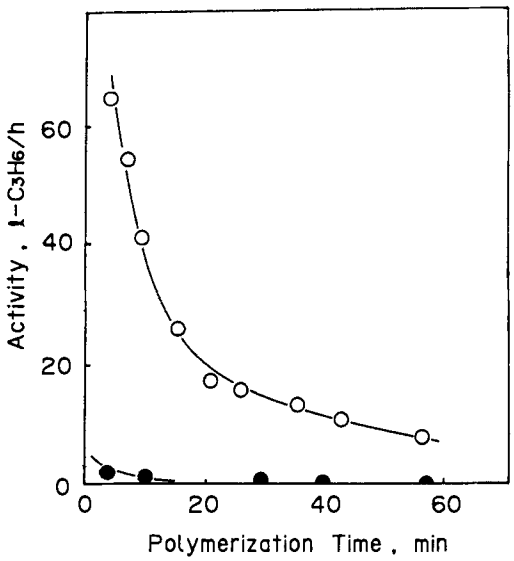

Fig. 1 Kinetic curves of propylene polymerization at 60°C; [Ti]= 0.1 mmol/l; [$AlEt_3$]=1.0 mmol/l; (○) $MgCl_2/TiCl_4$-$AlEt_3$; (●) $TiCl_3$ (AA)-$AlEt_3$

Table 1 Comparison of polymerization performance[a)]

Catalyst	Activity (g/mmolTi·h)	I.I[b)] (wt%)	Iso. value[c)] (%)
$MgCl_2/TiCl_4$-$AlEt_3$	968	33.9	89
$TiCl_3$(AA)-$AlEt_3$	23	75.9	91

a) Polymerization conditions are the same as in Fig. 1.
b) Weight fraction of polymers insoluble in boiling heptane.
c) Determined from the triad peaks of primary carbon resonance using the fraction insoluble in boiling heptane.

As is apparent from the given results, the $MgCl_2/TiCl_4$ catalyst system was highly active in the yield per 1 mmol of Ti in comparison with the $TiCl_3$ catalyst system, but the stereospecificity (isotactic index, I.I.) of polymer produced was quite low. However, one should notice that, as shown in Table 1, the yield of polymers insoluble in boiling heptane (isotactic polymers) per unit of Ti atom was extremely high in comparison with that of $TiCl_3$ and the isotacticity value of this

polymer by ^{13}C-NMR (triad) was almost as high as that of isotactic polymers obtained with the $TiCl_3$ catalyst system, which suggests that there are highly stereospecific (isotactic) active centers in the $MgCl_2/TiCl_4$ catalyst system as well as in the $TiCl_3$ catalyst system. So it is reasonable to assume that a highly active and highly stereospecific catalyst could be obtained by using very selectively only the stereospecific (isotactic) active centers in the $MgCl_2/TiCl_4$-$AlEt_3$ catalyst system.

In order to obtain more detailed information on polymerization with the $MgCl_2/TiCl_4$ catalyst system, the effect of the concentration of $AlEt_3$, [Al], was studied at 50°C slurry polymerization for 30 min. Table 2 and Figs. 2-7 show the polymerization results obtained by changing $AlEt_3$ concentration from 2.9 to 14.5 mmol/l under constant Ti concentration of 0.58 mmol/l (therefore, [Al]/[Ti] molar ratio was changed in the range of 5-25).

From these studies, the following was noted.

Overall polymer yields were constant and independent of [Al] in all experiments and I.I. of the produced polymer, as shown in Fig. 2, was almost unchanged (around 35%) in the range between 8.7 and 14.5 mmol/l of [Al]([Al]/[Ti]=15-25 mol/mol), but elevated slightly (42-44%) at lower [Al] of 5.8 ([Al]/[Ti]=10)-2.9 mmol/l ([Al]/[Ti]=5) by slight changes in the yields of heptane-insoluble and -soluble polymers in Fig. 3.

Molecular weight of boiling heptane-insoluble polymers and boiling heptane-soluble polymers (hereafter, represented as C_7-insoluble and C_7-soluble polymers, respectively) remained almost constant, except those produced under the condition of lowest [Al](2.9 mmol/l, [Al]/[Ti]=5), which were significantly higher than others as shown in Fig. 4.

The polydispersity($\bar{M}w/\bar{M}n$) could be regarded to be almost constant, except the slight decrease of C_7-insoluble polymers at the lowest [Al](Fig. 5). GPC curves of C_7-soluble polymers (Fig. 6) were all symmetric and showed no significant difference among themselves except for a slight shift to a higher molecular weight at the lowest [Al]. On the other hand, as shown in Fig. 7, GPC curves of isotactic polymers were all asymmetric and they seemed to be divided into two peaks at around 10^5 and 10^5-10^6 molecular weight. With lowering of [Al]/[Ti] or [Al], these asymmetric curves moved to a higher molecular weight, changing shapes by increasing the portion of higher molecular

Table 2 The effect of the concentration of $AlEt_3$ in the $MgCl_2/TiCl_4$-$AlEt_3$ catalyst system[1)]

No.	[Al]/[Ti] (mol/mol)	I.I. (wt%)	Yield				GPC					
			Overall		C_7-insol.	C_7-sol.	Overall		C_7-insol.		C_7-sol.	
			(g)	(g/mmolTi)	(g/mmolTi)	(g/mmolTi)	$\bar{M}n \times 10^{-4}$	$\bar{M}w/\bar{M}n$	$\bar{M}n \times 10^{-4}$	$\bar{M}w/\bar{M}n$	$\bar{M}n \times 10^{-4}$	$\bar{M}w/\bar{M}n$
101	5	42	54.8	378	159	219	2.57	7.27	9.52	3.47	1.93	4.41
102	10	44	51.2	353	155	198	2.62	6.77	7.61	4.27	1.61	4.47
103	15	35	58.2	401	140	261	2.53	6.72	7.84	4.54	1.46	4.69
104	20	35	55.9	386	135	251	1.77	10.2	7.75	4.77	1.42	4.67
105	25	37	55.0	379	140	239	2.19	8.18	7.49	4.34	1.36	4.59
106[2)]	25	84	42.9	296	249	47	5.78	8.14	9.36	4.96	1.25	5.13

1) n-decane 250 ml, 50°C, 30 min, [Ti]=0.58 mmol/l

2) $MgCl_2/TiCl_4$-$AlEt_3$/EB, [EB]/[Ti]=7 mol/mol

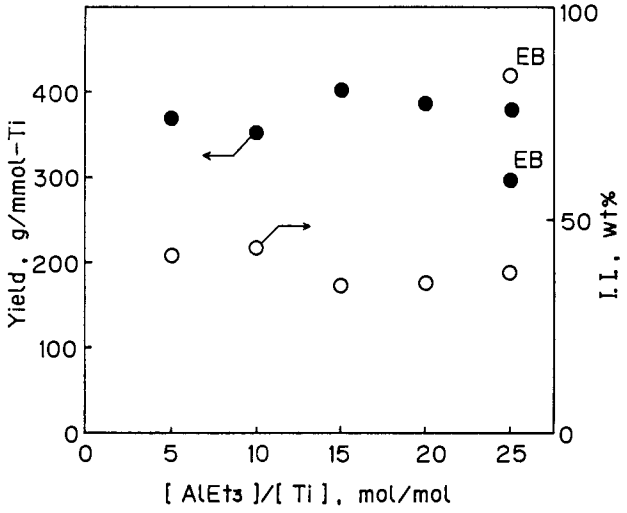

Fig. 2 Effect of $[AlEt_3]/[Ti]$ on the yield (●) and Isotactic Index (I.I.) of produced polymer (○) with $MgCl_2/TiCl_4$-$AlEt_3$. $●^{EB}$ and $○^{EB}$: $MgCl_2/TiCl_4$-$AlEt_3$/EB. Polymerization conditions are the same as those in Table 2.

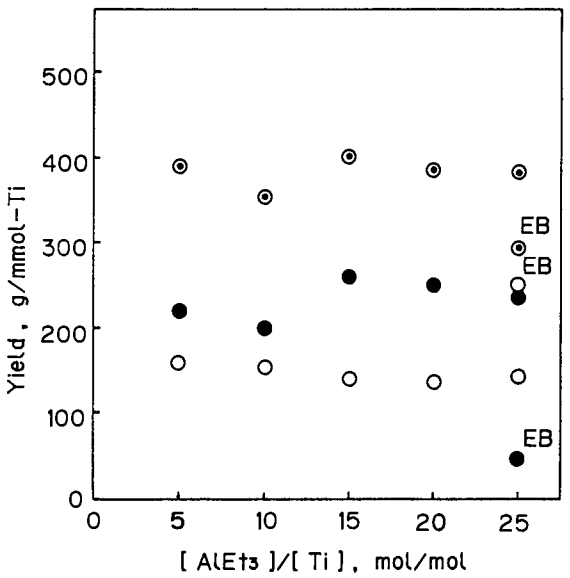

Fig. 3 Effect of $[AlEt_3]/[Ti]$ on the polymer yields (overall polymers (◉), C_7-soluble polymers (●), C_7-insoluble polymers (○)) with $MgCl_2/TiCl_4$-$AlEt_3$. Polymerization conditions are the same as those in Table 2.

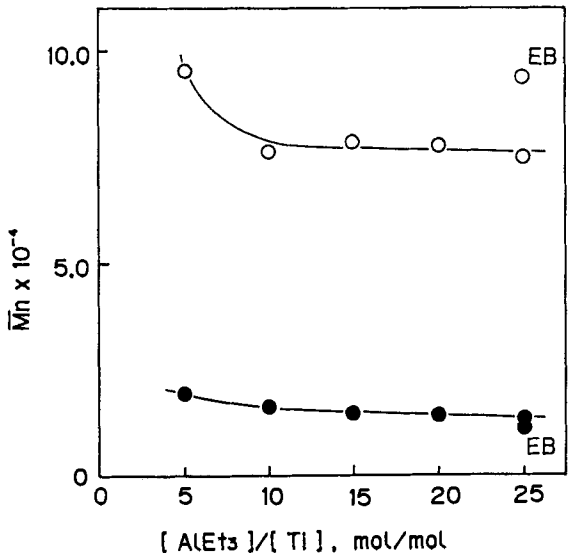

Fig. 4 Effect of $[AlEt_3]/[Ti]$ on $\bar{M}n$ of the produced polymers (C_7-soluble polymers (●), C_7-insoluble polymers (○)) with $MgCl_2/TiCl_4$-$AlEt_3$. Polymerization conditions are the same as those in Table 2.

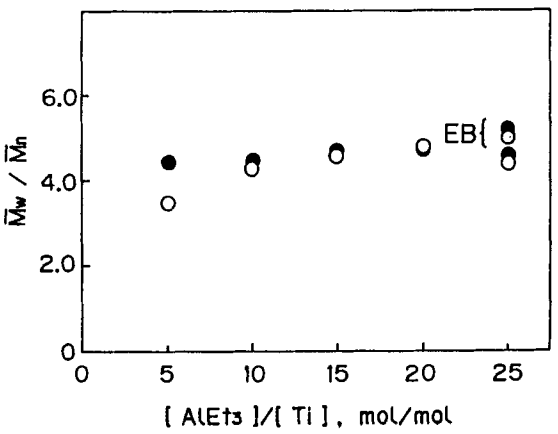

Fig. 5 Effect of $[AlEt_3]/[Ti]$ on $\bar{M}w/\bar{M}n$ (C_7-soluble polymers (●), C_7-insoluble polymers (○)) in $MgCl_2/TiCl_4$-$AlEt_3$. Polymerization conditions are the same as those in Table 2.

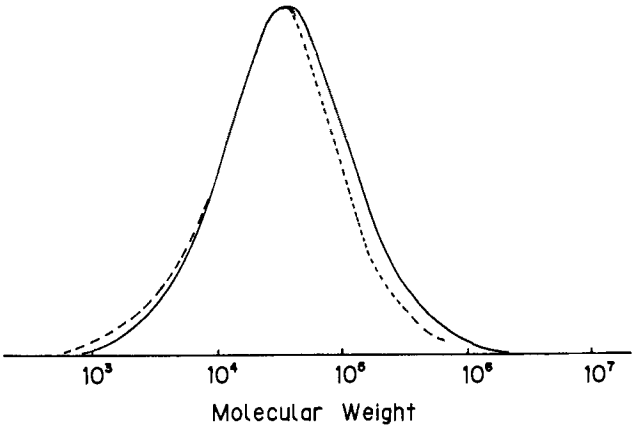

Fig. 6 Effect of $[AlEt_3]/[Ti]$ on the GPC curves of C_7-soluble polymers with $MgCl_2/TiCl_4$-$AlEt_3$. $[AlEt_3]/[Ti]$=5(——); $[AlEt_3]/[Ti]$= 10, 15, 20 and 25(-------). Polymerization conditions are the same as those in Table 2.

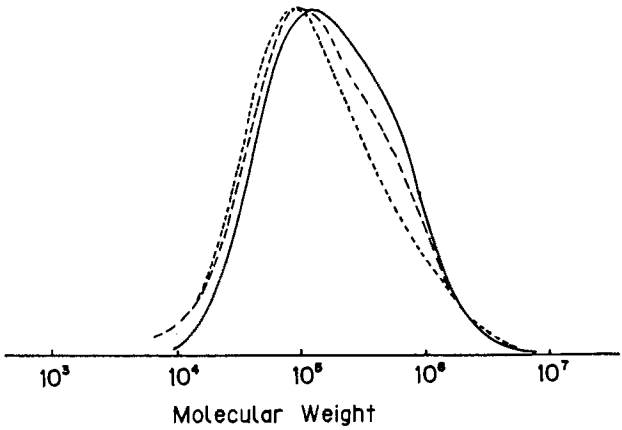

Fig. 7 Effect of $[AlEt_3]/[Ti]$ on the GPC curves of C_7-insoluble polymers with $MgCl_2/TiCl_4$-$AlEt_3$. $[AlEt_3]/[Ti]$=5(——); $[AlEt_3]/[Ti]$= 10(– – –); $[AlEt_3]/[Ti]$=15, 20 and 25(-------).
Polymerization conditions are the same as those in Table 2.

weight(10^5-10^6). The aforementioned increase of $\bar{M}n$ of C^7-insoluble polymers at the lowest [Al] in Fig. 4 could be attributed to the significant increase of the contribution of the peak at higher molecular weight.

These changes in the shape of GPC curves of C_7-insoluble (isotactic) polymer may be explained as follows: There would be at least two separate groups of isotactic active centers which would produce C_7-insoluble (isotactic) polymers having different molecular weight. And, under conditions of higher [Al], a group of active centers to produce isotactic polymers of lower molecular weight could be formed preferentially; on the other hand, under conditions of lower [Al], the other group of active centers to produce isotactic polymer of higher molecular weight could become comparable to the first group.

In other words, there would be two groups of isotactic active centers of which one would have a lower propagation rate constant, k_p and/or higher chain transfer rate constant, k_{tr} and the former could be formed with the higher probability under conditions of higher [Al]. Considering that $TiCl_4$ is easily reduced by the reaction with $AlEt_3$,[2] it may be that active centers formed at lower [Al] consist of Ti atoms of higher valence state.

In summary, within the range of the present investigation, the $MgCl_2/TiCl_4$-$AlEt_3$ catalyst system showed very high activity per unit of Ti atom but low stereospecificity, and the concentration of $AlEt_3$ in this catalyst system was not important on either activity or stereospecificity. GPC curves of obtained polypropylene suggest that there are at least two groups of isotactic active centers to produce isotactic polymers of different molecular weights, and the proportion of the contribution of each group depends on the concentration of $AlEt_3$.

2. Propylene polymerization with the $MgCl_2/TiCl_4$-$AlEt_3$/ethyl benzoate(EB) catalyst system
-Effect of addition of EB

Next, ethyl benzoate(EB) was introduced to the polymerization system following $AlEt_3$ addition under the condition of [EB]/[Ti]=7 (mol/mol), [Al]/[Ti]=25(mol/mol) and [Ti]=0.58 mmol/l in order to examine preliminarily the role of EB. The results are listed at the

bottom of Table 2. These data were plotted with notation of EB in Figs. 2-5 for comparison with data without EB addition.

First, as shown in Fig. 2, by addition of EB, I.I. of the obtained polymer was markedly enhanced from 37 wt% to 84 wt%, but at the same time, the overall polymer yield was lowered considerably. One can see from Fig. 3 that the decrease of the overall polymer yield was attributable to the sharp decrease of C_7-soluble (atactic) polymers, which cancelled the increase of C_7-insoluble (isotactic) polymers, and the drastic increase of I.I. was attained by these very favorable changes of yields for both polymers. Namely, by addition of EB, the yield of C_7-soluble (atactic) polymers was lowered to 20%, while in contrast, the yield of C_7-insoluble (isotactic) polymers increased to 175% of those without EB. These characteristic effects observed by addition of EB could not be seen by changing $AlEt_3$ concentrations in the $MgCl_2/TiCl_4$-$AlEt_3$ catalyst system (Fig. 2, 3). Therefore, these effects could not be attributed to the decrease of "effective $AlEt_3$ concentration"[3] by the reaction of $AlEt_3$ with EB[4-6], but could be well explained by the fact that EB had direct but entirely different action to atactic and isotactic active centers, namely, EB poisoned atactic active centers very preferentially, while it associated with isotactic centers in such a manner as to enhance the activity.

EB showed a similar effect on molecular weight and polydispersity of the polymers. As for the polydispersity, $\bar{M}w/\bar{M}n$ values of both atactic and isotactic polymers were slightly enlarged (Fig. 5). On the other hand, $\bar{M}n$ of both polymers (isotacitc and atactic) were affected by EB in a different way, that is increase of $\bar{M}n$ for isotactic polymers and slight decrease of $\bar{M}n$ for atactic polymers (Fig. 4). Although the same increase of $\bar{M}n$ for isotactic polymers was observed in Fig. 4 at the lowest [$AlEt_3$] without EB, the behavior of the atactic polymers was opposite to that obtained by EB addition.

As the result of the preliminary examination on the $MgCl_2/TiCl_4$-$AlEt_3$/EB catalyst system, the following may be pointed out as the effects of EB addition.

1) Considerable increase in yield of isotactic polymers
2) Sharp decrease in yield of atactic polymers
3) Increase of $\bar{M}n$ of isotactic polymers, and some decrease of that of atactic polymers

Further investigation to obtain more detailed information on the

role of EB was carried out by changing the amount of EB added from 0 to 15 in terms of the molar ratio of [EB]/[Ti] under the conditions of [$AlEt_3$]/[Ti]=25, [Ti]=0.58 mmol/l, 50°C, 15 min polymerization. The results are listed in Table 3 and shown in Figs. 8-13.

Figure 8 shows the dependence of the yields and I.I. of all polymers on the amount of added EB. EB enhanced I.I. of the polymers markedly from 35% to maximum values of 90%, but with considerable loss of the yield of all polymers. Fig. 9 shows that the loss of all polymers was attributable to the successive decrease of C_7-soluble (atactic) polymers by EB addition which canceled the increase of C_7-insoluble (isotactic) polymers. The yield of C_7-soluble (atactic) polymers decreased to only 7% as much as that of a control at the highest amount of EB ([EB]/[Ti]=15). On the other hand, the yield curve of C_7-insoluble (isotactic) polymers showed maximum peak, at which the yield was 1.9 times that of a control. EB increased the yield of C_7-insoluble (isotactic) polymers within the whole range of concentrations of EB in the present experiments. However, Fig. 9 shows that the use of an excess amount of EB results in the loss of C_7-insoluble (isotactic) polymers, for example, by the complexing of EB to the isotactic active center; therefore the obtained yield curve could be considered to be the result of the mutual cancellation of the positive and negative effects of EB on the yield and the result of overcoming the positive effect within the present experiments. Fig. 10 shows that EB increased the polydispersity, $\bar{M}w/\bar{M}n$ value of the both polymers of C_7-insoluble (isotactic) and C_7-soluble (atactic) polymers with increase of the amount added (see also Figs. 12, 13). Fig. 11 shows that, with increase of the added amount, EB increased markedly the molecular weight of C_7-insoluble (isotactic) polymers, but decreased slightly the molecular weight of C_7-soluble (atactic) polymers indicating that EB had quite opposite actions on the two active centers.

Figures 12 and 13 reflect clearly the changes of $\bar{M}w/\bar{M}n$ and $\bar{M}n$ in Figs. 10 and 11 by addition of EB. Fig. 12 shows that, with increase in the amount of added EB, GPC curves of C_7-soluble (atactic) polymers shifted to lower molecular weight, broadening the peak area. As mentioned above, EB very effectively inactivates active centers to produce C_7-soluble polymers. Therefore, the above results may be explained as the preferential inactivation of active centers to produce C_7-soluble (atactic) polymers of higher molecular weight.

Table 3 Effect of addition of ethyl benzoate into the $MgCl_2/TiCl_4$-$AlEt_3$ catalyst system[1)]

No.	[EB]/[Ti] (mol/mol)	I.I. (wt%)	Yield				GPC					
			Overall		C_7-insol.	C_7-sol.	Overall		C_7-insol.		C_7-sol.	
			(g)	(g/mmolTi)	(g/mmolTi)	(g/mmolTi)	$\bar{M}n \times 10^{-4}$	$\bar{M}w/\bar{M}n$	$\bar{M}n \times 10^{-4}$	$\bar{M}w/\bar{M}n$	$\bar{M}n \times 10^{-4}$	$\bar{M}w/\bar{M}n$
201	0	35	26.5	230	81	147	2.05	7.93	6.96	4.81	1.47	3.53
202	2.5	58	25.9	225	131	94	2.33	10.5	7.10	4.08	1.22	3.70
203	5.0	78	22.4	195	152	43	5.26	7.00	8.37	4.68	1.52	3.74
204	10.0	85	20.4	177	150	27	5.17	8.78	9.62	4.57	1.05	5.44
205	15.0	90	12.0	104	94	10	6.36	9.99	11.1	5.52	0.96	6.91

1) n-decane 250 ml, 50°C, 30 min, [Ti]=0.58 mmol/l, $[AlEt_3]$=14.5 mmol/l

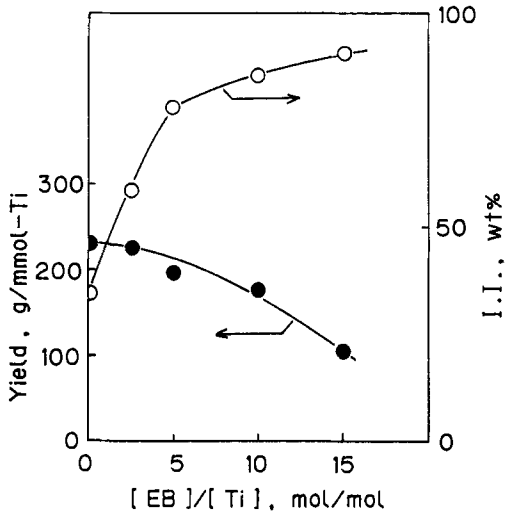

Fig. 8 Effect of [EB]/[Ti] on the yield (●) and Isotactic Index (I.I.) (○) of polymers produced with $MgCl_2/TiCl_4$-$AlEt_3$/EB. Polymerization conditions are the same as those in Table 3.

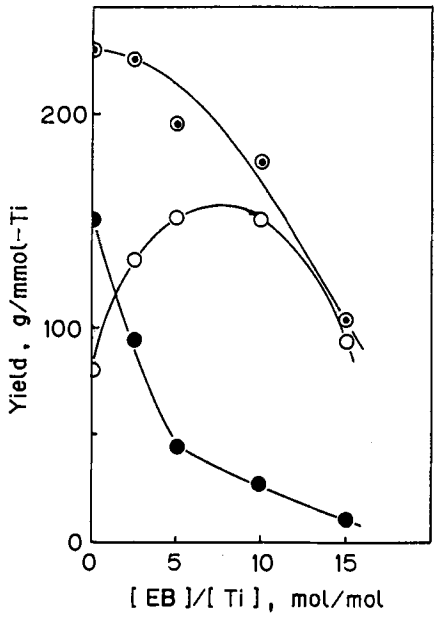

Fig. 9 Effect of [EB]/[Ti] on the yields (overall polymers (◎), C_7-soluble polymers (●), C_7-insoluble polymers (○)) with $MgCl_2/TiCl_4$-$AlEt_3$/EB. Polymerization conditions are the same as those in Table 3.

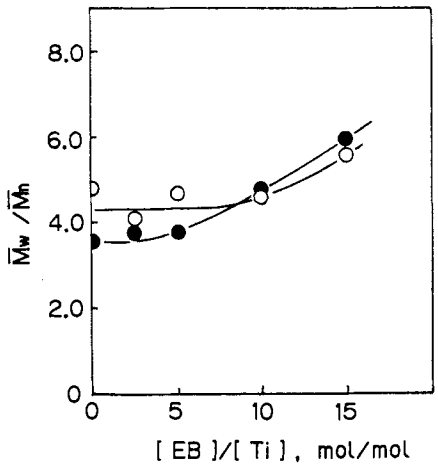

Fig. 10 Effect of [EB]/[Ti] on $\bar{M}w/\bar{M}n$ (C_7-soluble polymers (●), C_7-insoluble polymers (○)) in $MgCl_2/TiCl_4$-$AlEt_3$/EB. Polymerization conditions are the same as those in Table 3.

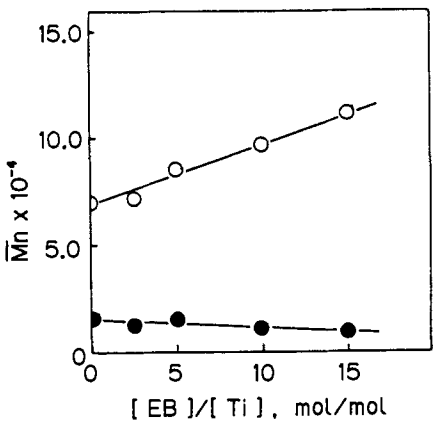

Fig. 11 Effect of [EB]/[Ti] on $\bar{M}n$ (C_7-soluble polymers (●), C_7-insoluble polymers (○)) in $MgCl_2/TiCl_4$-$AlEt_3$/EB. Polymerization conditions are the same as those in Table 3.

Fig. 13 shows that with the increase of the amount of added EB, asymmetric GPC curves of C_7-insoluble (isotactic) polymers shifted to higher molecular weight, broadening the peak area by increase of the relative contribution of the polymer portion having molecular weight of 10^5-10^6. One can see that these curves can be divided into two peaks in which the individual centers would be located at molecular weights of around 10^5 (L peak) and of 10^5-10^6 (H peak), respectively, and that these peaks are the same as those seen in Fig. 7 (no EB). As pointed out in the previous chapter, the contribution of the H peak to the GPC curves in Fig. 7 was increase with decreasing concentration of $AlEt_3$ or [Al]/[Ti] molar ratio in the $MgCl_2/TiCl_4$-$AlEt_3$ catalyst system. Therefore, it can be assumed that active centers to produce H peak are formed by the reaction of $AlEt_3$ and Ti catalyst under milder conditions such as lower [Al]/[Ti]. In the $MgCl_2/TiCl_4$-$AlEt_3$/EB catalyst system, increase of the amount of EB enhanced the relative contribution of H peak to L peak as shown in Fig. 13 (Note: However, the absolute yields of polymers of both L and H peaks decreased at higher concentrations of EB.). Considering the above, EB would bring about milder reaction conditions to form avtive centers to

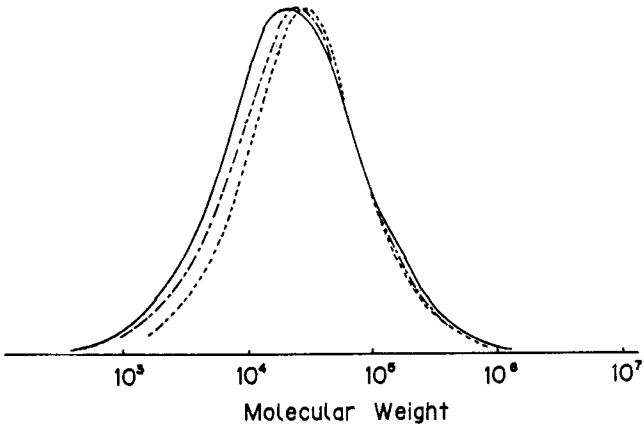

Fig. 12 Effect of [EB]/[Ti] on the GPC curves of C_7-soluble polymers with $MgCl_2/TiCl_4$-$AlEt_3$/EB. [EB]/[Ti]=0(·····); [EB]/[Ti]= 10 (-·-·-); [EB]/[Ti]=15(——). Polymerization conditions are the same as those in Table 3.

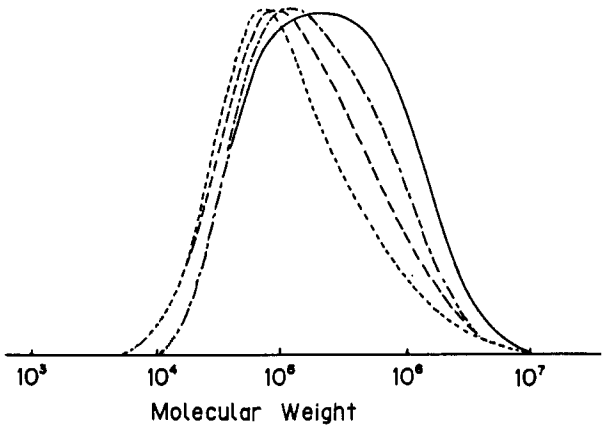

Fig. 13 Effect of [EB]/[Ti] on the GPC curves of C_7-insoluble polymers with $MgCl_2/TiCl_4$-$AlEt_3$/EB. [EB]/[Ti]=0(·····); [EB]/[Ti]=5 (-----); [EB]/[Ti]= 10 (-·-·-); [EB]/[Ti]=15 (——). Polymerization conditions are the same as those in Table 3.

produce H peak by lowering the concentration of $AlEt_3$ by reacting with $AlEt_3$ to form Al alchoxide compounds and/or by weakening the reactivity of $AlEt_3$ by complexing with it, and at the same time, an excess of EB would partially inactivate isotactic active centers.

As the conclusion of this chapter, the following can be said to be the role of EB. EB decreased the yield of atactic polymers very sharply with relative increase in the yield of isotactic polymers under the present conditions and consequently enhanced stereospecificity with minimum sacrifice of overall activity. EB inactivates atactic active centers very preferentially, and associates with isotactic active centers in a manner so as to enhance the activity first and then inactivate them gradually with increased concentration. Furthermore, GPC curves for C_7-insoluble (isoatactic) polymers suggest the presence of at least two separate groups of isotactic active centers, and EB appears to enhance the relative contribution of a group of active centers to produce polymers of higher molecular weight and consequently increased molecular weight and polydispersity of C_7-insoluble (isotactic) polymers.

3. Propylene polymerization with the $MgCl_2$-supported $TiCl_4$ catalyst system: Effect of the polymerization time

Hitherto, we have examined the effect of the concentration of $AlEt_3$ and the amount of added EB on propylene polymerization with the $MgCl_2/TiCl_4$-$AlEt_3$ catalyst system. These studies deal with polymers obtained by polymerization for 15 or 30 min.

As indicated earlier, the activity of the $MgCl_2/TiCl_4$-$AlEt_3$ catalyst system in propylene polymerization decreased with increase of polymerization time.[7),8)] Namely, the nature of the active centers of this catalyst system may change during the polymerization time. The effect of polymerization time was examined using polymerization data listed in Table 4 for 5, 10, 20 and 30 min with $MgCl_2/TiCl_4$-$AlEt_3$ at [Al]/[Ti]=25(mol/mol), 50°C and $MgCl_2/TiCl_4$-$AlEt_3$/EB at [Al]/[EB]=7 (mol/mol), 50°C. Fig. 14 shows the changes in activity by monitoring the consumption of propylene monomers with a flow meter in polymerizations No.304 and No.308 in Table 4. Two catalyst systems showed different overall polymerization activity but almost the same rate of decay in activity. Fig. 15 shows the dependence of I.I. of overall polymers on the polymerization time. I.I. remained almost unchanged in each catalyst system in spite of considerable decay in

Table 4 Effect of polymerization time on $MgCl_2/TiCl_4$-$AlEt_3$ and $MgCl_2/TiCl_4$-$AlEt_3$/EB[1)]

No.	[EB]/[Ti]	Time	I.I.	Yield			
				Overall		C_7-insol.	C_7-sol.
	(mol/mol)	(min)	(wt%)	(g)	(g/mmolTi)	(g/mmolTi)	(g/mmolTi)
301	0	5	32	23.1	159	51	108
302	0	10	34	33.5	231	79	152
303	0	20	35	45.8	316	111	205
304	0	30	37	55.0	379	140	239
305	7	5	82	15.2	105	86	19
306	7	10	83	23.6	163	135	28
307	7	20	84	33.8	233	196	37
308	7	30	84	42.9	296	249	47
309[2)]	0-7	30	61	49.1	339	207	132

1) n-decane 250 ml, 50°C, [Ti]=0.58 mmol/l, [Al]=14.5 mmol/l
2) EB was added at a laps of 5 min.

activity during polymerization. EB increased yield of C_7-insoluble (isotactic) polymers at the same ratio at any given moment during polymerization, and therefore the increase of the yield for C_7-insoluble (isotactic) polymers by addition of EB to the $MgCl_2/TiCl_4$-$AlEt_3$ catalyst system can not be explained by the elongation of the life time of isotactic active centers by the association of EB, but may be explained by the increase of the concentration of isotactic active centers and/or by the increase of the propagation rate constant by the introduction of EB.

Till now, EB was introduced to the polymerization system at the beginning of polymerization. Can the same effect of EB addition also be seen in the case in which EB is introduced to the polymerization system after the formation of active centers in the $MgCl_2/TiCl_4$-$AlEt_3$ catalyst system, i.e. after the beginning of polymerization? The answer to this question was obtained in the following way. Fig. 16 shows the time dependence of catalyst activity. Two solid line curves were given with $MgCl_2/TiCl_4$-$AlEt_3$ catalyst system and $MgCl_2/TiCl_4$-$AlEt_3$/EB catalyst system (EB was added at the beginning). Next, polymerization in which EB was introduced after 5 min under a molar

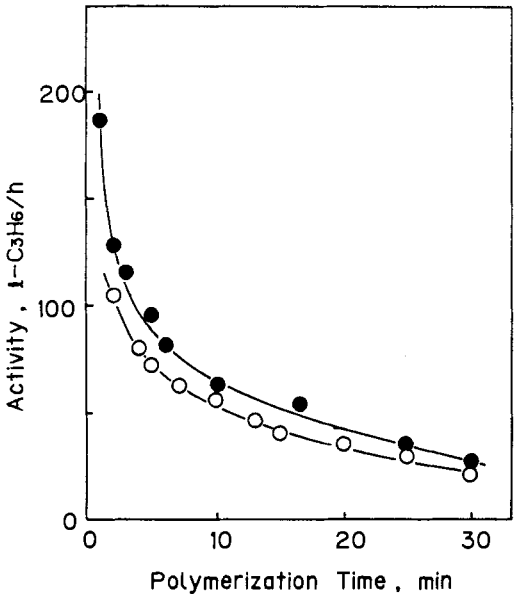

Fig. 14 Dependence of activities with polymerization time observed with $MgCl_2/TiCl_4$-$AlEt_3$(●) and $MgCl_2/TiCl_4$-$AlEt_3$/EB(○). Polymerization conditions are the same as those in Table 4.

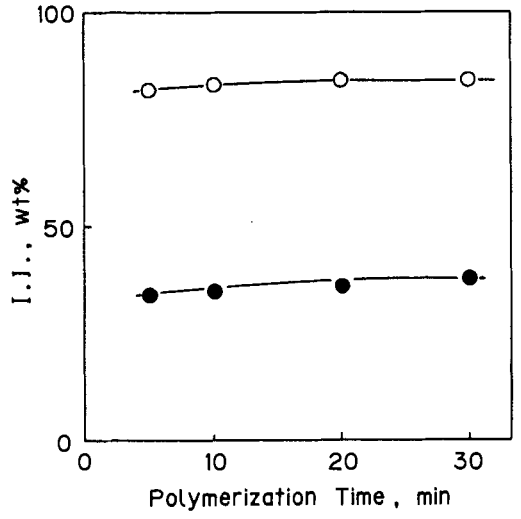

Fig. 15 Dependence of Isotactic Index (I.I.) on polymerization time observed with $MgCl_2/TiCl_4$-$AlEt_3$(●) and $MgCl_2/TiCl_4$-$AlEt_3$/EB(○). Polymerization conditions are the same as those in Table 4.

ratio of [EB]/[Ti]=7 with the $MgCl_2/TiCl_4$-$AlEt_3$ catalyst system was carried out for 30 min. The obtained data are listed in Table 4 (No.309) with the activity plotted by the symbol"●" in Fig. 16. One can see from Fig. 16 that after addition of EB, the plot of the overall catalyst activity shifted within 1 min from the curve for the $MgCl_2/TiCl_4$-$AlEt_3$ catalyst system to that for the $MgCl_2/TiCl_4$-$AlEt_3$/EB catalyst system. If, after the introduction of EB, all catalyst performances transferred from the former to the latter catalyst system, the polymers obtained by this experiment should be a mixture of the polymers produced in the "A" zone for 5 min with the $MgCl_2/TiCl_4$-$AlEt_3$ catalyst system and the polymers in the "B" zone for 25 min with the $MgCl_2/TiCl_4$-$AlEt_3$/EB catalyst system as seen in Fig. 16. The data for "A" was already given in Table 4 (No.301). The data for "B" was calculated from a comparison of the data for 5 min ("C") and 30 min ("D") (Nos.305, 308 in Table 4) with the $MgCl_2/TiCl_4$-$AlEt_3$/EB catalyst system. The calculated data for the mixture of polymers "A" and "B" are given as "X" in Table 5 together with "A," "B," "C" and "D." The observed data "Y" in table 5 (No.309 in Table 4) was consistent with data "X" calculated from "A" and "B."

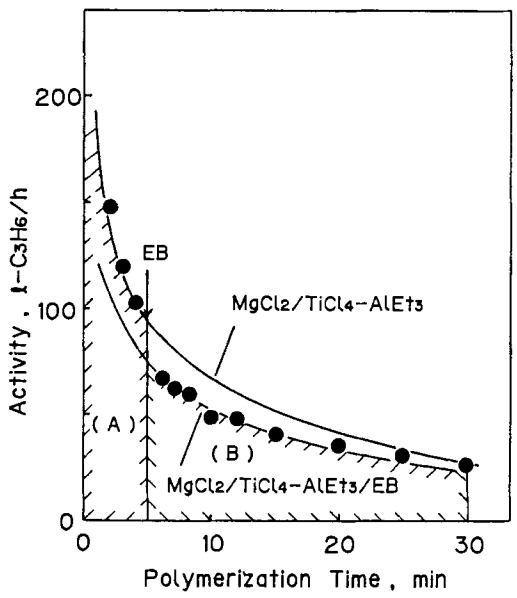

Fig. 16 Kinetic curves of propylene polymerization. EB added to the $MgCl_2/TiCl_4$-$AlEt_3$ system 5 min after start of polymerization.

Table 5 EB addition to the $MgCl_2/TiCl_4$-$AlEt_3$ catalyst system 5 min after start of polymerization

Catalyst system	[EB]/[Ti] (mol/mol)	0-5 min I.I. (wt%)	0-5 min Yield(g/mmonTi) Overall	0-5 min Yield(g/mmonTi) C_7- insol.	0-5 min Yield(g/mmonTi) C_7- sol.	0-30 min I.I. (wt%)	0-30 min Yield(g/mmolTi) Overall	0-30 min Yield(g/mmolTi) C_7- insol.	0-30 min Yield(g/mmolTi) C_7- sol.	5-30min I.I. (wt%)	5-30min Yield(g/mmolTi) Overall	5-30min Yield(g/mmolTi) C_7- insol.	5-30min Yield(g/mmolTi) C_7- sol.
(1)[1]	0	"A" 32	159	51	108								
(2)[2]	7	"C" 82	105	86	19	"D" 84	296	249	47	("B" 85	191	163	28)
(1)-(2)[3]	0-7					"Y" 61	339	207	132				
						("X" 61	350	214	136)				

1) $MgCl_2/TiCl_4$-$AlEt_3$
2) $MgCl_2/TiCl_4$-$AlEt_3$/EB
3) EB was added to 1) after 5 min.
"A," "C," "D," "Y": same as No.301, 305, 308, 309 in Table 3
"B": calculated from "C" and "D"
"X": calculated from "A" and "B"

As a conclusion, the answer to the question asked above is "Yes, the same effect can be seen." This indicates that active centers of the $MgCl_2/TiCl_4$-$AlEt_3$ catalyst system can be easily coverted to those of the $MgCl_2/TiCl_4$-$AlEt_3$/EB catalyst system and that the action of EB on active centers proceeds very quickly and easily.

4. The early stage of propylene polymerization with the $MgCl_2/TiCl_4$-$AlEt_3$ and $MgCl_2/TiCl_4$-$AlEt_3$/EB catalyst systems[9,10]

In chapter 2, we pointed out that both the increase of the yield of C_7-insoluble (isotactic) polymers and the sharp decrease of the yield of C_7-soluble (atactic) polymers were the most important effect of EB addition on the performance of the $MgCl_2/TiCl_4$-$AlEt_3$ catalyst system. On the other hand , the results of chapter 3 showed that suppression of the activity decay in isotactic active centers was not the reason for the increase of the yield of C_7-insoluble (isotactic) polymers, and therefore, the above-mentioned effects by EB addition may be attributed to the change in concentration of active centers([C*]) and/ or the change in the propagation rate constant(k_p) by EB addition.

As described above, both $MgCl_2/TiCl_4$-$AlEt_3$ and $MgCl_2/TiCl_4$-$AlEt_3$/EB catalyst systems showed considerable change in activity with polymerization time (Fig. 14), so in these catalyst systems, [C*] and/ or k_p change during polymerization. However, even these catalyst systems were found to have constant activity at the very early stage of 60°C polymerization for both C_7-insoluble and C_7-soluble polymers (within 1 min of start of polymerization as shown in Fig. 17). All corresponding data are listed in Tables 6 and 7. In this short period, [C*] and k_p of these catalyst systems can be considered constant. Moreover, also in this period, the characteristic effects of EB (the increase of C_7-insoluble polymers and the sharp decrease of C_7-soluble polymers) were observed as shown in Fig. 17, indicating that the conclusion concerning the role of EB obtained from early-stage polymerization at 60°C can be extrapolated to polymerization for 15 or 30 min at 50°C.

Using kinetic-molecular weight methods,[11] the value of [C*] can be determined from the following equation expressing the relationship between the number of polymer chains, [N], and the polymer yield, Y.

$$[N] = [C^*] + (k_{tr} \cdot [C^*]/R) \cdot Y \qquad (1)$$

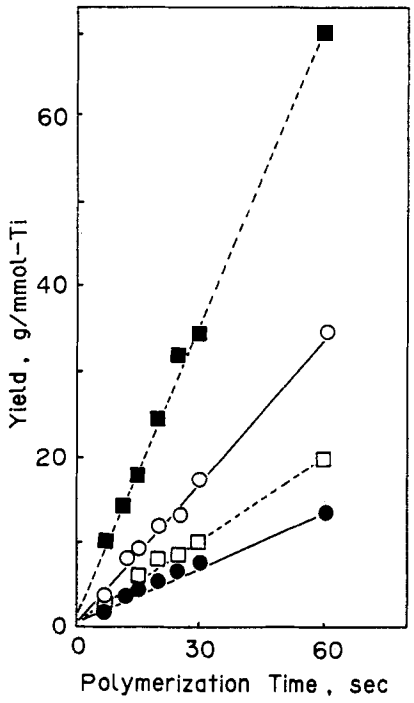

Fig. 17 Time dependence of polymer yield with $MgCl_2/TiCl_4$-$AlEt_3$ (Cat 1) and $MgCl_2/TiCl_4$-$AlEt_3$/EB (Cat 2). C_7-soluble polymers with Cat 1(■); C_7-insoluble polymers with Cat 1(□); C_7-soluble polymers with Cat 2(●); C_7-insoluble polymers with Cat 2(○). Polymerization conditions are the same as those in Table 6.

Table 6 Short-time polymerization of propylene with $MgCl_2/TiCl_4$-$AlEt_3$ [1)]

Time	Yield	I.I.	$\bar{M}n \times 10^{-4}$		$[N] \times 10^2$ (mol/molTi)	
(sec)	(g/mmolTi)	(wt%)	Overall	C_7-insol.	Overall	C_7-insol.
7.5	12.5	20.6	1.17	2.00	107	13
12	18.5	24.1	1.38	2.35	139	19
15	24.1	26.3	1.07	2.35	224	27
20	32.8	24.8	1.13	2.20	290	37
25	40.5	21.2	1.36	2.15	297	40
30	44.0	22.5	1.24	2.20	352	45
60	89.2	21.8	1.39	2.30	640	84

1) n-decane 500 ml, [Ti]=0.4 mmol/l, [$AlEt_3$]=10 mmol/l, 60°C

Table 7 Short-time polymerization of propylene with $MgCl_2/TiCl_4$-$AlEt_3$/EB[1)]

Time	Yield	I.I.	$\bar{M}n \times 10^{-4}$ (g/mol)			$\bar{M}w/\bar{M}n$			[N]$\times 10^2$ (mol/molTi)	
(sec)	(g/mmolTi)	(wt%)	Overall	C_7-insol.	C_7-sol.	Overall	C_7-insol.	C_7-sol.	C_7-insol.	C_7-sol.
7	5.6	63.0	2.93	5.76	1.50	3.77	2.64	2.66	6.10	14.0
12	12.3	68.3	3.51	6.52	1.48	3.94	2.74	2.90	12.9	26.4
15	13.8	67.2	2.62	6.49	1.51	4.38	2.87	3.04	14.3	30.0
20	17.4	68.9	3.61	6.79	1.42	4.10	2.80	3.02	17.7	38.0
25	20.0	66.9	3.32	6.52	1.43	4.06	2.74	2.88	20.4	46.8
30	24.2	71.4	3.01	6.54	1.51	3.63	2.82	2.55	26.5	45.7
60	48.0	71.6	3.32	7.43	1.56	4.39	3.42	3.07	46.2	87.2

1) n-decane 500 ml, 60°C, [Ti]=0.4 mmol/l, [$AlEt_3$]=10 mmol/l, [EB]=2.5 mmol/l

where R is the polymerization rate, [N] is obtained from Y and the number average molecular weight, $\bar{M}n$. Figs. 18 and 19 show the relationship between [N] and Y with the $MgCl_2/TiCl_4$-$AlEt_3$ catalyst system and the $MgCl_2/TiCl_4$-$AlEt_3$/EB catalyst system, respectively. The concentrations of the isotactic, atactic or overall active centers, $[C^*]_{iso}$, $[C^*]_{ata}$ or $[C^*]_{overall}$, were determined from the intercepts of Figs. 18 and 19 according to Eq.(1). R can be expressed by Eqs.(2) and (3).

$$R = k_p \cdot [M] \cdot [C^*] \qquad (2)$$

$$Y = R \cdot t \qquad (3)$$

where [M] is the propylene concentration in the solvent ([M]=0.24 mol/l under the present experimental conditions) and t is the polymerization time. R was obtained from the slope of the straight lines in Fig. 17, and k_p was determined from Eq.(2). The chain transfer rate, k_{tr}, was obtained from the slope of the straight lines in Figs. 18 and 19 and Eq.(1). All kinetic parameters a listed in Table 8. A comparison of the $MgCl_2/TiCl_4$-$AlEt_3$ catalyst system with the $MgCl_2/TiCl_4$-$AlEt_3$/EB catalyst system in Table 8, shows that addition of EB to the $MgCl_2/TiCl_4$-$AlEt_3$ catalyst system changed the concentration of isotactic active centers, $[C^*]_{iso}$, slightly, but increased $k_{p(iso)}$ markedly from 500-1500 (l/mol·sec) to 2100-6300 (l/mol·sec). On the other hand, the concentration of atactic active centers, $[C^*]_{ata}$ dramatically decreased from 14-58mol% to 2-6mol%, while $k_{p(ata)}$ remained unchanged.

In conclusion, regarding short-time polymerization, the increase in yield of isotactic polymers by addition of EB is considered to be mainly due to the increase of $k_{p(iso)}$, and not to the increase of $[C^*]_{iso}$; on the contrary, the sharp decrease in yield of atactic polymers seems to be due to the large decrease of $[C^*]_{ata}$, and not to the decrease of $k_{p(ata)}$.

SUMMARY

Some studies on propylene polymerization with the catalyst system of $MgCl_2$-supported $TiCl_4$ catalyst ($MgCl_2/TiCl_4$) in conjunction with $AlEt_3$ or $AlEt_3$ and ethyl benzoate (EB) have been made to elucidate the role of ethyl benzoate (EB), which is known to increase the stereospecificity of produced polypropylene.

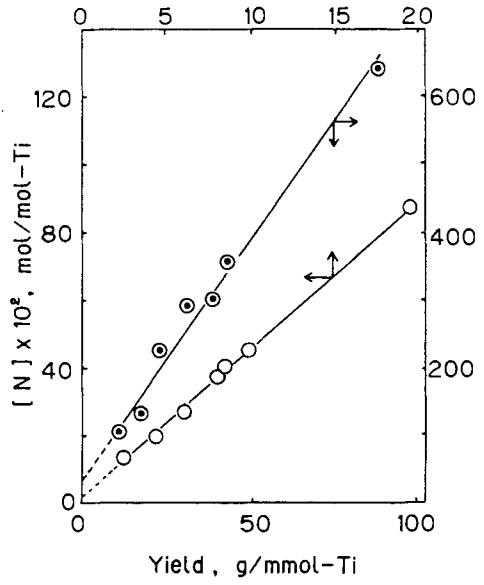

Fig. 18 Relationship between the polymer yield and the number of polymer chaines produced per mol of Ti, [N] in $MgCl_2/TiCl_4$-$AlEt_3$ (overall polymers (◎), C_7-insoluble polymers (○)).

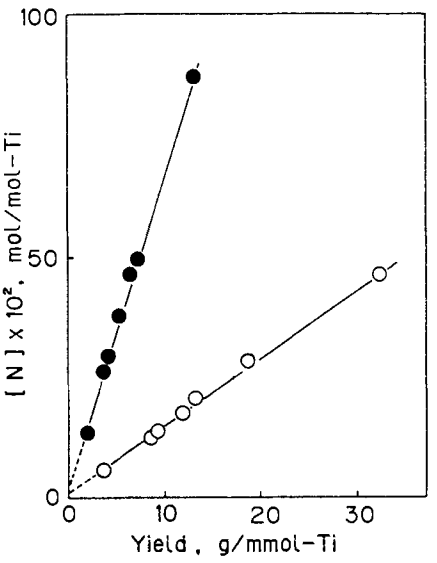

Fig. 19 Relationship between the polymer yield and the number of polymer chains produced per mol of Ti, [N] in $MgCl_2/TiCl_4$-$AlEt_3$/EB (C_7-soluble polymers (●); C_7-insoluble polymers (○)).

Table 8 Kinetic parameters of propylene polymerization with $MgCl_2/TiCl_4$-$AlEt_3$ and $MgCl_2/TiCl_4$-$AlEt_3$/EB

Catalyst systems	Fractions	Polymn. rate (mol/molTi·sec)[a)]	I.I. (wt%)	[C*] (mol%)	k_p (l/mol·sec)
$MgCl_2/TiCl_4$ -$AlEt_3$	overall	35	21-26	20-60	240-730
	C_7-insol.	8		2-6	500-1500
	C_7-sol.	27		14-58	200-800
$MgCl_2/TiCl_4$ -$AlEt_3$/EB	overall	20	63-76	4-7	1200-2100
	C_7-insol.	15		1-3	2100-6300
	C_7-sol.	5		2-6	350-1000

a) mol of propylene / mol of Ti·sec

First, propylene was polymerized with the $MgCl_2/TiCl_4$-$AlEt_3$ catalyst system (without EB). This catalyst system showed very high activity per unit of Ti atom but low stereospecificity, and the concentration of $AlEt_3$ was not important to the activity or stereospecificity in a considerably wide range.

Next, propylene polymerization was done with the $MgCl_2/TiCl_4$-$AlEt_3$/EB catalyst system (with EB). As a result, EB was found to considerably increase the yield of isotactic polymers, at the same time sharply decreasing the yield of atactic polymers and consequently, enhance stereospecificity. These results can be explained by the fact that EB has entirely different actions on isotactic and atactic active centers, associating with isotactic active centers in such a way as to enhance their activity, and in contrast, inactivating atactic active centers very preferentially.

Finally, from the results of kinetic study on short-time polymerization of propylene with both catalyst systems, it can be said that the increase of isotactic polymers by adding EB was mainly due to the increase of $k_{p(iso)}$, and not by increase of $[C^*]_{iso}$; on the contrary, the large decrease in the yield of atactic polymer was due to the large decrease in $[C^*]_{ata}$, and not to the decrease of $k_{p(ata)}$. Furthermore, the concentration of $AlEt_3$ or EB was found to affect the polydispersity and molecular weight of the obtained polypropylene, particularly of isotactic polypropylene.

REFERENCES

1. Japan Kokai 75-126590, Mitsui Petrochemical Industries, invs.: A.Toyota, N.Kashiwa; Chem. Abstr. 84-122575w; Japan Kokai 77-151691, Montedison S.P.A. and Mitsui Petrochemical Industries, invs.: L.Luciani, N.Kashiwa, C.Barbe and A.Toyota
2. A.Schindler, Makromol. Chem., 118, 1 (1968).
3. T.Keii, E.Suzuki, M.Tamura and Y.Doi, "Transition Metal Catalyzed Polymerizations," MMI Press, Harwood Academic Publishers, New York, 1983, p.97.
4. A.W.Langer, T.J.Burkhardt and J.J.Steger, Polymer Science and Technology vol. 19, "Coordination Polymerization," Plenum Press, New York, 1983, p.225.
5. R.Spitz and J.L.Lacombe, J. Polym. Sci., 22, 2611 (1984).
6. Y.V.Kissin and A.J.Sivak, ibid., 22, 3747 (1984).
7. J.C.W.Chien, C.I.Kuo and T.Ang, ibid., 23, 723 (1985).

8. J.C.W.Chien and C.I.Kuo, ibid.,23, 761 (1985).
9. N.Kashiwa and J.Yoshitake, Makromol. Chem., Rapid Commun., 4, 41 (1983).
10. N.Kashiwa and J.Yoshitake, Polym. Bull., 12, 99 (1984).
11. P.J.T.Tait, "Transition Metal Catalyzed Polymerizations," MMI Press, Harwood Academic Publishers, New York, 1983, p.115.

STRUCTURE, COMPOSITION AND ACTIVITY OF SUPPORTED TITANIUM-MAGNESIUM CATALYSTS FOR ETHYLENE POLYMERIZATION

V.A.ZAKHAROV, S.I.MAKHTARULIN, D.V.PERKOVETS, E.M.MOROZ,
T.B.MIKENAS and G.D.BUKATOV
Institute of Catalysis, Novosibirsk 630090, USSR

ABSTRACT

Studied is the effect of the substructure of magnesium chloride on the composition and activity of Ti-Mg catalysts prepared by different methods: (i) adsorption of $TiCl_4$ on highly dispersed magnesium chloride prepared from nonsolvated buthylmagnesiumchloride, (ii) adsorption of $TiCl_4$ on magnesium chloride activated by milling, and (iii) co-milling of magnesium chloride with $TiCl_4$. $TiCl_4$ is shown to react with the defects of the magnesium chloride structure. The concentration of these defects is associated with the size of the coherent scattering range, which is determined from X-ray data. Evidences have been obtained that the surface of magnesium chloride is nonuniform with respect to the interaction with $TiCl_4$ and VCl_4. The resulting V^{4+}, Ti^{4+} and Ti^{3+} surface compounds also are nonuniform in the coordination state and catalytic properties. The state of Ti^{3+} ions after the interaction of Ti-Mg catalysts with trialkylaluminum has been examined. It is assumed that active centers of these systems are in the surface associates of Ti^{3+} ions.

INTRODUCTION

In recent years, highly active catalysts of olefin polymerization, which contain titanium chloride supported over a highly dispersed anhydrous magnesium chloride (titanium-magnesium catalysts, TMC), occupy great deal of attention. As reported in[1)], the amount of $TiCl_4$ tightly bound to magnesium chloride is determined by the extent of the support crystallinity. Some data on the substructure, the composition and the activity of TMCs obtained by co-milling

of $TiCl_4$ with magnesium chloride can be found in[2,3].

Despite that the number of active centers in supported TMCs is rather high, the composition of these centers has not been so far reliably established. It has been proposed[4,5] that isolated Ti^{3+} ions observable by EPR are the active centers of these systems. An alternative opinion is that the active centers of TMCs are either in the surface associates or in highly dispersed $TiCl_3$ particles which are stabililized on the surface of $MgCl_2$[6].

In this work we report on the effect of the magnesium chloride substructure on the composition and the activity of supported Ti-Mg catalysts prepared by different methods. We have studied the interaction of $TiCl_4$ and VCl_4 with magnesium chloride and the composition of the compounds that are formed during the interaction of supported titanium chloride with organoaluminum co-catalysts. Based on the data obtained, the catalytic properties and the composition of resulting titanium compounds are discussed.

EXPERIMENTAL

Three types of catalysts were used. Catalyst A was prepared by adsorbing $TiCl_4$ from its solution in hexane on the support, which was prepared by the interaction of magnesium with n-butylchloride in the hexane at the molar ratio $RCl/Mg > 2$[7]. The support had no alkylmagnesium bonds; it consisted predominantly of magnesium chloride. Catalyst B was prepared by milling anhydrous highly crystalline magnesium chloride and by further treating with the solution of $TiCl_4$ in hexane. The milling was performed in a steel ball planetary mill. Catalyst C was obtained by co-milling anhydrous highly crystalline magnesium chloride with titanium tetrachloride (5% Ti by mass of $MgCl_2$) in a ball planetary mill.

After the interaction with $TiCl_4$, all catalysts were washed with hexane.

The polymerization of ethylene was carried out in hexane at 80°C for 1 hr at ethylene pressure of 3.5 atm and hydrogen pressure of 1 atm. The concentration of the catalyst was 0.03-0.1 g/l and and that of the co-catalyst — tri-iso-butylaluminum — 0.5 g/l.

RESULTS AND DISCUSSION

1. Influence of the preparation method and magnesium chloride substructure on the composition and the activity of the catalysts.

1.1. Substructure and composition of the catalysts.

In the case of catalyst A, a highly dispersed support is formed directly in the course of the transformation of butylmagnesium chloride to magnesium chloride[1,7]. It is characterized by a rather large surface area (30-100 m^2/g) and by a small size of crystallites (the coherent scaterring regions — c.s.r.) found from X-ray data (100-140 Å in the direction of 110 and 20-40 Å in the direction of 001). This size of crystallites may correspond to the surface area of 350-400 m^2/g, which largely exceeds the area found for these species from adsorption data (30-100 m^2/g). This fact is due to that the primary catalyst particles with size 200-400 Å are characterized by a significant number of distortions of the crystalline structure. Therefore, the sizes of the c.s.r. determined by X-ray method are far smaller than the sizes of primary particles. In this case, the size of c.s.r. can characterize the defectness of magnesium chloride primary particles. The amount of $TiCl_4$, that is strongly bound to the support during adsorption, decreases as the size of the c.s.r. grows[1]. Thus, we can conclude that at adsorption $TiCl_4$ interacts with the defects of the $MgCl_2$ structure.

Catalyst B. Data on the effect of the duration of milling on the substructure of the support and on the titanium content in the catalyst is given in Fig. 1. The size of c.s.r. sharply decreases with increasing the time of milling; it is 100-120 Å after 24-48 hrs and then remains unchanged. By this time, the surface area attains its maximum value (115 m^2/g) but has a tendency to decrease with further increasing the time of milling. The size of c.s.r. equal to 100-120 Å corresponds to 200 m^2/g, which is noticeably higher than the value found for the species from adsorption data (77-115 m^2/g). The content of titanium in catalyst B drastically increases when the time of milling is increased up to 24 hrs. Upon further increasing the time of milling, the content of titanium and the size of c.s.r. do not change, although the surface area becomes approximately 1.5 times smaller. The surface concentration of $TiCl_4$ in these species is $7.2 \cdot 10^{-4}$-$11.6 \cdot 10^{-4}$ mmol/m^2 which corresponds to a mean distribution of one $TiCl_4$ molecule over the area of 145-232 $Å^2$

Thus, only a small part of the surface of magnesium chloride is occupied by $TiCl_4$. This seems to be due to the presence of a limited number of centers (probably structural defects), which can strongly be bound to $TiCl_4$, on the surface of magnesium chloride activated by milling.

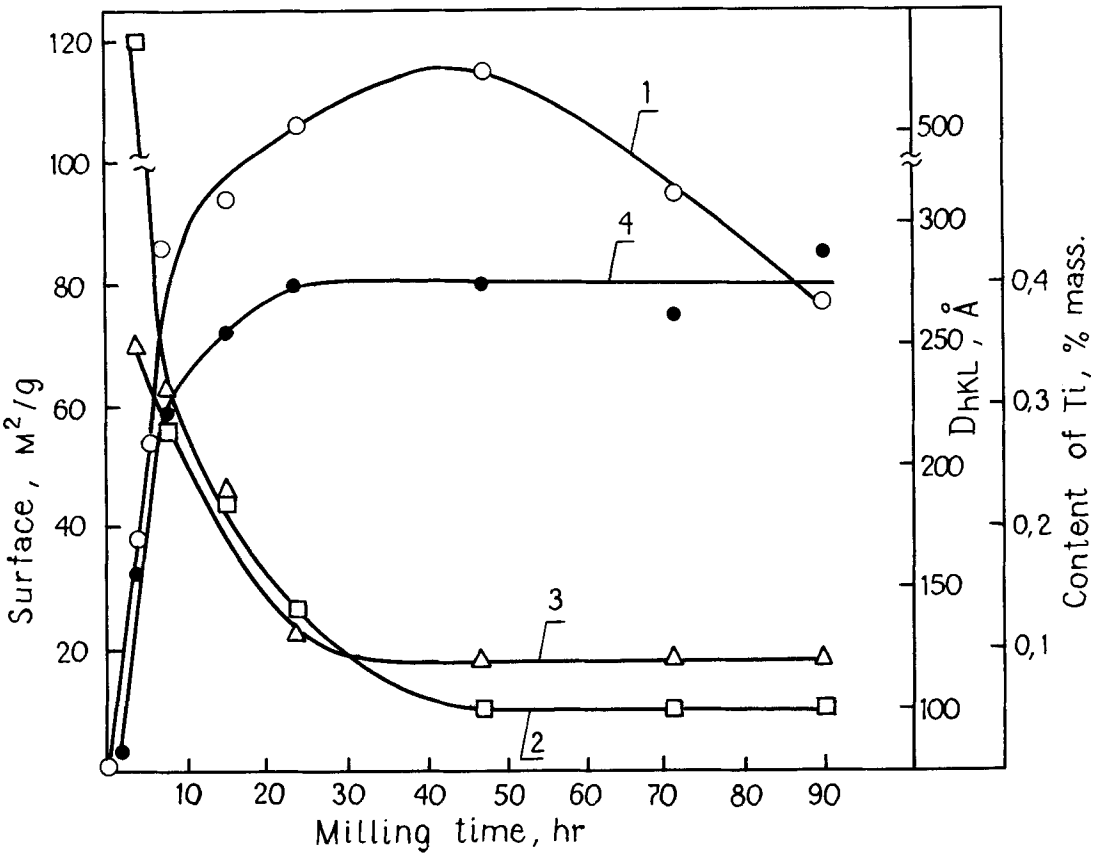

Figure 1. Effect of the milling time of magnesium chloride on its substructure and titanium content in catalyst B. 1 — surface area; 2 and 3 — the size of c.s.r. in the direction of 001 and 110, respectively; 4 — titanium content.

The data on the substructures of supports and the compositions of catalysts A and B are compared in Table 1.

Table 1. Data on the substructures of the supports and on the compositions of the catalysts (samples with the maximum Ti content)

Catalyst	Support surface area, m^2/g	Size of c.s.r.		Ti content	
		110	001	% mass	$\frac{mmol\ Ti}{m^2} \times 10^4$
A	95	130	30	1.2	26
B	115	120	100	0.4	7.2
C	119[1)]	50[1)]	65[1)]	4.5	78

[1)] Data on $TiCl_4/MgCl_2$ catalyst.

Both supports have similar surface areas; however, the content of titanium in catalyst A is much higher than in catalyst B. This difference seems to result from the specificity of the structure of magnesium chloride obtained by method A, which is reflected by a smaller size of c.s.r. in the direction of 001 . The support of catalyst A is characterized by a higher number of defects, as compared to catalyst B, and, hence, has a higher concentration of the surface sites which can strongly bind $TiCl_4$.

Catalyst C. Data on the influence of the time of milling on the substructure of catalyst C and on the titanium content are shown in Figure 2. As the time of milling is increased, the c.s.r. drastically decreases; even after 16 hrs it achieves a minimum size (50-65 Å) and then remains unchanged. The change of the catalyst surface with increasing the milling time is of a more complicated character, that is, the surface area is maximum (180 m^2/g) even after 8 hrs and then starts to decrease. The titanium content attains its maximum after 16-24 hrs and further remains constant, whereas the surface area falls by a factor of two. In general, the types of the dependences plotted in Figure 2 are similar to those obtained for catalyst B (Figure 1). However, the presence of $TiCl_4$ at magnesium chloride milling noticeably speeds up the process of support dispergation and finally leads to more profound changes in the substructure and the composition of the catalyst. In particular,

the maximum surface area and the minimum size of c.s.r. of catalyst C are achieved after 8-16 hrs of the milling, to be compared with 24-48 hrs for catalyst B. The maximum content of titanium in catalyst C (4.5% mass Ti or $96 \cdot 10^{-4}$ mmol/m^2) is approximately one order

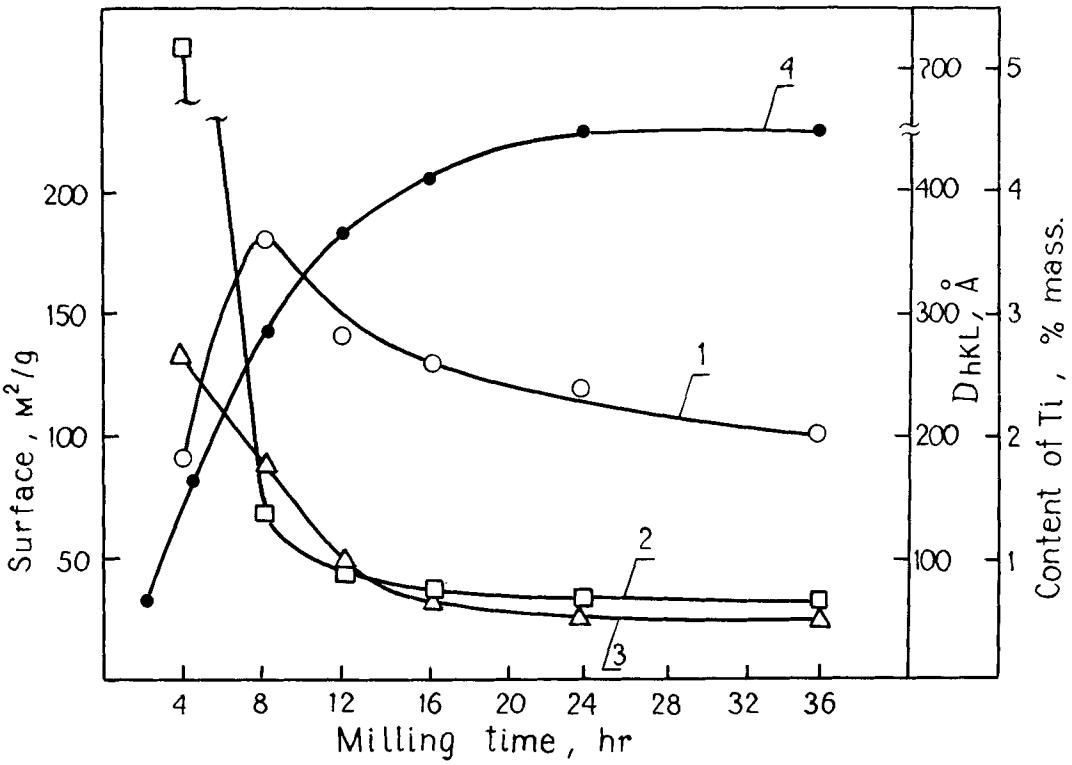

Figure 2. Effect of the co-milling of magnesium chloride with $TiCl_4$ on the substructure and titanium content in catalyst C. 1 — surface area; 2 and 3 — the size of c.s.r. in the direction of 001 and 110, respectively; 4 — the content of titanium.

of magnitude higher than its content in catalyst B. Evidently, during the course of milling there arises a high nonequilibrium concentration of defects in the $MgCl_2$ structure, through which titanium chloride interacts with magnesium chloride. When milling is performed in the absence of $TiCl_4$ (catalyst B), partial relaxation of

defects occurs before the interaction of $TiCl_4$ with magnesium chloride. We believe that during the co-milling part of titanium chloride enters either the sub-surface layer or the bulk of magnesium chloride particles. Titanium ions in the bulk of magnesium chloride seem to be inaccessible to the organoaluminum co-catalyst. To verify this idea, we have analyzed the oxidation state of titanium ions in catalysts A, B and C after their interaction with triethylaluminum (Table 2). As found, in the case of catalysts A and B, which have

Table 2. Data on the number of Ti^{3+} and Ti^{2+} ions resulting from the interaction Ti-Mg catalysts with triethylaluminum (Al/Ti= 5; T=20°C)

Catalyst	Ti content, % mass	Ti^{3+} and Ti^{2+} contents, % molar	
		Ti^{3+}	Ti^{2+}
A	1.2	80	20
B	0.4	100	0
C	1.65[1)]	30	-
	4.5[2)]	10	1

[1)] 4-hour milling

[2)] 24-hour milling

been obtained by adsorption of $TiCl_4$ on magnesium chloride, major part of titanium is accessible to triethylaluminum and is reduced producing Ti^{3+} and Ti^{2+} compounds. In the case of catalyst C, a significant part of titanium is inaccessible to and is not reduced with triethylaluminum under identical conditions. Part of accessible titanium decreases with increasing the milling time and the titanium content in the catalyst. The above comparison of catalysts A and B (Table 1) has indicated the relationship between the quantity of

the titanium chloride in these catalysts and the size of c.s.r. in the direction of 001 . For catalysts A, B and C prepared by different methods, there is a linear correlation between the value reciprocal of the size of c.s.r. in the direction 001 and the amount of $TiCl_4$, which can strongly binds with magnesium chloride (Figure 3).

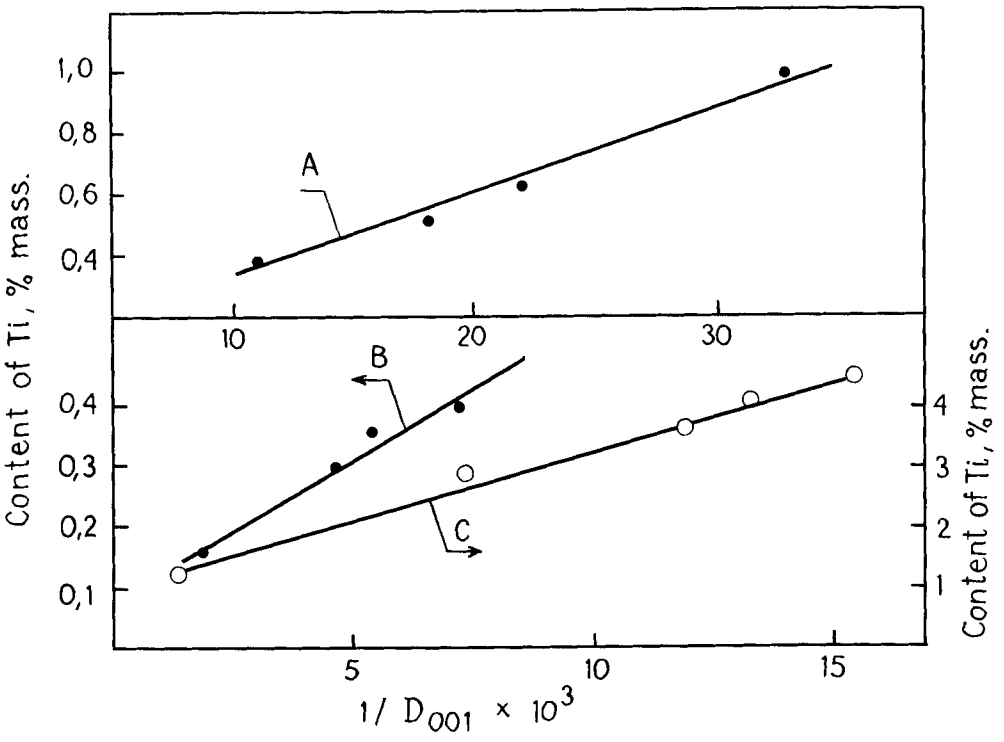

Figure 3. The content of Ti in catalysts A, B and C vs. inverse size of c.s.r. in the direction of 001 .

Probably, there is a correlation between the size of c.s.r. in this direction and the concentration of defects of magnesium chloride, which interact with $TiCl_4$.

1.2. Catalyst activity.

Figure 4 illustrates the kinetic curves of ethylene polymerization on catalysts A, B and C. The shape of the curves depends on

the catalyst preparation procedure. Catalyst A rapidly achieves its maximum activity, which remains constant during the long period of time (Figure 4, curve 1). For catalysts B the shape of the kinetic

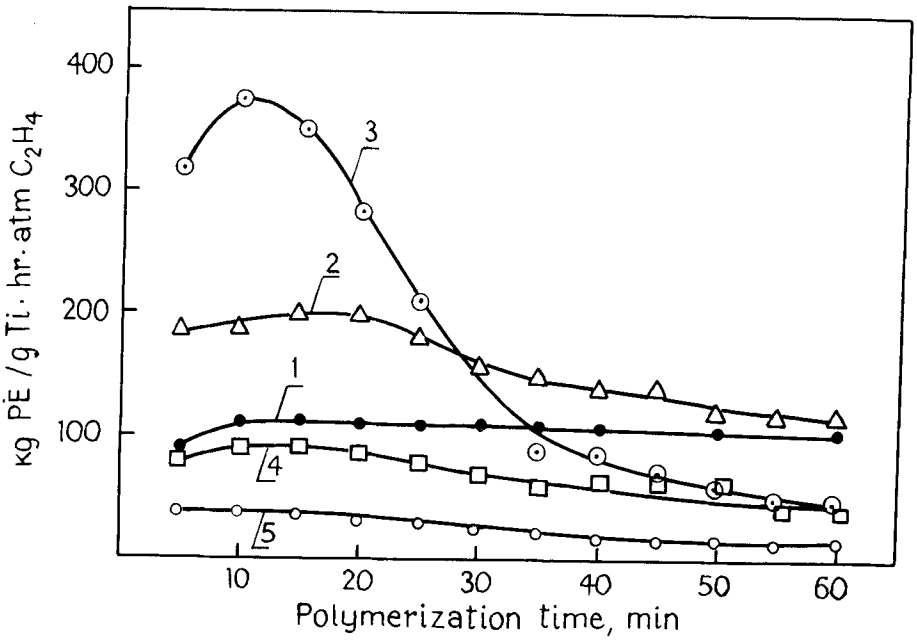

Figure 4. Kinetic curves for ethylene polymerization: 1 — catalyst A; 2 and 3 — catalyst B, milling time 4 and 48 hrs, respectively; 4 and 5 — catalyst C, milling time 4 and 24 hrs, respectively.

curves depends on the milling time. At a short period of milling catalyst B is characterized by quite stable activity (Figure 4, curve 2). At a long period of milling the activity is maximum in the initial period and then sharply falls down to the stationary value (Figure 4, curve 3). For catalysts C, the kinetic curves are unstationary too; but in all cases the activity is maximum in the initial period of the reaction (Figure 4, curves 4 and 5). Therefore, in further catalyst estimations either the maximum activities, which are achieved during the first 10-20 min of polymerization, or stationary activities have been used.

Data on the dependence of the activities of catalysts B and C on the milling time are shown in Figure 5. The maximum activity of

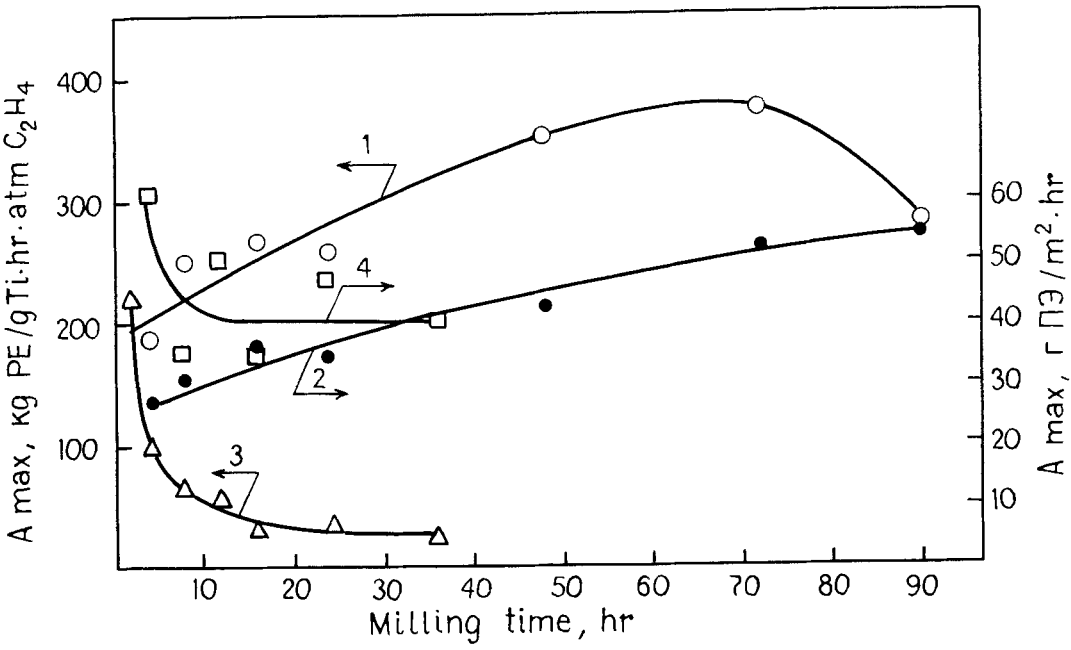

Figure 5. Effect of milling time on the activity: 1 and 2 — catalyst B; 3 and 4 — catalyst C.

catalyst B referred to the weight unit of titanium increases with the milling period up to 72 hrs (Figure 5, curve 1). Further the activity tends to decrease. The maximum activity of catalysts C drastically falls as the time of milling increases (Figure 5, curve 3). This means that during the co-milling of magnesium chloride with $TiCl_4$ part of titanium, which can participate in the formation of active centers, sharply decreases as the content of Ti in the catalyst is increased. Thus, a sharp growth of the content of titanium occurs predominantly due to the stabilization of inactive forms of titanium chloride. As mentioned above, the most probable reason for this is the insertion of titanium chloride into the bulk of the ma-

gnesium chloride species. In this case, titanium chloride becomes inaccessible to the organoaluminum co-catalyst and the monomer. The maximum specific activity of catalyst B per unit of catalyst surface area continuously grows with the time of milling (Figure 5, curve 2). Hence, the surface concentration of active centers continuously grows during the milling. The specific activity of catalyst C is maximum at the minimum time of milling and then decreases to some constant value (Figure 5, curve 4). Catalysts B and C have similar specific activities (30-55 and 40-60 g/m^2 hr, respectively). Thus, the surface concentrations of active centers in these systems also are similar.

In conclusion, it is expedient to estimate part of working titanium (the number of active centers) for titanium-magnesium catalysts prepared by different methods (Table 3). The number of active

Table 3. Data on the activity and number of active centers (C_p) at ethylene polymerization on Ti-Mg catalysts

Catalyst	Ti content, % mass	Activity, kg/g Ti·hr·atm C_2H_4	C_p [1] mol/mol Ti
A	0.05	670 (stationary)	0.47
	1.0	120 (stationary)	0.09
B	0.40	470 (maximal)	0.33
		107 (stationary)	0.075
C	0.55	210 (maximal)	0.15
		35 (stationary)	0.025
	4.5	100 (maximal)	0.071
		29 (stationary)	0.021

[1] Calculated with the use of the propagation rate constant $1 \cdot 10^4$ l/mol·S found by employing ^{14}CO

centers is high (0.47 mol/mol Ti) for catalyst A with a low titanium content (see section 2.1) and for catalyst B (0.33 mol/mol Ti) in the initial period of polymerization. In the other cases, the predominant part of Ti is inactive. This nonuniformity of Ti states can originate both at the first step of catalyst formation, that is during the interaction of titanium chloride with magnesium chloride, and at the subsequent step of the formation of active centers, that is, during the interaction of the catalyst with the organoaluminum co-catalyst.

2. Formation of the active component and of active centers of Ti-Mg catalyst.

2.1. Interaction of titanium and vanadium chlorides with magnesium chloride.

X-ray data. The interaction of $TiCl_4$ with highly dispersed magnesium chloride (catalyst A) was shown[1)] to result in some increase in the structural order of the support, which is characterized by the growth of the size of c.s.r. The similar effect has also been reported in[8)]. This effect is observed also at a dry mixing of highly dispersed magnesium chloride with a solid complex, $TiCl_4 \cdot C_6H_5COOC_2H_5$, and $TiCl_3$ (Table 4). Additional data about the interaction of $TiCl_4$

Table 4. Data on the change of the magnesium chloride substructure during its interaction with titanium chloride

Sample	Ti content, % mass	Size of c.s.r., Å	
		001	110
$MgCl_2$	-	20	130
$MgCl_2$+$TiCl_4$	1.2	40	170
$MgCl_2$+$TiCl_4 \cdot C_6H_5COOC_2H_5$	3.0	40	175
$MgCl_2$+ α-$TiCl_3$	3.9	40	170

with magnesium chloride comes from radial atomic distribution analysis (Figure 6, Table 5). The defectness of the initial support struc-

ture manifests itself in the increase of the interatomic distances, as compared to those characteristic of crystalline magnesium chloride (Table 5). The area of the peak of the first coordination sphere

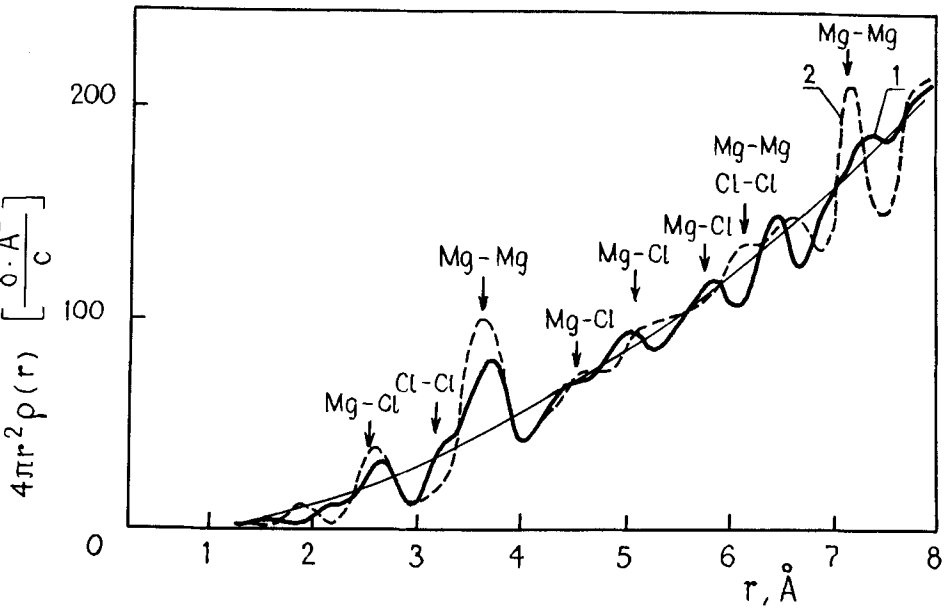

Figure 6. Radial atomic distribution curves for the support (1) and the catalyst A (2)

Table 5. Interatomic distances in the support and in the catalyst A, as found from atomic radial distribution data

Sample	Interatomic distances, Å						
	Mg-Cl	Mg-Mg	Mg-Cl	Mg-Cl	Mg-Cl	Mg-Mg	Mg-Mg
$MgCl_2$ crystal.	2.48	3.59	4.45	5.05	5.72	6.22	7.18
$MgCl_2$ support	2.52	3.60	4.50	5.10	5.75	6.30	7.25
$TiCl_4/MgCl_2$	2.49	3.59	4.43	4.95	5.70	6.15	7.18

corresponding to the Mg-Cl distance is 25% lower than the calculated area. This also indicates the presence of distortions in the structure, such as chlorine vacancies and the shift of magnesium cations from normal positions. During the interaction of the support with $TiCl_4$, these cations may diffuse into normal octahedral positions. This process corresponds to a sharp growth of the peaks that characterize the Mg-Mg distance (Figure 5). Chlorine ions from titanium chloride may occupy anion vacancies. It is also possible that titanium ions are located in the octahedra made of chlorine ions in the sub-surface layer of magnesium chloride, since the Ti-Cl distances (2.45 Å) are similar to the Mg-Cl distances in magnesium chloride. At supporting titanium chloride the Cl-Cl distance grows.

Calorimetric data. The results of the determination of the heat effect observed during adsorption of various amounts of $TiCl_4$ on a highly dispersed magnesium chloride (catalyst A) are shown in Figure 7. A sharp decreasing of the heat effect with increasing

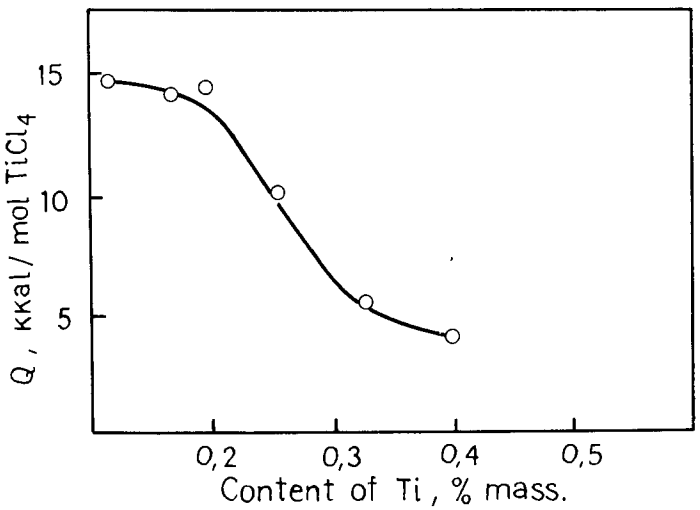

Figure 7. Heat effect of the interaction of $TiCl_4$ with magnesium chloride vs. amount of titanium chloride (catalyst A)

the titanium content points to the nonuniformity of surface adsorption sites and titanium complexes that are formed on the surface. In the range of low concentrations (less than 0.2% mass Ti or one molecule of $TiCl_4$ per area of 200 $Å^2$), the high heat effect ($\simeq$ 14 kcal/mol) corresponding to the chemisorption heat is observed. An increase in the titanium content leads to a drastic lowering of the heat effect down to 4 kcal/mol. Such a low heat effect, which is similar to the heat of physical adsorption, does not correspond to the observable strong binding of $TiCl_4$ with the magnesium chloride sample up to the Ti content of 1.2% mass. It seems that in this range of titanium concentrations (0.3-1.2% mass), a strong interaction of titanium chloride with magnesium chloride also occurs and, correspondingly, is characterized by a high heat effect (H_1). However, some portion of the heat of this interaction (H_2) is used either for the reconstruction of the support substructure (see X-ray data) or for the formation of more complex surface structures containing titanium chloride. As a result, in the experiment a small difference between the two values is observed: $Q=H_1-H_2 \simeq$ 4 kcal/mol.

Catalytic properties and EPR data. The nonuniformity of surface titanium compounds shows itself in the catalytic properties of these systems as well. Figure 8 illustrates the effect of the titanium content in catalyst A on the activity in ethylene polymerization. In the range of titanium concentrations from 0.4 to 1.2% mass, the catalytic activity is constant. It sharply increases as the titanium content is lowered down to 0.2%.

Valuable information about the peculiarities of the coordination state of the transition metal in these systems can be obtained by applying EPR method to the study of the catalyst prepared by supporting VCl_4 on the highly dispersed magnesium chloride, similar to that used for the preparation of catalysts A[9]. The maximum amount of VCl_4, which can strongly be adsorbed by the support at 20°C, is 1.2% mass V or $4 \cdot 10^{-3}$ mmol VCl_4/m^2. Similar data have been obtained for $TiCl_4$ adsorbed on the same support (1.1% mass Ti or $4 \cdot 10^{-3}$ mmol $TiCl_4/m^2$). The dependence of the activity of V-Mg catalyst on the content of vanadium (Figure 8, curve 2) is the same as that for Ti-Mg catalyst. We can, therefore, conclude that VCl_4 and $TiCl_4$ interact with magnesium chloride in the same manner.

As follows from EPR data at a low content of vanadium (0.1% mass) in the $VCl_4/MgCl_2$ system, vanadium is in the form of isolated

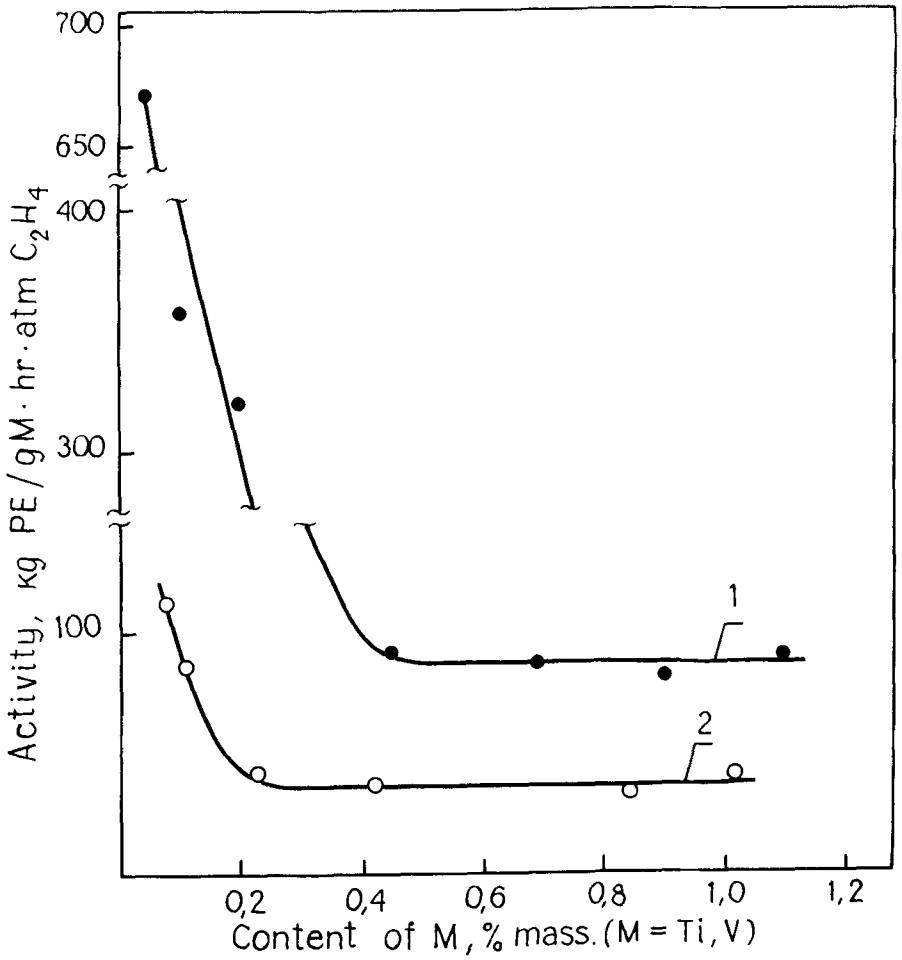

Figure 8. Activity vs. the transition metal content in catalysts A: 1 — $TiCl_4/MgCl_2$, 2 — $VCl_4/MgCl_2$

paramagnetic complexes, which produce a characteristic signal in the EPR spectrum. Upon further increasing the content of vanadium in the catalyst the signal intensity does not change. Only the treatment of these species with pyridine sharply enhances the intensity of EPR signals at the expense of pyridinate VCl_4 complexes formed. Thus, at a vanadium concentration of less that 0.2% mass ($< 6 \cdot 10^{-4}$

mmol VCl_4/m^2), VCl_4 is present as isolated surface complexes in the $VCl_4/MgCl_2$ system. At higher concentrations of vanadium, VCl_4 is in the form of associates containing exchange-bound V^{4+} ions. The similar conclusion about two stabilization states of $TiCl_4$ can be made for the $TiCl_4/MgCl_2$ system. Data on the catalytic properties of Ti-Mg and V-Mg catalysts (Figure 8) indicate that the active centers of these systems are formed both from isolated V^{4+} and Ti^{4+} complexes (range of low concentrations) and from surface associates of these ions (range of high concentrations of Ti and V). However, the yield of active centers formed from the isolated ions is noticeably higher.

2.2. On the composition of active centers of Ti-Mg catalysts.

The formation process of active centers in supported Ti-Mg catalysts of type A has been studied previously in [6] by EPR. As found, during the interaction of this catalyst with triethylaluminum, $TiCl_4$, which is adsorbed on the surface of magnesium chloride, is readily reduced even at low temperatures. As a result, three-valent Ti compounds different in the coordination state are formed. These are: isolated Ti^{3+} ions in the octahedral and tetrahedral chlorine surroundings, Ti^{3+} ions involved in the weak exchange interaction and highly dispersed particles or surface $TiCl_3$ associates. The latter type of compounds produce EPR signals only after the catalyst treatment with pyridine due to the formation of pyridinate complexes of Ti^{3+} compounds. Furthermore, small amounts of Ti^{2+} ions can also be formed. Data on the influence of the composition of Ti-Mg catalysts and of the conditions of their interaction with the organoaluminum co-catalyst on the catalytic properties and on the yield of various Ti^{3+} compounds suggest that isolated Ti^{3+} ions are side-products and cannot serve as active centers[6]. It is assumed that the active centers of these systems are in the composition of highly dispersed particles or of surface $TiCl_3$ associates and, therefore, are not detectable by EPR technique.

Catalyst A with the titanium content of 1.2% mass, in which, according to kinetic data, the number of active centers is 0.05-0.10 mol/mol Ti has been studied in [6]. Thus, major part of titanium in these samples is inactive. More detailed information about the composition of the active centers can be obtained from the investigation of the catalysts with low titanium contents, and a higher activity and,correspondingly, a higher number of the active centers

(Figure 8, curve 1). For catalysts, that contain 0.05-0.2% mass Ti and have the activity of 320-670 kg/g Ti · h · atm, the concentration of active centers is 0.22-0.47 mol/mol Ti.

Catalyst A with 0.08% of Ti produces no EPR signal. Neither the treatment of this sample with triethylaluminum (Al/Ti=5) produces signals corresponding to Ti^{3+} ions in the EPR spectrum. However, a subsequent treatment of the latter sample with pyridine leads to the appearance of the EPR signal ascribed to the pyridinate complex of Ti^{3+}, which is similar to the signal described in [6]. The signal intensity corresponds to the complete reduction of $TiCl_4$ to Ti^{3+}. Thus, in the catalyst A with a low Ti content and a high concentration of active centers, almost the whole of the titanium that has reacted with triethylaluminum is in the form of associates of Ti^{3+} ions characterized by a strong exchange interaction. Isolated Ti^{3+} ions are not formed at all in this system. Evidently, the active centers are located in the surface associates of Ti^{3+} ions.

Thus, at the first step of the formation of these catalysts, when $TiCl_4$ is supported on the highly dispersed magnesium chloride, isolated surface complexes of $TiCl_4$ can be formed provided that the titanium content is low (see section 2.1). But after the interaction of this catalyst with the organoaluminum co-catalyst, isolated surface compounds of Ti^{4+} transform to Ti^{3+} associates, which contain the active centers of these catalysts.

ACKNOWLEDGEMENT

The authors would like to acknowledge the assistance of Yu.D.Pankratiev (calorimetric measurements) and V.A.Poluboyarov (EPR study).

REFERENCES

1. S.I.Makhtarulin, E.M.Moroz, E.E.Vermel, V.A.Zakharov, React. Kinet. Catal. Lett., 9, 269 (1978).
2. N.Kashiwa, Polymer J., 12, 603 (1980).
3. P.Galli, P.Barbe, G.Guidetti, R.Zannetti, A.Martorana, A.Marigo, M.Bergozza, A.Fichera, Eur. Polym. J., 19, 19 (1983).
4. K.Soga, M.Terano, Makromol. Chem., 182, 2439 (1981).
5. J.C.W.Chien, I.C.Wu, C.I.Kuo, J. Polym. Sci., Polym. Chem. Ed., 20, 2461 (1982).

6. V.A.Zakharov, S.I.Makhtarulin, V.A.Poluboyarov, V.F.Anufrienko, Makromol. Chem., 185, 1781 (1984).
7. USSR Patent 726702, inv.: V.A.Zakharov, S.I.Makhtarulin, Yu.I. Yermakov, V.E.Nikitin, Chem. Abstr., 95, 220 579X (1981).
8. R.Spitz, J.L.Lacombe, A.Guyot, J. Polym. Sci., Polym. Chem. Ed., 22, 2625 (1984).
9. T.B.Mikenas, V.A.Zakharov, Visokomol. Soed. (in Russian), 26, 483, (1984).

This page intentionally left blank

ETHYLENE POLYMERIZATION WITH MODIFIED SUPPORTED CATALYSTS

SHANGAN LIN HAIHUA WANG QIXING ZHANG ZEJIAN LU YUN LU
Institute of Polymer Science, Zhongshan University, Guangzhou, China

ABSTRACT

Slurry polymerization of ethylene giving high yields of polyethylene under ambient or enchanced pressure with catalyst of $TiCl_4/MgCl_2/AlEt_3$ (named " GZ-Catalyst ") prepared by comilling method has been studied.

With modified catalyst comprising $TiCl_4$, $Ti(O\text{-}n\text{-}Bu)_4/MgCl_2/AlEt_3$ (named " ZS-Catalyst "), the yield of ethylene polymerization or ethylene/propylene copolymerization are raised up quite distinctly. For preparation of ultra high molecular weight polyethylene (UHMWPE), a modified catalyst of $TiCl_4/MgCl_2/AlEt_3$, RMgCl (named " HE-Catalyst") was found to be especially highly active. With catalyst comprising $TiCl_4$, $Ti(O\text{-}n\text{-}Bu)_4/MgCl_2$, $ZnCl_2/AlEt_3$ (named " YJ-Catalyst ") or with catalyst comprising $TiCl_4/MgCl_2/AlEt_3$,$ZnEt_2$ (named " ZE-Catalyst "), ethylene polymerization in absence of hydrogen gives lower molecular weight polymer. A noval modified catalyst of $TiCl_4$, $NdCl_3/MgCl_2/AlEt_3$ (named " SN-Catalyst ") is highly active for polymerization of ethylene as well as stereospecific polymerization of styrene and copolymerization of these two monomers.

The effects of polymerization conditions and kinetics of ethylene polymerization with each of the above catalysts have been studied.

Slurry polymerization of ethylene was carried out giving high yield of polyethylene under ambient or enhanced pressure (Table 1-4, Figure 1-2), with supported catalyst of $TiCl_4/MgCl_2/AlEt_3$ (named " GZ-Catalyst ") prepared by comilling method[1].

With modified catalyst comprising $TiCl_4$, $Ti(O\text{-}n\text{-}Bu)_4/MgCl_2/AlEt_3$ (named " ZS-Catalyst ")[2], the catalytic efficiency of ethylene polymerization is raised up quite distinctly (Table 1-4, Figure 1-2).

The kinetics of ethylene polymerization with GZ-1 and ZS-1 supported catalysts in the absence of hydrogen were studied[3]. The

polymerization rate V_p-time kinetics curves are of quick stationary type (Figure 1). The degree of polymerization, the specific active center [Ti] concentration [C^*], (e.g., $[C^*]=[Ti]_{active}/[Ti]_{total}$), the propagation rate constant k_p, apparent activation energies E and life time of chain growing $\bar{L}$ were determined (Table 2).

Table 1. Comparation of GZ-1 and ZS-2 catalysts for ethylene polymerization

Polymerization temperature (°C)	Catalytic efficiency (kg PE/g Ti)		Catalytic efficiency ratio (ZS-2/GZ-1)
	GZ-1	ZS-2	
60	10	30	3
45	12.3	18	1.4
35	8.1	11.4	1.4
25	5.1	7.8	1.5

Polymerization conditions: Cat[Ti]= 5-10x10^{-3} mmol/dm^3 (gasoline), Al/Ti = 150 mol/mol, 810 mmHg, 2 h, stirring rate = 520 rpm, (for 250 ml-reactor containing 100 ml purified gasoline as diluent).

For preparation of ultra high molecular weight polyethylene (UHMWPE), a modified supported catalyst of $TiCl_4/MgCl_2/AlEt_3$,RMgCl (named " HE-Catalyst ") was found to be especially highly active[4]. In recent years, highly active catalysts of titanium system containing organomagnesium compounds for ethylene polymerization have been reported[5-8], but none has been communicated in literatures about the usage of organomagneium compound as a promoter for catalysts of titanium system with $MgCl_2$ as carrier so as to increase the catalytic efficiency to a very high level (Table 3-4, Figure 2).

It is considered that the promotive effect of C_6H_5MgCl should arise from two factors[9]: 1), factor of increasing porosity of supported catalyst after treatment with C_6H_5MgCl, as shown by the SEM micrographs of various catalysts with or without C_6H_5MgCl as promoter; 2), factor of ligand's electronic effects. an increase of electron density of active center Ti ion owing to the pushing electronic effect of the R group (C_6H_5- group) in RMgCl ligand with its Cl group acts as a " chlorine bridge " connecting to the active center Ti ion. This favors the coordination and insertion of ethylene monomer toward the active Ti ion and Ti-C bond sucessively during the chain propagation reaction.

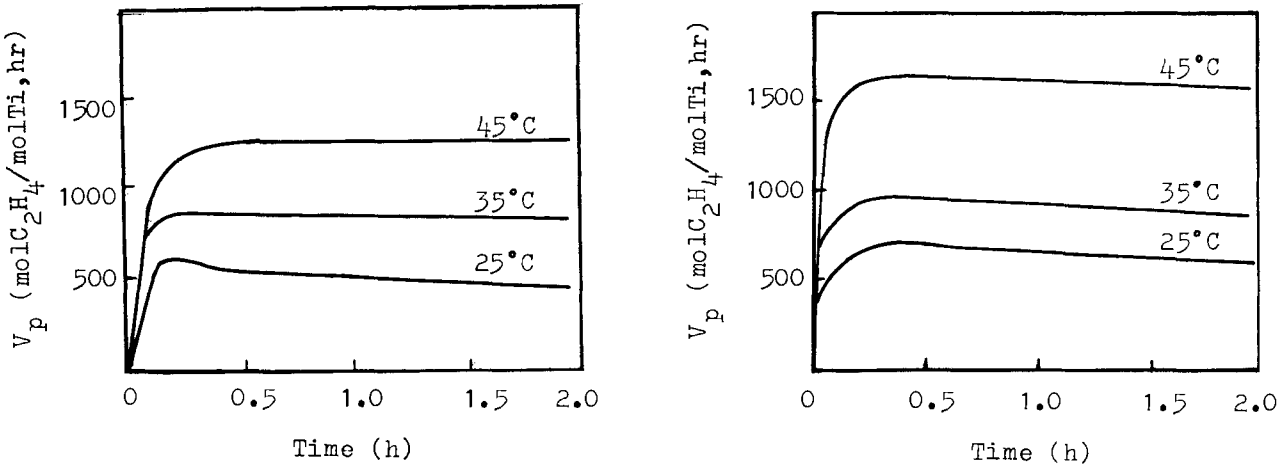

a), GZ-1 catalyst

b), ZS-2 catalyst

Figure 1. Ethylene polymerization kinetics curves with GZ-1 and ZS-2 catalysts. Polymerization condition: the same as in Table 1.

Table 2. Experimental results and kinetics parameters of ethylene polymerization with GZ-1 and ZS-2 catalysts

Catalyst system	T (°C)	V_p $\frac{mol C_2H_4}{molTi.min}$ (stationary)	$[C^*]$ $\frac{[Ti]active}{[Ti]total}$ (mol%)	k_p $\frac{dm^3}{mol.min}$ ($x10^{-3}$)	ΔE $\frac{kJ}{mol}$	$\bar{P}_n$ ($x10^{-3}$)	$\bar{L}$ (min)
$TiCl_4/MgCl_2/AlEt_3$ (GZ-1)	45	180	6.3	24.3	10.2	33.8	11.8
	35	114	3.8	22.4		45.3	15.1
	25	62	2.1	18.5		50.7	17.0
$TiCl_4$ $Ti(OBu)_4/MgCl_2/AlEt_3$ (ZS-2)	45	249	8.4	23.5	3.7	34.0	11.5
	35	154	4.2	23.0		43.3	12.0
	25	108	2.7	22.1		57.7	14.4

Polymerization condition: the same as in Table 1 and Figure 1.

Table 3. The promotive effect of C_6H_5MgCl on increasing catalytic efficiency of GZ and ZS type high active supported catalysts for ethylene polymerization

Catalyst system	$Ti(O\text{-}n\text{-}Bu)_4/TiCl_4$ (mol/mol)	Catalytic efficiency (kg PE/g Ti)	Increment of catalytic efficiency (%)
GZ-1	0/100	10	—
GZ-1+C_6H_5MgCl	—	21	110
ZS-1	5/ 95	18	—
ZS-1+C_6H_5MgCl	—	28	56
ZS-2	10/ 90	30	—
ZS-2+C_6H_5MgCl	—	35 (75*)	17 (150*)
ZS-5	20/ 80	15	—
ZS-5+C_6H_5MgCl	—	19	27

Polymerization condition: Cat[Ti]=4.3×10^{-2} mmol/dm^3 (gasoline), Al/Ti=70 mol/mol, Mg/Ti=1 mol/mol, 810 mmHg, 60°C, 2 h, (*: 70°C, 4 h).

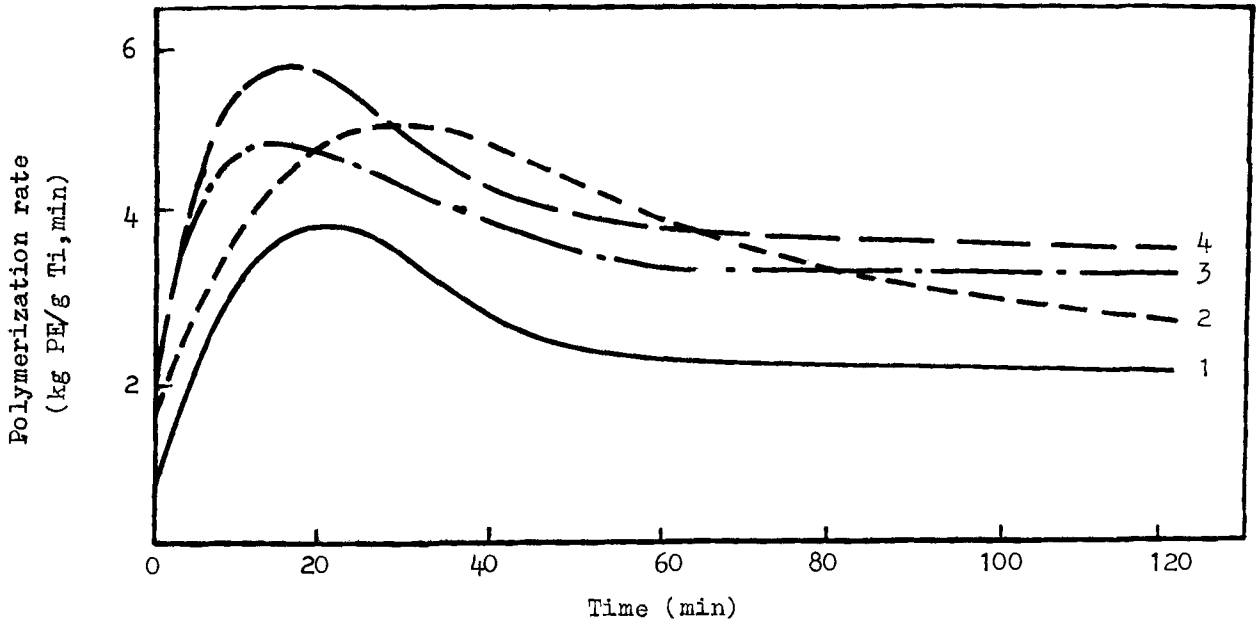

Figure 2. Kinetics curves of ethylene polymerization with variou highly active supported catalysts: 1), GZ-1; 2), GZ-1+C_6H_5MgCl; 3), ZS-3; 4), ZS-3+C_6H_5MgCl.
Polymerization condition: Cat[Ti]=4.3×10^{-2}mmol/dm^3 (gasoline), Al/Ti=70 mol/mol, Mg/Ti=1 mol/mol, 810 mmHg, 60°C, 2 h.

Table 4. The promotive effect of C_6H_5MgCl on ethylene polymerization under pressure (4 kg/cm^2)

Catalyst system	$Ti(O\text{-}n\text{-}Bu)_4/TiCl_4$ (mol/mol)	Catalytic efficiency (kg PE/g Ti)	Catalyst+C_6H_5MgCl	Catalytic efficiency (kg PE/g Ti)
GZ-1	0/100	290	GZ-1+C_6H_5MgCl	531
ZS-3	11/ 89	445	ZS-3+C_6H_5MgCl	550 (824*)
ZS-4	18/ 82	480	ZS-4+C_6H_5MgCl	530

Polymerization condition: Cat[Ti]=6.25x10^{-3} mmol/dm^3 (gasoline), [$AlEt_3$]=7 mmol/dm^3, Mg/Ti=1 mol/mol, 77°C, 2 h, (*: under 6 kg/cm^2 pressure).

Ultra high molecular weight polyethylene synthesized with HE-Catalyst displays high impact-resistance properties, and its physical behaviors were characterized extensively[10-12].

Another modified supported catalyst of $TiCl_4/MgCl_2/AlEt_3$, $ZnEt_2$ (named " ZE-Catalyst ") was prepared[13], with which ethylene polymerization was carried out in the absence of hydrogen. The catalytic efficiency increases and the molecular weight of polyethylene decreases with increasing of Zn/Ti molar ratio as shown in Figure 3. The kinetics parameters were determined (see Table 5) and were compared with those kinetics of GZ-1 and GZ-1+C_6H_5MgCl catalysts etc.

The chain transferring reaction rate constants of $AlEt_3$ and $ZnEt_2$ as transferring agents and the coresponding apparent activation energy of the chain transferring reaction were determined for GZ-1 and ZE catalytic polymerization (in Table 5) as shown in Table 6[13].

From Table 5 and 6, it is noted that ethylene polymerization with ZE-2 catalyst in which $ZnEt_2$ acts as an efficient polymerization rate promotor as well as chain transferring agent, gives very high yield of polyethylene of lower molecular weight. The apparent specific active center Ti concentration $[C^*]$ value is exceedingly high while value of apparent activation energy of chain transferring reaction $\Delta E_{tr,ZnEt}$ is especially lower than $\Delta E_{tr,AlEt}$. The chain transferring reaction may be represented as in the following scheme:

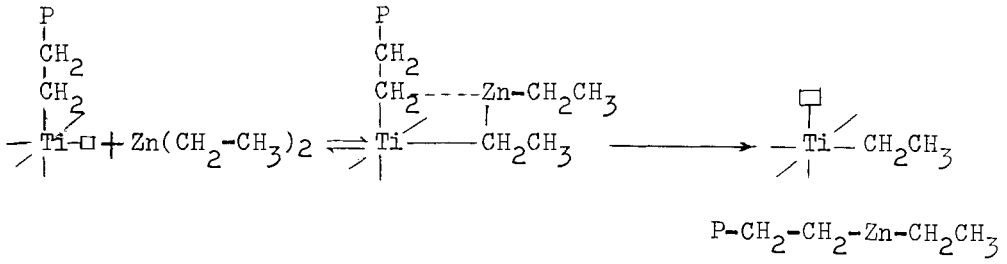

Since $ZnCl_2$ can react with $AlEt_3$ to give $ZnEt_2$, by using $ZnCl_2$ instead of $ZnEt_2$ as an ingredient of catalyst composition, a novel modified supported catalyst of $TiCl_4$, $Ti(O\text{-}n\text{-}Bu)_4/MgCl_2$, $ZnCl_2/AlEt_3$ (named " YJ-Catalyst ") was prepared for ethylene polymerization[14]. The molecular weight of polyethylene can be controlled in the absence of hydrogen by adjusting Zn/Ti molar ratio while the catalytic efficiency maintains more stationarily at quite high level as illustrated in Table 7 and Figure 4.

With fixation of Zn/Ti molar ratio at 8, the catalytic efficiency and molecular weight can be affected by adjusting the amount of

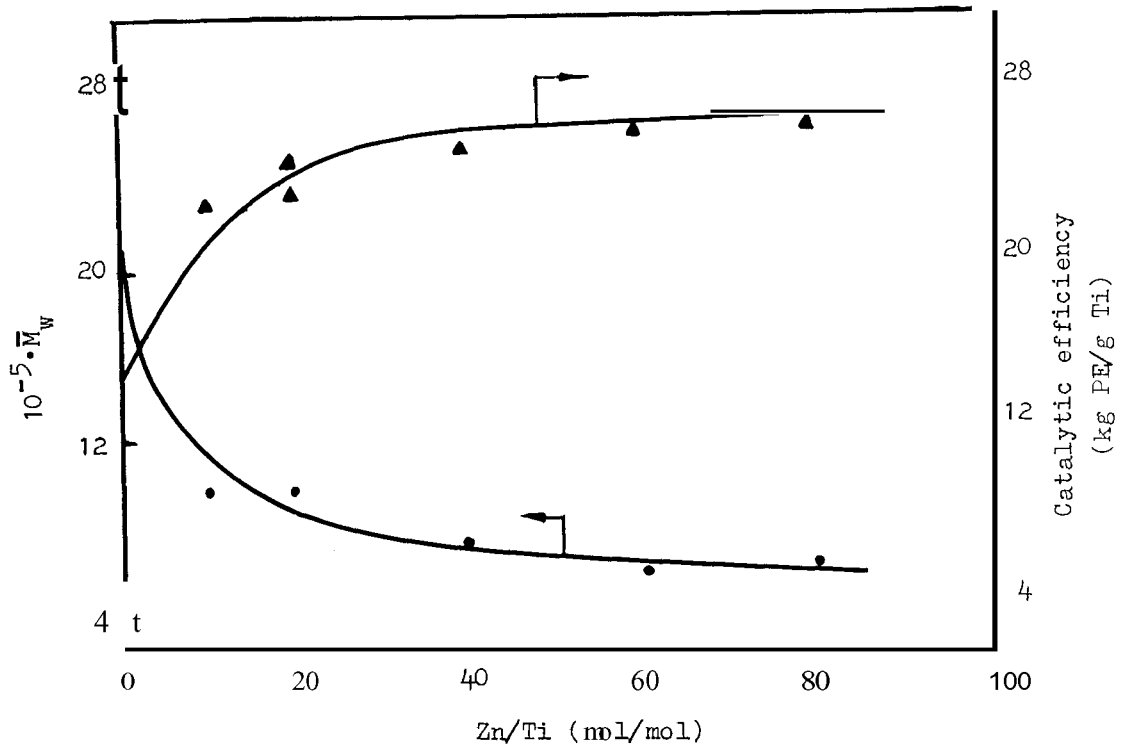

Figure *3*. Affection of Zn/Ti molar ratio on molecular weight ($\bar{M}_w$) and catalytic efficiency of ethylene polymerization with ZE catalyst (e.g., $TiCl_4/MgCl_2/AlEt_3$,$ZnEt_2$ system). Polymerization condition: Cat[Ti]=1.0×10^{-4}mmol/dm^3 (gasoline), Al/Ti=150 mol/mol, 810 mmHg, 45°C, 2 h.

Table 5. Comparative experimental results and kinetics parameters of ethylene polymerization

Catalyst system	T (°C)	V_p $\frac{mol C_2H_4}{molTi.min}$ (stationary)	$[C^*]$ $\frac{[Ti]\,active}{[Ti]\,total}$ (mol%)	k_p $\frac{dm^3}{mol.min}$ ($x10^{-3}$)	ΔE $\frac{kJ}{mol}$	$\overline{P}_n$ ($x10^{-3}$)	$\overline{L}$ (min)
$TiCl_4/MgCl_2/$	45	180	6.3	24.3	10.2	33.8	11.8
$AlEt_3$	35	114	3.8	22.4		45.3	15.1
(GZ-1)	25	62	2.1	18.5		50.7	17.0
$TiCl_4/MgCl_2/$	45	175	6.5	20.8	7.8	32.2	12.0
$AlEt_3$,PhMgCl	35	97	3.5	19.3		43.5	15.7
(HE-1) Mg/Ti=1	25	53	2.0	17.0		58.8	22.1
$TiCl_4/MgCl_2/$	45	418	89	3.70	11.6	8.2	17.8
$AlEt_3$,$ZnEt_2$	35	268	58	3.16		10.4	22.5
(ZE-2) Zn/Ti=20	25	148	31	2.76		10.7	22.4
$TiCl_4/NdCl_3/$	50	393	4.0	26.7	9.2	26.1	8.3
$MgCl_2/AlEt_3$	40	303	4.5	23.8		37.9	11.8
(SN-1)	34	125	12.5	21.7		72.3	23.0

Polymerization condition: Cat[Ti]=5-10 mmol/dm^3 (gasoline), Al/Ti=150 mol/mol, 810 mmHg, 2 h, stirring rate = 520 rpm (for 250 ml-reactor containing 100 ml purified gasoline as diluent).

Table 6. Chain transferring rate constant k_{tr} and apparent activation energy ΔE_{tr}

Catalyst system	T (°C)	$k_{tr,AlEt_3}$ ($\frac{dm^3}{mol.min}$)	$\Delta E_{tr,AlEt_3}$ ($\frac{kJ}{mol}$)	$k_{tr,ZnEt_2}$ ($\frac{dm^3}{mol.min}$)	$\Delta E_{tr,ZnEt_2}$ ($\frac{kJ}{mol}$)
$TiCl_4/MgCl_2/AlEt_3$ (GZ-1) Zn/Ti=0	45	7.05	51.8	—	—
	35	3.50			
	25	2.08			
$TiCl_4/MgCl_2/AlEt_3,ZnEt_2$ (ZE-2) Zn/Ti=20	45	—	—	27.5	25.5
	35			18.7	
	25			14.7	

Polymerization condition: the same as in Table 5.

Table 7. Affection of Zn/Ti molar ratio on catalytic efficiency and molecular weight ($\bar{M}_w$) of ethylene polymerization with YJ catalyst (e. g., $TiCl_4$, $Ti(O\text{-}n\text{-}Bu)_4/MgCl_2$, $ZnCl_2/AlEt_3$ system)

Zn/Ti (mol/mol)	Catalytic efficiency (kg PE/g Ti)	$\bar{M}_w$ ($\times 10^{-3}$)
0	261	465
2	274	356
4	280	331
6	272	312
8	278	280

Polymerization condition: Cat[Ti] = 15×10^{-3} mmol/dm^3 (gasoline), [$AlEt_3$] = 8 mmol/dm^3, 4 kg/cm^2, 75°C, 2 h.

Table 8. Correlation of the amount of YJ catalyst to catalytic efficiency and molecular weight ($\bar{M}_w$)

Cat[Ti] ($\times 10^{-3}$ mmol/dm^3)	Catalytic efficiency (kg PE/g Ti)	$\bar{M}_w$ ($\times 10^{-3}$)
4	384	188
8	262	196
22	262	214

Polymerization condition: Zn/Ti=8 mol/mol, [$AlEt_3$] = 10 mmol/dm^3, 4 kg/cm^2, 85°C, 2 h.

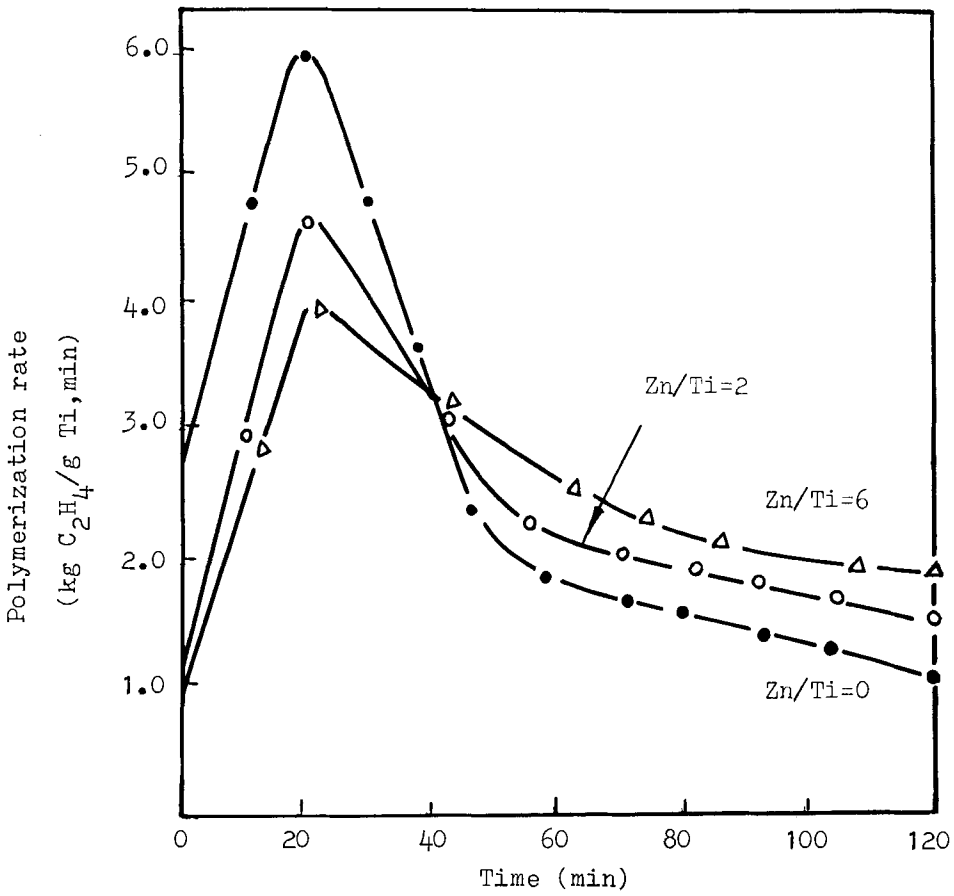

Figure 4. Kinetics curves of ethylene polymerization with YJ catalyst (e.g., $TiCl_4$, $Ti(O\text{-}n\text{-}Bu)_4/MgCl_2$, $ZnCl_2/AlEt_3$). Polymerization condition: the same as in Table 7.

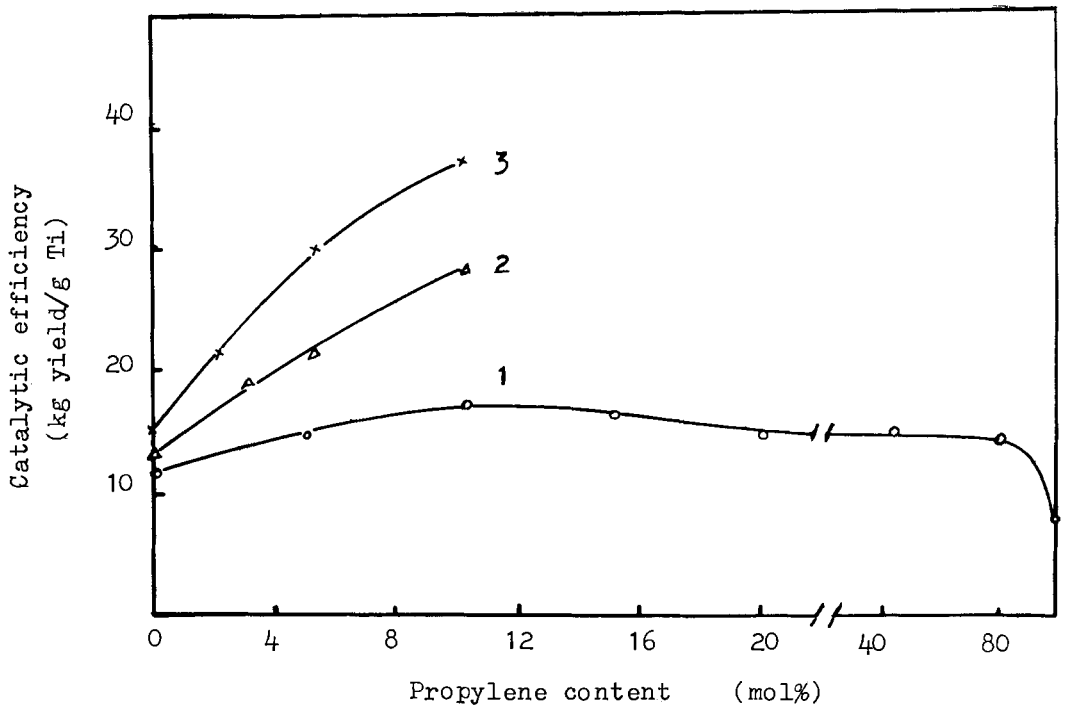

Figure 5. Dependence of feeding ratio of C_2H_4/C_3H_6 on catalytic efficiency. Copolymerization condition: 1), 60°C, Cat[Ti]=0.15 mmol/dm^3; 2), 60°C, Cat[Ti]=0.10 mmol/dm^3 3), 50°C, Cat[Ti]=0.10 mmol/dm^3.

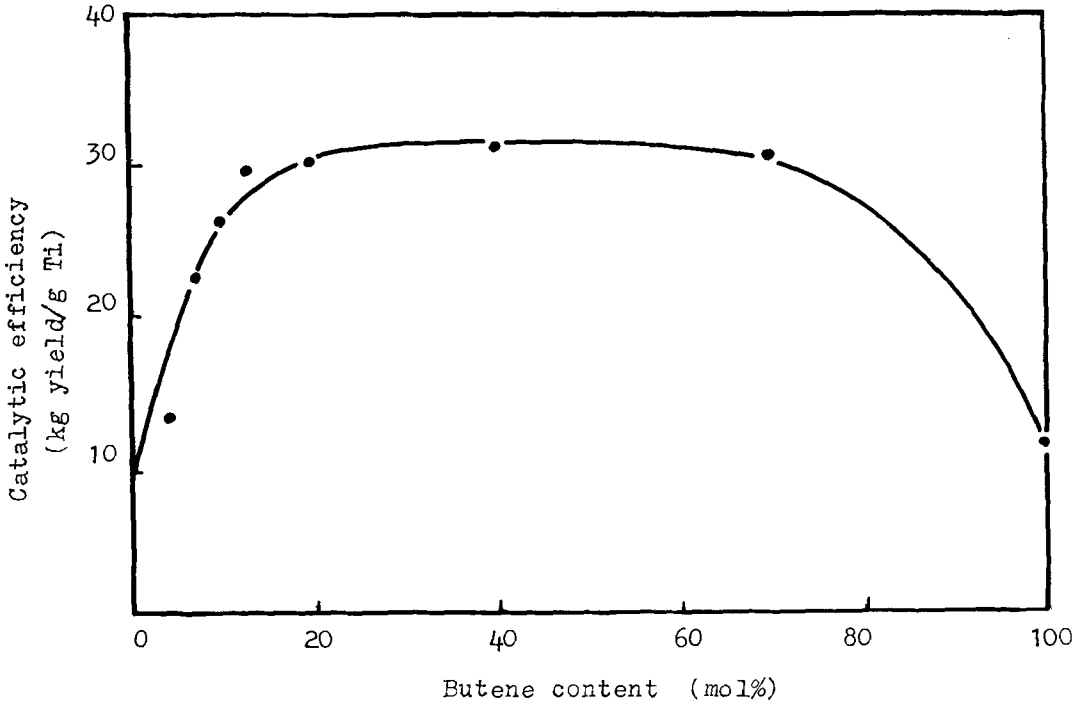

Figure 6. Affection of ethylene/butene molar ratio on catalytic efficiency of copolymerization of ethylene with butene.
Copolymerization condition: Cat[Ti]=0.1 mmol/dm^3 (gasoline), Al/Ti=150 mol/mol, 55°C, 1.5 h.

catalyst used (Table 8).

As shown in Table 5, the last modified supported catalyst of $TiCl_4$, $NdCl_3/MgCl_2/AlEt_3$ (named " SN-1 Catalyst ") was exploited in which a small amount of rare earth compound $NdCl_3$ was used as an ingredient. The feature of SN-1 Catalyst is of high value of rate constant (k_p) and high catalytic efficiency for ethylene polymerization[15]. SN-1 Catalyst is also very active for homopolymerization of styrene and copolymerization of ethylene and styrene[15]. Highly isotactic polystyrene was prepared with far higher catalytic efficiency than the results reported in literatures. Copolymerization gives good yield which consists styrene-unit content from 4 to 85 mol% of copolymer products. By the way, ZS-Catalyst is also very effective for copolymerization of ethylene and propylene[16]. The catalytic efficiency is even higher than that of homopolymerization of ethylene with the same catalyst and polymerization conditions as shown in Figure 5. With the similar modified supported catalyst, ethylene/butene-1 copolymerization[17] can be carried out with good yields as well (see Figure 6).

REFERENCE

1. S. Lin, et al., Acta Scientiarum Naturalium Universitatis Sunyatseni, 1976 (2), 64.
2. H. Wang, Q. Zhang, J. Yan, S. Lin and Y. Lu, Plastics Industries (Chinese), 1983 (3), 9.
3. Y. Lu, Z. Liu, J. Chen and S. Lin, Acta Scientiarum Naturalium Universitatis Sunyatseni, 1983 (4), 1.
4. Y. Lu, H. Wang, Q. Zhang and S. Lin, Plastics Industries (Chinese), 1983 (5), 1.
5. E. W. Duck, D. Crent, Europ. Polym. J., 10, 77, (1974).
6. L. Petkov, R. Kyrtcheva, Ph. Radenkov and D Dobreva, Polymer, 19, 567, (1978).
7. R. N. Haward, A. N. Roper and K. L. Fletcher, Polymer, 14, 365, (1973).
8. D. G. Boucher, L. W. Parsons and R. N. Haward, Makromol. Chem., 175, 3461 (1974).
9. H. Wang, Q. Zhang, J. Xu, Y. Lu and S. Lin, Chem. Jour. Chinese Univ. 5, 585, (1984).
10. S. Lin, Y. Lu, H. Wang, Q. Zhang, K. Liang, J. Xu, H. Luo and K. Liao, Proceediigs of China-U.S. Bilateral Symposium on Polymer Chemistry and Physics, p 417, Science Press, Beijing, 1981.

11. K. Liang, X. Tang, Y. Lu and S. Lin, Chem. Jour. Chinese Univ., 1985 (3).
12. K. Liao, S. Lin, Acta Scientiarum Naturalium Universitatis Sunyatseni, 1985 (1), 131.
13. S. Lin, J. Chen and Y. Lu, Polymer Communications, to be published.
14. H. Wang, Q. Zhang and S. Lin, Petrochemical Technology (Chinese), 13, 324, (1984).
15. S. Lin, X. Zhou, Z. Lu, Z. Zhao and Y. Lu, China-Japan Bilateral Symposium on the Synthesis Materials Science of Polymers, Preprints, page ii 1-4, Beijing (1984).
16. Z. Lu, A. Liao, K. Liang, Y. Lu and S. Lin, ibid., page 19-20.
17. Z. Lu, S. Lin, Research work of this laboratory.

This page intentionally left blank

SYNTHESIS OF EP-RUBBER USING TI-CATALYSTS

K.SOGA, T.SANO, R.OHNISHI, T.KAWATA, K.ISHII, T.SHIONO and Y.DOI
Research Laboratory of Resources Utilization, Tokyo Institute of Technology, Nagatsuta, Midori-ku, Yokohama 227, Japan

ABSTRACT

Based on the theory of catalyst design, which we established, we developed an efficient Ti-based catalyst for the production of an EP rubber. The catalyst was prepared by milling the $Ti(OBu)_4/MgCl_2$ mixture in heptane, followed by treatment with $AlEt_2Cl$. The catalyst combined with $Al(i\text{-}Bu)_3$ showed a markedly high activity for ethylene-propylene copolymerization and gave quality EP rubber.

Addition of hydrogen to the system controlled molecular weight without diminishing polymerization activity. The optimum conditions of the copolymerization were also investigated.

INTRODUCTION

Many patents and publications claim the synthesis of random and block copolymers from ethylene and propylene[1]. The copolymer composition strongly depends upon the catalytic systems. Soluble catalysts such as $VOCl_3$ and VCl_4 combined with $AlEt_2Cl$(DEAC) give a random or moderately alternating copolymer, while heterogeneous catalysts which seem to contain multiple active species usually give block copolymers[2-4]. The copolymers of ethylene and propylene are very important in commercial products and industrial efforts have been directed towards finding novel and more efficient catalysts for the synthesis of the desired copolymer. However, much remains to be studied regarding the nature of the active sites.

From a detailed study of the copolymerization of ethylene with various olefins and diene compounds by using a simplified catalytic system composed of titanium, we recently found an important correlation between the oxidation states of titanium and the polymerization activities of these monomers, i.e., the Ti^{3+} species are active for all these monomers, whereas the Ti^{2+} species are

active only for ethylene[5-8]. Therefore, it is of great importance for the production of linear low density polyethylene (LLDPE) and an ethylene/propylene/diene copolymer (EPDM) to prevent over-reduction of the Ti^{3+} species.

On the other hand, the activity of Ziegler-Natta catalysts for olefin polymerization has been substantially increased by supporting the titanium compound on $MgCl_2$[9-35]. However, the initial high activity usually decreases to a great extent during the course of polymerization. Such a decline in polymerization rate was also found when activated $TiCl_3$ was used as the catalyst. We have previously carried out a detailed kinetic study[36] on propylene polymerization using activated $TiCl_3$ combined with $AlEt_3$(TEA), and found that the rate of polymerization decreases exponentially with time as described by Eq.(1),

$$\frac{R_t - R_\infty}{R_o - R_\infty} = e^{-kt} \qquad (1)$$

where R_o, R_t and R_∞ are the rates of polymerization at t = 0, t and , and k is constant. By differentiating Eq.(1), we obtain

$$-\frac{d R_t}{dt} = k(R_t - R_\infty) \qquad (2)$$

Ambroz et al.[37] examined the same catalytic system and found that a considerable amount of Cl^- is extracted from $TiCl_3$ during the course of polymerization, resulting in the reduction of Ti^{3+} to Ti^{2+}. The rate of Cl^- extraction was given by Eq.(3),

$$-\frac{d[Cl^-]}{dt} = k'([Cl^-]_t - [Cl^-]_\infty) \qquad (3)$$

where $[Cl^-]_t$ and $[Cl^-]_\infty$ are the concentrations of Cl^- in the catalyst at t = t and ∞, and k' is constant. The apparent activation energies of k and k' were estimated to be approximately 2 ~ 3 kcal/mol.

Assuming that the Cl^- extraction is responsible for the decline

in polymerization rate, $-(dR_t/dt)$ should be proportional to $-(d[Cl^-]_t/dt)$. Then, Eq.(3) becomes identical to Eq.(2). These results strongly imply that Cl^- extraction from the surface of $TiCl_3$ results in the deactivation of the active species. It may be considered that a similar deactivation also takes place in the $MgCl_2$-supported $TiCl_4$ catalyst.

As is well known, no apparent deactivation takes place during propylene polymerization with a soluble $Ti(OBu)_4/AlEt_2Cl/MgCl_2$[in 2-ethyl-1-hexanol(2-EHA)]/toluene system[33]. The stability of this catalyst may also be interpreted in terms of the above model.

Based on the above theoretical background, we developed an efficient Ti-based catalyst for the production of an EP rubber.

EXPERIMENTAL

Materials Commercial extra pure grade heptane, ethylene and propylene were purified following the usual procedures. Research grade $MgCl_2$(Toho Titanium Co. Ltd.), alkylaluminums and $Ti(OBu)_4$ were commercially obtained and used without further purification. Nitrogen (Nihon Sanso Co. Ltd., 99.9995% purity) was used after passing through a molecular sieve 3A column.

Preparation of the Catalyst The mixture of $Ti(OBu)_4$(0.15mol) and $MgCl_2$(0.15mol) in 50 cm^3 of heptane was ground in a ball mill at 20°C for 24 h under a nitrogen atmosphere, followed by washing with abundant heptane. The resultant mixture was treated with a DEAC solution (10 mol-%) in heptane ([Al]/[total Ti] = 1) at 20°C for 16 h, washed frequently with heptane and dried i.vac. at 20°C to give the catalyst.

Copolymerization and Analytical Procedures The copolymerization of ethylene and propylene was usually carried out in a 300 cm^3 glass reactor equipped with a magnetic stirrer. A given amount of an alkylaluminum was added to the reactor containing 50 cm^3 of heptane, followed by introduction of the mixture of ethylene and propylene. After 10 min at the reaction temperature, a given amount of the catalyst was added. The mixture of ethylene and propylene was continuously supplied under a total pressure of 1 atm. The copolymerization was terminated by adding a dilute hydrochloric acid solution in methanol. The precipitate was dried i.vac. at room

temperature. The amounts of titanium and magnesium contained in the catalyst were determined by atomic absorption spectrophotometry (Shimadzu AA-6105). The composition of the copolymer was determined by ^{13}C NMR spectra[38,39] measured at 120°C using a JEOL JNM PS-100 spectrometer equipped with the PFT-100 Fourier transform system operating at 25.14 MHz. The molecular weight distribution of the copolymer was measured at 120°C by GPC (Shodex LC HT3) using o-dichloro-benzene as solvent. DSC measurements were made using a Du Pont 990 Thermal Analyzer at a heating rate of 10°C/min.

RESULTS AND DISCUSSION

Stability and Structure of the Catalyst The catalyst whose surface area measured by the BET method with nitrogen adsorption was 60 m^2/g contained 2.3 wt-% of titanium. The polymerization of propylene was first conducted at 40°C by using the catalyst combined with TEA.

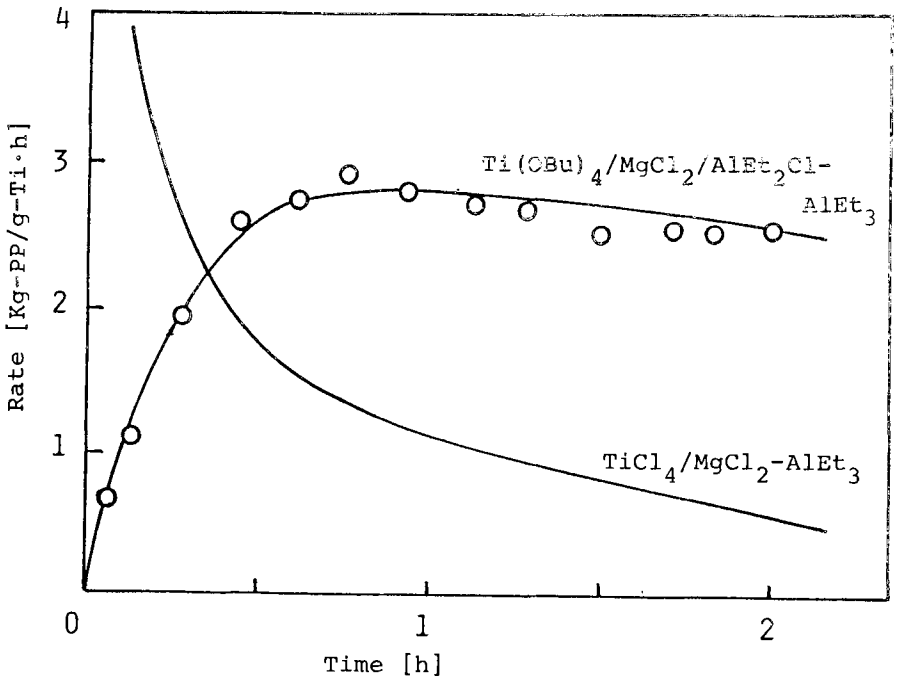

Figure 1. Rate curves of propylene polymerization

The kinetic curve of propylene polymerization is illustrated in Fig.1 together with that obtained with the use of the conventional supported catalyst ($TiCl_4/MgCl_2$, $43m^2/g$, Ti content: 0.84 wt-%) for reference. The present catalyst seems to be very stable as compared with the usual supported catalyst. The isotacticity of the polypropylene formed with the present catalyst was approximately 70 %, which was improved greatly (approximately 95 %) by adding 0.18 mmol of ethylbenzoate[40].

As is well known, the soluble $Ti(OBu)_4$/TEA/toluene system is incapable of propylene polymerization even in the presence of $MgCl_2$ (dissolved in 2-EHA)[33]. However, considerable activity appears by using DEAC in place of TEA. Similar results were also obtained in ethylene polymerization with Battelle-type catalysts: Addition of $MgCl_2$ to the $Cr(CH_3COO)_3 \cdot (CH_3CO)_2O$/DEAC or $Cr(OBu^t)_4$/DEAC system resulted in a remarkable increase in polymerization activity. However, no apparent enhancement was observed when TEA was used in place of DEAC[41,42].

These results strongly indicate that some ligand exchange reactions take place between the original transition metal compounds and DEAC, followed by forming the active complexes between the resultant transition compounds and $MgCl_2$ through Cl bridges[35].

The formation of the active species in the present catalyst might be schematically shown as in Fig.2.

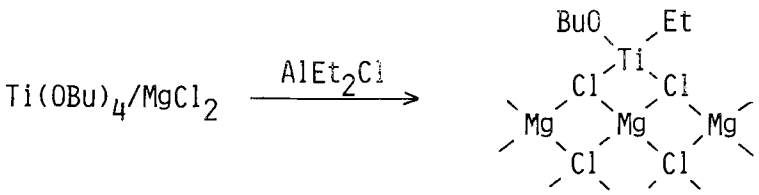

Figure 2. Plausible model of active species

Copolymerization of Ethylene with Propylene The copolymerization of ethylene with propylene was carried out at 30°C under a total pressure of 1 atm by using the catalyst combined with various alkylaluminums(Table 1). The activity was strongly dependent upon

the alkylaluminums used as cocatalyst. So far as polymerization activity and copolymer composition are concerned, little difference was observed between TEA and triisobutyl aluminum (TIBA). However, the copolymer obtained with TEA showed very weak absorption at 721 cm^{-1} attributed to a crystalline polyethylene, indicating that trace amounts of the Ti^{2+} species may be formed in this catalytic system.

Table 1. Copolymerization results over the $Ti(OBu)_4/MgCl_2/AlEt_2Cl$ catalyst

Run No.	Catalyst [$mmol/dm^3$]	Cocatalyst [$mmol/dm^3$]	Polymer Yield [g]	Activity [Kg/g-Ti h]	$C_3^=$ content [mol %]
1	0.156	$Al(i\text{-}Bu)_3$ 7.78	1.19	3.20	31.5
2	0.134	$AlEt_3$ 6.72	1.06	3.28	33.0
3	0.082	$AlEt_2Cl$ 4.14	0.00^7	0.04	—
4	0.310	$Al_2Et_3Cl_3$ 7.25	0.04	0.06	—

Polymerization conditions; 30°C, 1 h, total pressure = 1 atm [$C_2^=/C_3^=$ (gas phase) = 2/3], heptane = 50 cm^3.

The copolymerization was thus carried out in some detail using TIBA as cocatalyst. Typical results obtained are summarized in Table 2. The highest activity was obtained at 30°C with 5 $mmol/dm^3$ of TIBA. The content of propylene in the copolymer slightly decreased when the copolymerization was carried out either at low concentrations of TIBA (Runs No.5 and 6) or at low temperatures (Runs No.12, 13 and 14), the precise reason for which is, however, not clear at present. The number average molecular weight of the copolymer was 2.1×10^4 with a $Q(\bar{M}w/\bar{M}n)$ value of 9.7.

Table 2. Copolymerization results over the $Ti(OBu)_4/MgCl_2/AlEt_2Cl$ - $Al(i\text{-}Bu)_3$ catalyst

Run No.	Cocatalyst [mmol/dm^3]	Polymerization conditions	Activity [Kg/g-Ti·h]	$C_3^=$ content [mol %]
5	1	30°C × 1 h	5.4	31.0
6	3	〃	5.3	35.7
7	5	〃	11.3	47.5
8	10	〃	10.3	42.5
9	50	〃	9.3	41.8
10	5	30°C × 10 min	14.9	43.0
11	〃	30°C × 30 min	12.4	46.2
7	〃	30°C × 1 h	11.3	47.5
12	〃	0°C × 1 h	7.9	35.5
13	〃	10°C × 1 h	9.1	40.5
14	〃	20°C × 1 h	10.7	40.8
7	〃	30°C × 1 h	11.3	47.5
15	〃	40°C × 1 h	10.1	41.2

Polymerization conditions; [Ti] = 0.1 mmol/dm^3, total pressure = 1 atm [$C_2^=/C_3^=$(gas phase) = 2/3], heptane = 50 cm^3.

Figs.3, 4 and 5 show the IR and ^{13}C NMR spectra as well as the DSC curve of the copolymer obtained under best conditions (Run No.7). Although weak absorption at 995 cm^{-1} in Fig.3 indicates the presence of small amounts of isotactic PP block, the DSC curve hardly displays an absorption at around 135°C, indicating that the sequences of propylene units are fairly short. On the other hand, the intensities of the peaks at 34.9($S_{\alpha\beta}$), 33.6($T_{\gamma\gamma}$) and 27.9 ppm($S_{\beta\gamma}$), which are assigned to the carbons in the sequences with inverted propylene units, are negligible in Fig.4. The absence of propylene inversion in the copolymer is considered to be due to high regiospecificity of the catalytic system. The present copolymerization can be therefore analyzed as a binary copolymerization of ethylene (E) and propylene (P).

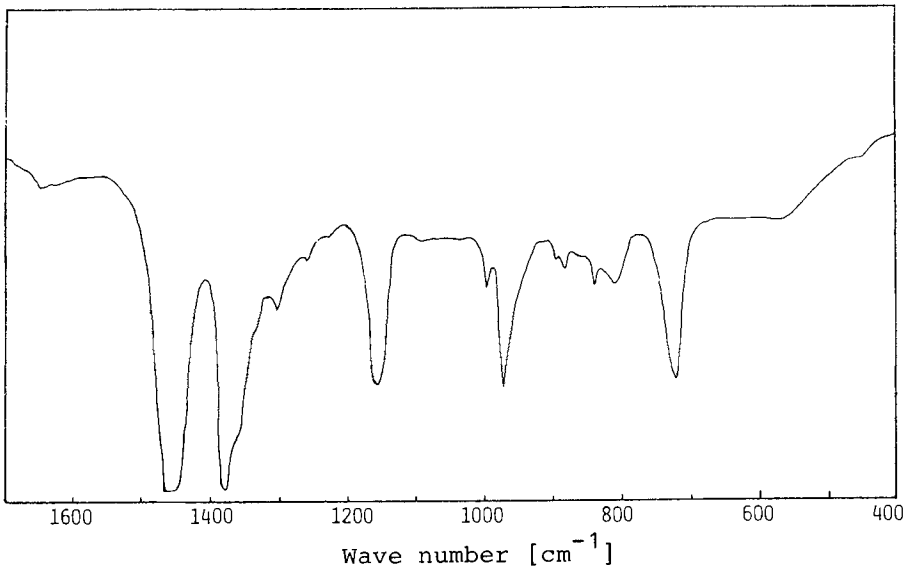

Figure 3. IR spectrum of sample 7

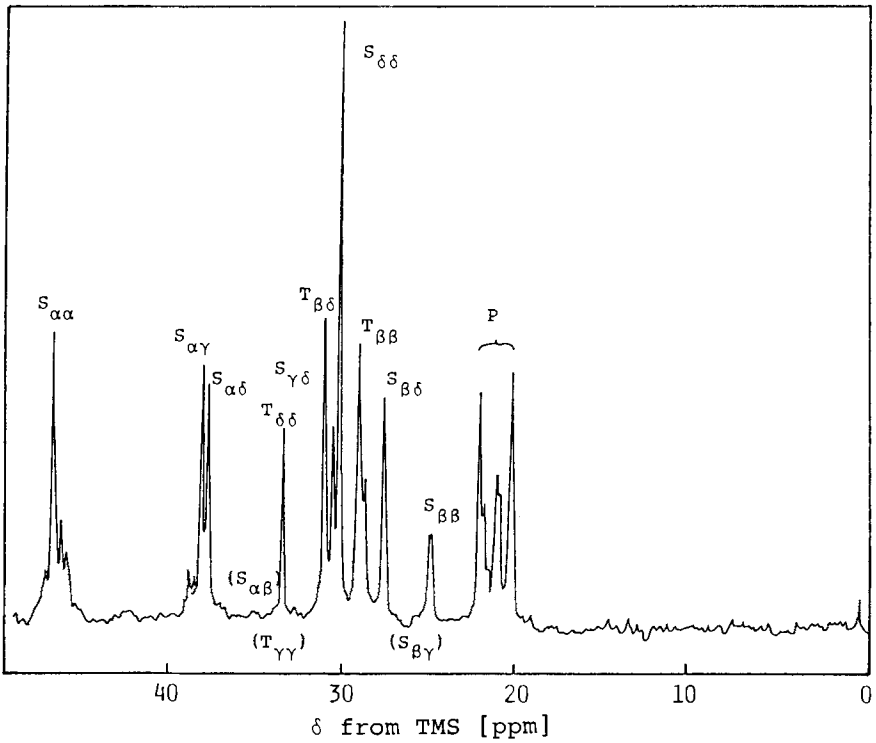

Figure 4. ^{13}C-NMR spectrum of sample 7

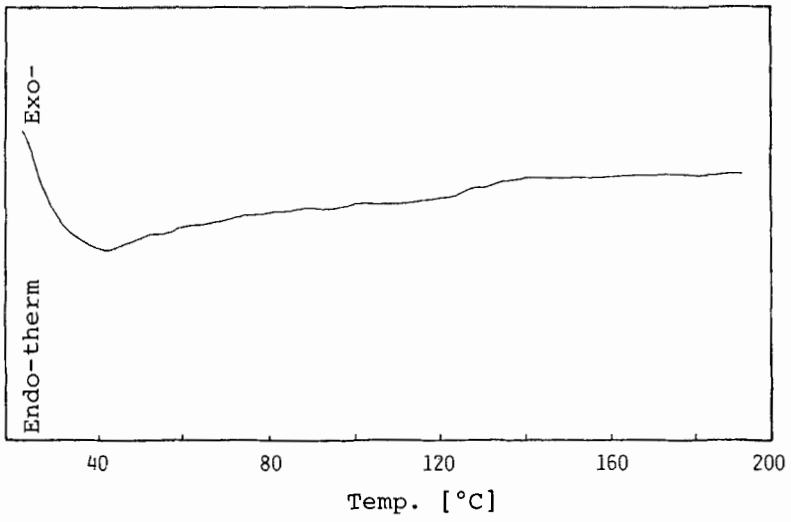

Figure 5. DSC curve of sample 7

The dyad and triad sequence distributions were determined using the following relations.

$$PP = I\,(S_{\alpha\alpha}) \tag{4}$$

$$EP = I\,(S_{\alpha\gamma}) + I\,(S_{\alpha\delta}) \tag{5}$$

$$EE = 1/2\,[\,I\,(S_{\beta\delta}) + I\,(S_{\delta\delta})\,] + 1/4\,I\,(S_{\gamma\delta}) \tag{6}$$

$$PPP = I\,(T_{\beta\beta}) \tag{7}$$

$$PPE = I\,(T_{\beta\delta}) \tag{8}$$

$$EPE = I\,(T_{\delta\delta}) \tag{9}$$

$$PEP = I\,(S_{\beta\beta}) = 1/2\,I\,(S_{\alpha\gamma}) \tag{10}$$

$$PEE = I\,(S_{\alpha\delta}) = I\,(S_{\beta\delta}) \tag{11}$$

$$EEE = 1/2\,I\,(S_{\delta\delta}) + 1/4\,I\,(S_{\gamma\delta}) \tag{12}$$

The monomer composition in the copolymer was calculated from the dyad and triad sequence distributions using Eqs.(13) and (14).

$$P = PP + 1/2\,PE = PPP + PPE + EPE \tag{13}$$

$$E = EE + 1/2\,PE = EEE + EEP + PEP \tag{14}$$

The observed sequence distributions of connecting monomer units may be interpreted in terms of a first-order Markovian process of a binary copolymerization involving the following four propagation steps.

$$\text{--- E-Ti} + C_2H_4 \xrightarrow{k_{11}} \text{--- EE-Ti} \quad (15)$$

$$\text{--- E-Ti} + C_3H_6 \xrightarrow{k_{12}} \text{--- EP-Ti} \quad (16)$$

$$\text{--- P-Ti} + C_2H_4 \xrightarrow{k_{21}} \text{--- PE-Ti} \quad (17)$$

$$\text{--- P-Ti} + C_3H_6 \xrightarrow{k_{22}} \text{--- PP-Ti} \quad (18)$$

Here kij is the rate constant of step ij, and the subscripts 1 and 2 refer to ethylene and propylene. Assuming a statistical stationary condition in the copolymerization, we can calculate the monomer reactivity ratios r_1 and r_2 by using Eqs.(19) and (20), where X is the ratio of ethylene concentration to propylene concentration in the feed.

Table 3. Monomer composition, sequence distribution and reactivity ratio of sample 7

P	0.56	PPP	0.26
E	0.44	PPE	0.21
		EPE	0.11
PP	0.32	PEP	0.10
PE	0.48	EEP	0.14
EE	0.20	EEE	0.18
	r_1	5.25	
	r_2	0.21	
	$r_1 \cdot r_2$	1.11	

$$r_1 = \frac{k_{11}}{k_{12}} = \frac{2(EE)}{(PE)X} \qquad (19)$$

$$r_2 = \frac{k_{22}}{k_{21}} = \frac{2(PP)X}{(PE)} \qquad (20)$$

The results obtained are shown in Table 3. The monomer reactivity ratios were determined as $r_1 = 5.25$ and $r_2 = 0.21$, i.e., $r_1 r_2 = 1.11$, indicating that the present copolymerization proceeds quite randomly.

The copolymerization was then carried out in a 5 dm^3 stainless reactor using 0.1 mmol of the catalyst, 1 mmol of TIBA and 1 dm^3 of heptane at 40°C for 30 min under a total pressure of 2.5 bar by supplying the mixed gas (C_2H_4/C_3H_6 = 1/1) continuously at a rate of 5 $dm^3\ min^{-1}$ (Run No.16). A transparent random copolymer with a propylene content of 38 mol % was obtained having a specific activity of 75.2 kg-polymer g-$Ti^{-1} \cdot h^{-1}$. The effect of hydrogen on the copolymerization was also examined by supplying the above system with hydrogen gas at a rate of 0.5 $dm^3\ min^{-1}$. A similar copolymer was obtained with a specific activity of 90.6 kg-polymer g-$Ti^{-1} \cdot h^{-1}$ (Run No.17).

Fig.6 shows the molecular weight distribution curves of the copolymers. Addition of hydrogen to the system could thus control the molecular weight without diminishing (rather increasing) the polymerization activity.

In conclusion, we succeeded in preparing a stable catalyst by milling the $Ti(OBu_4)/MgCl_2$ mixture in heptane, followed by treatment with DEAC. The catalyst combined with TIBA showed a very high activity for ethylene-propylene copolymerization to give a quality EP rubber.

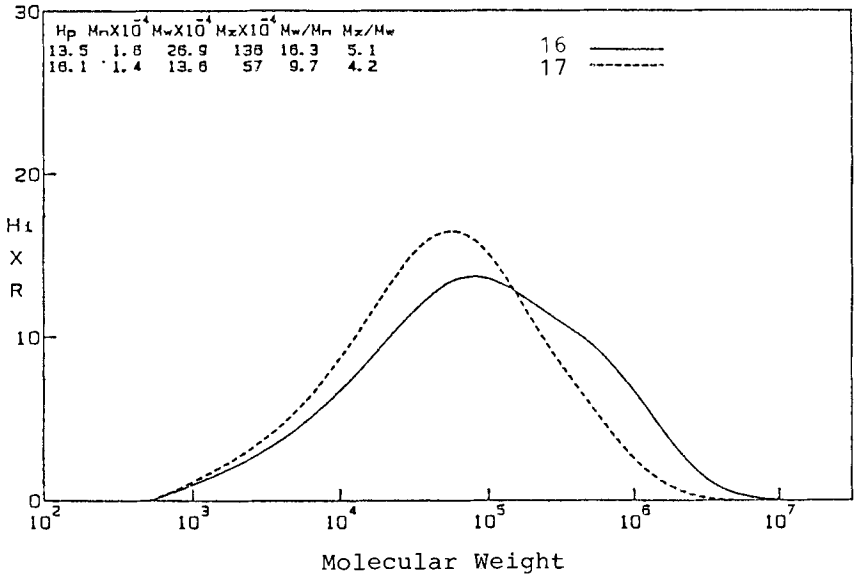

Figure 6. GPC chromatograms of samples 16 and 17

REFERENCES

1. J.Boor,Jr., "Ziegler-Natta Catalysts and Polymerization", Academic Press Inc., New York, 1979
2. G.Natta, A.Valvassore, G.Mazzanti and G.Sartori, Chim.Ind., 40, 717(1958)
3. E.Junghanns, A.Gumboldt and G.Bier, Makromol.Chem., 58, 18(1962)
4. W.L.Carrick, F.J.Karol, G.L.Karapinka and J.J.Smith, J.Am.Chem.Soc., 82, 1502(1960)
5. K.Soga, T.Sano and R.Ohnishi, Polym.Bull., 4, 157(1981)
6. K.Soga, S.Chen and R.Ohnishi, ibid, 8, 473(1982)
7. K.Soga, M.Ohtake, R.Ohnishi and Y.Doi, Polym.Commun., 25, 171(1984)
8. K.Soga, M.Ohtake, R.Ohnishi and Y.Doi, Makromol.Chem., 186, in press (1985)
9. Petrochemicals Ltd., Brit.Pat. 841, 822(1955)

10. Shell, Brit.Pat. 904, 510(1960)
11. W.A.Hewett, J.Polym.Sci., B, 5, 855(1965)
12. K.Soga, S.Katano, Y.Akimoto and T.Kagiya, Polym.J., 5, 128(1973)
13. R.N.Haward, A.N.Koper and K.L.Fletcher, Polymer, 14, 365(1973)
14. J.C.W.Chien and J.T.T.Hsieh, J.Polym.Sci., Polym.Chem.Ed., 14, 1915(1976)
15. A.Munoz-Escalona and J.Villalba, Polymer, 18, 179(1977)
16. K.Gardner, I.W.Parsons and R.N.Haward, J.Polym.Sci., Polym.Chem.Ed., 16, 1983(1978)
17. E.Suzuki, M.Tamura, Y.Doi and T.Keii, Makromol.Chem., 180, 2235(1979)
18. E.W.Duck, D.Grant and E.Kronfli, Eur.Polym.J., 15, 625(1979)
19. K.Soga, K.Izumi, M.Terano and S.Ikeda, Makromol.Chem., 181, 657(1980)
20. S.S.Ivanchev, A.A.Baulin and A.G.Rodionov, J.Polym.Sci., Polym.Chem.Ed., 18, 2045(1980)
21. N.Kashiwa, Polym.J., 12, 603(1980)
22. H.L.Hsieh, Polym.J., 12, 596(1980)
23. K.Soga and M.Terano, Polym.Bull., 4, 39(1981)
24. P.Galli, L.Luciani and G.Cecchin, Angew.Makromol.Chem., 94, 63(1981)
25. Y.Giannini, Makromol.Chem.Suppl., 5, 216(1981)
26. T.Keii, E.Suzuki, M.Tamura, M.Murata and Y.Doi, Makromol.Chem., 183, 2285(1982)
27. N.Kashiwa and J.Yoshitake, Makromol.Chem., Rapid Commun., 3, 211(1982); Makromol.Chem., Rapid Commun., 4, 41(1983)
28. G.D.Bukatov, S.H.Shepelev, V.A.Zakharov, S.A.Sergeev and Yu.I.Yermakov, Makromol.Chem., 183, 2657(1982)
29. J.C.W.Chien, J.C.Wu and I.J.Kuo, J.Polym.Sci., Polym.Chem.Ed., 20, 2091(1982)
30. A.D.Caunt, J.A.Licchelli, I.W.Parsons, R.N.Haward and M.R.Y.Al-Hillo, Polymer. 24, 121(1983)
31. P.C.Barbe, L.Noristi, G.Baruzzi and E.Marchetti, Makromol.Chem., Rapid Commun., 4, 249(1983)
32. Union Carbide Corp., Japan Kokai, 54-142192(1979)
33. Y.Doi, K.Soga, M.Murata, E.Suzuki, Y.Ono and T.Keii, Polym.Commun., 24, 244(1983)

34. K.Soga, Y.Doi and T.Keii, Proc. 8th Intern. Congr. Catalysis, West Berlin, Vol.5, p349(1984)
35. K.Soga, 189th ACS Meeting, Miami Beach, Fla, April 28-May 3, 1985, in press by D.Riedel Publishing Co. New York
36. T.Keii, K.Soga and N.Saiki, J.Polym.Sci., C16, 1507(1967)
37. J.Ambroz, P.Osecky, J.Mejzlik and O.Hamerik, ibid, c16, 423(1967)
38. C.J.Carman, R.A.Harrington and C.E.Wilkes, Macromolecules, 10, 536(1977)
39. J.C.Randall, ibid, 11, 33(1978)
40. K.Soga, T.Shiono, K.Ishii, A.Nogami and Y.Doi, Makromol.Chem., in press
41. K.Soga, S.Chen, T.Shiono and Y.Doi, Polymer, in press
42. K.Soga, S.Chen, T.Shiono and Y.Doi, Makromol.Chem., in press

DESIGN OF SUPPORTED ZIEGLER-NATTA CATALYSTS USING SiO_2 AS CARRIER

A. MUÑOZ-ESCALONA, J. G. HERNANDEZ and J.A. GALLARDO
Laboratorio de Polimeros. Centro de Química. IVIC.
Apartado 1872, Caracas 1010A. Venezuela.

ABSTRACT

The systematic preparation of supported Ziegler-Natta catalysts for ethylene polymerization was investigated. Catalysts were synthesized by a series of reactions of SiO_2 with $TiCl_4$, $AlR_{3-x}Cl_x$, $ZnEt_2$ and RMgI compounds. The main co-catalysts used for activation were $AlEt_2Cl$, $AlEt_3$ and $Al(iso\text{-}Bu)_3$. Silicas Davison 951 and 952 having different surface areas, porosities and mechanical properties were employed as carriers. It could be shown that, for the catalysts prepared by simple impregnation of SiO_2 with $TiCl_4$ and by co-impregnation with $TiCl_4$ and $AlEt_2Cl$, the carriers control the kinetic behavior of the catalysts. Thus, catalysts based on Davison 951 silica showed an acceleration type kinetic curve while those based on Davison 952 give a decay kinetic curve. Catalysts obtained by re-impregnation methods showed the highest activities when $Al(iso\text{-}Bu)_3$ was used for synthesis and for activation. In this case, the catalytical behavior is controlled by a layer of very active $TiCl_3$ crystallite formed as a consequence of the large amount of $TiCl_4$ used. Catalysts with activities as high as 18.000 g. PE x g. Ti^{-1} x $h.^{-1}$ x $atm.^{-1}$ and having a good control of the polymer morphology could be obtained.

INTRODUCTION

In the past ten years great efforts have been made to synthesize highly active catalysts for olefin polymerization. Systems based on the support of $TiCl_4$ on carriers having high surface areas, such as: SiO_2, Al_2O_3 or SiO_2 - Al_2O_3, followed

by activation with alkyl aluminum compounds have been reported in the technical and scientific literature[1-4]. These catalysts exhibit higher activities than the conventional ones based on $TiCl_3$ and also better ability in controlling the nascent polymer morphology[5,6].

Highly active catalysts have also been prepared using anhydrous $MgCl_2$ as support. Due to the low surface area of $MgCl_2$, this and the $TiCl_4$, alone or together with other compounds, have to be ball-milled intensively in order to activate the $MgCl_2$ and to introduce sufficient amount of titanium in its crystal lattice[7,8]. The result is a very high active catalyst for ethylene and propylene polymerization, showing, however, the catalysts poor morphology. This is a very important factor, because as it has been reported[9] the catalyst imposes its shape and size to the polymers particle. Therefore, undesirable amounts of fine polymer particles could be obtained in the reactor, specially when insufficient activity is present and consequently the replication factor (i.e. polymer size to catalyst size relationship) is very low. Improvement of the catalyst morphology can be achieved, however, by treatment with high Al/Ti ratios[10].

The ability of the catalyst to control the shape and size of the nascent polymer particles has been named replication phenomenum. The catalyst particles are formed by more or less loosely bounded aglomeration of subparticles, which at the same time consist of primary particles, leaving cracks and poros inside. The monomer diffuses through the particles and polymerization takes place at the active centers located at the surface of the primary particles. The poros and cracks are filled by the growing polymer, leading to the fissuring, rupture and expansion of the aggregate and of the whole particle, exposing new active centers to polymerization. Therefore, the size, shape and texture (type of aggregation, porosity, etc.) of the catalyst particles control not only the resulting polymer morphology[11], but also the polymerization kinetic, as established by Natta's finding[12]. The acceleration type

kinetic curves obtained during propylene polymerization with ungrounded samples of α- $TiCl_3$ have been understood on the basis of these explanations.

In regard to ethylene polymerization with supported Ziegler-Natta catalysts very little is shown in the literature on how carriers influence the polymerization activity and stabilize the active sites, and also how the catalyst morphology influences the kinetic behavior and the morphology of the resulting polymers.

EXPERIMENTAL

General outline procedures for the preparation of the supported catalysts have been described elsewhere[6]. Two grades of silica, Davison 951 and 952, both from Grace Davison USA, having very different characteristics were used as carriers. The 951 silica shows a high surface area (610 $m^2 \times g.^{-1}$), microporosity (0.90 ml x $g.^{-1}$ porous volume) and good mechanical strength; while the 952 exhibits lower surface area (220 $m^2 \times g.^{-1}$), macroporosity (1.60 ml x $g.^{-1}$) and breaks-up easily[6].

Before being used, the silicas were treated with diluted H_2SO_4 and HCl solutions, washed with plenty of distilled water and finally dried at 150°C under vacuum for 4 hours.

A group of catalysts were prepared by simple reaction of $TiCl_4$ with both silicas, following procedures described in reference 6 and summarized later on in this paper.

A second group of catalysts were obtained by reaction of SiO_2 simultaneously with each of the following pairs of reagents diluted in n-heptane: $TiCl_4$ and $AlR_{3-x}Cl_x$, $TiCl_4$ and ZnR_2, and $TiCl_4$ and MgXR, as described in schemes 1-3. Similar procedures were employed for preparing a third group of catalysts identical to those prepared in the second group, excepting that they were heat treated at 450°C under vacuum for 4 hours followed by re-impregnation with the same mixture of reagents.

Careful precautions were taken to ensure anaerobic and anhydrous conditions in all steps of the catalysts preparation.

The catalysts prepared were subsequently characterized by determining their surface area by BET method, surface acidity (Lewis and Breston acid centers) by Webb method based on the amount of chemisorbed NH_3 gas, and metal content by colorimetric and atomic absorption methods (see references 5 and 6 and also references therein for more details).

Polymerization of ethylene was carried out at 50°C under a constant monomer pressure of 5 atm. in 1 liter stirred glass autoclave reactor using 0.5 liter of n-heptane as a solvent.

The reactor was stirred at 1.200 rpm's speed in order to minimize mass transfer control of polymerization rates. Both catalyst components, supported Ti and co-catalyst, were introduced separately in the reactor, putting first in a glass ampoule the Ti containing catalyst, and then the alkyl aluminium compound in the solvent, when it was saturated with ethylene at the selected polymerization pressure. The Al/Ti ratio was kept constant at 10 and the polymerization was timed just after breaking the ampoule containing the catalyst. The polymerization rate was determined from the rate of monomer consumption (volume of ethylene flow into the reactor) measured by a method similar to that described by Schnecko et. al.[13]. This method has a very good reproducibility and the error in the rate measurements does not exceed $\pm$ 1%. After 2-3 hours polymerization time the reaction was quenched by introducing a solution of ethanol containing hydrochloric acid. The polymers obtained were washed several times with ethanol and dried in vacuum at 50°C.

The intrinsic viscosity of the polyethylenes was measured at 135 $\pm$ 0.05°C in decalin and molecular weight were calculated following procedures given in references 5 and 6.

Finally, catalysts and resulting polymers were observed

under the scanning electron microscope (SEM) by joining them to SEM stubs with conductive-adhesive silver paint. Particles size distribution were then obtained from the micrographs taking a population of 500 particles.

RESULTS AND DISCUSSION

Catalysts prepared by simple reaction of SiO_2 with $TiCl_4$

The first group of catalysts were synthesized by simple reaction at room temperature of both silicas with $TiCl_4$ in n-heptane for 1 hour. The supported solids were filtered and washed with n-heptane, until no trace of metals could be detected in the solutions. Finally, they were dried at 50°C under vacuum for more than 1 hour to obtain catalysts No. 515 (951 silica) and 548 (952 silica), respectively.

Due to the reaction of $TiCl_4$ with hydroxyl groups, the surface areas of both silicas decreased. Silica 951 undergoes greater reduction in its available surface area as a result of plugging of its microporos. This did not happen to that extension with silica 952, because it has macroporos (see Table 1). In regard to the amount of Ti supported, silica 951 can load a greater amount (6.7%) as compared to silica 952 (4.9%) due to their differences in surface areas.

The kinetic behavior of both catalysts were very different as shown in Figure 1. Catalyst 515 based on silica 951 presents an acceleration type curve, while catalyst 548 shows a decay curve. As a consequence of that, catalyst 515 has lower activity than catalyst 548 based on SiO_2 952 (see Table 2). These results may be explained considering the differences in mechanical properties and porosities of the two supports. Ethylene monomer diffuse more easily into catalyst 548, as a result of its higher porosity, than it does into the catalyst 515. Therefore, the polymer growths inside of the particles of catalyst 548 breaking them up into smaller fragments, due to its lower mechanical strength, generating new active centers for polymerization. This process does not take place in so

TABLE 1. PHYSICO-CHEMICAL CHARACTERIZATION OF CATALYSTS PREPARED BY REACTION OF $TiCl_4$ AND CO-REACTION OF $TiCl_4$ AND $AlEt_2Cl$ ON SiO_2

Catalyst Preparation	Catalyst No.	Surface Area ($m^2 xg.^{-1}$)	Surface Acidity ($mmol.NH_3 xg.\ cat.^{-1}$)	Ti (w%)	Al (w%)	Al/Ti (mol)	Total Amount of Metals (mols x 100 g. $cat.^{-1}$)
SiO_2 (951)	-	610	0.35	-	-	-	-
SiO_2(951) + $TiCl_4$	515	350	8.7	6.7	-	-	0.14
SiO_2(951) + $TiCl_4$-$AlEt_2Cl$ t-1h[a)]	543	280	12.3	4.5	3.4	1.3	0.22
Cat. 543, T = 450°C, 4h Vacuum	545	260	7.8	1.9	0.8	0.75	0.069
SiO_2(952)	-	240	0.40	-	-	-	-
SiO_2(952) + $TiCl_4$	548	190	3.5	4.9	-	-	0.10
SiO_2(952) + $TiCl_4$-$AlEt_2Cl$ t=3h[a)]	(541)	150	9.4	5.5	2.3	0.75	0.20
SiO_2(952) + $TiCl_4$-$AlEt_2Cl$ t=1h[a)]	541	150	9.5	3.5	3.7	1.9	0.21
Cat. 541, T = 450°C, 4 h Vacuum	542	150	7.1	2.6	0.5	0.3	0.073

a) t = reaction time

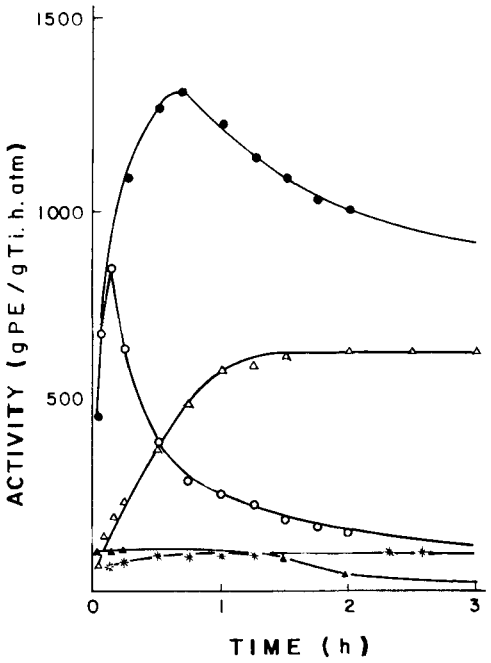

Figure 1. Catalytic activity vs. time for the catalysts: (●) 548, (△) 515, (o) (541)[1] (▲) 541 and (*) 543. Polymerization conditions: P=5atm. T=50°C, Al/Ti=10. Co-catalyst $AlEt_2Cl$

great extension in case of catalyst 515, where the catalyst particles become encapsulated with polymer and as a result its activity tends to be lower.

Figures 2 and 3 show the kinetic curves obtained using different co-catalysts ($AlEt_3$, $AlEt_2Cl$ and $Al(iso\text{-}Bu)_3$) for both catalysts. The same catalystic behavior can be seen with all types of co-catalysts used, i.e. acceleration curves for catalysts based on SiO_2 951 and decay curves for catalysts based on SiO_2 952, resulting the $Al(iso\text{-}Bu)_3$ the best co-catalyst, producing 22.8 Kg. PE x g. Ti^{-1} with catalyst 548 and 5.4 Kg. PE x g. Ti^{-1} with catalyst 515 (see Table 2).

Table 2. Influence of co-catalysts on the catalytic activity of catalysts obtained by simple impregnation and co-impregnation of SiO_2 Davison 951 and 952 with $TiCl_4$ and $TiCl_4$-$AlEt_2Cl$. Polymerization time = 2h., P = 5 atm., T = 50°C, Al/Ti = 10.

Catalyst Preparation[a]	Catalyst No.	Catalytic Activity (Kg. PExg.Ti^{-1})		
		$AlEt_2Cl$	$AlEt_3$	$Al(iso-Bu)_3$
SiO_2(951)+$TiCl_4$	515	4.9	3.5	5.4
SiO_2(952)+$TiCl_4$	548	11.2	11.7	22.8
SiO_2(951)+$TiCl_4$-$AlEt_2Cl$	543	0.04	-	-
SiO_2(952)+$TiCl_4$-$AlEt_2Cl$ t=1h[b]	541	0.81	-	-
SiO_2(952)+$TiCl_4$-$AlEt_2Cl$ t=3h[b]	(541)[1]	3.2	-	-

a) See schemes 1 and 2 for details
b) t = reaction time

Catalysts prepared by co-impregnation of SiO_2 with $TiCl_4$ and $AlEt_2Cl$

As it has been published many years ago by Tornqvist et. al.[14], the reduction of $TiCl_4$ with $AlEt_2Cl$ leads to the formation of a solid solution of $AlCl_3$ in the crystal lattice of the $TiCl_3$ formed. The isomorphous substitution of the Ti atoms for aluminium may produce the activation of the titanium by disrupting its crystal lattice and due to the electronic influence of the Al through chlorine atom bridges. Bearing in

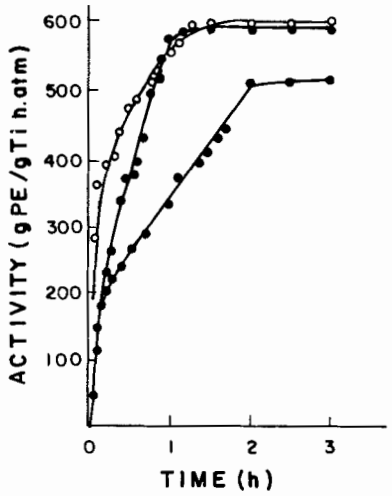

Figure 2. Catalytic activity of the catalyst 515 vs. time using the following co-catalysts: (o) Al (iso-Bu)$_3$, (●) $AlEt_2Cl$ (●) $AlEt_3$. Polymerization conditions: P=5atm. T=50°C, Al/Ti=10

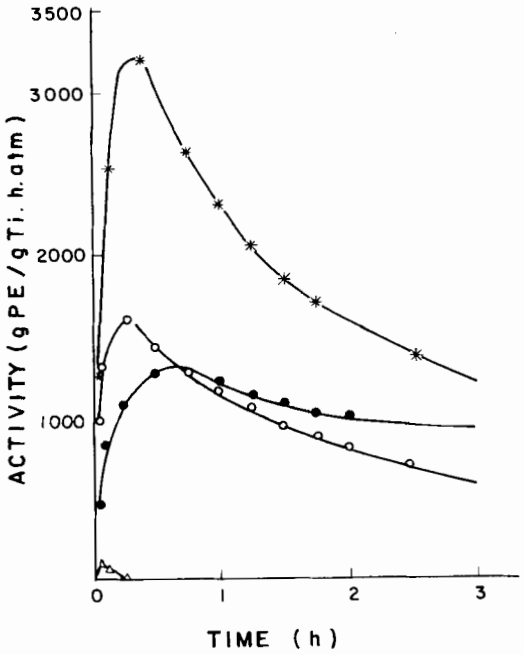

Figure 3. Catalytic activity vs. time of catalyst 548 using the following co-catalysts: (*) Al(iso-Bu)$_3$, (o) $AlEt_3$(●) $AlEt_2Cl$ and (Δ) $ZnEt_2$. Polymerization conditions: P=5atm. T=50°C, Al/Ti = 10

mind these ideas, we tried to produce a bimetallic complex by co-impregnation of both silicas with dilute solutions of $TiCl_4$ and $AlEt_2Cl$ in n-heptane, following procedures described in schemes 1 and 2. Catalysts 541 and $(541)^1$ based on silica 952 and catalyst 543 based on silica 951 were prepared. Catalysts 541 and $(541)^1$ differ by the co-impregnation time, been 1h. for the 541 and 3h. for the $(541)^1$. Under these conditions both metals compete for the hydroxyl groups of the silicas and could be supported. The supported amounts are shown in Table 1. As a result, the surface areas of both silicas undergo higher reduction compared to the simple impregnation with $TiCl_4$. The surface acidities, however, increase. The kinetic curves follow the same pattern, i.e. those catalysts obtained with silica 951 give rise to acceleration curves, while those based on silica 952 decay one (See Fig. 1). It is noteworthy, that the catalytic activity of catalysts obtained by co-impregnation are much lower than the ones prepared by simple reaction with $TiCl_4$ (Fig. 1 and Table 2). This could be explained by the umbrella effect of the aluminium and its chlorine atoms attached to it, which cover the titanium atoms. On the other hand, catalysts based on silica 952 (541 and $(541)^1$) are more active than the ones based on silica 951, although the latter have higher surface areas. The result may be explained by admitting that the mechanical properties and porosities of the carriers still influence the catalytic behavior at this step of the preparation.

Catalysts prepared by re-impregnation of modified SiO_2 with $TiCl_4$ and alkyl aluminium compounds

The catalysts prepared by co-impregnation of silicas 951 and 952 with $TiCl_4$ and $AlEt_2Cl$ were calcinated at 450°C under vacuum for 4h. to obtain catalysts 545 and 542 respectively (see schemes 1 and 2). By this treatment, part of the supported metals are removed from the silica, leaving behind on its surface metal oxide partially chlorinated (see Table 1), having, as a consequence, a high population of chloride vacancies. Furthermore, these catalysts were re-impregnated by

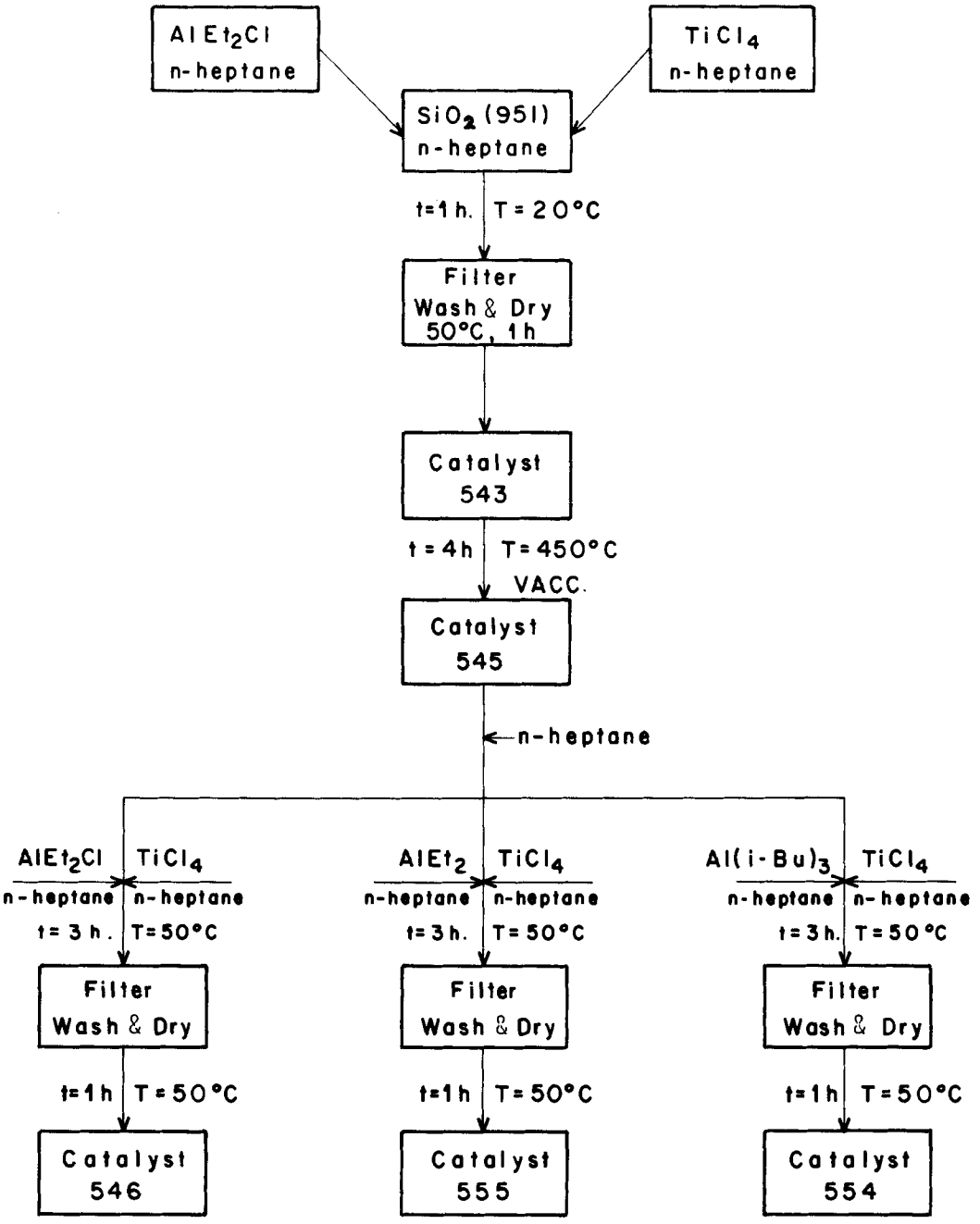

Scheme 1. Catalyst preparation by supporting $TiCl_4$ and alkyl aluminium compounds over SiO_2 951.

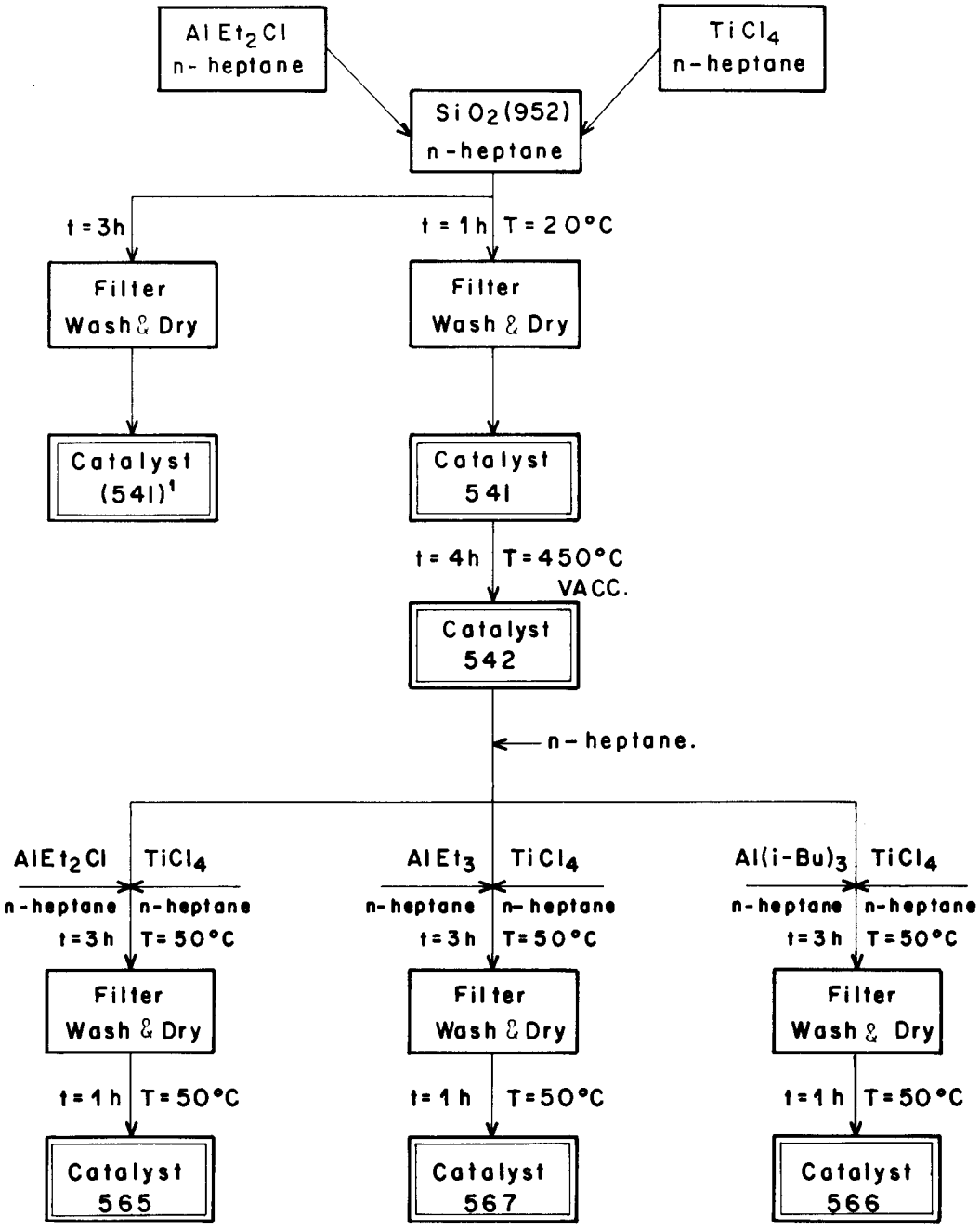

Scheme 2. Catalyst preparation by supporting $TiCl_4$ and alkyl aluminium compounds over SiO_2 952.

reacting them with diluted solutions of $TiCl_4$ in n-heptane together with solutions of $AlEt_2Cl$, $AlEt_3$ and $Al(iso\text{-}Bu)_3$, respectively, in order to obtain catalysts 546, 555 and 554 based on silica 951 and the series 565, 567 and 566 based on silica 952. The physico-chemical characterization of these catalysts is presented in Table 3. The surface areas were further reduced due to the re-impregnation, falling down to 150 $m^2xg.^{-1}$ and 110 $m^2xg.^{-1}$ for the two series of catalysts. The surface acidities and amount of supported Ti, on the contrary, increase. Catalytic activities as a function of polymerization time are given in Figs. 4 and 5 for the two series of catalysts. The polymerization rates decay rapidly with time for catalysts based on silica 952 and 951. It is very interesting to point out the change in the kinetic behavior of the catalysts based on silica 951, changing from acceleration curves to decay ones. These results suggest that the catalytic behavior is now controlled by the solid layer formed on the surface of the silica, rather than by the silica itself. The physical and chemical nature of this layer has to be very complicated, but it may be speculated here that it could be very porous allowing monomer diffusion inwards. In addition to that, it may be formed by very active $TiCl_3$ cystallites produced by the transformation of existing α-$TiCl_3$ under the action of $TiCl_4$, which behaves as a catalyst.

Catalytic activities as high as 18.000 g. PE x $g.Ti^{-1}xh.^{-1}xatm^{-1}$ could be obtained with catalyst 554 using $Al(iso\text{-}Bu)_3$ as co-catalyst (see Fig. 4). This catalyst system has, therefore, potential as a high mileage if the over-reduction of the titanium is depressed by adequate formulation of the co-catalyst system[15]. In Fig. 5 the kinetic curves for the catalysts prepared with silica 952 are presented. The productivities of these catalysts activated with different co-catalysts are given in Table 4. The best catalysts are those synthesized using $Al(iso\text{-}Bu)_3$ both for re-impregnation and also as co-catalyst.

TABLE 3. PHYSICO-CHEMICAL CHARACTERIZATION OF CATALYSTS PREPARED BY REIMPREGNATION OF MODIFIED SiO_2 WITH $TiCl_4$ AND ALKYL ALUMINIUM COMPOUNDS

Catalyst Preparation	Catalyst No.	Surface Area ($m^2 xg.^{-1}$)	Surface Acidity ($mmol.NH_3 xg.cat.^{-1}$)	Ti (w%)	Al (w%)	Al/Ti (mol)	Total Amount of Metals (mols x 100 g. $cat.^{-1}$)
SiO_2 (951) + $TiCl_4AlEt_2Cl$ T=450°C, t=3h vacc.	545	260	7.8	1.9	0.8	0.75	0.069
Cat. 545 + $TiCl_4$-$AlEt_2Cl$	546	150	15.3	8.8	3.1	0.63	0.30
Cat. 545 + $TiCl_4$-$AlEt_3$	555	146	7.7	7.3	3.9	0.95	0.30
Cat. 545 + $TiCl_4$-$Al(iso\text{-}Bu)_3$	554	150	10.9	7.8	0.5	0.11	0.18
SiO_2 (952) + $TiCl_4$-$AlEt_2Cl$ T = 450°C, t=3h vacc.	542	150	7.1	2.6	0.5	0.30	0.073
Cat. 542 + $TiCl_4$-$AlEt_2Cl$	565	117	9.3	9.4	0.5	0.10	0.22
Cat. 542 + $TiCl_4$-$AlEt_3$	567	103	8.8	9.1	5.5	1.10	0.39
Cat. 542 + $TiCl_4$-$Al(iso\text{-}Bu)_3$	566	115	10.2	2.7	2.7	0.50	0.31

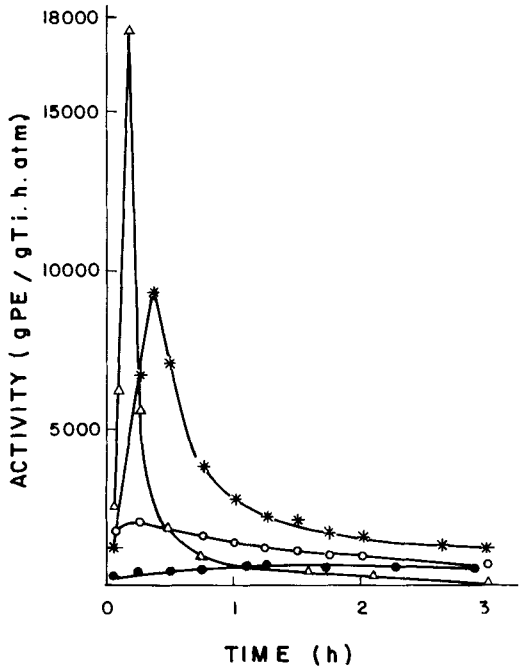

Figure 4. Catalytic activity vs. time for the catalysts: (●) 515, (o) 546, (*) 555 and (▵) 554. Polymerization conditions: P=5atm., T=50°C, Al/Ti=10: Co-catalyst = $Al(iso\text{-}Bu)_3$

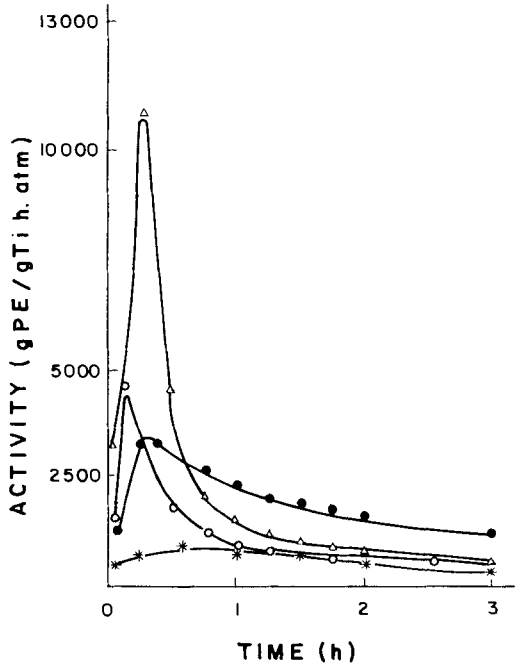

Figure 5. Catalytic activity vs. time for catalysts: (●) 548, (o) 565, (*) 567 (▵) 566. Polymerization conditions: P=5atm., T=50°C, Al/Ti=10. Co-catalyst = $Al(iso\text{-}Bu)_3$

Table 4. Influence of the co-catalyst on the catalytic activity of the catalysts obtained by re-impregnation of silica Davison 951 and 952 with $TiCl_4$ and alkyl aluminium compounds

Polymerization conditions: T=50°C, P=5atm., Al/Ti=10, Time=2h.

Catalyst Preparation[a]	Catalyst No.	Catalytic Activity (Kg. PExg.Ti^{-1})			
		$AlEt_2Cl$	$AlEt_3$	$Al(iso\text{-}Bu)_3$	$ZnEt_2$
Catalyst 545+ $TiCL_4$-$AlEt_2Cl$	546	6.6	20.8	15.4	10.5
Catalyst 545+ $TiCl_4$-$AlEt_3$	555	8.2	10.1	34.8	2.2
Catalyst 545+ $TiCl_4$-$Al(iso\text{-}Bu)_3$	554	14.6	11.0	16.8	15.2
Catalyst 542+ $TiCl_4$-$AlEt_2Cl$	565	2.7	18.1	14.1	-
Catalyst 542+ $TiCl_4$-$AlEt_3$	567	1.2	13.1	7.1	-
Catalyst 542+ $TiCl_4$-$Al(iso\text{-}Bu)_3$	566	4.1	14.5	25.0	-

a) See schemes 1 and 2 for details.

Catalysts prepared by co- and re-impregnation of $SiO_2$951 with $TiCl_4$-$ZnEt_2$ and $TiCl_4$-RMgI mixtures

Owing to the fact that silica 951 with the highest surface area produces a very active catalytic system by the re-impregnation method, catalysts based on this silica were syn-

thesized using $TiCl_4$-$ZnEt_2$ and $TiCl_4$-RMgI mixtures, following procedures already described. In Scheme 3, the steps to obtain catalysts No. 556, 557 and 558 are presented. Replacing $ZnEt_2$ by RMgI the corresponding catalysts No. 562, 563 and 568 were also synthesized (see Table 5). For the co-impregnation step the mixture $TiCl_4$-MeMgI was used, while for re-impregnation the mixture $TiCl_4$-HexMgI was preferred. Table 5 shows the physico-chemical characterization of all catalysts. It can be seen that catalysts prepared by $TiCl_4$-RMgI have higher surface areas and acidities than those based on $TiCl_4$-$ZnEt_2$. It is also noteworthy, that the surface area of catalyst No. 563 obtained by calcination of catalyst 562 increases due to the heat treatment.

The kinetic curves obtained with the re-impregnation catalysts (No. 558 and 568) are shown in Figs. 6 and 7. Both catalysts present a decay curve, and the best co-catalyst for activation is now the $AlEt_3$. The productivities are given in Table 6 reaching values as high as 61,2 Kg.PE x $g.Ti^{-1}$, with the catalyst containing Mg, after 2h, 50°C and 5 atm. polymerization pressure. Furthermore, this catalyst is very sensitive to the type of co-catalyst used for activation. Thus, very low activities could be obtained when $AlEt_2Cl$ and $Al(iso\text{-}Bu)_3$ were used for activation, while $AlEt_3$ give very good results, emerging as the best co-catalyst. Similar results, have been found with catalysts based on $TiCl_4$ supported over $MgCl_2$.

Viscosity average molecular weights

Very high molecular weights were obtained with all catalysts, when no H_2 was used as chain transfer agent for molecular weight control, as shown in Table 7.

Morphology of catalysts and polymer particles

A good catalyst must have very high activity in order to produce high purity polymer, it must also have an excellent

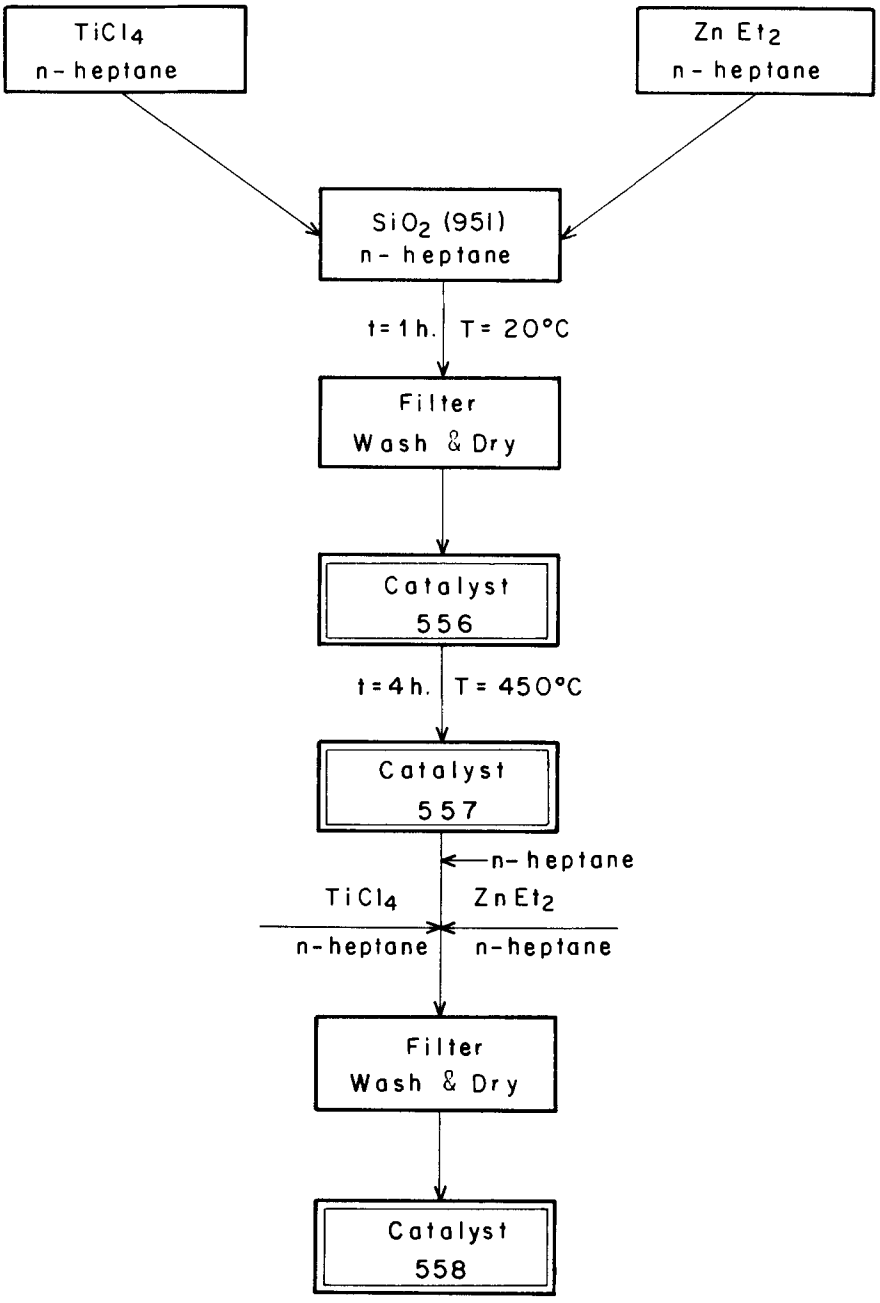

Scheme 3. Catalysts preparation by supporting $TiCl_4$ and $ZnEt_2$ over SiO_2 951.

TABLE 5. PHYSICO-CHEMICAL CHARACTERIZATION OF CATALYSTS PREPARED BY CO- AND RE-IMPREGNATION OF SiO_2 951 WITH $TiCl_4$-$ZnET_2$ AND $TiCl_4$-RMgI MIXTURES

Catalyst Preparation	Catalyst No.	Surface Area ($m^2 xg.^{-1}$)	Surface Acidity (mmol.NH_3xg. cat.$^{-1}$)	Ti (w%)	Zn (w%)	Mg (w%)	M/Ti (mol)	Total Amount of Metals (mols x 100 g. cat.$^{-1}$)
SiO_2 + $TiCl_4$-$ZnEt_2$	556	240	5.4	3.3	9.0	-	2.0	0.21
Cat. 556, T = 50°C t = 4h. vacc.	557	230	3.2	3.1	4.0	-	0.95	0.13
Cat. 557 + $TiCl_4$-$ZnEt_2$	558	54	6.9	3.0	9.6	-	2.3	0.21
SiO_2 + $TiCl_4$-MeMgI	562	310	13.9	3.6	-	2.3	1.26	0.17
Cat. 562, T = 50°C t = 4h. vacc.	563	400	6.2	3.5	-	0.7	0.39	0.10
Cat. 563 + $TiCl_4$-MexMgI	568	102	14.2	4.7	-	5.9	2.5	0.34

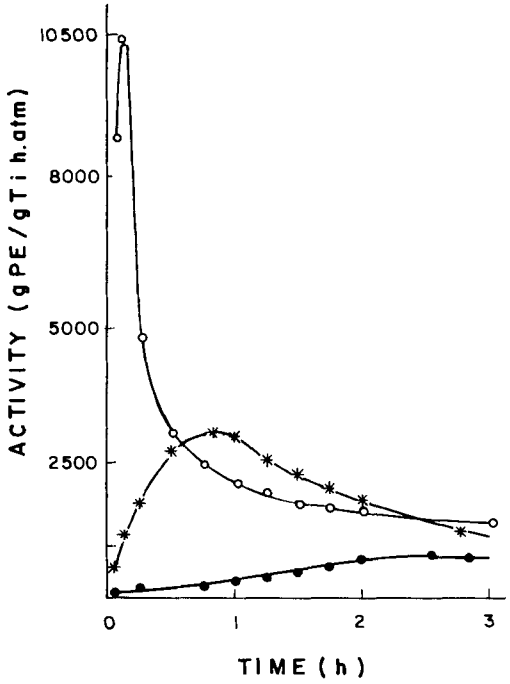

Figure 6. Catalytic activity vs. time for catalyst 558 using the following co-catalysts: (*) $Al(iso\text{-}Bu)_3$, (●) $AlEt_2Cl$ and (o) $AlEt_3$. Polymerization conditions: P=5atm., T=50°C, and Al/Ti=10

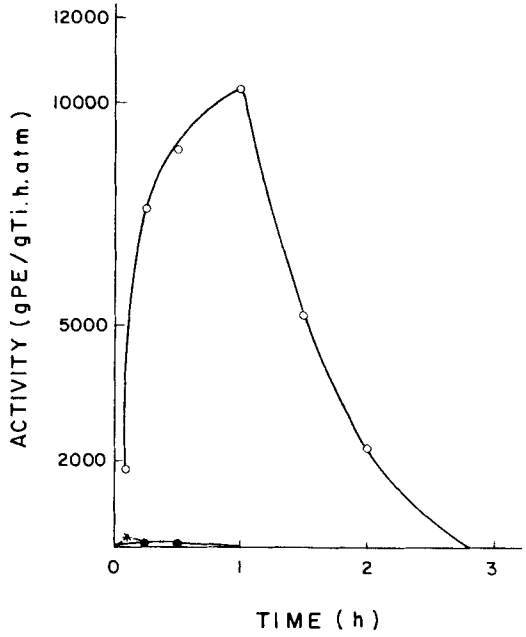

Figure 7. Catalytic activity vs. time for catalyst 568 using the following co-catalysts: (*) $Al(iso\text{-}Bu)_3$, (●) $AlEt_2Cl$ and (o) $AlEt_3$. Polymerization conditions: P=5atm., T=50°C and Al/Ti=10

Table 6. Influence of the co-catalysts on the activity of catalysts prepared by co- and re-impregnation of silica 951 with $TiCl_4$-$ZnEt_2$ and $TiCl_4$-RMgI mixtures.
Polymerization temperature = 50°C, P = 5 atm., Al/Ti = 10, Time = 2h.

Catalyst No.	Catalytic activity (Kg.PE x g.Ti^{-1})		
	$AlEt_2Cl$	$AlEt_3$	$Al(iso\text{-}Bu)_3$
558	4.3	27.5	24.8
568	0.31	61.2	0.13

Table 7. Viscosity average molecular weights.

Catalyst No.	$\bar{M}_v$ x 10^{-6}
515	0.5
548	0.6
541	1.9
543	1.8
555	1.5

control of polymer morphology. These characteristics should be of main concern in the catalyst synthesis. By controlling the average size and size distribution of the polymer particles, as well as the bulk density, the reactor productivity can be enhanced and many problems in plant operations can be eliminated. This can be done by synthesizing catalysts with good morphological characteristics. The ability of the catalysts synthesized to control the size of the nascent polymer particles

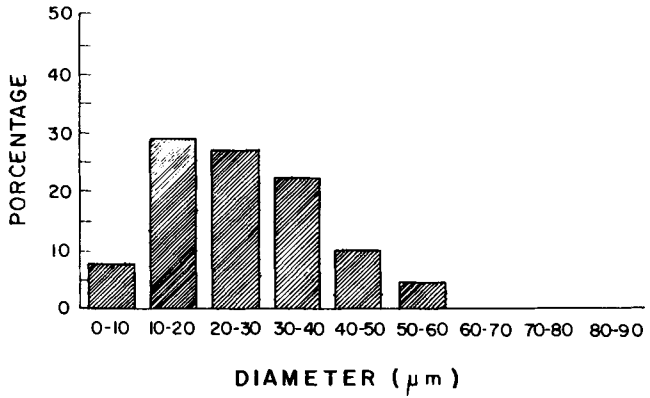

Figure 8.a Particle size distribution of silica 951

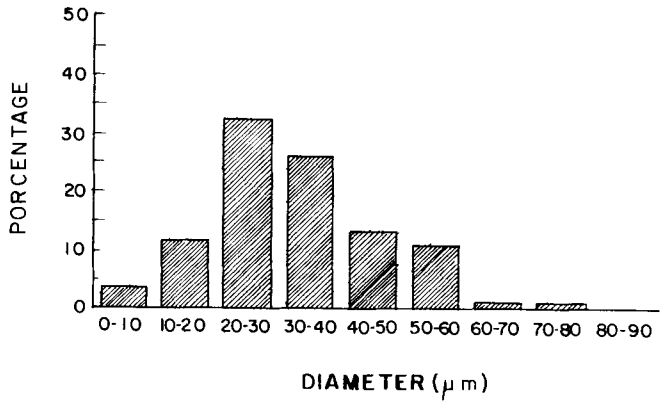

Figure 8.b Particle size distribution of catalyst 555 prepared with SiO_2(951)+$TiCl_4$-$AlEt_2Cl$ calcination at 450°C and re-impregnation with $TiCl_4$-$AlEt_3$

were tested. Figure 8 shows the particle size distribution of silica 951 and of the resulting catalyst 545.

By reacting silica 951 with $TiCl_4$ and $AlEt_2Cl$ its size increases slightly, and its surface becomes more rough[15]. The Figure 9 polymer particle size distribution of the resulting polymer is shown. It can be seen that most polymer particles are bigger than 500 μm and that only a small percentage can be considered as fine.

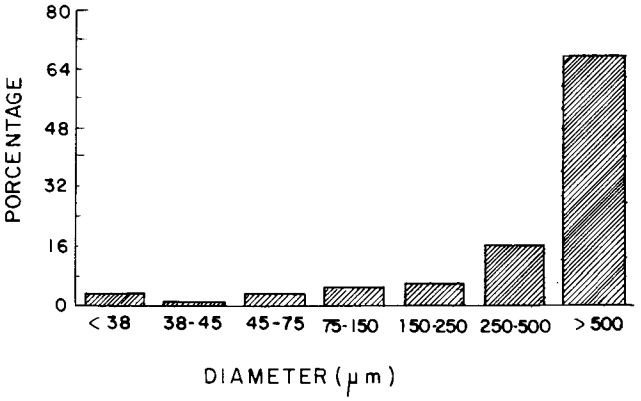

Figure 9. Particle size distribution of the polyethylene obtained with the catalyst 555 using $Al(iso\text{-}Bu)_3$ as co-catalyst.

ACKNOWLEDGMENT

The authors wish to thank Investigación y Desarrollo, C.A.-INDESCA (Maracaibo, Venezuela) for secretarial assistance in the preparation of the manuscript and particularly to its General Manager, Dr. I. Rodon for reading it and correcting the English text.

REFERENCES

1. J.C.W. Chien, J. Catal., 23 71 (1971).
2. J. Murray, J.J. Sharp and J.A. Hockey, J. Catal 18, 52 (1970).

3. K. Soga, T. Sano and R. Onishi, Polym. Bull., 4, 157 (1981).
4. A. Muñoz-Escalona, A. Martin and J. Hidalgo, Eur. Polym. J., 17, 367 (1981).
5. A. Muñoz-Escalona in "Transition Metal Catalyzed Polymerizations. Alkenes and Dienes", Edited by R.P. Quirk. Harwood Academic Publishers, London, 1983, p.323.
6. A Muñoz-Escalona, J.G. Hernández and J.A. Gallardo, J. Appl. Polym. Sci., 29, 1187 (1984).
7. J.W.C. Chien, J.C. Wu and C.I. Kuo, J. Polym. Sci Polym. Chem. Ed. 20, 2019 (1982).
8. B. Goodall in "Transition Metal Catalyzed Polimerizations Alkenes and Dienes", Edited by R.P. Quirk. Harwood Academic Publishers, London, 1983, p. 355.
9. J. Boor, Jr., "Ziegler-Natta Catalysts and Polymerization", Academic Press, New York, 1979, p. 180.
10. A. Muñoz-Escalona, P. Frias and A. Sierraalta. Org. Coat. Plast. Chem (ACS) 44, 170 (1981).
11. A. Muñoz-Escalona, C. Villamizar and P. Frías in "Structure-Properties Relationship of Polymeric Solids". Edited by A. Hiltner, Plenum, New York, 1983, p. 95.
12. T. Keii, "Kinetics of Ziegler-Natta Polymerization", Chapman and Hall, London, 1972.
13. H. Schnecko, M. Reinmuller, K. Weirauch, W. Lintz and W. Kern. Makrom. Chem. 69, 105 (1963).
14. E.G.M. Tornqvist, Ann. N.Y. Acad. Sci. 455, 477 (1969).
15. A. Muñoz-Escalona, J.G. Hernández and J.A. Gallardo. To be presented in next ACS meeting in Chicago, September 1985.

FUNCTION OF THE BINARY AND TERNARY COMPLEXES IN THE PROPYLENE POLYMERIZATION CATALYSTS

A. GUYOT, R. SPITZ, L. DURANEL (*) and J.L. LACOMBE (*)
CNRS - Laboratoire des Matériaux Organiques
BP 24 - 69390 LYON VERNAISON (France)

ABSTRACT

Infrared analysis of the precatalysts $MgCl_2$-Aromatic ester-$TiCl_4$ indicate the presence of binary complexes between the aromatic ester and either $MgCl_2$ or $TiCl_4$, but some shifts of the $\nu_{C=O}$ and $\nu_{C=C}$ bands support the idea of ternary complexes ; the activity of the catalysts seems to be related to these ternary complexes.

The binary complexes of the cocatalyst solution between AlR_3 and the aromatic ester have a composition and a stability depending on the nature of the components : the reduction towards alcoxy aluminium compounds involves an intermolecular reaction with free AlR_3 ; its rate is decreased in the presence of olefin.

Reversible equilibrium between the cocatalyst solution and its components adsorbed on or complexed with the precatalyst does govern the activity and stereospecificity of the catalyst. Stable activity can be obtained if a proper choice of these components is made. However, in any case, the stereospecificity is decreasing during the process, owing to ageing of the complex solution.

(*) Present address : ATO CHEM - SNEA(P) - BP 34 LACQ
64170 ARTIX (France)

INTRODUCTION

The most recent generation of polymerization catalysts for the synthesis of polypropylene, so-called high mileage-catalysts [1, 2], includes at least four components : a $MgCl_2$ support, $TiCl_4$, a trialkylaluminium AlR_3, and one or eventually two electron donors, most often aromatic esters and more recently phenyl silane derivatives. The catalytic system involves two different parts : one is a so-called solid precatalyst including $MgCl_2$, $TiCl_4$ and one electron donor ; the second, the cocatalytic solution involves AlR_3 and one electron donor : for each part, the same or two different electron donors can be used. The performance of the catalytic system, both activity or productivity and stereospecificity, are very much dependent on the details of the preparation of both the precatalyst and the cocatalytic solution.

Donor-acceptor complexes can be formed between the aromatic esters and each of the three other components. In previous papers [3], FTIR techniques have been used to study the interaction between triethylaluminium (TEA) and ethylbenzoate (EB) forming a 2-1 complex which is rather stable in the polymerization conditions. It was shown that the function of EB was not limited to the selective poisoning of the atactic catalytic sites, as previously suggested [1, 2] ; both the catalytic activity and the isospecificity were shown to be governed by the reversible interaction between the solid precatalyst and the species present in the cocatalytic solution. In this paper, a more extensive study of the complex formation between a set of alkylaluminium and a set of electron donors is presented, together with the consequences of the choice of the partners upon the stability of the complexes and their effect on polymerization.

The study of the precatalyst is still in the infancy. It has been shown that the best performances are obtained if the support is first grinded in the presence of the electron donor, before being impregnated with $TiCl_4$. The possible presence of ternary complexes $MgCl_2$-EB-$TiCl_4$ has been suggested [4, 5]. Some complementary results are presented here.

INFLUENCE OF THE NATURE OF THE COMPONENTS ON THE PERFORMANCE OF THE CATALYST

In the catalytic system, two kinds of components can be varied: the alkylaluminium and the electron donor. The following examples show that a proper choice of these components may lead to very dramatic effects.

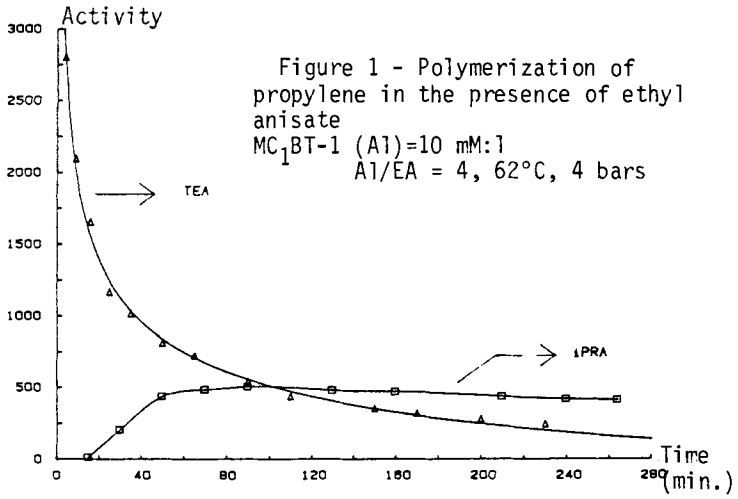

Figure 1 - Polymerization of propylene in the presence of ethyl anisate
MC_1BT-1 (Al)=10 mM:l
Al/EA = 4, 62°C, 4 bars

So, in Figure 1 are shown the kinetic curves for propylene polymerization using the same precatalyst, the same electron donor in the cocatalytic solution, but different alkylaluminium, namely triethylaluminium (TEA) and isoprenylaluminium (IPRA). The latter is a ill-defined mixture resulting from the reaction of isoprene or triisobutylaluminium, and is believed to be a polyaluminium compound ; a possible schematic representation of its formula might be :

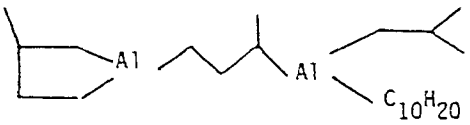

The use of IPRA leads to an induction period, and shows development of the activity up to a stable level, while with TEA a very high activity is reached immediately, but decreases down to very low level.

Table I - POLYMERIZATION RESULTS WITH VARIOUS ESTERS IN THE COCATALYTIC SOLUTION

Electron donor in the Precatalyst	Al compound	Ester	Duration mn	P	II
EB	TEA	EA	60	1040	51.6
EB	TEA	EPT	60	1300	93.8
EB	TEA	EB	60	1570	92.4
EB	TEA	EB	60	1270	92.8
MPT	IPRA	-	90	1200	63.2
MPT	IPRA	EA	90	280	89.6
MPT	IPRA	EPT	90	530	87.6
MPT	IPRA	EB	90	640	81.3

Conditions : 60° C
4 bars of polypropylene
(Al) = 10 mM/l
Al/ester : 4

EA : ethylanisate
EB : ethylbenzoate
EPT : ethylparatoluate

As shown in Table I, important changes in both activity (productivity P) and isospecificity (Isotactic index II) result from a change in the nature of the electron donor (ester) in the cocatalytic solution with both TEA or IPRA. The more striking differences are observed in the presence of IPRA, where productivity and isospecificity show inverse variations with the polarity of the electron donor.

In table II, precatalysts prepared using different electron donors are used in similar conditions (in the presence of TEA). No clear correlation is obtained with the Lewis basicity of the ester, but there is a trend to correlate the catalytic acticity, and maybe more, the isospecificity, with the steric hindrance of the second substituant of the ester.

It is certainly difficult to explain all these data ; it must also be noted that it may be dangerous also to strictly compare the results of different series of experiments which may differ from both the purity of the reactants and details of the experimental

procedure. However, the interactions between the different components which give rise to the formation of various complexes, and the behavior of these complexes will be usefull elements in the discussion of results.

Table II - PROPYLENE POLYMERIZATIONS IN THE PRESENCE OF PRECATALYSTS CONTAINING VARIOUS ESTERS
Co-catalytic solution : TEA - MPT

Ester in the precatalyst	Lewis basicity (pk)	Steric hindrance order	P	II
EB	4.2	1	1570	92.4
MPT[a)]	4.35	2	1360	90.5
EA	4.5	3	870	85.6
pClMB[b)]	4	3	890	88.2
MB[c)]	-	1	1360	93.6

a) pClMB : p.chloromethylbenzoate
b) MPT : methylparatoluate
c) MB : methylbenzoate

COMPLEXES IN THE COCATALYTIC SOLUTION

Several studies have already dealt with the description of complexes between AlR_3 and the aromatic esters, and also with the chemical reaction between the components [2-6-11] ; it is generally accepted that the reaction leads to the reduction of the ester producing an aluminium alkoxide. However, many published data are of little value for that discussion, because the experiments were carried out in conditions very different from those used in the polymerization conditions, i.e. upon rather high dilution and in the presence of monomer. In our previous study [2-8], FTIR was used to show that a 2/1 complex was formed between TEA and EB, the equilibrium being fuly displaced towards the complex, so that the free ester band at 1720 cm^{-1} was observed only if the Al/EB ratio

was lower than 2. The yellow complex was shown to be slowly decomposed at room temperature to a colorless aluminium alkoxide, the reaction rate was enhanced upon heating or by increasing either the TEA concentration or the TEA/EB ratio ; on the other hand, the decomposition was inhibited in the presence of hexene.

Similar results were obtained with the TEA/EA system (ethyl anisate), except that the stoiechiometry of the complex was 1-1. Figure 2 shows the IR spectra of systems with various TEA/EA ratios larger than 1.

Figure 2 - Infrared spectra of a TEA-EA solution for various Al/ester ratios

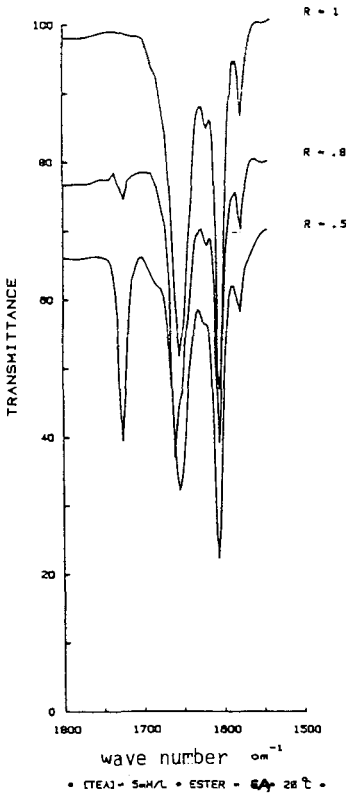

Figure 3 - Infrared spectra of a IPRA-EA solution for various Al/ester ratios

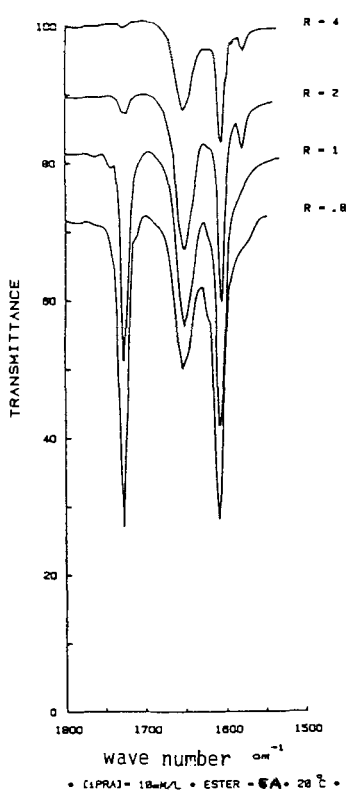

In the case of TEA/MPT, two complexes with stoiechiometry 2/1 and 1/1 are likely to exist, because for a ratio 1/1 of TEA/MPT, about 10 % of the ester appears to be uncomplexed, probably because there is 10 % of the 2/1 complex and 80 % of the 1/1 complex.

In the case of the IPRA/EA system (figure 3), the carbonyl band of the free ester is observed for ratios Al/EA lower than 4, but, more probably, the complexation equilibrium is less displaced than for TEA, owing to the large steric hindrance around the Al atoms.

A thorough study of the reduction of the ester has been carried out, using both UV and IR spectroscopy. For the exact stoiechiometry, it begins to appear upon ageing at 20°C (figure 4), decomposition being complete after about 4 hours when the $\nu_{C=O}$ band of the complex at 1655 cm^{-1} is no longer visible. More detailed results will be published elsewhere. It has been confirmed that the reaction rate is enhanced in concentrated solution, and upon heating, but is inhibited in the presence of the monomer. The effect of the Al/ester ratio leads to conclude to an intermolecular reaction : the complex (either 2/1 or 1/1) is reacted with an uncomplexed AlR_3 molecule : an aluminium alcoxide is formed and the AlR_3 molecule is liberated again. The inhibition of the reaction by an olefine may be explained by the competitive complexation of the excess AlR_3 by the olefin ; the existence of such complexes was postulated by Simon [6] and might be supported by our previous observation [8] of the exaltation of the intensity of the $\nu_{C=C}$ band of the olefin at 1640 cm^{-1} in the presence of TEA.

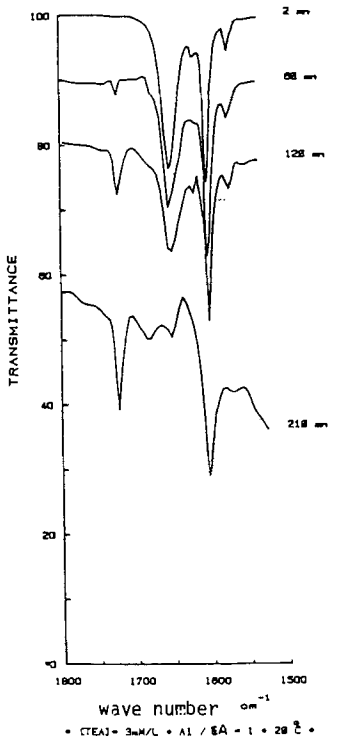

Figure 4 - Evolution of a TEA-EA solution for ratio 1 during time

Comparing the stability of the complexes of EA with either TEA or IPRA, it is interesting to note that the former is more stable at low Al/EA ratio, but less stable at higher ratios (figure 5 and 6).

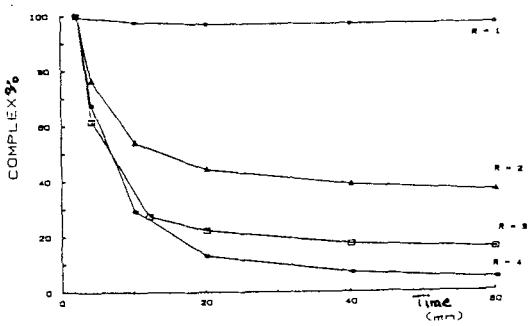

Figure 5 - Reduction kinetics of EA by TEA for various complexation ratios (R)
(Al)= 1.3 M/l - 30° C

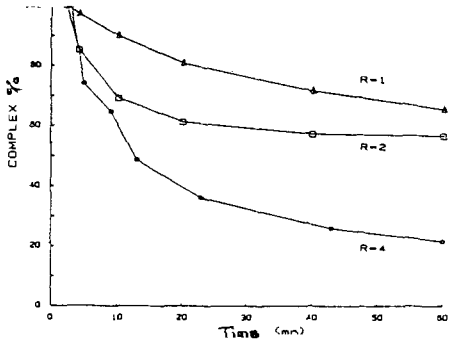

Figure 6 - Reduction kinetics of EA by IPRA for various complexation ratios (R)
(Al) = 0.8 M/l - 30° C

CONTROL OF THE ISOSPECIFICITY BY THE COCATALYTIC SOLUTION

Both the activity and the isospecificity of the catalytic system are chiefly depending on the Al/ester ratio in the cocatalytic solution ; both uncomplexed AlR_3 and complexes are present in the solution and can be reversibly adsorbed on the precatalyst ; this statement initially established with the TEA/EB system [5] was shown to be true for other systems such as TEA/EA or TEA/EPT.

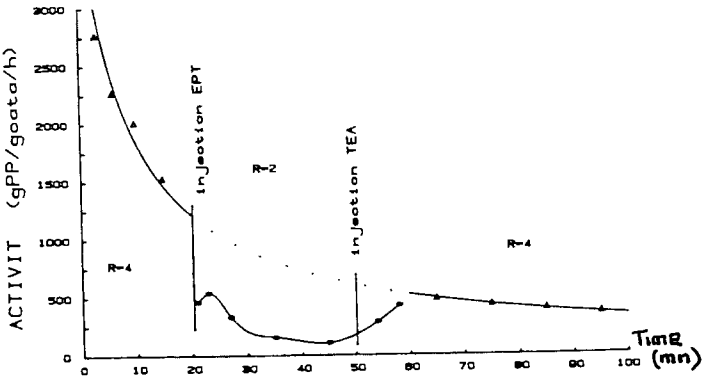

Figure 7 - Reversible desactivation by PTE in the presence of TEA
MC_1BT-1, (Al) = 3 mM/l
63° C, 4 bars

So, as shown in figure 7, the activity decreases if the Lewis base is added, so that the r = Al/EPT ratio drops from 4 to 2, but, upon addition of additional TEA to restore the ratio at 4, the activity increases again to reach the level expected for that ratio in a normal experiment. Upon addition of the free ester, a new equilibrium is established inside the cocatalytic solution first, and then between that solution and the catalyst. Even if the equilibrium is largely displaced towards the formation of the complex, a small amount of free ester remains in the solution, which is about proportional to the inverse of ratio r (the exact dependence being a function of the stoiechiometry of the complex). That free ester is expected to poison the active site, because, as shown later on by the value of the chemical shift of the IR carbonyl band, the complex of the ester with $TiCl_4$ is very strong. For a long time, the function of the ester was believed [1-2-9-12] to selectively poison the non isospecific catalytic centers. This view was challenged by experiments of Kashiwa [13] who has shown that the addition of esters leads to an increase in the yield of the isospecific sites producing high molecular weight isotactic polypropylene. Some of our experiments did confirm the statement by Kashiwa. As shown in figure 8, using the same precatalyst and the same TEA concentration at comparable polymerization conditions, upon increasing the EPT/TEA ratio (decreasing r), the productivity of the

isotactic sites goes through a maximum while the productivity of the atactic sites is continuously decreasing.

Figure 8 - Total, isotactic, atactic productivity versus ester/Al ratio
$MC_1BT)1$, TEA, PTE, (Al) = 5 mM/l
63°C, 4 bars

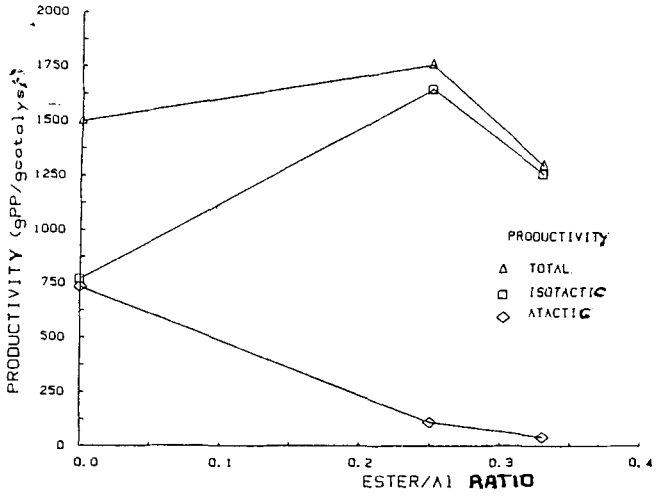

We propose that the active sites are at least bimetallic one, i.e. involve titanium atoms on the precatalyst surface, what will give a complex with alkylaluminium coming from either free alkylaluminium or ester-complexed alkylaluminium [21]. Owing to the steric hindrance, the sites involving alkylAl from ester complexed alkylaluminium are more likely to be isospecific. Upon decreasing r, less free alkylaluminium is present and, due to the reversible equilibrium, a large proportion of the site will be associated with the ester complexed AlR_3. So, we propose that aspecific sites may be reversibly transformed into isospecific sites. The final decrease in the productivity of the isospecific sites shown in figure 8 could be caused by poisoning with free esters. The continuous decrease in the aspecific site productivity could have two reasons : poisoning of the sites upon adsorption of free ester, and change of these sites into isospecific sites upon association with the ester-complexed AlR_3.

Upon ageing, i.e. during polymeriztion, the reduction of the ester by AlR_3, even if it is partially inhibited by the presence of the monomer, is expected to take place to some extent. Contradictory results are reported in the literature about the effect of the reduction products on the polymerization ; according to Langer et al [7], it is detrimental to the isospecificity of the catalyst ; we did observe the same result [3] ; but recently Kissin and Sivak [10], reported that the alkoxide produced about the same effect as the precursor ester, also forming a complex with AlR_3 (although the complexation equilibrium is much more shifted towards the free components) ; they suggest that the benefic effect for the isospecificity of the catalyst might be due more to the alkoxide than to the esters. Recently also, Sergeev et al [11] suggest that the interaction of the active sites with either the free ester or tertiary alkoxy derivatives are responsible for the high stereospecificity ; however, carefull examination of the data of these authors show that, in several cases, they observed a decrease in the isospecificity upon ageing the mixture of AlR_3 and ester prior to polymerization. So, if there is some reduction of the ester during polymerization, a decrase in the isospecificity of the catalytic system is to be expected with polymerization time. The results reported in Table III show that this is actually the case with the two typical systems studied here. The average II of the whole polymer decreases with polymerization time. From the data of experiments stopped at different times, the average II of time interval may be calculated ; the results reported in the last column of Table III show that the decrease in isospecificity is rather important. That decrease seems to be more important in the case of IPRA ; the reason is that the catalytic activity of the catalyst is continuously decreasing in the case of TEA, so that productivity decreases at the same time as isospecificity ; while in the case of IPRA, the activity remains stable and the contribution of the polymer produced in the last steps of the reaction is more important. On the contrary, one may think that the actual isospecificity of the catalyst with IPRA may be higher than with TEA, if the main driving force for the isospecificity is the steric hindrance ; the lower initial isospecificity shown in Table III for the IPRA system is due to the fact that, in that case, there is an

Table III - CHANGES IN ISOSPECIFICITY DURING POLYMERIZATION

Cocatalytic solution	T(°C)	Time (min)	P	II	Calculated values Interval (min)	P	II
TEA EPT	63	20	980	93.7	0-20	980	93.7
		60	1570	92.4	20-60	590	90.1
		240	3340	86.1	60-240	1770	80.6
IPRA EA	60	90	550	92.2	0-90	550	92.2
		270	2000	77.3	90-270	1450	71.6

Precatalyst ester : EB ; [Al] : 10 mM/l ; Al/ester = 4 ;
Polyropylene pressure : 4 bars

induction period (figure 1) and, during that period, the reduction of the ester may be more rapid (see figures 5and 6) than with TEA system which is working immediately with high catalytic activity.

COMPLEXES IN THE PRECATALYSTS

Precatalysts are generally prepared through grinding of dry $MgCl_2$ with the electron donor, followed with impregnation with an excess of $TiCl_4$ and then washing with hydrocarbon or treating under vacuum. In these operations, two kinds of binary complexes are formed between the electron donor and $MgCl_2$ and $TiCl_4$ respectively. But, in addition, the formation of ternary complexes is possible, as already suggested by Chien [4] and us [5].

The complex between $MgCl_2$ and EB was studied by Simon [14 - 15] who showed that it can be characterized by DSC. Upon grinding of both components, a part of the EB becomes strongly bonded to $MgCl_2$, and cannot be extracted with heptane or under vacuum. In our experiments, $MgCl_2$ was previously grinded to give a material with high surface area (55 m^2/g) and then grinded again in the presence of the electron donor (weight ratio/$MgCl_2$ ester around 10) and finally washed with heptane. The infrared spectrum of this complex (figure 9) shows a large shift of the $\nu_{C=O}$ band at 1685 cm^{-1} (for methylparatoluate MPT as an ester) instead of 1725 cm^{-1} for the free ester. In the case of EB, the $\nu_{C=O}$ band is at 1695 cm^{-1}.

Figure 9 - IR spectra of complex $MgCl_2$/PTM

Figure 10 - IR spectra of complex $TiCl_4$/PTM

The binary complex between $TiCl_4$ and MPT can be prepared independently from heptane solution ; it is a yellow solid needle-like material with a low surface area (3 m^2/g), slightly soluble in hot heptane and volatile in high vacuum. Its infrared spectrum (figure 10) shows two bands at 1610 and 1565 cm^{-1} attributed to complexed $\nu_{C=C}$ (aromatic ring) and $\nu_{C=O}$ band. These bands are observed at 1592 and 1560 cm^{-1} for the $TiCl_4$-EB complex.

Several studies did conclude [16-18] that the $TiCl_4$-EB complex cannot be identified with the active sites, because the polymerization activity of that complex in the presence of AlR_3 was poor. In our previous study [5], we have challenged this statement, because the yellow color of the catalyst, similar to that of the complex, disappears if the catalyst is heated under vacuum and that a large part of the catalytic activity is destroyed upon such a treatment. During the present study, we did prepare a catalyst through grinding $MgCl_2$ in the presence of a purified complex $TiCl_4$-MPT. That catalyst, containing 2.6 % of Ti, leads to a productivity of 870 and an isotacticity index of 84.3 (Table IV); these performances, although somewhat inferior to that of the regular catalyst are by no means negligible and show that the pure complex may lead to active sites, if its dispersion state is high enough ; however, it may be argued that the grinding process which was rather long in that case, did change the structure of the complex : actually, catalysts prepared by impregnation of $MgCl_2$ with a solution of the complex have a very poor catalytic activity.

Table IV - POLYMERIZATION RESULTS FOR VARIOUS CATALYSTS

Catalyst	Ester	% ester	% Ti	C=O	Vp(cm^3)	P[a]	II
MC_1BT_1	EB	12	5		0.36	1570	92.4
MC_2BT_{14}	MPT	10	1.8	1682	0.36	310	89.4
MC_2BT_6	MPT	9	2.3	1678	0.18	730	90.5
MC_2BT_{23}	MPT	12	4.5	1674	0.30	1360	92.4
MK_1B-4	MPT	9.4	2.6			870	84.3

a) productivity in propylene polymerization : 1 h at 63°C ; propylene pressure : 4 bars ; [Al] : 10 mM/l ; Al/EPT : 4

Figure 11 - IR spectra of various supported catalysts

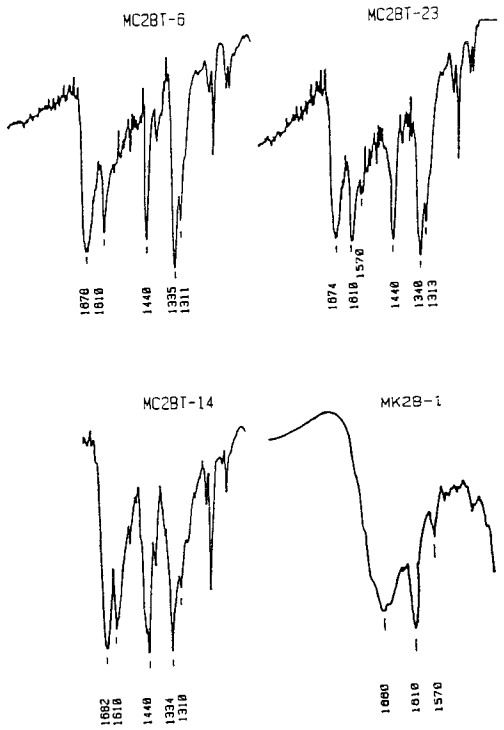

The infrared spectra of the catalysts mentioned in Table IV are shown in figure 11. In the carbonyl region, the spectra are intermediates between the spectra of the to binary complexes with shifts from each one, but are closer to the spectrum of $MgCl_2$-MPT complex. The shift in the main band is the largest when the amount of Ti fixed on the catalyst is the largest. The bands at 1570-1575 cm^{-1} are visible either in the case of catalyst MK2B-1 (grinding with $TiCl_4$-MPT complex) or with catalyst MC2BT-23 which has the highest Ti content, and which is the most active. The differences in the catalytic activities and also of the Ti contents of the catalysts of series MC2BT (prepared using MPT as an ester) are more easily explained on the basis of the morphology of the precatalyst (this point is discussed elsewhere [19] and the corresponding data

will be published separately). However, they tend to support the idea that a part of the ester might be coordinated with both Mg and Ti, and that the most active centers could involve ternary complexes.

It is interesting to note finally that the best performances (Table II and IV) are obtained when the ester used in the preparation of the precatalyst is ethylbenzoate, which the only ester which is complexed preferentially with 2 molecules of AlR_3. Then, EB could be more easily complexed with both $MgCl_2$ and $TiCl_4$ than other esters. It might be the reason for the choice of difunctional esters (phtalate, maleates...) in the recent patents [20] which seems to correspond to the performances of the "superactive third generation catalysts" reported by Galli [1].

REFERENCES

1 P. GALLI, P.C. BARBE and L. NORISTI - Angew. Makromol. Chem. - 120 73 (1984)

2 P. PINO and B. ROTZINGER - Makromol. Chem. Suppl. - 7 41 (1984)

3 R. SPITZ, J.L. LACOMBE, M. PRIMET and A. GUYOT in R.P. Quirck "Transition Metal Catalyzed Polymerization" MMI Symposium Ser. - 4 89 (1983)

4 J.C.W. CHIEN and J.C. WU - J. Polym. Sci. Polym. Chem. Ed. - 20 2445 and 2461 (1982)

5 R. SPITZ, J.L. LACOMBE and A. GUYOT - J. Polym. Sci. Polym. Chem. Ed. - 22 2641 (1984)

6 A. SIMON and A. GROBLER in R.P. Quirck "Transition Metal Catalyzed Polymerization" MMI Symposium Ser. - 4 403 (1983)

7 A.W. LANGER, T.J. BURKHARDT and J.J. STEGER - ibid ref. 6, p. 421

8 R. SPITZ, J.L. LACOMBE and M. PRIMET - J. Polym. Sci. Polym. Chem. Ed. - 22 2611 (1984)

9 A.W. LANGER, T.J. BURKHARDT and J.J. STEGER - in C.C. Price and E.D. Vandenberg "Coordination Polymerization" - Plenum Press N.Y. 1983, p 225

10 Y.V. KISSIN and A.J. SIVAK - J. Polym. Sci. Polym. Chem. Ed. - 22 3747 (1984)

11 S.A. SERGEEV, G.D. BUTAKOV and V.A. ZHAKAROV - Makromol. Chem. - 185 2377 (1984)

12 N. KOSHIWA - ibid ref. 6, p. 379

13 N. KASHIWA andJ. YOSHITAKE - Makromol. Chem. - 185 1133 (1984)

14 B. KESZLER, G. BODOR and A. SIMON - Polymer 21 1037 (1980)

15 B. KESZLER, A. GROBLER, E. TAKACS and A. SIMON - Polymer 22 818 (1981)

16 N. KASHIWA - Polymer J. - 12 603 (1980)

17 E. RYTTER, S. KVISLE and O. NIRISEN - Preprints IUPAC Macromolecules Symposium - Florence 2 32 (1980)

18 Y.Y. VERMEL, V.A. ZAKHAROV, Z.K. BUKATOVA, G.P. SHKURINA, I.G. YECHEVSKAYA, E.M. MOROZ and S.V. SUDAKOVA - Vysokomol. Soedin - A22 22 (1980)

19 L. DURANEL - Thesis (Lyon) 1984

20 Europ. Patent 86471 (1982) to Montedison and 86473 (1982) To Mitsui

21 R. SPITZ, L. DURANEL and A. GUYOT - ACS Meeting Chicago (sept. 1985)

This page intentionally left blank

STUDIES ON OLEFIN POLYMERIZATION

SHIPEI TANG
Beijing Research Institute of Chemical Industry,
He Ping Li, Beijing, China

ABSTRACT

Two methods of kinetics studies for propene polymerization were carried out with different kinds of high activity catalysts. The reliability and the influencing factors of the CO inhibition method were emphasized.

By changing electron donors in the preparation of the high activity catalyst, main parameters, such as activity, isotactivity, can all be improved significantly.

The "replica" relationship of the catalyst and polyolefine particle morphology were studied. PP has much better "replica" relationship than PE does. The reason was elucidated.

Bulk density is one of the most important characteristics for polyolefines, and is also a parameter most difficult to control. Comparison of bulk density for PE and PP was made, and the dependence of bulk density on several parameters for PE were elucidated. Means, such as prepolymerization, was found to be quite effective to improving the bulk density.

In polyolefine manufacturing processes, gas phase process was studied and believed to be the most advanced and preferred process of all PP processes.

On the basis of studies on olefin polymerization, a few important points are discussed and elucidated in the present paper.

THE KINETICS STUDY AND CATALYST ACTIVITY

In the study of the Ziegler-Natta polymerization kinetics, especially since the discovery of the high activity catalyst, there has been increasing interest in the investigation of C* (active center concentration) and k_p, both from academic and industrial

point of view. The well-known complex-type, i.e., Solvay type, $TiCl_3$ catalyst system, which is characterized by its rather high stereospecificity and activity, has already been employed in commercial production, but few works concerning its kinetic behavior have been published.[1)]

A complex-type catalyst, $TiCl_3 \cdot TiCl_4 \cdot nBu_2O$—$Et_2AlCl$, developed by BRICI (Beijing Research Institute of Chemical Industry), composed of $TiCl_3 \sim 80\%$, $TiCl_4 \sim 8\%$, nBu_2O $5 \sim 7\%$, specific area >100 M^2/g, was used for kinetic study. The viscosity-kinetic method for C* determination was used.[2)] Owing to the fact that both the molecular weight and isotacticity of PP obtained in the absence of H_2 were too high for determining M_n by GPC, viscometric method was employed. For the sake of improving the accuracy of M_n, the influence of MWD on M_n should be taken into consideration. In our experiment M_w/M_n obtained in the presence of H_2 by GPC were examined to be log-normal distribution. Thus, by the M_w/M_n value (5.4) determined in our studies in presence of a small amount of H_2 and that (1.205) originally determined in literature in establishing the viscosity-MW equation, M_n can be corrected according to the equation $K_n = K(M_w/M_n)^{0.5a(a+1)}$. The results are shown in Table 1.

Table 1. Determination of C* and k_p of different catalysts
$P_{C_3} = 860$mm Hg, in hexane

Catalyst	Polymn. temp. °C	R_p $gC_3H_6/gTiCl_3 \cdot h$	$C^* \cdot 10^2$ mol/mol Ti	k_p $dm^3/mol \cdot s$
$TiCl_3 \cdot TiCl_4 \cdot nBu_2O$	40	51.4	2.42	5.00
—Et_2AlCl	50	52.6	3.01	6.27
	60	62.1	5.17	8.18
Conventional $TiCl_3 \cdot 0.33AlCl_3$ —Et_2AlCl	50	14.4	2.06	2.55

$$\frac{C^*_{complex}}{C^*_{conventional}} \cong 1.5; \quad \frac{k_{p\ complex}}{k_{p\ conventional}} \cong 2.5$$

Hence it is concluded that the higher catalyst activity of complex-type $TiCl_3$ over the conventional one is not only due to its higher C*, but to a great extent to its higher k_p.

Nevertheless, the above viscosity-kinetic method is not satisfactory because of its larger error, although some M_n correction is made. The CO inhibition method in gas phase polymerization is believed to be the better one.[3] But the reliability of the method and the factors influencing the C* determination are not reported yet. The same complex-type catalyst was used in our studies [4] (Fig. 1). In order to elucidate the function of Et_2AlCl in the CO inhibition course, we interrupted the gas phase polymerization of propene, then the catalyst-PP mixture was washed with hexane several times, propene was introduced into the reactor again, and CO was added (Fig. 2). 48~60% of alkylaluminium was washed out.

The rate recovered only slowly after dropping to the minimum, and maintained there for about 10 minutes. The results illustrate that the chain transfer of the free alkylaluminium in the system plays a leading role for rapidly recovering polymerization rate after being depressed by CO.

The inhibition method involves the use of an inhibitor to "titrate" the active centers, and evaluate C* by the amount of CO, when the rate is depressed to zero. Therefore, the key of the reliability of the method lies in whether there is a stoichiometrical reaction between CO and C*. We found that regardless of the amount of CO added to the reactor, even if it was as high as 0.20 mole referring to the total Ti, the residual CO content in the gas phase at the later stage of polymerization was always smaller than that in the raw material propene (Fig. 3).

This phenomenon may be attributed to the active centers regenerated by alkylaluminium being inhibited again by the remaining CO, i.e., to the "repeating inhibition" by CO.

C* has been inhibited completely within 2 minutes after addition of CO. We compared the residual amount of CO analyzed by gas chromatography at this moment with the calculated residual amount of CO according to determined [Ti*] (Table 2). It is shown that, the CO moles consumed closely coincide with the determined [Ti*] moles, [CO]/[Ti*], i.e., [CO]/[C*], being $0.93 \sim 0.94 \cong 1$. This further proved that the influence of "repeating inhibition" could be avoided and the stoichiometrical relation that each active

center is inhibited by only one CO molecule is established by our determination.

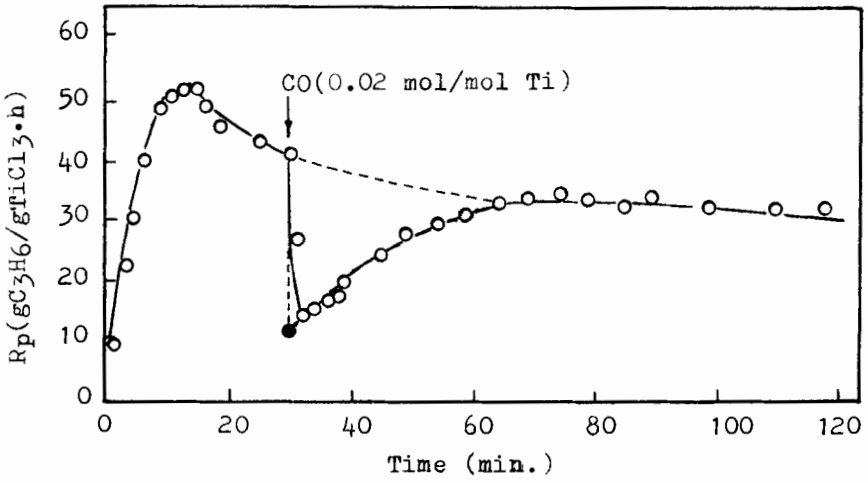

Figure 1. Change of R_p with the addition of CO during the gas phase polymerization of propene (50°C)

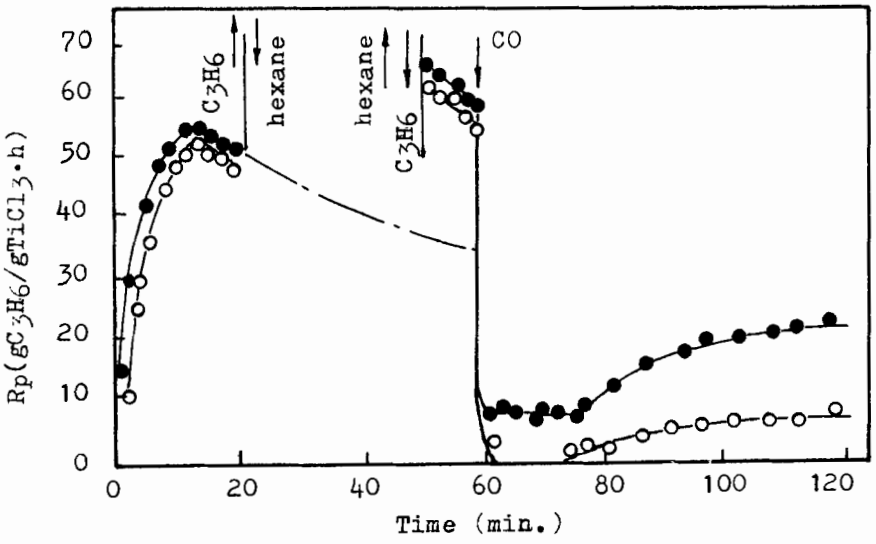

Figure 2. Change of R_p with the addition of CO after washing free alkylaluminium (50°C)

● CO/Ti = 0.02 mol/mol, o CO/Ti = 0.03 mol/mol

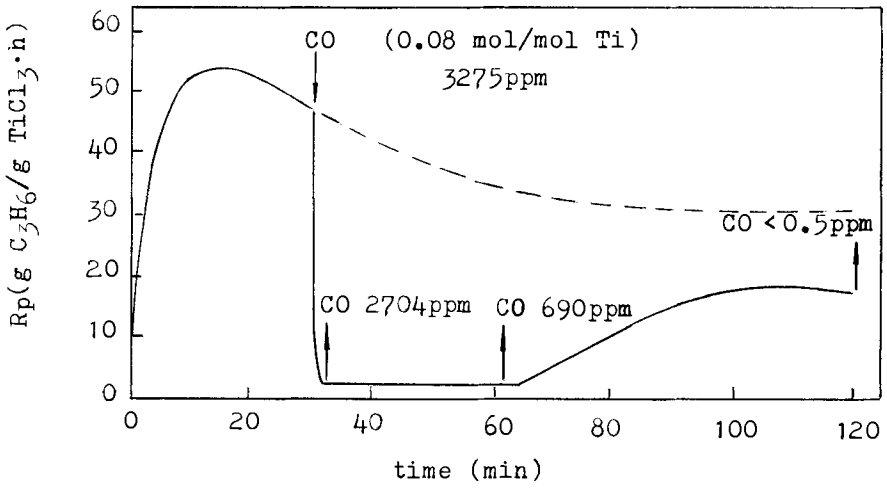

Figure 3. Change of residual CO content in the gas phase with the addition of excessive amount of CO

Table 2. Comparison of consumed CO from GC analyses with that calculated from C* in gas phase polymerization of propene

Runs	CO amount added (moles refer to total Ti moles)	CO consumed from GC analyses (moles refer to determined [Ti] moles)	CO amount calculated from C* (moles refer to determined [Ti] moles)	$\frac{[CO]}{[C^*]}$
1	0.08	0.0271	0.0289	0.94
2	0.08	0.0270		0.93

The C* obtained by this method, which is 2.90×10^{-2} mol/mol Ti at 50°C, is quite close to the data from the previous viscosity-kinetic method. In figure 4, it is proved experimentally that the rate decay coincides well with the C* decay, and therefore resulted from it, while the k_p remained constant.

We employed the CO inhibition method to $TiCl_4/MgCl_2/C_6H_5COOC_2H_5$-$AliBu_3$ catalyst system in propene gas phase polymerization. At 30°C

C* is 18.3×10^{-2} mol/mol Ti and k_p is 240dm^3/ mol•s, but at 50°C, an even lower value of C* is obtained. This implies that the diffusion control effect occurs because of the high activity of the catalyst and the low monomer concentration in the gas phase, hence the method is not reliable in this case.

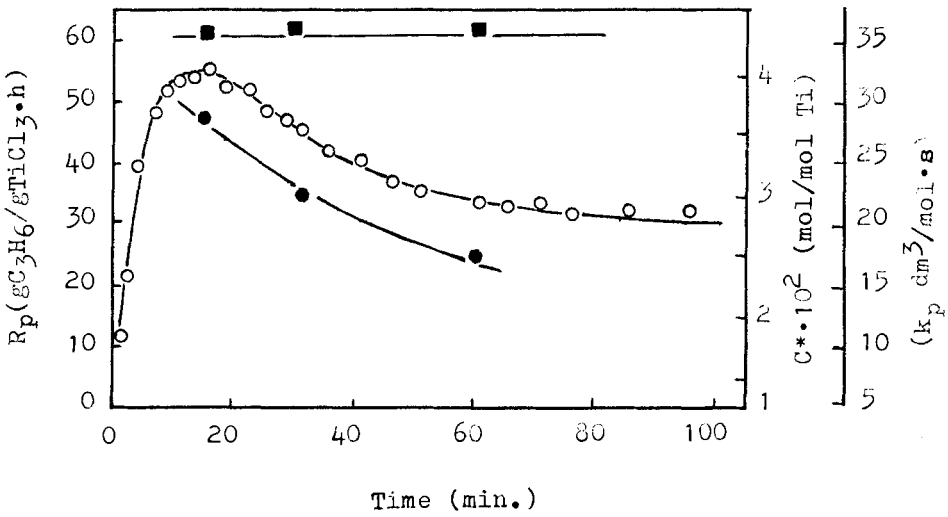

Figure 4. Change of R_p, C* and k_p with polymerization time (50°C)
○ R_p ● C* ■ k_p

For both PE and PP, we have developed various high activity catalysts, an activity of 1,000 kg polymer/g Ti in slurry polymerization has been achieved in both cases. In liquid propene bulk polymerization, an activity as high as 3,000～6,000 kg PP/g Ti is obtained. In the case of PE, the high activity can be attributed to the high C*, which is known as $50 \sim 70 \times 10^{-2}$ mol/mol Ti. Comparing with the C* of propene polymerization determined above, the high activity of propene polymerization must be due to the high k_p value, which would be considerably higher than that of ethene polymerization, although it seems that no direct determination and comparison are reported for ethene and propene polymerization using the same $MgCl_2$ supported catalyst and some workers believe that k_p is higher in ethene polymerization than that in propene polymerization. Anyway it is reasonable to say that, a PP catalyst capable of enhancing C* to a high extent will bring the catalyst activity to a brand-new level.

THE ELECTRON DONOR IN THE CATALYST SYSTEM

It has been proved that by changing electron donors the catalyst activity, the isotacticity of the polymer and kinetic behavior are all improved significantly (Table 3).

Table 3. Catalyst characteristics using different donors
80°C, 34 kg/cm^2, 2 h, propene bulk polymerization

Catalyst	Electron donors used in catalyst preparation	Electron donors used in polymn.	Activity kgPP/gTi	Total II, %	Kinetic behavior
$TiCl_4/MgCl_2$	ethyl benzoate EtOH	methyl p-toluate	846	95.4	rate decays rapidly within the first hour
$TiCl_4/MgCl_2$	ethyl hexyl alcohol phthalic anhydride diisobutyl phthalate	$Ph_2(MeO)_2Si$	1,760	98.8	rate keeps essentially steady even within six hours

These improvements are believed to be very successful commercially, but from the viewpoint of science, unknowns still remain. Among several $MgCl_2$ supported catalyst preparation methods, it has been proved by us and other workers that no matter what type of Mg compound (either $MgCl_2 \cdot ROH$ or Mg compound solubilized in a medium and then precipitated out again, or MgRx, $Mg(OR)_2$ etc.,) is used $MgCl_2$ matrix will ultimately reform. Some electron donors remain on the matrix while some disappear from the solid phase. Moreover, it is found that the electron donor also plays an important role in the precipitation step of $MgCl_2$ from solution. Perhaps this is one of the reasons why in the LLDPE catalyst preparation, where no stereospecificity problem exists at all, it is still necessary to add some electron donors to the catalyst system. The rule of the solubilization of $MgCl_2$ in various media, and the rule and particle control of the precipitation of $MgCl_2$ from solution, and the possible synergetic effect between the electron donors used in catalyst pre-

paration and in polymerization etc., are not quite clear yet.

"REPLICA" RELATIONSHIP

For the sake of energy saving, the elimination of the pelletizing step is now of increasing interest in the polyolefine industry. Therefore, good and uniform morphology of the polymer particle is becoming a very significant characteristic. According to our practice, by using a catalyst of $TiCl_4/MgCl_2$ system in propene polymerization, the spherical or spheroidal morphology of the catalyst and the polymer can be more easily kept in "replica" relationship than in the case of the ethene polymerization, as shown in Figure 5.6)

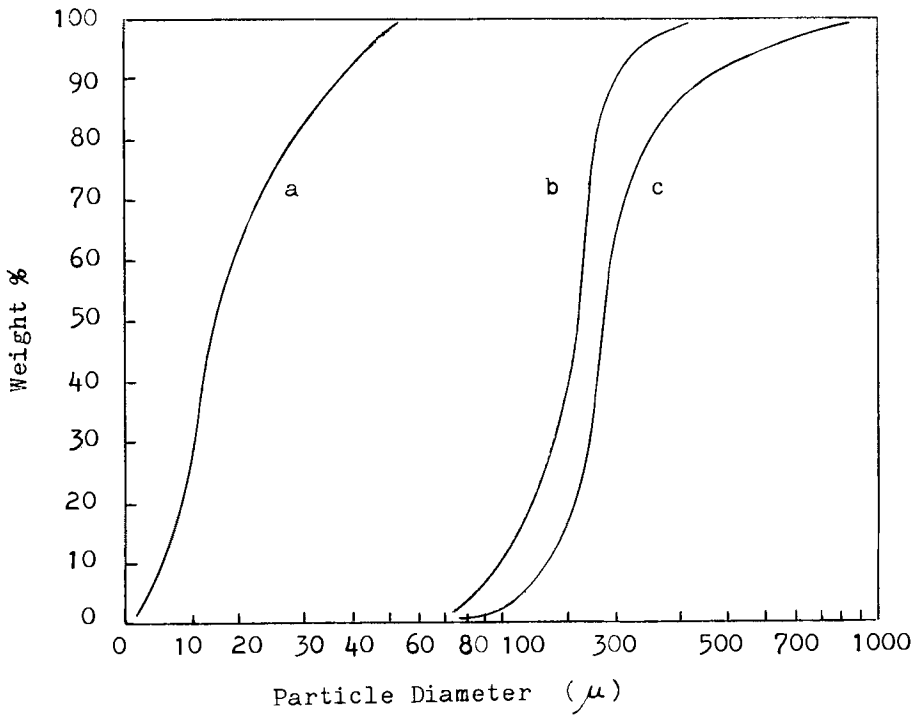

Figure 5. The "replica" relationship between the catalyst and polypropylene

70°C, 2 h

a $TiCl_4/MgCl_2 \cdot iC_8H_{17}OH$/donor catalyst

b PP(7kg/cm^2, in hexane)

c PP(30kg/cm^2, propene bulk polymerization)

The PP and catalyst particle size ratio is ~20 times, while in the case of complex-type catalyst and conventional $TiCl_3 \cdot 0.33AlCl_3$ catalyst, they are ~15 and ~7 times respectively in the hexane slurry polymerization. Nevertheless, quite different from PP, the PE particles obtained by using the same spherical catalyst have rather rough surface, loose structure and low bulk density, its morphology is much worse than the catalyst itself. The reason is probably attributed to ethene penetrating faster into the $MgCl_2$ catalyst subparticles than propene, and thus breaking it down. When SiO_2 supported Cr catalyst is used in ethene polymerization under drastic conditions, the morphology is even worse and a lot of PE fines are produced. This is due to the inherent brittle nature of SiO_2, which is different from $MgCl_2$. To slow down the initial rate and maintain good "replica" relationship, prepolymerization is proved to be an effective means. Even under drastic polymerization conditions, such as 20 kg/cm^2, 70°C, prepolymerization can keep the particles intact.[7] This subject will be discussed in more detail in the following section.

THE BULK DENSITY

This is one of the most important characteristics of concern to polyolefine manufacturers, since the direct processing of polyolefine particles is now being increasingly interested. By our experience, bulk density is the parameter most difficult to control and reproduce. Many factors influence it, which have not yet been figured out. For example, impurities in the raw material for catalyst preparation will deteriorate it. When employing the same kind of spherical catalyst, it is found that the PP obtained exhibits a much higher bulk density than PE. (Table 4)

Table 4. The bulk density of polyolefines produced by the same catalyst $TiCl_4/MgCl_2 \cdot EtOH/EB—AlEt_3$
$7 kg/cm^2$, 70°C, 2 h, in hexane

Monomer	Catalyst activity, kg/gTi	Bulk density, g/cm^3
ethene	830	0.30 - 0.35
propene	220	0.40 - 0.45

The high initial polymerization rate of ethene, together with

its lower concentration in hexane leads to the conclusion that the monomer diffusion and mass transfer into the catalyst is thus the main reason for PE's low bulk density. By varying the catalyst preparation conditions, catalysts having different Ti% and surface area can be obtained, lower Ti% and higher surface area both are favorable to the diffusion of the ethene molecules and hence to a higher bulk density (Fig. 6).[8)]

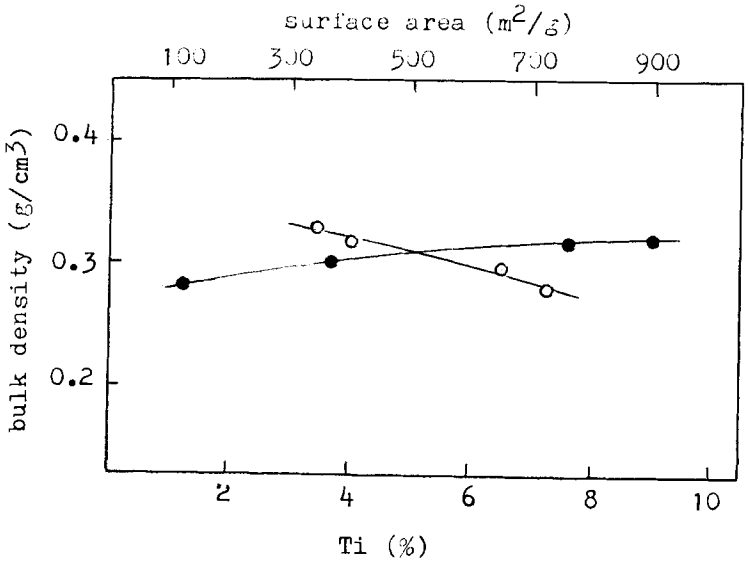

Figure 6. Dependence of bulk density of polyethylene on Ti content and surface area of $TiCl_4 \cdot MgCl_2 \cdot EtOH$-$AliBu_3$

o Ti (%) ● Surface area

Lower polymerization temperature increases ethene concentration in hexane and lowers the polymerization rate; the longer polymerization time allows ethene to fill up the inside of the catalyst, hence they both improve the bulk density (Fig. 7).[8)]

Prepolymerization of olefines to a certain extent in mild conditions (room temperature and atmospheric pressure), exhibited obvious increase of bulk density.(Table 5).[9)] In the course of prepolymerization, olefine polymerizes and forms a loose skeleton in the catalyst, or some polymers aggregate around the outer surface of the catalyst, thus slow down the initial rate and favor the increase of bulk density. It is found surprisingly that, in case of propene

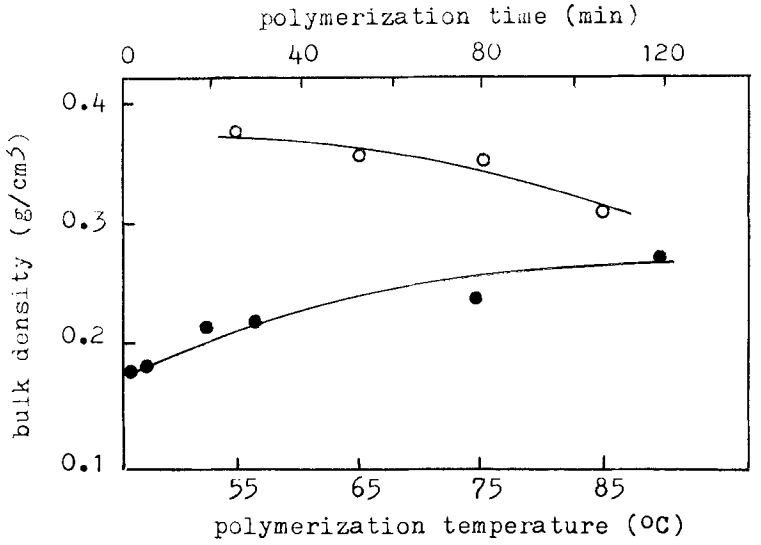

Figure 7. Dependence of the bulk density of polyethylene on the polymerization temperature and time

o Polymerization temperature ● Polymerization time

Table 5. The increase of bulk density of polyolefines by prepolymerization

For ethene: 70°C, 7 kg/cm^2, 2 h, in hexane

For propene: 80°C, 34 kg/cm^2, 2 h, bulk polymerization

	Runs	Bulk density, g/cm^3		Total II, %	
		Without prepolymn.	With prepolymn.	Without prepolymn.	With prepolymn.
PE	$TiCl_4/MgCl_2$·EtOH —$AlEt_3$				
	Cat. sample 1	0.29	0.33		
	Cat. sample 2	0.27	0.29		
	Cat. sample 3	0.24	0.30		
PP	$TiCl_4/MgCl_2$·donor —$AlEt_3$·donor				
	Cat. sample 1	0.38	0.43	97.6	99.5
	Cat. sample 2	0.39	0.43	98.3	99.4
	Cat. sample 3	0.39	0.44	98.1	99.4

polymerization, besides bulk density, isotacticity is also significantly increased by prepolymerizing the catalyst.

In the case of ethene—1-butene copolymerization (LLDPE) in hexane slurry polymerization using $TiCl_4/MgCl_2 \cdot iC_8H_{17}OH—AliBu_3$ catalyst system, bulk density is found to be a function of polymerization temperature and of 1-butene concentration (Fig. 8).[10] It shows that, introducing 1-butene into the polymerization system slows down the rate, and thus increases bulk density of LLDPE polymer.

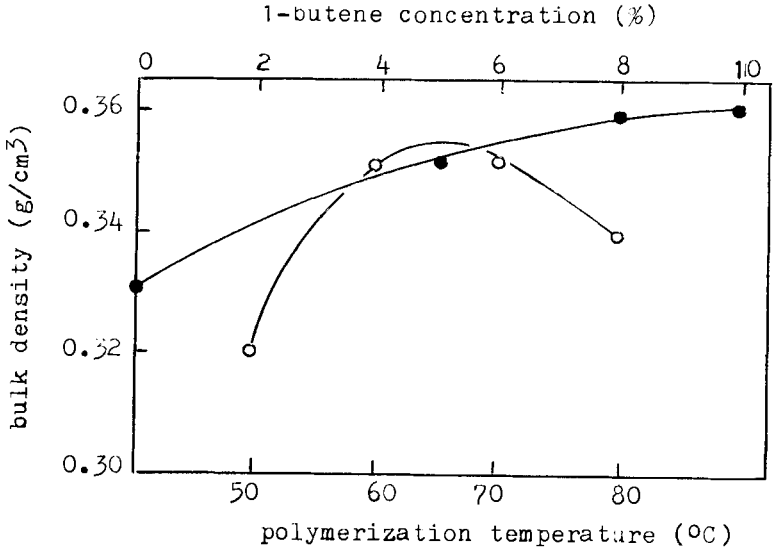

Figure 8. Dependence of bulk density of LLDPE on the polymerization temperature and 1-butene concentration

- o Polymerization temperature (1-butene 5%)
- ● 1-Butene concentration (70°C)

As to propene polymerization, monomer concentration and diffusion problems are much more advantageous over that of ethene, leading to much higher bulk density of PP.

THE GAS PHASE POLYMERIZATION PROCESS

For PE, the gas phase process has been extensively commercialized. But for PP, it is far less available in industry than either solvent slurry process or liquid propene bulk process. From our laboratory studies, there are no appreciable differences in the

kinetic curves and the C* values for the gas phase polymerization and the solvent slurry polymerization under the same working conditions (Fig. 9), but the k_p value is 5~7 times larger for the former. Consequently, the activation energy of the former is smaller (Table 6).

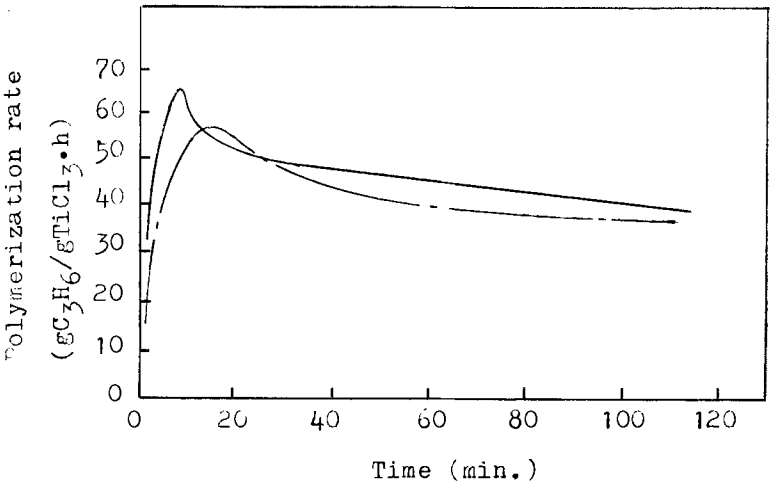

Figure 9. Comparison of polymerization rate—time curves of slurry and gas phase polymerization of propene ($TiCl_3 \cdot TiCl_4 \cdot nBu_2O$—$Et_2AlCl$, P_{C_3} 860mm Hg, 50°C)

——— Gas phase polymerization

——— Solvent slurry polymerization

The decrease of E_a and E_p of gas phase polymerization may be attributed to the elimination of the resistance of solvent molecules. All above data are in favor of the gas phase polymerization. Gas phase process also exhibits the advantage of the simplicity in shifting from one melt flow index grade to another, and the advantage of safety (because of no large quantity hold-up of liquid propene in the reactor). However, there must be some bottlenecks which delayed the development of propene gas phase polymerization process and caused it to lag behind. For instance, first, how to prevent the dead spots in gas phase reactor causing agglomeration, as can be substantially avoided in a slurry process ? Second, since collision and abrasion between the solid particles in a gas phase

Table 6. Activation energy of propene polymerization by different polymerization methods

$TiCl_3 \cdot TiCl_4 \cdot nBu_2O — Et_2AlCl$

Polymn. method	Temp. interval °C	E_a Apparent activation energy kcal/mol	E_p Activation energy of chain propagation kcal/mol	E kcal/mol
Solvent slurry polymn.	40 - 60	11.30	5.10	6.20
Gas phase polymn.		5.46	2.08	3.38

reactor are more severe, is it possible to obtain spherical polymer by using the corresponding catalyst following the "replica" relationship as can be done in a slurry process ? Thus, a fluidized bed reactor is considered to be better than a stirred vessel reactor in these respects. In the last two or three years the gas phase process have been developing successfully. In my opinion, the gas phase process is the most advanced and preferred process of all the PP manufacturing processes.

Acknowledgement: The author wishes to deeply acknowledge his colleages in BRICI for their permission to adopt the experimental data and their valuable suggestions.

REFERENCES

1. P.Tait, "Preparation and Properties of Stereoregular Polymers", Ed. by R.W.Lenz, Reidel Publ. Co., 1979, p 94.
2. S.P.Tang, Z.Z.Tan, S.M.Wang, A.R.Zhang, Polymer communications (China) 1984, (1).
3. Y.Doi, T.Keii, Ind. Eng. Chem., Rapid Commun., 1982, 21, (4), 581.
4. Y.E.Li, S.P.Tang, Polymer Communications (China), 1984, (2).
5. B.Q.Mao, L.L.Yang, et al., (BRICI) 2nd Symposium on Petrochemical Catalysts, Anching, China, 1983, Oct..
6. H.Y.Wang, G.Z.Chien, et al., (BRICI) unpublished work (1985).
7. M.Z.Jin, Q.Chen, (BRICI), International Chemical Congress of

Pacific Basin Societies, Honolulu, 1984, Dec..
8. X.Y.Song, Y.Xie, Petrochemical Technology (Shiyouhuagong), 1984, 13, (4), 235.
9. J.L.Li, et al., (BRICI), unpublished work (1985).
10. X.Y.Yang, et al., Petrochemical Technology (Shiyouhuagong), 1985, 14, (7).

This page intentionally left blank

SUPPORTED ORGANOMETALLIC CATALYSTS FOR ETHYLENE POLYMERIZATION

Yu.I.YERMAKOV, V.A.ZAKHAROV and G.A.NESTEROV
Institute of Catalysis, Novosibirsk 630090, USSR

ABSTRACT

The state of art in the field of polymerization catalysts, in which direct precursors of active sites are obtained by interacting organometallic transition metal compounds with surfaces of oxide supports, is considered. These catalysts are widely used to study fundamental aspects of organometallic chemistry on the surface of oxides including aspects of the mechanism of olefin polymerization. Some of the supported organometallic catalysts are employed in industry for the production of the high-density polyethylene.

INTRODUCTION

Supported organometallic catalysts can be defined as systems obtained by supporting organometallic complexes of transition elements on various carriers. This is a relatively new and broad class of catalytic systems. To our knowledge, the first systems of such type were prepared by supporting Mo, W and Cr hexacarbonyls over Al_2O_3 by Banks et al.[1] at research center of Philips Petroleum in Bartlesville (Oklahoma) in the middle of 60-s. So-obtained systems containing Mo and W catalyzed metathesis of olefins (thus this remarkable reaction was discovered). The Cr-containing system was active in the deep polymerization of ethylene. Later on the researchers from different countries made use of nearly all known metal carbonyls, both mono- and polynuclear to prepare supported systems (see reviews [2-4]).

Application of organometallic complexes with other organic ligands, such as benzyl, allyl and cyclopentadienyl ligands, which can be involved in the protolysis of metal-carbon bond opened up new possibilities of obtaining supported organometallic catalysts[5-10] (see Table 1). These systems were used to catalyze a number of re-

actions[11,12], for example, polymerization of olefins and diens, metathesis of olefins and hydrogenation. However, their application to ethylene polymerization is most comprehensively studied; the re-

Table 1. Transition metals used for catalyst preparation in the form of their homoleptic MR_x compounds capable of interacting with surface hydroxyls (≡ -OH)$_n$ + MR_x → (≡ -O)MR_{x-n} + nHR). The elements given in circles are active in ethylene polymerization. Dotted circle means scarce polymerization activity

III	IV	V	VI	VII	VIII
	Ti	V	Cr		Ni
	Zr	Nb	Mo		Ph, Pd
La, Ce, Pr, Nd Sm,Py,Ho,Tm,Yb	Hf		W		Pt
Th, U					

sults of the investigation of these catalysts can be found in some earlier published[11-14] and in quite recent[15] reviews. For this reason, we do not think there is a need to consider here all aspects of preparation, performance and application of supported organometallic polymerization catalysts. In this report we focuse on the data obtained in recent years and only briefly outline some preparation methods and properties of supported systems.

INTERACTION OF ORGANOMETALLIC COMPOUNDS WITH THE SURFACE OF OXIDES AND REACTIVITY OF THE SURFACE COMPLEXES FORMED

We consider only those systems, which are formed from the compounds able to take part in protolytic interaction with surface hydroxyl groups of oxides. Alkyl and allyl transition metal complexes (as well as cyclopentadienyl complexes of Cr) react with oxide supports via the scheme:

$$(\equiv E - OH)_n + MR_x \rightarrow (\equiv E - O)_n - MR_{x-n} + nHR \qquad (1)$$

here ≡ is the oxide surface; E = Si, Al; n = 1 ÷ 3; x = 2 ÷ 4; M is a transition metal; R is an organic ligand.

The occurence of reaction (1) has been established from IR and NMR spectroscopy data, as well as from the chemical analysis of the decomposition products of surface complexes[16-18]. The reaction stoicheometry and the surface composition of the complexes obtained depend upon the supported compound, the type of supports and the temperature of the preliminary dehydration (T_d) of the support, which determines the surface concentration of hydroxyl groups[11]. The optimal T_d, at which the highest catalytic activity is achieved, depends on the type of supported organometallic compounds. For example, T_d is ca. 100 °C for $Zr(C_3H_5)_4/SiO_2$ and ca. 800 °C for $Cr(C_5H_5)_2/SiO_2$ systems. As T_d rises, the molecular mass of the polymer formed has a tendency to decrease. Furthermore, by varying T_d, is possible to change drastically the properties of active sites. For example, if $Cr(C_3H_5)_3$ is supported over SiO_2 at T_d 300-500 °C, one obtains the active centers for deep ethylene polymerization. At $T_d \sim 600$ °C these are mainly the centers, at which ethylene is converted to a complicated mixture of liquid olefins with a branched structure, most probably, due to the simultaneous occurence of oligomerization metathesis and isomerization reactions.

Surface organometallic complexes of transition elements are reactive compounds. They can easily transform to surface hydrides at heating:

$$(\equiv E - O)_n M\text{-}R_m \xrightarrow{H_2,\ 25 \div 150\ °C} (\equiv E - O)_n M\text{-}H_m + nHR \qquad (2)$$

(M : Ti, Zr, Hf, R : C_3H_5, $CH_2C_6H_5$). An intermediate formation of surface hydrides seems to be the main route leading to the formation of active sites of the propagation reaction:

$$(\equiv E - O)_n M\text{-}H + C_2H_4 \longrightarrow (\equiv E - O)_n M\text{-}CH_2CH_3 \qquad (3)$$

As evidenced by IR[16,17] and NMR[18] data, alkylation of surface hydrides Ti and Zr, accompanied by ethylene polymerization occurs even at 150 K.

Apparently, active centers in classical chromium-oxide catalysts of ethylene polymerization are also produced via the formation of hydrides. The scheme of hydride formation proposed recently involves an oxidative addition of surface hydroxyls to low-valent chromium ions[19]:

Thus, in this case low-valent chromium ions (Cr^{+2} or Cr^{+3}) are the source of surface hydrides, that is of the direct precursors of active centers. The fact that the active centers in these catalysts are formed from low-valent chromium ions was demonstrated in earlier works[20], in which the number of propagation centers had been compared with an average oxidation number of chromium ions in operating catalysts. Finally, surface organometallic compounds are formed as active polymerization centers in classical chromium-oxide catalysts too. Thus, informally, these catalysts also belong to "supported organometallic" systems.

Surface organic and hydride metal complexes are more stable than the corresponding compounds in the solution. For instance, while allyl compounds of Zr and Cr decompose in the solution even at 0 °C, allyl complexes on the surface of the oxides are stable at 25–50 °C. Surface hydride complexes of Ti, Zr and Hf are stable even at 150–300 °C. This provides the possibility to use such complexes as catalysts for ethylene polymerization in the solution at 150–250 °C.

Table 2. The properties of samples obtained via the interaction of $Ti(CH_2C_6H_5)_4$ with SiO_2 as a function of the hydrogen treatment temperature (content of Ti is 1%)

Temperature of treatment by H_2, °C	Amount of hydrogen evolved at thermodesorption	Average* oxidation number of Ti ions	Predominant surface species formed
150	2.3	3.4	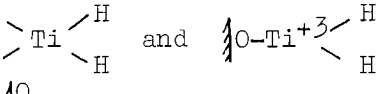
300	1.2	3.4	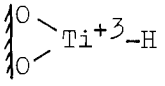
600	0.1	2.7	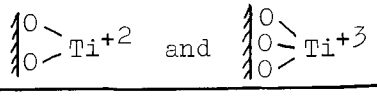

*Calculated from the amount of oxygen consumed for sample oxidation

Data on the content of hydrides in the sample obtained by treating the $Ti(CH_2C_6H_5)_4/SiO_2$ system with hydrogen at different temperatures are given in Table 2. Even when heated in H_2 at 300 °C mainly 1 Ti-H species are present on the surface. The treatment of the catalyst with hydrogen at 600 °C produces low-valent Ti ions, which deserve attention as possible active sites of some catalytic reactions.

Table 3. Data on the number of propagation centers (C_p) corresponding to maximum polymerization activities (V_{max}) of various supported organometallic catalysts. The data were calculated from the propagation rate constant (K_p) measured using ^{14}CO as radioactive quenching agent. Ethylene polymerization temperature was 80 °C.

Catalyst	V_{max} $\frac{g\ C_2H_4}{mmol\ M\ h\ atm}$	C_p, mol/mol M	$K_p \cdot 10^{-3}$, l/mol·s
$Ti(CH_2C_6H_5)_4/Al_2O_3$	200	0.032	0.95
$Zr(CH_2C_6H_5)_4/Al_2O_3$	1500	0.11	2.2
$Zr(C_3H_5)_4/Al_2O_3$	380	0.027	2.2
$Zr(C_3H_5)_4/SiO_2$	76	0.058	0.2
$Zr(C_3H_5)_4/SiO_2$ [a]	400	0.35	0.18
$Zr(C_3H_5)_3Cl/SiO_2$	200	0.016	2.2
$Zr(C_3H_5)_3Cl/SiO_2$ [a]	600	0.05	2.0
$Zr(CH_2C_6H_5)_2Cl_2/SiO_2$	900	0.048	3.0
$Zr(BH_4)_4/SiO_2$ [b]	600	0.28	0.3
$Cr(C_5H_5)_2/SiO_2$	650	0.12	10

a) Catalyst was activated by treatment with H_2 at 150 °C.

b) Catalyst was activated by heating at 220 °C.

Hydride surface complexes can take part in a great number of reactions: they react with olefins and diens, can easily be in-

volved in the isotope exchange with D_2 and be decomposed in water. Note, that there is a correlation between the content of hydride hydrogen in catalysts and their catalytic activity, both in ethylene polymerization[16] and in hydrogenation of olefins and benzene[21].

Only part of surface organometallic complexes can be transformed to the active centers of olefin polymerization. Evidence for this comes from the data obtained by method of radioactive quenching technique with the use of CO^{14} (see Table 3). Optimal conditions of catalyst treatment, that provide a maximum yield of active centers, depend on the composition of catalytic systems. For example, to attain the maximum activity of the $M(C_3H_5)_4/SiO_2$ system (M = Zr, Hf), hydrogen treatment at 100-150 °C has to be used. For $M(BH_4)_m/SiO_2$ (or Al_2O_3) (M = Ti, Zr, Hf, U) heating at 150-250 °C is needed, while for MR_x/SiO_2 (M = Ti, Zr; R = benzyl or norbornyl) it is UV-irradiation.

NEW MODIFICATIONS OF SUPPORTED ORGANOMETALLIC CATALYSTS

1). The use of new organometallic complexes.

The use of carbonyl, allyl, benzyl and cyclopentadienyl complexes of Groups 4, 6 and 8 metals for the preparation of supported organometallic catalysts is a technique which may be considered now as conventional one. Consider now some new ways of the preparation of these catalysts based on the broadening of the class of compounds used for supporting.

The attempts to use σ-organometallic complexes of Groups 4-5 elements with such ligands as neophyl[23] ($-CH_2C(CH_3)_2C_6H_5$), norbornyl[24] and naphthyl[25] for preparation of supported polymerization catalysts have been reported quite recently. However, little is as yet published on the results of the study of these systems. The system obtained by supporting Ti, Zr, Hf and U tetrahydroborate complexes[26,27] has been studied in more detail. For these complexes, simple methods of synthesis (the milling of metal chlorides with $LiBH_4$ and further isolation of tetrahydroborates by sublimation) have been developed[28]. The complexes are thermally more stable than σ-organometallic or allyl complexes and can easily be dissolved in aliphatic solvents. They react with surface hydroxyl groups via the scheme:

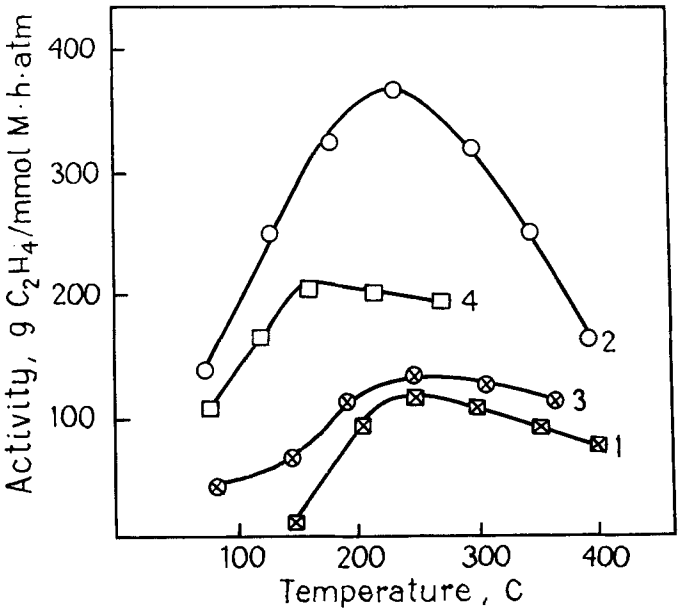

Figure 1. The activities of $Zr(BH_4)_4/SiO_2$ (1), $Zr(BH_4)_4/Al_2O_3$ (2), $U(BH_4)_4/SiO_2$ (3) and $Ti(BH_4)_3/Al_2O_3$ (4) catalysts vs the temperature of heating in vacuum (the supports were dehydroxylated at 400 °C, for sample (3) at 700 °C). Polymerization of C_2H_4 at 80 °C and 6 atm.

$$(\text{≡E-OH})_n + M(BH_4)_m \longrightarrow (\text{≡E-O})_n\text{-}M(BH_4)_{m-n} + \frac{n}{2} H_2 + nBH_3 \qquad (4)$$

$(n = 1,2;\ m = 3,4)$

The occurrence of reaction (4) is confirmed by IR[27], NMR[27a] data and by the analysis of the reaction products. The similar conclusion has been made from the study of the interaction between $Zr(BH_4)_4$ and surface hydroxyl groups formed during the oxidation of the aluminium film[29]. The evolving BH_3 can either recombine producing diborane or react with hydroxyl groups:

$$(\text{≡E-OH})_n + BH_3 \longrightarrow (\text{≡E-O})_nBH_{3-n} + H_2 \qquad (5)$$

The heating of the anchored hydroborate complexes leads to the formation of M-H bonds (IR absorption bands at 1560-1570 cm^{-1} for Ti-H, at 1665 cm^{-1} for Zr-H and at 1730 cm^{-1} for Hf-H). This formation is the necessary step for providing the catalytic activity. This latter significantly depends on the temperature of sample pre-heating (see Figure 1).

Based on IR, NMR and chemical analysis data the decomposition of surface tetrahydroborate complexes can be described as:

$$(\equiv E\text{-}O)_n M(BH_4)_{m-n} \longrightarrow (\equiv E\text{-}O)_n M\begin{matrix}(BH_4)_x \\ (H)_y\end{matrix} + H_2 + B_2H_6 \qquad (6)$$

Surface hydrides produced by decomposition of surface tetrahydroborate complexes are highly stable up to 300 °C, as suggested by IR spectroscopy. Compare to the known individual hydride compounds, which possess a far lower thermal stability, e.g. $[(C_5H_5)_2TiH]_2$ and $(C_5H_5)_2Zr(H)BH_4$ complexes decompose[30,31] even at 100 °C. The high thermal stability of surface hydrides seems to be due to their rigid fixation on the surface, which precludes the possibility of their decomposition via bimolecular reactions.

In recent works, Burwell and co-workers[3,32,33] have mentioned that catalysts obtained by supporting organometallic derivatives of actinides, $M(C_5H_5)_2(CH_3)_2$ (M=U or Th) induce the polymerization of ethylene. The interaction of these compounds with alumina[34] has been studied in detail. As found, this reaction follows mainly the route of the $M\text{-}CH_3$ bond protolysis by surface hydroxyls. Burwell et al.[3] report also on the high activity of the catalysts obtained in hydrogenation, which is almost similar to the activity of noble metals.

Organometallic compounds of lanthanides (Yb, Lu) in the solution also were shown[35] to be catalytically active in ethylene polymerization. It would be interesting to examine whether the activity of these complexes increases at their supporting on the surface of oxides. However, we are unaware of any reliable evidence for this fact (note, that, to our opinion, first reports of the activity of soluble allyl and benzyl complexes are erroneous because an observable low activity is determined by heterogeneous products of their decomposition[36]. Recently, supported catalysts[37] from $M[C_5H_4\text{-}CH(CH_3)_2]_3$ (M - La, Ce, Pr, Nd, Sm, Dy, Ho, Tm, Yb) have been prepared at the Institute of Catalysis; but the attempts to activate these systems for ethylene polymerization have been no success.

Now let us dwell on the use of diene complexes of transition metals synthesized recently by Wilke, Bogdanovich et al.[38,39]. The catalysts obtained by supporting $M(isoprene)_3$ (M = Mo or W) over SiO_2 are efficient in olefin metathesis[40] at low temperatures (see Figure 2). Diene complexes are quite convinient for use owing to the

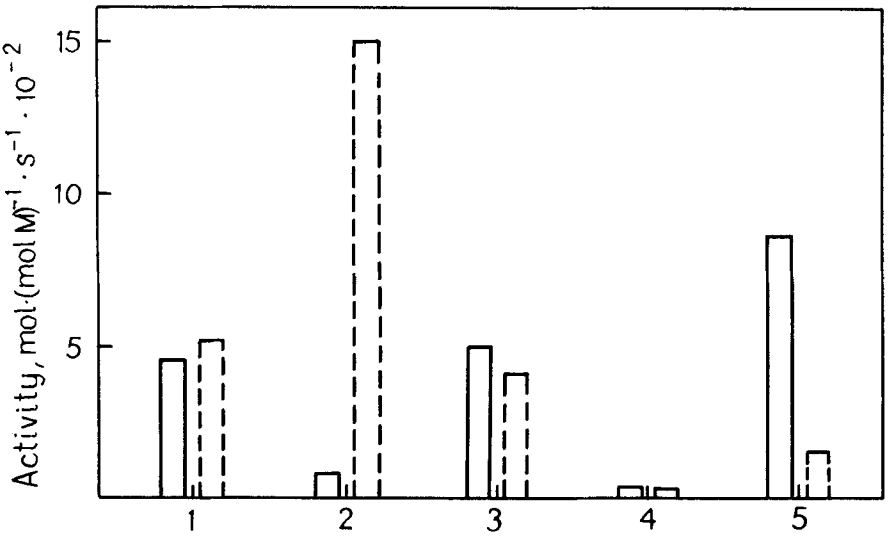

Figure 2. Activities of the catalysts obtained by supporting Mo(isoprene)$_3$ or W(isoprene)$_3$ (dotted line) over SiO_2 in propylene metathesis at 100 °C (1) catalyst in the "initial" state, that is without an additional treatment after supporting the complexes; (2) treatment with hydrogen at 100 °C; (3) treatment with hydrogen at 500 °C; (4) treatment with oxygen at 400 °C; (5) treatment of the oxidized catalysts with hydrogen at 500 °C. Data obtained by A.N. Startsev and V.N.Rodin.

ease of their preparation and to the higher stability as compared to allyl complexes.

Data on the application of organometallic complexes to catalyst preparation allows one to compare systems in both metal and ligand series (Table 4). This comparison is based on the data on the activities registered under identical conditions (experiments made at the Institute of Catalysis). Catalysts were activated in optimal conditions (it is not excluded, certainly, that we failed to find optimal conditions for some of the systems). From the data obtained we may conclude that:

1. In all cases the activity increases when passing from Ti to Zr and Hf. This is due to the increase in the number of active centers, which in turn, seems to result from the growth of the stability of hydride and organometallic complexes in the order Ti → Zr → Hf.

2. Upon varying organic ligands, the complexes which can easily

Table 4. Activity of various supported catalysts prepared with the use of homoleptic MR_x compounds in C_2H_4 polymerization. Activity in g C_2H_4/mmol M·h·atm

R	Ti on		Zr on		Hf on		Cr on
	SiO_2	Al_2O_3	SiO_2	Al_2O_3	SiO_2	Al_2O_3	SiO_2
Allyl			180	280			300
Benzyl	30	370	70	2400	20	1300	
Naphthyl	35	90					
Norbornyl	0	850	40	500			
Cyclopenta-dienyl							250
BH_4	45	220	300	1000	100	280	

form hydride surface complexes, possess the highest activity.

Note, that the stability of surface organometallic complexes increases in the order: allyl < benzyl < naphthyl < norbornyl.

The systems on alumina are more active than those on silica (it is important to tell that for the purpose of polymerization granules of oxide supports with large pores should be used, such granules decompose to elementary particles during the polymerization process and, thus, provide the participation of the whole support surface in the reaction preventing its blocking by the polymer[41].

2. Application of new supports

The work has been carried out recently at the Institute of Catalysis on the use of supports with low surface areas for the preparation of supported organometallic systems. The objective of this research was to obtain polymerization-filled composite materials, in which the polymer and the support would be in commensurable proportions. Data on the polymerization activities of various systems are listed in Table 5. It is seen that the activity per 1 mol of the metal is noticeably lower than in the case of SiO_2. Still this activity is sufficient to obtain materials with several grams of the polymer per 1 g of the support. As is shown by scanning

Table 5. Data on catalysts prepared by interaction of $Zr(BH_4)_4$ with natural silicates. Dehydration temperature of supports was 300 °C[42].

Support and its BET surface	Content of Zr		Activity	
	mol/m^2	mol/g	g C_2H_4 / g cat·h·atm	g C_2H_4 / mmol Zr·h·atm
Tufa (2.6 m^2/g)	$4 \cdot 10^{-6}$	$11 \cdot 10^{-6}$	0.3	28
Pumice (2.7 m^2/g)	$4 \cdot 10^{-6}$	$11 \cdot 10^{-6}$	0.4	34
Kaolin (12.6 m^2/g)	$2 \cdot 10^{-6}$	$27 \cdot 10^{-6}$	0.3	11

electron microscopic data (Figure 3), the polymer evenly envelopes the surface of the mineral support. The starting materials are practically nonporous (see, e.g., micrographs of tufa particles in Figure 3a). In the sample, containing about 10% of the polymer (Figure 3b), the form and the size of particles do not change. Thin polymeric threads are observed, but their weight cannot achieve 10% of the total mixture. Thus, the predominant part of the polymer is in the form of the film (~ 0.1 μ) that covers tufa particles. As the content of the polymer increases up to 50%, faceted particles are no more observed; instead elongated and rounded particles appear in the material (see Figure 3c). A fibrous structure of the polymeric film is clearly seen at the cracks. At increasing the content of the polymer in the sample up to ca. 85%, the polymeric film cracks, and worm-like formations with a 0.5-2 μ diameter produced in the material. From the small size of these formations we may judge that they do not have the mineral support inside. Rather, they are polymeric structures which have come off the material surface. A dense coverage of inorganic materials with the polymeric film at the polymerization makes it possible to obtain a uniform by filled material of good mechanical strength, provided the content of the polymer in the mixture is 50-100% (by weight of the mineral support).

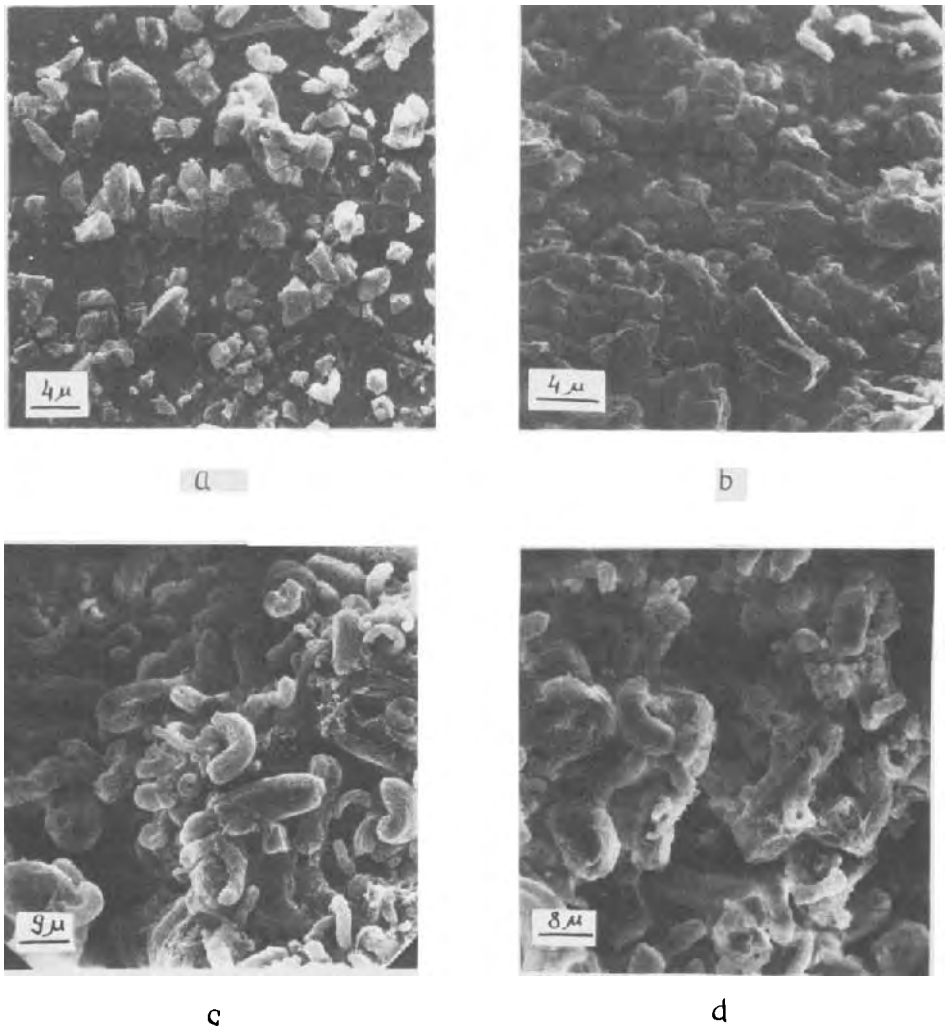

Figure 3. SEM micrograph of the samples of tufa (a) and filled polyethylene obtained on $Zr(BH_4)_4$/tufa with polyethylene content (b) 11% wt., (c) 50% wt., (d) 85% wt.

SUPPORTED ORGANOMETALLIC CATALYSTS AS OBJECTS OF THE STUDY OF THEORETICAL PROBLEMS OF CATALYSIS

One of the authors[43] has already considered why the systems obtained via anchoring metal complexes are advantageous for theoretical studies of catalysis problems. These advantages are primarily associated with the possibility of purposeful synthesis of ac-

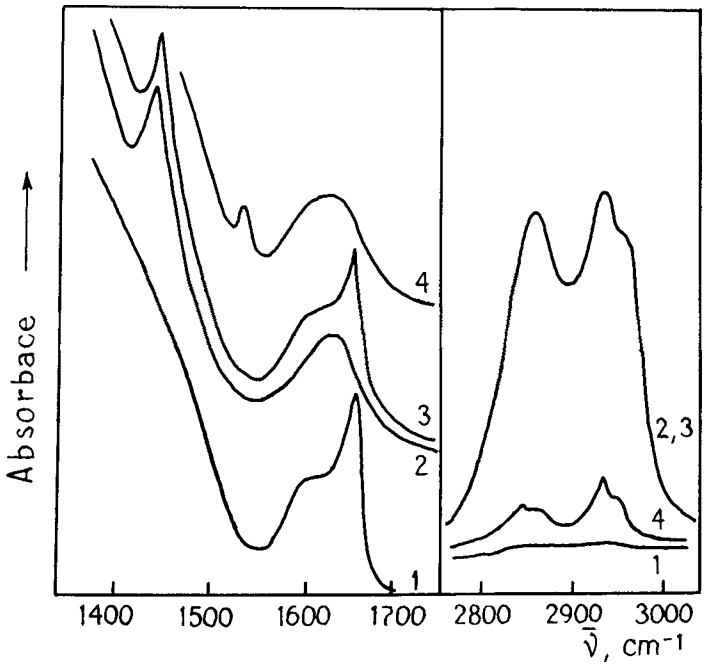

Figure 4. IR spectra of $Zr(BH_4)_4/SiO_2$ catalyst pretreated with ethylene and carbon monoxide: (1) $Zr(BH_4)_4/SiO_2$ activated by heating in vacuum at 220 °C; (2) ethylene adsorption on sample (1) at room temperature; (3) treatment of sample (2) with hydrogen at 100 °C; (4) CO adsorption on sample (1) at 40 °C.

tive centers and with the possibility to obtain more homogeneous surface compositions as compared to conventional methods of preparation. This latter fact ensures more unambiguous information obtained with the use of physical methods.

In the case of polymerization, the problems of primary concern are those related to the mechanism of the formation of active centers and to the mechanism of polymerization.

When investigating catalysts containing surface Ti, Zr or Hf hydrides, it is possible to follow the insertion of ethylene into the M-H bond. For example, ethylene adsorption on the catalyst even at 200 K leads to the disappearance of the adsorption bands corresponding to ν_{M-H} (1665 cm^{-1}, see curve 1 in Fig. 4) and to the appearance of absorption bands at 2800-3000 cm^{-1} and one band at 1465 cm^{-1} attributed to methyl and methylene groups of the polymer formed. These changes of spectra correspond to the following reac-

tions:

$$\equiv M\text{-}H \xrightarrow{C_2H_4} \equiv M\text{-}C_2H_5 \xrightarrow{nC_2H_4} \equiv M(C_2H_4)_nC_2H_5 \qquad (8)$$

The treatment of the catalysts by H_2 partly restores the bands of ν_{M-H}, which indicates the hydrogenolysis of the metal-alkyl bond (Figure 4, curve 3):

$$\equiv M\text{-}(C_2H_4)_n\text{-}C_2H_5 \xrightarrow{H_2} \equiv M\text{-}H + H(C_2H_4)_n - C_2H_5 \qquad (9)$$

Thus, surface hydride compounds are direct precursors of active centers.

CO adsorption of hydride complexes of Zr is of a reversible character up to 0 °C. The temperature rise up to 20 °C leads to irreversible changes in the IR spectra (see Figure 4, curve 4). The treatment of such samples with hydrogen at 100 °C does not result in the formation of the $\equiv M\text{-}H$ bonds. The data obtained evidence that CO inserts into the $\equiv Zr\text{-}H$ bond producing formyl complexes (ν_{CO} = 1540 cm^{-1}):

$$\equiv Zr\text{-}H \underset{300\ K}{\overset{CO}{\rightleftharpoons}} \equiv Zr\begin{matrix}CO\\H\end{matrix} \xrightarrow{>300\ K} \equiv Zr\begin{matrix}C\text{-}H\\O\end{matrix} \qquad (10)$$

When surface formyl complexes are decomposed by water, methanol is detected in the decomposition products.

As distinct from surface compounds, the interaction of CO with Zr and Ti hydride complexes in the solution does not yield formyl complexes, but gives the products of biomolecular interaction between intermediate formyl complexes and the metal hydride (see e.g. [44]).

The supports containing surface low-valent ions obtained by reduction of anchored organometallic complexes of Group 4 metals have been used recently to study the nature of the "strong interaction between the metal and the support" (SIMS). The discovery of this phenomenon[45], which implies unique properties of metal particles on TiO_2, La_2O_3 and other oxides capable of being reduced has been followed by a great flow of works aimed at an insight into its nature. However, one can notice that the similar change in the properties of supported metals has been described earlier[46-48] for catalysts containing metal particles stabilized on surface low-valent ions of Mo and W. These changes have been accounted for by

the interaction of dispersed metal particles with low-valent ions on the surface of oxides. It can reasonably be proposed that ions of Group 4 elements cause the similar variations in the properties of supported metal particles. To verify this idea, Ni, Pd or Pt were supported from their π-allyl complexes over SiO_2 modified by Ti, Zr or Hf hydrides or ions obtained from organometallic complexes. So-obtained catalysts reveal SIMS effects (for Ni-containing systems see[9]):

(i) increase of the stability of metallic particles to sintering;
(ii) increase of the activity in CO hydrogenation; and
(iii) decrease of the activity in hydrogenation of benzene and hydrogenolysis of ethylene.

Once the catalysts are oxidized and then reduced at moderate temperatures, these effects disappear as in the case of TiO_2 and ZrO_2 systems. An X-ray photoelectron spectrometer registeres the fall of the signal intensity from Ti and Zr ions when supporting Group 8 metals on Ti/SiO_2 and Zr/SiO_2 samples. All these data evidence that the reason for the variation in the properties of metallic particles on TiO_2 and ZrO_2 may also be their interaction with surface low-valent ions.

PRACTICAL VALUE OF SUPPORTED CATALYSTS OF ETHYLENE POLYMERIZATION

Now we compare various supported polymerization catalysts. If these systems, including classical chromium-oxide catalysts, are considered at the propagation step, they can be regarded as "supported organometallic" catalysts since their active centers are surface organometallic species. The role of the process of polyethylene production on chromium-oxide catalyst is as yet very high in the slurry technology of production of high-density polyethylene. In the new process of the gas phase polymerization developed by Union Carbide Co. the following catalysts are used:

a) $CrO_2(OSiPh_3)_2/SiO_2$ activated by diethylaluminiumetoxide. This catalyst provides a high yield of polyethylene with a broad molecular mass distribution (MMD). This catalyst can be substituted in the industrial process by the CrO_3/SiO_2 system subjected to a special activation.

b) $Cr(C_5H_5)_2/SiO_2$ also provides a high yield of polyethylene. Specific feature of the polymer is the narrow MMD. The catalyst has a

Table 6. Comparison of the properties of various supported catalysts used for the industrial production of polyethylene

Catalyst	Polymerization process	Activity under conditions of industrial application		Properties of the polymer obtained		
		$\frac{kg\ C_2H_4}{g\ cat \cdot h}$	$\frac{kg\ C_2H_4}{g\ M \cdot h}$	MMD	Melt index $\frac{g}{10\ min}$	Density g/cm^3
$CrO_2[O\text{-}Si(C_6H_5)_3]_2/SiO_2 + AlEt_2OEt$	gas-phase 20 atm, 100 °C	3	1000	broad	0-2	0.960-0.945
$Cr(C_5H_5)_2/SiO_2$	gas-phase 20 atm, 100 °C	5	350	narrow	0-60	0.965-0.950
$TiCl_4/MgCl_2 + AlEt_3$	slurry 12 atm, 70-90 °C	5-15	500-1000	narrow	0-60	0.965-0.925

unique property, that is the molecular mass can easily be regulated by H_2. It has not been succeeded so far to substitute this catalyst by catalysts obtained with the use of more simple inorganic chromium compounds.

Supported zirconium-organic catalysts are as active as chromium systems, and apparently, can be used in the technology of production of polyethylene of various types.

CONCLUSIONS

The interaction of organometallic systems with surface functional groups of the support is the direct method for the synthesis of nearest precursors of active centers of ethylene polymerization. The complete utilization of the supported metal in the formation of active centers is not yet achieved, but at present the number of active centers can reach up to 30% of the supported metal.

The interaction of organometallic complexes with surface hydro-

xyl groups makes it possible to obtain active catalysts for ethylene polymerization. It does not allow, however, preparation of sterespecific catalysts of α-olefin polymerization. The search for systems, obtained by the interaction of organometallic compounds with more complex functional groups, which would provide steric control of the propagation reaction in supported organometallic systems, seems to be of great importance for future development.

REFERENCES

1. R.L.Banks,and C.F.Cook, "Catalyst Technology: Discovery to Commercialization. Disproportionation of Propylene in Modern Aspects of Catalysis, Nauka, Novosibirsk, 1978, p. 149. Yu.I. Yermakov, editor.
2. D.C.Bailey and S.H.Langer, Chem.Rev., 81, 105 (1981).
3. R.L.Burwell, Jr., J.Catal., 86, 301 (1984).
4. Yu.I.Yermakov, L.N.Arzamaskova and V.L.Kuznetsov, Koord.Khim., 10, 877 (1984).
5. V.L.Shmonina, N.N.Stefanovskaya, E.I.Tinyakova and B.A.Dolgoplosk, Vysokomol.Soed., 12B, 566 (1970).
6. Yu.I.Yermakov, "Application of Organometallic Compounds of Transition Metals for the Synthesis of Supported Catalysts, Nauka, Novosibirsk, 1971, p. 5.
7. Yu.I.Yermakov, A.M.Lazutkin, E.A.Demin, Yu.P.Grabovski and V.A.Zakharov, Kinet.Katal., 13, 1422 (1972).
8. D.G.H.Ballard, Advan.Catal., 23, 263 (1973).
9. Ch.Wu, A.W.Dow, R.N.Johnson and W.L.Carrick, J. Polym. Sci., A-1, 2621 (1972).
10. Yu.I.Yermakov and B.N.Kuznetsov, Dokl. Akad. Nauk SSSR, 207, 644 (1972).
11. Yu.I.Yermakov, Catal.Rev.-Sci. Eng., 13, 77 (1976).
12. Yu.I.Yermakov, B.N.Kuznetsov and V.A.Zakharov, "Catalysis by Supported Complexes", Elsevier, 1981.
13. Yu.I.Yermakov and V.A.Zakharov, Advan. Catal., 24, 173 (1975).
14. V.A.Zakharov and Yu.I.Yermakov, Catal. Rev.-Sci. Eng., 19, 67 (1979).
15. Yu.I.Yermakov, J. Molec. Catal., 21, 35 (1983).
16. V.A.Zakharov, V.K.Dudchenko, E.A.Paukshtis, L.G.Karakchiev and Yu.I.Yermakov, J. Molec. Catal., 2, 421 (1977).

17. G.A.Nesterov, V.A.Zakharov, E.A.Paukshtis, E.N.Yurchenko and Yu.I.Yermakov, Kinet. Katal., 20, 428 (1979).
18. G.A.Nesterov, V.M.Mastikhin, O.V.Lapina and V.A.Zakharov, React. Kinet. Catal. Lett., 19, 175 (1982).
19. C.Groeneveld, P.P.M.M.Wittgen, H.P.M.Swinnen, A.Wernsen and G.C.A.Schuit, J. Catal., 83, 346 (1983).
20. Yu.I.Yermakov, V.A.Zakharov, Yu.P.Grabovski and E.G.Kushnareva, Kinet. Katal., 11, 519 (1976).
21. Yu.I.Yermakov, O.N.Alekseev and Yu.A.Ryndin, Kinet. Katal., in press.
22. V.A.Zakharov, V.K.Dudchenko, A.M.Kolchin and Yu.I.Yermakov, Kinet. Katal., 16, 808 (1975).
23. R.A.Settergnist, F.N. Teble and W.G.Peet, in "Coordination polymerization", Ed. by Ch.C.Price and E.J.Vandenberg, Plenum Press, 1983, p. 167.
24. M.A.Makarova, G.A.Nesterov, V.A.Zakharov, K.H.Thiele, A.Dimitrov and Yu.I.Yermakov, React. Kinet. Catal. Lett., 21, 239 (1982).
25. G.A.Nesterov, V.A.Zakharov and K.H.Thiele, React. Kinet. Catal. Lett., in press.
26. G.A.Nesterov, V.A.Zakharov, V.V.Volkov and K.G.Myakishev, Vysokomol. Soed., 10, 755 (1979).
27. G.A.Nesterov, V.A.Zakharov, E.A.Paukshtis, E.N.Yurchenko, V.V. Volkov and K.G.Myakishev, Kinet. Katal., 21, 736 (1980).
27a. G.A.Nesterov, V.A.Zakharov, V.V.Volkov and K.G.Myakishev, J. Molec. Catal., in press.
28. V.V.Volkov and K.G.Myakishev, Izv. Sib. Otd. Akad. Nauk SSSR, Ser. Khim. Nauk, 2, 77, (1977).
29. H.E.Evans and W.H.Weinberg, J. Am. Chem. Soc., 102, 9548 (1980).
30. I.I.Murus, W.I.Kennelly, I.R.Kolb and L.A.Shimp, Inorg. Chem., 11, 2540 (1972).
31. I.E.Bercau, R.M.Marvich, L.E.Bell and H.H.Brintzinger, J. Am. Chem. Soc., 94, 1219 (1972).
32. M.Yu.He, R.L.Burwell, Jr., and T.J.Marks, Organometallics, 566 (1983).
33. M.Yu.He, G.Xiong, P.J.Toscano, R.L.Burwell, Jr. and T.J.Marks, J. Am. Chem. Soc., 107, 641 (1985).
34. J.Toscano and T.J.Marks, J. Am. Chem. Soc., 107, 653 (1985).
35. P.L.Watson, J. Am. Chem. Soc., 104, 337 (1982).

36. Yu.I.Yermakov, V.A.Zakharov and K.Sh.Ovchinski, Kinet. Katal., 13, 248 (1972).
37. Yu.A.Noghin, Yu.A.Ryndin, Yu.B.Zverev and Yu.I.Yermakov, React. Kinet. Catal. Lett., in press.
38. V.Gausing and G.Wilke, Angew. Chem., 93, 201 (1981).
39. H.Bounemann, B.Bogdanovich, Angew. Chem. int. Ed. Eugl, 22, 732 (1983).
40. A.N.Startsev, B.Bogdanovic, G.Wilke, V.N.Rodin and Yu.I.Yermakov, Chem. Commun., in press.
41. Yu.I.Yermakov, V.A.Mikhalchenko, V.S.Beskov, Yu.P.Grabovski and I.V.Emirova, Plast. Massy, 9, 6 (1970).
42. N.V.Semikolenova, G.A.Nesterov and V.A.Zakharov, Vysokomol. Soed., in press.
43. Yu.I.Yermakov, Pure Appl. Chem., 52, 2075 (1980).
44. J.H.Tueben, E.J.M. De Boer, A.H.Klazinge and E.Kler, J. Mol. Catal., 13, 107 (1981).
45. S.J.Tauster, S.C.Fung and R.L.Garten, J. Am. Chem. Soc., 100, 170 (1978).
46. Yu.I.Yermakov, B.N.Kuznetsov and Yu.A.Ryndin, React. Kinet. Catal. Lett., 2, 151 (1975).
47. M.S.Ioffe, B.N.Kuznetsov, Yu.A.Ryndin and Yu.I.Yermakov, 6-th Intern. Congress on Catalysis, London, 1976, preprint A5.
48. Yu.I.Yermakov, B.N.Kuznetsov and Yu.A.Ryndin, J. Catal., 42, 73 (1976).
49. Yu.I.Yermakov, Yu.A.Ryndin, O.S.Alekseev and M.N.Vassileva, J. Chem. Soc., Chem. Commun., 1480 (1984).

This page intentionally left blank

CHELATE COMPLEXES OF NICKEL: CATALYSTS FOR THE OLIGOMERIZATION/POLYMERIZATION OF ETHYLENE

W. Keim
Institut für Technische Chemie und Petrolchemie der Rheinisch-Westfälischen Technischen Hochschule Aachen, Worringer Weg 1,
D5100 Aachen, FRG

ABSTRACT

A number of uni-component complexes for the oligomerization/polymerization of ethene are presented. The complexes are chosen among square planar nickel complexes, which possess a five-membered chelate ring containing at least one phosphorous atom. Best results were obtained with P O-chelates yielding highly linear oligomers (α-olefins) and polymers. The use of amino-bis(imino)phosphoranes as ligands gave polymers, whose physical properties lie between those of high-pressure polyethylene and EPDM.

Introduction

The oligomerization/polymerization of ethene can be carried out with a variety of catalyst systems. Best known are catalysts consisting of a transition metal salt combined with a reducing agent. But also uni-component complexes have been reported to catalyse oligomerizations/polymerizations. The question arises whether both catalyst preparation methods will lead to identical catalytic intermediates (Figure 1).

The use of uni-component complexes as starting material offers a variety of advantages, especially for understanding. For instance, spectroscopic in situ investigations are less complex compared to those using Ziegler-Natta type catalysts. A further advantage rests in the amenability to tailor the ligand field in the complexes thus providing structural data. But one always must keep in mind that the uni-component complex itself is not the true catalyst and serves only as precursor.

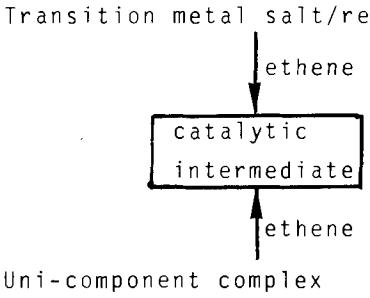

Figure 1. Different ways for catalyst preparation

Results

Some years ago, we initiated a program to investigate the oligomerization of mono olefins by nickel complexes (1-3). For our catalyst selection the model shown in Figure 2 was chosen

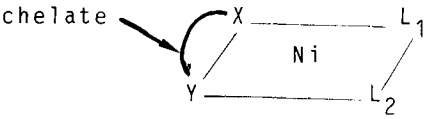

square planar
X = Y and X ≠ Y
X = donor, Y = acceptor
L_1 and L_2 must dissociate easily

Figure 2. Model for mono olefin oligomerization

Square planar nickel complexes provide appropriate orbitals to interact with incoming olefins. Chelate ligands favor square planar structures. In addition, the chelate should minimize the chance of coordinating olefins formed during the catalytic cycle. The ligands X and Y were chosen among soft and hard ligands. The ligands L_1 and L_2 should easily dissociate, thus providing empty coordination sites for the olefins to be oligomerized. The effect of the change on the metal and the attainment of an 18-valence shell of electrons are also two strong forces in determining preferred coordination number.

According to Figure 3 the complex 1 was synthesized which consists of a mixture of two isomers (4).

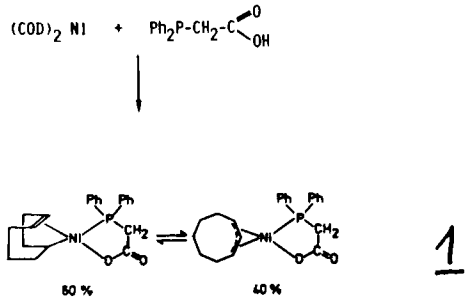

1

Figure 3. Synthesis of P⌒O-chelate complex 1

The addition of ethene to a toluene solution of 1 yielded linea α-olefins.

Table 1. Results of batch oligomerization of ethylene with catalyst 1

T, °C	$^{c}C_2H_4$, mol L^{-1}	$10^{-3}C_{cat.}$, mol^{-1}	conversn, %	N, s^{-1}	$\beta C_{10}-C_{20}$
75	0.38	2.3	53	0.14	0.39
75	0.83	2.53	59	0.23	0.30
75	2.41	2.34	50	0.47	0.29
75	4.72	2.47	41	0.57	0.29
75	7.00	2.70	32	0.62	0.30
75	8.95	3.39	30	0.57	0.34
75	11.22	2.64	15	0.48	0.50
75	4.58	0.99	24	0.71	0.24
75	4.22	5.00	65	0.53	0.37
60	4.83	2.27	9	0.17	0.16
85	4.95	2.29	62	1.12	0.10
95	4.75	2.32	69	1.83	0.10

Capillary GC analysis after 35-min total reaction time; products are > 99 % linear; α-olefin content > 95 %.

In Table 1 the results of the oligomerization experiments are summarized. After the autoclaves are charged at room temperature and immersed into a heat bath, thermal equilibrium is reached within 3-5 min, upon which the catalytic reaction commences immendiately as recorded by the pressure drop. At 25°C 1 shows no activity. From the initial rates specific turnover numbers N (mol of ethylene per mol of Ni per s) are calculated. The rate is first-order in catalyst concentration. Plotting 1/N over reciprocal ethylene concentration results in a straight line; only at very high concentrations of C_2H_4 is a deviation observed, probably due to a solvent effect of the substrate itself. This so-called Lineweaver-Burk diagram is in good agreement with the proposed Michaelis-Menten-type mechannism (5). The oligomers are practically 100 % linear and the α-olefin content ranges from 95 % to 99$^+$ %. This underlines the remarkable selectivity of 1 for ethylene only.

Interestingly, if complex 1 is suspended in n-hexane only high density linear polyethylene of molecular weights up to one million is formed. Similar results are obtained on supporting 1 to Al_2O_3 and using n-hexane as solvent. It is noteworthy that the polymerization can be carried out in water. This makes this type of complexes to potential candidates for the oligomerization/polymerization of functional group containing monomers.

A reaction mechanism accounting for the products obtained is shown in Figure 4.

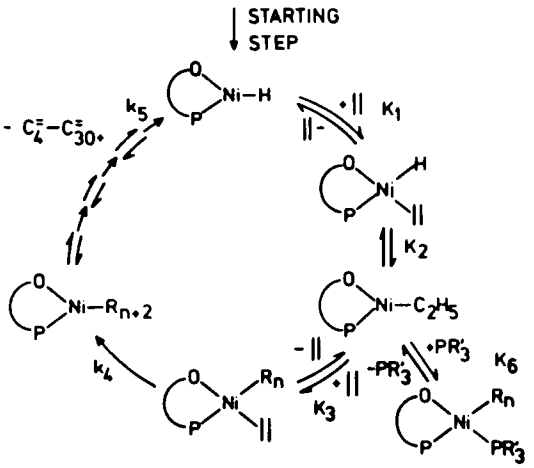

Figure 4. Reaction mechanism for ethene oligomerization

A widely accepted mechanism for olefine oligomerization invokes metal hydrides as active species. The formation of a nickel-hydride from 1 can easily be explained according to equation (1)

(1) 1 ⟶  + C_8H_{12} $\overset{P}{O}$ = $\emptyset_2PCH_2COO$

Indeed, 7 % 1,5-cyclooctadiene, 34 % 1,4-cyclooctadiene, 8 % 1,3- cyclooctadiene and 31 % Cyclooctene could be detected by GC analysis. However, all attempts to identify a nickel-hydride - even under reaction conditions using high pressure NMR (6) - failed. Therefore, one is forced to refer to analogous systems were hydrides have been isolated (7) or argue with known model reactions of metal-hydrides. It is not possible to completely rule out other mechanisms as depicted in Figure 5.

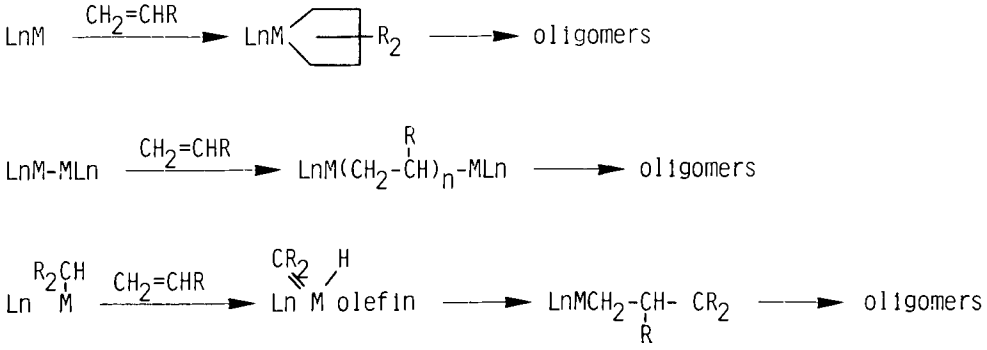

Figure 5. Possible reaction mechanisms for olefine oligomerization (7).

The use of $\emptyset P(CH_2COOH)_2$ and $P(CH_2COOH)_3$ in combination with $(cod)_2Ni$ yielded only high density polyethylene.

Further insight in the delicate nature of the chelate ligand necessary elucidated experiments using ligands such as $\emptyset_2P(CH_2)_nCOOH$ (n = 2,3), $\emptyset_2PCH_2CH_2OH$, $\emptyset_2PCH_2CH_2SH$, $\emptyset_2PCH_2CH_2NH_2$. All those ligands, upon reaction as desribed in Figure 3, yielded inactive systems.

Applying $\emptyset_2P(CH_2)_nCOOH$ (n = 2,3) could result in a too large chelate ring. (6 or 7 membered rings versus a 5 membered ring in 1)

To understand the requirements of the ligand field better it appeared of interest to investigate the demands of the P,O-chelate in more detail. According to equation 2 complex 2 could be isolated and its square planar structure - as requested by the model in Figure 1 - could be confirmed by x-ray analysis (5).

(2) $(cod)_2Ni + Ph_3P + Ph_3P{=}CH{-}CO{-}Ph \xrightarrow[-2\,cod]{}$ 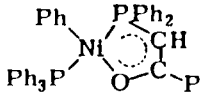 2

Reaction of a toluene solution of the complex 2 with ethylene (50 bar) at 50°C affords n-olefins which are up to 99 % linear and consists of up to 98 % of α-olefins. The olefins up to C_{30} analyzed by gas chromatography are present in a geometrical distribution. Activities of 6000 mol ethylene per mol of complex 2 are achieved. When the reaction of 2 with ethylene is carried out in n-hexane as suspension medium, again, high molecular linear polyethylene is formed.

As evident from Table 2 the β-value of the oligomers formed is determined by the ethene pressure used. The temperature has only a minor effect.

Table 2. Effect of pressure and temperaturure on the β-value of the ethene oligomerization using complex 2

Pressure C_2H_4 (bar)	conversion (%)	β-value
10	20	2.3
30	100	2.0
50	100	1.5
100	100	0.7

Temperature* (°C)	conversion (%)	β-value
30	-	-
50	10	1.1
80	100	1.2
100	100	1.2
120	decomposition	-

* 50 bar ethene applied.

For a mechanistic discussion it is assumed that a reaction path as outlined in Figure 4 is operating. The formation of a nickel-hydride can proceed as shown in equation 3.

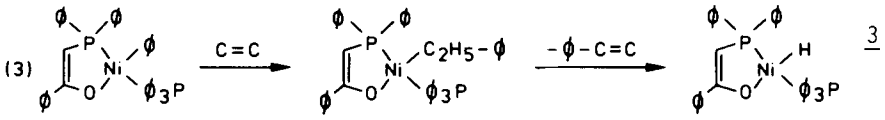

3

Indeed, styrene could be isolated in accordance with equation 3. Again, the proof of the nickel-hydride intermediate is pending.

Starting from the postulated intermediate 3 a pathway as indicated in Figure 6 could be invoked to describe the competition of ethene and $Ø_3P$ for free coordination sides.

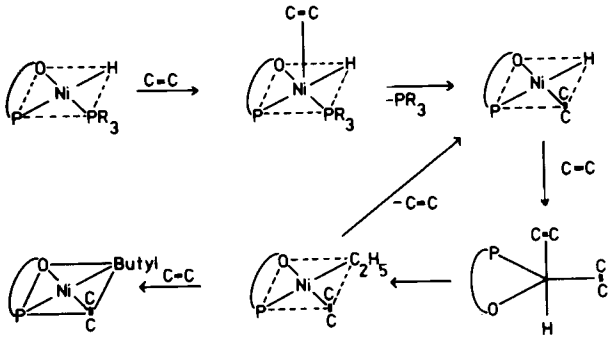

Figure 6. Competition of ethene and $Ø_3P$ for coordination sides

In a kind of "windshield wiper" exchange $\emptyset_3P$ will coordinate and dissociate. If such a picture is operable addition of $\emptyset_3P$ should effect the product selectivity. Indeed, by adding $\emptyset_3P$ to 2 the β-value can be altered (see Table 3).

Table 3. Effect of adding $\emptyset_3P$ to complex 2

$\emptyset_3P$ added (mol)	β-value	activity (TON)
pure complex	0.7	5000
0.2	0.9	4500
1	2.0	3500
4	7.4	500

70°C, 100 bar

Such a $\emptyset_3P$ coordination-dissoziation finds further support by in situ NMR measurements under reaction conditions at 100 bar ethene pressure (6). Here the $\emptyset_3P$ dissociation can be observed by P^{31}-measurements. In this way, the addition of $\emptyset_3P$ is a further handle to control the β-value. Furthermore, addition of equimolar amounts of Et_3P to 2 leads to inactive systems. This can be explained by considering a blocking of coordination sides for ethene because the basic Et_3P is strongly bound. Interestingly, adding $(\alpha\text{-naphthyl})_3P$ yields linear polyethylene.

In a general approach, complexes of type 1 and 2 can be broken up into a chelate part and into an organyl part

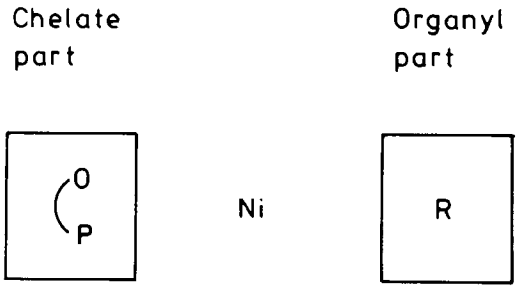

What impact on ethene oligomerization do changes in the organyl and the P⌒O-chelate part have? To answer this question a variety of complexes were synthesized. For the "ylid"-complexes reaction paths as shown in Figure 7 were chosen (8).

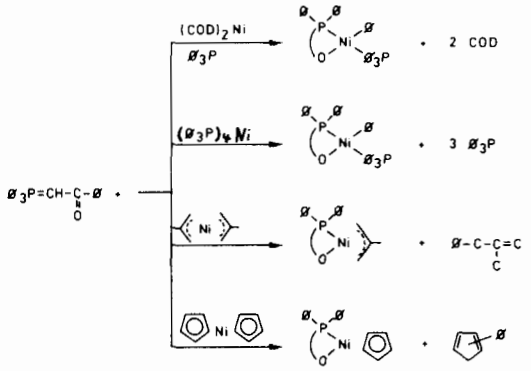

Figure 7. Synthesis routes for "ylid"-complexes

Figure 8 summarizes a number of complexes in which the P⌒O-chelate was slightly changed keeping the five-ring chelate constant.

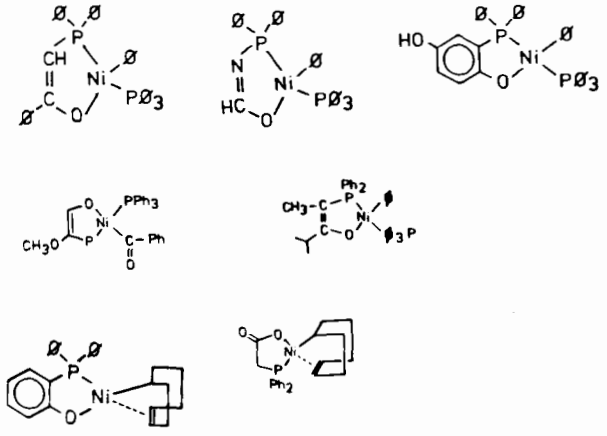

Figure 8. Complexes with changes in the P⌒O-chelate part

All complexes are highly active in ethene oligomerization and give similar results regarding linearity and α-olefin content. Figure 9 lists two groups of complexes in which the organyl part was altered.

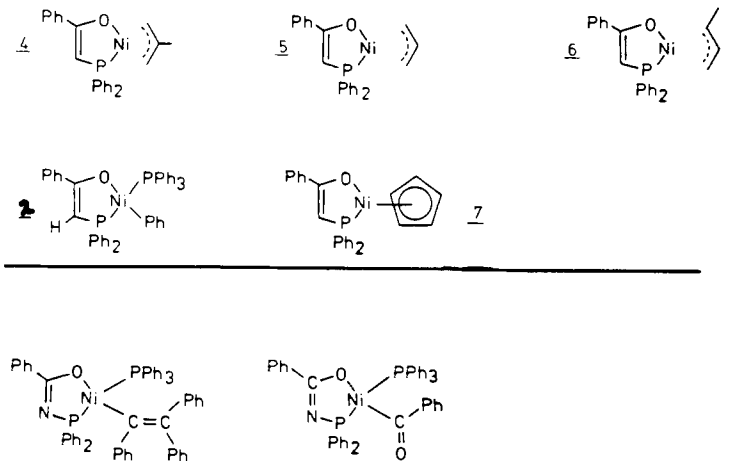

Figure 9. Complexes with changes in the organyl part

All seven complexes are highly active. Again, all compounds show only minor changes in product selectivity regarding linearity and α-olefin content. However, there are great differences at which temperatures the complexes will become active. The induction periode and the temperature leading to the active intermediates follow the order 2 >> 6 > 4 ~ 5 >> 7. Temperatures up to 120°C and induction periods of up to 15 minutes are needed to convert the uni-component starting complex 7 into an active system. These results can be understood by comparing the ease of nickel-hydride formation. Complex 2 easily inserts ethene yielding the nickel-hydride as shown in equation 3. To form nickel-hydride intermediates from the allyl complexes 4, 5, 6 butadiene or allene must be eliminated, a reaction whose equilibrium lies on the side of the complex (equation 4 and 5).

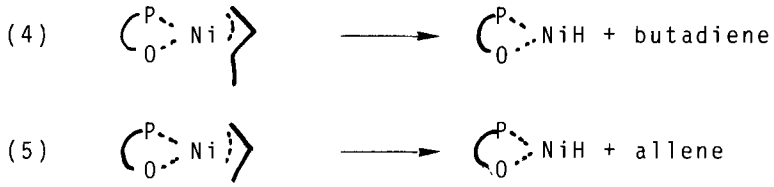

Complex 7 needs temperatures above 120°C explainable by the difficulty to displace the C_5H_5-ring. Addition of $\emptyset_3P$ to 4, 5, 6, 7 lowers the activation temperature. It can be assumed that from all uni-component complexes of Figure 9 similar active intermediates proposed as the nickel-hydride complex 3 will be derived.

All our results and observations over many years are in agreement with the following statement:

> The unicomponent starting complexes, which will lead to active and selective linear ethylene oligomerization/polymerization catalysts must be square planar and must possess a five-membered P O-chelate ring.

Based on the above statement it appeared of interest to include the bigger atom arsenic in our investigations. Using $\emptyset_2AsCH_2COOH$, which has the same pka-value as $\emptyset_2PCH_2COOH$, in combination with $(cod)_2Ni$ yielded practically inactive systems. However, with the ylid $\emptyset_3AsCHCO\emptyset$ the complex 8 could be isolated (9).

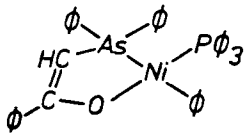

8

The x-ray structure confirms a square-planar arrangement of the ligands with a slight tilt to tetrahedral probably due to the bigger bite of the arsenic atom. The reaction of 8 with ethene leads already at 25°C to an active catalyst. The oligomers are > 95 % linear but the α-olefin content is lowered to 60-80 % indicating isomerization properties.

In our search for active P N-ligands we found that the reaction of $(cod)_2Ni$ with amino bis(imino)phosphorane results in active catalysts for the polymerization of ethene. Figure 10 summarizes the reaction conditions and the polymer data obtained (10).

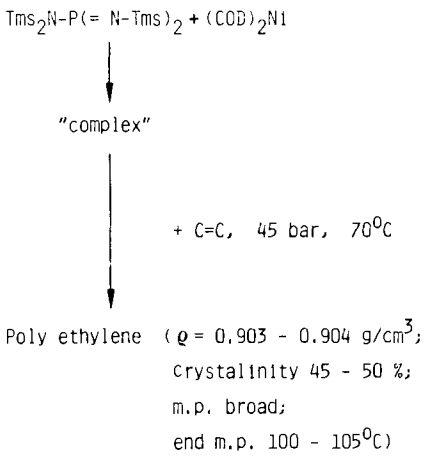

Figure 10. Ethene polymerization with amino bis(imino)phosphorane ligands

Activities of 1000 mol ethylene per mol of nickel are achieved. The physical properties of the short-chain branched polymer lie between those of high-pressure polyethylene and "EPDM". For a detailed description of the polymer and its mechanistic formation the work of Dr. Fink and Möhring, Max-Planck-Institut für Kohlenforschung, which is also included in this book, must be consulted.

All our attempts to isolate the "complex" in Figure 10 failed so far. However, using bis(η^3-allyl)nickel the complex 9 could be isolated according to equation 6.

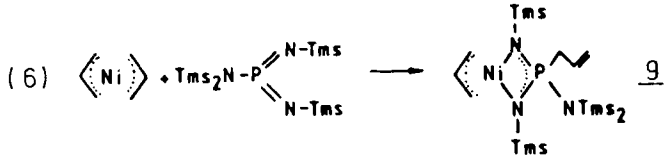

An y-ray analysis showed that 9 has a square planar structure. Disappoitingly, complex 9 is inactive in ethylene polymerization. Even addition of hydrogen didn't lead to an active system. But the in situ combination of bis(η^3-allyl)nickel with $(Me_3SiN)_2PN(SiMe_3)_2$ gave active catalysts. These results once more show that isolated complexes are not identical with catalytically active intermediates and one must be very cautious to refer to them as catalysts as often is done. Uni-component complexes, however, can be used in model reactions, which allow us to postulate intermediates - even catalytic species.

REFERENCES

1 a. W. Keim, A. Behr, M. Röper in Comprehensive Organometallic Chemistry, Vol. 5, 371-462 (1982)

2 b. W. Keim, Chimia 35, 344 (1981)

3 W. Keim "Fundamental Research in Homogeneous Catalysis", Plenum Press, Vol. 4, 131-145 (1984)

3 W. Keim Chem.-Ing.-Tech. 56, 850 (1984)

4 M. Peuckert, W. Keim Organometallics 2, 594 (1983)

5 F.H. Kowaldt, C. Krüger, W. Keim Angew. Chem. 90, 6, 493 (1978)

6 Togehter with Prof. Heaton at Canterbury unpublished

7 W. Keim in "Catalytic Transition Metal Hydrides", Annals of the New York Academy of Sciences, Vol. 415, 191-201 (1983)

8 W. Kein unpublished

9 W. Keim, A. Behr, B. Limbäcker, C. Krüger Angew. Chemie Int. Ed. 22, 6, 503 (1983)

10 W. Keim, R. Appel, A. Storeck, C. Krüger, R. Goddard Angew. Chemie Int. Ed. 20, 116 (1981)

This page intentionally left blank

MOLECULAR BEHAVIOUR OF SOLUBLE CATALYSTS FOR OLEFIN POLYMERIZATION
Part I: Ethylene insertion with soluble Ziegler Catalysts

G. FINK, W. FENZL and R. MYNOTT
Max-Planck-Institut für Kohlenforschung, D-4330 Mülheim a. d. Ruhr, Federal Republik of Germany

ABSTRACT

The development of the oligomer distribution during the polymerization of ^{13}C enriched ethylene by soluble Ziegler catalyst systems of the type $Cp_2TiMeCl/AlMe_nCl_n$ was followed by ^{13}C NMR spectroscopy. It is shown that the rate of formation of new chains can be monitored directly from the spectra. The concentrations of Ti-propyl and Ti-pentyl species during the polymerization were followed; both attain a steady state concentration. These results give a greater insight into the way that the oligomer distribution develops and into the dependence on the chain length of the first insertion steps.

INTRODUCTION

One suitable method for obtaining information on catalytically active systems without disturbing the reaction is ^{13}C NMR spectroscopy.

In an earlier publication[1] we reported our studies on the polymerization of ^{13}C-enriched ethylene using the soluble $Cp_2TiEtCl/AlEtCl_2$ catalyst in an NMR sample tube. Experiments using a batch reactor have shown that this Ti-Et system is a much more active polymerization catalyst than Ti-Me systems (see Fig. 1). The lowest curve (solid line) is for the $Cp_2TiMeCl/AlMeCl_2$ catalyst system, with which the polymerization proceeds much mor slowly. This catalyst is ideally suitable for the ^{13}C NMR investigations reported here and with the right choise of experimental parameters it has proved possible to obtain considerable detail of the reaction path of the insertion.

APPLICATION OF ^{13}C-ENRICHED ETHYLENE

In these experiments we used ethylene to over 90 atom % ^{13}C. Besides providing a considerable gain in sensitivity over ethylene with ^{13}C at natural abundance this allows the carbons in the polymer chain derived from ^{13}C-enriched ethylene to be distinguished from those from the Ti-Me or Al-Me carbons on the basis of their signal intensities. Whereas ^{13}C-^{13}C spin-spin couplings are observed in natural abundance ^{13}C NMR spectra only as very weak satellites, in enriched samples they may cause the signals to appear as multiplets. The proton-decoupled spectrum of enriched ethylene free in solution is a singlet because the two ^{13}C nuclei are magnetically equivalent. Once incorporated into a chain, these carbons are no longer chemically equivalent and the coupling between neighbouring ^{13}C nuclei is observed.

Table 1 summarizes the multiplet structures expected for a Ti-alkyl chain formed by the repeated insertion of ethylene enriched to 91 atom % ^{13}C at both carbons starting with a Ti-methyl at the natural isotopic abundance. For those molecules containing ^{13}C in the α-position there is a probability of 91 % that the β-carbon will also be ^{13}C and the α-carbon signal will therefore be split into a doublet. The remaining 9 % of the molecules have ^{12}C β-neighbours and show no coupling. The α-carbon signal is thus observed to be a doublet superimposed on a small signlet slightly shifted to the left of centre as a result of isotope shifts. The β-carbon has a probability of 82.8 % that both the α- and γ-carbons are ^{13}C anda triplet will be observed, while those isotopomers with only the α- or only the γ-carbon ^{13}C (combined probability 16.4 %) will give a doublet.

Inspection of the ^{13}C chemical shifts of the n-alkanes shows that the α-, β- and γ-carbons have characteristic shift ranges, but that for acrbon atoms from the δ-position to the chain centre the environments become too similar to produce any significant differences in their chemical shifts. These carbons in the middle of the chain have resonances at approximately 30 ppm. Similarly, for Ti-alkyls, the presence of the metal substituent on the α-carbon will produce no significant effect beyond the γ-carbon. Thus a signal at 30 ppm indicates that chains at least eight carbon atoms long are present; the larger its relative intensity the greater the fraction of even longer chains which are present. This peak is labelled in the spectra

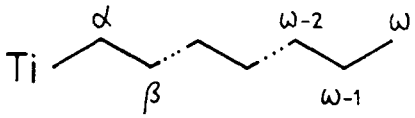

	α	β — (ω-2)	(ω-1)
Rel. Intensity	0.91	0.91	0.91
Fraction with 0	9.0	0.8	8.9
" 1	91.0	16.4	90.1
" 2	-	82.8	1.0
^{13}C neighbours (%)			

Ethylene: 91 atom % ^{13}C

Table 1. Multiplet structures expected for a Ti-alkyl chain formed of ethylene enriched to 91 atom % ^{13}C at both carbons starting with a T isotopic abundance

with the symbol 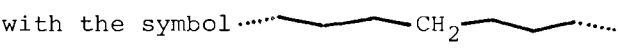 .

POLIMERIZATION

Figure 2 illustrates the first of a series of ^{13}C NMR spectra of the system reacting with ethylene. The upper spectrum was recorded at 213 K before the start of the reaction. The lower spectrum was measured after the sample had been kept at 258 K for 30 minutes and shows that the first insertion steps have occured as indicated by the small peaks of the β-carbons of Ti-propyl and Ti-pentyl. The ethylene signal at 123 ppm remains a sharp singlet and is unshifted, demonstrating that even at the chosen ratio Ti : Al : C_2H_4 = 1.0 : 0.95 : 0.7 no interaction with the catalyst is detectable.

In Figure 3, after a reaction time of 70 minutes, the α, β, γ, ω-2 and ω-1 signals of the different chains up to Ti-heptyl are to be discerned. In addition, the presence of a small peak at 30.7 ppm due to central CH_2-groups indicates that chains with a least 9 carbon atoms are present. Figure 4 shows the situation after 110 minutes. The signals reveal the developing oligomer distribution and the size of the peak of the central CH_2-groups has increased considerably. By the time that the reaction has been proceeding for approximately 3 hours (Fig. 5) this peak has become the major feature of the oligomer spectrum, showing that most chains are longer than Ti-nonyl.

Let us now consider how this result could arise when the initial concentration ratio Ti : C_2H_4 was 1.0 : 0.7. If <u>all</u> the initially added Ti had been active then at the end of the reaction on average less than <u>one</u> ethylene per Ti-CH_3 would have undergone insertion. In this case we would find mostly Ti-propyl chains and possibly a small quantity of Ti-pentyl chains. This assumes that all the ethylene has been consumed, but as can be seen in Fig. 5, there are much longer oligomer chains present even though there is a considerable amount of unreacted ethylene left.

The observation that longer oligomer chains have been formed is very important since it proves that not all the Ti has been able to undergo insertion. A large amount of Ti-CH_3 groups must therefore still be present. This is confirmed by the corresponding signal at 64 ppm, which represents a considerable concentration of Ti-methyl groups because the methyl group has <u>natural</u> ^{13}C abundance. This leads again to the conclusion, that the primary complex formed between Ti-

and Al-compound cannot be already the active species. Figure 6 gives a brief synopsis of the true reaction scheme which has been deduced from our previous experiments[2)4)5)] and which is confirmed by the experiments in this paper. The most important component of this reaction scheme for soluble Ziegler catalyst systems is the formation of the active species in two successive equilibrium steps. The first equilibrium lies well to the right, the second well to the left. Consequently at low ratios Al/Ti there is only a very small concentration of active species C^{*}. A further consequence is that the propagation process itself is then an intermittent process which causes the molecular weight distribution to undergo a particular type of development[4)5)].

The ^{13}C NMR spectrum recorded towards the end of the reaction (after 14.5 hours at 258 K) is illustrated in Fig. 7. In addition to the oligomer distribution and the strong "polyethylene" peak, the following features should be noted:

(I) Comparing the intensities of all Ti-α-peaks (i.e., Ti-α-propyl, Ti-α-($\geq$ pentyl)) at 90 ppm with the intensity of the Ti-methyl peak at 64 ppm and taking into account the ^{13}C abundances of 91 % and 1.1 %, respectively, one obtains the true concentration ratio of about 0.1 : 1.0. This indicates that only 10 % of the initial Ti-methyl compound has been involved in insertion reactions. This is to be expected from the location of the successive equilibria at the chosen ratio of Ti/Al = 1 : 1.

(II) The signal of the ω-carbon at approximately 14 ppm is very weak since it is at the natural abundance of ^{13}C.

(III) The (ω-1) peak for Ti-heptyl and longer chains is clearly a doublet, produced by coupling with only <u>one</u> adjacent ^{13}C nucleus (see Table 1).

Both (II) and (III) prove that the insertion has occurred into the Ti-carbon bond.

(IV) After the long reaction time of 15.5 hours, small quantities of α-olefines are formed as indicated by the weak signals at 114 and 140 ppm. This means that a transfer reaction to the monomer <u>via</u> H-β-elimination has occurred.

The experiment described above has provided general information on the course of the polymerization reaction. We have carried out further investigations aimed at obtaining more details on the chain propagation itself. Figure 8 illustrates the series of spectra recorded for a sample of $Cp_2TiMeCl/AlMe_2Cl/^{13}C_2H_4$ in the ratio 1 : 2 : 2, to increase the concentration of active species. The potential of this approach is apparent. These spectra, each measured over a period of an hour, were recorded successively in order to follow the development in chain growth. The regions depicted are for the Ti- α resonances and for the signals for the β to ω -1 positions.

First of all it is to notice in Figure 8 the rapid increase of the peak of the central CH_2-groups. This is again in full agreement with our reaction scheme because now we have more active species.

Furthermore it is to see in this presentation, that we were successfull in better separating the peaks of the different chain carbon atoms.

Hence, we discover that the propyl chains (as to see by the Ti-α- or Ti-β-propyl positions in the spectrum) and the pentyl chains (as to see by the Ti-(β+γ)- or (ω-1)-pentyl positions in the spectrum) remain constant during the reaction; i.e., here is visible a steady state of the concentration of these chains.

The integration[+)] of the Ti-propyl, the Ti-pentyl peaks and the peaks of β-heptyl and longer chains leads to the important result in Figure 9: after the starting phase of the chain development the concentrations of propyl chains and pentyl chains attain a steady state. The reason for is the dependence on the chain length of the first insertion steps.

For this steady state now the equations hold written at the top of the diagramm. The evaluation shows, that the ratio of the propagation constants k_{propyl} and k_{pentyl} is about equal 2. That means, the insertion into a Ti-propyl chain is twice faster than the insertion into a Ti-pentyl chain.

[+)] This is a preliminary evaluation because the β- and γ-resonances of the Ti-pentyl species lie very close together. A detailled separation by spectra simulation is in working.

This confirms exactly our former results of oligomer kinetics by means of a plug flow reactor and GPC analysis[3)5)], where we did find that k_{propyl} has a value of 96 l/mol·sec and k_{pentyl} has a value of 48 l/mol·sec.

EXPERIMENTAL

The ^{13}C NMR spectra were recorded on a Bruker WM-300 spectrometer at a frequency of 75.5 MHz. Samples were measured in 10 mm tubes dissolued in D_8-toluene which had been dried over $LiAlH_4$, degassed several times and distilled in vacuum. Chemical shifts were recorded relative to the CD_3-signal of the D_8-toluene solvent as internal reference and converted to the TMS scale (δ_{CD_3} = 20.47 at 258 K).

For preparation of the NMR-samples see ref. 1.

REFERENCES

1. G. Fink and R. Rottler, Angew. Makromol. Chemie 94, 25 (1981).
2. G. Fink and W. Zoller, Makromol. Chem. 182, 3265 (1981).
3. G. Fink and G. Döllinger, J. Appl. Polymer Sci.: Appl. Polymer Symp. 36, 67 (1981).
4. G. Fink and D. Schnell, Angew. Makromol. Chemie 105, 15 (1982).
5. G. Fink and D. Schnell, Angew. Makromol. Chemie 105, 31 (1982).

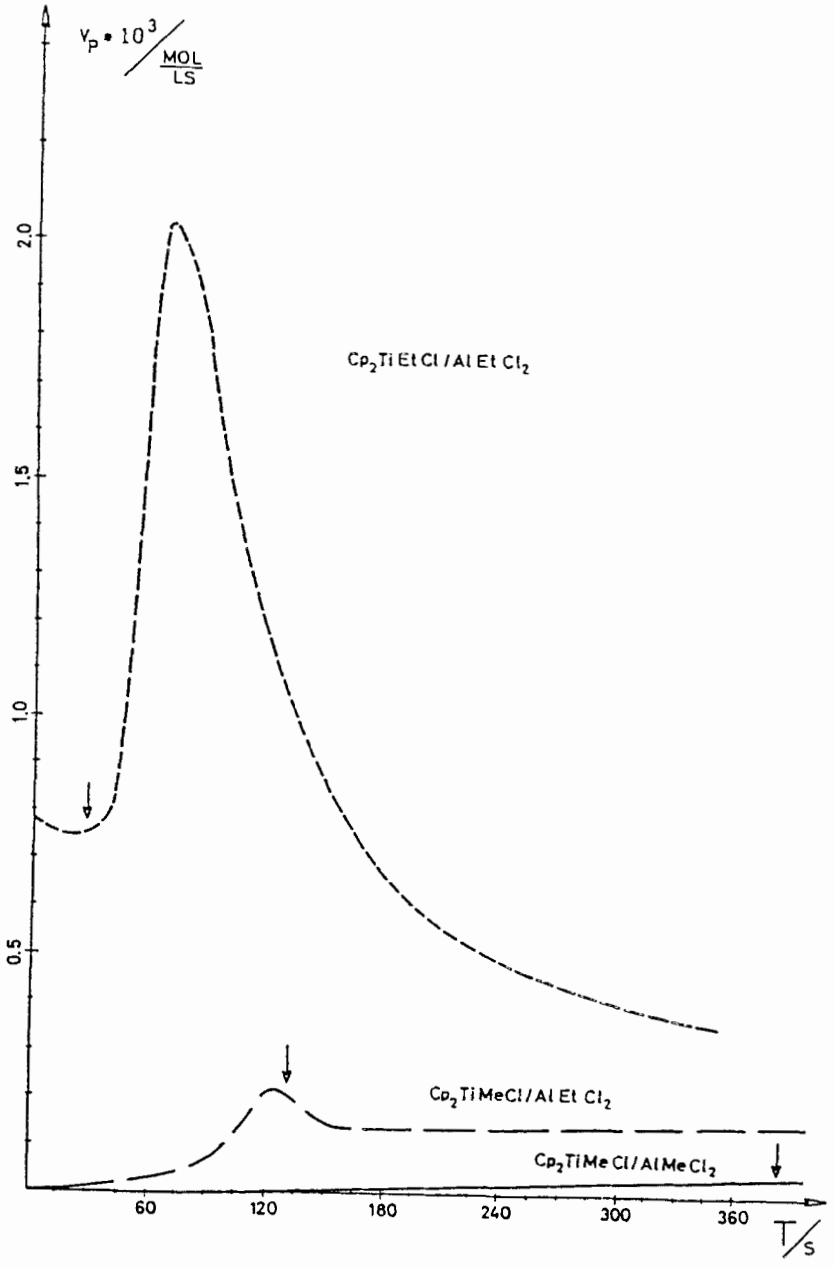

Figure 1. Overall polymerization rate of ethylene versus time for various Ti/Al catalysts determined in a batch reactor by following the rate of consumption of ethylene. (For experimental method see reference[2]). Al/Ti = 4; $[Ti] = 3.10^{-3}$ mol/l; $[C_2H_4] = 0.089$ mol/l; solvent toluene; T = 283 K.

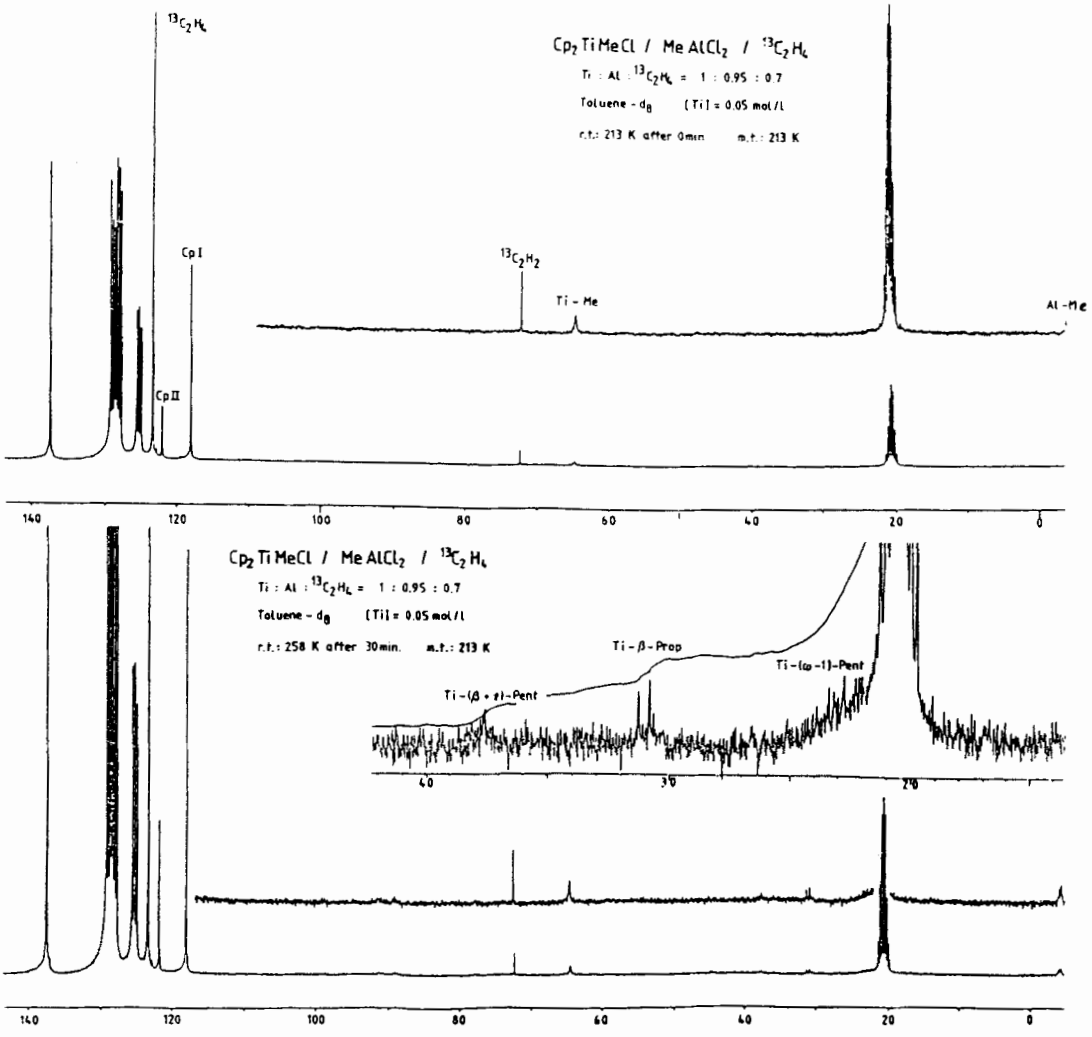

Figure 2. 75.5 MHz ^{13}C NMR spectra of the system $Cp_2TiMeCl/AlMeCl_2$ reacting with $^{13}C_2H_4$ in toluene-d_8 recorded at 213 K; $[Cp_2TiMeCl]$ = 0.05 mol/l; [Ti] : [Al] : $[^{13}C_2H_4]$ = 1 : 0.95 : 0.7. Upper spectrum: at start of reaction (0 minutes). Lower spectrum: after the sample had reacted for 30 minutes at 258 K and then been cooled rapidly to 213 K.

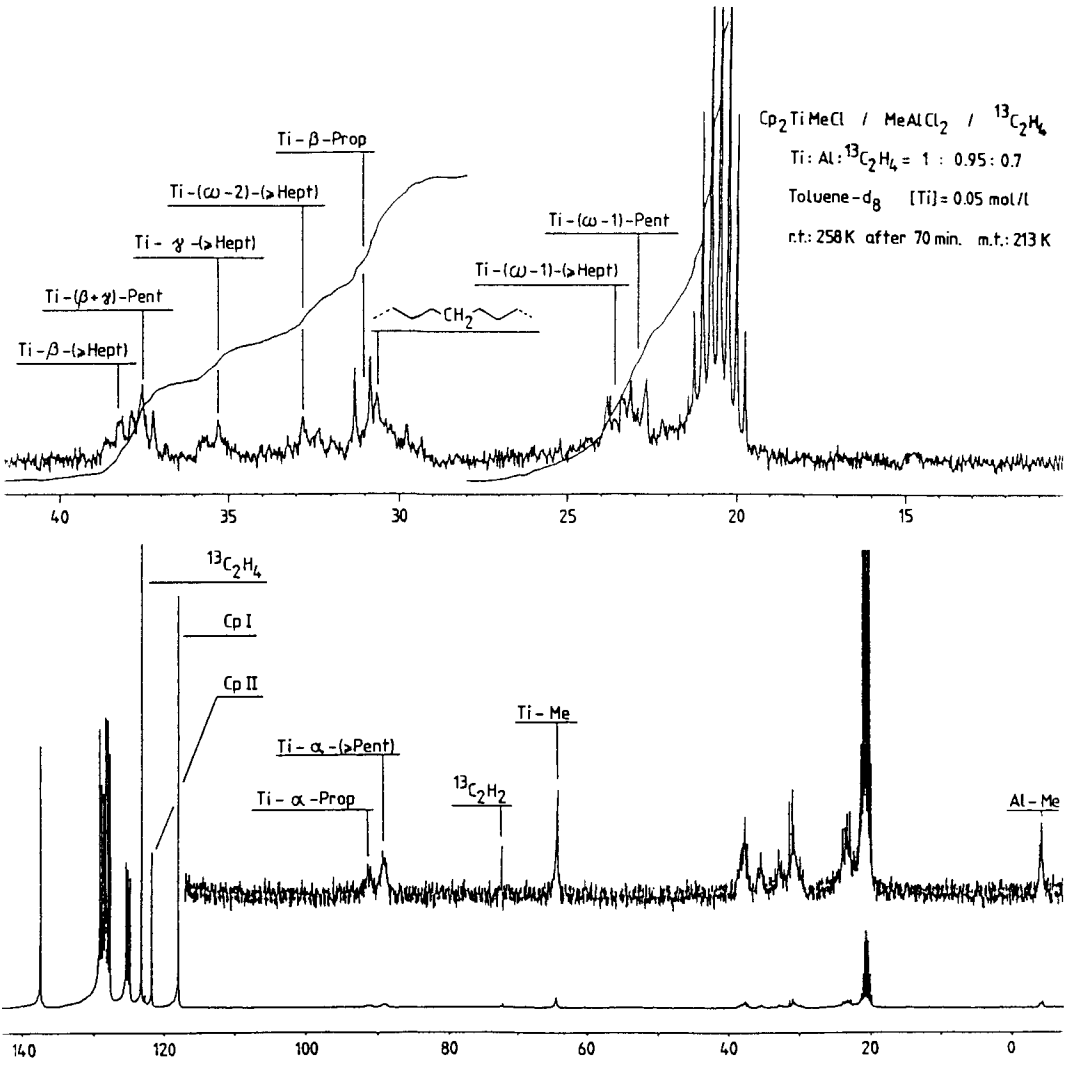

Figure 3. As for Fig. 2, but after a total reaction time of 70 minutes at 258 K.

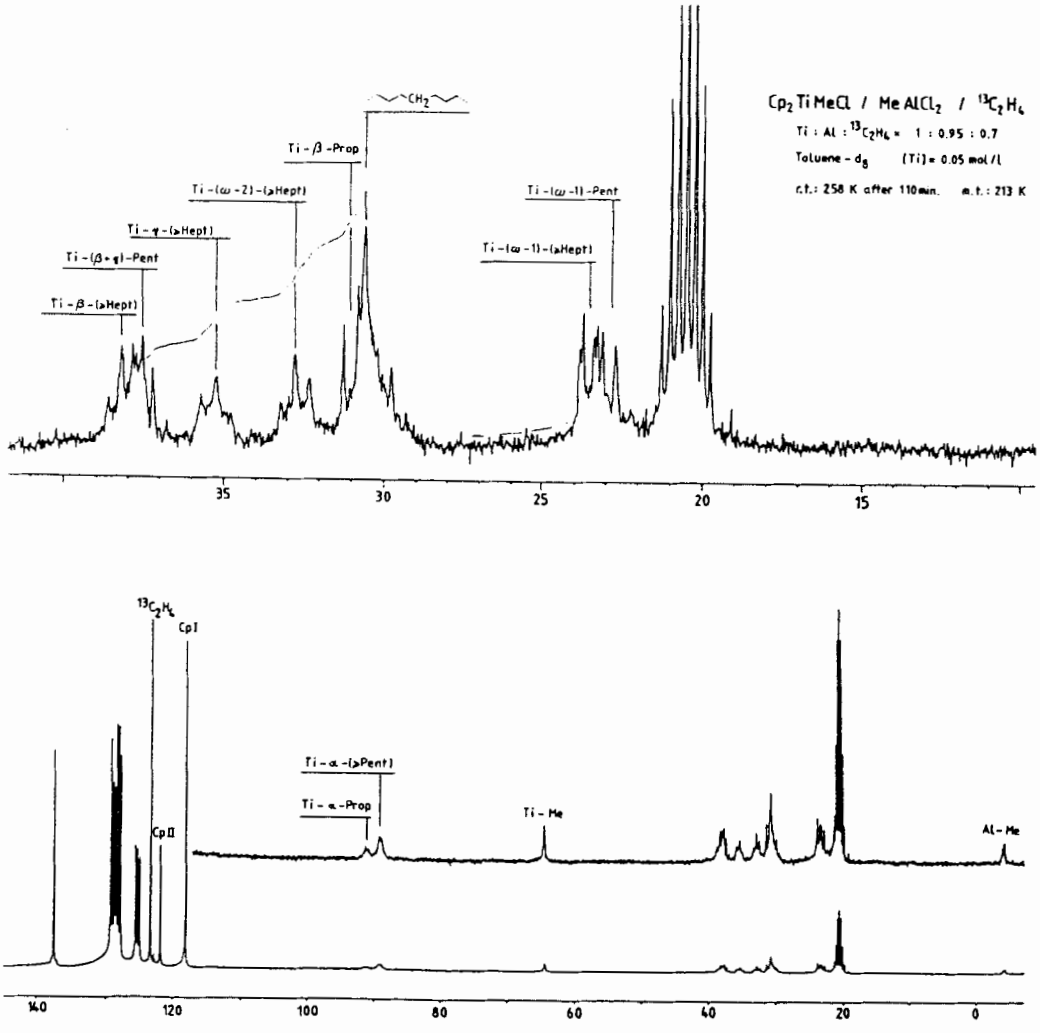

Figure 4. As for Fig. 2, but after a total reaction time of 110 minutes at 258 K.

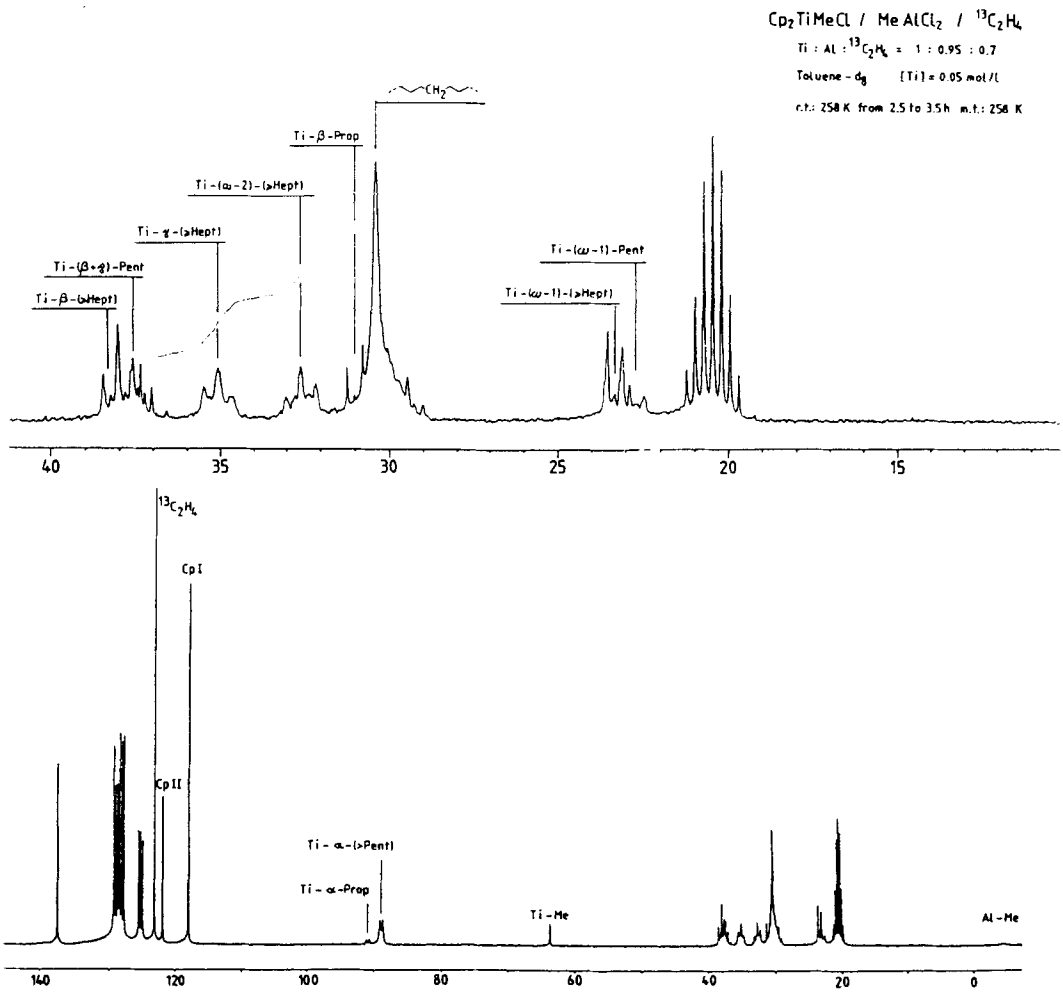

Figure 5. ^{13}C NMR spectrum of the system $Cp_2TiMeCl/AlMeCl_2$ reacting with $^{13}C_2H_4$ in toluene-d_8 at 258 K.
$[Cp_2TiMeCl]$ = 0.05 mol/l;
$[Ti] : [Al] : [^{13}C_2H_4] = 1 : 0.05 : 0.7$.
Spectrum recorded at 258 K at between 2.5 and 3.5 hours of reaction time.

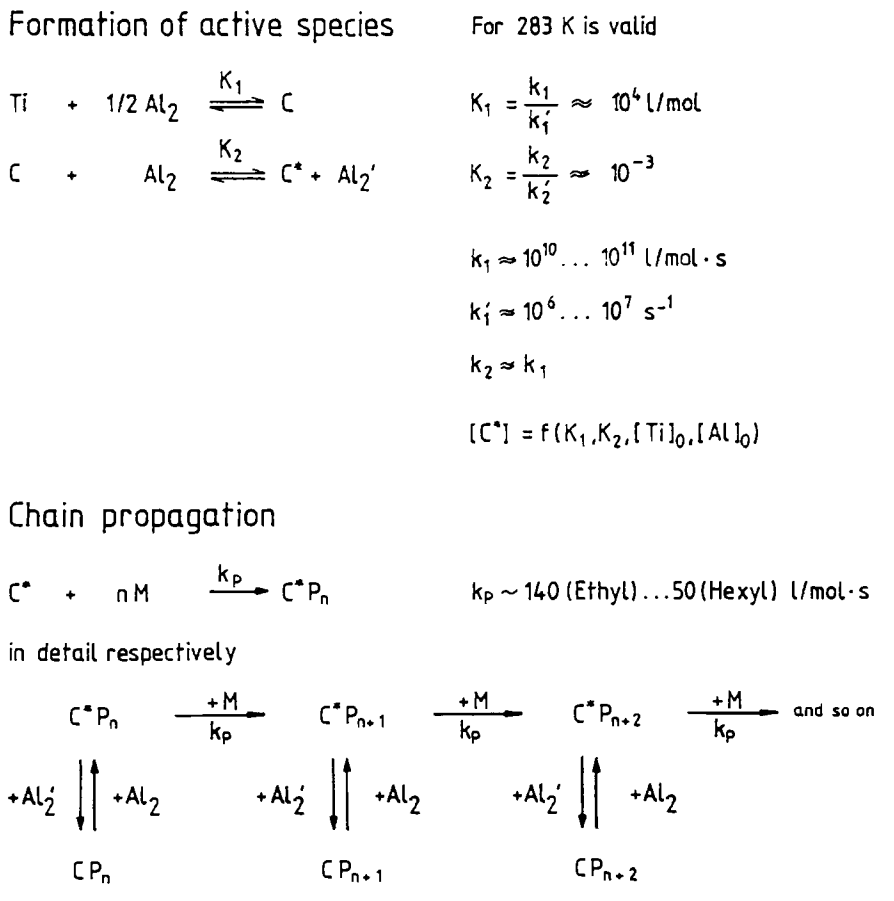

Figure 6. Reaction scheme of the successive equilibria using soluble Ziegler catalysts for ethene polymerization (Cp_2TiRCl/AlR_xCl_y/ toluene).

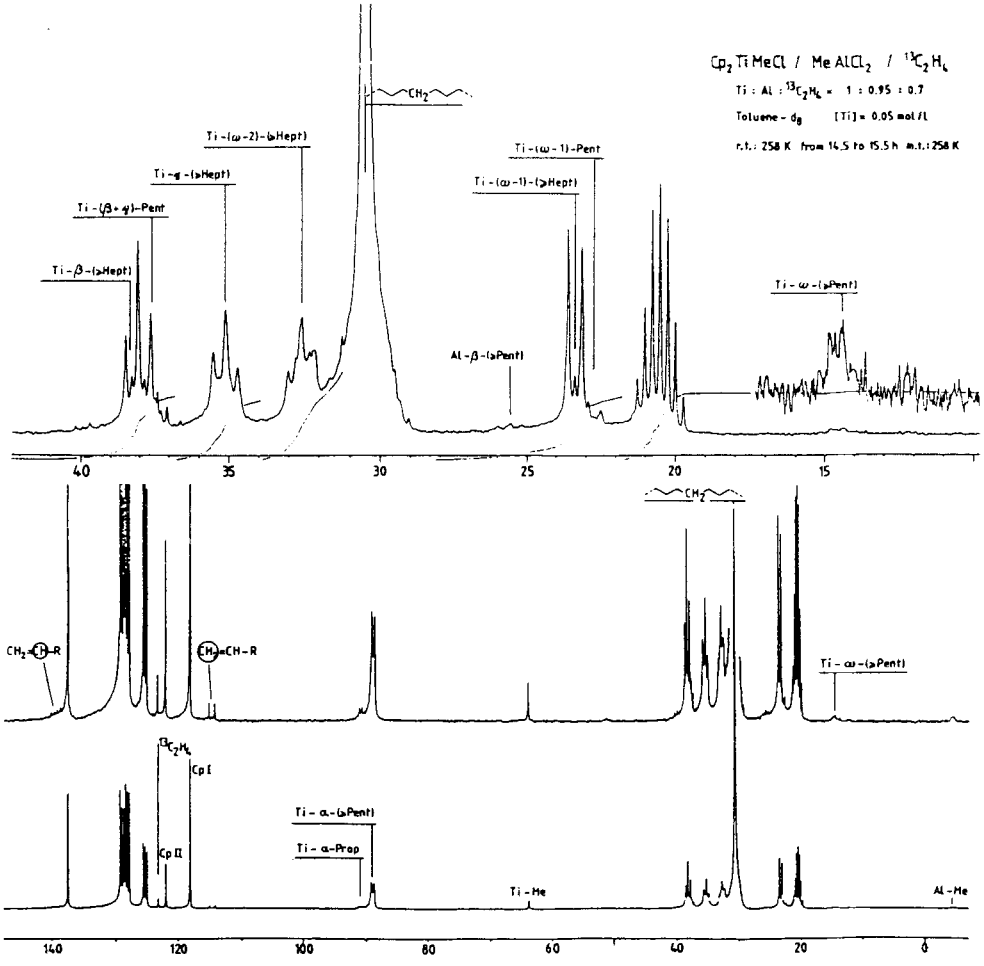

Figure 7. ^{13}C NMR spectrum of the system $Cp_2TiMeCl/AlMeCl_2$ reacting with $^{13}C_2H_4$ in toluene-d_8 at 258 K.
$[Cp_2TiMeCl]$ = 0.05 mol/l;
$[Ti] : [Al] : [^{13}C_2H_4] = 1 : 0.95 : 0.7$.
Reaction time from 14.5 to 15.5 h.

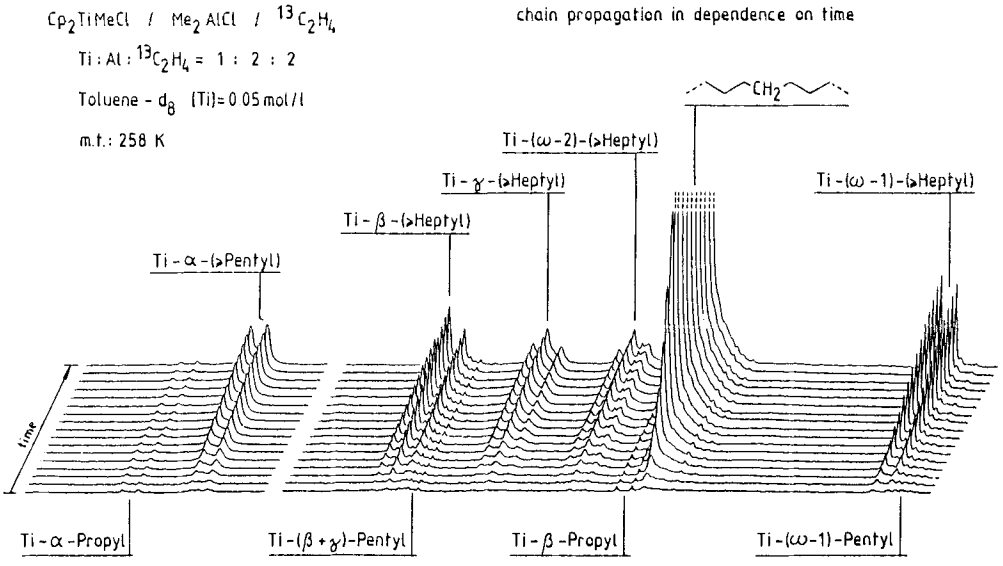

Figure 8. 75.5 MHz ^{13}C NMR spectra of the system $Cp_2TiMeCl/AlMe_2Cl$ reacting with $^{13}C_2H_4$ in toluene-d_8 at 258 K.
Initial $[Cp_2TiMeCl]$ = 0.05 mol/l;
$[Ti] : [Al] : [^{13}C_2H_4] = 1 : 2 : 2$.
These spectra, each measured over a period of an hour, were recorded successively in order to follow the development in chain growth. The regions depicted are for the Ti-α resonances and for the signals for the β to ω-1 positions.

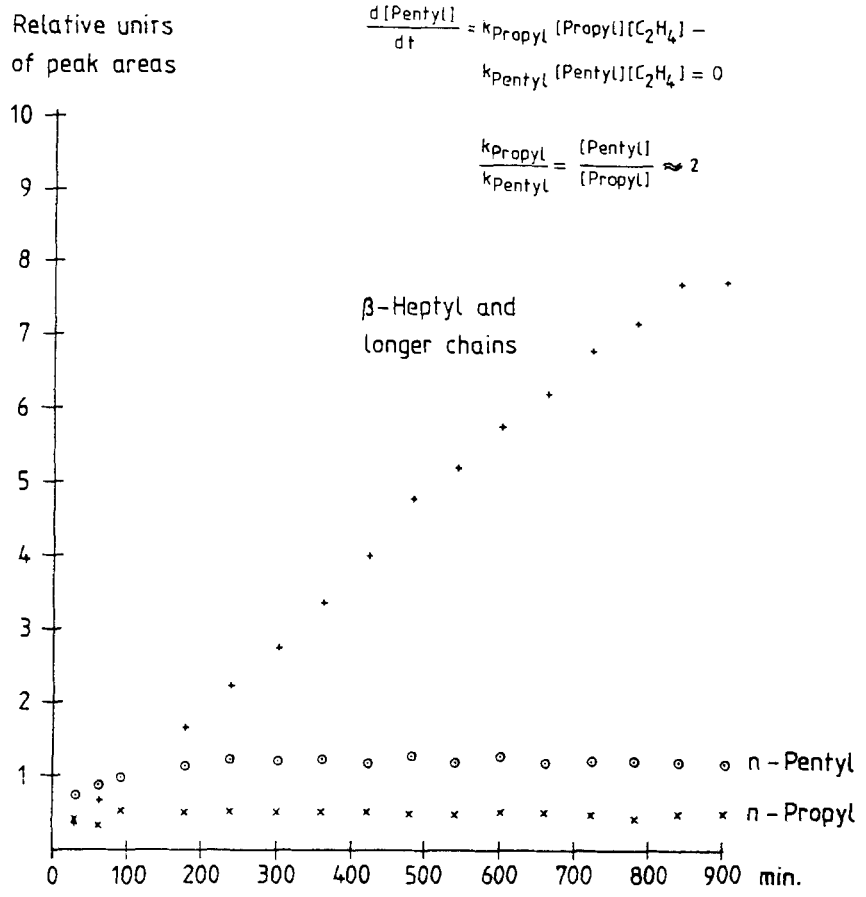

Figure 9. Integration of the spectra (preliminary evaluation) of Fig. 8; steady state concentrations for Ti-propyl and Ti-pentyl chains.

PART II: A NEW TYPE OF α-OLEFIN POLYMERIZATION WITH NI(O)/PHOSPHORANE CATALYSTS

G. FINK and V. MÖHRING
Max-Planck-Institut für Kohlenforschung, D-4330 Mülheim a. d. Ruhr, Federal Republik of Germany

ABSTRACTS

The soluble catalyst system Ni-compound/bis(trimethylsilyl)-amino-bis(trimethylsilylimino)phosphorane is able to polymerize α-olefins only by 2-ω-linkage of the monomers.

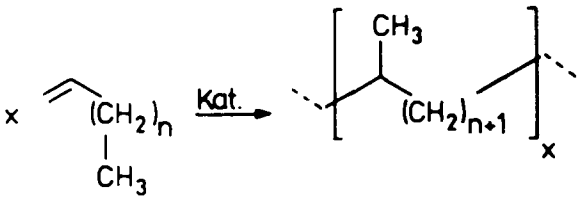

This reactions leads to only methyl branched chains in which the methyl groups have the regular distance of n+1 CH_2-groups. A migration of the catalyst complex along the side chain of the α-olefin is discussed.

INTRODUCTION

The polymerization of ethylene with the catalyst system Ni-compound/bis(trimethylsilyl)amino-bis(trimethylsilylimino)phosphorane (Figure 1 above) generates according Keim[1] short chain branched polyethylene. Now we found, that this system can be used for α-olefin polymerization too and that surprisingly the structure of the products does not correspond with the usual 1.2-linkage of the monomers to comblike polymers, but with a 2.ω-linkage (Figure 1 middle line).

STRUCTURE OF THE POLYMERS

The branching structure of these poly-α-olefins is unusual. Polymerizing of α-olefins leads to only methyl branched polymer

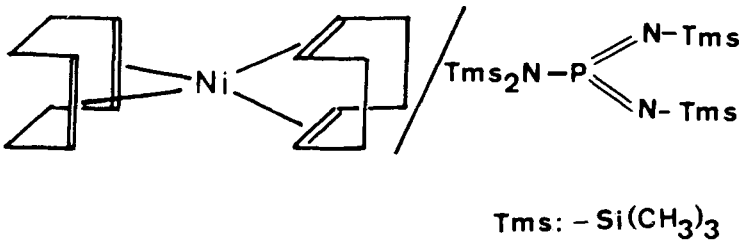

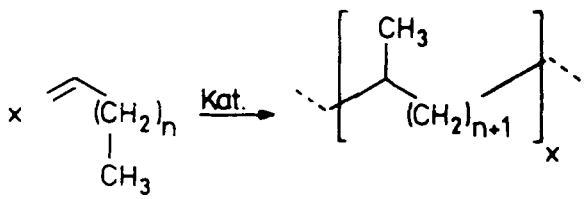

Figure 1 Ni(0)/Phosphorane catalyst (above)

2.ω- linkage of the linear α-olefin (below)

chains, in which moreover the methyl groups have the regular distance of n+1 CH_2-groups. Furthermore, these distances can be varied according to the length of the side chain of the α-olefin.

The structure of these products is proved unambiguous by ^{13}C NMR analysis.

Two examples are shown in Figures 2 and 3. The assignment of the signals was carried out by means of the increment rules of Lindemann/Adams[2]. All signals, which are expected in 2.ω-linkaged α-olefin polymers, have been found in the spectra.

The analysis of the ^{13}C NMR spectra of polymers formed with deuterated α-olefins demonstrated, that the propagating chain is bound to the next α-olefin by $C_\omega \longrightarrow C_2$-linkage; during this process the C_1-atom of the double bond forms the later methyl branching in the polymer.

Gel permeation chromatographical and ^{13}C NMR spectroscopical determination of the molecular weights of the formed poly-α-olefins shows further, that independent of the length of the used monomer the gram-molecular weight has always the same value (for instances at 298 K about 1000 g/mol). In other words, and this is shown in Figure 4, the polymerization degree is decreased linear with elongated α-olefin.

MIGRATION MECHANISM

Considering all results[3] we developed a mechanism which can explain this special structure of the poly-α-olefins. The central topics of the reaction scheme in Figure 5 are:

i) the monomer can insert only in a primary Ni-alkyl on the end of the propagating chain.

ii) there is regioselectivly only $C_\omega \longrightarrow C_2$-linkage of the propagating chain with the next monomer.

iii) between two insertion steps a migration of the Ni-catalyst complex takes place along the polymer chain; during this migration indeed transfer reactions to the monomer occur but no insertion reactions.

A more detailled mechanistic proposal is shown in Figure 6. Again for the example of the buten-1-polymerization an alternating

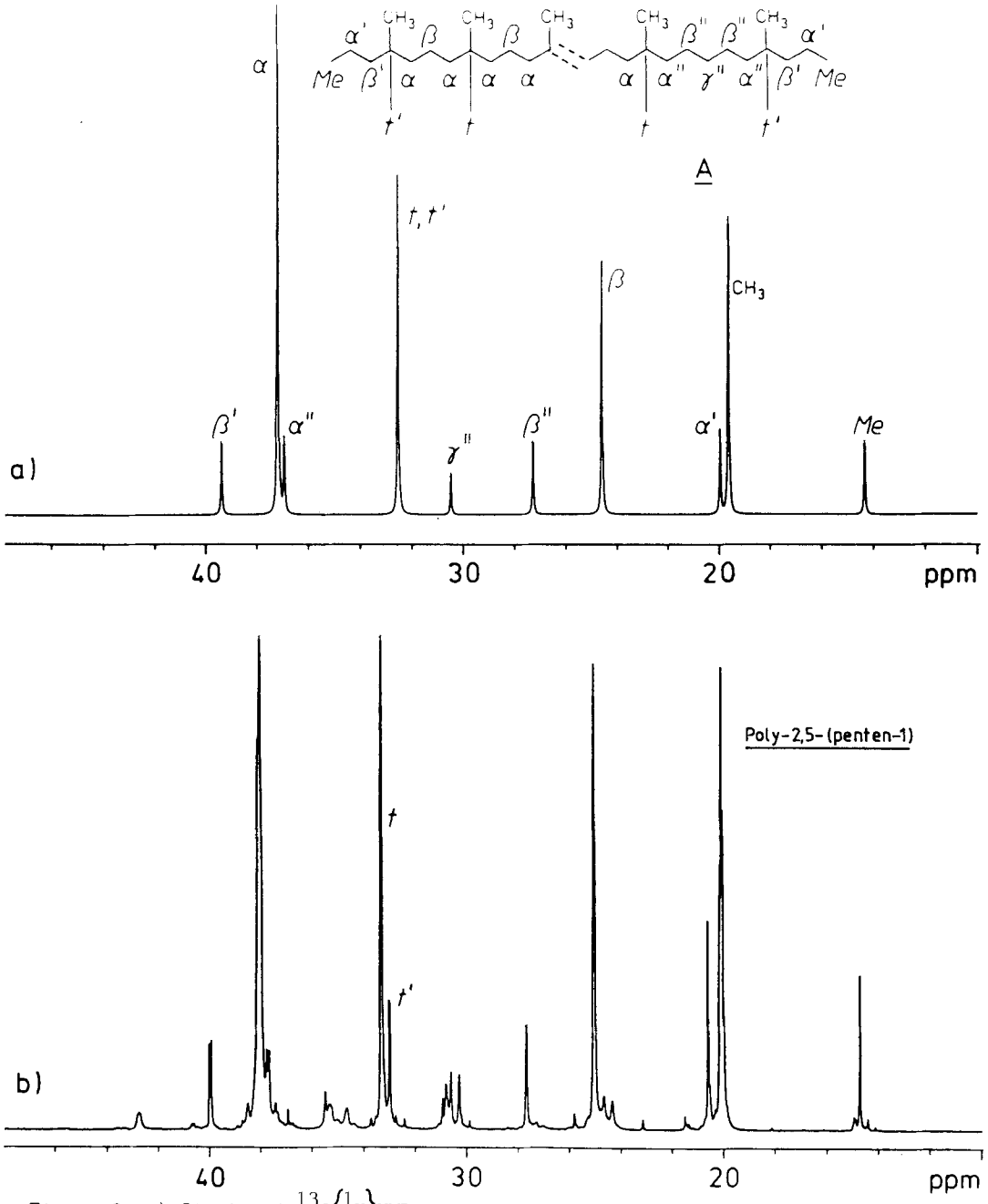

Figure 2 a) Simulated $^{13}C\{^{1}H\}$ NMR spectrum of a polymer with the designed structure (with chain beginning A and chain end)

b) $^{13}C\{^{1}H\}$ NMR spectrum of poly-2.5-(pentene-1) (75.5 MHz, [D_6] benzene, 303 K)

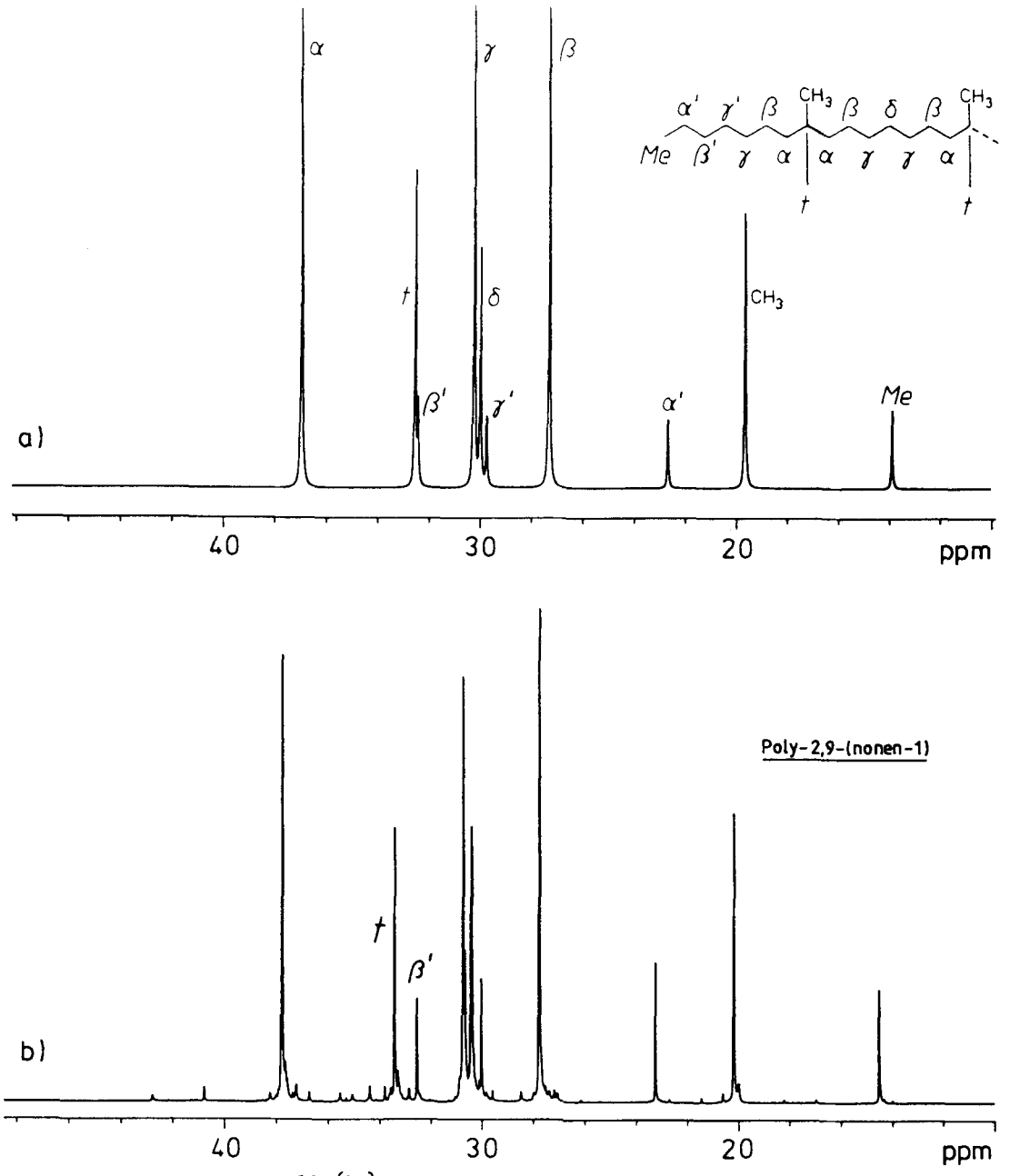

Figure 3 a) Simulated $^{13}C\{^1H\}$ NMR spectrum of a polymer with the designed structure (with chain end)

b) $^{13}C\{^1H\}$ NMR spectrum of poly-2,9-(nonene-1) (75.5 MHz, [D_6] benzene, 303 K)

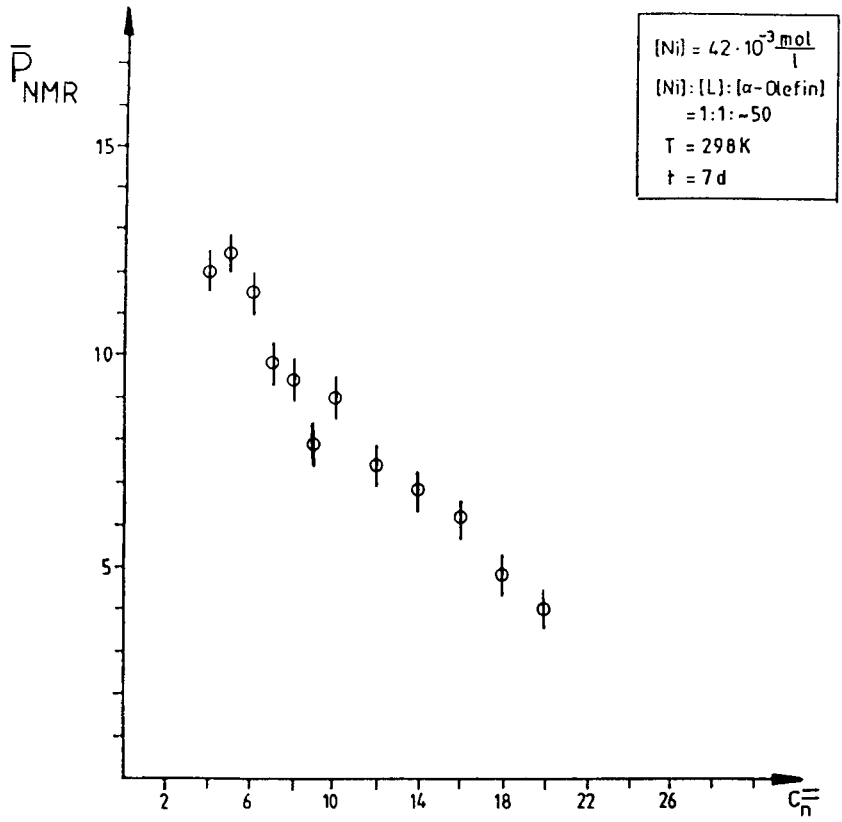

Figure 4 Dependence of the polymerization degree on the C number of the used monomer

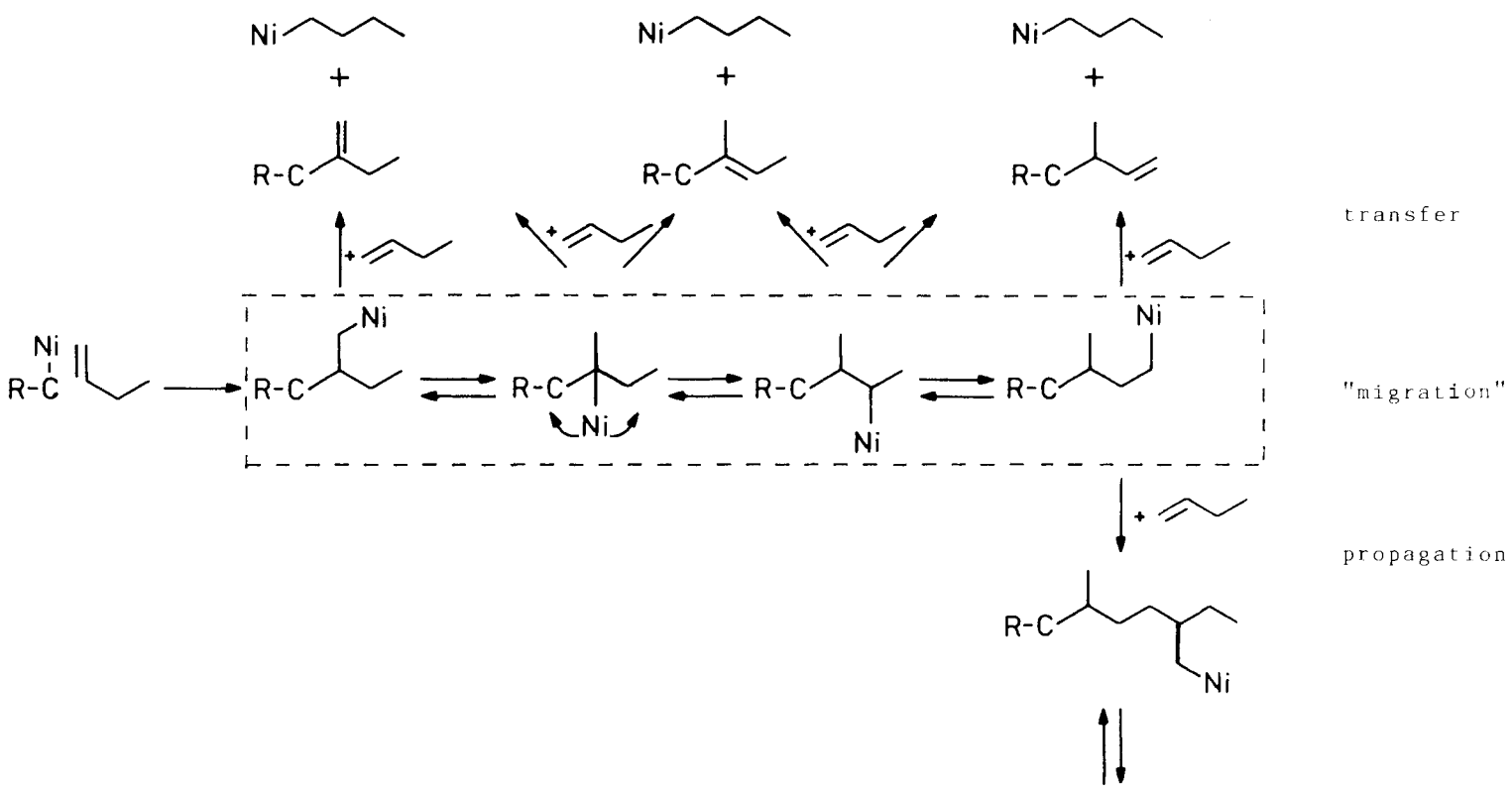

Figure 5 Reaction scheme with migration mechanism for the butene-1 polymerization as an example

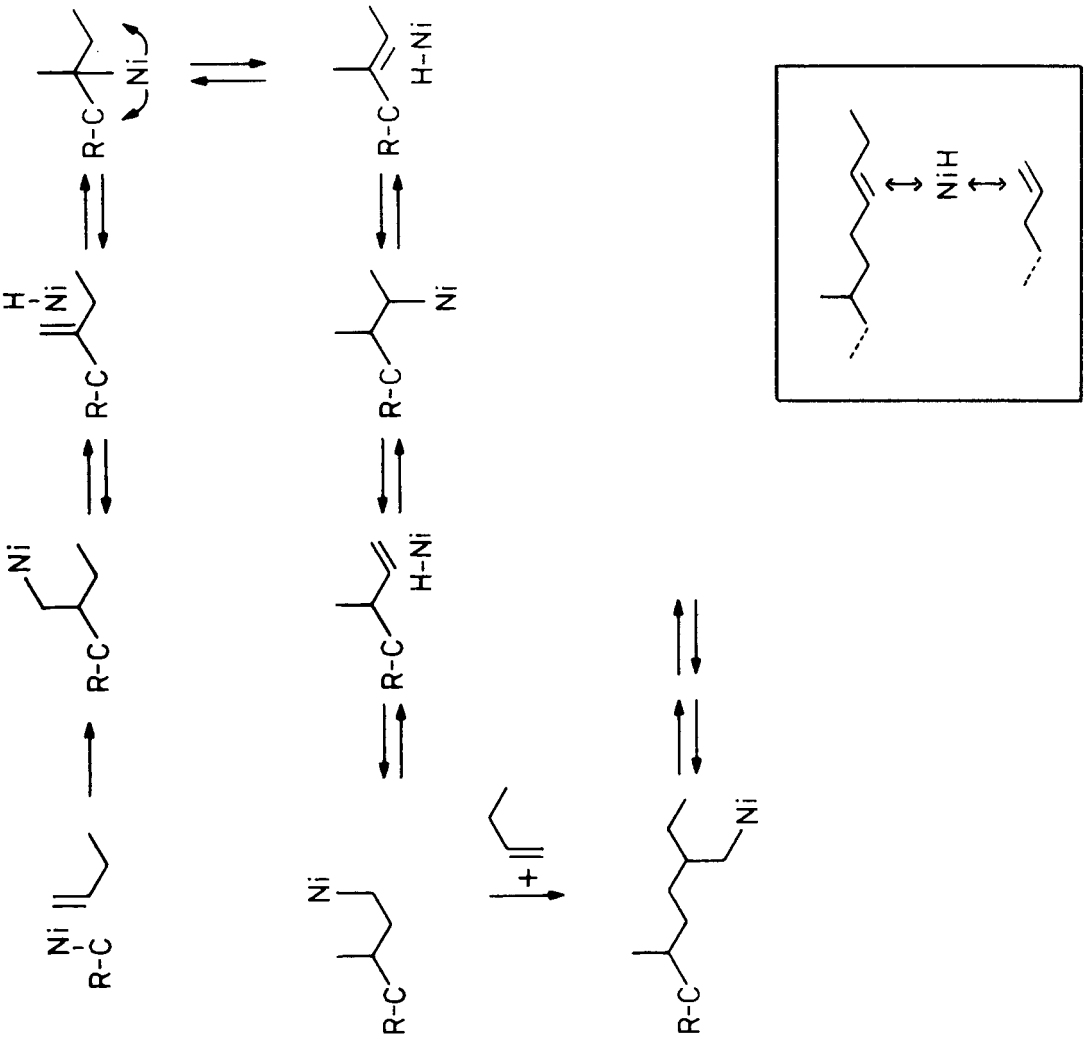

Figure 6 Proposal of a reaction scheme involving an intermediate Ni-hydride (butene-1 polymerization)

addition-elimination process is formulated with the formation of Ni-alkyl/Ni-hydrid species via a 1.2-Hydrid shift.

This intermediate Ni-hydrid could act additionally as transferring species (as demonstrated in the box below in Figure 6), whereby according the momentary position of the Ni-catalyst complex in the polymer chain via β-H-elimination the different detectable double bonds (vinylidene, vinylene and vinyl groups) could result.

As a consequence of the reversibility of the migration steps the Ni catalyst complex moves not only forward to the "right" end of the chain, but also moves back in direction to the beginning of the formed polymer chain. The longer the chain, the more from statistical reasons the probability increases for the migration in both directions. So, the dependence of the polymerization degree on the length of the α-olefin may be caused through a limit of the chain length. Beyond this chain length then the probability for the formation of a primary Ni-alkyl on the end of the chain and in this way the possibility of the insertion of the next monomer become zero.

REFERENCES

1. W. Keim, R. Appel, A. Storeck, C. Krüger, and R. Goddard, Angew. Chem. 93, 91 (1981).
2. L. P. Lindemann and J. Q. Adams, Anal. Chem. 43, 1245 (1971).
3. V. Möhring, Dissertation, Universität Düsseldorf, 1985.

This page intentionally left blank

STRUCTURE OF POLY-α-OLEFINS AND REACTION MECHANISM OF ZIEGLER-NATTA POLYMERIZATION.

ADOLFO ZAMBELLI and PAOLO AMMENDOLA
University of Salerno, 84100 - Salerno, Italy.

ABSTRACT

Several problems concerning the mechanism of polymerization of α-olefins, in the presence of Ziegler-Natta catalytic systems, have been solved by investigating the structure of the resulting macromolecules. The stereochemical structure of polypropylene, as well as that of ethylene-propene copolymers, shows that isotactic polymerization is due to the asymmetry of the active sites. These results have been confirmed by analyzing the stereochemical structure of suitably ^{13}C enriched end groups resulting from chain initiation on different alkyl groups. It has been also shown that isotactic polymerization involves anti-Markownikoff addition. The relative reactivities of a number of α-olefins ranging from ethylene to 3-ethyl-1-pentene have also been rationalized by considering the structure and the conformation of the monomer together with that of the growing chain end.

INTRODUCTION

It is generally accepted that the active sites involved in isotactic specific polymerization of 1-alkenes in the presence of heterogeneous catalytic systems consisting of titanium halides (TiX_n) and organometallic compounds such as AlR'_3 or AlR'_2Y or ZnR'_2

(R'=hydrocarbon radical, X,Y=halide ligands) are titanium atoms bonded to at least one hydrocarbon radical (R)[1]. The coordination number of the Ti atoms of the active sites, the presence of other ligands, the role of the organometallic cocatalyst other than alkylating the surface of TiX_n by ligand exchange, are more or less speculative since a direct determination of the structure of the sites has not yet been achieved[1]. The growing of the macromolecules involves consecutive antimarkownicoff[2-5] suprafacial[6] additions of the "active titanium carbon bond" of the catalytic sites (Ti-R) to the monomer. In the initiation step R=R', i.e. the hydrocarbon radical bonded to the titanium of the active sites comes from the organometallic cocatalyst and can be detected on the end groups of the resulting macromolecules[2,7-11]. Of course, in the i^{th} chain propagation step R is the growing polymer chain having degree of polymerization i-1. The stereoregular structure of the polymers of prochiral 1-alkenes entails that during the propagation steps, the addition is highly enantioselective[12]. It is worthwhile to observe that for polymerizations of this sort there is no clear cut between initiation and propagation steps. For instance the addition of a titanium isobutyl bond to propene could be considered the initiation step of a polymerization performed in the presence of a catalytic system consisting of TiX_n and $Al(iC_4H_9)_3$.

$$Ti\text{-}CH_2\text{-}CH(CH_3)_2 \xrightarrow{+C_3H_6} Ti\text{-}CH_2\text{-}CH(CH_3)\text{-}CH_2\text{-}CH(CH_3)_2.$$

The same addition should be considered the first propagation step[7,8] in the presence of a catalytic system consisting of TiX_n and $Al(CH_3)_3$

$$Ti\text{-}CH_3 \xrightarrow{+C_3H_6} Ti\text{-}CH_2CH(CH_3)_2 \xrightarrow{+C_3H_6} TiCH_2CH(CH_3)CH_2CH(CH_3)_2.$$

As a consequence information concerning the polymerization mechanism and the structure of the active sites can be derived both by determining the regiochemical and the stereochemical sequence of the monomer units inside the polymer chains[5,14-16] and by determining the structure of the polymer end groups resulting from the beginning addition steps[7-9,15]. Additional information can also result from the structure of the end groups arising from the chain transfer or chain termination processes[5,10]. During this communica

tion we will mainly review the data concerning the structure of the end groups of isotactic poly-1-alkenes reported in the literature, together with some new data we have recently obtained. Their meaning in view of the reaction mechanism will be also discussed.

ADDITION OF Ti-CH_3 and Ti-C_2H_5 TO PROPENE AND 1-BUTENE.

Addition of Ti-CH_3 to propene produces a isobutyl group[7,8]. The two methyls of the isobutyl end groups of polypropylene are diastereotopic due to the chiral carbon of the 2,4 dimethylpentyl group resulting from the subsequent addition to propene of the titanium-iC_4H_9 produced in the initiation step[17-19] (see also Fig.1). The different stereochemical environments of the considered methyls can be detected by means of ^{13}C NMR analysis[5,7,8]. When Ti-CH_3 is ^{13}C enriched, two diastereomeric selectively 5 ^{13}C enriched 3,4 dimethyl pentyl groups could result from the considered subsequent additions (see Figure 1).

In Figure 2 a it is reported the methyl region of the ^{13}C NMR spectrum of highly isotactic polypropylene obtained in the presence of $\delta TiCl_3$-$Al(^{13}CH_3)_2I$[7,8]. The resonances of the enriched methyls of the considered diastereomeric end groups are at 20.6_7ppm ($\nu\delta t$) and 21.7_8ppm ($\nu\delta e$) from HMDS[7,8]. The intensities of the considered resonances show that the population of the a end groups is higher than that of the b ones. Looking at Figure 1, one can easily visualize that this result means that both the addition of Ti-$^{13}CH_3$ and of Ti-$CH_2CH(CH_3)$-$^{13}CH_3$ to propene are more or less enantioselective and that the direction of enantioselectivity is the same for both the additions. It is relevant that, excepting the isotopic effect, the considered additions do not involve chiral alkyl groups. Therefore the different reactivity of the enantiofaces of propene, experimentally observed towards both the addition of Ti-CH_3 and of Ti(i-C_4H_9), implies a driving force coming from some chiral feature of the active sites other than the presence of a chiral carbon at the last unit of the growing chain end.

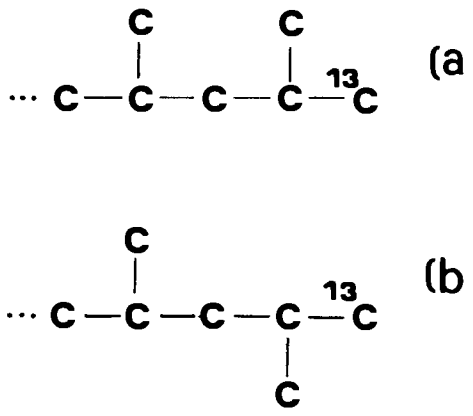

Figure 1. All trans projections of diastereomeric 5 ^{13}C enriched 2,4 dimethylpentyl end groups. Accordingly to a previously proposed nomenclature[19] the enriched carbon occupy the δt(=syndiotactic) position in a and the δe(=isotactic) position in b relative to methyl 2'.

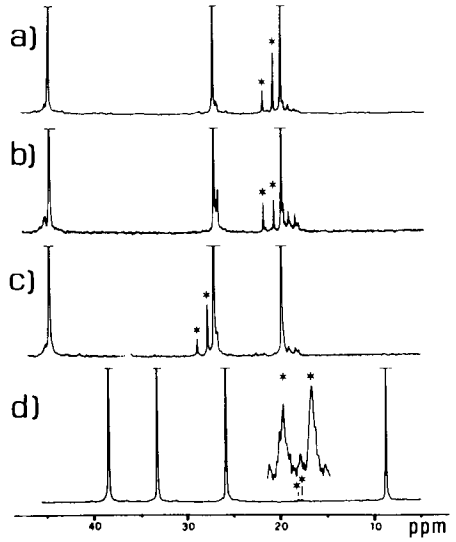

Figure 2. ^{13}C NMR spectra of a) isotactic polypropylene prepared in the presence of δ-$TiCl_3$-$Al(^{13}CH_3)_2I$. b) isotactic polypropylene prepared in the presence of δ-$TiCl_3$-$Al(^{13}CH_3)_3$-$Zn(^{13}CH_3)_2$; c) isotactic polypropylene prepared in the presence of δ-$TiCl_3$-$Al(^{13}CH_2CH_3)_3$-$Zn(^{13}CH_2CH_3)_2$; d) isotactic polybutene prepared in the presence of δ-$TiCl_3$-$Al(^{13}CH_3)_3$-$Zn(^{13}CH_3)_2$. Reprinted with permission of the authors from Ref.8.

In fact such a chiral carbon comes off at the growing chain end only after the considered insertion steps.

In Figure 3 it is reported the ^{13}C NMR spectrum of highly isotactic poly-1-butene obtained in the presence of δ-$TiCl_3$-$Al(C_2H_5)_3$-$Zn(C_2H_5)_2$ selectively ^{13}C enriched on the methylene carbons[20].

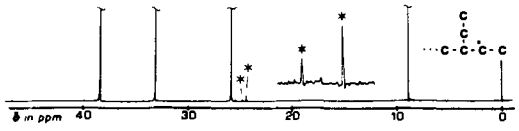

Figure 3. ^{13}C NMR spectrum of isotactic poly-1-butene prepared in the presence of δ-$TiCl_3$-$Al(^{13}CH_2CH_3)_3$-$Zn(^{13}CH_2CH_3)_2$. Reprinted with permission of the authors from ref.20.

The different intensities of the resonances of the enriched methylene carbons occupying diastereotopic positions, relative to the 2'ethyl substituent of the 5 ^{13}C 2-4 diethylhexyl end groups ($\nu\delta t=24.1_8$ppm; $\nu\delta e=24.5_6$ppm from HMDS), confirm that the addition to the enantiofaces of a prochiral substrate may be enantioselective even before the active sites involve any chiral growing chain end. Figure 2d shows the ^{13}C NMR spectrum of isotactic poly-1-butene obtained in the presence of δ-$TiCl_3$-$Al(^{13}CH_3)_3$-$Zn(^{13}CH_3)_2$[8]. One can observe, from the sharp resonances of the carbons of the inner monomer units of the chains, that this poly-1-butene is isotactic to an extent comparable with the sample of Figure 3. However the resonances (at 17.8_4 and 18.1_3ppm from HMDS) of the enriched methyls of the 4' ^{13}C 2-ethyl, 4-methylhexyl end groups have, roughly, the same intensity. This fact implies, at least, that the addition of Ti-CH_3 to 1-butene is not enantioselective. The ^{13}C NMR spectrum reported in Figure 2 b[8] (highly isotactic polypropylene prepared in the presence of δ-$TiCl_3$-$Al(^{13}CH_3)_3$-$Zn(^{13}CH_3)_2$) shows that even addition of Ti-CH_3 to propene is not enantioselective

when the catalytic system does not include iodine ligands (compare Figure 2 a). Figure 2 c shows the ^{13}C NMR spectrum of highly isotactic polypropylene prepared in the presence of δ-$TiCl_3$-$Al(C_2H_5)_3$ and $Zn(C_2H_5)_2$ selectively ^{13}C enriched on the methylene carbons[8]. The resonances of the enriched methylenes of the 5 ^{13}C-2,4-dimethyl hexyl groups occur at 27.7$_2$ppm (δt) and 28.8$_2$ppm (δe) from HMDS and have different intensities, showing that addition of Ti-C_2H_5 to propene as well as to 1-butene (see Figure 3) is enantioselective. By considering alone polymerization of propene, one could guess that there is no need of any chiral feature of the active sites, other than a chiral alkyl bonded to the titanium of the active sites, in order to explain the results reported in Figures 2 b and 2 c. As a matter of fact one could explain the relative intensities of the observed resonances of the enriched carbons assuming that additions to propene of Ti-CH_3, Ti-C_2H_5 and Ti-(i-C_4H_9) are not enantioselective, while addition of chiral Ti-$CH_2CH(CH_3)C_2H_5$ is partially enantioselective. Likewise, the presence of a chiral carbon at the last unit of the growing chain end should be the driving force of the high enantioselectivity of the following chain propagation steps. The partial enantioselective addition of Ti-CH_3 and Ti-(i-C_4H_9) to propene inferred from the spectrum reported in Figure 2 a could be simply due to the presence of different halide ligands on the catalytic system. Actually, the active sites could become chiral as a result of a partial exchange of the halide ligands between the surface of $TiCl_3$ and $Al(CH_3)_2I$. This fact could well produce a supplementary driving force for enantioselective addition. It is true that the presence of different halide ligands enhances the driving force of the steric control[21]. However, as reported in Ref. 22, the additions of Ti-CH_3 and Ti-(i-C_4H_9) are partially enantioselective even in the presence of the catalytic system TiI_3-$Al(^{13}CH_3)_3$. The isotactic specific sites present in this catalytic system should reasonably have the same simmetry properties as the sites present on the $\delta TiCl_3$-$Al(CH_3)_3$ system.

On the other hand the above explanation is also conflicting with the results reported in Figure 3 and 2 d. The different intensities of the resonances at 24.1_8 and 24.5_6 ppm of Figure 3 entail that addition of $Ti-C_2H_5$ and $Ti-CH_2CH(C_2H_5)_2$ to 1-butene are enantioselective although the considered alkyls are achiral, and the catalytic system contains only one sort of halide ligands[20]. In addition, according to this reasoning, it appears almost impossible to understand that the addition of the same chiral $Ti-CH_2CH(CH_3)-C_2H_5$ to propene (Figure 2 c) looks enantioselective, while the addition to 1-butene (Figure 3) does not[8]. Notice that the two monomers have the same simmetry properties.

A comprehensive interpretation of all the experimental facts reported in this and in the following sections implies that the isotactic specific sites are originally chiral (i.e. independently from the presence of an active bond between titanium and any chiral alkyl). The driving force of the enantioselective additions eventually comes from this "original" chirality but the actual extent of the enantioselectivity depends on additional features which, at least in part, shall be considered in the next sections. The structures of the end groups detected in the spectra reported in this and in the following sections, also show that the addition is antimarkownicoff.

ADDITION OF $Ti-(i-C_4H_9)$, $Ti-CH_2CH(CH_3)C_2H_5$ AND $Ti-CH_2CH(C_2H_5)_2$ TO PROPENE AND 1-BUTENE IN COMPARISON WITH THE SUBSEQUENT CHAIN PROPAGATION STEPS.

A further splitting of the resonances of the enriched carbons of the previously discussed end groups should be considered, in view of the stereochemical effect on the chemical shift of the enriched carbons by the substituent of the third monomer unit incorporeted into the growing polymer chain[17]. Actually, when, e.g., propene is polymerized in the presence of the moderately syndiotactic specific system $VCl_4-Al(^{13}CH_3)_2Cl$ four resonances are detected for the diastereomeric enriched ^{13}C 2,4,6 trimethylheptyl end

groups reported in Figure 4.

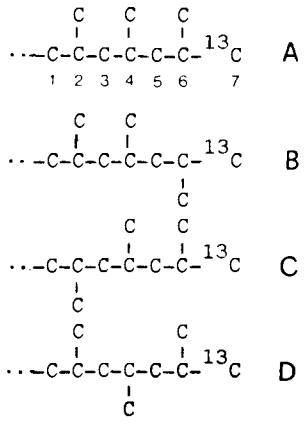

Figure 4. Diastereomeric end groups detected on atactic polypropylene. Relative to methyls 2' and 4' the enriched carbons occupy the placements a) $\delta t\zeta t(\nu=20.6_7 ppm)$; b) $\delta e\zeta e(\nu=21.7_6 ppm)$; c) $\delta t\zeta e(\nu=20.8_7 ppm)$; d) $\delta e\zeta t(\nu=21.5_4 ppm)$. HMDS scale.

A similar splitting should also be considered for selectively enriched $7^{13}C$ 2,4,6-trimethyloctyl; $6'^{13}C$ 2,4-diethyl,6-methyloctyl and $7^{13}C$ 2,4,6-triethyloctyl end groups,in view of the stereospecific additivity rules of the chemical shift of branched hydrocarbons reported in the literature[19]. On the other hand, in the spectra of Figures 2 a, 2 b and 2 c,only the resonances of the $\delta t\zeta t$ and $\delta e\zeta e$ enriched carbons are detected. Only two resonances are similarly detected for the enriched carbons in the spectra of Figures 2 d and 3.

These findings imply that addition of the quoted Ti-R to both propene and 1-butene are enantioselective to an extent comparable with that of the subsequent chain propagation steps. The extent of the enantioselectivity of the chain propagation steps in the presence of any of the catalytic systems reported in section 2 may be higher than 99% and can be evaluated by determining the stereochemical sequence of the configuration of the substituted carbons

of the polymer chain. Isotactic macromolecules prepared in the presence of catalytic systems based on δ-$TiCl_3$ tipically consist of sequences of m diads spanned by pairs of r diads ···mmmrrm···mrrmm···[16] On the whole the amount of r diads may be lower than 2%. The occurrence of pairs of r diads, more often than isolated r diads, confirms that the driving force of the enantioselectivity is the "original" chirality of the active sites[23]. The same conclusion can be reached by considering that, as previously reported in the literature[15], the steric control of the addition to propene crosses intervening ethylene units in ethylene-propene copolymerization.

ADDITION OF Ti-C_6H_5 TO PROPENE.

All the additions discussed up to now, including the propagation steps, involved primary alkyl ligands bonded to Ti. In Figure 5 is reported the aromatic region of the ^{13}C NMR spectrum of highly isotactic polypropylene prepared in the presence of δ-$TiCl_3$-$Zn(C_6H_5)_2$[9]. The resonances of the o, m and p aromatic carbons are detected at 124.8_8, 126.2_3 and 123.6_5ppm from HMDS. A unique resonance is detected at 145.6ppm for the quaternary aromatic carbon.

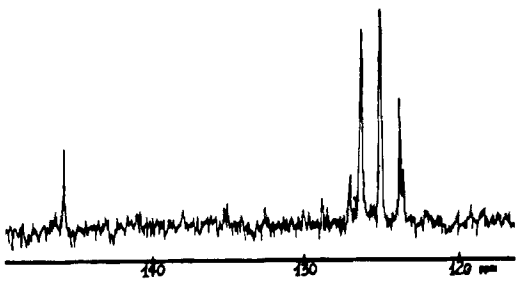

Figure 5. Aromatic region of ^{13}C NMR spectrum of highly isotactic polypropylene prepared in the presence of δ-$TiCl_3$-$Zn(C_6H_5)_2$ HMDS scale. Reprinted with permission of the authors from Ref.9.

On the other hand the resonance of the quaternary carbon is splitted in the spectrum of the mixture of (RR, SS) and (RS, SR) 2,4,6-trimethylhexyl benzene[9]. The chemical shift of the quaternary carbon δt with respect to the 4' methyl is at 145.6ppm from HMDS, while that of the δe quaternary carbon is at 146.2ppm[9]. It can be concluded that addition of Ti-C_6H_5 is highly enantioselective in the same direction as the following addition of Ti-$CH_2CH(CH_3)C_6H_5$. Even this addition is antimarkownicoff.

ADDITION OF Ti-CH_3 TO STYRENE AND VINYLCYCLOHEXANE.

The ^{13}C NMR spectrum of isotactic polystyrene prepared in the presence of δ-$TiCl_3$-$Al(^{13}CH_3)_3$ is reported in Figure 6b[24]. The resonances of the enriched methyls of the 5 ^{13}C 2,4-diphenylpentyl end groups coming from the chain initiation steps are at 19.2_2 and at 21.5_2ppm.

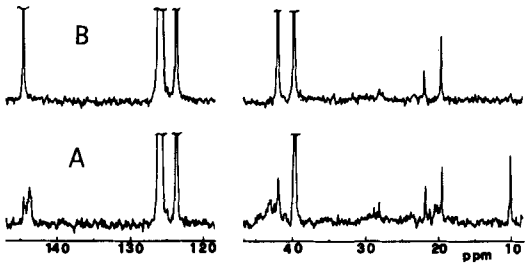

Figure 6. ^{13}C NMR spectra of a) butanone soluble and b) butanone insoluble-benzene soluble fractions of polystyrene prepared in the presence of δ-$TiCl_3$-$Al(^{13}CH_3)_3$.

The assignment of the resonance at 19.2_2ppm to the δt methyls and of the resonance at 21.5_2ppm to the δe methyls is achieved by considering the spectra of model compounds previously reported in the

literature[25] and the additivity rules of the chemical shift of ^{13}C[26]. The structure of the observed end groups and the different intensities of the observed methyl resonances, show that the addition is antimarkownicoff and enantioselective. Similar conclusions are reached by observing the spectrum of isotactic polyvinylcyclohexane prepared in the presence of δ-$TiCl_3$-$Al(^{13}CH_3)_3$-$Zn(^{13}CH_3)_2$[24]. It can be observed that the enantioselectivity of the addition of Ti-CH_3 increases while increases the steric demand of the substituent of the monomer. It is negligible for propene and 1-butene, but it is clearly observable for styrene and vinylcyclohexane. Most probably such an effect has not been observed previously for 3-methyl-1-butene, 3-methyl-1-pentene and 3-ethyl-1-pentene[10,11] due to lack of resolution (see also the next section) of the spectra.

ADDITION TO 3-METHYL-1-PENTENE.

Addition of Ti-R' to chiral 1-alkenes may led to diastereomeric monomer units depending on the attacked monomer diastereoface (see Figure 7).

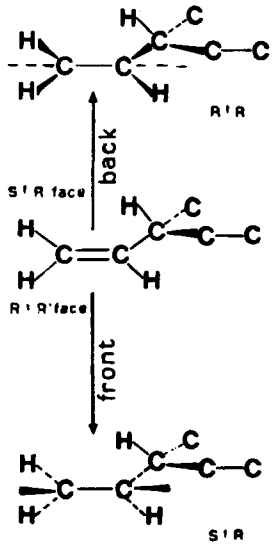

Figure 7. Diastereomeric monomer units arising from attack of the frontface and the back face of (R) 3-methyl-1-pentene on the growing polymer chain.

In Figure 8 it is reported the ^{13}C NMR spectrum of isotactic poly (R,S)-3-methyl-1-pentene prepared in the presence of δ-$TiCl_3$-$Al(^{13}CH_3)_3$-$Zn(^{13}CH_3)_2$[10].

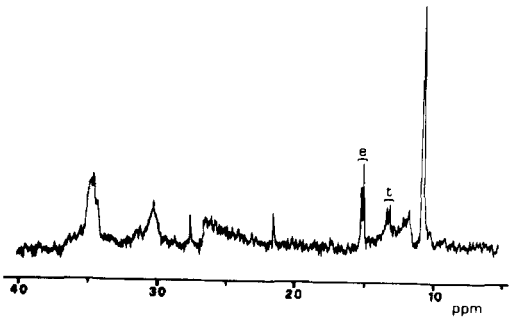

Figure 8. ^{13}C NMR spectrum of the acetone insoluble-benzene soluble fraction of poly (R,S)-3-methyl-1-pentene prepared in the presence of δ-$TiCl_3$-$Al(^{13}CH_3)_3$-$Zn(^{13}CH_3)_2$. The resonances of the enriched methyls of the diastereomeric 2'^{13}C 2,4-dimethylpentyl end groups are labelled with e and t. The e $^{13}CH_3$'s come from the front attack (i.e. (R')(R) or (S')(S) faces), the t $^{13}CH_3$'s from the back attack (i.e. (S')(R) or (R')(S) faces) of Figure 8.
Reprinted with permission of the authors from Ref.10.

The resonances centered at 15.1_8ppm and at 13.3_3ppm from HMDS are due to the enriched methyls of the diastereomeric 2'^{13}C 2,4-dimethylpentyl end groups resulting from the addition of Ti-$^{13}CH_3$ to the monomer diastereofaces. The different intensities of the two considered resonances and the assignment reported in Figure 8 shows that the front attack of Figure 7 is faster than the back attack[10]. The rate of attack of Ti-CH_3 to the diastereofaces of 3-methyl-1-pentene, in comparison with that of the attack to 3-methyl-1-butene and 3-ethyl-1-pentene previously reported in the literature[11], suggests that, in the active state, the conformation of the 1-alkenes branched on C_3 might be either H skew$^+$ or H skew$^-$ (more or less

distorted). These conformations could lead to acceptable non bonded interactions between the incoming 1-alkenes and the ligand environment of the active sites[11,27]. A similarly different rate of attack to the diastereofaces of 3-methyl-1-pentene was found also during the chain propagation steps[10], and justifies the "stereoselective" behaviour of polymerization of chiral C-3 branched 1-alkenes[10-28].

RELATIVE REACTIVITIES OF SOME 1-ALKENES

Quantitative ^{13}C NMR analysis of the enriched end groups resulting from binary copolymerizations in the presence of δ-$TiCl_3$ and selectively ^{13}C enriched cocatalysts, affords a fast and reliable method for determining relative reactivity of 1-alkenes. We have determined in such way, the relative reactivities (toward addition of Ti-CH_3) of ethylene; propene; 1-butene; 3-methyl-1-butene; 3-methyl-1-pentene; and 3-ethyl-1-pentene, in the presence of δ-$TiCl_3$-$Al(^{13}CH_3)_3$-$Zn(^{13}CH_3)_2$ [29-31]. The results, reported in Reference 29, can be qualitatively understood by considering the steric restrictions coming from the enantioselective character of the considered additions and the just mentioned conformational restrictions.

In similar manner one can test the trend of the relative reactivity of a pair of 1-alkenes when changing the hydrocarbon radical bonded to the titanium atom of the active sites[31].

CONCLUSION

Considerable information on the reaction mechanism of stereospecific polymerization of 1-alkenes can be achieved by determining the stereochemical structure of the polymers. Under this respect the structure of the end groups deserves particular attention. The results here reported show that in the presence of heterogeneous isotactic-specific catalytic systems, the addition to the monomer is antimarkownicoff even in the case of vinyl aromatic monomers such as styrene. The enantioselectivity of the addition, which ensures the isotactic steric control, is due to the "original" chirali

ty of the active sites and increases while increasing the size of any of the ligands of the catalyst components and the steric demand of the substituent of the monomer.

Finally the addition to chiral C-3 branched 1-alkenes is diastereoselective, most probably due to restrictions concerning the conformation of the monomer in the active state.

Concerning the "original" chirality of the active sites, it is possible to speculate that it could come from the asymmetric configuration of the transition metal or else from the asymmetric spatial arrangements of ligands outside the coordination sphere, or even simply from restricted rotation of the active transition metal-carbon bond (at least when R'≠CH_3). The ···mmrrmm··· steric defects of the stereochemical sequence of the configurations of the substituted carbons of the polymer chains should arise from a failure of enantioselective addition. ···mmrmm··· defects should be caused e.g. by inversion of the configuration of the active site during the macromolecular growth, or by migration of the growing polymer chain from D preferring to L preferring sites[32].

REFERENCES

1. J.Boor Jr., "Ziegler-Natta Catalysts and Polymerization", Academic Press, New York, 1979.
2. G.Natta, P.Pino, E.Mantica, F.Danusso, G.Mazzanti and M.Peraldo, Chim.Ind., Milan, 38, 124 (1956).
3. P.Longi, G.Mazzanti, A.Roggero and M.P.Lachi, Makromol.Chem., 61, 63 (1963).
4. Y.Takegami, T.Suzuki and T.Okazaki, Bull.Chem.Soc.Japan, 42, 1060 (1969).
5. A.Zambelli, P.Locatelli and E.Rigamonti, Macromolecules, 12, 156 (1979).
6. T.Miyazawa and Y.Ideguchi, J.Polymer Sci., Part B, 1, 389 (1963).
7. A.Zambelli, P.Locatelli, M.C.Sacchi and E.Rigamonti, Macromolecules, 13, 798 (1980).

8. A.Zambelli, M.C.Sacchi, P.Locatelli and G.Zannoni, Macromolecules, 15, 211 (1982).
9. P.Locatelli, M.C.Sacchi, I.Tritto, G.Zannoni, A.Zambelli and V. Piscitelli, Macromolecules, in press.
10. A.Zambelli, P.Ammendola, M.C.Sacchi, P.Locatelli and G.Zannoni, Macromolecules, 16, 341 (1983).
11. A.Zambelli, P.Ammendola and A.J.Sivak, Macromolecules, 17, 461 (1984).
12. Isotactic polymerization of 1-alkenes involves that the insertion of the monomeric unit into the active metal-carbon bond of the active sites is selective toward the enantiofaces of the prochiral monomer. The chain propagation approaches the "enantiomorphic sites" statistic model (R.A.Shelden, T.Fueno, T.Tsunetsugu and J.Furukawa. J.Polymer Sci., Part A, 3, 23 (1965)). Accordingly the enantioselectivity is quantitatively defined $P_{DD}(=P_{LL})$. See also Ref. 13.
13. A.Zambelli, P.Locatelli, M.C.Sacchi and I.Tritto, Macromolecules, 15, 831 (1982).
14. A.Zambelli, "NMR Basic Principles and Progress", Springer, New York, 1971, vol.4, p.101.
15. A.Zambelli, G.Bajo and E.Rigamonti, Makromol.Chem., 179, 1249 (1978).
16. C.Wolfsgruber, G.Zannoni, E.Rigamonti and A.Zambelli, Makromol. Chem., 176, 2765 (1975).
17. A.Zambelli, P.Locatelli and G.Bajo, Macromolecules, 12, 154 (1979).
18. C.J.Carman, A.R.Tarpley Jr. and J.H.Goldestein, Macromolecules, 6, 719 (1973).
19. A.Zambelli and G.Gatti, Macromolecules, 11, 485 (1978).
20. P.Locatelli, I.Tritto and M.C.Sacchi, Makromol.Chem., Rapid Commun., 5, 495 (1984).
21. Y.Doi, T.Kohara, H.Koiwa and T.Keii, Makromol.Chem., 176, 2159 (1975).
22. M.C.Sacchi, P.Locatelli, I.Tritto and A.Zambelli, Makromol. Chem., Rapid Commun., 5, 661 (1984).

23. G.Natta, J.Inorg.Nucl.Chem., 8, 589 (1958).
24. P.Ammendola, T.Tancredi and A.Zambelli, Macromolecules, submitted for publication.
25. H.Sato and Y.Tanaka, "NMR and Macromolecules", (J.C.Randall ed.), ACS Symposium Series, Washington D.C., 247, 181 (1984).
26. D.M.Grant and E.G.Paul, J.Am.Chem.Soc., 86, 2984 (1964).
27. P.Ammendola, G.Guerra and V.Villani, Makromol.Chem., 185, 2599 (1984).
28. G.Natta, P.Pino, G.Mazzanti, P.Corradini and U.Giannini, Rend. Acc.Naz. Lincei (VIII), 19, 397 (1955).
29. P.Ammendola and A.Zambelli, Makromol.Chem., 185, 2451 (1984).
30. P.Ammendola, A.Vitagliano, L.Oliva and A.Zambelli, Makromol. Chem., 185, 2421 (1984).
31. P.Ammendola, L.Oliva, G.Gianotti and A.Zambelli, Macromolecules, in press.
32. The enantiomorphic sites of different configuration are labelled according to Ref. 12.

STRUCTURE AND REACTIVITY OF "LIVING" POLYPROPYLENE

Y.DOI, S.SUZUKI, F.NOZAWA and K.SOGA
Research Laboratory of Resources Utilization, Tokyo Institute of Technology, Nagatsuta, Midori-ku, Yokohama 227, Japan
T.KEII
Numazu College of Technology, Ooka 3600, Numazu 410, Japan

ABSTRACT

"Living" polypropylene of uniform chain length was prepared by low-temperature polymerization of propene with some soluble vanadium-based catalysts. The chain end structure of living polypropylene was studied by ^1H NMR analysis of iodine-bonded polypropylene. ^1H NMR analysis revealed that the majority of active centers exist as a secondary vanadium-carbon bond during the chain propagation of living polypropylene. The mechanism of the living coordination polymerization is discussed based on kinetic and stereochemical data.

INTRODUCTION

The synthesis of "living" polyolefins with Ziegler-Natta catalysts is one target of research in the field of coordination polymerization[1]. As has been proved in research on anionic polymerization, "living" polymers are of great importance as a tool for the synthesis of tailor-made polymers such as terminally functionalized polymers and block copolymers[2]. In addition, "living" polymers are also useful in the understanding of the mechanism on the propagation reaction of a growing chain end with monomers.

The first example of "living" polypropylene of uniform chain length was found by Doi et. al.[3,4] in the syndiotactic-specific polymerization of propene with a soluble catalyst composed of tris (2,4-pentanedionato) vanadium and dialkyl aluminium halide as $Al(C_2H_5)_2Cl$. Kinetic studies on the living polymerization of propene have reached the following conclusions: (i) The living polymerization of propene takes place at low temperatures below

-65°C[3]. (ii) The formation of active centers is instantaneous[5]. (iii) The chain propagation reaction takes place via an insertion of coordinated propene into a vanadium-polymer bond and the rate is inflenced by the aluminium component as co-catalyst[3,5]. (iv) The molecular weight distributions of polypropylenes produced are as narrow as 1.05 to 1.20 of $\bar{M}w/\bar{M}n$[3,4]. The syndiotactic regularities of monodisperse polypropylenes are influenced by the kind of aluminium component[6,7]. The living polypropylene end of the vanadium-carbon bond has been found to react with some additives such as I_2 and CO to give terminally functionalized polypropylenes[8-10]. In addition, this new type of living polypropylene has been applied to the synthesis of well defined block copolymers of propylene-ethylene[11], propylene-tetrahydrofuran[8], propylene-styrene[12], and propylene-methyl methacrylate[13].

This paper is a report of recent advances we have made on the living coordination polymerization of propene with some soluble vanadium-based catalysts.

RESULTS AND DISCUSSION

1. Synthesis of "Living" Polypropylene

Two different types of vanadium compound, tris (2,4-pentanedionato) vanadium, $V(acac)_3$, and tris (2-methyl-1,3-butanedionato) vanadium, $V(mbd)_3$, were used for the synthesis of living polypropylene.

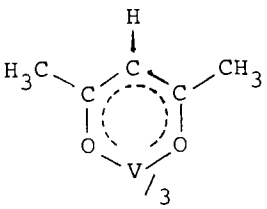

$V(acac)_3$

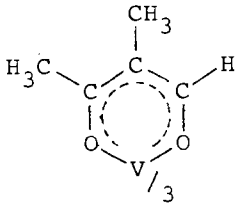

$V(mbd)_3$

Figure 1 shows time dependences of polymer yield, $\bar{M}n$ and $\bar{M}w/\bar{M}n$ of polymers, and the number of polymer chains produced per vanadium atom [N] in the polymerization of propene with a toluene solution of

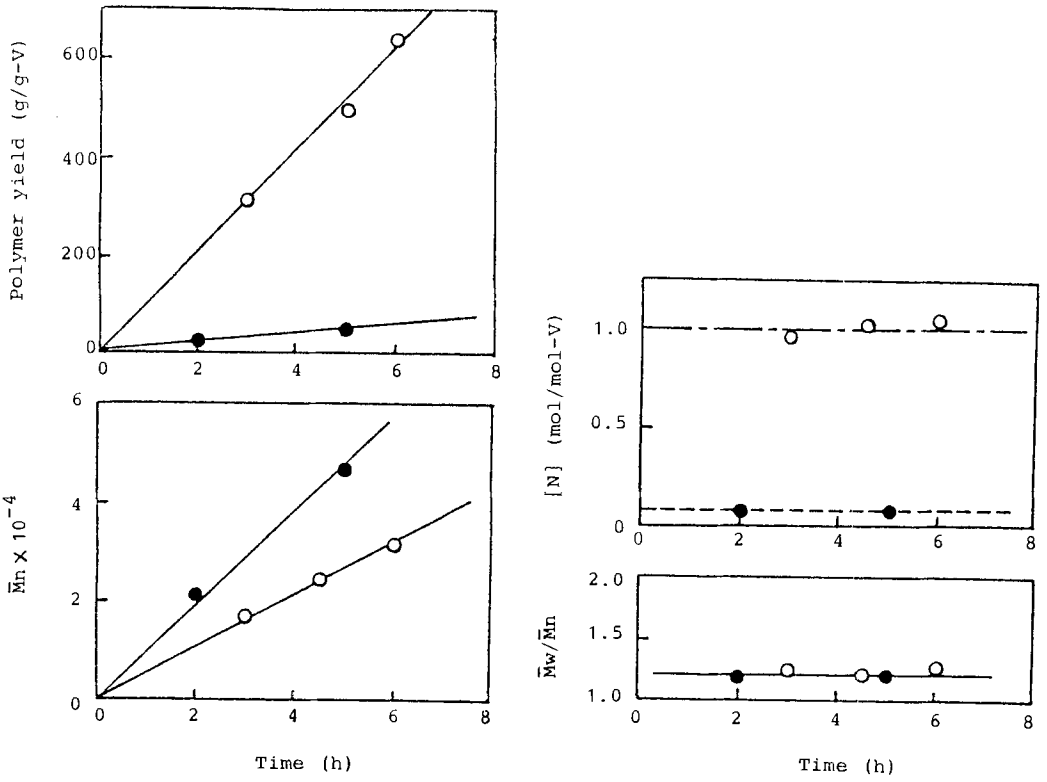

Figure 1. Time dependence of yield, $\bar{M}_n$ and $\bar{M}_w/\bar{M}_n$ of polypropylene and of the number of polymer chains produced per vanadium atom [N] in the polymerization of propene at -70°C with the $V(mbd)_3/Al(C_2H_5)_2Cl$ catalyst (○) and the $V(acac)_3/Al(C_2H_5)_2Cl$ catalyst (●).

Polymerization conditions: propene=830 mmol, $Al(C_2H_5)_2Cl$=20 mmol, toluene solution=100 cm^3, $V(mbd)_3$=0.05 mmol, $V(acac)_3$=0.5 mmol.

$V(acac)_3/Al(C_2H_5)_2Cl$ or $V(mbd)_3/Al(C_2H_5)_2Cl$ catalyst at -70°C. Both the yield and $\bar{M}n$ of polymers increased proportionally to polymerization time, which indicates that any chain-terminating processes are not present in those polymerization systems. The molecular weight distributions of polypropylenes were unimodal and their polydispersities ($\bar{M}w/\bar{M}n$) were as small as 1.2, independent of time. The number of polymer chains produced per vanadium atom [N] remained almost constant during the course of polymerization. In a living polymerization, the number of polymer chains [N] is consistent with the number of active centers. Here, it should be noted that the value of [N] in the polymerization with the $V(mbd)_3/Al(C_2H_5)_2Cl$ catalyst is almost unity (1.0 ± 0.1) during the course of polymerization. This is the case of living polymerization where all of the vanadium species function as active centers.

Temperature effects of polymerization activity and moleculare weight distribution (MWD) of polypropylene were examined in the range of -78°C to 3°C in the polymerization of propene with both catalysts $V(acac)_3/Al(C_2H_5)_2Cl$ and $V(mbd)_3/Al(C_2H_5)_2Cl$. For both catalysts, the MWD of polypropylene obtained at temperatures below -65°C was close to the Poisson distribution, while the MWD at higher temperatures above -60°C became broader ($\bar{M}w/\bar{M}n$ = 1.5 ~ 2.3). Some chain-terminating processes took place at higher temperatures. It has been concluded that the living polymerization of propene occurs at temperatures below -65°C.

The polymerization of propene was performed at -78°C with various types of dialkylaluminium monohalides in the presence of $V(acac)_3$. The results are shown in Figure 2. For all the aluminium compounds in Figure 2, the $\bar{M}n$ of produced polypropylene increased proportionally to polymerization time and the polydispersity ($\bar{M}w/\bar{M}n$) was as small as 1.15 ± 0.05, indicative of the formation of living polypropylene. The rate of increase in Mn, i.e. the rate of propagation of a living polymer chain expressed by $\bar{M}n/(42 \cdot t)$, is influenced by the kind of aluminium component.

The stereoregularities of monodisperse polypropylenes were determined from the ^{13}C NMR spectra. The result is listed in Table 1. The syndiotactic triad fraction [rr] is also dependent upon the kind of aluminium component.

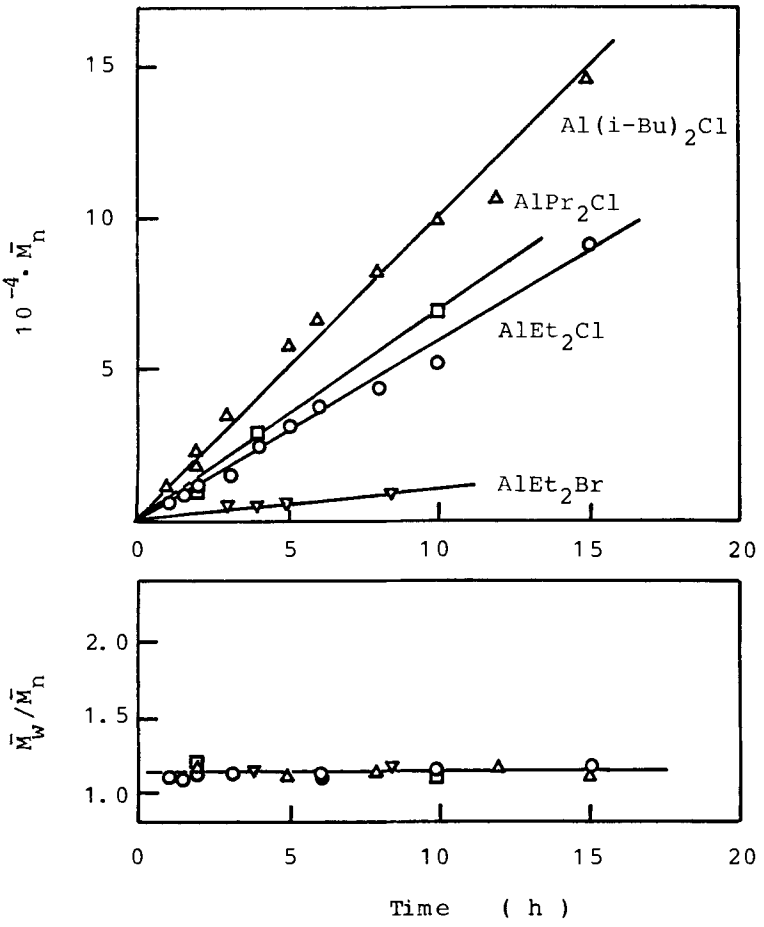

Figure 2. Time dependence of $\bar{M}_n$ and $\bar{M}_w/\bar{M}_n$ of polypropylene obtained at -78°C in the presence of different soluble catalysts composed of V(acac)$_3$ and aluminium alkyls. (Δ): Al(i-C_4H_9)$_2$Cl, (□): Al(C_3H_7)$_2$Cl, (○): Al(C_2H_5)$_2$Cl, (▽): Al(C_2H_5)$_2$Br.

Polymerization conditions: propene=830 mmol, V(acac)$_3$=0.5 mmol, aluminium alkyl=5 mmol, toluene solution=100 cm^3.

Table 1. Stereoregularities and molecular weights of polypropylenes prepared with soluble vanadium-based catalysts at -78°C.

V-component	Al-component	Polym.time in h	Stereoregularity				Mol. wgt.	
			[rr]	[rm]	[mm]	[r]	$10^{-4}\bar{M}_n$	$\bar{M}_w/\bar{M}_n$
$V(acac)_3$	$Al(C_2H_5)_2Cl$	3.0	0.65	0.32	0.03	0.81	1.50	1.1
$V(acac)_3$	$Al(C_3H_7)_2Cl$	2.0	0.63	0.33	0.04	0.79	0.76	1.1
$V(acac)_3$	$Al(i\text{-}C_4H_9)_2Cl$	3.0	0.52	0.38	0.10	0.71	3.50	1.1
$V(acac)_3$	$Al(C_2H_5)_2Br$	8.5	0.48	0.38	0.14	0.67	0.81	1.2
$V(mbd)_3$	$Al(C_2H_5)_2Cl$	6.0	0.64	0.30	0.06	0.79	1.70	1.2

acac: 2,4-pentanedionato, mbd: 2-methyl-1,3-butanedionato, r: syndiotactic(racemic)dyad, m: isotactic(meso)dyad.

These kinetic and stereochemical results are direct evidence of the bimetallic structure of the active center in which alkylaluminium components are involved as important ligands.

2. Structure of "Living" Polypropylene End

The structure of living polypropylene end was studied by ^{1}H NMR analysis of iodine-terminated polypropylenes of low molecular weights. As reported in previous papers[8,9], the living polypropylene end of vanadium-carbon bond reacts instantaneously with the iodine molecule to give an iodine-bonded monodisperse polypropylene. The analysis of iodine-bonded polypropylene offers direct information on the structure of living polypropylene end, since active vanadium is replaced by an iodine atom.

For the purpose of chain-end structure analysis, an iodine-bonded propylene oligomer was prepared by the reaction of iodine with a living propylene oligomer of 12 propylene units ($\bar{P}n$ = 12) obtained at -78°C with the $V(acac)_3/Al(C_2H_5)_2Cl$ catalyst. Figure 3 shows the ^{1}H NMR spectrum of iodine-bonded propylene oligomer. Except for the strong resonances of 0.7 - 1.7 ppm arising from protons in the polypropylene segment, two weak signals, a (d, 1.95 and 1.98) and b (m, 4.30), are observed at the lower magnetic field of the spectrum. As reported in a previous paper[9], these new signals are assignable to the resonances of protons in the chain-end group bonding to iodine atom as formed by reaction 1,

$$*V^{3+}\text{-}\underset{\underset{(\,1\,)}{}}{\overset{\overset{CH_3}{|}}{CH}}\text{-}CH_2\text{-}(P) + I_2 \longrightarrow I\text{-}\underset{\underset{(\,2\,)}{}}{\overset{\overset{\overset{a}{CH_3}}{|}}{\underset{\underset{b}{}}{CH}}}\text{-}CH_2\text{-}(P) + V\text{-}I \qquad (1)$$

where $*V^{3+}$ represents an active vanadium center and (P) denotes the polypropylene chain.

The chain-end structure (2) is formed by the reaction of I_2 with a secondary vanadium-carbon bond (1) arising from a secondary insertion of propene into a vanadium-polymer bond. On the other hand, the addition of I_2 to a primary vanadium-carbon bond (3) gives the chain-end structure (4) following the mechanism of reaction (2).

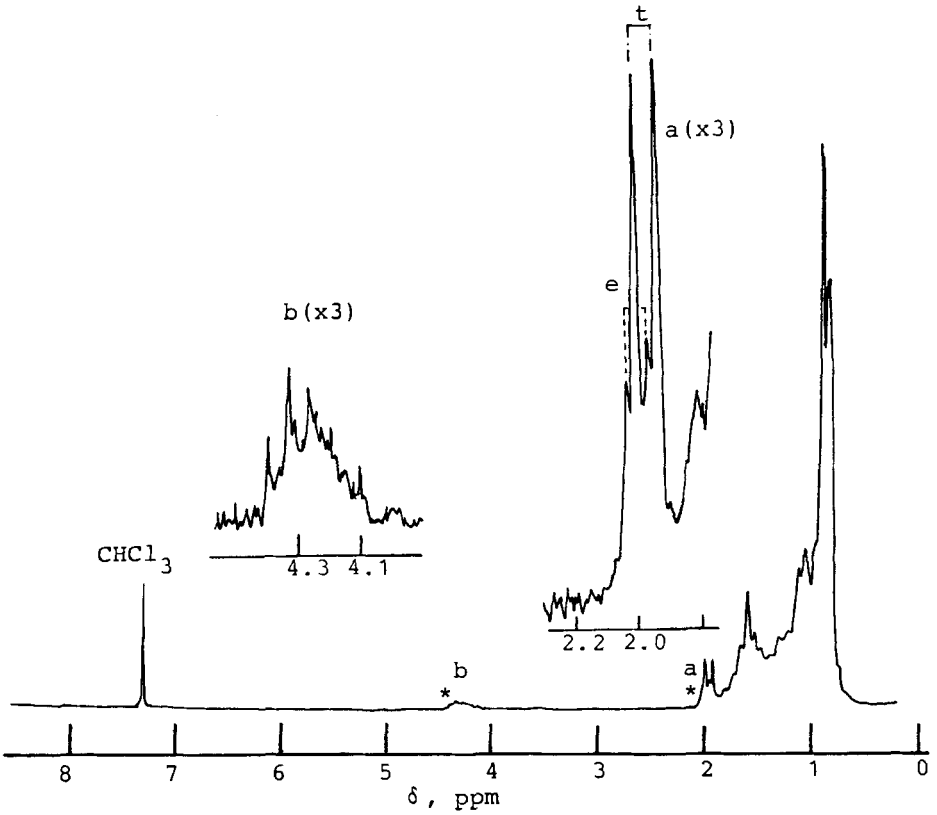

Figure 3. 100 MHz ^{1}H NMR spectrum of iodine-terminated propylene oligomer ($\overline{P}_n$= 12). Chemical shifts are in ppm down-field from TMS.

$$*V^{3+}\text{-}CH_2\text{-}\underset{\underset{(3)}{}}{\overset{CH_3}{\overset{|}{C}}}H\text{-}(P) + I_2 \longrightarrow I\text{-}\underset{\underset{(4)}{}}{\overset{\alpha}{CH_2}}\text{-}\overset{CH_3}{\overset{|}{C}}H\text{-}(P) + V\text{-}I \qquad (2)$$

The doublet resonance of α-methylene proton in the chain-end structure (4) is expected to appear at 3.1 - 3.2 ppm on the basis of the ^1H NMR spectra of some model compounds such as $CH_3\text{-}CH(CH_3)\text{-}CH_2\text{-}I$ ($\alpha\text{-}CH_2$ proton: d, δ 3.10). However, we could not detect any signal at around 3.1 ppm in the spectrum in Figure 3. These results are direct evidence that the majority of active vanadium complexes exist as secondary vanadium-carbon bonds during the syndiotactic-specific propagation of living polypropylene.

The signal a of methyl proton in the last inserted propylene unit consists of two doublet resonances (see Figure 3). The weak doublet resonance (d, δ1.98, $J_{H\text{-}H}$ = 6.8H_Z) in the lower field is related to the erythro (isotactic) placement of the last propylene units (2-e), whereas the strong doublet resonance (d, δ1.95, $J_{H\text{-}H}$ = 6.8 H_Z) in the higher field is related to the threo (syndiotactic) placement of the same units (2-t), as represented by

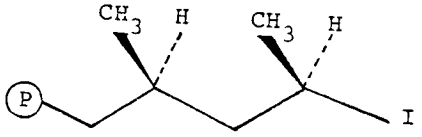

(2-e)

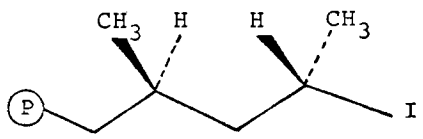

(2-t)

Then, the intensity ratio, $I_t/(I_t + I_e)$, represents the degree of syndiotactic regularity of the last propylene units formed via the secondary insertion into a vanadium-polymer bond. The value of $I_t/(I_t + I_e)$ was determined as being 0.79 $\pm$ 0.05 from the spectrum in Figure 3, and was almost identical with the syndiotactic diad fraction ([r] = 0.81) of propylene units in a long polymer chain (Pn = 690) obtained with the same catalyst.

It has been found that the syndiotactic regularity of propylene units in the secondary insertion step is not influenced by the sequence length of a living polymer chain but dependent upon the kind of aluminium component used as co-catalyst[14].

3. Reactivity of "Living" Polypropylene End

The propagation rate of living polypropylene chain can be expressed by Eq.(3) in the polymerization of propene with the catalyst $V(acac)_3/Al(C_2H_5)_2Cl$[3]:

$$R_p = \frac{\overline{P}_n[N]}{t} = k_s \left(\frac{K_M[M]}{1 + K_M[M]}\right)[N] \qquad (3)$$

where [M] denotes the concentration of propene monomer and [N] represents the number of living polypropylene chains, i.e. the number of active centers. The values of the constants k_s and K_M found at -78, -65 and -48°C are listed in Table 2, together with their activation energies.

Table 2. Rate constants k_s and K_M of elementary steps (Eq.3) observed in the polymerization of propene with the catalyst $V(acac)_3/Al(C_2H_5)_2Cl$.

Temp. (°C)	k_s (s^{-1})	E_{k_s} (kcal/mol)	K_M (dm^3/mol)	E_{K_M} (kcal/mol)
-78	0.053	8.1	0.37	0.8
-65	0.12		0.35	
-48	0.89		0.28	

Eq.(3) can be interpreted in terms of the mechanism (4) that the rate-determining step of the chain propagation is the insertion of the coordinated propene monomer into a vanadium-polymer bond.

$$*V^{3+}\text{-}P_i + C_3H_6 \underset{}{\overset{K_M}{\rightleftharpoons}} \overset{C_3H_6}{*V^{3+}\text{-}P_i} \xrightarrow{k_s} *V^{3+}\text{-}P_{i+1} \qquad (4)$$

The constants K_M and k_s denote the equilibrium constant for propene monomer coordination and the rate constant for the insertion of the coordinated monomer. The coordination energy of monomer to the

vanadium was as small as 0.8 kcal/mol, and the activation energy of the insertion step was determined to be 8.1 kcal/mol.

We propose here a model for the chain propagation of living polypropylene bonded to an active vanadium center, as depicted in Figure 4. A tetracoordinated V^{3+} complex is proposed as an active center, in which bidentate dionato, chloride and alkyl ligands are coordinated to the V^{3+} ion and dialkylaluminium chloride in dimer form is bound via a chloride ligand. After propene coordination, the active complex changes from tetra- to pentacoordination. The activity and stereospecificity of active the vanadium complex may be regulated by the bound aluminium component which influences both electronic and geometric structures of vanadium-carbon bond. The pentacoordinated V^{3+} complex was originally proposed by Zambelli and Allegra[15].

Molecular hydrogen was found to function as a chain transfer agent for living polypropylene[16]. In the presence of H_2 the polydispersity ($\bar{M}w/\bar{M}n$) of polymers increased with polymerization time and approached 2.0, corresponding to a most probable distribution of chain length. The chain transfer with H_2 could be expressed by Eq.(5).

$$*V^{3+}- P_i + H_2 \xrightarrow{k_t} *V^{3+}- H + P_i- H \qquad (5)$$

The rate constant for chain transfer reaction with H_2, k_t, was determined to be 0.2 $bar^{-1} h^{-1}$ at -78°C.

The reaction of living polypropylene end with additives such as I_2, amine and CO is of importance for the synthesis of terminally functionalized polypropylenes which exhibit new characteristic properties or function as initiators for block copolymer synthesis.

As described in the preceding section, an iodine-bonded polypropylene was prepared by the reaction of I_2 with the living polypropylene end. The reaction was completed within a few minutes at -78°C to yield a monodisperse polypropylene ($\bar{M}w/\bar{M}n$ = 1.15). The element analysis of iodine-terminated polypropylene indicated that I_2 reacted quantitatively with a vanadium-polymer bond to give a new iodine-polymer bond along the scheme (1). The iodine-bonded monodisperse polypropylene was reacted with an excess amount of ethylene

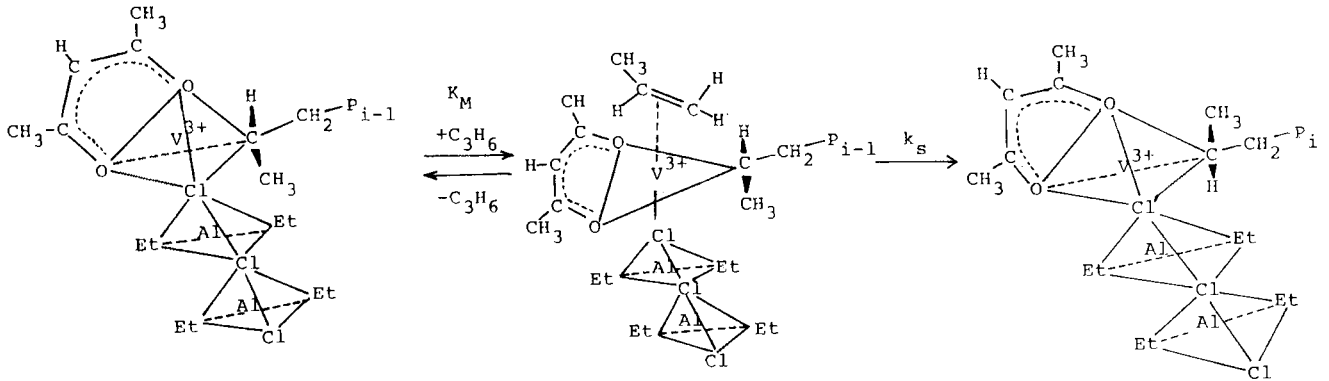

Figure 4. Proposed structure of active complex and mechanism for chain propagation in the living coordination polymerization of propene with the soluble $V(acac)_3/Al(C_2H_5)_2Cl$ catalyst.

diamine for 120 h at room temperature in THF solution, followed by washing with aqueous alkaline solution. This reaction resulted in the formation of a NH_2-functional polypropylene (5).

$$\underset{(\,2\,)}{I\text{-}CH(CH_3)\text{-}CH_2\text{-}(P)} + H_2NCH_2CH_2NH_2 \xrightarrow[THF]{r.t.} \xrightarrow[H_2O]{NaOH} \underset{(\,5\,)}{H_2N\text{-}CH_2\text{-}CH_2\text{-}NH\text{-}CH(CH_3)\text{-}CH_2\text{-}(P)} \qquad (6)$$

The reaction of CO with the living polypropylene was performed by adding carbon monoxide of 1 or 30 bar into the toluene solution of living polypropylene produced with the catalyst of $V(acac)_3/Al(C_2H_5)_2Cl$ at -78°C, followed by hydrolysis with aqueous hydrochloric acid. The IR spectra of the CO-terminated bolypropylenes after hydrolysis showed an absorption band at 1723 cm being attributable to the stretching vibration of CO groups. The number of CO groups per one polypropylene chain was found to be almost unity, which indicates that every living polypropylene chain reacts quantitatively with one molecule of CO. The reaction of CO with a living polypropylene end has been represented by the following scheme [10].

$$\underset{(\,1\,)}{*V^{3+}\text{-}CH(CH_3)\text{-}CH_2\text{-}(P)} + CO \xrightarrow{-78°C} *V^{3+}\text{-}C(=O)\text{-}CH(CH_3)\text{-}CH_2\text{-}(P)$$

$$\xrightarrow{HCl} \underset{(\,6\,)}{H\text{-}C(=O)\text{-}CH(CH_3)\text{-}CH_2\text{-}(P)} + V^{4+}\text{-}Cl \qquad (7)$$

REFERENCES

1. J.Boor,Jr., "Ziegler-Natta Catalysts and Polymerizations" Academic Press, New York 1979
2. M.Morton, "Anionic Polymerization: Principles and Practice" Academic Press, New York 1983
3. Y.Doi, S.Ueki, and T.Keii, Macromolecules, 12, 814(1979)
4. Y.Doi, S.Ueki, and T.Keii, Makromol. Chem., 180, 1359(1979)
5. Y.Doi, S.Ueki, S.Tamura, S.Nagahara, and T.Keii, Polymer, 23, 258(1982)
6. Y.Doi, Macromolecules, 12, 1012(1979)
7. Y.Doi, T.Koyama, and K.Soga, Makromol. Chem., 185, 1827(1984)
8. Y.Doi, Y.Watanabe, S.Ueki, and K.Soga, Makromol. Chem., Rapid Commun., 4, 533(1983)
9. Y.Doi, F.Nozawa, M.Murata, S.Suzuki, and K. Soga, Makromol. Chem., in press
10. Y.Doi, M.Murata, and K.Soga, Makromol. Chem., Rapid Commun., 3, 225(1984)
11. Y.Doi, S.Ueki, and T.Keii, Makromol. Chem., Rapid Commun., 3, 225(1982)
12. Y. Doi, S.Ueki, and T.Keii, "Coordination Polymerization" edited by C.C.Price and E.J.Vandenberg, Plenum Pub., New York 1983, p.249
13. Y.Doi, T.Koyama, and K.Soga, Makromol. Chem., 186, 11(1985)
14. Y.Doi, F.Nozawa, and K.Soga, Makromol. Chem., in press
15. A.Zambelli, and G.Allegra, Macromolecules, 13, 42(1980)
16. Y.Doi, S.Ueki, and T.Keii, Polymer, 21, 1352(1980)

LIGAND EFFECTS ON METALLOCENE CATALYZED ZIEGLER-NATTA POLYMERIZATIONS

JOHN A. EWEN
Fina Oil and Chemical Company, Box 1200, Deer Park, Texas 77536.

ABSTRACT

The effects of the chiralities, steric requirements and basicities of ligands attached to soluble Ti and Zr metallocene catalysts on propylene and ethylene homo- and copolymerizations have been reviewed. Isotactic polypropylene configurational structures are controlled by chiral cyclopentadienyl (Cp) ligands and chiral chain-ends; possibly both individually and simultaneously. Ethylene–propylene copolymerization reactivity ratios are predominantly influenced by ligand steric effects. The polymerization rates and polymer molecular weights obtained in Zr catalyzed ethylene polymerizations vary according to both Cp basicities and steric requirements. Novel polypropylene microstructures, narrow polydispersities ($\overline{M}_w/\overline{M}_n$), bimodal polyethylene molecular weight distributions and tailored copolymer composition distributions have been obtained.

INTRODUCTION

Ligand effects on catalyst selectivities, polymerization rates and stabilities are of both practical and fundamental importance. Surprisingly, few investigations of substituted cyclopentadienyl (Cp) ligand effects have been published during the decade following the discovery of the versatile group 4b metallocene/methylalumoxane catalyst systems.[1,2)]

The polymerization behaviour of a series of titanoncene and zirconocene derivatives having substituents on the Cp rings are reviewed in this paper. The ligand effects provide insight into the polymerization reaction mechanisms and have enabled the syntheses of polypropylenes (PP) with novel microstructures,[3)] ethylene/propylene copolymers (EP) with controlled composition distributions[4,5)] and high density polyethylenes (HDPE) with both narrow and bimodal molecular weight distributions (MWD).[6)]

The metallocenes have proven to be a nearly ideal system for the study of ligand effects on Ziegler-Natta polymerizations since the basicities, steric requirements and chiralities of the ligands attached to titanium and zirconium centers strongly influence the polymerizations. In addition, the catalysts and reaction intermediates possess controlled, well-defined ligand environments.[3,7,8)]

EXPERIMENTAL

Catalyst and cocatalyst syntheses, kinetic and polymerization procedures, polymer molecular weight determinations and PP ^{13}C NMR structural characterizations have been described previously.[3,9)] EP copolymer molecular weights were estimated from GPC data by empirical interpolation between the calculated values for PP and HDPE. RCps were prepared under a N_2 atmosphere from stoichiometric quantities of LiCp and the corresponding alkyl bromides in THF; allowing the solutions to warm to ambient from dry ice/acetone temperature. RCps were aromatized with n-BuLi and reacted with $ZrCl_4$ without isolation of the intermediates. The air stable complexes were purified by vacuum sublimation and found to be spectroscopically pure by ^1H NMR. 1:1 alumoxane/trimethyl aluimnum (TMA) mixtures were synthesized with $CuSO_4.5H_2O$ as described earlier.[3)] The cocatalyst for the HDPE polydispersity and some EPR comonomer composition distribution studies was synthesized by incremental hydrolysis of 30 cc portions of a stock solution (600 cc of 14.5% TMA in hexane) with 0.3 cc water at 100 °C in a high pressure reactor.[4-6)] The cocatalyst solutions obtained with this latter procedure contained insoluble white material and resulted in relatively broad polymer MWDs of 3-4.

RESULTS

Polymerization Scheme.[3)] It has been previously shown that propylene polymerization rates for catalysts derived from $Cp_2Ti(Ph)_2$ vary linearly with the product of monomer, transition metal and total Al concentrations with < 11% propylene conversion and < 100 mM Al. Catalyst turn overs were typically between 0.1 to 5 sec^{-1}. Polypropylene MWDs tend assymptotically to the most probable value for a single polymerization species with time at < -30 °C and

molecular weights vary linearly in direct proportion with the catalyst turn over numbers.

Scheme I

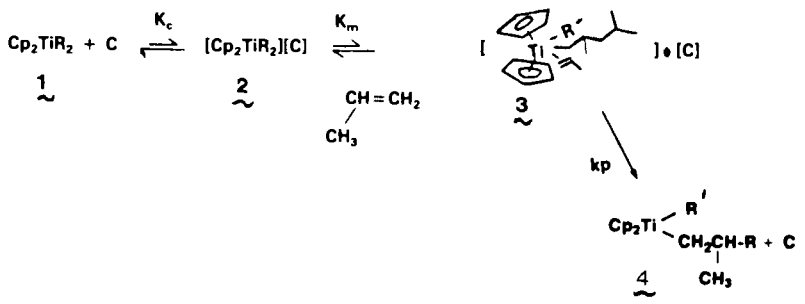

Scheme I, for $Cp_2Ti(IV)$ polymerizations of propylene, is representative of the kinetics for all of the polymerizations.

Under pseudo-first-order conditions:

$$R_p = k_{obsd}[C_3H_6][C][M] \quad (1)$$

with

$$k_{obsd} = k_p K_c K_m/(1 + K_m[C_3H_6] + K_c[C]) \quad (2)$$

and

$$K_m[C_3H_6] + K_C[C] << 1 \quad (3)$$

The oligomeric alumoxane = $[Al(CH_3)\text{-}O\text{-}]_n$ is represented as C. The propagation kinetics indicate low pseudo-equilibrium (competing processes) and equilibrium levels of species 2 and 3 respectively under the polymerization conditions. Species 1 and 4 are presumably at high concentrations since intercepts of linear plots of the number of polymer chains/Ti vs time are consistent with 100% and 40% of the Ti having growing chains at -30 and -60 °C respectively; providing there is only one chain per Ti.[3)]

Species 1 and 4 are formally d^0 16-electron, coordinatively unsaturated, pseudo-tetrahedral, bent metallocenes in the four oxidation state. Structure 2 represents the catalyst in its resting state. Intermediate 3 is shown with the monomer coordinated at a $1a_1$ orbital with the three non-Cp ligands and the transition metal in a common plane.[7a)] The carbon–carbon double bond is cis to and

coplanar with the metal alkyl sigma-bond prior to a concerted "1-2" cis-insertion.[3,10] The bonding mechanism between the metallocene and the cocatalyst is unknown.

Polypropylene stereoregulation. Two alternative configurational microstructures for isotactic polypropylene (PP) are represented by Structures I and II

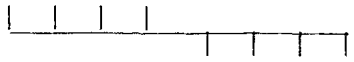

(I)

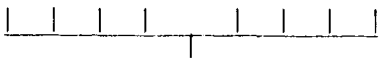

(II)

The pairs of adjacent methine carbons are predominantly meso (m) dyads of the same relative configuration. The m dyads are connected by one (Structure I) and two (Structure II) racemic (r) dyads, respectively.

Ligand effects on stereoregulation are apparent from the influence they have on the mechanisms by which asymmetry is transfered to the growing polymer chain. Stereoregulation can be due to a chiral stereorigid Cp ligand, to a conformationally stable chain-end methine group or to both mechanisms simultaneously.

Table 1. Structures of metallocenes and their stereochemical control mechanisms in propylene polymerizations.

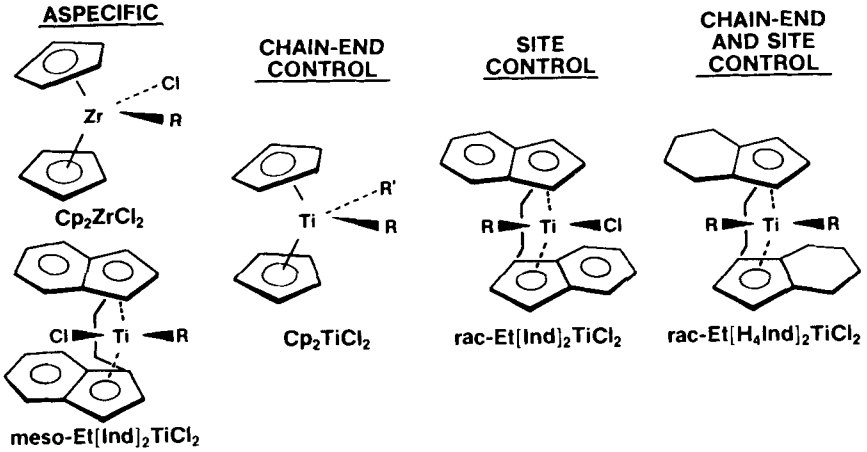

The structures of the metallocenes used to investigate the mechanisms of stereochemical control are portrayed in Table 1.

Chain-end control. Figure 2 is an example of the ^{13}C NMR spectrum of the methyl pentad region for isotactic polypropylene obtained with $Cp_2Ti(Ph)_2$. Only nine bands for the ten unique steric arrangments of five adjacent monomer units are observed since the mmrm and rmrr pentads have the same chemical shifts.[11)]

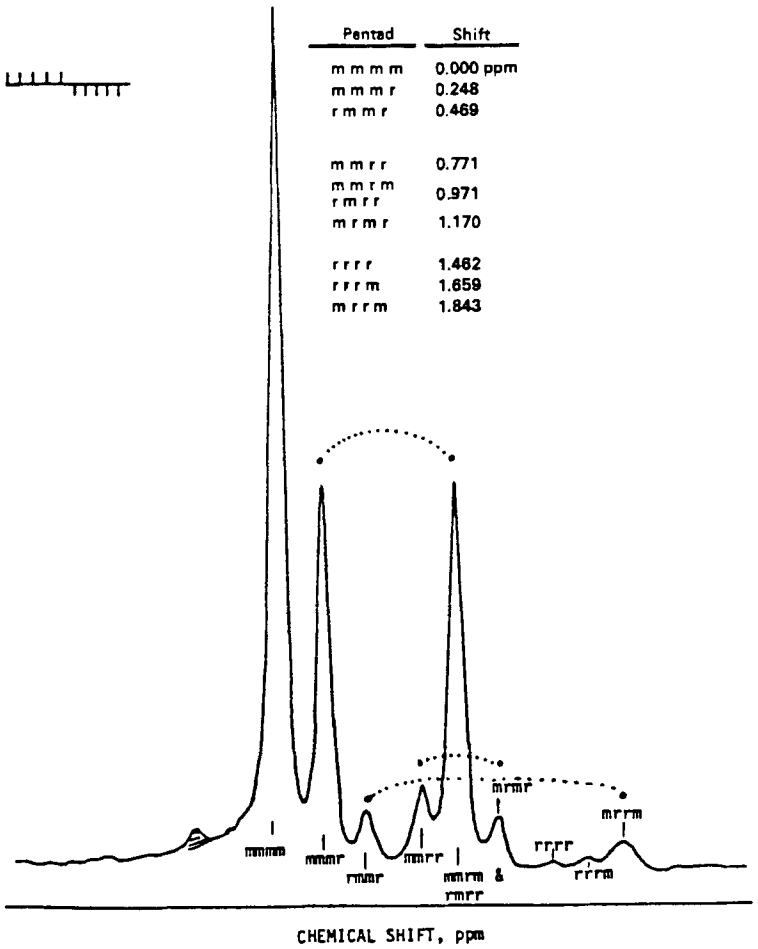

Figure 2. ^{13}C NMR spectrum isotactic stereoblock polypropylene obtained with $Cp_2Ti(Ph)_2$ at -30 °C.[3)]

The three most intense pentad bands correspond to the longer isotactic sequences (mmmm) and the stereoblock junctures (mmmr and mmrm). The predominant pentads identify the polymer ...mmmmrmmmmrmmmm... stereosequences in accord with Structure I. The connected pentads in Figure 2 have equal intensities within experimental error; as required by the structural model. Further, all the pentad intensities can be calculated using one adjustable parameter and Bovey's[23] theoretical Bernoullian statistical equations for chain-end controlled stereospecific polymerizations.[3] Sructure I is obtained since steric inversions during propagation result in the new absolute configuration of the last inserted monomer unit becoming the most probable one in the succeeding enchainment.

The stereoblock polymers with less than 95 %-m placements did

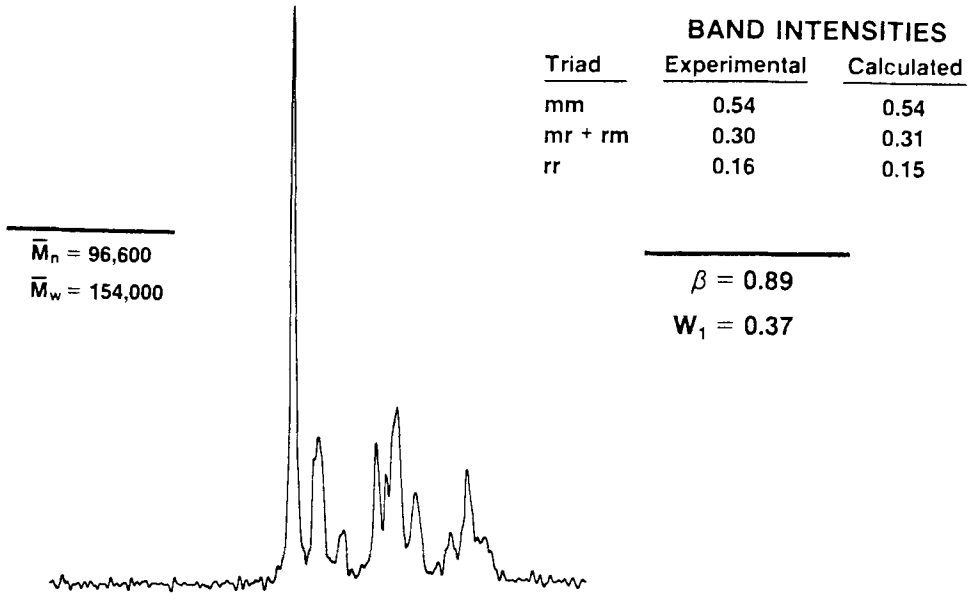

Figure 3. ^{13}C NMR spectrum of methyl region for polymer mixture obtained with meso- and rac-Et[Ind]$_2$TiCl$_2$ at -60 °C. (m.pt. = 94 °C).

not exhibit sharp melting points. Final m.pts. for the samples obtained at -30 °C (83%-m) and at -60 °C (85%-m) were 55 °C and 62 °C respectively.

Site control. The ^{13}C NMR spectrum for the methyl region of PP

obtained with a mixture meso- and rac-Et[Ind]$_2$TiCl$_2$ at -60 °C is displayed in Figure 3.

Heptad effects preclude accurate measurement of the pentad intensities for this particular spectrum. The experimental and calculated triad band intensities are shown, however, to be in accord with a 2 parameter model for a mixture of 63% isotactic and 37% atactic PP with the chiral catalyst having a probability parameter of 0.89.

Calculation of 3 observables with 2 parameters does not prove the site control mechanism. Indeed, this mixture of atactic and isotactic material "falsely" satisfies the enantiomorphic-site control triad (2[rr]/[mr] =1) and pentad (mmmr:mmrr:mrrm = 2:2:1) tests.[3] Convincing evidence for isotactic material with Structure II due to an enantiomorphic-site control mechanism and an atactic fraction consisting of an ideally random structure was obtained by calculating the nine pentad intensities with a 2 parameter model after fractionation of the original sample.[3]

The catalyst chirality dictates stereoregulation in the chiral catalyst site control mechanism. This results in the occasional steric inversions in the chain being predominantly reversed in succeeding monomer enchainments.

Dual control. The dual control model assumes mixed stereoregulation in which the stereochemistry is controlled by the enantiomorphic-site and by the chain-end simultaneously. The mathematical framework for this dual control model was laid out by Price[12] and the pentad equations listed in Table 2 were derived by Stehling.[26]

The spectrum of polypropylene obtained with rac-Et[H$_4$Ind]$_2$TiCl$_2$ at 0 °C is recorded in Figure 4 and Table 3. The sample had $\bar{M}_n$ = 37,100 and $\bar{M}_w/\bar{M}_n$ = 2.1 (Figure 5). This indicates that it was produced by a soluble catalyst.[13] Triad analysis and mechanistic model tests are consistent with the material having the enantiomorphic site control structure (Structure II) to a first approximation.

The pentad intensities are better accounted for with a 2 parameter model in Table 3. (The 4 parameters are defined in terms of each other.[3]) The relative intensities of the mmrr and mmrm bands prove that enantiomorphic-site is the predominant mechanism.

The lesser degree of stereochemical control by the chain-end is not surprising since this mechanism is only modestly effective or ineffective near and above the PP glass transition temperatures.[3)]

Isotactic polypropylene obtained with rac-Et[$IndH_4$]$_2TiCl_2$ at −60 °C contains 95%-m placements. The polymer had a melting point of 144 °C. The only clearly discernible bands other than the mmmm pentad

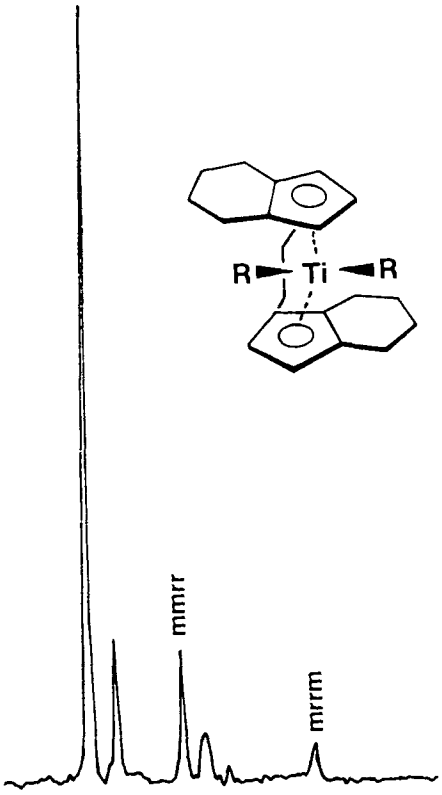

$P_a = 0.909$ $F_a = 0.887$
$P_b = 0.285$ $F_b = 0.113$

BAND INTENSITIES

Pentad	Experimental	Calculated
mmmm	0.56	0.61
mmmr	0.15	0.13
rmmr	0.019	0.01
mmrr	0.12	0.10
mmrm + rmrr	0.070	0.04 + 0.03 = 0.07
mrmr	0.013	0.017
rrrr	0.006	0.004
rrrm	0.013	0.0125
mrrm	0.049	0.048
	1.00	1.00

Figure 4. ^{13}C NMR spectra of the methyl pentad region of polypropylene obtained with rac-Et[$IndH_4$]$_2TiCl_2$ at 0 °C.(m.pt.= 99°C)

Table 2. Summary of dyad, triad and pentad intensities for the one site mixed-control model.[a)]

C type	Intensities
m	$(2 - P_a - P_b)^{-1}[P_a(1 - P_b) + P_b(1 - P_a)]$
r	$(2 - P_a - P_b)^{-1}[2(1 - P_a)(1 - P_b)]$
mm	$(2 - P_a - P_b)^{-1}[(1 - P_b)P_a^2 + (1 - P_a)P_b^2]$
mr	$(2 - P_a - P_b)^{-1}[2(1 - P_a)(1 - P_b)(P_a + P_b)]$
rr	$(2 - P_a - P_b)^{-1}[(1 - P_a)(1 - P_b)]$
mmmm	$F_a P_a^4 + F_b P_b^4$
mmmr	$F_a[P_a^3(1 - P_b) + P_b^3(1 - P_a)] + F_b[P_b^3(1 - P_a) + P_a^3(1 - P_b)]$
rmmr	$F_a P_b^2(1 - P_a)(1 - P_b) + F_b P_a^2(1 - P_a)(1 - P_b)$
mmrr	$2F_a P_a^2(1 - P_a)(1 - P_b) + 2F_b P_b^2(1 - P_a)(1 - P_b)$
mmrm	$F_a[P_a^2 P_b(1 - P_a) + P_b^2 P_a(1 - P_a)] + F_b[P_a^2 P_b(1 - P_a) + P_b^2 P_a(1 - P_b)]$
rmrr	$F_a[P_a(1 - P_a)^2(1 - P_b) + P_b(1 - P_a)^2(1 - P_b)] + F_b[P_a(1 - P_a)(1 - P_b)^2 + P_b(1 - P_a)(1 - P_b)^2]$
mrmr	$2P_a P_b(1 - P_a)(1 - P_b)$
rrrr	$(1 - P_a)^2(1 - P_b)^2$
rrrm	$F_a[P_a(1 - P_a)^2(1 - P_b) + P_b(1 - P_a)^2(1 - P_b)] + F_b[P_a(1 - P_a)(1 - P_b)^2 + P_b(1 - P_a)(1 - P_b)^2]$
mrrm	$F_a P_a^2(1 - P_a)(1 - P_b) + F_b P_b^2(1 - P_a)(1 - P_b)$

where $F_a = (1 - P_b)(2 - P_a - P_b)^{-1}$
and $F_b = (1 - P_a)(2 - P_a - P_b)^{-1}$

a)Equations derived by F. C. Stehling.[26)] Parameters were defined in ref. 3)

were two relatively small bands with a 1:1 intensity ratio which had the mmmr and the mmrm pentad chemical shifts. This is in accord with the polymer having Structure I and is evidence that the chain-end was the dominating chiral center for stereochemical control. The low level of steric imperfections compared to the mmmm band precluded detailed analyses of the other methyl pentads.

Table 3. Experimental and calculated intensities for polypropylene obtained with rac-Et[$IndH_4$]$_2TiCl_2$ at 0 °C.

C-type	Experimental	Band Intensities[a] One Species; Mixed Control	Difference
m	0.83	0.86	-0.03
r	0.17	0.14	0.03
mm	0.73	0.74	-0.01
mr	0.20	0.19	-0.01
rr	0.068	0.065	0.003
mmmm	0.56	0.61	0.05
mmmr	0.15	0.13	-0.02
rmmr	0.02	0.01	0.01
mmrr	0.12	0.10	0.02
mmrm	0.070	0.04 ≥ 0.07	0.00
mrmr		0.03	
rmrm	0.013	0.017	0.004
rrrr	0.006	0.004	0.002
rrrm	0.013	0.0125	0.01
mrrm	0.049	0.048	0.001

[a] For mixed control model $P_a = 0.909$; $F_a = 0.887$; $P_b = 0.285$; $F_b = 0.113$. Parameters defined in ref.3). Polymerization conditions were - 60 °C; .014 mmoles Ti; 4.1 mmoles Al; 1 h; 4.8 moles C_3H_6; 400 cc toluene;0.15 g yield and 0 °C; 0.0042 mmoles Ti; 36 mmoles Al; 5.05 moles C_3H_6; 400 cc toluene; 5.5 h and 0.60 g yield.

The difference in the stereoregulation mechanisms for rac-Et[$IndH_4$]$_2TiCl_2$ and rac-Et[Ind]$_2TiCl_2$ is attributed to the chain being cis to a bulky non-Cp ligand in the former complex (conformationally stable chain-end) and cis to a small chloride ligand in the latter (freely rotating chain-end).

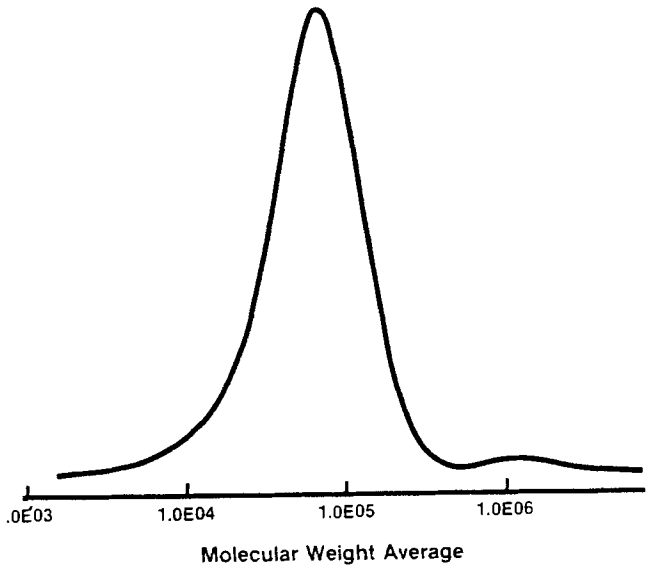

Figure 5. GPC elution curve of polypropylene produced with $Et[IndH_4]TiCl_2$ at 0 °C. $\bar{M}_n$ = 37,100 and $\bar{M}_w/\bar{M}_n$ = 2.1. The impurity centered at 10^6 MW represents less than 2% of the total polymer.

The different chain-end environments for the two chiral Ti catalysts may be a consequence of the relative basicities of the Cp ligands. The chloride ligands in rac-$Et[IndH_4]_2TiCl_2$ are most probably labilized towards ligand exchange (electron donating Cps) resulting in two chains per site. The Cl anions are bound more tightly to Ti in rac-$Et[Ind]_2TiCl_2$ (electron withdrawing Cps) resulting in only one chain per site. rac-$Et[Ind]_2TiCl_2$ is more stable than rac-$Et[IndH_4]_2TiCl_2$ at -60 °C during polymerization and, as a result, gives moderately higher PP yields.

Ethylene/propylene copolymerizations. The structures of the intermediates[7b] for the Zr complexes synthesized to investigate the Cp steric effects on ethylene/propylene copolymerizations are shown in Table 4. The alkyl substituted Cp ligands are more sterically hindered than Cp_2ZrCl_2 at the monomer coordination site.

The Si-bridged derivative is strained, with a reduced Cp-Zr-Cp angle (10 degrees) and has an enlarged R-Zr-L angle.[14] This change in geometry creates a monomer coordination site which is less

Table 4. Structures of reaction intermediates for zirconocenes with substituted Cps.

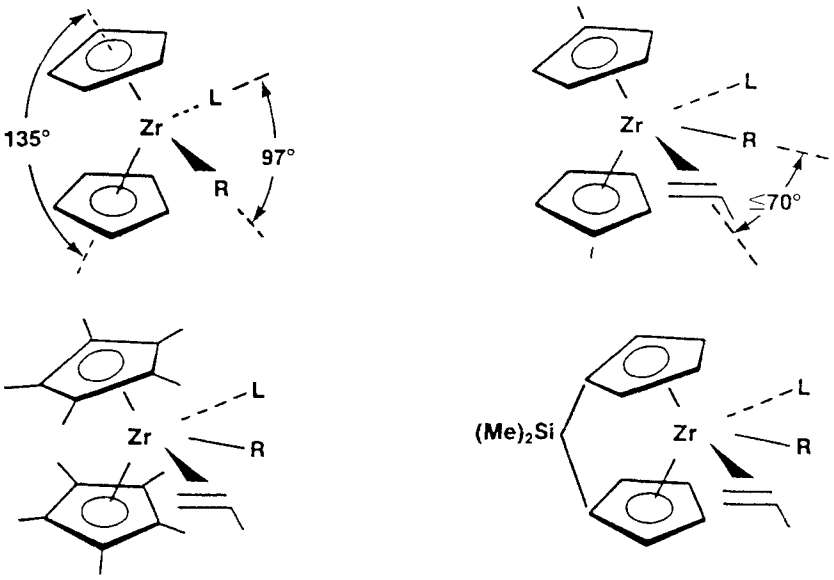

sterically hindered by both the Cp ligands and the chain ends. Cp^* has the opposite effect. The ligand steric effects are clearly more pronounced for the coordination of bulkier monomers.

A ^{13}C NMR spectrum of an EP copolymer produced with a $Cp_2Ti(IV)$ based catalyst has been reported previously[19] and the EP chemical shift ssignments have been summarized by Carmen et. al.[15] For the EP copolymers produced with Ti, the peaks at 34.9, 33.6 and 27.9 ppm due to carbons in sequences with inverted propylene units were negligibly small. Table 5 contains some typical polymerization conditions and polymer yields for copolymerization with single and mixed caralysts.

The dyad and triad sequence distributions in the copolymer samples were were determined from the secondary and tertiary carbon atom peak areas with the equations reported by Knox et. al.[16] The polymer compositions were calculated from the dyad and triad distribution equations (Eqs. 4 and 5).

Table 5. Representative yields, polymerization conditions and compositions of ethylene/propylene copolymers prepared with metallocene complexes.[a)]

Metallocene, mmol	Al, mmol	time, h	Yield g	Polymer mole-% C_3H_6
$Cp_2Ti(Ph)_2$ (3.13)	16	1.5	14.4	35
$Cp^*_2ZrCl_2$[b)] (0.312)	16	1.5	76	3.4
$Cp_2Ti(Ph)_2$ (3.37) + $Cp^*_2ZrCl_2$ (0.274)	16	1.0	62	6.0

[a)] Reaction conditions: 402 cc toluene; 200 cc C_3H_6 (<10% conversion); 50 °C; $P(C_2H_4)$ = 25 psig. [b)] Cp^* = Me_5Cp.

$$P = PP + 1/2PE = PPP + PPE + EPE \quad (4)$$

$$E = EE + 1/2PE = EEE + EEP + PEP \quad (5)$$

The triad sequence distributions can be calculated in terms of the first-order Markovian satistical process for of a binary

$$E\text{-}M + C_2H_4 \xrightarrow{k_{11}} EE\text{-}M \quad (6)$$

$$E\text{-}M + C_3H_6 \xrightarrow{k_{22}} EP\text{-}M \quad (7)$$

$$P\text{-}M + C_2H_4 \xrightarrow{k_{21}} PE\text{-}M \quad (8)$$

$$P\text{-}M + C_3H_6 \xrightarrow{k_{22}} PP\text{-}M \quad (9)$$

copolymerization involving the propagating steps in Eqs. 6 to 9.

Here k_{ij} is the rate constant for step ij, and the subscripts 1 and 2 refer to ethylene and propylene, respectively. If steady state conditions are assumed the monomer reactivity ratios r_1 and r_2 can be calculated from the dyad sequence distributions:

$$r_1 = k_{11}/k_{12} = 2EE/PE.X \qquad (10)$$

$$r_2 = k_{22}/k_{21} = 2PP.X/PE \qquad (11)$$

where X is the solution molar ratio of ethylene to propylene (determined by GC analysis) during polymerization. The calculated values are compared in Table 6.

Table 6. Reactivity ratios of metallocenes in EP copolymerizations.

Catalyst	r_1	r_2	$r_1.r_2$	Method
$Cp_2Ti{=}CH_2.DMAC$[a]	24	0.0085	0.20	NMR
$Cp_2Ti(Ph)_2$	19.5	0.015	0.29	IR
$[Cp_2ZrCl]_2O$	50	0.007	0.35	NMR
Cp_2ZrCl_2	48	0.015	0.72	IR
$Me_2SiCp_2ZrCl_2$[b]	24	.029	0.70	IR
$Cp^*_2ZrCl_2$[c]	250	.002	0.50	IR
$(MeCp)_2ZrCl_2$[b]	60			IR

[a] Tebbe reagent with DMAC = dimethylaluminum chloride. [b] Copolymer probably contains significant levels of H-H and T-T propylene regioirregularities. [c] Approximate "copolymerization parameter" (r_1) determined from IR measurements and assuming an ideal Bernoullian copolymerization with $r_1.r_2 = 1$.

Determination of the reactivity ratio products using IR measurements and the Fineman and Ross equation[17] and using alumoxanes that were obtained by direct water hydrolysis with the IR methods gave closely analogous results for r_1 but with higher $r_1.r_2$ values. Comparison of the values obtained by NMR and IR for the two

$Cp_2Ti(IV)$ and two $Cp_2Zr(IV)$ complexes (clearly the same intermediates with the same transition metal and same Cp ligand) demonstrates this point. Similar discrepancies between the Fineman and Ross IR procdure[17] and the Carman and Wilkes NMR method[18] were noted by other workers[19] after this study was completed.[4] Anomolously high $r_1 \cdot r_2$ values can be obtained if more than one distinct polymerization species are present.[21,22] MWD studies (vide infra) indicate this is the case in metallocene catalyzed polymerizations where the cocatalyst is obtained by direct water hydrolysis of TMA as opposed to hydrolysis with $CuSO_4.5H_2O$.

The large variation in the four zirconocene r_1 values as a function of the Cp ligand steric requirements (Table 6) is consistent with the steric effects on coordination being more severe for propylene than ethylene.

The moderately alternating copolymer structure obtained with $Cp_2Ti(IV)$ and the more random copolymer structure for $Cp_2Zr(IV)$ are consistent with the former catalyst having, predictably, greater non-bonded interactions between the CH_3 groups of coordinated C_3H_6 and propylene chain-end units. The decrease in the L-Zr-R angle in $Cp^*_2Zr(IV)$ relative to $Cp_2Zr(IV)$ results in the former complex producing a more alternating copolymer, as expected. The opposite effect with $Me_2SiCp_2Zr(IV)$ may have been masked by neglecting the regioirregularities with this relatively unhindered species.

The Cp^* ligand offers a unique opportunity for synthesizing HDPE/LLDPE and elastomer/medium density PE reactor blends with heterogeneous catalysts in the sense of two catalysts rather than two phases. An example of a reactor blend with the latter composition distribution obtained with a mixture of $Cp^*_2Zr(IV)$ and $Cp_2Ti(IV)$ is shown in Table 5. $Cp^*_2Zr(IV)$ and $Me_2SiCp_2Zr(IV)$ mixtures give analogous results from ligand effects alone but with lower molecular weights for the elastomeric fractions.

The copolymer triad sequence distributions, with the exception of the two weakly populated and experimentally less certain P centered triads, could be calculated fairly satisfactorily using a first-order Markovian analysis.[20]

High density polyethylene. The effects of Cp substituents on polyethylene molecular weights using zirconocenes under equivalent conditions are listed in Table 7.

Table 7. Representative yields and molecular weights of HDPE prepared with zirconocene complexes.[a)]

Metallocene,	Yield, kg/g-M.h.atm	$10^{-3}.\bar{M}_w$	MWD
$(MeCp)_2ZrCl_2$	467	212	3.8
$(EtCp)_2ZrCl_2$	306	171	3.8
Cp_2ZrCl_2	252	140	3.5
$Cp^*_2ZrCl_2$	71	63	4.7

a)Reaction conditions: 402 cc toluene; 80 °C; $P(C_2H_4)$ = 60 psig; Al/Zr = 24,000; time = 30 min. The alumoxane, obtained by hydrolysis with water, results in a lower $\bar{M}_n$ and a broader MWD than usual.

The molecular weights vary linearly with the polymerization rates (over 3 fold) for the four complexes at this particular set of conditions. A balance between the importance of both steric and electronic Cp ligand effects is apparent from comparisons of Cp_2ZrCl_2 with the complexes having alkyl Cp substituents.

The bulky Cp^* ligands decrease the polyethylene propagation rate (Eq. 2) by reducing both K_c and K_m (Scheme I). The reduction in molecular weight is not a consequence of increased termination rates. It has been shown previously that the higher basicity of Cp^* decreases k_t (termination by β-hydride elimination) relative to Cp in propylene polymerizations by decreasing the acidity of the metal.[3)]

The monoalkyl substituted Cps show the interesting result that the catalyst with MeCp is more active and gives a higher molecular weight than the catalysts with EtCp and Cp ligands. The MeCp

Table 8. Molecular weights and polydispersities obtained with individual and mixed complexes.[a)]

Complex, mg	Conditions	Yield,g	$10^{-3}.\bar{M}_n$	$\bar{M}_w/\bar{M}_n$	GPC
$Cp^*_2Zr(CH_3)_2$ (0.10)	A	20.6	42.0	3.31	Unimodal
$Cp_2Ti(Ph)_2$ (1.02)	A	13.2	184	3.03	Unimodal
$Cp^*_2Zr(CH_3)_2$ (.102) + $Cp_2Ti(Ph)_2$ (.906)	A	20.1	58.6	5.51	Bimodal
$Cp_2Zr(CH_3)_2$ (0.015) + $Cp_2Ti(Ph)_2$ (5.18)	B	10.7	63.0	7.8	Bimodal
$Cp_2Zr(CH_3)_2$ (0.151) + $Cp_2Ti(Ph)_2$ (5.50)	B	13.1	16.5	5.4	Bimodal

[a)]Polymerization conditions: (A) 511 cc toluene; 50 psig ethylene; 20 cc of cocatalyst with 0.64 M total Al; 50 °C; t = 30 minutes for individual complexes and 15 minutes for mixed complexes.
(B) 441 cc toluene; 60 psig ethylene; 15 mmoles total Al in cocatalyst; 80 °C; t = 40 minutes

catalyst receives the benefit of increased electron density at the metal (increasing k_p/k_t) with relatively little opposing steric effects on ethylene coordination.

The data collected in Table 8 shows that the narrow molecular weight distributions obtained with individual metallocenes can be broadened considerably by adding controlled amounts of more than one catalyst to the polymerization system. Further, the higher molecular weights obtained with Ti relative to Zr under identical polymerization conditions have permitted the use of mixed metal catalysts for the syntheses of materials with GPC elution curves having resolved bimodality (Figure 6). Simply varying the Ti/Zr ratio permits tailoring of $\bar{M}_n$ between 16,000 and 63,000.

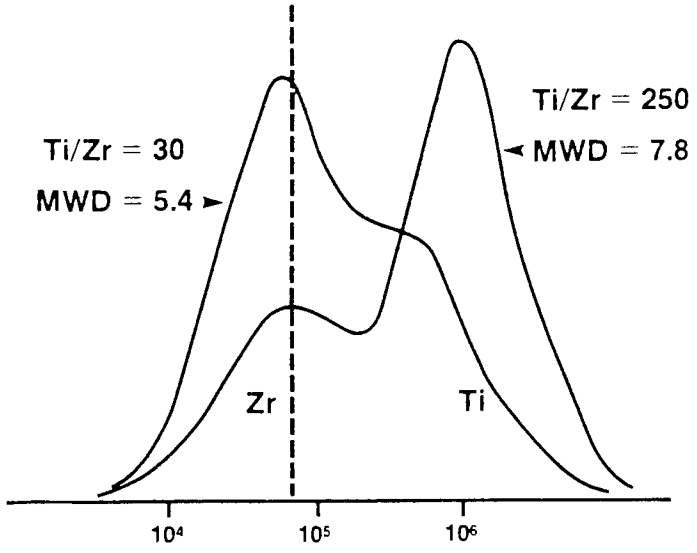

Figure 6. GPC elution curves of HDPE produced with $Cp_2Ti(Ph)_2$ and Cp_2ZrCl_2 mixtures.

DISCUSSION

Chain-end control. Three alternative mechanisms in which transfer of asymmetry from an enantiomorphic active site have

Table 2. Concentration dependencies of stereoregularities from mechanisms that predict the isotactic-stereoblock PP structure.

Mechanism	R(m)/[Ti*]	R(r)/[Ti*]	m/r
Isomerization	$k_p[C][C_3H_6]$	k_r	$k'[C][C_3H_6]$
	$(k_p[C_3H_6])$	(k_r)	$(k'[C_3H_6])$
Al Transfer	$k_p[C][C_3H_6]$	$k_r[C]$	$k'[C_3H_6]$
	$(k_p[C_3H_6])$	$(k_r[C])$	$(k'[C_3H_6]/[C])$
Ti Transfer	$k_p[C][C_3H_6]$	$k_r[Ti^*]$	$k'[C][C_3H_6]/[Ti^*]$
	$(k_p[C_3H_6])$	$(k_r[Ti^*])$	$(k'[C_3H_6]/[Ti^*])$
Chain-end	$k_m[C][C_3H_6]$	$k_r[C][C_3H_6]$	k'
	$(k_m[C_3H_6])$	$(k_r[C_3H_6])$	(k')

endo exo

The decreased steric interactions with $Me_2SiCp_2ZrCl_2$ most probably results in a significantly higher level of exo complexes and hence regioirregularities in copolymerizations. Neglect of these in the copolymer analyses may have obscured the anticipated Cp effects on comonomer sequence distributions.

Mixed-control. The good agreement between the theoretical and measured pentad intensities and the shift in the importance of the mechanisms of stereochemical control with temperature were cited as evidence of a mixed-control model. The trace impurity shown in Figure 5 suggests this mechanism is on less secure grounds than the chain-end and site control models and warrants further investigations. The pentad intensities listed in Table 3, however, could not be calculated with precedented mixed homopolymer models.

Carbon-carbon bond formation. A concerted bimetallic "1-2" insertion mechanism has been assumed as a working hypothesis. A carbene propagation mechanism is inconsistent with both the H/D kinetic isotope effects on ethylene polymerizations with $Cp_2Ti(IV)$[16a] and with the elegant polyacetylene isotopic labelling experiments by Katz and Yannoni et. al.[16b]

"Agostic" C-H-Ti bridges creating chirality at the methylene carbon of the chain-end is inconsistent with the lack of isotope effects on the polymer stereoregularity when cis-CD_3CD=CHD was substituted for propylene.[3]

Catalyst/cocatalyst interaction. The steric bulk of the alumoxane presumably prevents the soluble Cp_2MRL.alumoxane species from deactivating by bimolecular reductions. The catalyst/cocatalyst bonding interactions in species 3 (Scheme I) were suggested by Kaminsky et. al.[25] to create an inner-sphere, hexacoordinate complex with oxygen coordinated at the transition metal. The 18 electron rule requires that, in this model, the coordinated methylalumoxane oxygen in species 2 dissociate prior to monomer coordination.[3,7] The unhydrolyzed aluminium alkyl (TMA), which is essential for good polymerization rates,[26] can presumably free the catalyst monomer coordination site for polymerization by competing with Ti and Zr for the alumoxane oxygens.

been proposed to result in Structure I. They involve isomerizations of chiral active sites,[21] Al transportation of polymer chains between enantiomeric sites[22] and exchanges of polymer chains between soluble racemic Ti complexes.[3] All three require that the chemical processes changing the environment of the chain-end be slower than the monomer insertion rates. The pentad intensity distributions predicted for these mechanisms is the same as that for a chain-end control mechanism on condition that the chemical processes cause inversions sufficiently frequently so as to make errors in stereoregulation at a particular chiral catalyst site relatively negligible.

The three alternating chiral site control mechanisms for structure I are kinetically distinguishable since they predict the polymer stereoregularity (m/r) will have the reactant concentration dependencies listed in Table 2 where m/r is the ratio of rates for m and r propagations and rates are in terms of catalyst turn over numbers. The expressions in parentheses correspond to reactions zero-order in Al. The alternating chiral site control mechanisms can be discarded since the polymer stereoregularity is independent of all the reactant concentrations.[3]

The chain-end Ti stereochemical control mechanism with "1-2" insertion[3] takes effect at about the glass transition temperature for PP. $\Delta\Delta G^{\ddagger}$ is less than 2 kcals/mole, as it is for the chain-end controlled syndiotactic VCl_4 "2-1" insertion polymerization of propylene.[23] Both chain-end control systems occur with a reversed enantioface stereoselectivity, i.e., with Si and Re face coordination of the monomer being promoted by R and S chain-end configurations respectively. Ti would be syndiotactic specific and V isotactic isotactic specific if the diastereoface selectivities were changed to R,Re and S,Si. Finally, it is remarked that the Cossee and Arlman proposal of syndiotactic propagation with catalyst isomerization as result of insertion[24] predicts syndiotactic polymers with pentad distributions analogous to the isotactic site-control model with m and r reversed in the distribution equations.

Regiospecificty. Molecular models indicate the Cp ligands affect regiospecificity through steric interactions with the propylene methyl group favoring the formation endo isomers.

Rearrangements to monohapto or allyl Cps to create additional coordination vacancies are ruled out since the relative polymerization rates of $Et[Ind]_2TiCl_2$ and $Et[IndH_4]_2TiCl_2$ indicate that monomer coordination is not accelerated by the "indenyl ligand effect". [27]

Cp effects. Significant Cp steric and electronic ligand effects are apparent in the ethylene, propylene and ethylene/propylene homo- and copolymerizations that have been discussed. The ligand steric and electronic effects are both important with the Zr catalysts. The steric effects dominate the Ti polymerizations to the point where $Cp^*_2Ti(IV)$ complexes are practically inactive towards ethylene polymerizations.

ACKNOWLEDGEMENTS

I am indebted to Fina Oil and Chemical Company for financial assistance which made this work possible. I also thank Dr. H. C. Welborn and Dr. F. C. Stehling for valuable contributions to the work covered in this review.

REFERENCES

1. A. Andresen, H. Cordes, J. Herwig, W. Kaminsky, A. Merck, R. Mottweiler, J. Pein, H. Sinn and H. Vollmer, Angew. Chem. Int. Ed. Engl. 15, 630 (1976).
2. H. Sinn and W. Kaminsky, Adv. Organomet. Chem., 18, 99 (1980).
3. J. A. Ewen, J. Amer. Chem. Soc., 106, 6355 (1984).
4. J. A. Ewen and H. C. Welborn, "Reactor Blend Polyolefins"; European Patent Publication No. 128,046 (Dec. 12, 1984).
5. J. A. Ewen and H.C. Welborn, "Polyolefin Density and Molecular Weight Control"; European Patent Publication No. 129,368 (Dec. 27, 1984)
6. J. A. Ewen and H. C. Welborn, "Polyethylene Having a Broad Molecular Weight Distribution"; European Patent Publication No. 128,046 (Dec. 12, 1984).
7. (a) C. J. Ballhausen and J. P. Dahl, Acta Chem. Scand., 15, 1333 (1961). (b) J. W. Lauher and R. Hoffmann, J. Am. Chem. Soc., 98, 1729 (1976).

8. M. E. Silver and R. C. Fay, Organometallics, 2, 44, (1983).
9. H. Kopf and W. Kahl, J. Organometal.Chem.,64, C37 (1974).
10. (a) J. Soto, M. Steigerwald and R. H. Grubbs, J. Amer. Chem. Soc., 104, 4479 (1982). (b) T. J. Katz, S. M. Hacker, R. D. Kendrick and C. S. Yannoni, J. Amer. Chem. Soc., 107, 2180 (1985).
11. A. Zambelli, P. Locatelli, G. Bajo, and F. A. Bovey, Macromolecules, 8, 687, (1975).
12. F. P. Price in "Markov Chains and Monte Carlo Calculations in Polymer Science", G. G. Lowry, ed., Dekker, N.Y., pp187-256.
13. Y. Doi, J. Kinoshita, A. Morinaga, T. Keii, J. Polym. Sci., Polym. Chem. Ed., 13, 2491 (1975).
14. J. A. Smith, J. V. Severl, G. Huttner and H. H. Brintzinger, J. Organometal. Chem., 173, 175 (1976).
15. C. J. Carman, R. A. Harrington and C. E. Wilkes, Macromolecules, 10, 536 (1977).
16. G. J. Ray, P.E. Johnson and J. R. Nox, Macromolecules, 10, 773 (1977).
17. M. Fineman and S. D. Ross, J. Polym. Sci.,5, 259 (1950).
18. C. J. Carman, C. E. Wilkes, Rubber Chem. Technol., 48, 705 (1975).
19. V. Busico, L. Mevo, G. Palumbo, A. Zambelli and T. Tancredi, Makromol. Chem., 184, 2193 (1985).
20. J. C. Randall, "Polymer Sequence Determination ^{13}C NMR Method", Academic Press, New York, 1977.
21. G. Natta and I. Pasquon, Adv. Catal., 11, 30 (1959).
22. J. P. Kennedy and A. W. Langer, Fortschr. Hochpolym.-Forsch., 3, 508, (1969).
23. A. Zambelli, P. Locatelli, A. Provasoli and D. R. Ferro, Macromolecules,13, 267 (1980).
24. E. J. Arlman and P. Cossee, J. Catal.,3, 103 (1964).
25. W. Kaminsky, M. Miri, H. Sinn and R. Woldt, Makromol Rapid Commun., 4, 417 (1983).
26. R. Job, personal communication.
27. M. E. Rerek, L-N Ji and F. Basolo, J. Chem. Soc., Chem. Commun., 1208 (1983).

PREPARATION OF SPECIAL POLYOLEFINS FROM SOLUBLE ZIRCONIUM COMPOUNDS WITH ALUMINOXANE AS COCATALYST

W. KAMINSKY
Institut für Technische und Makromolekulare Chemie, Universität Hamburg, Bundesstr. 45, D-2000 Hamburg 13, FRG

ABSTRACT

The Ziegler-Natta catalyst containing soluble zirconium compounds and methylaluminoxane not only shows a very high activity of $25 \cdot 10^6$ g PE/g Zr·h but also produces polyolefins with special properties. It is possible to get polyethylene with density between 0,90 and 0,98 g/cm^3 by incorporation of butene and a melting point of 140 ^{o}C.

With bis(cyclopentadienyl)zirconiumdichloride as transition metal component we can polymerize propylene to pure atactic polypropylene with molecular weights up to 600 000. Also EPDM elastomers are formed by copolymerization. Changing the zirconium compound into the chiral ethylene(bistetrahydroindenyl)zirconiumdichloride leads to a catalyst which produces only isotactic polypropylene. The atactic part is less than 0,5 %.

All products show a very narrow molecular weight distribution M_w/M_n of 2. The mechanism for the polymerization will be discussed.

INTRODUCTION

The soluble Ziegler-Natta-Catalyst formed from bis(cyclopentadienyl)zirconium compounds and the coactivator methylalumoxane with the structure $(Al(CH_3)O)_{6-20}$ gives activities up to $25 \cdot 10^6$ g polyethylene/g Zr·h. Assuming that every zirconium atom is an active center, the turnover time for one ethylene insertion step is only $5 \cdot 10^{-5}$ s [1-3].

Every active center inserts more than 20 000 ethylene molecules per second at 90 °C. It is also possible to use titanium or hafnium compounds as transition metals, but then the activity is smaller.

The catalysts are the more active the higher the degree of oligomerization of the aluminoxane, and possess a polymerization activity which lasts for days. At temperatures below -20 °C the transfer reaction is so slow, that the molecular weight is only a function of the polymerization time, as is found in living polymer systems. The molecular weight of the polyethylene can be varied over a wide range between 10 000 and 2 000 000 by changing the polymerization temperature between 20 and 100 °C and the zirconium concentration. In addition, the molecular weight can be influenced by addition of hydrogen. In contrast to most heterogeneous catalysts, only traces of hydrogen were needed to lower the molecular weight of the polymer. The molecular weight distribution M_w/M_n is only 2.

Natural substances like starch, cellulose and lignin can, due to their free water, form aluminoxane analogous structures on addition of trimethylaluminium. After addition of the metal compound starch grains or cellulose fibers treated in this manner have a considerable polymerization activity when suspended in toluene. By this procedure physical and chemical properties of natural and synthetic polymers can be combined.[4,5]

In the same manner it is possible to cover cellulose, lignin or inorganic materials like $CaCO_3$, $CaSO_4 \cdot 0,5\ H_2O$ or Al_2O_3 with polyethylene or other polyolefins.

COPOLYMERIZATION OF ETHYLENE AND HEXENE

By incorporation of hexene-1 into the polyethylene matrix LLDPE is produced. In **here** there is a remarkable dependence of the activity upon the hexene proportion (Table 1). As long as less than 50 mol-% hexene are engaged the polymerization rates are in the same order as for homopolymerization of ethene (e.g. 10^8 g polymer/g Zr·h). When the amount of hexene in the solution is exceeding that of ethene the polymerization rate will increase drastically (for app. 65 mol-%: $Rp = 1,8 \cdot 10^8$); further increase of the hexene proportion leads to a final de-

Table 1. Conditions and activity of ethylene (E) and hexene (H) copolymerization at 60 °C in toluene with $Cp_2Zr(CH_3)_2$/methylaluminoxane ($1{,}7 \cdot 10^{-2}$ mol Al/l)

Activity kg PEH	Yield g	E (bar)	H (mol/l)	Zr (mol/l)	Time (h)	H in Polymer (mol-%)
1970	6,0	4	0,12	$1 \cdot 10^{-7}$	1,00	0,4
2300	7,0	4	0,36	$1 \cdot 10^{-7}$	1,00	1,0
2800	8,5	4	0,72	$1 \cdot 10^{-7}$	1,00	6,5
2630	8,0	4	1,20	$1 \cdot 10^{-7}$	1,00	12,5
1580	16,0	4	0,36	$1 \cdot 10^{-6}$	0,20	1,4
1900	14,5	4	0,72	$1 \cdot 10^{-6}$	0,15	11,5

crease in the polymerization rate (Figure 1). Different reaction temperatures and concentrations of zirkonocene show all similarily a distinct maximum of the reaction rate. The activation energy for the growth rate is for app. 67 mol-% hexene En = 47,5 kJ/mole.

In spite of the great extent of hexene (max. 95 mol-%) it is incorporated to a by far smaller degree than ethylene (max. app. 20 mol-%) due to its high steric demands. According to the method of Finemann-Ross[6] the copolymerization parameters r_1 and r_2 were calculated from the insertion rates. At 20 °C they were found to be r_1 = 55 for ethylene and r_2 = 0,005 for hexene, respectively (Table 2).

Table 2. Ethylene-hexene-copolymerization parameters (Zr) = 10^{-6} mol/l, ethylene 4 bar, hexene 25-95 mol-%.

T	r_1	r_2	k_{11} (l/mol·s)	k_{22} (l/mol·s)
20 °C	55	0,004	150	0,2
40 °C	54	0,005	1 450	0,6
60 °C	52	0,005	3 460	1,5
70 °C	79	0,005	5 750	-

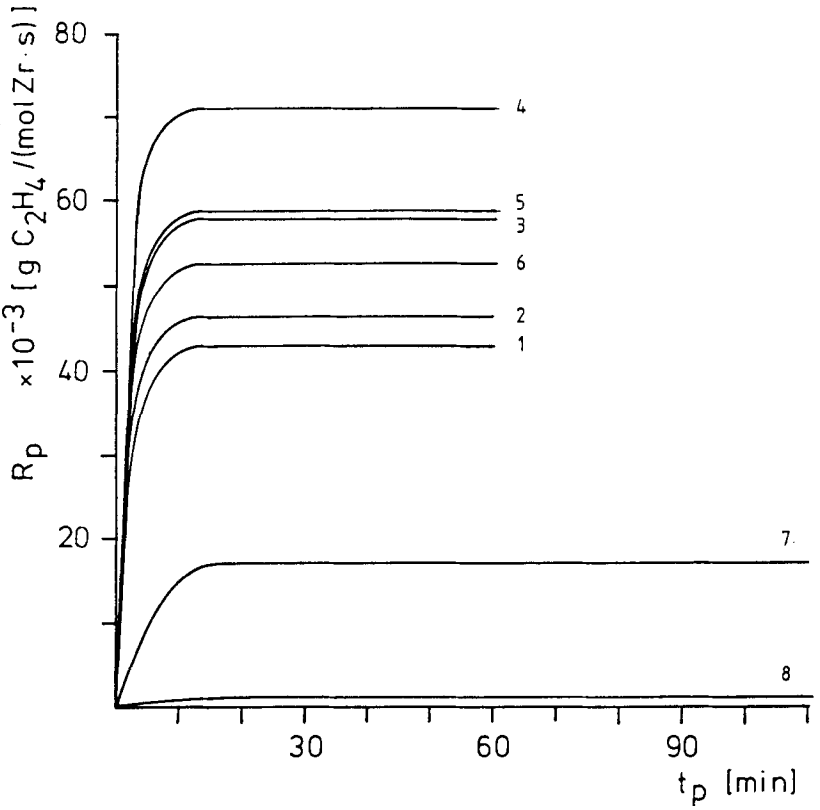

Figure 1. Ethylene-hexene-copolymerization rate versus time in toluene with different hexene concentrations

1	0 g/l	4	60 g/l
2	10 g/l	5	100 g/l
3	30 g/l	6	200 g/l

These figures go along well with those from ^{13}-nmr-sequence-analyses. Figure 2 shows the ^{13}C-nmr--spectrum of a ethylene-hexene-copolymer with a high hexene content. The hexene units are distributed at random into the polyethylene matrix. The content of hexene diads is relatively low. At 70-80 ^{o}C there is even less insertion of the comonomer (r_1 = 80). A drop in zirkonocene concentration by a factor of 10 will lead to less incorporation of the α-olefin.

As for homopolymerizations of ethylene an increase in the aluminoxane concentration will cause an increase in activity, even for hexene concentrations of app. 75%. From this the re-

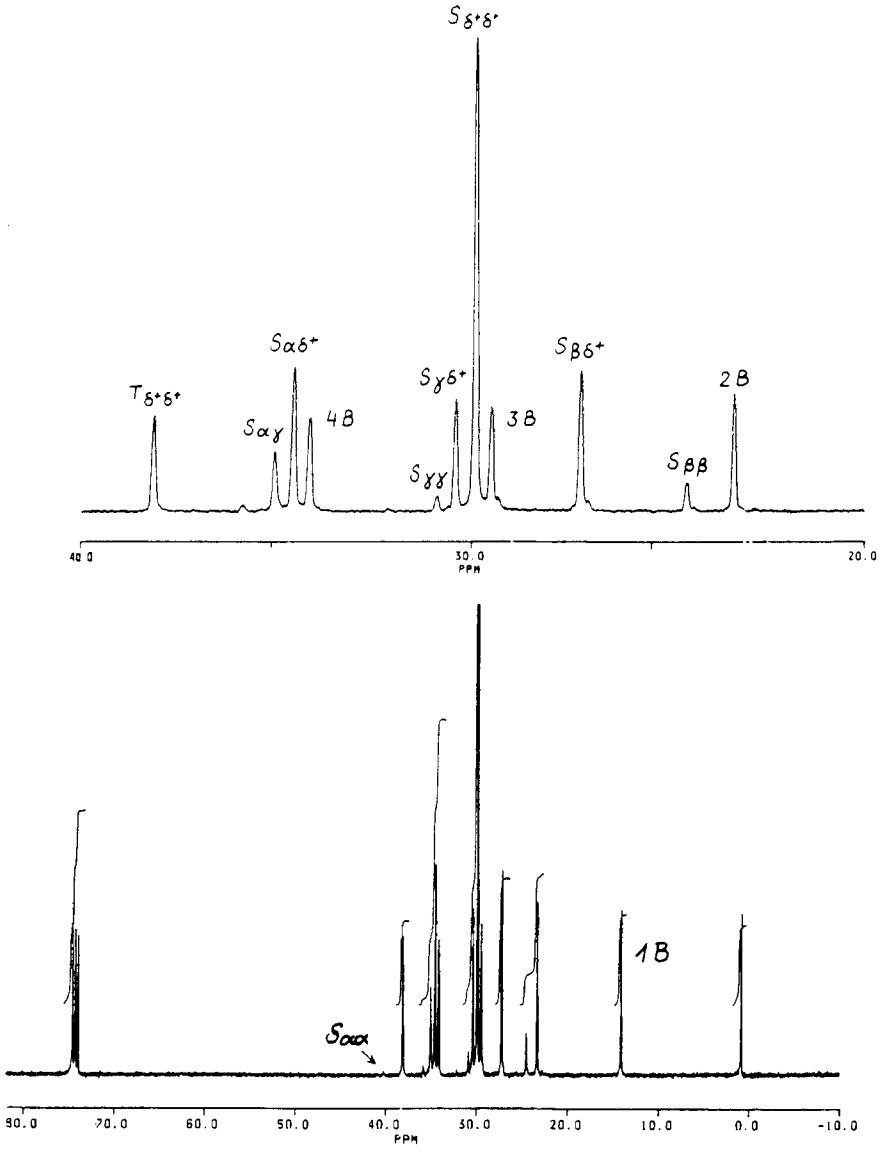

Figure 2. ^{13}C-nmr-spectrum (90 MHz) of ethylene-hexene-copolymer with 23 mol-% of hexene, solvent: 1,2-dideuterotetrachlorethane , 120 ^{o}C , nomenclature by Carman and Randall[7,8]

action order with respect to aluminoxane has been calculated to be 0.8. An exchange between biscyclopentadienylzirconiumdimethyl and the corresponding dichloride has no marked influence on the reaction pathway.

Another striking feature of hexene as comonomer is its tendency for interrupting chains. 50 mol-% hexene lead at 60°C to a molecular weight of 100 000 instead of 200 000 for ethylene homopolymerization. This is achieved without any loss of activity. Right along with this decrease in molecular weight there is an increase in the proportion of vinyliden groups in the copolymer, as can be seen by ir-spectroscopy (Table 3).

Table 3. Concentration of unsuturated endgroups in the ethylene-hexene-copolymers (IR-measurements)

Hexene in Copolymer mol-%	Trans-vinyl/ 1 000 C	Vinyl/ 1 000 C	Vinylidene/ 1 000 C
0	0,03	0,12	0,02
1	0,02	0,15	0,06
1,9	0,03	0,20	0,15
4,6	0,04	0,14	1,00
7,7	0,04	0,11	1,20

It is supposed that the unsaturated endgroups are formed predominantly via chain transfer towards the monomer units and that hydrogen transfer to the transition metal is only of minor importance. Molecular weight distributions of copolymers are relatively narrow; a typical figure of $\frac{M_w}{M_n}$ is 2, which corresponds well with the predominance of one kind of active centers.

In addition to ir ^{1}H-^{13}C-nmr spectrochemical investigations there have been performed DSC experiments which lead to correlation diagrams between melting points and comonomer amounts. Insertion of 6 weight-% hexene causes a drop of the melting point by 17 degrees to 119 °C.

Wide angle X-ray scattering is a profound means for investigating the crystallinity of copolymers. Although the samples have been drastically frozen from 160 °C to 0 °C during the production of films, the effect of the butyl side chains was still manifest. Copolymers with amounts of hexene higher than 20 mol-% are nearly completely amorphous.

Polyhexenes have been produced at polymerization temperatures of 20, 40, and 60 °C. They show much lower activities than copolymers. A typical figure is 14 kg/mol Zr·h. Molecular weights are extremely small. A polymer produced at room temperature has a viscosity index of 0,05 dl/g, whereas a product from the polymerization at 60 °C has a boiling point of app. 80 °C under 0,01 Torr reduced pressure.

The proportion of vinyliden groups is extremely high (app. $\frac{10}{1000}$ C-atoms) and decreases with decreasing reaction temperature Melting points of polyhexenes cannot be determined, even not for those with higher molecular weights. This is due to their entirely amorphous character.

EPDM-terpolymers need higher amounts (20-50 wt.-%) of α-olefins (esp. propene) if suitable elastomeric properties are to be achieved. This can be realized by special polymerization conditions. App. 4-6 wt.-% diene in the polymer are necessary for a proper vulcanization with sulfur and special additives.

Activities for typical EPDM polymerization lie between 10-100 kg polymer/g Zr·h. An increasing amount of propene in the reaction mixture will cause them to fall down continuously. Nevertheless, these figures are higher than those of common vanadium catalysts.

Emphasis should be given to the fact that it might take 10 hours time till the system has reached its maximum polymerization rate and that it then will keep up this rate for several days.

The induction phase can be shortened with smaller amounts of propene and diene.

POLYPROPYLENE

Only atactic polypropylene is formed with Cp_2ZrIV-compounds, $Cp(CH_3)_5$-$CpZrCl_2$ or $(Cp(CH_3)_5)_2ZrCl_2$. For low temperatures Ewen[9] reported that small amounts of isotactic polypropylene are obtained with Cp_2ZrPh_2. The atactic polypropylene shows a narrow molecular weight distribution of 1,6 to 2,5.

If the π-bonded cyclopentadienyl ligands of the zirconium compound are changed for ethylene-bridged indenyl-rings a stereorigid chiral-zirconium is formed (Figure 3).

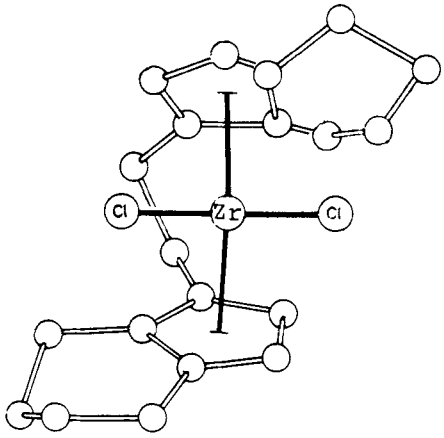

Figure 3. Structure of rac-ethylene(bistetrahydro-indenyl) zirconiumdichloride[10,11].

Contrary to the analogous titan compound the chiral zirconocene forms solely the racemic mixture and no additional meso-form.

Using the chiral rac-ethylenebis(indenyl)-or tetrahydroindenyl)zirconiumdichloride together with methylaluminoxane as catalyst we were able to obtain pure isotactic polypropylene. Table 4 shows the polymerization conditions and activity[12].

Table 4. Polymerization of 70 ml propylene with rac-Et $(Ind)_2ZrCl_2$ (I) or rac-Et$(TH\text{-}Ind)_2$ (II) and $1{,}6 \cdot 10^{-2}$ mol Al/l methylaluminoxane in 330 ml toluene.

Catalyst (mol/l)		T (°C)	Time (min)	Yield (g)	Activity (kg PP/mol Zr·h)
$7 \cdot 10^{-7}$	I	15	620	3,6	1 500
$7 \cdot 10^{-7}$	I	21	500	31	16 000
$7{,}7 \cdot 10^{-6}$	I	32	20	31	12 000
$8{,}4 \cdot 10^{-6}$	II	-20	360	1,5	80
$8{,}4 \cdot 10^{-6}$	II	-10	270	4,5	300
$8{,}4 \cdot 10^{-6}$	II	0	255	12,5	880
$8{,}4 \cdot 10^{-6}$	II	8	180	13,0	1 300
$8{,}4 \cdot 10^{-6}$	II	15	170	26,7	2 900
$8{,}4 \cdot 10^{-6}$	II	20	120	31,3	4 750
$8{,}4 \cdot 10^{-6}$	II	60	90	38,7	7 700

The (indenyl)zirconocene is more active than the (tetrahydroindenyl)zirconocene. The activity increases with increasing polymerization temperature and reaches a value of 16 000 kg isotactic polypropylene per mol Zr and h. The properties of the obtained polypropylene are shown in Table 5.

Table 5. Properties of isotactic polypropylene obtained with the zirconium catalyst.

T (°C)	$\bar{M}_w$	M_w/M_n	Soluble Prod.	Isotact. Ind.
- 10	305 000	2,6	0,25 %	90,0
0	144 000	2,4	0,2 %	88,1
15	62 000	2,0	0,7 %	87,3
20	45 000	1,9	1,0 %	86,0
32	57 000	-	-	95

The toluene soluble part consists of less than 0,2 weight percent and therefore lies below that of isotactic polypropylene produced with supported catalysts. The high index of isotacticity, determined via the method of Luongo, together with the frequency of triads in nmr experiments (95,9 mm; 3,2 mr; 0,9 rr) suggest that propene is exclusively head to tail bonded with the same overall configuration. Only every 50th propene unit has the wrong configuration.

Molecular weights are strongly dependent on reaction temperature as is shown in Figure 4.

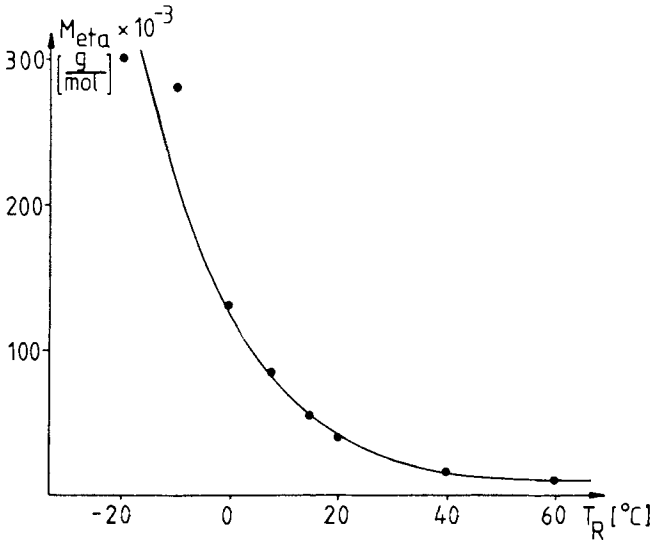

Figure 4. Molecular weight of isotactic polypropylene in dependence of the polymerization temperature.

By variation of reaction temperature in the range from -20 °C to 60 °C molecular weights from 300 000 to 1 500 are yielded.

Furthermore, a separation of the racemic mixture of the zirconocene compound into optically active pure enantiomeric forms could be performed, leading for the first time to optically active polypropylene. Table 6 represents different values for the specific rotations of soaked polymer suspensions as have been found for various solvents and after different pretreatment. Being bound to the optically active center, the polymer chain is formed dominantly in only one screw sense.

Table 6. Measurements of specific rotations.
Instrument: Perkin Elmer 243; employed wavelength: Na-D-line (589 nm); specific rotation: $\alpha \overset{T}{=} \frac{\alpha_{meas.} \cdot 100}{d \cdot l}$;
l = length of sample tube = 1 dm; d = concentration in $\frac{g}{100\ ml}$
specific rotation of the employed catalyst: $\alpha \overset{RT}{436} = +297\ ^{o}$

Sample	Solvent	d	$\alpha_{meas.}$	$\alpha \overset{T}{589}$
atactic PP	decalin	1,775	-0,025	-1,4
isotactic PP	decalin	0,285	-0,350	-123
isotactic PP	o-xylene	0,280	-0,700	-250
isotactic PP	toluene	53,0	$\pm$0	-
isotactic PP	dcaa*	0,210	$\pm$0	-
isotactic polybutene	decalin	0,114	+0,150	+130

* dichloroaceticacid, helix-destroying solvent

After getting rid of the metal center, the so formed helix (3/1) remains stable, unless treated under higher temperatures or being completely dissolved. In these cases the optical activity will be lost by racemization into helices of both screw senses.

A transparent foil of app. 0,1 mm thickness from the optically active polypropylene displays after orientation an angle of rotation of -65 ^{o}.

REFERENCES

1. H. Sinn, W. Kaminsky, Adv.Organomet.Chem. 18, 99 (1980)
2. W. Kaminsky, M. Miri, H. Sinn, R. Woldt, Makromol.Chem. Rapid Commun. 4, 464 (1983)
3. J. Herwig, W. Kaminsky, Polymer Bull. 9, 464 (1983)
4. W. Kaminsky, Naturwissenschaften 71, 93 (1984)
5. W. Kaminsky, H. Lüker, Makromol.Chem., Rapid Commun. 5, 225 (1984)
6. M. Fineman and S.D. Ross, J.Polym.Sci., 5, 259 (1950)
7. C.J. Carman, Rubb.Chem.Technol., 44, 781 (1971)
8. E.T. Hsieh and J.C. Randall, Macromolecules 11 33 (1978)
9. J.A. Ewen, J.Am.Chem.Soc., 106, 6355 (1984)
10. F.R.W.P. Wild, L. Zsolnai, G. Huttner, and H.H. Brintzinger, J.Organomet.Chem., 232, 233 (1982)
11. F.R.W.P. Wild, M. Wasiucionek, G. Huttner, and H.H. Brintzinger, J.Organomet.Chem., in press
12. W. Kaminsky, K. Külper, H.H. Brintzinger, and F.R.W.P. Wild, Angew.Chem., 97, 507 (1985)

KINETIC STUDIES ON ZIEGLER-NATTA POLYMERIZATION - AN INTERPRETATION OF RESULTS

P.J.T. TAIT
Department of Chemistry, UMIST, Manchester M60 1QD, England

ABSTRACT

The phenomenological behaviour shown by many Ziegler-Natta catalyst systems is outlined and the factors controlling the observed rate-time profiles are discussed in the light of existing kinetic models. Results for C^* and derived values of $\bar{k}_p$ are presented for the polymerization of propylene and 4-methylpentene-1 by $MgCl_2$/EB/$TiCl_4$-$Al(i\text{-}Bu)_3$ catalysts. The concentrations and activities of polymerization centres giving rise to atactic and isotactic polymer in propylene polymerization are evaluated. The higher overall rates observed in both propylene and 4-methylpentene-1 polymerization are discussed in terms of C^* and $\bar{k}_p$ values. Increased values of C^* obtained for higher α-olefin polymerization are also presented.

INTRODUCTION

The kinetics of Ziegler-Natta polymerization have provided a facination for polymer chemists ever since the first discovery of these catalysts. As a result very many kinetic studies have appeared in the published scientific literature. Of the earlier publications which have helped to formulate our present understanding of the mechanism of these polymerizations it is appropriate to mention on this occasion the studies by Natta and by his coworkers[1,2], by Chien[3], and by Keii et al[4-6] on the polymerization of propylene; by Grieveson et al[6-8] and by Böhm[9-11] on the polymerization of ethylene; by Yermakov et al[12-15] on the polymerization of both ethylene and propylene; and by Tait et al[16-23] on the polymerization of α-olefins such as 4-methylpentene-1.

More recently many additional publications have appeared. Such studies have demonstrated that the kinetics of Ziegler-Natta polymerization are remarkably complex, involving centres of differing activity[24,25], differing stereospecificity and differing stability.

Additionally, physico-chemico processes such as adsorption have been shown to be important[16-23] and, under appropriate circumstances, diffusion processes may operate also[26]. At the present time with the advent of second and third generation high activity supported catalysts[27,28] the overall kinetic behaviour is recognized to be even more complicated with the added complications of third component participation and related reactions[29].

PHENOMENOLOGICAL BEHAVIOUR

Early research by Natta and Pasquon[2] using α-$TiCl_3$ catalysts clearly established that breakdown of the $TiCl_3$-matrix took place during the polymerization and that the steady state polymerization rate was more or less independent of the initial size of the $TiCl_3$ particles. This behaviour both provided a simplification and a complication in kinetic studies of Ziegler-Natta catalysts: a simplification in that steady state rates could be readily observed; a complication in that the actual surface area of the polymerization catalyst could not be measured directly.

This breakdown, during the early stages of the polymerization reaction of the $TiCl_3$ matrix to yield primary catalyst particles, together with the chain initiation reactions, however, is very important in that it gives rise to the characteristic rate-time profiles exhibited by these catalyst systems.

Rate-time profiles are significant in Ziegler-Natta polymerizations in that their particular shape may be characteristic sometimes of a particular catalyst system. The importance of such profiles has been discussed previously by Keii[5] and Tait[22,24]. For first generation catalysts such profiles can often be considered to consist of three periods, viz., an acceleration period, a decay period, and a stationary period. However a number of different types of rate-time profiles are possible and some typical examples are shown in Figure 1.

Type A behaviour is shown by many first generation catalyst systems, e.g., α-$TiCl_3$, VCl_3, δ-$TiCl_3$ 0.33 $AlCl_3$, etc. catalysts when used with dialkylaluminium halides as cocatalysts for the polymerization of propylene in hydrocarbon media. Type B behaviour is often observed when trialkylaluminium compounds are used as cocatalysts under similar conditions. In both cases there is a definite settling period during which the rate increases to a maximum value followed by a period during which the rate either remains

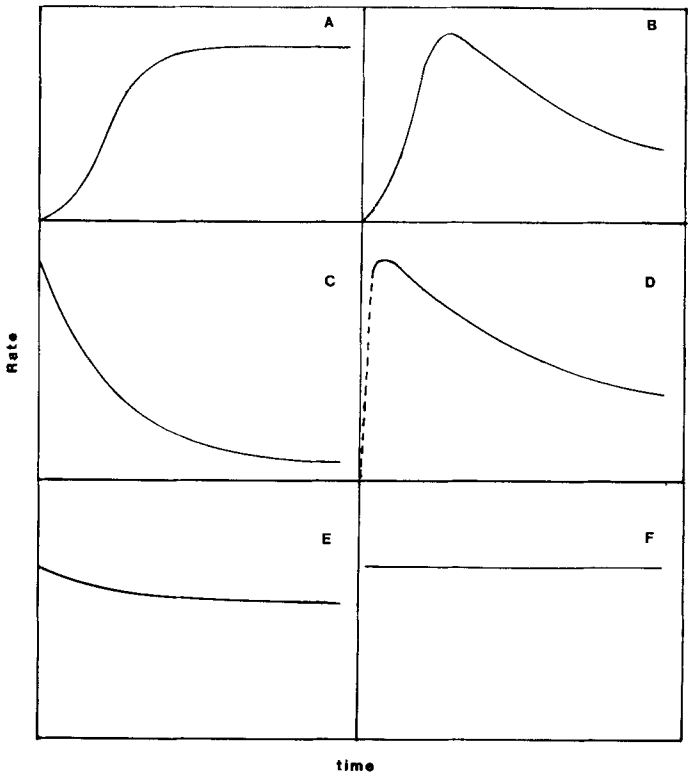

Figure 1. Some typical rate-time profiles.

constant or decreases with time. The use of trialkylaluminium as cocatalyst normally produces a more active but less stable catalyst system. Many high activity supported catalyst systems show either C or D type behaviour in which the rate may either start at a maximum value or rise very rapidly to a maximum value and then decrease rapidly with time, e.g., $MgCl_2/EB/TiCl_4$-$AlEt_3$ catalyst systems when used for either propylene or ethylene polymerization (EB $\equiv$ ethyl benzoate). Type C behaviour has also been observed in the polymerization of styrene by catalysts derived from $TiCl_4$ and $AlEt_3$[30,31] and by many homogeneous catalyst systems, e.g., $Cp_2TiEtCl$-$AlEtCl_2$ in ethylene polymerization[32], and certain modified catalyst systems, e.g., $VOCl_2 \cdot 2THF$-AlR_3 in vinyl chloride polymerization[33]. Solvay & Cie ether treated catalysts in propylene polymerization show E type behaviour where the settling period is more or less eliminated and breakdown of the porous catalyst particles is practically instantaneous on treatment with an alkylaluminium compound. Thereafter the rate only decreases very gradually with

time[34]. The use of phthalate esters in $MgCl_2$ supported catalysts can yield type F behaviour in the polymerization of 4-methylpentene-1 (4-MP-1). Here no settling period is observed and the rate remains almost completely constant with time[35].

The principal factors giving rise to the observed types of rate-time profiles are as follows.

(a) Catalyst Matrix Type and Preparation.

The stability of the catalyst matrix has a profound effect on the rate-time profile and this is evidenced by the presence or absence of a settling period. Solvay & Cie ether treated type catalysts have highly porous structures and catalyst matrix breakdown takes place very rapidly on treatment with alkylaluminium chloride to produce primary catalyst particles with good time stability. A typical plot of rate versus time is shown in Figure 2[34].

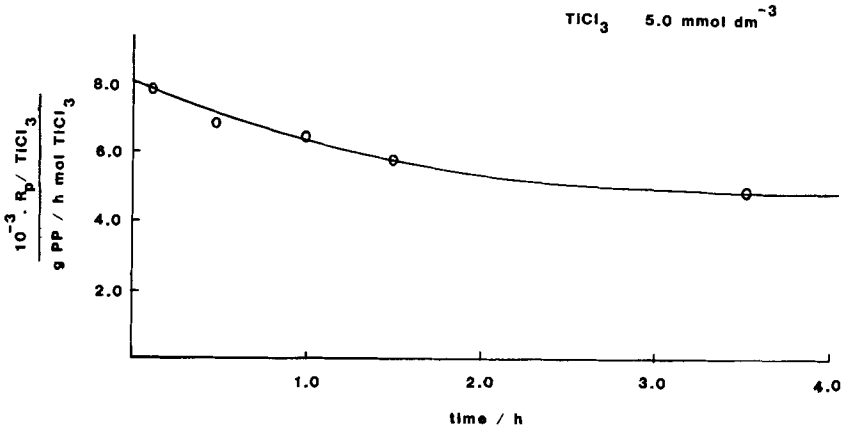

Figure 2. Plot of rate versus time for the polymerization of propylene at 60 °C using a Solvay & Cie ether treated $TiCl_3$ catalyst. $[TiCl_3]$ (JV161) = 5.0 x 10^{-3} mol/dm^3; $[AlEt_2Cl]:[TiCl_3]$ = 2:1.

When using $MgCl_2$/electron donor/$TiCl_4$ catalyst systems the type and concentration of the donor used can have an important effect on the observed rate-time behaviour. Figure 3 illustrates the rate-time behaviour of two $MgCl_2$/electron donor/$TiCl_4$ catalysts for the polymerization of 4-MP-1, one containing ethyl benzoate and the other a phthalate ester[35,36].

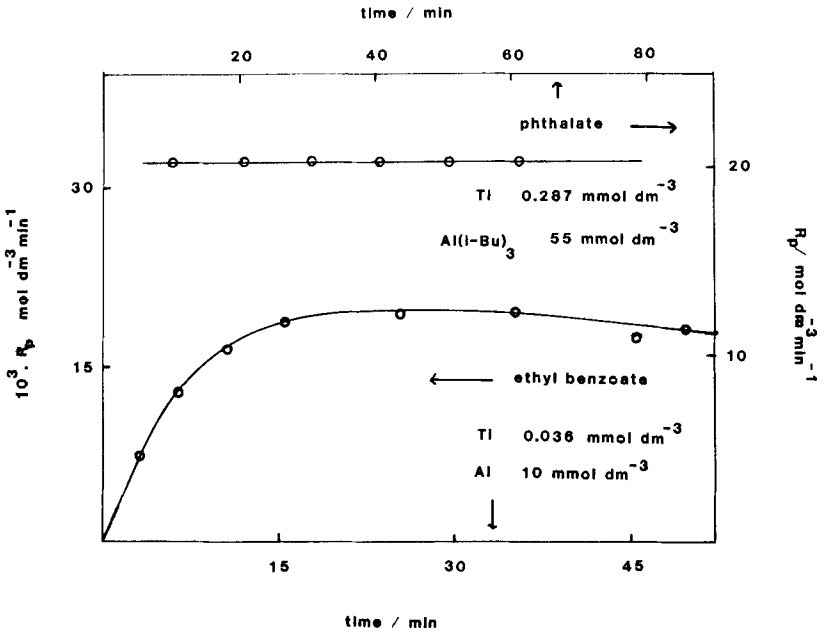

Figure 3. Plots of rate versus time for the polymerization of 4-MP-1 using $MgCl_2$/electron donor/$TiCl_4$-Al(i-Bu)$_3$ catalysts.

b) Alkylaluminium.

Rate-time profiles are affected by both the type of alkylaluminium compound used as cocatalyst, e.g., whether a trialkylaluminium or a dialkylaluminium halide is used, and by the concentration of alkylaluminium as is observed in the polymerization of propylene by δ-$TiCl_3 \cdot 0.33\ AlCl_3$-$AlR_3$ or AlR_2Cl catalyst systems in hydrocarbon media. The observed behaviour is complex arising from alkylation, reduction, extraction (i.e., $AlCl_3$), and catalyst modification reactions.

Variation of the trialkylaluminium concentration can bring about profound changes in rate-time profiles for $MgCl_2$/electron donor/$TiCl_4$ catalyst systems as is shown in Figure 4.

This behaviour of believed to arise from adsorption reactions and has been analysed by Keii[37]. The presence or absence of an electron donor in the cocatalyst affects also the actual rate-time behaviour which is observed.

(c) Monomer.

For polymerization using $MgCl_2$/electron donor/$TiCl_4$ catalysts it is not often realized that the actual monomer may affect the observed rate-time profiles. In particular α-olefins such as 4-MP-1 exhibit different rate-time profiles from those shown in either ethylene or

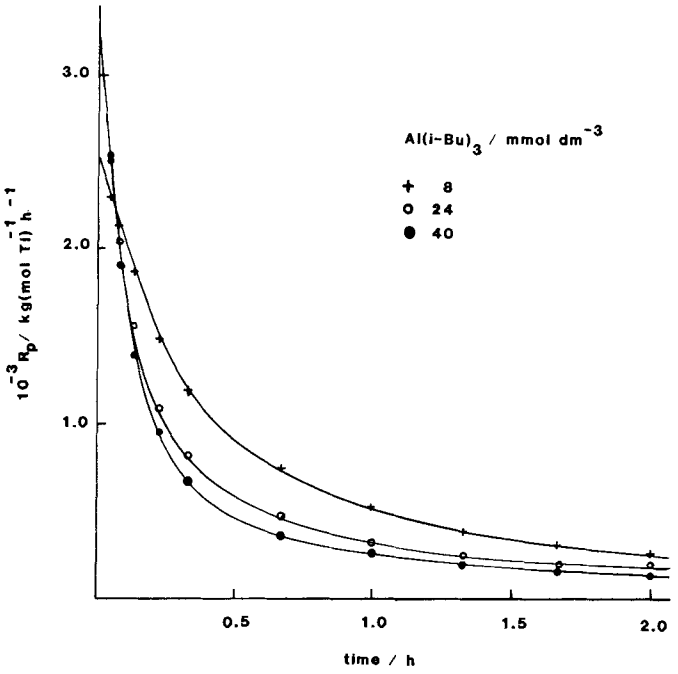

Figure 4. Plots of rate versus time for the polymerization of propylene at 60 ^{o}C using a $MgCl_2$/EB/$TiCl_4$ catalyst for varying concentrations of triisobutyl aluminium.

propylene polymerization. For polymerization using 4-MP-1 very stable polymerization systems can be obtained involving fairly high concentrations of active centres[36]. Figure 5 shows a typical plot for the polymerization of ethylene and 4-MP-1 using similar types of catalyst. An analysis of this type of behaviour will be detailed in a forthcoming publication[38].

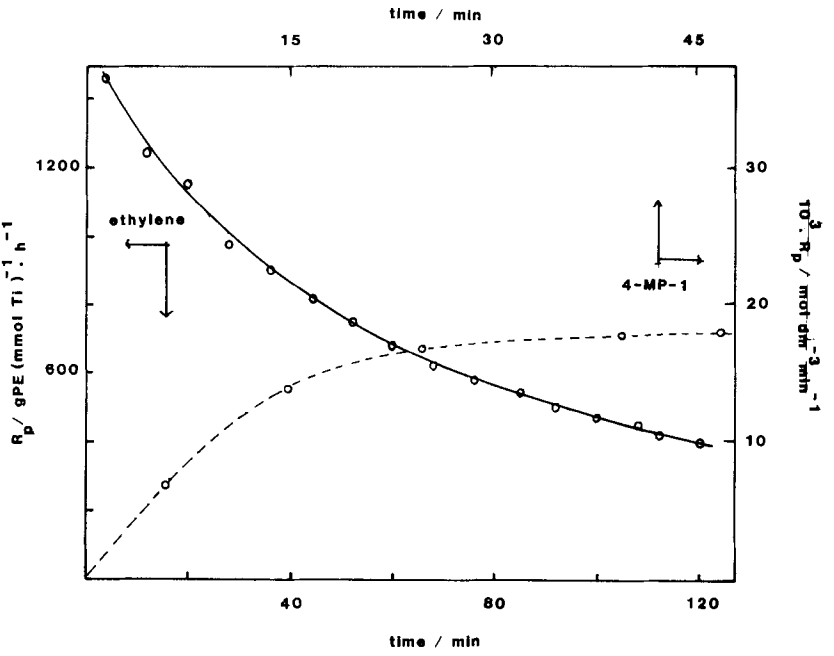

Figure 5. Plots of rate versus time for the polymerization of ethylene and 4-MP-1 using $MgCl_2/EB/TiCl_4$ catalysts.
ethylene ——— at 60 °C, 4-MP-1 ------ at 40 °C.

(d) Pressure.

The pressure of monomer may also affect the observed rate-time profiles as is shown in Figure 6.

Many catalyst systems which exhibit steady rate-time profiles for polymerization at atmospheric pressure show decay type profiles when used at significantly higher monomer pressure, i.e., 5-10 bar.

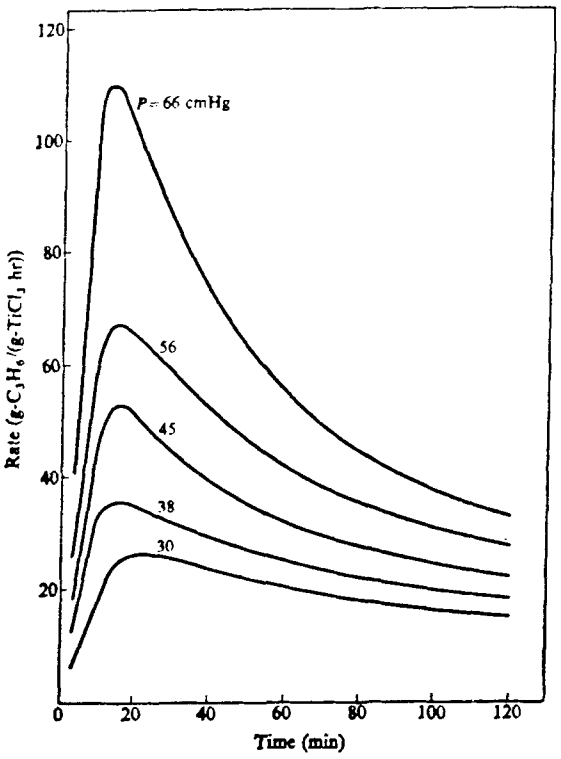

Figure 6. Kinetic curves obtained by Keii et al[5,39] at 44 °C and various pressures ($TiCl_3$ = 2 g/dm^3, $AlEt_3$ = 15 mmol/dm^3 in 250 cm^3 n-heptane).

(e) Polymerization Medium.

Normally Ziegler-Natta polymerizations are carried out in hydrocarbon media. When however, polymerizations are conducted in aromatic solvents very different rates and rate-time profiles are observed. This effect is illustrated in Figure 7 for the polymerization of propylene in toluene medium by a δ-$TiCl_3 \cdot 0.33\ AlCl_3$ catalyst. For the catalyst system under observation the observed behaviour is believed to arise from the finite solubility of the $AlCl_3$ in the catalyst matrix in the toluene medium (containing excess alkylaluminium) which leads to catalyst matrix breakdown. This breakdown generates additional active centres giving enhanced rates of polymerization but the catalyst system is not so stable with time and shows decay type characteristics.

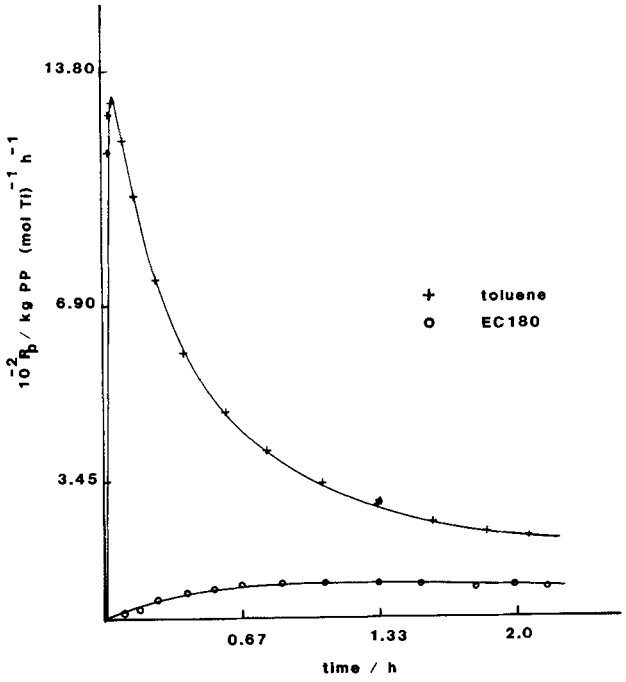

Figure 7. Rate-time profile for the polymerization of propylene in toluene and EC180 media.

(f) Temperature.

Although most published results are limited to the temperature range of 30-100 ^{o}C the overall effect of increased temperature appears to be destabilization of the catalyst systems above certain critical temperature values. However this effect will be discussed in a later section of this paper.

It is evident that this complex behaviour is controlled by both chemical and physical factors and these may include the following.

(a) Catalyst particle size and morphology. The effective particle size and particle size distribution as functions of time will determine the numbers of exposed transition metal atoms which can be involved in catalyst forming reactions at any particular time.

(b) Catalyst centre forming and catalyst destroying reactions. These reactions will control the instantaneous concentration of potential or actual active centres.

(c) Complexation reactions between active centres and alkylaluminium species, between active centres and donor molecules, and between alkylaluminium species and donor molecules. These reactions will control the relative numbers of potential and actual active centres.
(d) Diffusion phenomena.

KINETIC MODELS

The complex behaviour outlined in the previous section arises from variations with time in intrinsic catalyst activity (i.e., in k_p values), in active centre concentration of the relevant species, and in available monomer concentration. Thus a number of kinetic models (9, 13, 17, 23) have been formulated to account for the kinetic behaviour of heterogeneous Ziegler-Natta polymerization reactions in terms of these parameters. However little attention has been paid to the occurrence of centres of differing intrinsic activity.

Normally the instantaneous rate of polymerization (R_p) at a given time is represented by either (1),

$$R_p = k_p C^* [M] \quad (1)$$

where [M] is the bulk concentration of monomer; C^* is the concentration of active centres and k_p is the relevant propagation rate constant, or by (18),

$$R_p = k_p C^* \theta_M \quad (2)$$

where θ_M is the fraction of active centres covered by adsorbed monomer (or complexed by monomer); C^* is the total concentration of active centres (potential and actual); and k_p is the propagation rate constant for adsorbed monomer. Thus equation (1) may be regarded as a special case of equation (2) where the value of θ_M is very low.

It is important to recognise that the theory advanced previously (18) for adsorption kinetics involved what we now recognise as a two-stage propagation sequence, i.e., adsorption or complexation of monomer followed by an insertion reaction of complexed monomer. The more general relevance of this type of sequence has become more apparent in the light of the observed behaviour in higher α-olefin polymerization[36] and in copolymerization studies of ethylene and higher α-olefins using $MgCl_2$/electron donor/$TiCl_4$ catalysts[40].

Additionally the earlier theory[18] considered competitive adsorption between monomer [M] and alkylaluminium (chloride or

dichloride) species (A) and active centres (S), viz.,

$$S + M \underset{}{\overset{K_M}{\rightleftharpoons}} S...M \tag{3}$$

$$S + A \underset{}{\overset{K_A}{\rightleftharpoons}} S...A \tag{4}$$

The fraction of active centres with adsorbed monomer (θ_M) and the fraction with adsorbed alkyl (θ_A) may be expressed in terms of Langmuir-Hinshelwood isotherms as:

$$\theta_M = \frac{K_M[M]}{1 + K_M[M] + K_A[A]} \tag{5}$$

and

$$\theta_A = \frac{K_A[A]}{1 + K_M[M] + K_A[A]} \tag{6}$$

One advantage of such a treatment is that it can be extended readily for the case where a donor (D) is present, i.e.,

$$\theta_M = \frac{K_M[M]}{1 + K_M[M] + K_A[A] + K_D[D]} \tag{7}$$

where K_D is the relevant adsorption constant[21].

In the likely situation where a number of types of active centre of differing activity is present then equation (1) becomes

$$R_p = \sum_{i=1}^{n} R_{p_i}$$

$$= [M] \sum_{i=1}^{n} k_{p_i} C^*_{p_i} \tag{1a}$$

and equation (2) becomes

$$R_p = \sum_{i=1}^{n} R_{p_i}$$

$$= \sum_{i=1}^{n} k_{p_i} C^*_{p_i} \theta_{M_i} \tag{2a}$$

The simplest cases being where there are only two types of active centres of differing activity.

ACTIVE CENTRE DETERMINATIONS ON $MgCl_2$/EB/$TiCl_4$ CATALYST SYSTEMS

(1) Polymerization of Propylene - Use of ^{14}CO.

Only very limited information may be obtained on the distribution of centres of differing activity in Ziegler-Natta catalysis. However, when combined with extraction procedures, the use of ^{14}CO radio-labelling is of importance in that it allows differentiation between centres producing soluble (and hence largely atactic) polymer from those producing insoluble (and thus mainly isotactic) polymer[24,41].

Polymerizations of propylene were carried out at 785 mmHg pressure using a $MgCl_2$/EB/$TiCl_4$ catalyst containing 0.7% Ti, prepared by ball-milling dried $MgCl_2$ with EB and $SOCl_2$ for 72 h ($MgCl_2$:EB:$SOCl_2$ = 6:1:0·3); Al(i-Bu)$_3$ was used as cocatalyst[42].

The polymerization system shows a typical rate-time profile of type C (See Figure 1). Active centre concentrations were performed using ^{14}CO which was added 2 min after the start of the polymerization. Values of C_p^* for different temperatures together with corresponding values of k_p are listed in Table 1. For comparison corresponding values of C_p^* and k_p obtained using δ-$TiCl_3$.0.33 $AlCl_3$ and Solvay & Cie ether treated catalysts are shown in Table 2[24].

Table 1. Values of C_p^* and k_p at different polymerization temperatures

Temp.	$C_p^* \times 10^2$/mol/mol			k_p/dm^3/mol/s		
	Total	Insol	Sol	Total	Insol	Sol
40	7.14	3.44	3.70	369	703	59
50	8.03	4.93	3.10	669	1034	89
60	10.30	6.68	3.61	858	1256	122
70	11.31	7.47	3.84	1341	1952	163

Note: (a) C_p^* (total) was determined using the unextracted polymer.

(b) C_p^* (insol) was determined using the insoluble part of polymer samples extracted by boiling n-heptane for 24 h.

(c) C_p^* (sol) = C_p^* (total) - C_p^* (insol).

(d) Polymerization time before injection of ^{14}CO was 2 min.

Table 2. Values of C_p^* and k_p for different catalyst systems for propylene polymerization at 60 °C.

Catalyst System	$C_p^* \times 10^3$/mol/mol			k_p/dm^3/mol/s		
	Total	Insol	Sol	Total	Insol	Sol
δ-$TiCl_3$ 0.33 $AlCl_3$ -$AlEt_2Cl$	10.0	7.5	2.2	8.2	10.5	1.1
Solvay & Cie -$AlEt_2Cl$	7.9	6.7	1.1	17.0	20.0	1.6
-$AlEt_3$	20.8	13.2	5.7	47.5	58.4	38.2

The following conclusions are evident.

(a) When using a $MgCl_2$/EB/$TiCl_4$ type catalyst only a maximum of 11.3% Ti (mol/mol) at 70 °C is involved in active centres for propylene polymerization (c.f., results reported later for the polymerization of 4-MP-1). This value compares with a value of about 1% Ti for δ-$TiCl_3$ 0.33 $AlCl_3$-$AlEt_2Cl$ type catalysts when used under comparable conditions at 60 °C.

(b) Very high values of k_p are obtained during the initial stages of the polymerization, and values of k_p are much higher than those obtained for δ-$TiCl_3$ 0.33 $AlCl_3$-$AlEt_2Cl$ type catalysts. It should be remembered that these values will be average values where centres of more than one kind produced atactic (soluble) and isotactic (insoluble) polymer.

(c) Values of k_p(insol) are greater by a factor of about ten than those obtained for k_p(sol). This is in good agreement with values reported earlier for δ-$TiCl_3$ 0.33 $AlCl_3$-$AlEt_2Cl$ type catalysts[24].

Although at first sight it appears surprising that k_p(insol) should be greater than k_p(sol), the reason is very likely that the more exposed and less sterically crowded centres can coordinate more strongly with the olefin in the transition state thus leading to a slower insertion reaction. This explanation is consistent with the two-stage propagation model discussed earlier[21].

(d) Values of C_p^* (insol) increase with temperature in the temperature range examined whilst those for C_p^*(sol) remain more or less constant. Activation energies for the polymerization system

are listed in Table 3.

Table 3. Activation Energies

	Activation Energy/kcal/mol		
	E_a	E_p	ΔE
Total	12.3	8.8	3.5
Insoluble	12.6	6.9	5.7
Soluble	7.6	7.1	0.5

The significance of these values will be discussed elsewhere[42].
(e) Values for both k_p(insol) and k_p(sol) increase with temperature as is expected.

(2) Polymerization of 4-methylpentene-1 - use of MeOT quenching.

The polymerization of 4-MP-1 using a $MgCl_2$/EB/$TiCl_4$-Al(i-Bu)$_3$ catalyst system has already been reported and the results analysed[39]. The rate-time profile is very different from that observed in propylene and ethylene polymerization and is of type A shown in Figure 1. Active centre concentrations were determined using a tritium quenching technique[18,41]. Values of C_p^* and $\bar{k}_p$ are listed in Table 4 together with corresponding values for Stauffer 1.13 (δ-$TiCl_3$ 0.33 $AlCl_3$ donor modified) and VCl_3 catalyst systems. Corrections for the kinetic isotope effect and for chain transfer with adsorbed alkylaluminium were carried out as described previously[18]. It is important to recognise that the use of tritiated alcohols to determine active centre concentrations is non-selective and thus the values of the chain propagation constant which are obtained are average values only ($\bar{k}_p$).

An examination of Table 4 reveals that the polymerization system $MgCl_2$/EB/$TiCl_4$-Al(i-Bu)$_3$/4-MP-1 behaves somewhat differently from $MgCl_2$/EB/$TiCl_4$-Al(i-Bu)$_3$/propylene, ethylene systems.

Table 4. Comparative values of active centre concentrations and rate constants for chain transfer and chain propagation and adsorption constants for various catalyst systems.

Catalyst System	$C_o^* \times 10^2$ / mol/mol	k_a / min^{-1}	K_A / $dm^3\ mol^{-1}$	K_M / $dm^3\ mol^{-1}$	$10^{-3}\ \bar{k}_p$ / min^{-1}
$MgCl_2$/EB/$TiCl_4$ -Al(i-Bu)$_3$ (catalyst contains 3.4% Ti)	29	10	13	2.6	4.67
Stauffer 1.13 -Al(i-Bu)$_3$	9.7	0.20	16	0.38	1.29
VCl_3 -Al(i-Bu)$_3$	0.038	0.067	5.1	0.16	3.10

[4-MP-1] = 2.00 mol dm^{-3}; temperature = 40 °C.

(a) The much higher rate of polymerization in comparison to that observed when using Stauffer 1.13 catalysts, i.e., R_p values of 1110 and 3.6 mol min^{-1} (mol Ti)$^{-1}$ respectively) arises mainly from the much higher C_p^* values (x43) together with a smaller increase in the value of $\bar{k}_p$ (x3.6). The higher values of C^* in higher α-olefin polymerization is consistent with the rate enhancement effects observed in copolymerization studies and with the concept of a two-stage propagation step. A further presentation and discussion of this effect will be given elsewhere[35,40].

(b) The use of tritiated alcohol in the determination of C^* allows evaluation of k_a, K_A and K_M, the values of which cannot be obtained from ^{14}CO radio-labelling.

(i) Much higher values of k_a are observed in comparison with corresponding values from δ-$TiCl_3$ 0.33 $AlCl_3$ type catalysts although the values of K_A are more or less the same. Evidently the more active centres (higher $\bar{k}_p$ values) in $MgCl_2$/EB/$TiCl_4$ type catalysts transfer growing chains much more rapidly with adsorbed alkyl-aluminium.

(ii) Higher values of K_M are also observed indicating that the

more active centres in $MgCl_2/EB/TiCl_4$ type catalysts have a greater affinity for coordination with monomer leading to higher θ_M values and hence a higher rate of polymerization. This effect is additional to that described in (a) above.

It is thus apparent that considerable progress has been and is being made towards a better and more comprehensive understanding of the intrinsic nature of Ziegler-Natta catalysis from the use of kinetic studies, a field of investigation which owes much to the pioneering research carried out by Professor T. Keii and his coworkers. The future promises to be as exciting as the past and we can confidently await further progress in our understanding and in the development of these fascinating polymerization systems.

ACKNOWLEDGEMENT

I wish to acknowledge the help and assistance of a number of current research students whose research work has been used in the preparation of this paper; viz. Y. Akinbami, A.L. Burns, S. Davies, M. Abu Eid, A.E. Enenmo, M.I. Osammor, and S. Wang.

REFERENCES

1. G. Natta, J. Polym. Sci., 34, 21 (1959).
2. G. Natta and I. Pasquon, Advan. Catal., 11, 1 (1959).
3. J.C.W. Chien, J. Polym. Sci., A1, 425 (1963).
4. T. Keii, K. Soga and N. Saiki, J. Polym. Sci., C16, 1507 (1967).
5. T. Keii, "Kinetics of Ziegler-Natta Polymerization", Kodansha, Tokyo, 1972.
6. T. Keii, J. Res. Ind. Catal., Hokkaido Univ., 28, No. 3, 243 (1980).
7. M.N. Berger and B.M. Grieveson, Makromol. Chem., 83, 80 (1965).
8. B.M. Grieveson, Makromol. Chem., 84, 93 (1965).
9. L.L. Böhm, Polymer, 19, 545 (1978).
10. L.L. Böhm, Polymer, 19, 553 (1978).
11. L.L. Böhm, Polymer, 19, 562 (1978).
12. Y.I. Yermakov and V.A. Zakharov, in "Coordination Polymerization; A Memorial to K. Ziegler", J.C.W. Chien (Ed.), Academic Press, New York, 1975, p.91.
13. V.A. Zakharov, G.D. Bukatov, N.B. Chumaevski and Y.I. Yermakov, Makromol. Chem., 178, 967 (1977).

14. V.A. Zakharov, G.D. Bukatov and Y.I. Yermakov, Makromol. Chem., 176, 1959 (1975).
15. G.D. Bukatov, V.A. Zakharov and Y.I. Yermakov, Makromol. Chem., 179, 2093 (1978).
16. P.J.T. Tait and I.D. McKenzie, IUPAC Symposium on Macromolecular Chemistry, Budapest, 1969, Preprints Vol. 2, p.59.
17. D.R. Burfield, I.D. McKenzie and P.J.T. Tait, Polymer, 13, 302 (1972).
18.a) I.D. McKenzie, P.J.T. Tait and D.R. Burfield, Polymer, 13, 307 (1972).
18.b) D.R. Burfield and P.J.T. Tait, Polymer, 13, 315 (1972).
19. R.D. Burfield, P.J.T. Tait and I.D. McKenzie, Polymer, 13, 321 (1972).
20. I.D. McKenzie and P.J.T. Tait, Polymer, 13, 510 (1972).
21. D.R. Burfield and P.J.T. Tait, Polymer, 15, 87 (1974).
22. D.R. Burfield, I.D. McKenzie and P.J.T. Tait, Polymer, 17, 130 (1976).
23. P.J.T. Tait in "Coordination Polymerization; A Memorial to K. Ziegler", J.C.W. Chien (Ed.), Academic Press, New York, 1975, p.155.
24. P.J.T. Tait in "Preparation and Properties of Stereoregular Polymers", R.W. Lenz (Ed.), D. Reidel Publishing Co., Dordrecht, 1980, p.85.
25. T. Keii, Makromol. Chem., 185, 1537 (1984).
26. T.W. Taylor, K.Y. Choi, H. Yuan and W.H. Ray in "Transition Metal Catalysed Polymerizations: Alkenes and Dienes", R.P. Quirk et al (Ed.), Harwood Academic Publishers, New York, 1983, p.191.
27. Montecatini Edison Co., Br. Pat., 1 286 867 (1968).
28. Mitsui Petrochemicals Ind., Ital. Pat., 912 345 (1968).
29. B.L. Goodall in "Transition Metal Catalyzed Polymerizations: Alkenes and Dienes", R.P. Quirk et al. (Ed.), Harwood Academic Publishers, New York, 1983, p.355.
30. G.M. Burnett and P.J.T. Tait, (Unpublished data). P.J.T. Tait, Ph.D. Thesis, University of Aberdeen, 1959.
31. F. Danusso, D. Sianesi and B. Calcagno, Chim. & Ind., 40, 628 (1958).
32. L.F. Borisova, E.A. Fushman, E.I. Vizen and N.M. Chirkov, Europ. Polymer J., 9, 953 (1973).

33. A.G. Chesworth, R.N. Haszeldine and P.J.T. Tait, Polymer, 14, 224 (1973).
34. A.D. Caunt, S. Davies and P.J.T. Tait (To be published).
35. P.J.T. Tait and A.E. Enenmo, (To be published).
36. P.J.T. Tait and M. Abu Eid, Proc. XI Iberoamerican Symposium on Catalysis, Lisbon, Vol. 1, 163 (1984).
37. T. Keii, Makromol Chem., 183, 2285 (1982).
38. P.J.T. Tait (To be published).
39. T. Keii, K. Soga and N. Saiki, J. Polymer Sci., C16, 1507 (1967).
40. P.J.T. Tait and Y. Akinbami (To be published).
41. P.J.T. Tait in "Transition Metal Catalysed Polymerizations: Alkenes and Dienes", R.P. Quirk et al. (Ed.), Harwood Academic Publishers, New York, 1983, p.115.
42. P.J.T. Tait and S. Wang (To be published).

CATALYSIS AND THE UNIPOL PROCESS

FREDERICK J. KAROL and FELIX I. JACOBSON
Union Carbide Corporation, UNIPOL Systems Department, P.O. Box 670, Bound Brook, NJ 08805, USA

ABSTRACT

Production of low-density polyethylene (LDPE) is undergoing the kind of revolution not seen in the field since the discoveries by Ziegler and Natta. Union Carbide has developed a unique and versatile low-pressure, fluid-bed process (UNIPOL) that yields vastly improved polyethylene resins, linear low-density polyethylenes (LLDPE), at greatly reduced costs. Proprietary catalysts are key to success of the UNIPOL process. Catalysts have an important effect on productivity, polymer molecular weight, polymer molecular weight distribution, copolymerization kinetics, and degree of stereoregularity. Moreover the size, shape, and porosity (morphology) of the catalyst particle play an important role in regulating the morphology of the resultant polymer.

Today, Union Carbide and its more than twenty-five licensees are operating or constructing polyethylene plants based on the UNIPOL process in fifteen countries. By 1986 the combined capacity of UNIPOL reactors will be sufficient to supply 25% of the world's total demand for polyethylene. A recent development has been the production of polypropylene by the UNIPOL process. This is a result of a cooperative undertaking between Union Carbide and Shell Chemical, USA, and combines for the first time a high activity catalyst with simplicity and improved economics of gas-phase, fluidized-bed technology. A new polypropylene plant of 80,000 tons per year based on the UNIPOL process is starting production in 1985 at Seadrift, Texas.

UNION CARBIDE--WORLD LEADER IN POLYETHYLENE TECHNOLOGY

The polyethylene industry and scientific community recently celebrated its golden jubilee in London.[1)] Since its discovery in the 1930s polyethylene has grown to be the world's largest thermo-

plastic. Indeed, world plant-capacities for polyolefins are very large (Table I).[2)]

By 1986 the combined capacity of UNIPOL reactors in operation or under construction around the world will be sufficient to supply 25% of the world's total demand for polyethylene. Fifty-three reactors will be in place in 15 countries on six continents. Linear low-density polyethylene (LLDPE) has already revolutionized the polyethylene industry, and will continue to impact significantly on the future of the entire polyolefins business. The UNIPOL process is recognized as a significant technological accomplishment. Union Carbide received the prestigious Kirkpatrick Award for UNIPOL in 1979.[3)] Changes in polyethylene process and product technologies in the last decade, brought about through polymerization catalysis, are so significant that this period will no doubt be called "Catalysis and The Polyethylene Revolution." Key to the success of the UNIPOL process is the proprietary catalysts that operate at low pressures and low temperatures, and which are suitable for use in a gas-phase, fluid-bed reactor. It is primarily by means of catalyst composition that resin properties are controlled in the UNIPOL process. High-pressure technology, dominated by concerns for reactor engineering and reactor control of polymer properties is rapidly giving way to a new technology in which catalysis and chemical control of product properties are key factors.

PROCESS DESCRIPTION AND BENEFITS OF UNIPOL PROCESS

In the UNIPOL process (Figure 1, 2), gaseous ethylene, a comonomer and a catalyst are reacted in the presence of a chain transfer agent at temperatures of about 100°C or less and pressures of 2.1 MPa (300 psi) or less to produce a polyethylene product that is removed directly from the reactor as a granular, solid material. Gaseous ethylene, comonomer and chain transfer agent are fed continuously into a fluidized bed reactor. Catalyst is added separately. Circulated by a small compressor, the gas stream fluidizes the polymer bed, provides reactants for polymerization, and removes exothermic heat of reaction. The circulating gas stream passes through a cooler before being returned to the reactor.

Granular polyethylene is removed through a gas-lock chamber. Only a small amount of residual monomer accompanies the product into this chamber, and this is purged safely from the resin. Overall,

the combined conversion rate of ethylene and comonomer is approximately 97% to 99%. The average catalyst residence time is three to five hours during which the polymer particles grow to an average size of 500-1000 microns. The granular product, with or without conventional additives, is ready for packaging and shipping to the customer without any further processing. The size and the shape of the polymer granules are such that their bulk density and solid flow characteristics are suitable for subsequent materials handling and processing operations by the customer. For pelleted product, the granular material may be fed to conventional pelleting equipment or to proprietary Union Carbide pelleting systems.

PROCESS OPTIONS

The UNIPOL Process is available in three versions, i.e., Grass Roots Plant, Waterborne Option, and Facility Modernization System (FMS) (Figures 3-4). The Waterborne Option involves construction of UNIPOL LLDPE plants on ocean-going barges and delivered as turnkey operations anywhere in the world accessible by deep water. The FMS Option offers high-pressure LDPE producers a highly efficient way to enter the LLDPE market immediately and minimizes investment costs by making maximum use of existing plant facilities.

Waterborne Option

Union Carbide has completed the first "Waterborne" plant for Ipako S.A., Argentina (Figure 5). The plant was constructed in the shipbuilding facilities of Ishikawajima-Harima Heavy Industries near Nagoya, Japan. It has a design capacity of 135,000 metric tons-per-year of LLDPE. The plant was delivered to Ipako's waterside site in Bahia Blanca, Argentina in late 1981. Construction of the plant from keel-laying to shipyard commissioning was completed in just eight months. The plant was in full commercial operation by December 1981--just 22 months from signing of the sales agreement. This represents a reduction in construction time of at least a year from that required for land-based construction of a traditional polyethylene plant.

FMS Option

UNIPOL FMS offers process and product technology equal to that formerly possible only with a "grass roots" UNIPOL facility. Northern Petrochemical Company in Illinois chose FMS to upgrade its existing high-pressure facility to produce LLDPE. With this approach

a cost-efficient, low-pressure UNIPOL reactor system can be "dropped in" to an outmoded high-pressure polyethylene plant and tied into existing process and support facilities. The old reactor is then shut down, and the "new" plant started up, capable of producing not only LLDPE, but a full range of polyethylenes.

Table 1. World-Plant Capacities for Polyolefins[2)]

	MM Tons/Yr.			
YEAR	LDPE	LLDPE	HDPE	PP
1980	16.10 ⟶		8.48	6.86
1981	16.10	0.44	9.27	7.04
1982	14.48	1.78	8.70	7.27
1983	13.92	2.91	9.40	7.93
1984	14.22	3.92	9.80	8.19
1985	14.62	4.65	10.07	8.81

Total 1984 Capacity ∿36 MM Tons (79 MMM lbs)

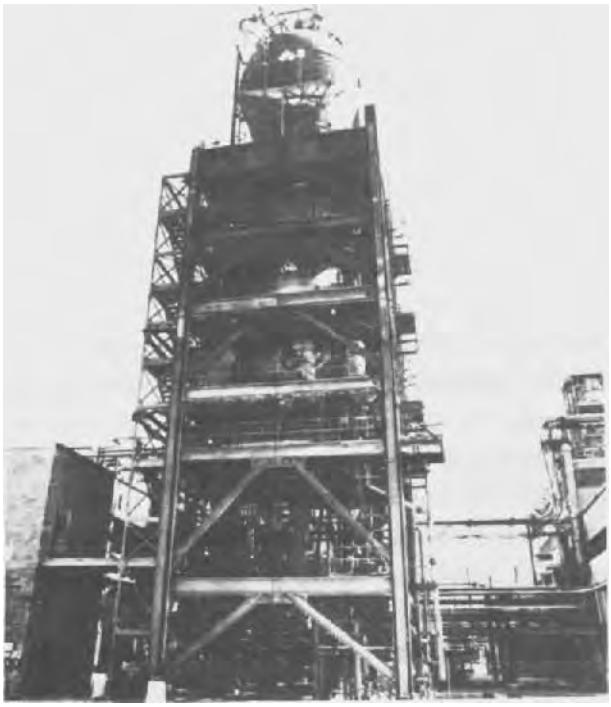

Figure 1:
Fluid-Bed Plant at Seadrift, Texas for Polyethylene Production

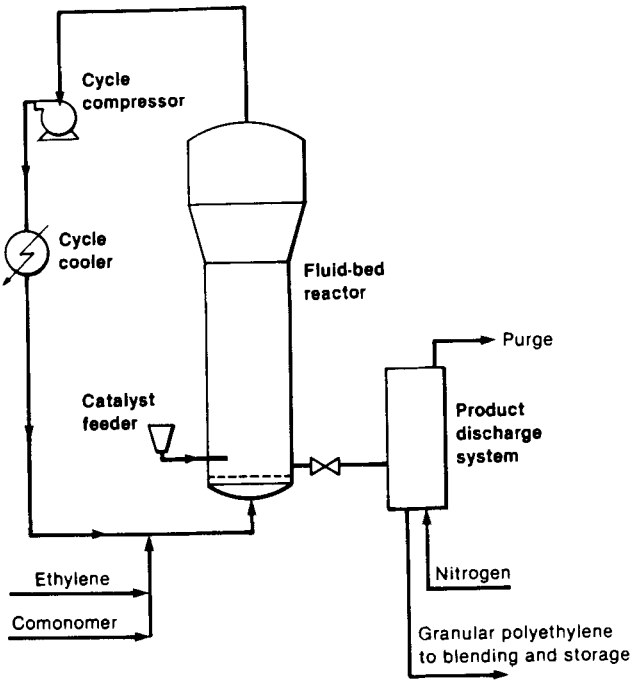

Figure 2: Schematic of Low-Pressure, Fluid-Bed Process for Polyethylene Production

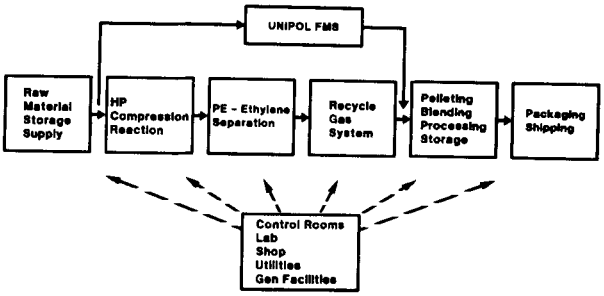

Figure 3: UNIPOL Facilities Modernization System (FMS)

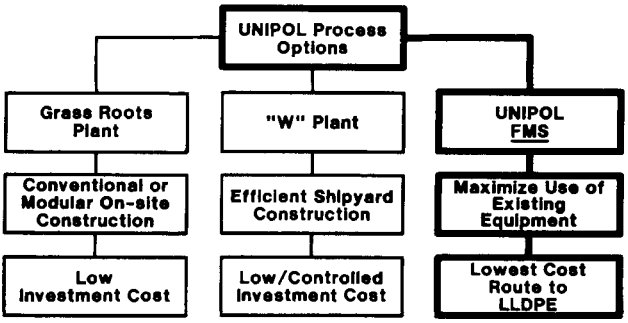

Figure 4: UNIPOL Process Options

Figure 5:
Ipako Barge-Mounted Plant

POLYETHYLENE PRODUCTS FROM UNIPOL PROCESS

The UNIPOL process commercially produces ethylene homopolymers, and copolymers with several alpha olefins including butene-1 and hexene-1. The process can produce products over the entire density range of polyethylene. Catalyst and process technology know-how permit control of polymer molecular weight or melt index from less than 0.1 g/10 min to melt indexes well above 100. Likewise, polymer molecular weight distribution may be adjusted from M_w/M_n as narrow as 3 to as broad as 30.

The development and commercialization in the United States of LLDPE products from the UNIPOL process have occurred at a rapid rate (Table II-III).[4] By contrast it took traditional LDPE twenty years to reach a billion pounds annual consumption--HDPE over a decade. The pace was set with introduction of general purpose LLDPE products in 1978. Shortly thereafter film producers, using retrofit technology, were able to modify LDPE fabrication equipment to handle LLDPE products at competitive rates. Use of higher alpha-olefins such as hexene-1 as a comonomer, led to a line of new, high-strength LLDPE products. Through the use of specially-designed air rings with specially-formulated UNIPOL LLDPE products, a series of clarity-grade products was introduced in 1983. A new family of easy-flow

LLDPE products has recently been developed and introduced to the marketplace. Shortly a line of HMW-LLDPE resins will also be seen in the marketplace.[5)]

The film industry represents two-thirds of the U.S. polyethylene market. Film made from LLDPE resin offers high tensile strength, improved puncture resistance, and higher elongation, as well as better toughness and improved properties at both low and high temperatures.

Injection molding is the second largest market for polyethylene accounting for 10% of consumption. LLDPE has virtually replaced conventional LDPE in all major injection molding applications due to its exceptional toughness and high environmental stress-crack resistance (ESCR).

For blow molders, LLDPE resins provide superior ESCR and higher modulus/lower gas permeability. These improved properties allow blow molders to go after new small-bottle and food-container markets. Blow-molded LLDPE drum liners either meet or exceed industry standards for low temperature toughness and ESCR.

Rotational molders have turned to LLDPE because its high impact strength and improved ESCR provide a competitive alternative to more expensive resins. In addition, using a high melt index LLDPE resin, a rotomolder can reduce cycle time by more than 25% and still maintain maximum toughness.

Pipe and tubing extruders have moved up to LLDPE because of its outstanding physical properties. Exceptional burst strength, high modulus values, excellent ESCR, low temperature toughness, and overall thermal stability are some reasons LLDPE is finding widespread use in the extrusion market.

LLDPE is rapidly penetrating such specialty markets as power and communications cable insulation and jacketing systems. These resins offer improved high and low temperature toughness, excellent ESCR and good dielectric properties. LLDPE is already the U.S. "standard" for communications cable jacketing.

Table II. LDPE and LLDPE Markets in USA (1980-1985)[4]

	MM Tons/Yr			
YEAR	LDPE	LLDPE	% LDPE	% LLDPE
1980	2.59	0.28	90	10
1982	2.32	0.66	78	22
1983	2.40	0.85	74	26
1984	2.35	1.10	68	32
(1985)	(2.30)	(1.41)	(62)	(38)

Table III. Introduction of UNIPOL Process LLDPE Products[5]

1978	General Purpose LLDPE
1979	Retrofit Film-Fabrication Technology
1982	High-Strength LLDPE
1983	Clarity Technology for LLDPE
1984	Easy-Flow LLDPE
1985	Ultra-Strength HMW-LLDPE

UNIPOL PROCESS FOR POLYPROPYLENE

Polypropylene by the UNIPOL process is the result of a cooperative undertaking between Union Carbide Corporation and Shell Chemical (a Division of Shell Oil Company) and combines for the first time a high-activity catalyst with the simplicity and improved economics of gas-phase, fluid-bed technology. Polypropylene made by this process contains such low catalyst ash and atactic polymer levels that no removal steps are required (Figures 6-7). Therefore, investment and operating costs associated with conventional extraction, purification, and drying steps are eliminated as well.[6]

The UNIPOL process offers the lowest investment and operating costs of any available polypropylene process. Featured are 10-15% lower investment and operating costs than that of any other "new generation" process being licensed. A new polypropylene plant (Figure 6) of 80 thousand tons per year based on the UNIPOL process started production recently in our Seadrift, Texas plant. This plant, based on the FMS concept, was constructed in only nine months.

In the production of polypropylene by the UNIPOL process, catalyst, propylene, and other reactants, such as hydrogen, cocatalysts, and comonomers, are continuously fed to a reaction system. This system consists of a reactor, a blower, and a heat exchanger. The reactor is a vertical fluid-bed reactor containing granular polypropylene about 0.025 inches, and a small amount of active catalyst. Usually polymerization conditions are 1.7-4.1 MPa (250-600 psi) pressure and 50-88°C. Typically, high-activity catalysts yield on the order of 20,000 lb of polypropylene/lb of catalyst.

The gaseous reactants pass through the reactor, providing fluidization and absorbing the heat of reaction. After passing through the fluidized bed of polypropylene, the gas enters an expanded section where fine particles are disengaged. The gas then passes through a heat exchanger where it is cooled. The cooled gas is then recirculated to the reactor. Polypropylene is removed directly from the reactor through a discharge system where unreacted monomer is separated and recycled. The resin is then purged of any residual hydrocarbons and conveyed out of the system.

Homopolymers and random copolymers are made using a single fluid-bed reactor. For production of in-situ impact copolymers, the polypropylene containing active catalyst is transferred from the homopolymer reactor to a second, smaller reactor, where the ethylene-propylene rubber phase is produced. Product recovery is similar to the system used for homopolymers. Only two reactors in series are required to make the full range of medium- to super-high impact products.

The UNIPOL process for polypropylene produces a full line of products consisting of homopolymers, and random and block copolymers (Table IV).[7] The process produces impact copolymers directly in the reactor thereby eliminating post-reaction blending. Because of independent control of (a) stereoregularity and molecular weight for homopolymers, (b) molecular weight, comonomer type/content for random copolymers, and (c) stereoregularity, molecular weight and ethylene content for impact (in-situ) copolymers, the process will allow the development of optimized products to satisfy demanding end-use requirements in the marketplace.

The UNIPOL process has gained worldwide recognition as the pre-eminent process for producing polyethylene. And the same simplicity, minimal equipment requirements and reduced space needs which UNIPOL brought to polyethylene, it has now brought to polypropylene.

Figure 6:
Union Carbide/Shell Chemical UNIPOL PP Plant at Seadrift, Texas

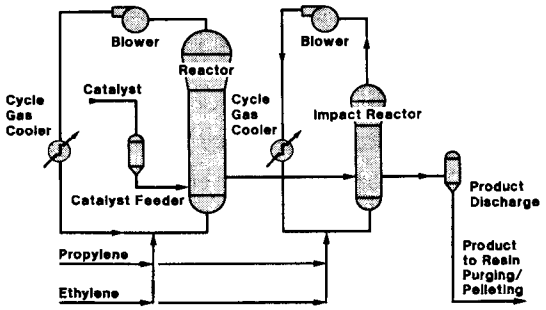

Figure 7:
Schematic of Union Carbide/Shell Chemical UNIPOL PP Plant

Table IV: UNIPOL PP Product Capabilities[7)]

Homopolymer
- High, Controllable Stereoregularity (II 93-98%)
- Broad MW Range (<0.1 to >100 MF)

Random Copolymers
- Broad Range of Comonomer Content ($\leq$7%)
- Not Limited to Ethylene
- Broad MW Range (<0.1 to >100 MF)

Impact (In-Situ) Copolymers
- Excellent Impact/Stiffness Balance
- Competitive to World Leaders Using Complex Technology
- Broad Range of Total Ethylene Content ($\leq$25%)
- Not Limited to Ethylene
- Broad MW Range (<0.1 to >50 MF)

CATALYSTS MAKE IT ALL POSSIBLE

Without suitable catalysts, the giant step in reducing the operating pressure for production of low density polyethylenes would not have been possible.[8-9)]

Polymerization catalysts must show attractive behavior in a number of areas, particularly catalyst productivity, polymer molecular weight and molecular weight distribution, comonomer incorporation, and polymer morphology (Table V). In propylene polymerization, control of polymer isotactic index is also important. Production of catalysts should be made as simple as possible in order to provide the basis for reproducible production of polyolefins.

Catalyst Productivity

Catalyst productivities based on the transition metal should be sufficiently high ($\geq 10^5$-10^6 kg polymer/kg transition metal) so that catalyst residues need not be removed from the polymer. Catalyst supports such as silica or magnesium chloride to improve polymerization activity by increasing the concentration of active sites are particularly effective. With chromium catalysts, chemical anchoring to silica supports to form new surface compositions has proven highly effective for providing catalysts showing very high ethylene polymerization activity. High-activity titanium catalysts

can be based on catalyst precursors prepared from bimetallic complexes (Mg, Ti), through insertion into defects of a $MgCl_2$ substrate, by formation of high surface area sponges, and by formation of solid solutions of $TiCl_3$ and $MgCl_2$ by cocrystallization. Typical examples of high activity catalysts described in the patent and scientific literature are listed in Table VI.[10, 11]

Molecular Weight and Molecular Weight Distribution

Molecular weight of the polyethylenes can be controlled by the reaction temperature and the concentration of chain transfer agent in the system. Hydrogen is an effective chain transfer agent with many catalysts. The specific catalyst type significantly affects molecular weight distribution. Many chromium-based catalysts provide polyethylenes of intermediate or broad molecular weight distribution while use of titanium-based catalysts lead to polyethylenes of relatively narrow molecular weight distribution. Considerable experimental data support the view that a diversity of chemically distinct active species is primarily responsible for the range of molecular weight distributions measured in ethylene and propylene polymerizations. Among the factors that could affect the diversity of active species are the specific transition metal compound including ligand environment and oxidation state, the type of cocatalyst and electron donor used to generate the catalytically active species, the physical state of the catalyst, and the nature of the catalyst substrate.

Comprehensive studies have evaluated the effect of π-bonded organic ligands attached to chromium on polymerization parameters of chromium catalysts.[10] In these studies differences in hydrogen response, comonomer incorporation, and polymerization activity with these catalysts suggested that the nature of the active sites was different due, at least in part, to changes in ligand environment (eq. 1):

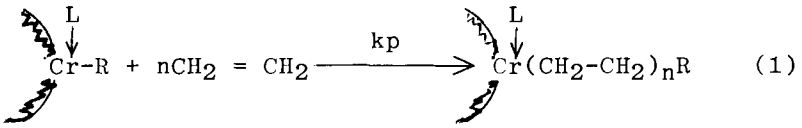

(1)

Table V: Catalyst Requirements in UNIPOL Process

- High Catalyst Productivities
- Control of Polymer Molecular Weight
- Control of Polymer Molecular Weight Distribution
- Good Comonomer Incorporation
- Good Polymer Morphology
- Simple, Reproducible Catalyst Preparation
- High Polymer Isotactic Index

Table VI: Examples of High Activity Catalysts for Olefin Polymerization

Titanium/Magnesium Composition	Metal Alkyl	Polymer
$TiCl_4/MgCl_2$ (Activated)	$(C_2H_5)_3Al$	PE
$TiCl_4/MgCl_2$/Electron Donor	"	"
$TiCl_4/Mg(OC_2H_5)_2$	"	"
$TiCl_4/MgCl_2$/Ethyl-p-Toluate	$(C_2H_5)_3Al$ + Ethyl-p-Toluate	PP
Chromium Composition		
CrO_3/SiO_2 + Modifiers	--	PE
$(C_5H_5)_2Cr/SiO_2$	--	PE

Comonomer Incorporation

Comonomer incorporation rates are highly dependent on the nature of the specific catalyst used to produce the copolymers. Improvements in comonomer incorporation lead to higher comonomer efficiency, and less dilution of the more reactive ethylene monomer. Generally heterogeneous catalysts, based on titanium or chromium, produce copolymers of broad compositional heterogeneity.

Morphology

Heterogeneous olefin polymerization catalysts can replicate their morphology into the morphology of the polymer particles. The catalyst particles act as a template for growth of the polymer particles. For high activity catalysts in olefin polymerization, the average particle size of the polymer is about 15-20 times larger than the size of the catalyst particle. Polymer particle growth can be influenced by the specific catalyst activity, the nature of the support matrix, the kinetic profile of the polymerization, and the nascent polymer viscosity.

Isotactic Index

Addition of electron donors to high activity catalysts for polypropylene production raises the isotactic index of the polymer. With many high activity catalysts, electron donors added to both the titanium precursor and the aluminum alkyl cocatalyst provide a route to polypropylene of very high isotactic content. In addition to raising the isotactic index of polypropylene, the addition of electron donors to high activity catalysts provides a means of stabilizing catalyst crystallites and a route to accelerating the rate of reaction of the magnesium/titanium compounds.

OUTLOOK FOR THE FUTURE

The UNIPOL gas-phase process has evolved, first to HDPE, then to low- and medium-density ethylene-propylene and ethylene-butene copolymers, and more recently, to LLDPE containing higher α-olefins. The capability of the UNIPOL process is being extended outside of the density and melt index limits normally associated with polyethylene. In particular, products with densities lower than 900 kg/m^3 offer significant new product opportunities where toughness and flexibility are special requirements. In addition, the process is now capable of producing a new line of easy-flow LLDPE resins that combine the excellent strength and drawdown characteristics of general-purpose LLDPE with the easy processability of a broad molecular-weight-distribution product.

Polypropylene by the UNIPOL process represents an extension of recent polypropylene technology trends to their most advanced level yet. Polypropylene technology using the UNIPOL process is capable of producing a full range of competitive homopolymer and copolymer products to serve all significant market segments. This technology offers considerable potential for new and improved products to meet future market demands.

Olefin polymerization catalysis continues to be a fertile area of research, with worldwide participation in both industrial and academic laboratories. The intensity of research, documented in patents and publications, has shed light on important features in catalysis. The polyethylene revolution has instilled great vitality to studies in olefin polymerization catalysis. This renewed vitality should provide an important stimulus for catalyst research in the 1980s and beyond. The combination of polymerization catalysis

and the UNIPOL process will provide worldwide focus for future new developments in the polyolefin arena.

REFERENCES

1. Abstracts of Papers Presented at Golden Jubilee Conference for Polyethylene, 1933-1983, London, June 8-10, 1983.
2. Digest of Polymer Developments, Springborn Laboratories, Inc., N. Platzer, Ed., Confidential Publ., October 1984, by permission of Editor.
3. Chem. Eng., 1979, 86 (Dec. 3), 80-85 (1979 Kirkpatrick Chemical Engineering Achievement Award [Union Carbide Corp.].
4. Plastics Industry Europe, Vol. 8, No. 18, End-September 1984.
5. D. E. James, Paper Presented at 11th CDC International Business Conference, Brussels, Belgium, April 17-18, 1985.
6. S. P. Sawin and C. J. Baas, Chem. Eng., 1985 (May 27) 42-43.
7. G. S. Cieloszyk and B. J. Garner, Paper Presented at Achema 1985, June 14, 1985 in Frankfurt, W. Germany.
8. F. J. Karol, Chemtech, pp. 222-228 (April 1983).
9. F. J. Karol, Paper Presented at 189th National Meeting of American Chemical Society, "History of Polyolefins," Miami Beach, Florida, April 28-May 3, 1985.
10. F. J. Karol, Catal. Rev.-Sci. Eng., 26 (3 & 4), 557-595 (1984).
11. R. D. Quirk, Ed., Transition Metal Catalyzed Polymerizations, MMI Press Symposium Series, Vol. 4, Parts A and B (1983).

This page intentionally left blank

HEAT AND MASS TRANSFER LIMITATIONS AND CATALYST DEACTIVATION EFFECTS IN OLEFIN POLYMERIZATION FOR GAS PHASE AND SLURRY REACTORS

S. FLOYD, G. E. MANN and W. H. RAY
Department of Chemical Engineering, University of Wisconsin, Madison, WI 53706

ABSTRACT

A detailed mathematical model for polymerization of olefins over solid catalysts, the Multigrain Model, is used as the basis for this study. This model takes account of the microstructure of the growing particle and considers diffusion of monomer in two distinct regimes. Using the model, polymerization rate behavior of the growing polymer particles in gas or slurry polymerization may be predicted. Criteria for the importance of intraparticle monomer diffusion and heat transfer under conditions of industrial interest are presented graphically. In addition, the mass and heat transfer resistances in the external film are evaluated for catalysts of varying activity. The effects of mass and heat transfer and catalyst decay on reaction rate profiles, activation energies and particle overheating phenomena are illustrated.

INTRODUCTION

The importance of diffusion resistances in polymerization of olefins has been speculated on for some time[1-9]. In particular, various authors have suggested that the rate of polymerization is diffusion controlled[1,3,5,9], that mass transfer has important effects on polymer properties[1,4], and that mass transfer effects result in the observed rate decay[10]. On the other hand, polymerization of olefins over heterogeneous catalysts has been usefully modelled without consideration of heat and mass transfer resistances by Keii et al.[11-13] and others[14,15], and experimental evidence has been presented which establishes beyond reasonable doubt that mass transfer effects are not responsible for the observed rate decay in many cases[12,16]. It is the purpose of this paper to present an

accurate model of polymerization over solid catalysts, and to quantitatively estimate the importance of mass transfer resistances in these systems. In addition, heat transfer effects will be considered and related to some commonly observed industrial problems. The relative importance of mass transfer resistances and activated catalyst decay on the observed polymerization rate behavior and activation energy will also be illustrated. Further, it will be shown that the catalyst particle size and the primary crystallite size are important design variables for modern high activity catalysts, if heat and mass transfer effects are to be avoided.

INTRAPARTICLE HEAT AND MASS TRANSFER LIMITATIONS

Since it is difficult to measure concentration gradients and temperatures within solid particles, numerous authors have attempted to elucidate heat and mass transfer effects through mathematical modelling. Perhaps the most realistic model is the Multigrain Model (schematically illustrated in Figure 1), which has been extensively used by Ray et al.[1,9,17], and by Laurence and Chiovetta[8].

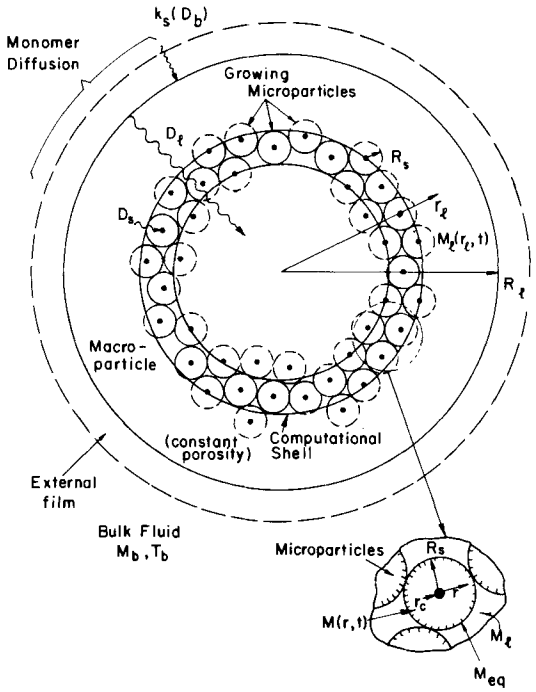

Figure 1 The Multigrain Model

The model is based on numerous observations (via scanning electron microscopy) by Hock and others[18,19] that the starting catalyst particle breaks up into its primary crystallites, around which the polymer grows. Thus, the large macroparticle is comprised of many small polymer particles (microparticles) which encapsulate these catalyst fragments. In this idealized picture, all microparticles at a given large particle radius are assumed to be the same size. For monomer to reach the active sites, there is both macrodiffusion in the interstices between microparticles and microdiffusion within the microparticles. Realistic values for the diffusivities of monomer in these regimes and some other parameters of interest are presented in Table 1.

To model the particle, we must write the partial differential equations for the monomer concentration and temperature in the two regions. From the concentration and temperature profiles we may calculate the reaction rates, yields and molecular weight distribution[1].

The governing equation for the diffusion of monomer in the macroparticle is

$$\epsilon_\ell \frac{\partial M_\ell}{\partial t} = \frac{1}{r_\ell^2} \frac{\partial}{\partial r_\ell} \left(D_\ell r_\ell^2 \frac{\partial M_\ell}{\partial r_\ell} \right) - R_v \tag{1}$$

where ϵ_ℓ is the large particle porosity, $M_\ell(r_\ell,t)$ is the monomer concentration in the pores of the macroparticle, and D_ℓ is the pseudobinary macrodiffusion coefficient. The reaction rate term, R_v, represents the total rate of consumption of monomer in an infinitesimal spherical shell at a given radius of the macroparticle. The boundary and initial conditions are

$$r_\ell = 0; \quad \frac{\partial M_\ell}{\partial r_\ell} = 0 \tag{2}$$

$$r_\ell = R_\ell; \quad D_\ell \frac{\partial M_\ell}{\partial r_\ell} = k_s (M_b - M_\ell) \tag{3A}$$

or

$$r_\ell = R_\ell; \quad M_\ell = M_S \tag{3B}$$

$$t = 0; \quad M_\ell = M_{\ell 0} \tag{4}$$

where M_b is the bulk monomer concentration in the reactor, k_s is the mass transfer coefficient in the external film, and M_S is the monomer concentration at the external solid surface. For the microparticles, the partial differential equation governing monomer diffusion is given as

$$\varepsilon_s \frac{\partial M}{\partial t} = \frac{1}{r^2} \frac{\partial}{\partial r} \left(D_s r^2 \frac{\partial M}{\partial r} \right) \tag{5}$$

$$r_c \leq r \leq R_s$$

where $M(r,t)$ is the monomer concentration in the microparticle, D_s is the pseudobinary microdiffusion coefficient and ε_s is the porosity. In the microparticles, all of the active sites are assumed to be at the surface of the catalyst core at $r = r_c$. Thus, the boundary and initial conditions are given by

$$r = r_c; \quad 4\pi r_c^2 D_s \frac{\partial M}{\partial r} = \frac{4}{3} \pi r_c^3 R_{cs} \tag{6}$$

$$r = R_s; \quad M = M_{eq}, \quad M_{eq}(M_\ell) \leq M_\ell \tag{7}$$

$$t = 0; \quad M = M_{s0} \tag{8}$$

where boundary condition (7) allows for the possibility of sorption equilibrium at the surface of the microparticles. Here r_c is the catalyst primary particle radius, R_s is the microparticle radius, and R_{cs} is the rate of polymerization at the catalyst particle surface given by

$$R_{cs} = k_p C_* M_c \tag{9}$$

where k_p is the propagation rate constant, C_* is the concentration of active catalyst sites, and M_c is the monomer concentration at the catalyst surface. The partial differential equations for the energy balances in the macroparticles and the microparticles are completely analogous to (1-8) and are shown in [20].

Considering the time-scales for heat and mass transfer to reach quasi-steady-state conditions, it is possible to show that the quasi-steady-state approximation is generally valid for the microparticles and for heat transfer in the macroparticles. This is fortuitous, since it enables analytic solutions to be written for the monomer

TABLE 1

Range of Multigrain Model Parameters for Polymerization of Propylene and Ethylene under Industrial Conditions[20)]

Property	Propylene (PP)		Ethylene (PE)	
	Slurry (n-heptane)	Gas	Slurry (n-hexane)	Gas
M_b (mol/ℓ)	4.0	1.0	2.0	1.0
T_b (K)	343	343	353	353
P(atm)	13	21	25	27
mol fraction monomer	0.49	1	0.266	1
$-\Delta H_p$ (kcal/mol)	20.5	24.8	22.7	25.7
E (kcal/mol)	10	10	10	10
k_p (ℓ/mol-site•s) (High Activity Catalyst)	660-2640	2640	2000-4000	4000
C_* (mol-sites/ℓ-cat)	10^{-3} - 10^{-1}	10^{-3} - 10^{-1}	10^{-3} - 10^{-1}	10^{-3} - 10^{-1}
k_e (cal/cm•s•K)	3.5×10^{-4}	2.6×10^{-4}	5.6×10^{-4}	4.8×10^{-4}
D_b (cm^2/s)	8×10^{-5}	4×10^{-3}	1×10^{-4}	6.0×10^{-3}
D_ℓ (cm^2/s)	10^{-6} - 10^{-5}	10^{-4} - 10^{-3}	10^{-6} - 10^{-5}	10^{-4} - 10^{-3}
D_s (cm^2/s)	10^{-8} - 10^{-6}	10^{-8} - 10^{-6}	10^{-8} - 10^{-6}	10^{-8} - 10^{-6}
R_s (cm)	10^{-6} - 10^{-4}	10^{-6} - 10^{-4}	10^{-6} - 10^{-4}	10^{-6} - 10^{-4}
R_ℓ (cm)	10^{-4} - 0.1	10^{-4} - 0.1	10^{-4} - 0.1	10^{-4} - 0.1

TABLE 1 (continued)

Notation:

M_b	:	Bulk Monomer Concentration
T_b	:	Bulk Temperature
$-\Delta H_p$	:	Heat of Polymerization
k_p	:	Propagation Rate Constant
C_*	:	Active Site Concentration
k_e	:	Effective Thermal Conductivity of Polymer Particle
D_b	:	Bulk Diffusivity of Monomer
D_ℓ	:	Large Particle Diffusivity
D_s	:	Small Particle Diffusivity
R_s	:	Small Particle Radius
R_ℓ	:	Large Particle Radius

concentration and temperature at the catalyst surface, in terms of these states in the pores of the macroparticle. Using the parameters from Table 1, the model predicts that the microparticles are at uniform temperature, as are the macroparticles under most circumstances. However, depending on the intrinsic activity of the catalyst, concentration gradients may exist in both the macroparticles and the microparticles. Figure 2 (taken from [20]) illustrates the regimes of significant and negligible diffusion resistance in the microparticles in terms of the observed activity of the catalyst. The quantity M_{eq}, the monomer concentration at the surface of the microparticles, is in equilibrium with the concentration in the pores of the macroparticle. For slurry polymerization, M_{eq} is assumed to be equal to the monomer concentration in the pores, while in gas phase, it would probably be roughly half that value[20]. It is worthwhile to note that the existence of microparticle diffusion resistance depends strongly on the primary crystallite radius, r_c. Since values of the small particle diffusivity range from 10^{-8}-10^{-6} cm^2/s (Table 1), for the small values of r_c typical of modern catalysts (~ 0.01 μ), micropar-

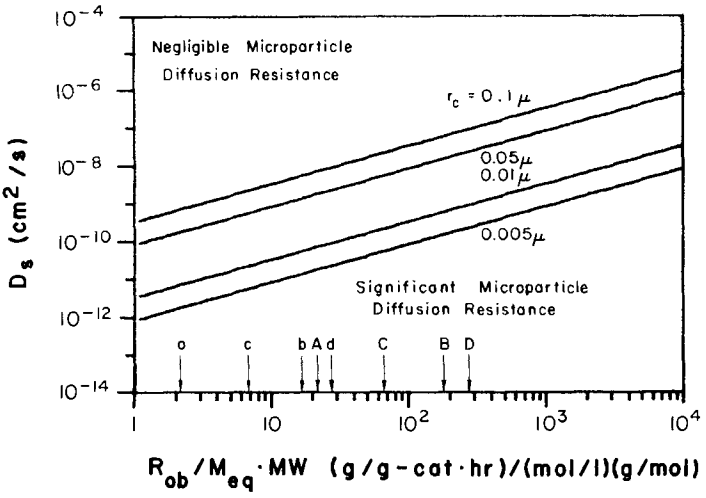

Figure 2 Regimes for microparticle diffusion resistance with catalyst primary particle size $0.005 \leq r_c \leq 0.1$ μ. Approximate values for typical catalysts if $M_{eq} = M_b$ for slurry and $M_{eq} = M_b/2$ for gas phase.

a,A Propylene slurry polymerization, low and high activity catalyst.
b,B Propylene gas phase polymerization, low and high activity catalyst.
c,C Ethylene slurry polymerization, low and high activity catalyst.
d,D Ethylene gas phase polymerization, low and high activity catalyst.

(Low activity: R_{ob} = 400 g/g-cat.hr, High activity: R_{ob} = 4000 g/g-cat.hr under representative industrial conditions)

ticle diffusion resistance should not limit the rate, at least for current industrial catalysts.

The possibility of significant macroparticle concentration and temperature gradients must also be considered. For slurry polymerization, the presence of the diluent liquid ensures internal temperature rises of less than a few degrees K. In gas phase polymerization, however, significant temperature gradients can result for large particles of high activity catalyst, as illustrated in Figure 3. However, for catalysts in use today, temperature gradients greater than a few degrees K would only be likely for catalyst particles greater than 50-60 microns diameter. Note that as the polymer particle grows, the heat of polymerization becomes diluted, so that

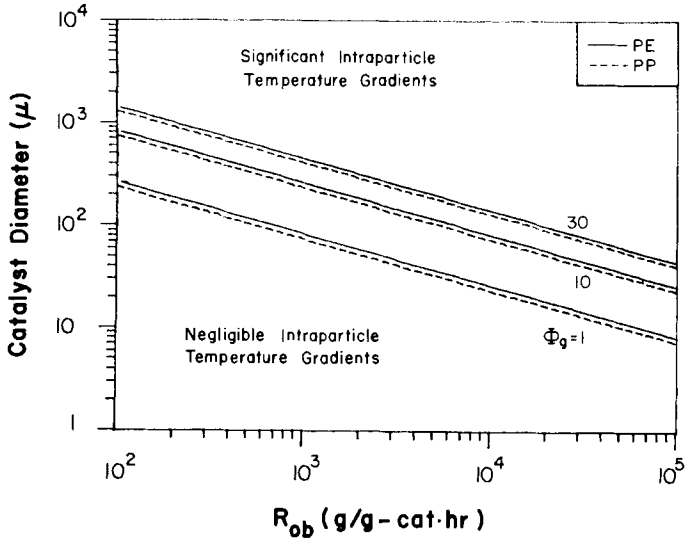

Figure 3 Regimes for significant macroparticle temperature gradients for ethylene and propylene polymerization. Catalyst size d_c versus observed rate for various macroparticle growth factors $\Phi_g = R_\ell/R_c$

the particle approaches isothermality. Figure 4 illustrates the regimes of heat and mass transfer resistances in the macroparticles for slurry and gas phase conditions. In gas phase polymerization, the large particle diffusivity D_ℓ is of the order of 10^{-4}-10^{-3} cm^2/s, and hence significant intraparticle mass transfer effects are unlikely, except for large particles of highly active catalyst. On the other hand, as seen from Table 1, large particle diffusivities in slurry polymerization are on the order of 10^{-6}- 10^{-5} cm^2/s, and in this region significant mass transfer resistance is present (at growth factor $\Phi_g = 1$) even for catalysts of relatively low activity. Note that macroparticle diffusion resistance is more severe (for the same observed rate) if the monomer concentration is low. Thus, one may not rule out significant intraparticle mass transfer resistance effects under laboratory conditions. As the polymer particle grows ($\Phi_g > 1$), the diffusion resistance becomes less, because the reaction rate per unit volume decreases. For the highest activity catalysts, however, diffusion might influence the polymerization rate for a significant time period. Hence, in the complete absence of catalyst deactivation, an acceleration-type polymerization rate behavior would

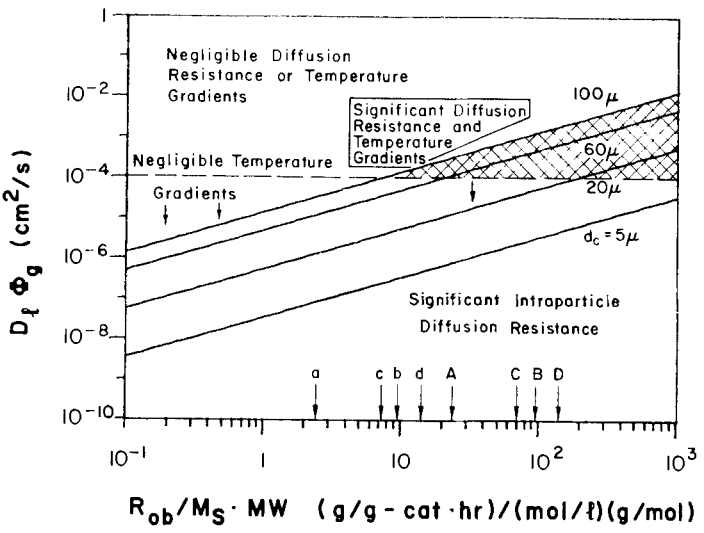

Figure 4 Regimes for macroparticle diffusion resistance and temperature gradients. $D_\ell \Phi_g$ versus observed catalyst activity. Approximate values for typical catalysts if $M_S = M_b$.

a,A Propylene slurry polymerization, low and high activity catalyst.
b,B Propylene gas phase polymerization, low and high activity catalyst.
c,C Ethylene slurry polymerization, low and high activity catalyst.
d,D Ethylene gas phase polymerization, low and high activity catalyst.

(Low activity: R_{ob} = 400 g/g-cat.hr, High activity: R_{ob} = 4000 g/g-cat.hr under representative industrial conditions)

be expected. This is illustrated in Figure 5 (solid line) for a catalyst of intrinsic activity 4000 g/g-cat/hr under industrial conditions. Acceleration-type rate behavior has been observed with some catalyst-monomer systems, especially for the polymerization of ethylene[21,22]. Note that with catalyst deactivation and reduced mass transfer limitation, decay type kinetics are observed (dashed line). Choi[23] has earlier observed these combined effects. Figures 6 and 7 illustrate kinetic and diffusion control for high activity catalysts with second and first-order chemical decay, respectively. As evident from these figures, kinetic control may be observed when $D_\ell = 1 \times 10^{-5}$ cm^2/s. When diffusion resistance is present, the effect of catalyst decay will be offset by increased diffusion of monomer

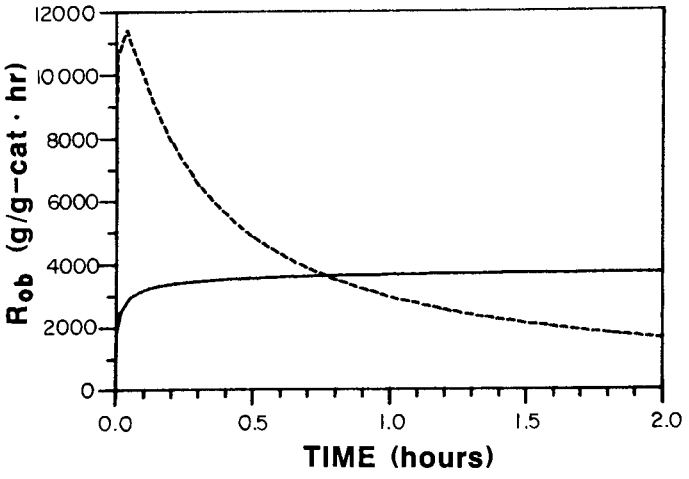

Figure 5 Kinetic and diffusion control for catalysts, average activity over a 2 hour period ~ 4000 g/g-cat.hr.
- - - - 2nd-order deactivating catalyst, $D_\ell = 5 \times 10^{-6}$ cm^2/s
——— non-deactivating catalyst, $D_\ell = 1 \times 10^{-6}$ cm^2/s

into the growing particle. Thus, the observed order of rate decay will be less than the true order in this circumstance. Under severe diffusion influence, hybrid-type rate curves rather than decay-type curves are observed (Curve 3 in Figs. 6 and 7). If such rate curves are observed, the possibility of intraparticle mass transfer limitations on the rate should be considered. It is of interest that a transition from decay-type rate curves to hybrid-type was observed by Boucher et al.[24], on lowering the cocatalyst concentration in ethylene slurry polymerization from 5 mmol/ℓ to 0.06 mol/ℓ. Since the reaction rate depends on cocatalyst concentration, it is possible that the rate could have become limited by mass transfer of cocatalyst in this case. This is especially true because the catalyst was not precontacted with cocatalyst, and the bulky cocatalyst (TEA) molecule should be more susceptible to diffusion influences than monomer. Of course, chemical explanations for such rate curves, such as a slow initiation step, may also be proffered. Conversely, when rate curves which decay sharply from the initial rate are observed,

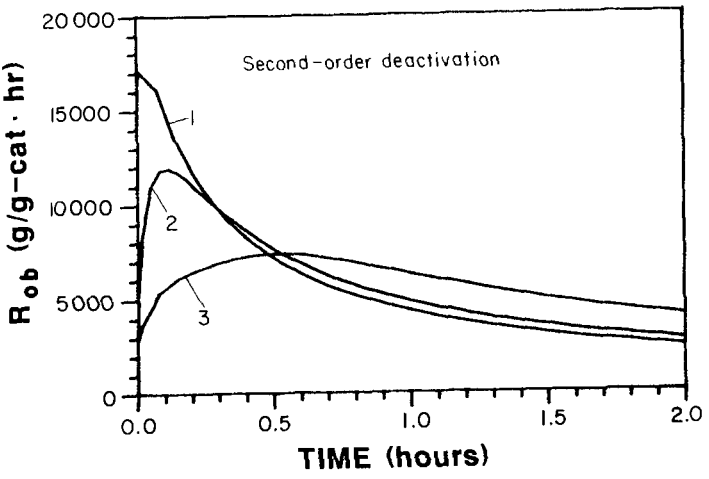

Figure 6 Kinetic and diffusion control for 2nd-order deactivating catalysts, average activity over 2 hour period ~ 5800 g/g-cat.hr. Curve 1: $D_\ell = 1x10^{-5}$ cm^2/s Curve 2: $D_\ell = 2x10^{-6}$ cm^2/s Curve 3: $D_\ell = 1x10^{-6}$ cm^2/s. Each curve has different intrinsic catalyst activity, but comparable observed activity.

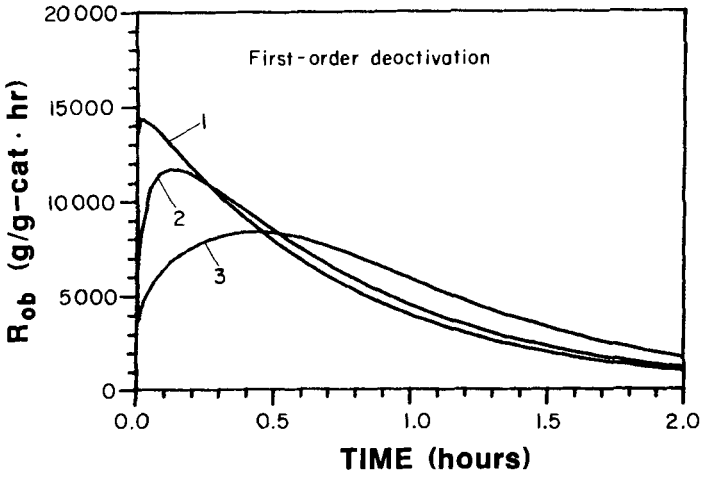

Figure 7 Kinetic and diffusion control for 1st-order deactivating catalysts, average over 2 hour period ~ 5300 g/g-cat.hr. Curve 1: $D_\ell = 1x10^{-5}$ cm^2/s Curve 2: $D_\ell = 2x10^{-6}$ cm^2/s Curve 3: $D_\ell = 1x10^{-6}$ cm^2/s. Each curve has different intrinsic catalyst activity, but comparable observed activity.

as in Ref. [12], it is likely that diffusion influence on the rate is minor.

From Figure 4 it can also be inferred that the size of the catalyst particles in Ziegler-Natta systems will influence the yields when mass transfer limitations are present. This is illustrated by example in Figure 8. The difference in the yields obtained from catalyst particles of different size depends upon the activity of the catalyst as well as the macroparticle diffusion coefficient. The higher the activity of the catalyst and the smaller the diffusion coefficient, the greater the effect of catalyst particle size on the yields.

From detailed simulations, the difference in the yields will be observable for high activity catalysts if the diffusion coefficient is less than around 5×10^{-6} cm^2/sec, while the difference will be observable for low activity catalysts only if the diffusion coefficient is less than approximately 1×10^{-6} cm^2/sec. If the diffusion coefficient is greater than around 5×10^{-6} cm^2/sec, it may be difficult to experimentally observe an effect of catalyst particle size on yields even with relatively high activity catalyst.

From Figure 8 it may be concluded that in order to prevent the yield of a catalyst from being influenced by the catalyst particle size, either the catalyst particle size range should be kept small or the effective diffusivity in the macroparticle should be kept large (e.g. through increased porosity).

EXTERNAL FILM RESISTANCES

We will now turn to examination of the heat and mass transfer resistances in the external film. To analyze this, we formulate a quasi-steady-state mass or energy balance for the polymer particle, using the observed reaction rate for the catalyst. For the external film mass transfer resistance we thus obtain

$$k_s A_p \Delta M = \rho_c V_c \frac{R_{ob}}{MW} \tag{10}$$

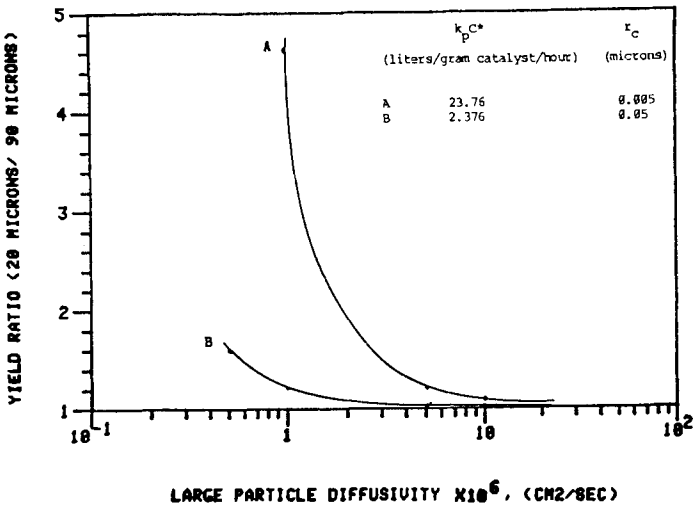

Figure 8 The effect of catalyst particle size on polymer yield as a function of macroparticle diffusivity, D_ℓ.

where ρ_c and V_c are the apparent density and volume of the catalyst macroparticle, MW is the molecular weight of monomer, A_p is the geometric surface area of the polymer particle, k_s is the mass transfer coefficient, and ΔM is the concentration drop. Various correlations may be used to estimate k_s, and the reader is referred to [25] for a discussion of these. In this paper, we will present results based on the Ranz-Marshall correlation, for both the mass and heat transfer coefficients. The Ranz-Marshall correlation for mass transfer is given as

$$Sh = 2 + 0.6\ Re^{\frac{1}{2}}\ Sc^{\frac{1}{3}} \tag{11}$$

and involves the particle-fluid relative velocity as well as the physical properties of particle and fluid. For slurry polymerization, the terminal velocity of the particle in the diluent liquid was assumed. This should give conservative estimates for the mass transfer resistance, because under agitated conditions, the mass transfer coefficient is considered to be greater than the value thus calculated by a factor up to 4. Figure 9 illustrates the predicted concentration drop across the external film for propylene slurry polymerization with low and high activity catalysts of various par-

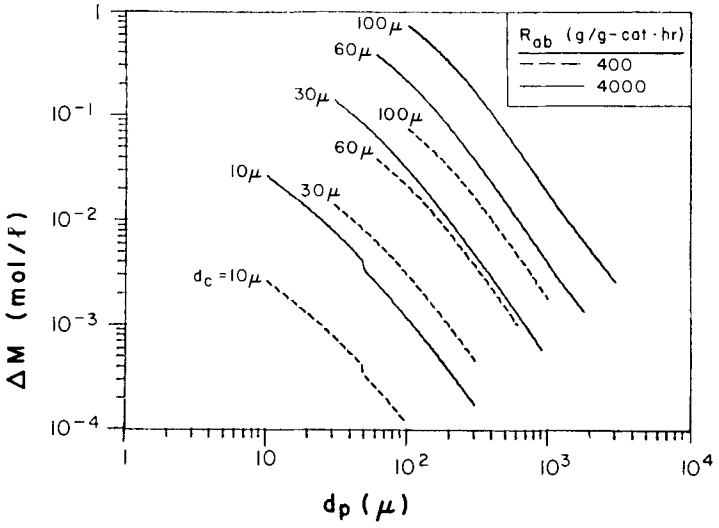

Figure 9 External film mass transfer resistance in propylene slurry polymerization as a function of polymer particle size, using the Ranz-Marshall correlation for Low (R_{ob} = 400 g/g-cat.hr) and High (R_{ob} = 4000 g/g-cat.hr) activity catalysts with various catalyst particle sizes

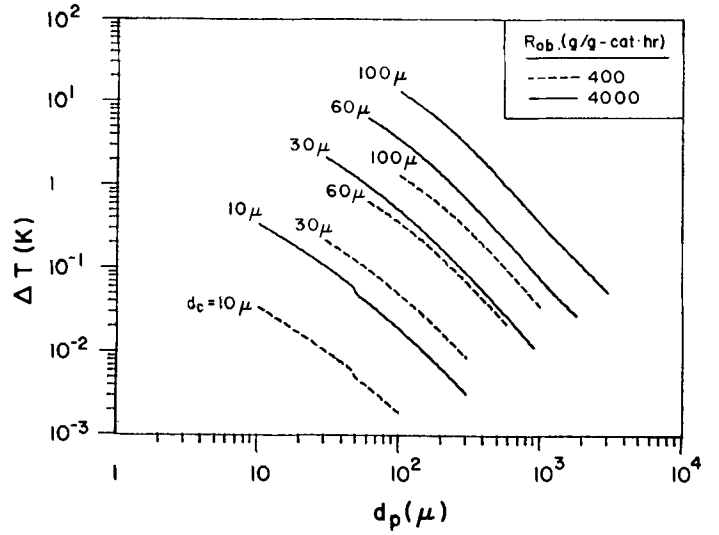

Figure 10 External film heat transfer resistance in propylene slurry polymerization as a function of polymer particle size, using the Ranz-Marshall correlation for Low (R_{ob} = 400 g/g-cat.hr) and High (R_{ob} = 4000 g/g-cat.hr) activity catalysts with various catalyst particle sizes

ticle sizes. The lines represent the growth of the polymer particle from a catalyst particle of indicated size. It can be seen that the mass transfer resistance even for high activity catalyst is quite insignificant compared to the bulk monomer concentration (under industrial conditions) of 4 mol/ℓ when the catalyst particle size is small. For large particles of high activity catalyst, a significant external film resistance will exist for a short period of time until the polymer particle grows to several times the original catalyst size. Figure 10 illustrates the external film temperature rise for propylene slurry polymerization. The temperature rise is around 2 K for 30 μ particles of high activity catalyst, but for larger particles, the initial ΔT might reach as high as 10 K. However, detailed simulations show that intraparticle diffusion resistance early in the polymerization causes this initial temperature rise to be smaller than would be predicted from the catalyst's intrinsic activity. For slurry polymerization, the assumption of an isothermal particle with temperature equal to the bulk liquid temperature is usually justified, unless the initial activity of the catalyst is very large.

Turning to gas phase polymerization, we employ a particle-fluid relative velocity of 2 cm/s, quoted by Wisseroth[26] for stirred bed reactors. In fluidized bed reactors, larger values would be appropriate[27]. Considering the case where hydrogen or a comonomer is present in the reactor, we predict the external film mass transfer resistance for ethylene gas phase polymerization as shown in Figure 11. Fortunately, this concentration drop turns out to be insignificant. Thus, the composition of monomer, comonomer, hydrogen etc. at the particle surface may be assumed equal to the composition in the bulk gas. On the other hand, Figure 12 shows that a significant temperature rise across the external film may be anticipated in gas phase polymerization. Specifically, an initial temperature rise of greater than 10 K is attained for 30 micron particles of high activity catalyst and 100 micron particles of low activity catalyst. The melting point of the polymer would be reached for particles of high activity catalyst larger than 60 μ. Since a catalyst particle distribution will generally contain some coarser particles and catalyst agglomeration may take place on injection, this effect can frequently result in polymer melting, sticking or agglomeration problems in industrial gas phase reactors. Clearly, these problems can be

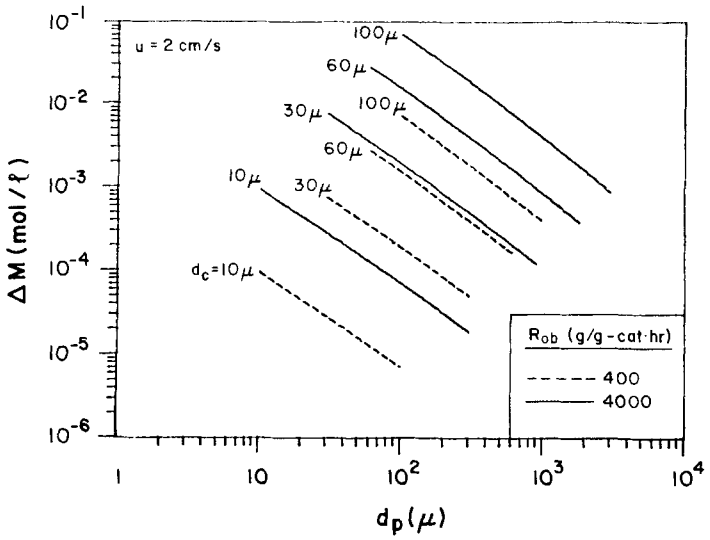

Figure 11 External film mass transfer resistance in ethylene gas phase polymerization (stirred bed conditions, u = 2 cm/s) as a function of polymer particle size, using the Ranz-Marshall correlation. Low (R_{ob} = 400 g/g-cat.hr) and High (R_{ob} = 4000 g/g-cat.hr) activity catalysts with various catalyst particle sizes.

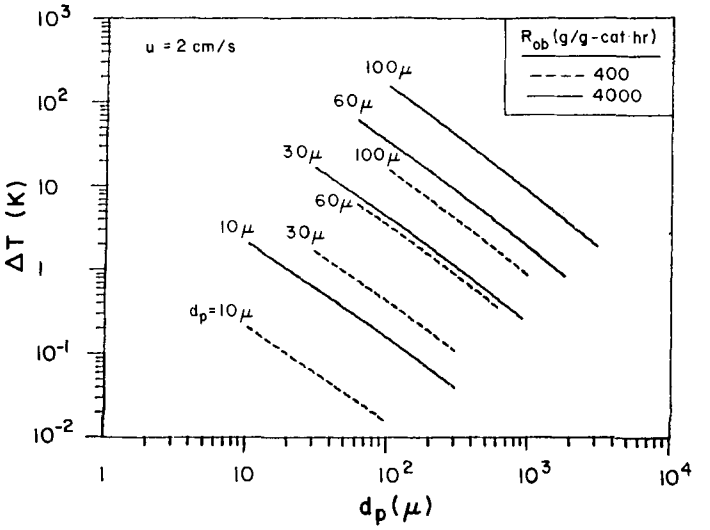

Figure 12 External film heat transfer resistance in propylene gas phase polymerization (stirred bed conditions, u = 2 cm/s) as a function of polymer particle size, using the Ranz-Marshall correlation. Low (R_{ob} = 400 g/g-cat.hr) and High (R_{ob} = 4000 g/g-cat.hr) activity catalysts with various catalyst particle sizes.

reduced by closer control of the catalyst particle size distribution. On the other hand, there is a limit to reducing the average size of the catalyst particles, because very fine particles create problems in handling and entrainment[28]. Furthermore, even at high yields, a minimum catalyst size is necessary to produce polymer particles which do not require pelletization. A more useful approach is to reduce the initial activity of the catalyst. As illustrated in Figure 13, when the active sites do not reach their full activity immediately, but become activated with a time constant τ_c, the temperature rise during the critical first few seconds can be reduced from polymer melting levels to as little as a few K. In practice, this retardation of initial activity can be achieved in several ways. Separate injection of catalyst components[29], premixing the catalyst with polymer particles[30], prepolymerizing[31], coating the catalyst with wax[32] and temporary deactivating agents[33] are some methods mentioned in the patent literature of industrial gas phase polymerization. In summary, the most important heat and mass transfer resistances in solid-catalyzed olefin polymerization are intraparticle mass transfer resistances in slurry and the external film temperature rise in gas phase. In the following sections, the effects of diffusion resistances and catalyst deactivation on the observed activation energy will be discussed.

THE EFFECT OF MASS TRANSFER LIMITATIONS ON THE EFFECTIVENESS OF ZIEGLER-NATTA CATALYSTS AND ON THEIR ARRHENIUS PLOTS

As indicated in the last section, the severity of the mass transfer limitations is highly dependent on the activity of the catalyst, the diameter of the catalyst, and on the magnitude of the diffusion coefficients governing the mass transfer. This dependence is illustrated in Figures 14a, 14b which shows the overall (microparticle plus macroparticle) catalyst effectiveness factors predicted by the multigrain model for propylene slurry polymerization with a high activity catalyst and a low activity catalyst under conditions for severe mass transfer limitation and for mild mass transfer limitation. Here the catalyst effectiveness factor is the rate at which polymer is produced divided by the rate at which the polymer would be produced if mass transfer limitations did not exist.

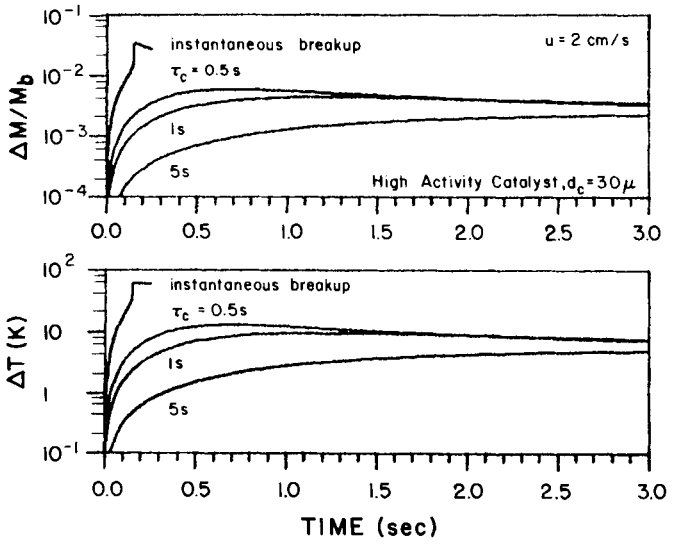

Figure 13 External film heat and mass transfer resistances in gas phase polymerization of ethylene under stirred bed conditions (u = 2 cm/s, using the Ranz-Marshall correlation) with high activity catalyst. Effect of characteristic breakup time of catalyst τ_c . Average rates (g/g-cat.hr); τ_c= 0.5 s : 4820, τ_c= 1 s : 3790, τ_c= 5 s : 1180.

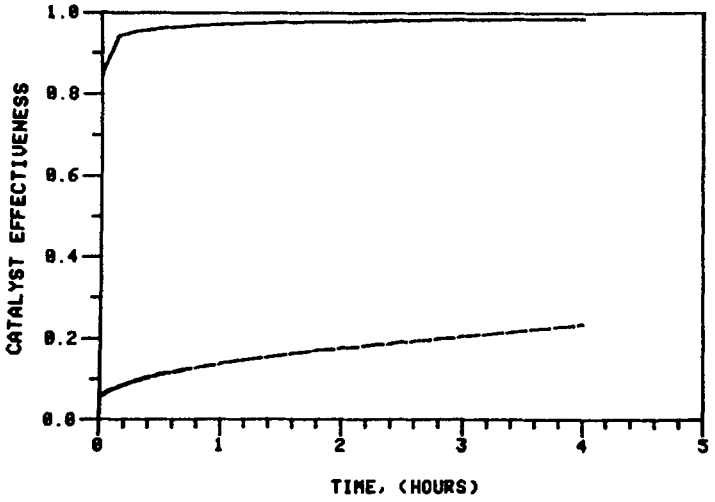

Figure 14a The overall effectiveness factor for a high activity catalyst under mild and severe mass transfer limitations without catalyst deactivation. k_pC^* = 23.76 liters/gram catalyst/hour; T = 70 C.

——— mild mass transfer limitation (D_ℓ = 5x10^{-6} cm^2/sec), D_s = 1x10^{-8} cm^2/ sec, d_c = 40 microns, r_c = 0.005 microns)

— — — severe mass transfer limitation (D_ℓ = 1x10^{-6} cm^2/sec) D_s = 1x10^{-9} cm^2/sec, d_c = 100 microns, r_c = 0.1 microns

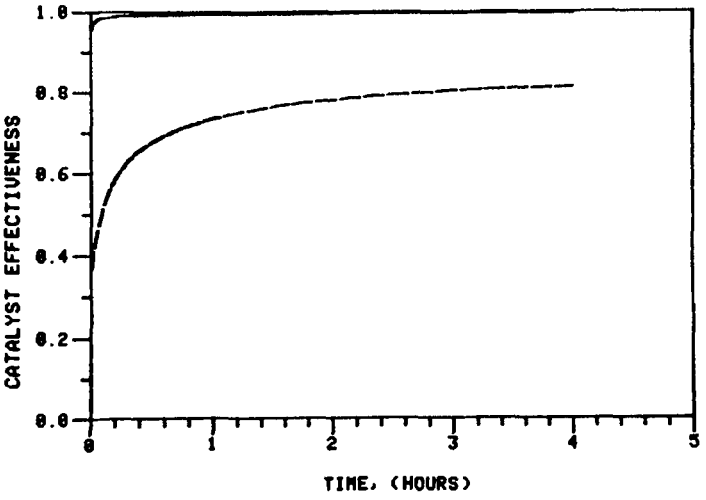

Figure 14b The overall effectiveness factor for a low activity catalyst under mild and severe mass transfer limitations without catalyst deactivation. $k_p C^* = 2.376$ liters/gram catalyst/hour; T = 70C.

——— mild mass transfer limitation ($D_\ell = 5 \times 10^{-6}$ cm^2/sec), $D_s = 1 \times 10^{-8}$ cm^2/ sec, $d_c = 40$ microns, $r_c = 0.005$ microns)

— — — severe mass transfer limitation ($D_\ell = 1 \times 10^{-6}$ cm^2/sec) $D_s = 1 \times 10^{-9}$ cm^2/sec, $d_c = 100$ microns, $r_c = 0.1$ microns

The high activity catalyst has an intrinsic rate of 4000 g/g-cat.hr in the absence of diffusion limitations, while the low activity catalyst has an intrinsic rate of 400 g/g-cat.hr. It is assumed that the concentration of the propylene in the slurry is 4 moles/liter. Note that both the high activity catalyst and the low activity catalyst can experience significant mass transfer limitations if the catalyst particles are large, the primary crystallite size is large, or the diffusion coefficients are small.

Figures 15a and 15b illustrate the effect of mass transfer limitations on the Arrhenius plots one obtains from a low activity Ziegler-Natta catalyst. If mass transfer limitations are negligible, one obtains a straight line Arrhenius plot, and the slope of the plot yields an activation energy equivalent to the true activation energy for the catalyst (which in these simulations is 10.0 kcal/mole.) Furthermore, the Arrhenius plot based on the initial reaction rates is nearly identical to the Arrhenius plot based on the reactions' four hour yields (in the absence of catalyst deactivation).

On the other hand, if mass transfer limitations are significant, one obtains a curved Arrhenius plot, and the slope of the plot at any point yields an activation energy less than the kinetic activation energy of the catalyst. Furthermore, with significant mass transfer limitations, the Arrhenius plot based on the initial reaction rates is noticably different from the Arrhenius plot based on the reaction's 4 hour yields. The difference is due to the fact that the mass transfer limitations are most severe during the initial phases of particle growth.

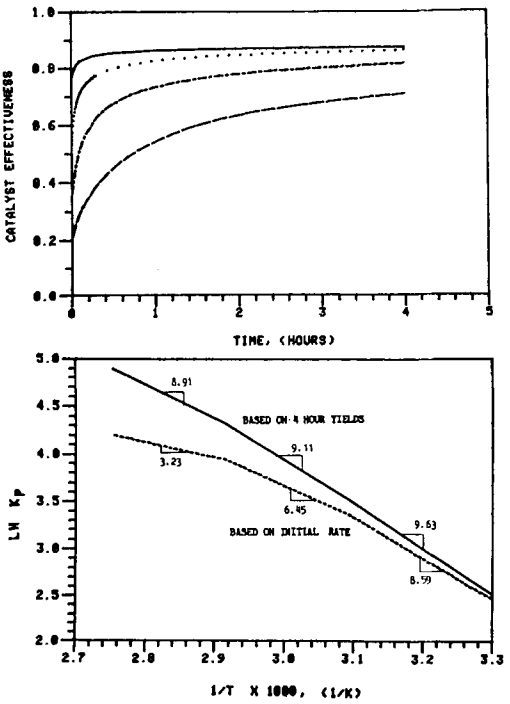

Figure 15a Effectiveness factors and activation energy plots for low activity catalyst with severe diffusion limitations, activated microscale diffusion, D_s, and no catalyst deactivation. $k_pC^* = 2.376$ liters/gram catalyst/hour at 70 C, $D_\ell = 1\times10^{-6}$ cm^2/sec, $d_c = 100$ microns $r_c = 0.1$ microns, $E_p = 10.0$ kcal/mole.

——— T = 30 C, $k_pC^* = 0.34$, $D_s = 8.1\times10^{-11}$

····· T = 50 C, $k_pC^* = 0.90$, $D_s = 3.1\times10^{-10}$

—·—·—·— T = 70 C, $k_pC^* = 2.38$, $D_s = 1.0\times10^{-9}$

— — — — T = 90 C, $k_pC^* = 5.33$, $D_s = 2.9\times10^{-9}$

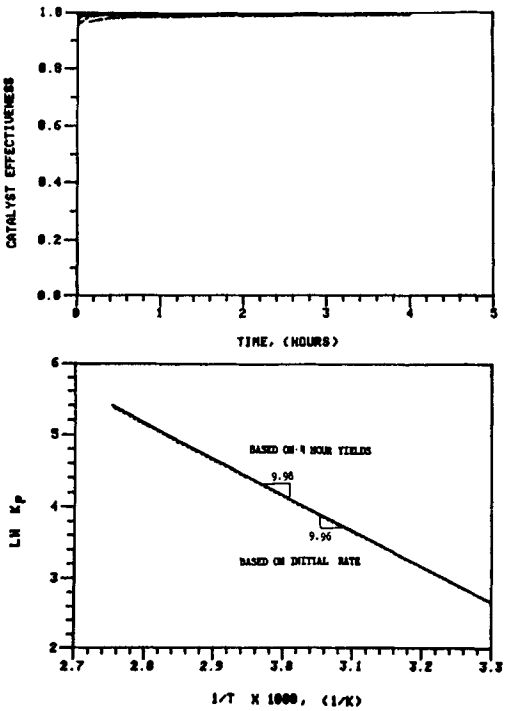

Figure 15b Effectiveness factors and activation energy plots for low activity catalyst with mild diffusion limitations, activated micro-scale diffusion, D_s, and no catalyst deactivation. $k_pC^* = 2.376$ liters/gram catalyst/hour at 70 C, $D_\ell = 5\times10^{-6}$ cm^2/sec, $d_c = 40$ microns $r_c = 0.005$ microns, $E_p = 10.0$ kcal/mole.

——— T = 30 C, $k_pC^* = 0.34$, $D_s = 8.1\times10^{-10}$

····· T = 50 C, $k_pC^* = 0.90$, $D_s = 3.1\times10^{-9}$

—.—.—.— T = 70 C, $k_pC^* = 2.38$, $D_s = 1.0\times10^{-8}$

— — — — T = 90 C, $k_pC^* = 5.33$, $D_s = 2.9\times10^{-8}$

Figures 16a and 16b illustrate the same effects for high activity catalyst. With a high activity catalyst, a maximum can occur in the Arrhenius plot under severe mass transfer limiting conditions. The drop in rate at the high temperatures results when the propagation constant becomes so large that the monomer cannot penetrate into the catalyst before being consumed. All of the reaction occurs at the catalyst surface and the catalyst below the surface is not used effectively.

As illustrated in Figure 17 where D_s is held constant with temperature, the same trends are observed whether or not the small particle diffusion coefficient is thermally activated (as it is in Figures 15 and 16).

In conclusion, the effectiveness factor and observed activation energy of Ziegler-Natta catalysts can be strongly affected by diffusion limitations. The severity of these limitations is highly dependent upon catalyst diameter, the catalyst primary crystallite size, the microscale diffusivity D_s and the macroscale diffusivity D_ℓ.

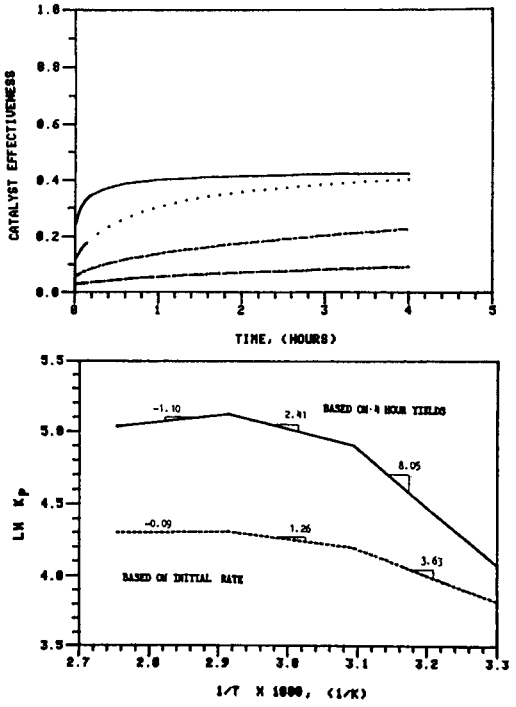

Figure 16a Effectiveness factors and activation energy plots for high activity catalyst with severe diffusion limitations, activated microscale diffusion, D_s, and no catalyst deactivation. $k_pC^* = 23.76$ liters/gram catalyst/hour at 70 C, $D_\ell = 1\times10^{-6}$ cm^2/sec, $d_c = 100$ microns, $r_c = 0.1$ microns, $E_p = 10.0$ kcal/mole.

——— T = 30 C, $k_pC^* = 3.40$, $D_s = 8.1\times10^{-11}$

····· T = 50 C, $k_pC^* = 9.00$, $D_s = 3.1\times10^{-10}$

—·—·—·— T = 70 C, $k_pC^* = 23.8$, $D_s = 1.0\times10^{-9}$

— — — — T = 90 C, $k_pC^* = 53.3$, $D_s = 2.9\times10^{-9}$

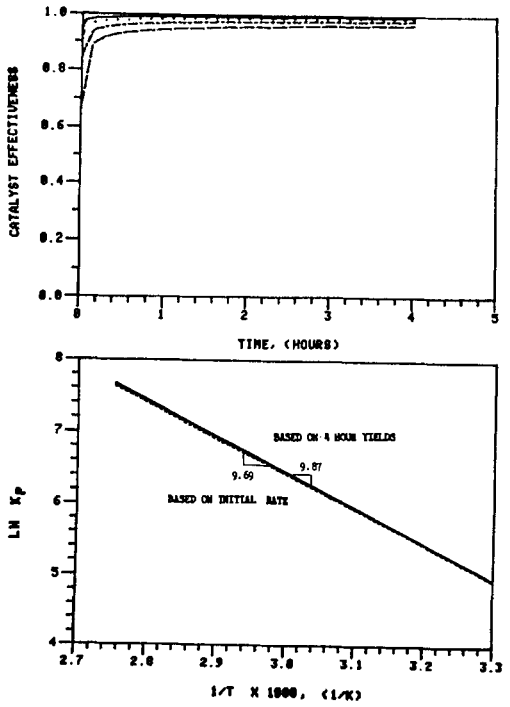

Figure 16b Effectiveness factors and activation energy plots for high activity catalyst with mild diffusion limitations, activated microscale diffusion, D_s, and no catalyst deactivation. k_pC^* = 23.76 liters/gram catalyst/hour at 70 C, $D_\ell = 5\times10^{-6}$ cm^2/sec, d_c = 40 microns, r_c = 0.005 microns, E_p = 10.0 kcal/mole.

——— T = 30 C, $k_pC^* = 3.40$, $D_s = 8.1\times10^{-10}$

····· T = 50 C, $k_pC^* = 9.00$, $D_s = 3.1\times10^{-9}$

—·—·—·— T = 70 C, $k_pC^* = 23.8$, $D_s = 1.0\times10^{-8}$

— — — — T = 90 C, $k_pC^* = 53.3$, $D_s = 2.9\times10^{-8}$

However as shown in [20], it is expected that considering the properties r_c, d_c, D_s, D_ℓ for present day catalysts, the catalyst particle diameter and macroscale diffusion will have the largest mass transfer effect on observed activation energies.

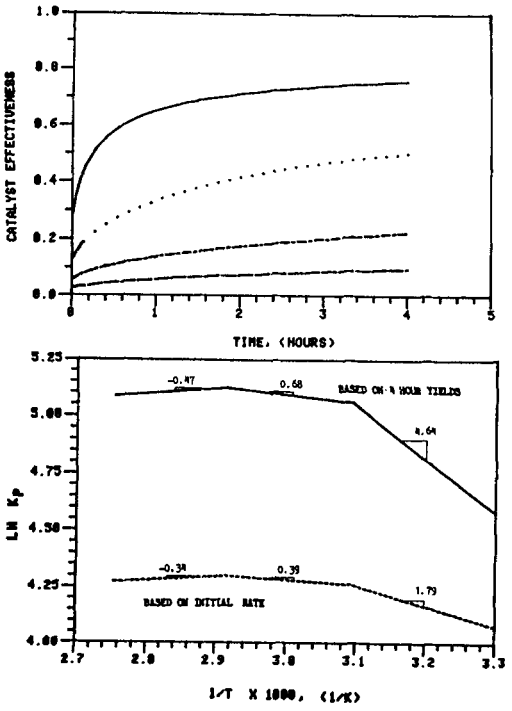

Figure 17 Effectiveness factors and activation energy plots for high activity catalyst with severe diffusion limitations, without activated microscale diffusion, D_s, and no catalyst deactivation. k_pC^* = 23.76 liters/gram catalyst/hour at 70 C, $D_\ell = 1\times10^{-6}$ cm^2/sec, d_c = 100 microns, r_c = 0.1 microns, E_p = 10.0 kcal/mole.

——— T = 30 C, $k_pC^* = 3.40$, $D_s = 1.0\times10^{-9}$

····· T = 50 C, $k_pC^* = 9.00$, $D_s = 1.0\times10^{-9}$

—.—.—.— T = 70 C, $k_pC^* = 23.8$, $D_s = 1.0\times10^{-9}$

— — — — T = 90 C, $k_pC^* = 53.3$, $D_s = 1.0\times10^{-9}$

THE EFFECT OF THERMALLY ACTIVATED CATALYST DECAY

Diffusion limitations are not the only factors that can make the Arrhenius plots of Ziegler-Natta systems nonlinear. Thermally activated catalyst decay can also cause observed activation energies to vary. Figure 18 demonstrates how the temperature dependence of catalyst decay can influence the Arrhenius plots for a high activity catalyst and a low activity catalyst. As can be seen, the curvature of the Arrhenius plots increases as the activation energy of the catalyst decay increases. A maximum occurs in the Arrhenius plots for both the high activity catalyst and the low activity catalyst when the activation energy of the decay constant exceeds 20 kcal/mole. Brockmeier[15] has reported activation energy values for catalyst decay of 14.7 kcal/mole for a Montiedison catalyst having a Propagation activation energy of 15.6 kcal/mole.

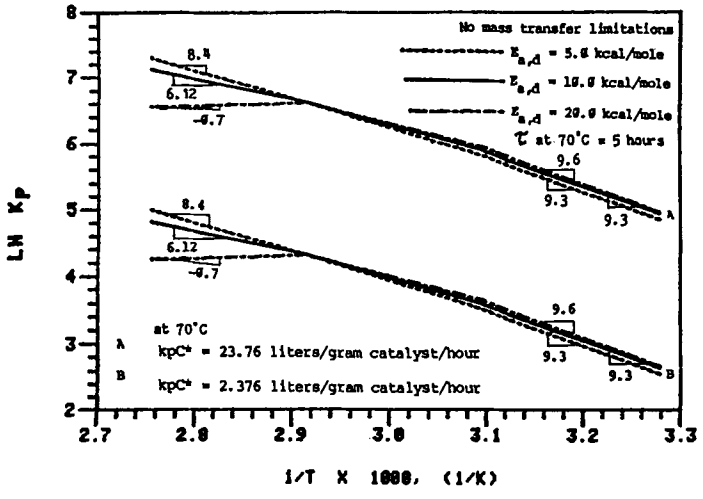

Figure 18 The effect of thermally activated catalyst decay on the Arrhenius plots for high activity catalyst (k_pC^* = 23.76 liters/gram catalyst/hour, E_p = 10 kcal/mole) and low activity catalysts (k_pC^* = 2.376 liters/gram catalyst/hour, E_p = 10 kcal/mole). Catalyst decay constant $k_d = k_{do}\exp^{(-E_{a,d}/RT)}$ where k_{do} is chosen such that the time constant for deactivation at 70 C is 5 hours.

Thus, thermally activated catalyst decay can cause nonlinearities in the Arrhenius plots for Ziegler-Natta systems as can mass transfer limitations. If the system is mass transfer limited, reducing the size of the catalyst particles and/or primary crystallites should increase the catalyst yields.

CONCLUSIONS

Although the degree of diffusion resistance that will be experienced during polymerization of olefins depends on the properties of individual catalysts, some general conclusions regarding the importance of diffusion resistances can be made from the present work. First, it is likely that microparticle diffusion limitations will only be significant with catalysts of high activity for which the primary particle size is larger than around 0.05 microns. This indicates that the primary particle size should be considered an important design variable for high activity catalyst systems. Temperature gradients in the microparticles will, however, be negligible for both gas and liquid phase polymerizations. In the macroparticles, significant temperature gradients appear likely to exist only for large, high activity particles in gas phase polymerization. On the other hand, significant concentration gradients in the macroparticles can exist at short times (i.e. at low growth factor) in slurry polymerization, even for catalysts of relatively low activity. For large particles of high activity catalyst, intraparticle mass transfer resistance can be rate limiting over longer periods, and in this case an effect of catalyst particle size on yield may be observed. In cases of severe diffusion control, acceleration or hybrid-type rate behavior may be observed. The rate limitation may result from mass transfer of cocatalyst as well as monomer, especially when catalyst and cocatalyst are not premixed. Conversely, when rate curves which decay sharply from $t = 0$ are observed, severe intraparticle mass transfer resistance is unlikely. In gas phase, macroparticle diffusivities are presumably high enough to avoid significant concentration gradients, although a low diffusivity during catalyst breakup is not inconceivable.

In summary, the degree of mass transfer limitations experienced in Ziegler-Natta systems is dependent on both the catalyst particle size and the size of the primary crystallites. It is of practical

significance that with severely diffusion limited catalyst, less than 50% of the transition metal sites may be effectively used. Finally, if a catalyst is severely diffusion-limited, the Arrhenius plots based on yield or initial rate will be nonlinear and may exhibit a maximum. However, it should be noted that such Arrhenius relations are also likely to arise through thermal activation of the catalyst decay. It is possible to distinguish between these sources of nonlinearity in the Arrhenius plots by extrapolating the polymerization rate to zero time. If the source of the nonlinearity is mass transfer resistance, the Arrhenius plot for the initial rate will differ significantly from that for long-time yields, and if the source is activated catalyst decay, the Arrhenius plots based on the initial reaction rates will be linear.

In general, it is safe to say that external film mass transfer resistances are of little practical importance. However, the initial temperature rise across the external film may be as high as 10 K in slurry polymerization for large particles of high activity catalyst. In gas phase, the initial temperature rise for high activity catalyst or agglomerated low activity catalyst can cause the melting point of the polymer to be reached. This appears to be the cause of sticking and agglomeration problems commonly observed in industrial gas phase reactors. Such problems can be mitigated by reducing the activity of the catalyst for a brief period during and after injection.

REFERENCES

1. E. J. Nagel, V. A. Kirillov and W. H. Ray, I. & E.C. Prod. Res. Dev., 19, 372 (1980).
2. J. W. Begley, J. Polym. Sci. A-1, 4, 319 (1966).
3. B. Fisa and R. H. Marchessault, Polym. Lett., 12, 561 (1974).
4. D. Singh and R. P. Merrill, Macromolecules 4 (5), 599 (1971).
5. N. F. Brockmeier and J. B. Rogan, A.I.Ch.E. Symp. Ser., 72, No. 160, 28 (1976).
6. J. C. W. Chien, J. Polym. Sci. Polym. Chem. Ed., 17, 2555 (1979).
7. H. Meyer and K. H. Reichert, Angew. Makromol Chem., 57 (888), 211 (1977).
8. R. L. Laurence and M. Chiovetta, Proceedings, Berlin Workshop on Polymer Reaction Eng., October 1982, p. 73. Edited by K. H. Reichert and W. Geisler, Hanser Verlag, Munich.

9. T. W. Taylor, K. Y. Choi, H. Yuan and W. H. Ray, "Physicochemical Kinetics of Liquid Phase Propylene Polymerization", Proceedings of the 1981 MMI Symposium on Transition Metal Catalyzed Polymerizations, Midland, MI. Published by Plenum Press (1983).
10. L. L. Böhm, Makromol. Chem., 89, 1 (1980).
11. T. Keii, "Kinetics of Ziegler-Natta Polymerization", Chapman and Hall, London, 1972.
12. Y. Doi, M. Murata, K. Yano and T. Keii, Ind. Eng. Chem. Prod. Res. Dev., 21, 580 (1982).
13. T. Keii, E. Suzuki, M. Tamura, M. Murata and Y. Doi, Makromol. Chem. 183 (10), 2285 (1982).
14. L. L. Böhm and H. Passing, Makromol. Chem., 177, 1097 (1976).
15. N. F. Brockmeier and J. B. Rogan, paper presented at A.I.Ch.E. Meeting, Anaheim, CA, May, 1984.
16. K. Y. Choi and W. H. Ray, J. Appl. Polym. Sci., 30, 1065 (1985).
17. (a) T. W. Taylor, Ph.D. Thesis, University of Wisconsin, 1983. (b) G. E. Mann, M.S. Thesis, University of Wisconsin, 1985. (c) S. Floyd, Ph.D. Thesis, University of Wisconsin, 1985.
18. C. W. Hock, J. Polym. Sci. A-1, 4, 3055 (1966).
19. R. J. L. Graff, G. Kortleve and C. G. Vonk, Polym. Lett., 8, 735 (1970).
20. S. Floyd, K. Y. Choi, T. W. Taylor and W. H. Ray, paper submitted to Journal of Applied Polymer Science, May, 1985.
21. P. Pino and B. Rotzinger, Makromol. Chem. Suppl., 7, 41 (1984).
22. V. A. Zakharov, V. N. Druzhkov, E. G. Kushnareva and Yu.I. Yermakov, Kinetika i Kataliz, 15 (2), 446 (1974).
23. K. Y. Choi, Ph.D. Thesis, University of Wisconsin, 1984.
24. D. G. Boucher, I. W. Parsons and R. N. Haward, Makromol. Chem. 175, 3461 (1974).
25. S. Floyd, K. Y. Choi, T. W. Taylor and W. H. Ray, paper submitted to Journal of Applied Polymer Science, May, 1985.
26. K. Wisseroth, private communication (1982).
27. D. Kunii and O. Levenspiel, "Fluidization Engineering", Wiley, N.Y., 1969.
28. U.S.P. 3,300,457 (1967) to B.A.S.F.
29. U.S.P. 3,652,527 (1972) to B.A.S.F.
30. U.S.P. 3,772,261 (1973) to Scholven-Chemie.

31. U.S.P. 3,922,322 (1975) to Union Carbide.

32. U.S.P. 4,200,715 (1980) to Gulf.

33. U.S.P. 4,130,699 (1978) to Standard Oil of Indiana.

ACKNOWLEDGEMENTS

The authors are indebted to the National Science Foundation, E.I. DuPont and Co., Exxon Chemical Co., and Mobil Chemical Co. for support of this research.

This page intentionally left blank

REACTION ENGINEERING ASPECTS OF ETHYLENE POLYMERIZATION WITH ZIEGLER-CATALYSTS IN SLURRY REACTORS

K.H.REICHERT, R.MICHAEL AND H.MEYER
Institut fuer Technische Chemie, Technische Universitaet Berlin, Straße des 17. Juni 135, D - 1000 Berlin 12, West Germany

ABSTRACT

The semicontinuous polymerization of ethylene in slurry with a supported Ziegler catalyst was studied in laboratory scale bubble columns and stirred vessels at constant temperature and pressure. By applying the model of resistance in series mass transfer and kinetic parameters of the polymerization in the three phase system were determined. For gas hold up and heat transfer in slurries with high solid content dimensionless correlations are given which consider energy input and some physical properties of the slurries. The diffusion of ethylene within porous catalyst and polymer particles may play a certain role under certain circumstances. The molecular weight distribution of the polyethylene formed is rather broad and depends to some extent on cocatalyst and hydrogen concentration.

INTRODUCTION

Mixing and heat transfer play a dominant role in multiphase polymerization like the polymerization of gaseous olefins with Ziegler catalysts in slurry reactors. Extensive studies regarding mass and heat transfer have been carried out with multi-phase systems mostly however with non reacting systems based on inorganic solids dispersed in water and air as gaseous phase. Little is published on mass and heat transfer for olefin polymerization in slurry reactors in the presence of high fractions of solid polymer. Data and results

presented in this paper refer to the Ph.D thesis of Michael[1] and Meyer[2] which deal with heat and mass transfer of ethylene polymerization in bubble column and stirred tank reactor and molecular weight distribution of high molecular weight polyethylene.

EXPERIMENTAL

The polymerization of ethylene was run in a laboratory scale bubble column and in a stirred tank reactor at constant temperature and pressure. For starting the polymerization the preactivated catalyst dispersion, consisting of $TiCl_4$ / $Mg(OC_2H_5)_2/Al(C_2H_5)_3$, was pumped into the pressurized reactor generally in the presence of polyethylene powder to avoid agglomeration of the catalyst particles at the beginning of polymerization. Heptane or other paraffinic mixtures were used as liquid phase. The absorption rate of ethylene was measured by using a thermal mass flow meter.
The molecular weight of polyethylene was determined by high temperature gel permeation chromatography using large porous inorganic column material by Merck AG (non commercial laboratory product). An infra red spectrometer was used as detector. Special attention must be given to the sample preparation and to the effect of sample concentration upon elution volume in the case of high molecular weight polymers. For details see Ph.D thesis of Meyer[2].Heat transfer in slurries was studied by inserting a heating shell into the reactor and measuring the heating performance as well as the temperatures of the wall of the heating shell and of the slurry at different distances. The gas hold up of the slurry was determined by measuring the height of the reactor content at work and at rest. The viscosities of the slurries were measured by using a rotational viscosimeter and a liquid having the same density as polyethylene. Particle size distribution were determined by Coulter-Counter technique. For details see Ph.D thesis of Michael[1].

RESULTS

Mass transfer gas-liquid:

The kinetic results were evaluated by using the model of resistance in series as summarized in the text book of Satterfield[3]. At stationary state of polymerization the following concentration profiles of ethylene in the three phase system can be assumed leading to an equation which shows that the main resistance of the process is equal to the sum of the three single resistances. See figure 1.

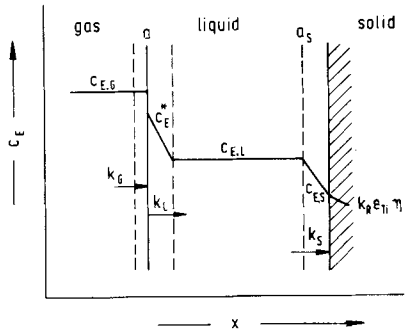

$$\frac{c_E^*}{R_V} = \frac{1}{k_L a} + \frac{1}{k_S a_S} + \frac{1}{k_R e_{Ti}\, \eta\, c_K}$$

$$a_S = f\, c_K$$

$$\frac{c_E^*}{R_V} = \frac{1}{k_L a} + \frac{1}{c_K}\left(\frac{1}{f\, k_S} + \frac{1}{k_R e_{Ti}\, \eta}\right)$$

Fig.1: Concentration profile of ethylene in the polymerizing three phase system.

Knowing the absorption rate of ethylene, R_V, at given catalyst concentration, C_K and saturation concentration of ethylene, c_E^*, the resistance of mass transfer gas-liquid, $1/k_L a$, can be determined if this model is fulfilled in the case of ethylene polymerization with heterogeneous Ziegler catalysts. As can be seen in figure 2 this is the case.

Straight lines result when the reciprocal absorption rate of ethylene is plotted versus the reciprocal catalyst concentration according to the equation derived from the model of resistance in series.

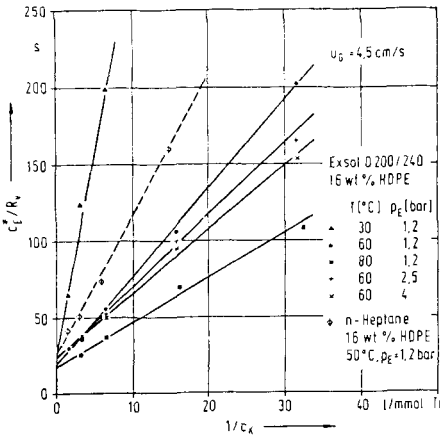

Reciprocal maximum polymerization rate versus reciprocal catalyst concentration at different temperature and ethylene pressure.

$$\frac{c_E^*}{R_V} = \frac{1}{k_L a} + \frac{1}{c_K}\left(\frac{1}{f k_S} + \frac{1}{k_R c_{Ti}^n}\right)$$

Fig.2: Influence of temperature and ethylene pressure on mass transfer and ethylene polymerization in bubble column

In this way the influence of temperature, T, ethylene pressure, p_E, superficial gas velocity of ethylene in bubble column, u_G, and polyethylene content, c_{HDPE}, on mass transfer coefficient gas-liquid, $k_L a$, was tested. The results are summarized in table 1.

T °C	p_E bar	u_G cm/s	c_{HDPE} wt.%	$k_L a$ 1/s
30	1,2	4,5	16	0,037
60	1,2	4,5	16	0,052
80	1,2	4,5	16	0,057
60	1,2	4,5	16	0,052
60	2,5	4,5	16	0,045
60	4	4,5	16	0,044
60	1,2	2,2	16	0,031
60	1,2	4,5	16	0,052
60	1,2	8,9	16	0,071
60	1,2	4,5	4	0,052
60	1,2	4,5	16	0,052
60	1,2	4,5	30	0,040

Tab.1: Volumetric mass transfer coefficient gas-liquid, $k_L a$, at different reaction conditions

The superficial gas velocity has the largest effect on volumetric mass transfer coefficient gas-liquid as expected while the influence of the polymer content on mass transfer gas-liquid is relatively small.

Most important parameter is the gas hold up, ε_G , of the multiphase system. It was found that the volumetric mass transfer coefficient gas-liquid is proportional to the gas hold up in the present case. The gas hold up in bubble column can be correlated fairly well by the following dimensionless equation in table 2 which is based on a semi-theoretical equation of Mersmann[4].

$$\frac{\varepsilon_G}{(1-\varepsilon_G)^4} = c \cdot u_G \cdot \left(\frac{\rho_C^2}{\sigma \Delta\rho g}\right)^{0,25} \cdot Fl^{0,065} \cdot \left(\frac{\rho_G}{\rho_C}\right)^{0,06}$$

with $c = 0,23$ for nonfoaming hydrocarbons

$c = 0,29$ for foaming hydrocarbons

$Fl = \sigma^3 \rho_C^2 / \eta_C^4 \Delta\rho g$ altered from $4,7 \cdot 10^5$ to $6,9 \cdot 10^{10}$

u_G/ρ_C altered from $0,1 \cdot 10^{-3}$ to $2,9 \cdot 10^{-3}$

$$\rho_C = \rho_S \cdot \phi_S + \rho_L (1-\phi_S)$$

$$\eta_C = \eta_L \left[1 + \frac{1,25\phi_S}{(1-\phi_S/\phi_{S,max})}\right]^2 \quad \text{after Eilers}$$

with $\phi_{S,max} > 0,3$ otherwise experimental values of η_C

$$\phi_{S,max} = \rho_B/\rho_S$$

ϕ_S : volume fraction of solid, ρ_B: bulk density

Tab.2: Correlation for gas hold up, ε_G, of the three phase system

The gas hold up can be influenced by the superficial gas velocity, u_G, and some physical properties of the multi-phase system like density, ρ_C, and viscosity, η_C, of the dispersion liquid-solid, the volume fraction of the solid, ϕ_S, and its maximum value, $\phi_{S,max}$, the surface tension gas-liquid, σ, and the difference of densities gas-liquid, $\Delta\rho$. These parameters have been altered in a large way. The results are plotted according to equation in figure 4.

From figure 4 it can be seen that foaming liquids like paraffinic mixtures (Exsol types of Esso and benzine) cause larger gas hold ups than non foaming pure liquids at the same gas through put and the same solid content of the polymerization reactor.

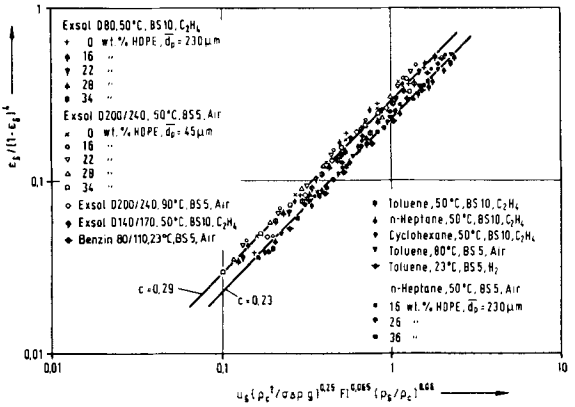

Fig.4: Correlation between gas hold up and gas through put as well as physical properties of the multi phase system gas-liquid-solid

Mass transfer liquid-solid:

For evaluating the mass transfer coefficient, k_S, dimensionless correlations of Sänger and Deckwer[5] were used which are able to correlate many experimental data from literature. The correlations are given in table 3 and refer to two different ranges of mass related energy dissipation rate, ε. For calculation of mass transfer coefficient liquid-solid, k_S, there must be known the mean diameter of the solid particles d_S, the diffusion coefficient of ethylene in the appropriate liquid phase, D_m, which was calculated by using the equation of Wilke and Chang[6], the kinematic viscosity of the liquid phase, η_L. The mass related energy dissipation rate, ε, is proportional to the product of superficial gas velocity, u_G, and gravitational constant, g, in the case of bubble column reactor. The specific surface of the solid particle, a_S, was determined by assuming spherical geometry. Using these values the time dependence of the three single resistances of the polymerization process can be calculated. They are summarized in table 3 for 0, 2 and 80 minutes of reaction.

Mass transfer liquid/solid

Sanger and Deckwer

$Sh = 2 + 0{,}649\ Sc^{0.333} (\varepsilon\ d_S^4 / \gamma_L^3)^{0.242}$

for $(\varepsilon\ d_S^4 / \gamma_L^3) > 1$

$Sh = 2 + 2{,}067\ Sc^{0.333} (\varepsilon\ d_S^4 / \gamma_L^3)^{0.379}$

for $(\varepsilon\ d_S^4 / \gamma_L^3) < 1$

with $Sh \equiv k_S\ d_S / D_m$; $Sc \equiv \gamma_L / D_m$; $\varepsilon = u_G\ g$

$a_S = 6\ \Phi_S / d_S$

t	d_S	k_S	a_S	$\frac{1}{k_S a_S}$	$\frac{1}{k_R e_{Ti} \eta c_K}$	$\frac{1}{k_L a}$
min	10^{-6}m	$10^{-4}\frac{m}{s}$	$\frac{1}{m}$	s	s	s
0	8	13	25	31	33	20
2	54	5,1	1573	1,2	33	20
80	80	4,6	20135	0,1	33	20

Data refer to : $T = 60°C$, $u_G = 4{,}5$ cm/s , $p_E = 4$ bar,
$c_K = 1{,}26 \cdot 10^{-4}$ mol Ti/l

Tab.3: Correlations for mass transfer liquid-solid and time dependence of the single resistances for mass transfer gas-liquid and liquid-solid as well as chemical reaction

The average particle diameter of the catalyst used was 8 µm. After 2 minutes of polymerization the polymer particles formed had a diameter of 54 µm and they grew further to an average diameter of 80 µm in 80 minutes as determined by Coulter-Counter technique. It was assumend that each catalyst particle forms one polymer particle. If more than one polymer particle is formed from one catalyst particle the mass transfer resistance liquid-solid, $1/k_S a_S$, will fall even more with time. The other two resistances can be assumed being constant with time at medium solid content in the reaction vessel. From these calculations one can conclude that at given conditions

mass transfer liquid-solid plays a role in the very beginning of ethylene polymerization but can be neglected when the reaction proceeds. If this is the case the activation energy of the polymerization can be determined from the slopes of the straight lines in figure 2. Plotting the corresponding values in an Arrhenius diagram a slightly bent curve results. The reason for this is that the overall rate constant, $k_R e_{Ti} \eta$, is a function of ethylene concentration. The maximum value of the constant is reached at an ethylene pressure of 4 bar in the present case. This is probably due to the fact that the efficiency of titanium, e_{Ti}, and/or the effectivness factor, η, are dependent upon ethylene concentration. If the experimental values of $k_R e_{Ti} \eta$ are corrected by taking into account the maximum values of e_{Ti} and η straight lines are obtained in the Arrhenius diagram.See figure 5.

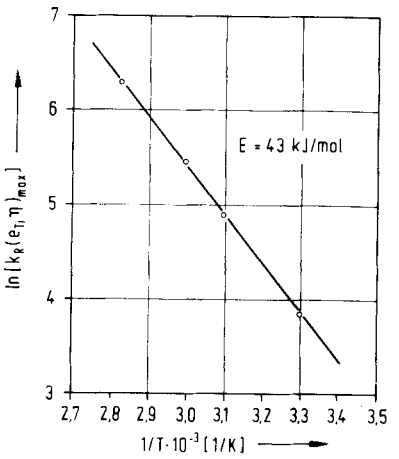

Arrhenius diagram at maximum catalyst activity

$$k_R(e_{Ti}\,\eta)_{max} = \frac{k_R\, e_{Ti}\,\eta}{e_{Ti}\,\eta\,/(e_{Ti}\,\eta)_{max}}$$

Fig.5: Arrhenius diagram for ethylene polymerization

An overall activation energy of 43 kJ/mol results. The overall rate constants are in the region of 38 to 340 l/mol s for temperatures between 30 and 80 ^{o}C. These values agree with data from literature for similar catalyst systems.

Diffusion in porous particles

Catalyst particles:

In order to estimate whether porous diffusion of ethylene is to be considered at reaction conditions given the Thiele modulus must be known. In the following table some data for the catalyst used are summarized.

Diffusion and Reaction in Porous Catalyst Particle

Thiele modulus for first order reaction in a spherical catalyst particle

$$\Phi = R\sqrt{\frac{k_v}{D_{eff}}} \geq 4$$

$$R = 4 \cdot 10^{-6}\,m \qquad (N_C = 1{,}4 \cdot 10^{8}\,(l^{-1}))$$

$$k_v = \frac{r_{eff,o}}{c_E}\,\frac{V_R}{V_C} = \frac{4 \cdot 10^{-3}\,mol/l\,s}{0{,}256\,mol/l}\,\frac{1\,l}{3{,}24 \cdot 10^{-5}\,l} = 480\,s^{-1}$$

with $r_{eff,o} = r_{max}$

$$D_{eff} = \frac{D\,\varepsilon}{\tau} = \frac{3{,}7 \cdot 10^{-9}\,m^2/s\;\;0{,}6}{5} = 4{,}4 \cdot 10^{-10}\,m^2/s$$

$$\eta = \frac{3}{\Phi}\left(\frac{1}{\tanh\Phi} - \frac{1}{\Phi}\right) \leq 0{,}6$$

Reaction data: $T = 60\,^{\circ}C$ $u_G = 4{,}5\,m/s$

$p_E = 4\,bar$, Exol D 200/240

$c_C = 1{,}26 \cdot 10^{-4}\,mol\,Ti/l$

$\rho_C = 1{,}53\,kg/l$

Tab.4: Thiele modulus for ethylene polymerization within porous Ziegler catalyst

The Ziegler catalyst used had an average particle radius, R, of 4 μm, the porosity, ε, is 0.6, the average particle number, N_C, is $1.4 \cdot 10^8$ per liter, having a volume, V_C, of $3.24 \cdot 10^{-5}$ liter. The tortuosity factor, τ, is not known. It was assumed a value of 5 for τ. The initial maximum rate of ethylene absorption, $r_{eff,o}$, at given reaction conditions was measured. A value of $4 \cdot 10^{-3}$ mol/l s was found. The ethylene concentration, c_E, at 4 bar and 60 °C is 0.256 mol/l in Exol D 200/240. The diffusion coefficient of ethylene, D, in the liquid phase at given conditions was calculated with the equation of Wilke und Chang[6]. With these data a minimum Thiele modulus of around 4 results indicating that at reaction conditions given porous diffusion of ethylene within the catalyst particles must be considered at the very beginning of polymerization.

Polymer particles:

After 80 minutes of polymerization the polymer particles had an average radius of 40 μm, a particle number, N_{PE}, of $1.4 \cdot 10^9$ per liter and a porosity of 0.6. The polymer volume, V_{PE}, is 0.367 liter. The reaction rate decreased to a volume of $2.7 \cdot 10^{-3}$ mol/l s. The resulting Thiele modulus depends on the model used for the growing polymer particles. In the case of the well known multigrain model porous diffusion must be considered. The polymeric flow model indicates that porous diffusion seems to play no significant role at conditions given and data used . See table 5.

For diffusion of ethylene in polyethylene a diffusion coefficient of $1.5 \cdot 10^{-11}$ m^2/s was used in the case of the multigrain model, refering to experimental data of Michaels[7] who studied the diffusion of different gases in high density polyethylene at different temperatures. Whereas in the case of the polymeric flow model free access of ethylene to the active species of the catalyst was assumed. In this case a diffusion coefficient of

$3.7 \cdot 10^{-9}$ m^2/s was used. It was also tried to disintegrate the active polymer particles and see if there is any effect on polymerization rate. Unfortunately the polymerization stopped very quickly when the slurry was pumped through a colloidal mill (ultra turax) which was placed in a bypass.

Diffusion and Reaction in Porous Polymer Particle

Thiele modulus for first order reaction in a spherical and porous polymer particle with relative uniform catalyst distribution

$$\Phi = R \sqrt{\frac{k_v}{D_{eff}}}$$

$R = 40 \cdot 10^{-6}$ m (after 80 min, $N_{PE} = 1,4 \cdot 10^9$ (l^{-1}))

$$\frac{k_{v,eff}}{k_v} = \frac{3}{\Phi} \left(\frac{1}{\tanh \Phi} - \frac{1}{\Phi} \right)$$

$$k_{v,eff} = \frac{r_{eff} \, V_R}{c_E \, V_{PE}} = \frac{2,7 \cdot 10^{-3} \text{ mol/l s} \;\; 1 \text{l}}{0.256 \text{ mol/l} \;\; 0,357 \text{l}} = 2,9 \cdot 10^{-2} \, s^{-1}$$

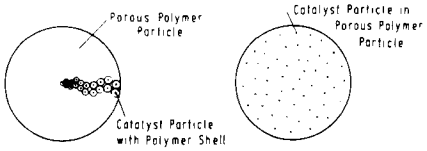

Multigrain Model	Polymeric Flow Model
$D_{eff} = \frac{1,5 \cdot 10^{-11} \; 0,6}{5}$	$D_{eff} = \frac{3,7 \cdot 10^{-9} \; 0,6}{5}$
$D_{eff} = 1,8 \cdot 10^{-12} \, m^2/s$	$D_{eff} = 4,4 \cdot 10^{-10} \, m^2/s$
$\Phi = 9,6$	$\Phi = 0,3$
$\eta = 0,3$	$\eta = 1$

Tab.5: Thiele modulus for ethylene polymerzation within porous polymer particles

Heat transfer:

Heat transfer was studied in bubble column reactors in a wide range of solid content, particle size of the solid and superficial gas velocity. The results achieved can be correlated well by a dimensionless equation given by Deckwer[8].

See table 6.

$$St = 0{,}1\,(Re\ Fr\ Pr^2)^{-0.25}$$

$St \equiv h/\rho_L\, c_{P,C}\, u_G$. $Re \equiv u_G\, d_B\, \rho_C / \eta_C$

$Fr \equiv u_G^2/g\, d_B$. $Pr \equiv c_{P,C}\, \eta_C / \lambda_C$

$\rho_C = \rho_S\, \Phi_S + \rho_L (1 - \Phi_S)$

$c_{P,C} = W_S\, c_{P,S} + W_L\, c_{P,L}$

$$\eta_C = \eta_L \left[1 + \frac{1{,}25\, \Phi_S}{(1 - \Phi_S/\Phi_{S,max})} \right]^2$$

$\Phi_{S,max} = \rho_B / \rho_S > 0.3$

$\lambda_C = \lambda_L [2\lambda_L + \lambda_S - 2\Phi_S(\lambda_L - \lambda_S)] / 2\lambda_L + \lambda_S + \Phi_S(\lambda_L - \lambda_S)$

$h = c\, \lambda_C^{0.5}\, \rho_C^{0.75}\, c_{P,C}^{0.5}\, \eta_C^{-0.25}\, u_G^{0.25}\, g^{0.25}$

$c = 0{,}12$

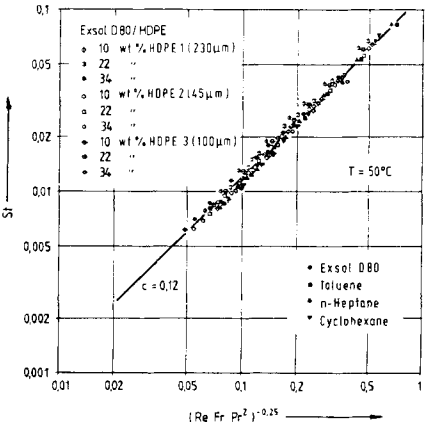

Tab.6: Dimensionless correlation for heat transfer in slurry reactors with high solid content.

For calculation of the Stanton-, Reynolds-, Froude- and Prandtl-number the physical data of the solid-liquid dispersion had to be used like density, ρ_C, heat capacity, $C_{P,C}$, dynamic viscosity, η_C, and thermal conductivity, λ_C. These data are usual mean values of the physical properties of the single phases by considering either the volume, Φ, or the weight fraction, W, of the corresponding solid and liquid phase (index S or L). d_B is the mean diameter of the gas bubbles. For maximum volume fractions of polyethylene, $\Phi_{S,max}$, larger than 0.3 the viscosity correlation of

Eilers[9] can be used to calculate the viscosity of the suspensions. The viscosity is influenced by the volume fraction of the solid phase, ϕ_S, and by the shape, the surface roughness and by the particle size distribution of the polyethylene particles. These parameters seem to be considered in the maximum volume fraction of polyethylene. From these results one can see that the heat transfer coefficient, h, is determined by the energy input ($u_G g$) and the physical data of the suspensions. The heat transfer coefficient is nearly independent of polyethylene concentration up to 20 weight percent. Above 20 weight percent it depends mainly on the viscosity of the dispersion. Small and non spherical polyethylene particles cause higher viscosities than large and uniform particles. See figure 6.

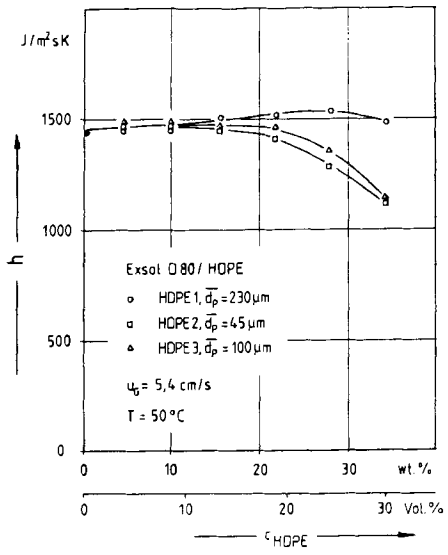

Fig.6: Influence of polyethylene concentration on heat transfer coefficient for particles of different size

Calculation for heat transfer within the polymerizing particles by Meyer[2] show that there is practically no temperature increase in the particles at normal polymerization conditions.

Molecular weight distribution:

As can be seen in figure 7 the molecular weight distribution of the polyethylene formed can be correlated well by a logarithmic normal distribution. Up to now it was not possible to derive the logarithmic dependence of the molecular weight distribution from kinetic models not even by considering mass transport influence

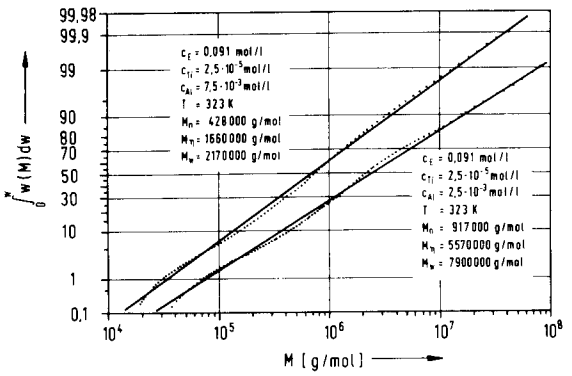

Fig.7: Molecular weight distribution of polyethylene

The molecular weight distribution is nearly constant with polymerization time at conditions studied. The polymerization was run in a stirred tank reactor at 750 revolutions per minute and a bubble column at 2 cm/s gas velocity. Data are given in figure 8.

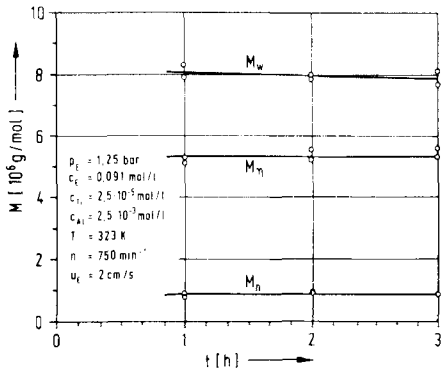

Fig.8: Molecular weights (weight, viscosity and number average) of polyethylene at different polymerization times.

It is not known in the present case if the polymer particles are still growing during the period of 3 hours. If they would grow the influence of diffusion should not play a significant role. The molecular weight distribution is influenced by the concentration of triethyl aluminium and to less extent by the concentration of hydrogen. See table 7.

From these data one has to consider chain transfer reactions with ethylene, aluminium alkyl and hydrogen. The chain transfer constants are of the following order: $K_{tr,E} = 1.4 \cdot 10^{-5}$, $K_{tr,Al} = 63 \cdot 10^{-5}$ and $K_{tr,H} = 8400\ 10^{-5}$ at 50 °C.

The number average molecular weight of polyethylene produced at 50 °C can be expressed by the correlation

$M_n = 2 \cdot 10^6 C_E / C_E + 45\ C_{Al} + 6000\ C_H$ in g/mol.

Meyer [2] developed a kinetic model for the slurry polymerization of ethylene by assuming a Langmuir-Hinshelwood mechanism.

c mol/l	M_n g/mol	M_η g/mol	M_w g/mol	M_w/M_n
c_E				
0,091	537000	2780000	3760000	7,0
0,218	1030000	5230000	7540000	7,3
0,346	1210000	6380000	8730000	7,2
$c_{Al}\,10^3$				
1,25	1130000	7160000	9580000	8,5
2,5	921000	5460000	7920000	8,6
5,0	537000	2780000	3760000	7,0
7,5	428000	1660000	2170000	5,1
c_H				
0	1210000	6390000	8730000	7,2
0,0031	37000	181000	255000	6,8
0,0063	18800	93700	124000	6,6
0,0071	17100	84000	112000	6,4

$c_{Ti} = 2{,}5 \cdot 10^{-5}$ mol/l , T = 50 °C

Tab.7: Molecular weights of polyethylene and its dependence on concentration of ethylene, C_E, triethyl aluminium, C_{Al}, and hydrogen, C_H

This leads to the following relation of the rate constant, k_V, and the concentrations of aluminium alkyl, C_{Al}, and hydrogen, C_H:

$$k_V \sim \frac{C_{Al}}{(1 + K_{Al}\, C_{Al} + K_H\, C_H)^2}$$

K_{Al} and K_H are the adsorption constants of aluminium alkyl and hydrogen. The adsorption of ethylene was neglected. Since k_V is proportional to the square root of the Thiele modulus the concentration of these chemicals may have an influence on porous diffusion. By increasing the concentration of aluminium triethyl or of hydrogen the rate constant will decrease and hereby the Thiele modulus also. This will lead to a more narrow molecular weight distribution if mass transfer is dominant. This of course does not exclude the model of multiplicity of active sites and its effect on molecular weight distribution. Even a combination of both models (diffusion

limitation and multiplicity of sites) is to be considered as has been done by Galvan and Tirell[10].

REFERENCE

1. R. Michael, Ph. D thesis, Technische Universitaet Berlin, 1984.
2. H. Meyer, Ph. D thesis, Technische Universitaet Berlin, 1983.
3. C.N. Satterfield, "Mass Transfer in Heterogeneous Catalysis", The Massachusetts Institute of Technology, 1977.
4. A. Mersmann, Chem.-Ing.-Tech., 49, 9, 679 (1977).
5. P. Sänger, W.-D. Deckwer, Chem.Eng.J. 22, 179 (1981).
6. C.R. Wilke, P. Chang, AIChE-J., 1, 2, 264 (1955).
7. A.S. Michaels, H.J. Bixter, J. Polym. Sci., 50, 413 (1961).
8. W.-D. Deckwer, Chem. Eng. Sci., 35, 1341 (1980).
9. H. Eilers, Kolloid - Z, 97, 3, 313 (1941).
10. R. Galvan, M. Tirell, private communication, paper submitted to Chem. Eng. Sci..

APPROACHES TO THE PROBLEM OF TACTICITY DETERMINATION IN POLYPROPYLENE

DAVID R. BURFIELD and PATRICK S.T. LOI

Department of Chemistry, University of Malaya,
Kuala Lumpur 22-11, MALAYSIA.

ABSTRACT

The determination of polypropylene isotacticity is still of importance today in the evaluation of commercial catalysts and in the search for detailed mechanistic understanding of the stereoregulating process. Whereas, methods based on NMR measurements provide the most definitive information secondary techniques which are simpler and faster to carry out still provide valuable information. This paper reviews the methods for tacticity determination based on solvent extraction, IR and recently proposed calorimetric techniques. The advantages and limitations of the methods are discussed. Some recent experimental results pertaining to the calibration of the IR method and to various aspects of the calorimetric measurements will also be presented.

INTRODUCTION

One of the fascinating features of polypropylene is the possibility of stereoisomer formation. Thus Natta[1,2] distinguished three possible stereoisomeric sequences resulting from the intrinsic asymmetric nature of the tertiary carbon atom in the propylene repeating unit. Sequences of monomer units of uniform configuration were termed *isotactic*, whereas sequences of alternating configuration were known as *syndiotactic* and random arrangements were designated *atactic*.

However, it was swiftly realised that although catalysts were available which could produce predominantly isotactic or syndiotactic polymers the *as-polymerized* samples were rarely

stereochemically pure and consisted of mixtures of isotactic (or, syndiotactic), stereoblock and atactic macromolecules. These fractions were initially separated by procedures based on solvent extraction and characterized on the basis of their X-Ray diffraction patterns[2]. The fundamental distinction between the different tacticities centres on their relative facility in crystallization. Thus isotactic polypropylene crystallizes readily, whereas, the atactic samples are obtained as amorphous materials.

As a consequence, effectively all of the early characterization methods were based on the measurement of parameters related to the crystallinity of the material and only indirectly related to the actual tacticity. Such parameters include solubility, IR absorbance, density, melting point, and X-Ray diffraction. Experimental methods employing these techniques have been briefly reviewed elsewhere[3].

NMR studies of polypropylene revolutionised the determination of tacticity when it was realised that the relative steric configuration of neighbouring units affected the chemical shifts of both proton and carbon atoms in the propylene repeating unit. It now became possible to quantitatively determine stereo-sequences within the polymer chain. For purpose of quantitative analysis it was necessary to introduce a nomenclature to specify two distinct arrangements known as *diads*[4]. An isotactic diad (symbol m) represented the situation where the neighbouring unit has the same stereochemistry as the specified unit, whereas, a syndiotactic diad (symbol r) represents a neighbouring unit of opposite configuration. Rapid developments in high field proton NMR and subsequently ^{13}C-NMR permitted the distinction of longer stereosequences as first triad, then pentad and subsequently heptad sequences became resolved. The nomenclature for these longer sequences are based on the diad definition, for example, for sequences of three repeat units, three distinct triads may be specified: isotactic (mm), syndiotactic (rr) and hetereotactic (mr) where the symbols refer to the configuration of the neighbouring units relative to the specified unit. Analogous designations are used for longer sequences. These developments have been

reviewed in a general way by a number of authors[5-7].

Elucidation of the tacticity of polypropylene samples is important from two viewpoints. Firstly, detailed structural information is increasingly becoming an important tool for understanding mechanisms of chain growth and the stereo-regulating abilities of catalyst systems. Secondly, since only the isotactic material is of commercial significance, the determination of tacticity is of crucial importance in evaluation of catalyst efficiency with respect to the formation of the isotactic product. This latter aspect is of particular relevance today, amidst the search for catalysts of ever higher activity.

Whereas, unquestionably the NMR method provides the most rigorous and fundamental evaluation of polymer tacticity yet the technique is specialised, time-consuming and requires expensive instrumentation. Consequently, secondary methods employing relatively simple and rapid evaluation techniques are still widely used and continue to make an important contribution to propylene polymerization studies. It is the purpose of this paper to discuss some of these secondary methods and to present some recent results which have some bearing on the usefulness of these techniques *vis à vis* the NMR characterization techniques.

EXPERIMENTAL

Polypropylene samples of varying stereoregularity and molecular weight were prepared by the use of a variety of conventional and supported catalysts in the presence or absence of transfer agents, as reported earlier[8,9].

NMR stereoregularities of the samples were determined by courtesy of Dr. Y.Doi by the techniques previously described[8].

Samples were prepared for IR examination by hot pressing a 50 mg sample between aluminium foil at 200°C, for approximately 5s. The pressure was then immediately released and the film allowed to cool to ambient temperatures. Samples were examined as soon as possible after pressing as small changes in the IR spectrum were found to occur for a period of several days, due to the effect of room temperature annealing. Polymer samples were annealed at elevated temperatures by heating the film, encased in aluminium foil, in an evacuated glass tube which

was thermostatted in an oil bath. The samples were annealed at a temperature approximately 5-10 K below the melting point as previously determined by a DSC scan. After annealing for 3 hours the sample was then allowed to cool slowly in the oil bath over a period of about 2 hours, whilst maintaining a high vacuum environment. Samples of very low isotacticity which did not form a coherent film were examined and annealed after casting onto a NaCl disk. IR spectra were run on a Perkin-Elmer Model 1330 spectrometer operated at a scan time of 12 min. Films were sandwiched between NaCl discs for examination. The orientation and position of the film did not significantly affect the results but significant differences were observed when comparing alternative instrumentation. The following baselines were used in evaluating various absorbance values: A_{840} - (910 cm^{-1} to 760 cm^{-1}), A_{970} and A_{995} - (1060 cm^{-1} to 910 cm^{-1}), A_{1160} - (1180 cm^{-1} to 910 cm^{-1}).

Solvent extraction of the PP samples was carried out with n-heptane, under nitrogen, for a period of 6 hours in a conventional soxhlet extractor. Residues were dried to constant weight under vacuum, whereas, heptane solubles were recovered by concentration followed by methanol precipitation.

Calorimetric examination of the PP samples was carried out with a Perkin-Elmer DSC-2C instrument, on polymer samples (c.a., 5 mg) encapsulated in standard aluminium pans. Details of the instrument calibration and experimental procedures have been described earlier[10]. All measurement runs were conducted at a scan rate of 20 K/min. Samples were held at 470 K for 5 minutes before conducting a cooling run.

RESULTS and DISCUSSION

Characterization of PP Tacticity by Solvent Extraction

The differential solubility of isotactic and atactic material proved to be of inestimable importance in the initial characterization of these polymers. Natta and co-workers[11] subsequently postulated an isotactic index which was equivalent to the percentage of a given sample insoluble in boiling n-heptane. This index is still widely utilised in evaluation of PP stereoregularity. Subsequently, a more detailed correlation

between isotacticity and solubility in various solvents was published[12] and this is reproduced below.

Table 1. Data of Natta[12] relating solvent fractionation to stereoregularity

Insoluble in	Soluble in	% Crystallinity	MPt. °C	% Irregularity
ether	n-pentane	15-27	106-114	26.1-29.5
n-pentane	n-hexane	25-37	110-135	17.3-27.8
n-hexane	n-heptane	41-54	147-159	17.2-12.2
n-heptane	2-ethylhexane	52-64	158-170	2.5- 3.4
2-ethylhexane	n-octane	60-66	174-175	0.4- 0.8
n-octane	-	64-68	174-175	0.4- 0.8
trichloroethylene	-	75-85	176	0

The validity of this method was evaluated by Quynn *et al*[13] in comparison with alternative methods for determining PP crystallinity, e.g., by density and IR methods. It was shown that whereas, the IR and density methods provide a consistent measurement of crystallinity, as judged by X-Ray diffraction measurements, the heptane insolubility index was somewhat dependent on the molecular weight of the sample and did not give a reliable guide of crystallinity.

Subsequently, in seeking to refute conclusions as to the effect of the nature of the base metal-alkyl on the stereospecificity of the catalyst, Firsov *et al*[14] showed that the isotacticity index based on solvent extraction did not correlate well with IR and X-Ray measurements. In particular their work showed that the extent of extraction was dependent on molecular weight as well as stereospecificity.

Recently, during the course of the synthesis of low molecular weight polypropylene samples[9] we have confirmed the validity of the above criticism by comparison of the stereoregularity of samples through solvent extraction and ^{13}C-NMR measurements (Table 2).

Table 2. Comparison of polypropylene stereoregularity from ^{13}C-NMR and solvent extraction measurements.

Sample[a]	[$ZnEt_2$][b] mmol/l	$\overline{Mn}_T$[c] x 10^{-4}	Isotactic[d] Index	(mm)[e]
5 Whole	0	30.2	71.4	0.79
HI		44.8		0.89
S		14.8		0.39
11 Whole	400	1.26	21.7	0.83
HI		11.3		1.00
S		0.84		0.77
6 Whole	600	0.91	28.0	0.87
HI		10.9		0.98
S		0.8		0.83

a - Whole sample, HI - Heptane insoluble, S - Heptane soluble; b - $TiCl_3$.Type 1.1/$AliBu_3$ catalyst; c - $\overline{Mn}$ as measured by tritium tracer technique[9]; d - % insoluble in boiling n-heptane; e - triad isotacticity by NMR.

It is clear from this table that for low molecular weight polymers the isotactic index as deduced by solvent extraction does not give meaningful results. Thus, whereas the isotacticity of the samples in the presence of high concentrations of transfer agent appears to be reduced from 71% to about 30%, the NMR measurements show that in fact the overall stereoregularity of the samples increase from about 79% to 87%. This is presumably associated with the deactivation of the less stereospecific, more exposed sites by interaction with the transfer agent. Examination of the molecular weights of the insoluble and soluble fractions show clearly that the latter are very much lower than the former and that this effect is accentuated as the overall molecular weight of the sample is reduced. It might be supposed that the molecular weight of the atactic polymers are intrinsically lower than the isotactic fraction.

This suggestion is not unreasonable since sites producing atactic polymer are probably more open to chain transfer with metal alkyl. However, it is plain from the results cited in the table that for low molecular weight samples the soluble fraction is quite stereoregular (mm = 0.77-0.83). This clearly shows that the solubility in boiling heptane is dependent not only on stereoregularity but also on molecular weight.

Admittedly the above data are drawn from an extreme case with low molecular weight polypropylene. A comparison of the heptane insolubles versus NMR stereospecificity taken from recent results[15] shows a better correlation (Table 3). In this case the isotactic index as determined by solvent

Table 3. Comparison of solvent extraction versus NMR tacticity from the data of Martuscelli *et al*[15]

Sample Code	Isotacticity Index		$\overline{Mn}$ x 10^{-4}	Crystallinity by X-Ray (%)
	% Heptane Insolubles	^{13}C-NMR		
LY-97.5	97.5	0.956	5.5	64
HY-97.5	97.5	0.953	5.8	68
HY-96	96.0	0.949	-	68
HY-90	90.0	0.879	-	57
VHY-97.5	97.5	0.953	7.2	65

extraction agrees within about 2% that determined from NMR. It is apparent therefore, that for high molecular weight highly isotactic material the solvent extraction method gives a good indication of isotacticity. This is perhaps not altogether surprising since pure isotactic polypropylene will be highly crystalline and as such not significantly soluble in boiling n-heptane which has a boiling point (98.4^{o}C) which is lower than the melting point of the isotactic material. Thus the top point of the isotacticity index is likely to be coincident by extraction and NMR methods. However, even in the absence of molecular weight effects the two measurements are likely to diverge increasingly as the true isotacticity

decreases. This follows since the solubility in n-heptane is actually a function of crystallinity and this parameter is not directly proportional to isotacticity as is discussed subsequently in this paper. It should be borne in mind too, that the effect of hot solvent extraction is not only to remove less isotactic material but also to anneal the residue, and thus increase the crystallinity of that material.

In summary, solvent extraction is a useful semi-quantitative technique which is capable of ranking samples in order of isotacticity providing that the molecular weights of the samples are comparable.

Stereoregularity Determination by IR Measurements

Next to solvent extraction techniques, methods based on IR measurement have proved the most widely used in determination of polypropylene isotacticity. This is probably a consequence of the ready availability of the instrumentation and ease and simplicity of sample preparation and measurement.

Whereas, the IR spectrum of isotactic polypropylene was first reported by Natta and coworkers[16,17], the first quantitative study seeking to relate isotacticity with IR absorption intensity was published by Luongo[18]. The results of this study are still widely quoted today. Luongo showed that the ratio of absorbances at 995 and 974 cm^{-1} was a function of the isotacticity of the sample. The absorbance at 995 cm^{-1} which is intense in highly isotactic material was attributed to a crystallinity band since it disappeared on heating the sample at 180°C - above the melting point of the isotactic polypropylene. Luongo established a calibration curve relating the absorbance ratio to isotactic content by using physical mixtures of supposedly completely isotactic and atactic material.

A review at that time[19] pointed out the limitation, that since the IR isotactic index was a function of crystallinity, the measurement would be dependent on the thermal history of the sample. Brader[20] sought to circumvent this problem by annealing samples for 15 min at 160°C in a carbowax bath, but in so doing introduced further errors through air oxidation of the unprotected samples. It was also shown[21,22] that the

intense band observed at 995 cm^{-1} as well as those at 1170 and 841 cm^{-1} in the spectrum of isotactic polypropylene are due to the conformation of the polymer chain rather than crystallinity *per se*. Subsequently, Hughes[22] sought to overcome the problems associated with the earlier methods by subjecting the polypropylene films to a 3 hour annealing at 165°C under argon. Utilising this method samples could be given a uniform thermal history, whereby, supposedly all the isotactic material could be converted to helices. Again, as with Luongo's original method a standard calibration curve was constructed using samples of apparently isotactic and atactic nature. Other indices have been proposed for measurement of isotacticity (or, crystallinity) based on the absorptions at 841 cm^{-1}[24,25] and 1220 cm^{-1}[26].

The most extensive studies relating to IR characterization of isotacticity have been carried out by Kissin and co-workers and much of this work has been summarised[27-29]. An important aspect of this work is the observation that the appearance of the various isotactic helix bands is dependent on the length of the isotactic sequences. Thus the critical sequence lengths for appearance of these bands are: 973 cm^{-1} (5 units), 998 cm^{-1} (11-12 units), 841 cm^{-1} (13-15 units) respectively. On the basis of this observation three indices of isotacticity were proposed based on the following absorbance ratios: A_{973}/A_{1460} (known as the spectral degree of isotacticity (α)); A_{998}/A_{973} (known as the macrotacticity M); and, A_{841}/A_{973}.

At this point it is perhaps worth pointing out that there seems to be some confusion between authors as to the significance of the absorbance at 973 cm^{-1}, which is observable[18,22] in the melt of isotactic samples as well as in purely atactic material[18,22] and has been attributed[22] to the chemical structure of head-to-tail sequence of propylene units. On this basis the band has been used as an internal reference for comparison with bands characteristic of isotacticity. On the other hand, Kissin *et al*[27] largely attribute this absorption to short isotactic helices which are still present in the melt and to some extent in atactic samples, and as such can be used as a measure of isotacticity in comparison with a reference

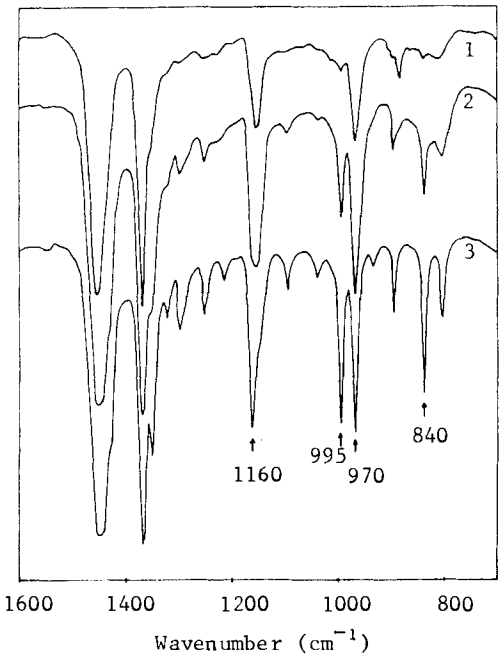

Figure 1. IR Spectra of polypropylene samples of varying tacticity showing bands used for calibration curves. (1 - mm = 0.35; 2 - mm = 0.58; 3 - mm = 1.00)

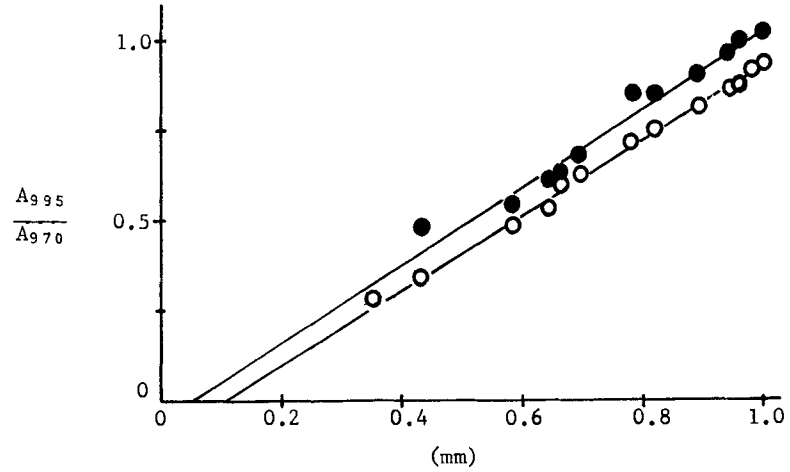

Figure 2. Calibration curve for IR absorbance ratio A_{995}/A_{970} versus NMR triad isotacticity. (● - Annealed; o - Hot pressed only)

band such as the absorbance at 1460 cm^{-1}. However, at the same time the absorption at 973 cm^{-1} is also used by them as a reference band in the other absorption ratios.

The use of the ratio A_{973}/A_{1460} is complicated by an overlapping syndiotactic absorption band at low isotacticity and by reduced sensitivity at the high isotacticity end of the scale. Insensitivity to state of aggregation and hence thermal history of the sample is the claimed advantage[27].

Owing to the uncertainty in the nature of the reference bands and in the linearity of the absorption coefficient of helix bands on isotacticity, as well as complications introduced by thermal history effects, the IR method must be regarded as essentially empirical. Unfortunately, the only calibrations available from the literature are derived on the basis of samples of nominal isotacticity. We have undertaken to establish IR calibration curves based on polypropylene samples whose stereostructure has been determined by ^{13}C-NMR. Figure 1 shows the IR spectra in the region 1600 -700 cm^{-1} for samples of varying isotacticity.

Several absorption ratios have been evaluated as measures of isotacticity in particular: A_{840}/A_{970}; A_{995}/A_{970}; A_{840}/A_{1160}; and A_{995}/A_{1160}. This corresponds to the use of the absorbances at 840 and 995 cm^{-1} as a measure of isotacticity with respect to internal reference bands of 970 and 1160 cm^{-1}. The ratio A_{970}/A_{1460} was not evaluated as the absorbance at 1460 cm^{-1} was generally too intense for precise determination. All four indices provide useable calibration curves (Figures 2-5) but the ratios A_{840}/A_{970} and A_{995}/A_{970} are to be preferred because of reduced scatter and the linearity of the calibrations. High temperature annealing of the polymer samples gives rise to a shift in the position of the calibration curves to a higher absorbance ratio but does not otherwise affect the shape of the curves. In the opinion of the authors there is in fact little to be gained by the added annealing step provided that standardised conditions are used for hot pressing the film, since this process effectively erases the previously thermal history of the sample. (It was noticed that slow annealing processes do occur in the pressed film, as evidenced by

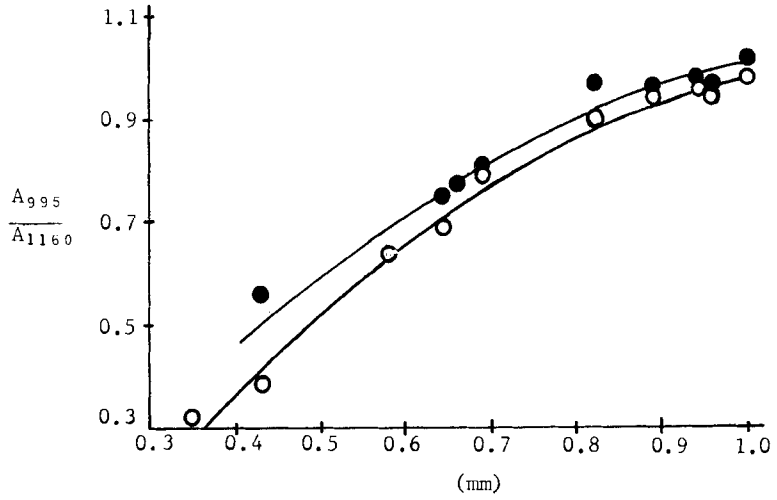

Figure 3. Calibration curve for IR absorbance ratio A_{995}/A_{1160} versus NMR triad isotacticity.

(●- Annealed; o - Hot pressed only)

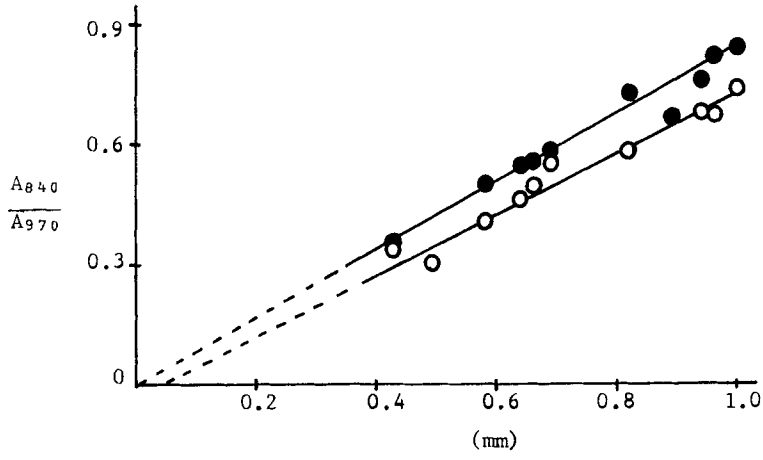

Figure 4. Calibration curve for IR absorbance ratio A_{840}/A_{970} versus NMR triad isotacticity.

(● - Annealed; o - Hot pressed only)

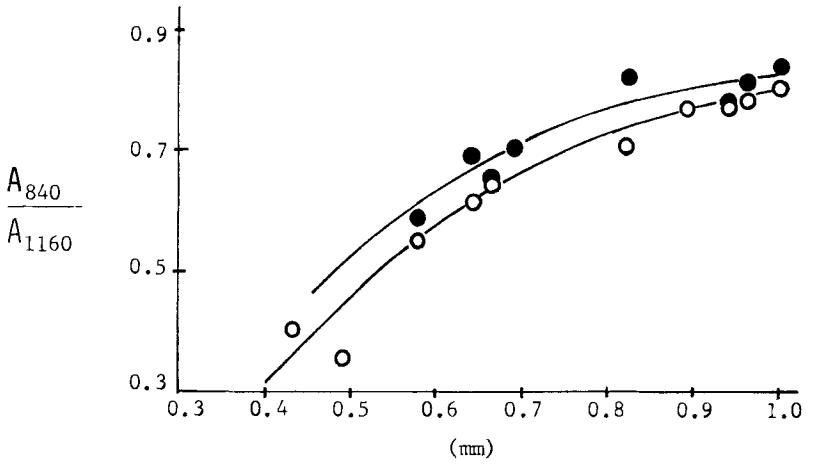

Figure 5. Calibration curve for IR absorbance ratio A_{840}/A_{1160} versus NMR triad isotacticity (● - Annealed; o - Hot pressed only)

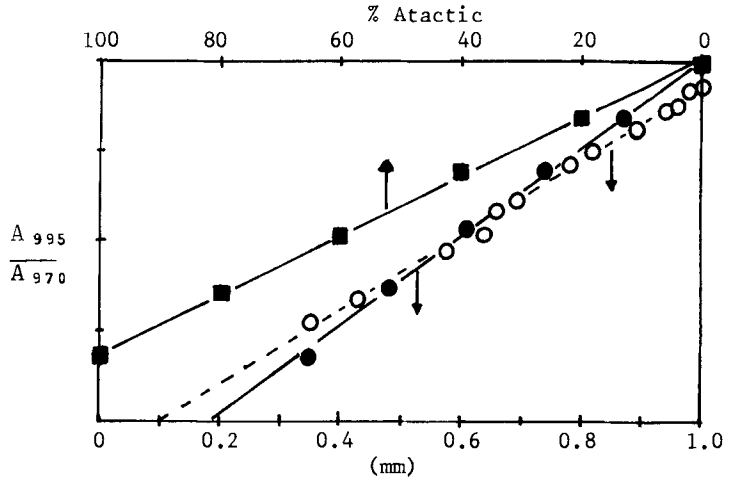

Figure 6. Comparison of literature calibration curve with current results.
(■ - Original data of Luongo[18];
● - Luongo data recalculated using mm = 0.35 and mm = 1.00 for the atactic and isotactic polymer;
o - Results from this work.)

changes in absorption ratio over a period of several days. Consequently all unannealed samples were run within 1-2 hours of pressing.)

Comparison of the present results with Luongo's original calibration is shown in Figure 6. It is quite clear that the % isotacticity determined by Luongo does not correspond well with the triad isotacticity as determined by NMR. However, if a isotacticity of mm = 0.35 is assigned to the atactic sample used by Luongo, then the calculated curve shows a reasonable correlation.

In summary, the IR technique proves to be a simple and rapid method for determination of isotacticity and the values deduced therefrom can be correlated with NMR triad isotacticities. Little advantage is gained in reproducibility or accuracy by annealing procedures.

Isotacticity from Calorimetric Measurements

As has already been observed, the secondary methods available for determination of polypropylene isotacticity are largely dependent on the different crystallization behaviour of the various tactic configurations. Thus highly isotactic material undergoes facile and extensive crystallization leading to high density[13], insolubility in hot heptane and characteristic IR spectra and X-Ray diffraction patterns[30,31]. Calorimetric studies afford an alternative method of probing the crystallinity of the polymers in relation to melting point or enthalpy of fusion. Early calorimetric methods[12,32,33] were mainly concerned with attempting to relate the melting point of the polymer to isotacticity. A clear trend is discernable (Table 1) as the melting point increases in step with isotacticity. However, the correlation for unfractionated samples is poor[33] and in any case the melting point is affected by thermal pretreatment. Using an alternative approach Tolchinskii *et al*[34] were able to establish a relationship between the area of the melting peak and the % amorphous (atactic) content. The drawback of this approach is that the melting curve is very broad, and consequently the precise area is difficult to define and is in any case very dependent on

the previous thermal history of the sample.

Recently[10], we have shown that an alternative calorimetric approach to measurement of isotacticity, is to monitor the crystallization behaviour of the polymer. This has two significant advantages over studies of the fusion process. Firstly, the thermal history is erased by high temperature treatment and secondly the crystallization temperature range in a dynamic cooling run is much narrower and more reproducible than in an analogous heating cycle. In particular, the onset temperature of crystallization (T_c) is highly reproducible and has been shown to be related to the isotacticity of the sample. Thus, by using fractionated polymer samples of known isotacticity, an empirical calibration has been established[10]. More recently[35], by extending our studies to a wider range of samples we have observed that polymers produced by supported catalysts show slight differences in crystallization behaviour from those prepared by conventional catalyst systems and this is illustrated in Figure 7. In simultaneous and detailed isothermal crystallization studies Martuscelli *et al*[15,36] have confirmed the dependence of the crystallization behaviour on the stereoregularity of the polymer chain and have shown that the overall rate of crystallization, at a given temperature, decreases with increase in stereochemical defects. From their studies it is apparent that the crystallization behaviour is dependent on the distribution as well as the number of stereochemical defects and this may explain the differences observed in Figure 7.

One drawback of employing the crystallization onset temperature as a measure of isotacticity is that it is only appropriate for samples that are fairly homogeneous in stereostructure such as the residue and soluble fraction from hot heptane extraction. This is illustrated in the table given below: The crystallization temperature of the whole sample (387.3 K) corresponds to an NMR triad isotacticity of about 0.94 according to the calibration curve (Figure 7). This is very far different from the calculated NMR value of 0.84 and shows that in the case of a mixture of polymers of grossly different stereoregularity the observed crystallization onset

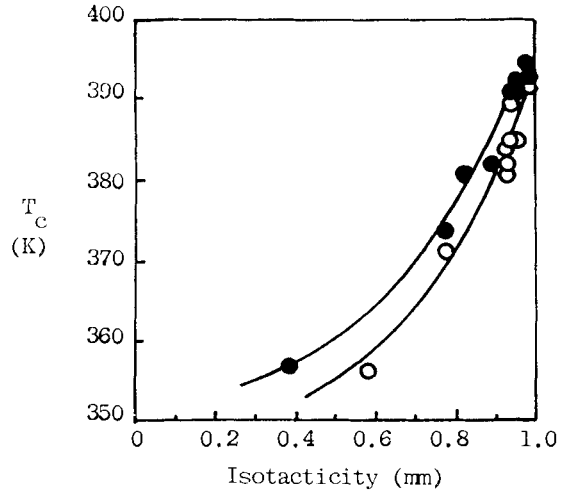

Figure 7. Correlation of crystallization onset temperature with isotacticity.
● - Conventional; o - Supported catalyst.

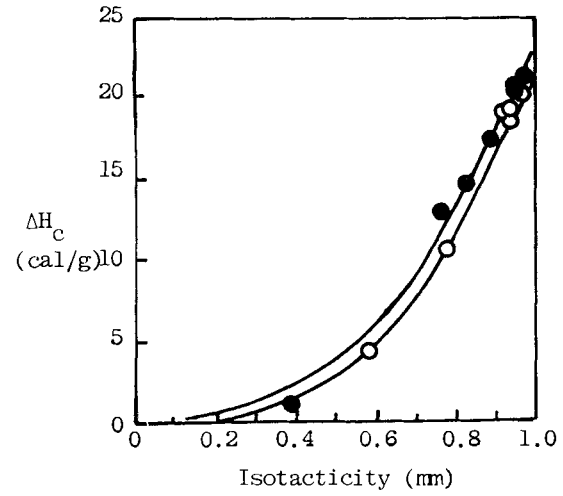

Figure 8. Correlation of enthalpy of crystallization with isotacticity.
● - Conventional; o - Supported catalyst

Table 4. Comparison of Crystallization Parameters for Whole and Fractionated Sample.

Sample	Tc (K)	H_c (cal/g)	mm (NMR)
Whole Sample	387.3	-17.1	(0.84)*
Heptane Insoluble (32%)	393.6	-23.5	1.00
Heptane Soluble (68%)	375.1	-13.5	0.77

* Calculated from weight fractions of insoluble and soluble fractions.

temperature is more representative of the fraction of higher stereoregularity.

However, in this case, much better agreement is observed from measurements of the enthalpy of fusion, which are found to be approximately additive. Thus calculation of the enthalpy of crystallization of the whole sample from the relationship:

$$\Delta H_{c_{Whole}} = W_{INSOL} \cdot \Delta H_{c_{INSOL}} + W_{SOL} \cdot \Delta H_{c_{SOL}}$$

where, W_{INSOL} and W_{SOL} represent the weight fractions of the insoluble and soluble fractions respectively, leads to a value of $\Delta H_{c_{Whole}} = -16.7$ cal/g. This is close to the experimentally observed value for the whole fraction of -17.1 cal/g.

Correlation of the enthalpy of crystallization with isotacticity (Figure 8) leads to an alternative method of tacticity determination by DSC measurement. This method has certain advantages in that: (i) there is little difference in behaviour of polymers from varying catalyst types; (ii) both whole and fractionated samples may be accommodated; and (iii) the enthalpy of crystallization may be measured more accurately than the onset temperature, with samples of low isotacticity.

Recently[37], in DSC studies of ethylene-propylene copolymers we have shown that the enthalpy of crystallization of the ethylene segments is proportional to the probability of forming

ethylene run sequences of a certain minimum length. Similar relationships are apparent in the present studies. Thus if it is assumed that: (i) only isotactic segments contribute to the observed crystallization exotherm; (ii) a minimum sequence length is required for crystallization; and (iii) the stereo-defects are incorporated in a random fashion then the following relationship should hold:

$$\Delta H_c = kP_{iso}^{n}$$

where, ΔH_c is the observed enthalpy of crystallization, k a constant, P_{iso} the fraction of isotactic units and n the critical sequence length for crystallization to occur. This relationship may be tested in the form:

$$\log(\Delta H_c) = \log k + \frac{n}{3} \log (mm)$$

where (mm) is the triad isotacticity. Figure 9 illustrates such a plot which has a slope of 2.69. This corresponds to a

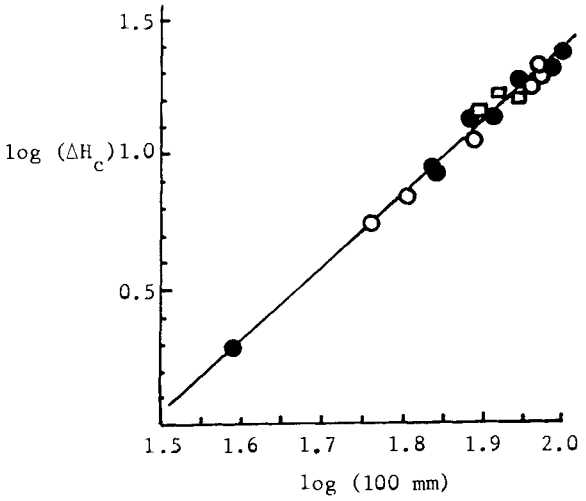

Figure 9. Relationship of enthalpy of crystallization to NMR triad isotacticity.

□ - Whole sample

● - Conventional catalyst, fractionated sample

o - Supported catalyst, fractionated sample

critical sequence run of n = 8 isotactic units. Interestingly, all samples including fractionated and whole polymers appear to fall on the same line and consequently this could be a useful calibration for relating isotacticity to enthalpy of crystallization.

In summary, whereas measurement of enthalpy of fusion and melting point appear to be of limited value in determining polymer stereoregularity, methods based on polymer crystallization are promising. In particular the enthalpy of crystallization may be directly related to the triad isotacticity of the polymer. Calorimetric methods are advantageous in only requiring small samples and being rapid in measurement. Further work is in hand to establish the reliability of these methods.

REFERENCES

1. G. Natta, J. Polym. Sci., 16, 143 (1955).
2. G. Natta and F. Danusso, J. Polym. Sci., 34, 3 (1959).
3. J. Boor, Jr., "Ziegler-Natta Catalysts and Polymerizations", Academic Press, New York, 1979, Chapter 3.
4. H.L. Frisch, C.L. Mallows and F.A. Bovey, J. Chem. Phys., 45, 1505 (1966).
5. J.C. Randall, "Polymer Sequence Determination", Academic Press, New York, 1977.
6. J.L. Koenig, "Chemical Microstructure of Polymer Chains". Wiley-Interscience, New York, 1980.
7. H.J. Harwood, "NMR Analysis of Stereoregular Homopolymers" in "Preparation and Properties of Stereoregular Polymers", R.W. Lenz and F. Ciardelli, Eds., D. Riedel, Boston, 1980.
8. D.R. Burfield and Y. Doi, Macromolecules, 16, 702 (1983).
9. D.R. Burfield, Polymer, 25, 1817 (1984).
10. D.R. Burfield and Y. Doi, Polymer Commun., 24, 48 (1983).
11. G. Natta, G. Mazzanti, G. Crespi and G. Moraglio, Chim. Ind., 39, 275 (1957).
12. G. Natta, J. Polym. Sci., 34, 531 (1959).
13. R.G. Quynn, J.L. Riley, D.A. Young and H.D. Noether, J. Appl. Polym. Sci., 2, 166 (1959).

14. A.P. Firsov, B.N. Kashprov, Yu. V. Kissin and N.M. Chirkov, J. Polym. Sci., 62, S104 (1962).
15. E. Martuscelli, M. Avella, A.L. Segre, E. Rossi, G. Di Drusco, P. Galli and T. Simonazzi, Polymer, 26, 259 (1985).
16. G. Natta, P. Pino, F. Danusso, G. Mazzanti, E. Mantica, and G. Moraglio, J. Am. Chem. Soc., 77, 1708 (1955).
17. G. Natta, Makromol. Chem., 16, 213 (1955).
18. J.P. Luongo, J. Appl. Polym. Sci., 3, 302 (1960).
19. S. Krimm, Advan. Polym. Sci., 2, 51 (1960).
20. J. Brader, J. Appl. Polym. Sci., 3, 370 (1960).
21. G. Zerbi, F. Ciampelli and V. Zamboni, J. Polym. Sci., Part C, 7, 141 (1964).
22. H. Tadokoro, M. Kobayashi, M. Ukita, K. Yasufuku, S. Murahashi, T. Torii, J. Chem. Phys., 42, 1432 (1965).
23. R. H. Hughes, J. Appl. Polym. Sci., 13, 417 (1969).
24. J.P. Sibilia and R.C. Winckelhofer, J. Appl. Polym. Sci., 6, S56, (1962).
25. W. Heinen, J. Polym. Sci., 38, 545 (1959).
26. P.J. Samuels, J. Polym. Sci., Part A, 3, 1741 (1965).
27. Yu. V. Kissin, V.I. Tsvetkova and N.M. Chirkov, Eur. Polym. J., 8, 529 (1972).
28. Yu. V. Kissin, Advan. Polym. Sci., 15, 92 (1975).
29. Yu. V. Kissin and L.A. Rishina, Eur. Polym. J., 12, 757 (1976).
30. G. Natta, Makromol. Chem., 35, 94 (1960).
31. J.D. Stroupe and R.E. Hughes, J. Am. Chem. Soc., 80, 2341 (1958).
32. B. Coleman, J. Polym. Sci., 31, 155 (1958).
33. R.L. Miller, J. Polym. Sci., 47, 975 (1960).
34. I.M. Tolchinskii, N.A. Nechiltailo, A.V. Topchiev, Plast. Mass., 7, 3 (1960).
35. D.R. Burfield, Y. Doi, J. Mejzlik, Preprints, Polymer 85 I.U.P.A.C. International Symposium on Characterisation and Analysis of Polymers, Melbourne, 1985 p.21.
36. E. Martuscelli, M. Pracella and L. Crispino, Polymer, 24, 693 (1983).
37. S.N. Gan, D.R. Burfield and K. Soga, Macromolecules (In Press).

A STUDY ON THE STATES OF ETHYLBENZOATE AND $TICL_4$ IN $MGCL_2$-SUPPORTED CATALYSTS BY THERMAL ANALYSIS

M. TERANO and T. KATAOKA
Toho Titanium Company, Chigasaki 3-3-5, Chigasaki-shi, 253 Japan
and T. KEII
Numazu College of Technology, Ooka 3600, Numazu-shi, 410 Japan

ABSTRACT

The method of thermal gravity-differential thermal analysis (TG-DTA), in combination with other methods such as IR and XD, was applied to study $MgCl_2$-supported Ziegler catalysts. Two types of supported catalysts $MgCl_2/TiCl_4$/Ethylbenzoate (EB), developed by Montedison and Mitsui Petrochemical, were studied.

Comparing the TG-DTA curves obtained with various mixtures of $MgCl_2$, $TiCl_4$, EB and $TiCl_4$·EB complex as well as the catalysts themselves, no interaction between $TiCl_4$ and EB in the $MgCl_2$ matrix of the two catalysts is suggested.

INTRODUCTION

Since the discovery of Natta, [1] $TiCl_3$ catalyst has been used traditionally in the polypropylene industry. New commercial catalysts, highly active $MgCl_2$-supported catalysts, were successfully developed by Montedison [2] and Mitsui Petrochemical, [3] though $MgCl_2$-supported catalyst was proposed earlier for ethylene polymerization.[4]

Many types of supported catalysts have now been proposed and the earliest catalysts noted above which are based on $MgCl_2/TiCl_4$·EB or $MgCl_2$/EB/$TiCl_4$ have been widely studied [5-12] and features of their activities are established.

However, the active structure of the catalyst itself as well as the mechanism of active species formation still remain unclear. That is, the states of $TiCl_4$, EB or $TiCl_4$·EB complex in the catalysts are not yet established.

The irreversible complexation of EB with $TiCl_4$ and the stability of $TiCl_4$·EB complex at room temperature strongly suggest the existence

of an $TiCl_4$·EB complex in the catalyst. However, this suggestion is in contradiction with the fact that washing of the catalyst with heptane results in lowering of Ti content.

At any rate, it is important to know the states of the catalyst components in connection with the discussion of polymerization centers. In this situation we propose here the application of a method of thermal analysis for elucidating the states of the catalyst components.

EXPERIMENTAL

Reagents. Pure heptane (from Toa Oil Co., Ltd.) and extra pure EB (from Kanto Chemical Co., Ltd.) were used after being dried by using the molecular sieve 4-A. Unhydrous $MgCl_2$ (from Toho Titanium Co., Ltd., S.A. : 11 m^2/g) and $TiCl_4$ (from Toho Titanium Co., Ltd.) were used without further purification.

Preparation. $TiCl_4$·EB complex: In a 200 ml glass flask were placed 80 ml of heptane and 0.10 mol of EB at 40°C under nitrogen followed by adding 0.10 mol of $TiCl_4$ dropwise and reacted with stirring at 40°C for 1 h. The yellowish solid product was then separated by filtration, washed with heptane and dried in a vacuum. The molar ratio of $TiCl_4$/EB in the resulting complex was 1.09.

Grinding: 315 mmol (30 g) of $MgCl_2$ with 11 m^2/g and, when necessary 45 mmol of each compound as placed in a 1 l stainless steel vibration mill pot with 50 balls (25mm) under nitrogen and vibrated for 30 h at r.t..

cat-A: 315 mmol of $MgCl_2$ and 15.4 g (45 mmol) of $TiCl_4$·EB complex were coground as described above.

cat-B: 6.1 g of the coground product of $MgCl_2$ and EB were treated in a 500 ml flask with 200 ml of $TiCl_4$ at 90°C for 2 h with stirring under nitrogen, followed by washing with heptane and dried in a vacuum.

Measurements. IR spectroscopy: IR spectra were recorded on a Hitachi 270-30 spectrometer with 2.5 mm KBr pellet containing each sample.

TG-DTA: The measurements were conducted on a Rigaku Thermoflex 8100 under nitrogen at a heating rate of 17 °C/min using α-Al_2O_3 as a reference substance.

XD: X-ray analysis was carried out in a special cell with a poly (ethylene terephthalate) film window on a Rigaku CN-2155D2

diffractometer with monochromatic copper radiation.

RESULTS AND DISCUSSION

1. Basic aspects of the interactions between every two components

The interactions between every two components were studied to obtain basic information about the $MgCl_2$-supported catalysts.

$TiCl_4$ and EB form an equimolar complex described under EXPERIMENTAL. Fig. 1 shows IR spectra of (1) EB and (2) $TiCl_4$·EB complex. The C=0 band is shifted from 1725cm^{-1} in (1) to 1568cm^{-1} and 1594cm^{-1} in (2) by the complex formation.

Fig. 1-(3) is the IR spectrum of the coground product of $MgCl_2$ and EB. The C=0 band appears at 1680cm^{-1}, which is similar to the results of Chien et al.[13]

Five grams of $MgCl_2$ with various surface areas were treated using 200 ml of $TiCl_4$ at 90°C for 2 h, followed by washing with 200 ml of heptane 10 times. Ti content on each $MgCl_2$ is shown in Table 1.

Table 1. Amounts of Ti supported on $MgCl_2$ with different surface areas

surface area of $MgCl_2$ (m^2/g)	Ti [a] (mmol/g-$MgCl_2$)
11	trace
60	0.17

[a] Five grams of $MgCl_2$ was treated with 200 ml of $TiCl_4$ at 90°C for 2 h followed by washing with 200 ml of heptane at 40°C 10 times; then Ti content was measured.

Only a trace amount of Ti is supported on $MgCl_2$ with a surface area of 11 m^2/g. But when $MgCl_2$ with 60 m^2/g which was prepared by grinding $MgCl_2$ with 11 m^2/g was used, the Ti content became 0.17 mmol/g-$MgCl_2$.

Table 2 shows Ti contents of (1) coground product of $MgCl_2$ and $TiCl_4$, and (2) washed product of (1). A much larger amount of Ti is able to be supported on $MgCl_2$ by grinding. But about 40% of supported Ti is removed by heptane washing, which suggests that about 40% Ti

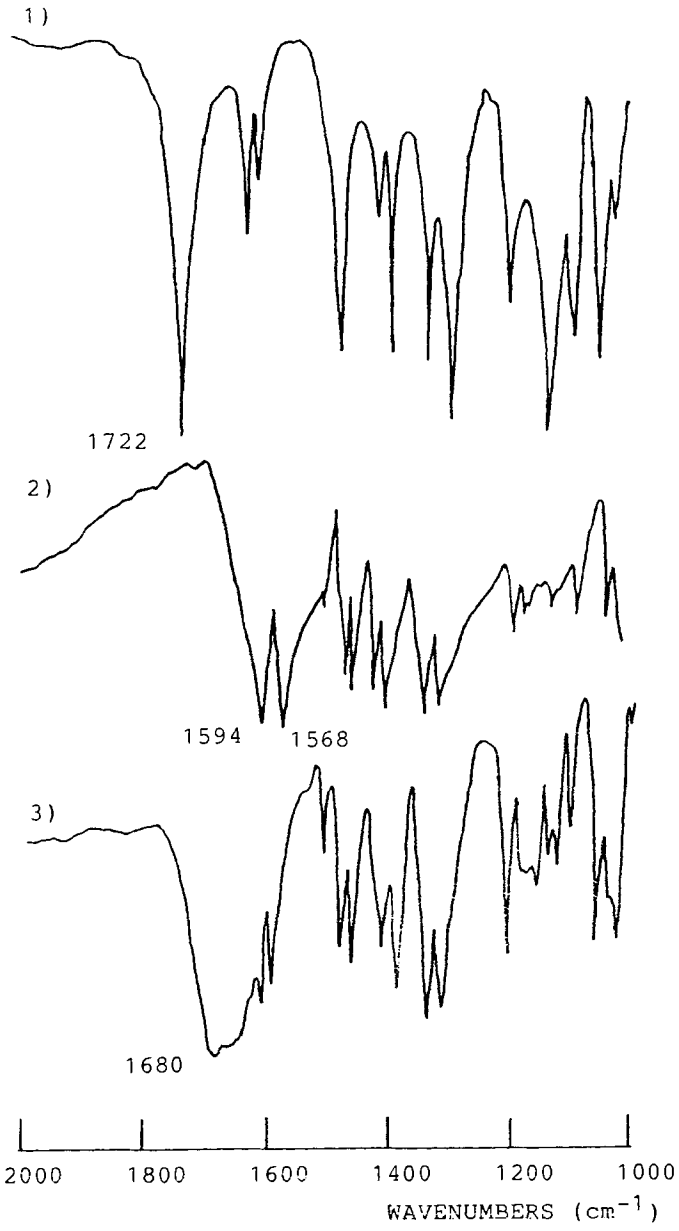

Figure 1. IR spectra of 1) EB, 2) $TiCl_4$·EB complex, and 3) coground product of $MgCl_2$ and EB

interacts only slightly with $MgCl_2$.

Table 2. Difference of Ti content by heptane washing

	Ti (mmol/g-$MgCl_2$)
(1) Coground product of $MgCl_2$ and $TiCl_4$	1.51 [b]
(2) Washed product of (1) [a]	0.88

[a] Five grams of the coground product was washed with 200 ml of heptane at 40°C 10 times.

[b] Calculated from the amounts of $TiCl_4$ and $MgCl_2$

2. Detailed study of $TiCl_4$ and EB in the $MgCl_2$-supported catalysts

The structure of the active site as well as polymerization mechanism of the $MgCl_2$-supported catalysts still remain unclear.

Here, $TiCl_4$ and EB in the catalysts are studied to obtain basic information concerning the above questions using TG-DTA and some other analytical instruments. First, interactions between every two components are investigated in detail. Then the following catalysts, which are famous as the earliest types of $MgCl_2$-supported catalysts developed by Montedison and Mitsui Pertochemical, are studied to clarify the states of $TiCl_4$ and EB in the catalysts.

cat-A; Prepared by grinding $MgCl_2$ with $TiCl_4$·EB complex.

cat-B; Prepared by treating the coground product of $MgCl_2$ and EB with $TiCl_4$, followed by washing with heptane.

Fig. 2 shows TG-DTA curves of (1) $TiCl_4$·EB complex, (2) coground product of $MgCl_2$ and EB, and (3) coground product of $MgCl_2$ and $TiCl_4$.

In the case of (1) the $TiCl_4$·EB complex, there are two large peaks at 128°C and 188°C with 50 ~ 60% weight decrease at the temperature range of 100°C to 200°C. These peaks are due to $TiCl_4$ (b.p.: 136°C) and EB (b.p.: 213°C) produced by the decomposition of the $TiCl_4$·EB complex. A small peak exists at about 365°C, which may be caused by a decomposition of a reformation product of $TiCl_4$·EB complex.

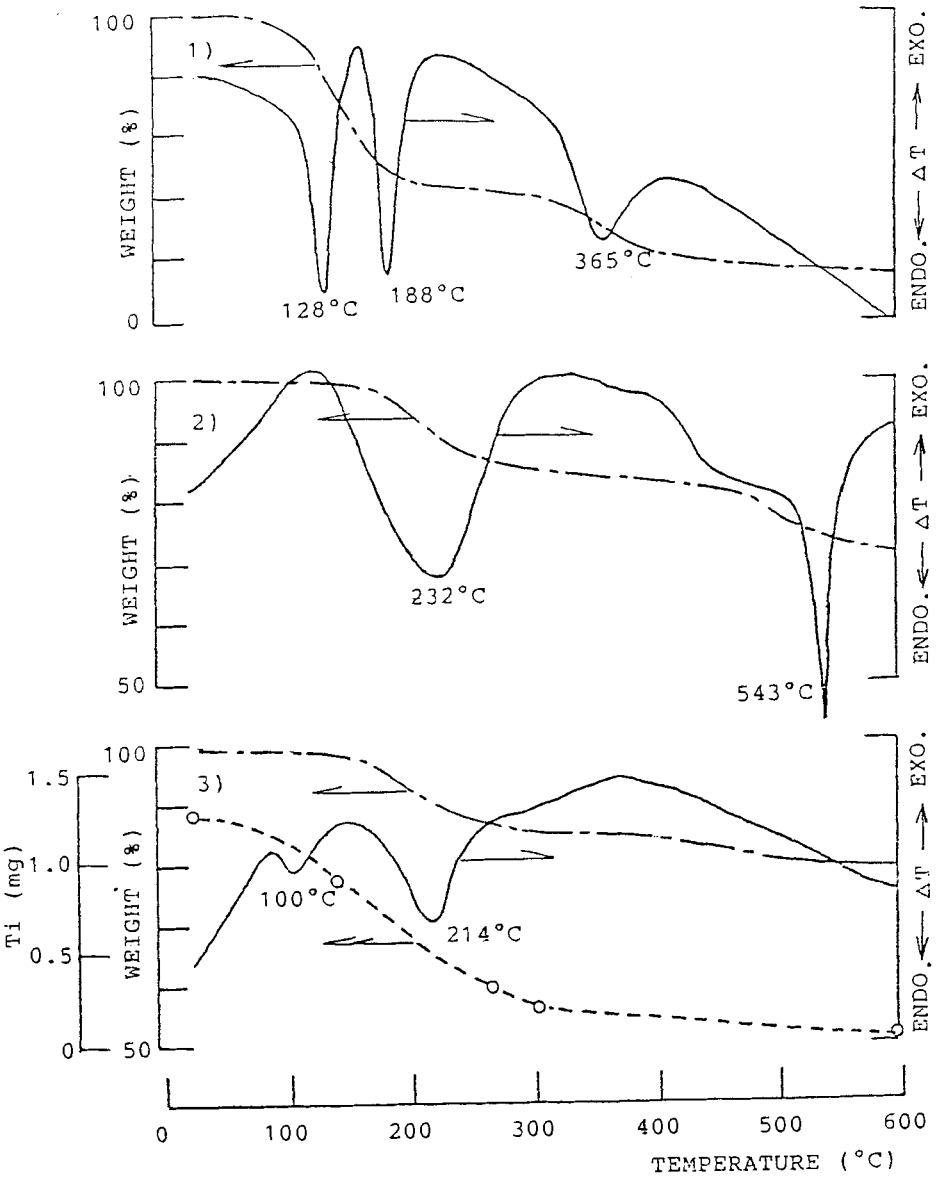

Figure 2. TG-DTA curves of 1) $TiCl_4$·EB complex, 2) coground product of $MgCl_2$ and EB, and 3) coground product of $MgCl_2$ and $TiCl_4$. DTA range: ±25 V, Sample weight: 1) 8.2 mg, 2) 18.9 mg, 3) 19.2 mg. —— - —— : TG, ———— : DTA, - - - - - - : Ti.

DTA curve of the coground product of $MgCl_2$ and EB has two peaks at 232°C and 543°C with weight decrease. These are probably due to EB on the surface and in the crystalline matrix of $MgCl_2$ respectively.

Fig. 2-(3) shows the change in Ti content as well as TG-DTA curve. The DTA curve has two peaks at 100°C and 214°C. They are caused by $TiCl_4$ having no interaction with $MgCl_2$ (100°C) and $TiCl_4$ fixed in the crystalline matrix of $MgCl_2$ (214°C), which agrees with the decrease in Ti content. This corresponds to the result in Table 2, where $TiCl_4$ decreased by washing, indicating the existence of $TiCl_4$ that does not interact with $MgCl_2$.

Fig. 3 shows TG-DTA curves of (1) mixed product of $MgCl_2$ and $TiCl_4$·EB complex, (2) cat-A and (3) cat-B with changes in Ti content.

There is a large peak at 130°C in (1), which is due to $TiCl_4$ produced by the decomposition of the $TiCl_4$·EB complex as in Fig. 2-(1). The peak seems to involve dissociation energy of the complex. In one case of the complex the peak of EB was at 188°C. The peak is shifted to 224°C and 543°C, similar to the peaks of the coground product of $MgCl_2$ and EB (see Fig. 2-(2)). This is because EB produced by the decomposition of $TiCl_4$·EB complex interacts with $MgCl_2$.

The change of Ti content in cat-A is similar to that in (1), but there is only a very small peak at 100°C by free $TiCl_4$ in (2). There is no peak at about 130°C by $TiCl_4$ produced from the complex, indicating that the $TiCl_4$·EB complex has already decomposed. That is, the complex decomposed when it was ground with $MgCl_2$. The peak at 237°C is mainly due to EB that has interacted with $MgCl_2$ as it is similar to the peak of the coground product of $MgCl_2$ and EB. But because of the decrease in Ti contents, the peak at 237°C seems to include also a desorption of $TiCl_4$. Thus, if the $TiCl_4$·EB complex is coground with $MgCl_2$, the complex decomposes and $TiCl_4$ and EB exist interacting only with $MgCl_2$.

Moreover, in (3) cat-B shows a TG-DTA curve similar to that of cat-A in (2). It indicates that the states of $TiCl_4$ and EB in cat-B are spontaneously the same as in cat-A, though cat-A and cat-B are regarded as different catalysts because of the difference of preparation methods.

Fig. 4 shows the IR spectra of (1) cat-A and (2) cat-B. The C=0 band of each spectrum appears not at 1580cm^{-1}, which suggests the interaction with $TiCl_4$, but at 1680cm^{-1} due to the interaction with $MgCl_2$. These results indicate that EB exists interacting with $MgCl_2$

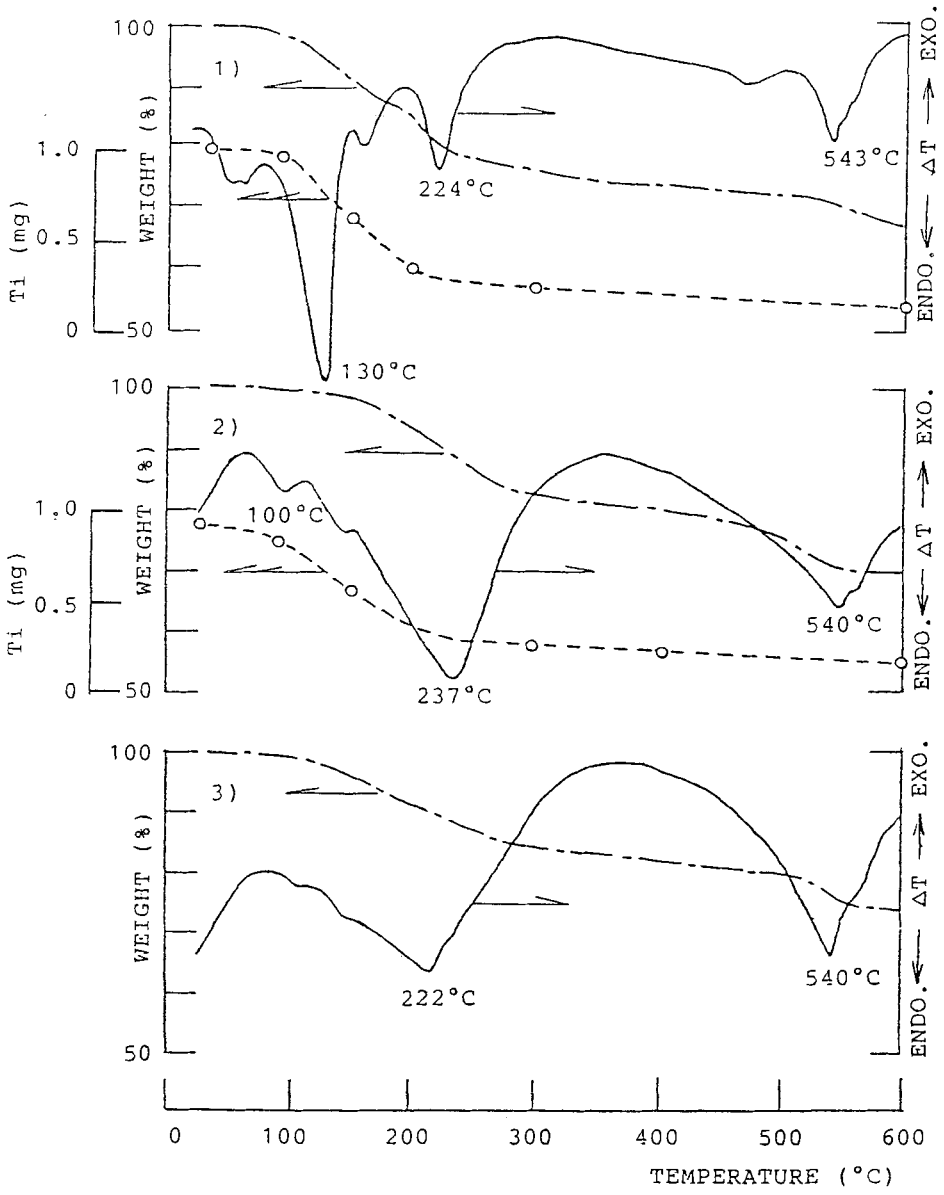

Figure 3. TG-DTA curves of 1) mixed product of $MgCl_2$ and $TiCl_4$·EB complex, 2) a catalyst prepared by grinding $MgCl_2$ with $TiCl_4$·EB complex (cat-A), and 3) a catalyst prepared by prepared by treating the coground product of $MgCl_2$ and EB with $TiCl_4$ (cat-B). DTA range: ± 25μV, sample weight: 1) 20.7 mg, 2) 19.3 mg, 3) 21.0 mg, —— - —— : TG, ———— : DTA, - - - - - - - : Ti.

in the two types of $MgCl_2$-supported catalysts and agree with those of TG-DTA.

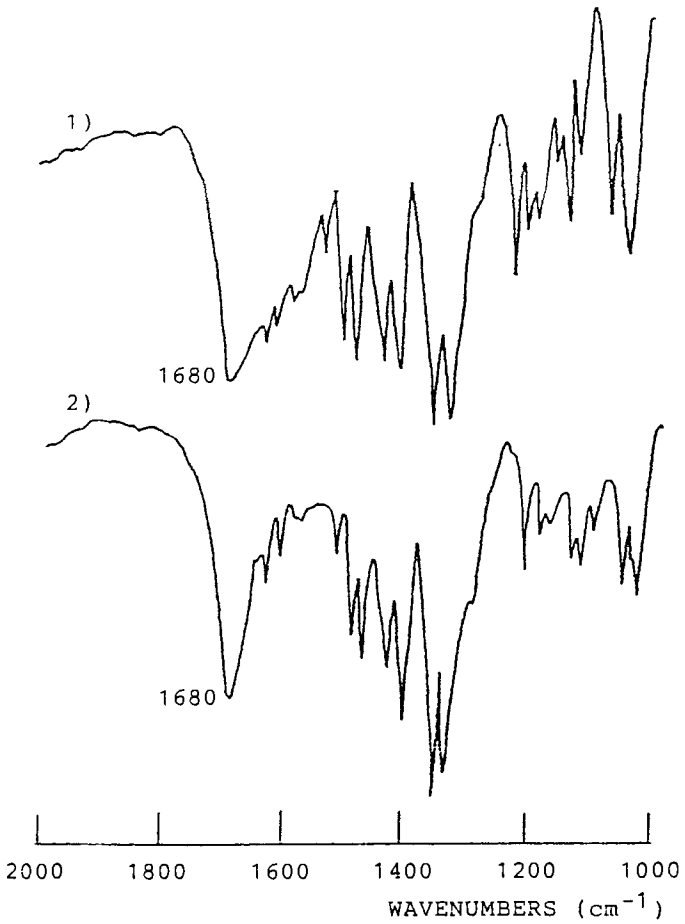

Figure 4. IR spectra of 1) a catalyst prepared by grinding $MgCl_2$ with $TiCl_4$·EB complex (cat-A), and 2) a catalyst prepared by treating the coground product of $MgCl_2$ and EB with $TiCl_4$ (cat-B).

To confirm the results, the following two types of experiments were conducted.

First, changes in contents of EB and Ti by washing the coground product of $MgCl_2$ and $TiCl_4$·EB complex (cat-A) were measured. The results are shown in Table 3.

Table 3. Differences of Ti and EB contents by heptane washing

	Ti (mmol/ g-$MgCl_2$)	EB (mmol/ g-$MgCl_2$)
(1) Coground product of $MgCl_2$ and $TiCl_4$·EB complex, cat-A	1.40	1.24
(2) Washed product of (1) [a]	0.64	1.05

[a] Five grams of coground product was washed with 200 ml of heptane at 40°C 10 times.

Ti content decreases about 55%, while EB content decreases only about 15%. If $TiCl_4$ and EB exist in complex form, their decrease by heptane washing must be the same in amount. So, the result suggests that they do not exist in complex form. This corresponds to the TG-DTA results which show that $TiCl_4$ and EB exist interacting only with $MgCl_2$.

Fig. 5 shows XD patterns of (1) ground $MgCl_2$, (2) coground product of $MgCl_2$ and $TiCl_4$, (3) coground product of $MgCl_2$ and EB, and (4) coground product of $MgCl_2$ and $TiCl_4$·EB complex. Ground $MgCl_2$ has four main peaks at $2\theta=15°$, 30°, and 50°.

The peaks at $2\theta=30°$, 35°, 50° in (2), and the peak at $2\theta=15°$ in (3) become smaller than those in (1). In (4), however, all peaks are smaller. Though it is possible to regard these results as being caused by using the complex, it may be more reasonable to consider that $TiCl_4$·EB complex decomposed, then $TiCl_4$ and EB act on $MgCl_2$ independently to decrease the intensity of X-ray peaks as if the effects of (2) and (3) are made up.

From the above resuts obtained by applying thermal analysis to the catalysts, we arrived at the conclusion that $TiCl_4$ and EB exist in the $MgCl_2$-supported catalysts interacting only with $MgCl_2$. Results obtained using other analytical equipment such as IR and XD, corresponded to those obtained using thermal analysis.

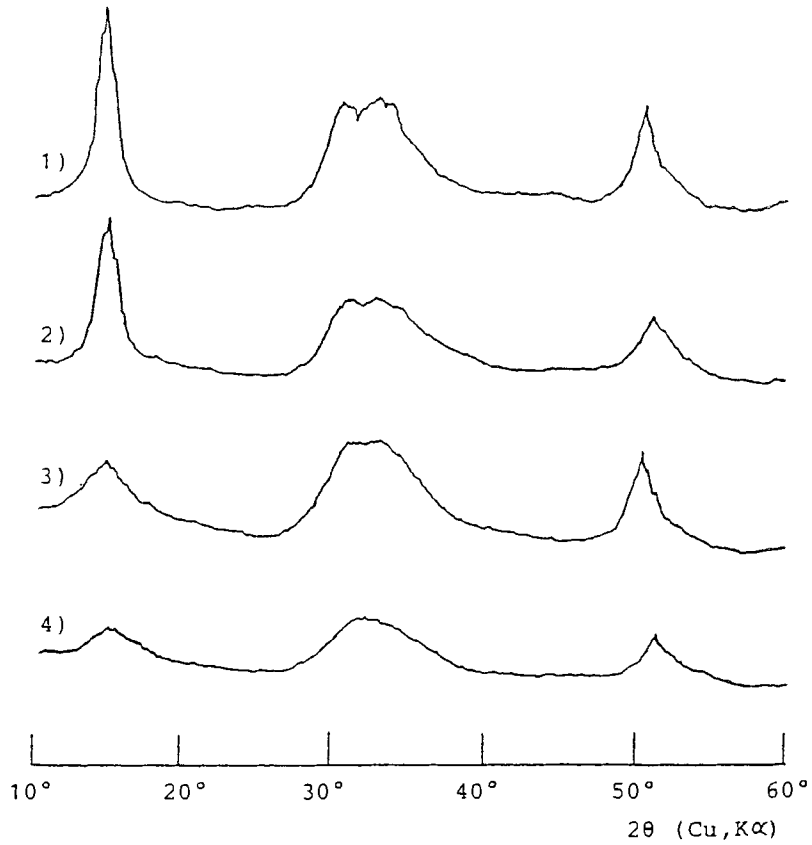

Figure 5. Powder X-ray diffraction patterns of 1) ground $MgCl_2$ (S.A. = 60 m^2/g), 2) coground product of $MgCl_2$ and $TiCl_4$, 3) coground product of $MgCl_2$ and EB, and 4) coground product of $MgCl_2$ and $TiCl_4$·EB complex (cat-A).

ACKNOWLEDGMENTS

The authors are grateful to Toho Titanium Co., Ltd. for permitting us to publish this paper, and to Mr. M. Hosaka for the experimental contribution to this work.

REFERENCES

1. G. Natta, P. Corradini, F. Danusso, E. Mantice, G. Mazzanti and G. Moraglio, J. Am. Chem. Soc., 77, 1708 (1955).
2. Montedison SPA, Japan Pat. 1076201.

3. Mitsui Petrochemical, Japan Pat. 1014471.
4. Shell, Japan Pat. 432533.
5. J.C.W. Chien and J.T.T. Hsieh, J. Polym. Sci, Polym. Chem. Ed., 14, 1915 (1976).
6. A. Munoz-Escalone and J. Villalba, Polymer, 18, 179 (1977).
7. K. Soga, M. Terano and S. Ikeda, Polym. Bull., 1,849 (1979).
8. E. Suzuki, M. Tamura, Y. Doi and T. Keii, Makromol. Chem., 180, 2235 (1979).
9. N. Kashiwa, Polym. J., 12, 603 (1980).
10. P. Galli, L. Luciani and G. Cecchin, Angew. Makromol. Chem., 94, 63 (1981).
11. S.A. Sergeev, G.D. Bukatov, E.M. Moroz and V.A. Zakharov, react. Kinet. Catal. Lett., 21, 403 (1982).
12. N.F. Brockmeier and J.B. Rogan, Ind. Eng. Chem. Prod. Res. Dev., 24, 278 (1985).
13. J.C.W. Chien, J.-C.Wu and C.-I. Kuo, J.Polym. Sci., Polym. Chem. Ed., 21, 725 (1983).

STUDIES ON THE COPOLYMERIZATION OF ETHYLENE AND α-OLEFINS WITH ZIEGLER- NATTA CATALYST SUPPORTED ON ALUMINA OR MAGNESIUM CHLORIDE

RAUL QUIJADA [1] and ANA MARIA RAMOS WANDERLEY [2]

1 - Centro de Pesquisas e Desenvolvimento da PETROBRÁS

2 - PETROQUISA - PETROBRÁS QUÍMICA S.A. e Instituto de Macromoléculas - Universidade Federal do Rio de Janeiro.

ABSTRACT

Two Ziegler-Natta catalytic systems were prepared from supports with different chemical structures, namely alumina and magnesium chloride. The activity was studied by comparing the homopolymerization of ethylene and its copolymerization with 1-butene, 1-hexene, 1-octene and 1-decene, respectively. Differences in both comonomer incorporation and physical properties of the polymers were investigated.

INTRODUCTION

The great success of the Ziegler-Natta catalysis during the last decade was the development of highly active catalytic systems for homopolymerization of ethylene and propylene, where the compound containing the transition metal is first deposited on a carrier. Various inorganic and organic substances have been proposed as carriers. The main characteristic of these new types of catalysts is their high activity in polymerization, allowing the elimination of the stages of catalyst desactivation and removal of the catalyst residues from the polymers as well as producing highly stereoregular products.

These supported catalysts continue to attract considerable attention in many industrial and academic laboratories specially looking for new type of polymers with particular characteristics. One example of this new type of polymer is the Linear low density polyethylene (LLDPE), obtained by polymerization under low pressure, using a catalyst system of the Ziegler type.

At the present state of development, low pressure ethylene polymerization is generally a highly efficient low-cost operation. Yet many unsolved problems face industry. Still better catalysts are needed, not so much for high activity but for better copolymerization capability, less sensitivity to feedstock impurities, better control of molecular weight distribution and better particle size control.

There is a gap between low density polyethylene (LDPE), produced by radical polymerization under high pressure, and high density polyethylene (HDPE), synthetised under low pressure, with transition metal catalysts when comparing physical and mechanical properties.

Early attempts to obtain such intermediate properties of the materials included physical mixtures of LDPE and HDPE or changes in operation conditions of the polymerization reactors[1] has been done, however, the results were not very satisfactory. Improvement of certain properties of blends are achieved in detritment of the others. Also, changes of operation conditions are limited by economic factors. Definitive solution for this problem was found by doing the copolymerization of ethylene with α-olefins, using transition metal catalysts. The introduction of α-olefins in the polymeric chain produces small ramifications, which decrease the density of the polymer. By this way, it is possible to obtain the Linear low density polyethylene (LLDPE). These copolymers show a large range of densities, with improvement in physical and mechanical properties.

LLDPE has been scarcely dealt with in scientific papers[2,3]; it is more often presented in patent literature[4,5,6] and trade journals. This material deserves much interest of the polyethylene consumers, since there is a practical demand to be made of polymers with density in the range between 0.92 and 0.94 g/cm^3 or lower. From this point of view and considering the little information published related with the use of active catalyst systems for copolymerization, we present in this paper an study of the ethylene copolymerization with 1-butene, 1-hexene, 1-octene and 1-decene. The final copolymers obtained are in the range of densities mentioned above and they were produced in slurry process, using Al_2O_3 an $MgCl_2$ supported Ziegler-Natta catalysts. The main interest of the study was related to the evaluation of the catalytic activity and the incorporation of comonomers to the main chain of the polymer.

EXPERIMENTAL

Materials. Commercial, extra pure grade hexane was purified by usual procedures. Extra pure grade titanium tetrachloride and triisobutylaluminum were commercially obtained and used without further purification. Argon and monomer gases were purified passing through columns of molecular sieves and BASF catalyst for removal of water and oxygen, respectively. The liquid comonomers were distilled in an inert atmosphere.

Alumina (γ -Al_2O_3) was produced through a process developed by PETROBRÁS Research Center (Brazilian Patent 8 005 302), by reacting aluminium sulphate and amonium bicarbonate at a controlled pH. It was later dried and calcinated at 700°C, with final properties of specific area around 250 m^2/g, pore volume > 1,0 cm^3/g and 85% of the pores with diameter above 100 A°.

Magnesium chloride ($MgCl_2$) was obtained from commercial $MgCl_2.6H_2O$; dehydrated at 110°C and 450°C under flow of argon and HCl, respectively. The anhydrous compound was then ground in a ball mill.

Preparation of the supported catalysts. Highly dispersed catalysts were obtained by treatment with $TiCl_4$, at reflux temperature, in absence of solvent. The adopted procedure is described in the literature[7].

Polimerization procedures. The polymerization reactions were carried out in a 1 gallon Parr reactor, where a measured amount of n-hexane, triisobutylaluminum and catalyst were introduced under argon atmosphere at room temperature. The comonomers and ethylene were fed into the reactor at 80°C, untill a constant pressure of 10-14 kg/cm^2 of ethylene was attained and kept for 1 or 2 hours. Kinetics results were recorded according to the rate of ethylene consumed during the experiment by using a calibrated rotameter; the results were checked by weighing the final product.

Hydrogen was used as regulator of molecular weight only in the reactions with $MgCl_2$ supported catalyst.

Analytical procedures. The incorporation of comonomer was determined by infrared spectroscopy using the methyl band at 1378 cm^{-1} from Perkin Elmer 467 Spectrophotometer. The chosen procedure[8] employed a compensation method with a polymethylene wedge. The density was measured in a DUPONT Differential Scanning

Calorimeter, DSC. The intrinsic viscosity was measured under argon atmosphere at 135°C in decaline containing 0,1% of Irganox and Irgafos mixture. Values of $[\eta]$ were determined through Solomon and Gostman's equation [9,10] from a single value of specific viscosity obtained at one definite concentration. The suitability of this equation was checked by comparing to values of intrinsic viscosity obtained by the Huggins equation [11]. The cristallinity of the copolymers was determined using the relationship: $D=\rho_c X + \rho_a (1-X)$ where: D = material density; ρ_c = polyethylene density 100% cristalline; ρ_a = polyethylene density 100% amorphous and X = cristallinity.

RESULTS

The copolymerization of ethylene with α-olefins using different support for the Ziegler-Natta catalysts are presented below.

1 - Alumina (γ-Al_2O_3) as the catalytic support.

Table I shows the results obtained in the ethylene copolymerization with 1-butene. In this series of reactions, the concentration of 1-butene in the feed was ranged from 6.7 up to 30.4 mole per cent in relation to the liquid phase.

Table I. Influence of the 1-butene concentration on copolymerization with ethylene using Al_2O_3 as support[(a)]

RUN	1-BUTENE CONCENTRATION (MOLE %)	CATALYTIC ACTIVITY x 10^{-3} (gPOLYM/gTi)	1-BUTENE INCORPORATION (MOLE %)	DENSITY (g/cm³)	CRISTALLINITY (%)	MELTING POINT (°C)	INTRINSIC VISCOSITY (dl/g)
A-1	-	49.276	-	0.9360	52.44	144	30.03
A-2	6.7	35.120	0.06	0.9300	48.78	140	21.35
A-3	11.5	32.145	0.90	0.9290	48.17	138	19.62
A-4	21.5	24.104	1.63	0.9258	46.22	135	14.08
A-5	30.4	17.559	2.41	0.9222	44.02	133	8.76

(a) Polymerization conditions: ethylene pressure: 13,5 Kg/cm²; temperature: 80°C; reaction time: 2h; catalyst: $TiCl_4/Al_2O_3$; cocatalyst: Al $(iC_4H_9)_3$; Al/Ti molar ratio: 50.

It was found that the addition of 1-butene decreases the catalytic activity and increases the comonomer incorporation to the polymer chain continuosly. Even when small quantities of 1-butene is incorporated in the main chain, the density of the polymer changes, decreasing gradually as the incorporation of the comonomer increases. Melting point decreases in a similar way, due to the introduction of branching in the macromolecule. Also, the intrinsic viscosity values experiment similar behavior, the α-olefin seems to act as a regulator of molecular weight, since hydrogen was not used for molecular weight control.

The results of the ethylene copolymerization with 1-hexene, 1-octene and 1-decene are shown in Table II. For comparison 1-butene is also included. It could be observed that the addition of comonomer decreases the catalytic activity when compared with the results obtained in the homopolymerization of ethylene under the experimental conditions. The shorter the alkyl subtituent, the more reactive is the comonomer. The incorporation of the α-olefins in the polymer chain follows the sequence:

1-butene > 1-hexene > 1-octene > 1-decene.

As could be expected, and also is known for 1-butene, when the α-olefin contents increases in the copolymer, the density, the melting point and the viscosity decreases.

Table II. Comparative results of the ethylene homopolymerization and copolymerization with α-olefins using Al_2O_3 as support[a]

RUN	COMONOMER	CATALYTIC ACTIVITY x 10^{-3} (gPOLYM/gTi)	COMONOMER INCORPORATION (MOLE %)	DENSITY (g/cm^3)	CRISTALLINITY (%)	MELTING POINT (^oC)	INTRINSIC VISCOSITY (dl/g)
A-1	-	49.276	-	0.9360	52.44	144	30.03
A-3	1-BUTENE	32.145	0.90	0.9290	48.17	138	19.62
B-1	1-HEXENE	29.742	0.17	0.9318	49.88	142	20.20
C-1	1-OCTENE	33.363	0.05	0.9338	51.09	142	22.74
D-1	1-DECENE	40.318	0.02	0.9348	51.71	143	22.79

(a) Polymerization conditions: ethylene pressure: 13,5 kf/cm^2; comonomer feed: 11-13 mole %; temperature: 80°C; reaction time: 2h; catalyst: $TiCl_4/MgCl_2$; cocatalyst: Al $(iC_4H_9)_3$; Al/Ti molar ratio: 50.

Figure 1 shows the results for the catalytic activity of the alumina-supported system with the variation of the feed composition.

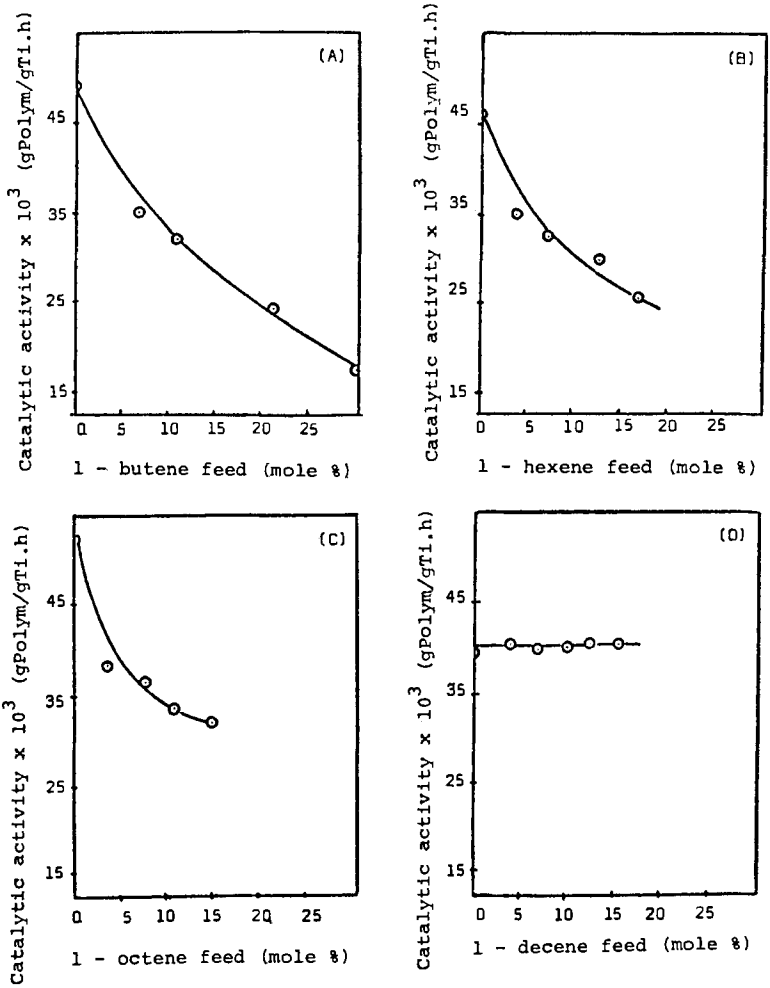

Figure 1. Variation of catalytic activity with comonomer feed in ethylene copolymerization using Al_2O_3 as support.

2 - Magnesium chloride ($MgCl_2$) as the catalytic support.

Table III shows the results of the copolymerization of ethylene and 1-butene. The concentration of 1-butene in the feed was studied in the range of 7,2 to 21,1 mole per cent. The higher values of the catalytic activity presented by this system when compared with alumina as support, shows a very efficient system not only for the homopolymerization but also for the copolymerization. It is interesting to observe that the addition of 1-butene decreases significatively the activily which remain practically constant for the investigated range of comonomer concentration.

Table III. Influence of the 1-butene concentration on copolymerization with ethylene using $MgCl_2$ as support (a)

RUN	1-BUTENE CONCENTRATION (MOLE %)	CATALYTIC ACTIVITY x 10^{-3} (gPOLYM/gTi)	COMONOMER INCORPORATION (MOLE %)	ELASTOMERIC SUBPRODUCT (%)	DENSITY (g/cm³)	CRISTALLINITY (%)	MELTING POINT (°C)	INTRINSIC VISCOSITY (dL/g)
E-1	-	1,048	-	0.5	0.9520	60.00	137	3.02
E-2	7.2	685	1.9	5.0	0.9370	53.05	126	1.97
E-3	10.5	592	2.19	6.0	0.9326	50.37	126	1.68
E-4	15.4	633	2.94	22.0	0.9314	49.63	125	1.52
E-5	19.8	646	3.56	24.0	0.9279	47.50	124	1.46
E-6	21.1	644	4.03	29.0	0.9261	46.40	123	1.44

(a) Polymerization conditions: ethylene pressure: 10,0 kg/cm ^{2}; hydrogen pressure: 4,0 kg/cm ^{2}; temperature = 80°C; reaction time: 1h; catalyst: $TiCl_4/MgCl_2$; cocatalyst: Al (iC_4H_9)$_3$; Al/Ti molar ratio: 10.0.

The influence of 1-butene concentration on the comonomer incorporation and on the various properties of the copolymer obtained can be clearly observed. Incorporation increases when the comonomer concentration in the reactor increases; consequently, the density decreases proportionally. The molecular weight is also influenced by the comonomer concentration. As it was mentioned before, for explaining this effect, one must consider the possible occurrence of chain transfer reactions with the comonomer, as point out by Böhm [2].

The presence of the α-olefin intensifies the controlling action of the hydrogen on the molecular weight.

Finally, this system promotes the formation of an elastomeric subproduct that is proportional to the amount of comonomer in the feed.

In the Table IV are shown the results related to the ethylene copolymerization with 1-hexene, 1-octene and 1-decene for a fixed α-olefin concentration. In contrast to what was observed with alumina-supported catalyst, the catalytic activity changes with the type of α-olefin chosen for study. For 1-butene and 1-octene there is a significant decrease of the activity. For 1-hexene there is an increase of the catalytic activity. Figure 2 shows this effect for each system. A similar phenomenum was also reported by Finogenova , without any explanation.

Table IV. Comparative results of the ethylene homopolymerization and copolymerization with α-olefins using $MgCl_2$ as support[a]

RUN	COMONOMER[b]	CATALYTIC ACTIVITY x 10^{-3} (gPOLYM/gTi)	COMONOMER INCORPORATION (MOLE %)	ELASTOMERIC SUBPRODUCT (%)	DENSITY (g/cm^3)	CRISTALLINITY (%)	MELTING POINT (°C)	INTRINSIC VISCOSITY (dl/g)
E-1	-	1.048	-	0.5	0.9520	60.00	137	3.02
E-3	1-BUTENE	592	2.19	6.0	0.9326	50.37	126	1.68
F-1	1-HEXENE	1,345	1.14	3.2	0.9410	55.49	131	1.60
G-1	1-OCTENE	606	0.60	2.0	0.9461	58.60	131	1.79
H-1	1-DECENE	1,187	0.32	3.6	0.9518	62.07	131	1.96

(a) Polymerization conditions shown in table III

(b) Comonomer feed: 11-13 mole %

As reported for alumina as support of the Ziegler-Natta catalyst, magnesium chloride support presented similar behavior concernig the comonomer incorporation order:

1-butene > 1-hexene > 1-octene > 1-decene

The density values show the dependence with the type of α-olefin being incorporated, related to the alkyl substituing group.

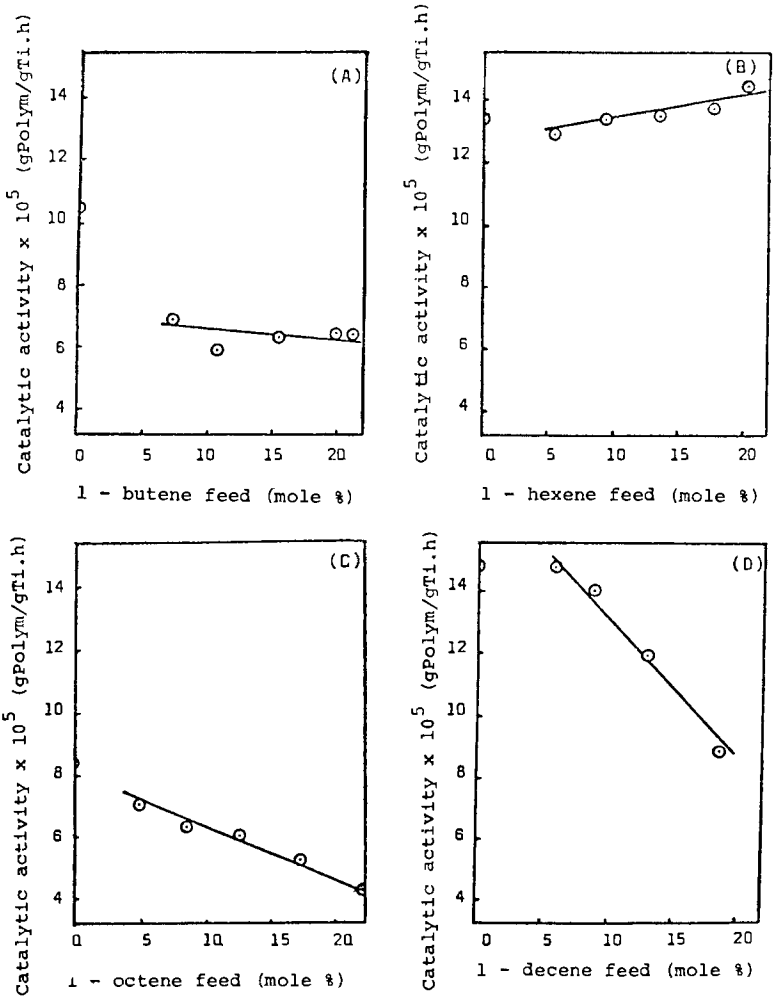

Figure 2. Variation of catalytic activity with comonomer feed in ethylene copolymerization using $MgCl_2$ as support.

3 - Determination of the reactivity ratios of the pair ethylene-α-olefins in Ziegler-Natta copolymerization using $MgCl_2$ as support.

Due to the great quantity of data obtained in this work, the reactivity ratios parameters values were calculated using Mayo-Lewis and Fineman-Ross methods. The results are presented in Table V.

Table V. Reactivity ratios of the α-olefins in copolymerization with ethylene using $MgCl_2$ as support

DETERMINATION METHOD	COMONOMERS							
	ETHYLENE/1- BUTENE		ETHYLENE/1-HEXENE		ETHYLENE/1-OCTENE		ETHYLENE/1-DECENE	
	r_2	r_1	r_2	r_1	r_2	r_1	r_2	r_1
MAYO-LEWIS	35.26	0.01	132.00	0.02	160.00	0	315.00	0
FINEMAN-ROSS	45.00	0.16	129.76	0.01	170.13	0	271.90	0

Bohm[12] found values of reactivity ratio for the pair ethylene-1-butene of 67 and 0.08 respectively at 85°C for his particular catalytic system. This means that the value obtained in our work is within the range accepted for this type of catalytic system. For the others pair of ethylene-α-olefins the higher values were expected due to the lower reactivity of the α-olefin with the larger substituent groups.

DISCUSSION

When looking at the results presented for alumina used as support in Tables I and II, we can conclude that the increase of the comonomer concentration is accompaned by a corresponding decrease in catalytic activity, due to the lower reactivity of the α-olefins, while the incorporation in the macromolecule increases.

Density and Cristallinity of the copolymers decreases due to the introduction of small side chains. The melting point also decreases due to the modification in size and perfection of the crystallites.

The α-olefins examined occupy the following order according to their effect on the parameters studied:

1-butene > 1-hexene > 1-octene > 1-decene

For $MgCl_2$ used as a support, Tables III and IV, the variation of catalytic activity was found to be a characteristic of each α-olefin investigated. The other parameters follow normal tendencies already discussed for alumina.

The formation of elastomeric subproduct in the reaction with this catalytic system may be related to the possibility of having two different types of active centers.

REFERENCES

1. W. Payer, Die Angew. Makromol. Chem., 94, 49 (1981).
2. L.L. Böhm, Makromol. Chem., 182, 3291 (1981).
3. L.T. Finogenova, V.A. Zakharov, A.A. Buniyat-Zade, G.D. Bukatov and T.K. Plaksunov, Polym. Sci. U.S.S.R, 22, 448 (1980).
4. F. Baxmann, J. Dietrich, A. Frese and O. Hahmann, German Patent 2214271.
5. Y. Miwa, T. Shimada, S. Hayashi, M. Ukita, H. Nakagawa and M. Matsumura, U.S. Patent 2093047.
6. M.Araki and K. Machita, Japan Patent 8008488.
7. J.C.W Chien and J.T.T. Hsieh, J.Polym. Sci., 14, 1915 (1976).
8. ASTM D 2238.
9. O.F. Solomon and J.Z. Cinta, J. Appl. Polym. Sci., 6, 683 (1962).
10. L.G. Gargallo, Bol. Soc. Chil. Quim., 1-2, 16 (1973).
11. J.H. Elliot, K.H. Horowitz and T. Hoodock, J. Appl. Polym. Sci., 14, 2947 (1970).
12. L.L. Böhm, J. Appl. Polym. Sci., 29, 279 (1984).

This page intentionally left blank

THE STRUCTURAL STUDY OF SUPPORTED ZIEGLER-NATTA CATALYSTS FOR THE POLYMERIZATION OF OLEFIN

XIAO SHIJING, CAI SHIMIAN, CHEN ZANPO and LIU HUANQIN
Institute of Chemistry Academia Sinica, Beijing

ABSTRACT

The interaction between $MgCl_2$ and electron donors and the structure of supported catalysts were studied by IR and XPS. Experimental data obtained demonstrated that the surface complexes between $MgCl_2$ and electron donor probably formed during milling. When the catalysts were made by treating the milled product ($MgCl_2$/PIP, $MgCl_2$/PYRR) with $TiCl_4$ a large quantity of PIP and PYRR came down from the support and $TiCl_4$/PIP and $TiCl_4$/PYRR complexes formed respectively, while the milled product was $MgCl_2$/EB, the characteristic bands of $MgCl_2$/EB in IR spectra were remained and this indicated that $MgCl_2$/EB kept unchanged during the treating.

When $TiCl_4$EB complex was milled togetter with $MgCl_2$, the complex decomposed and $MgCl_2$/EB surface complex formed. The other component $TiCl_4$ binds with $MgCl_2$ through chlorine bridge. However, no exchange between the complex and $MgCl_2$ support could be observed during the cogrinding of $MgCl_2$ and $TiCl_4$2PIP or $TiCl_4$2PYRR.

INTRODUCTION

Electron donor compounds such as esters, amines, ethers etc. can be used for the conventional coordination catalysts and have a considerable significance in the modification of supported Ziegler-Natta catalysts for the polymerization of propylene. The study of the interaction of catalyst components (electron donor, $MgCl_2$, $TiCl_4$) and the structure of the supported catalyst may lead to a better understanding the mechanism of stereospecific polymerization of α-olefins. Although some work in this field have been reported [1-5], the results are quite different. The main problem is that whether the electron donor on the surface of the catalyst coordinates to $MgCl_2$ or forms titanium complexes which bind to the coordina-

tive unsaturated Mg atoms located on the surface of $MgCl_2$ through chlorine bridge. It is also possible that the electron donor reacts with $MgCl_2$ and $TiCl_4$ simultaneously.

The examination of IR and XPS spectra of the complexes $MgCl_2(CH_3COOC_2H_5)_2$ and $TiMgCl_6(CH_3COOC_2H_5)_4$[6] showed that the results obtained by studying the surface structure of the supported catalyst by means of IR and XPS can be verified from each other, so that the reliable results may be obtained.

Supported catalysts with ester and amine as electron donor were prepared and the interaction between catalyst components and the structure of the catalysts have been studied.

EXPERIMENTAL

I. The preparation of titanium complexes

(i) $TiCl_4EB$ and $TiCl_4 2EB$, (EB ethyl benzoate.)

When $TiCl_4$ reacted with equivalent amount of EB in hexane a yellow precipitate was obtained.

When $TiCl_4$ was added to an excess of EB $TiCl_4 2EB$ was obtained.

(ii) The preparation of $TiCl_4 2PIP$ and $TiCl_4 2PYRR$, (PIP= Piperidine; PYRR=Pyrrolidine)

Complexes of $TiCl_4$ with amines were prepared by adding hexane solution of one of the ligands dropwise to the precooled hexane solution of $TiCl_4$ in the same solvent.

The complexes were filtered under anhydrous condition, washed with dry hexane, and then dried under vacuum at room temperature.

II. The preparation of the $MgCl_2$-supported titanium catalysts

Anhydrous $MgCl_2$ was ground for 9hrs. in a vibration ball mill and heat-treated at 420°C in vacuo before comilling with a electron donor for support use.

The supported catalysts were prepared by milling the pretreated $MgCl_2$ with electron donor for 24hrs. A portion of milled product was suspended in excess of $TiCl_4$ in a flask equipped with a stirrer and the suspension was stirred at 110°C for 2hrs. The solid portion was separated by filtration and washed with n-heptane several times at 80°C.

Some of the catalysts were prepared by cogrinding $MgCl_2$ with titanium complexes for 24-30hrs.

All procedure were carried out under dried inert gas. All reagents were purified according to conventional methods.

III. IR and XPS measurements

The IR spectra (200-4000 cm^{-1}) were recorded on a SP-2000 spectrophotometer. The IR samples were prepared in a dry nitrogen atmosphere as nujol mull.

XPS measurements were done on a ES-300 spectrometer and MgK exciting radiation. In order to prevent the specimen from decomposition the sample preparation for XPS measurements was performed in a glove box which was connected to the sample stage of the spectrometer and filled with argon. The sample holder which was inserted into the measuring chamber which was cooled by liquid nitrogen. Contaminated carbon C1S was taken as a reference of binding energy and the value was 285.0 ev.

RESULT AND DISCUSSION

1. IR spectra of titanium complexes

In order to investigate the behavior of titanium in the supported catalyst and to clarify whether the electron donors fix on $MgCl_2$ directly or form complexes with $TiCl_4$, IR spectra of the following titanium complexes and free ligands (EB, PIP, PYRR) were measured, so as to make a comparison with the supported catalysts.

(i) The IR spectra of $TiCl_4EB$ and $TiCl_42EB$ are shown in Figure 1. It is known that ethyl benzoate was coordinated to the $TiCl_4$ via $\geq C=O$ function group. The $\nu_{C=O}$ shifs to lower wavenumber due to the formation of complex. Thus, the two strong bands at 1595 cm^{-1} and 1566 cm^{-1} may be assigned to the characteristic absorption band of both complex $TiCl_4EB$ and $TiCl_42EB$.

(ii) The IR spectra of PIP, PYRR and their Ti complexes are shown in Figure 3. and 4. The ν_{N-H} in PIP and PYRR were found at 3290 cm^{-1} and 3300 cm^{-1} respectively. The characteristic band ν_{N-H} of the Ti complexes were shifted to lower wavenumbers spectral region by 115 cm^{-1} and 103 cm^{-1} respectively. These shifts indicate the formation of coordination which weakens the N-H bond.

2. The cogrinding effect of electron donor and $MgCl_2$

When the milling-soaking method is used, the catalyst preparation is usually a two-step process. In the first step anhydrous carrier was vibration-milled with electron donor. The milled products $MgCl_2$/EB, $MgCl_2$/PIP and $MgCl_2$/PYRR were obtained.

The role of EB as been described in our earlier work. This electron donor could accelarate the breaking of $MgCl_2$ crystallites

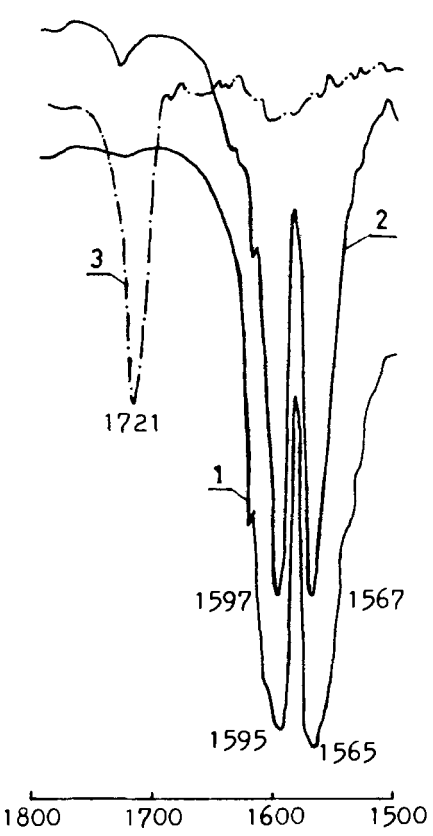

Fig. 1. Characteristic IR spectra of EB and their complexes. 1-$TiCl_4$EB; 2-$TiCl_4$2EB, 3-EB.

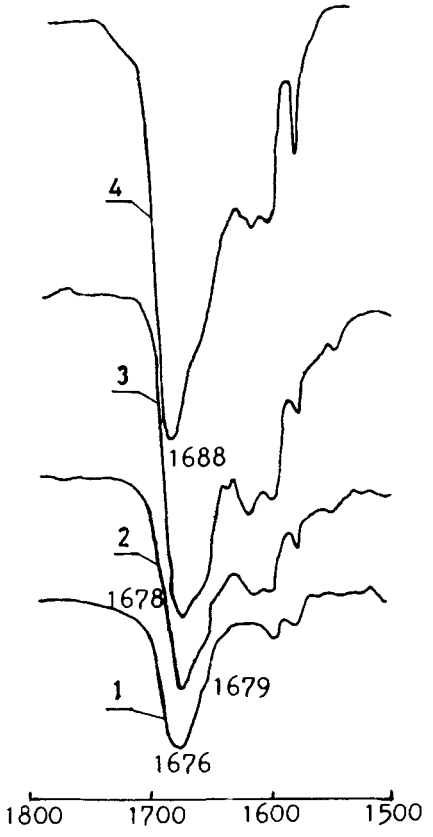

Fig. 2. Characteristic IR spectra of milled products and catalysts. 1-$MgCl_2$/EB/$TiCl_4$; 2-$MgCl_2$/$TiCl_4$2EB; 3-$MgCl_2$/$TiCl_4$EB; 4-$MgCl_2$/EB.

during the comilling with $MgCl_2$ and then EB coordinated on the fresh surfaces of $MgCl_2$ to form a surface complex. This was clearly proved by IR and X-ray diffraction data. Figure 2. shows the $MgCl_2$/EB spectrum. The strong peak at 1688 cm^{-1} can be obviously attributed to C=O absorption of the surface complex. The free EB absorption band at 1721 cm^{-1} was not found in the IR spectrum of $MgCl_2$/EB. This indicates that all EB has been bound to the surfaces of $MgCl_2$ during milling.

In the case of PIP and PYRR the N-H stretching frequences of the milled products of $MgCl_2$/PIP and $MgCl_2$/PYRR shifted by 50 cm^{-1}

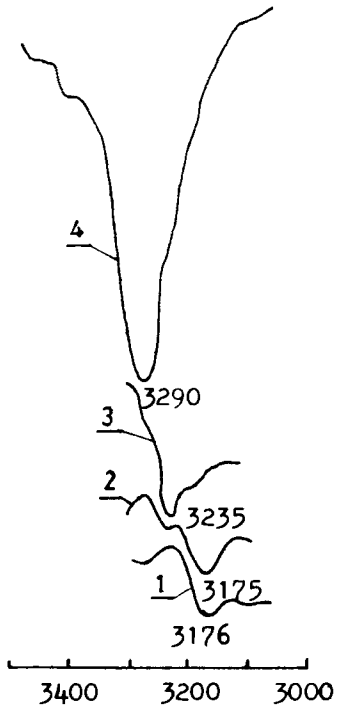

Fig. 3. Characteristic IR spectra of 1-$TiCl_4$2PIP, 2-$MgCl_2$/PIP/$TiCl_4$, 3-$MgCl_2$/PIP and 4-PIP.

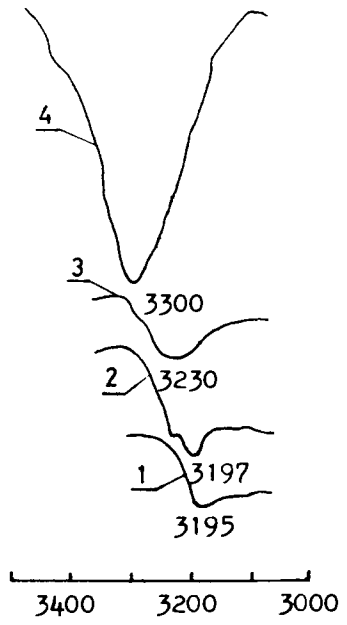

Fig. 4. Characteristic IR spectra of 1-$TiCl_4$2PYRR, 2-$MgCl_2$/PYRR/$TiCl_4$, 3-$MgCl_2$/PYRR and 4-PYRR.

and 70 cm^{-1} respectively to lower wavenumber region. The ν_{N-H} band of free PIP and PYRR were also absent in the IR spectra of these milled products. This fact shows that all PIP and PYRR have coordinated to $MgCl_2$ and formed surface complexes via its nitrogen atom during milling.

3. The interaction of milled products with $TiCl_4$

The second step of the catalyst preparation involved the treatment of milled product with neat $TiCl_4$ as described in experimental section. Thus the supported catalysts $MgCl_2$/PIP/$TiCl_4$ and $MgCl_2$/PYRR/$TiCl_4$ were obtained.

The absorption bands at 3235 cm^{-1} and 3157 cm^{-1} were found in the IR spectra of $MgCl_2$/PIP/$TiCl_4$ (see Figure 3). The former was much weaker than the latter which corresponds to the νN-H of

Table 1. ν_{N-H} of Ti complexes, milled products and catalyst (cm^{-1})

Compound	ν_{N-H}	Compound	ν_{N-H}
PIP	3290	PYRR	3300
$MgCl_2$/PIP	3235	$MgCl_2$/PYRR	3230
$MgCl_2$/PIP/$TiCl_4$	3175	$MgCl_2$/PYRR/$TiCl_4$	3192
$TiCl_4$2PIP	3176	$TiCl_4$2PYRR	3190
$MgCl_2$/$TiCl_4$-2PIP	3175	$MgCl_2$/$TiCl_4$-2PYRR	3185

$TiCl_4$2PIP. Similar case in the $MgCl_2$/PYRR/$TiCl_4$ (see Figure 4) was found. This indicates that in this step of catalyst preparation large amount of PIP and PYRR (Lewis base) was extracted by $TiCl_4$ (Lewis acid) forming the corresponding complex and the complex was then adsorbed on $MgCl_2$ surface vacancies.

This deduction was supported by DTA. Above the boiling point of PYRR, the complexed PYRR in $MgCl_2$/PYRR was released at 135°C, but the PYRR in $TiCl_4$2PYRR was released at 160°C and 230°C. This suggests that the bond between PYRR and $MgCl_2$ is weaker than that between PYRR and $TiCl_4$.

However, it is very interesting to compare the IR spectrum of the catalyst $MgCl_2$/EB/$TiCl_4$ prepared from $MgCl_2$/EB and $TiCl_4$ with that of $MgCl_2$/EB, as shown in Figure 2 and Table 2. The $\nu_{C=O}$ at 1679 cm^{-1} is for the former, and $\nu_{C=O}$ at 1688 cm^{-1} is for the latter. The difference between these two absorption bands is 9 cm^{-1}. This seems to be analogous to those of the complexes $MgCl_2$2EA and $TiMgCl_6$4EA (EA=$CH_3COOC_2H_5$)[6]. $\nu_{C=O}$ were found at 1696 cm^{-1} and 1704 cm^{-1} for $TiMgCl_6$4EA and $MgCl_2$2EA respectively. The difference of these two absorption bands is equal to 8 cm^{-1}. It has been indicated previously that all EA in the complex $TiMgCl_6$4EA were coordinated to Mg atoms[7]. Therefore EB in the catalyst might still be coordinated to $MgCl_2$ and the coordinative bond of the surface complex between $MgCl_2$ and EB might keep the same as in the $MgCl_2$/EB milled product.

4. Coground products of titanium complex with $MgCl_2$

The catalysts $MgCl_2$/$TiCl_4$EB, $MgCl_2$/$TiCl_4$2EB, $MgCl_2$/$TiCl_4$2PIP and $MgCl_2$/$TiCl_4$2PYRR were prepared by cogrinding the corresponding

Table 2. The IR spectra of compounds

Compound	$\nu_{C=O}$ (cm^{-1})	$\Delta\nu$ (cm^{-1})
$MgCl_2$/EB	1688	9 cm^{-1}
$MgCl_2$/EB/$TiCl_4$	1679	
$MgCl_2$2EA	1704	8 cm^{-1}
$TiMgCl_6$4EA	1696	

titanium complexes with $MgCl_2$ respectively. From the IR data it could be seen that the complexes containing C=O group changed during the milling with $MgCl_2$ not like the complexes containing N-H group. As shown in Figure 2., the IR spectra of $MgCl_2$/$TiCl_4$EB and $MgCl_2$/$TiCl_4$2EB were considerably similar to those of $MgCl_2$/EB and $MgCl_2$/EB/$TiCl_4$.

The characteristic bands of titanium complexes could not be found in these two catalysts. This indicated that the $TiCl_4$EB and $TiCl_4$2EB decomposed under the action of milling. All EB produced due to decomposition recombined with $MgCl_2$ during the milling. $TiCl_4$, the other decomposed product might be fixed on the surface of $MgCl_2$ through Cl bridge. This could be supported by the fact that no $\nu_{C=O}$ of free EB in these two catalysts.

However, the ν_{N-H} for $MgCl_2$/$TiCl_4$2PIP and for $MgCl_2$/$TiCl_4$2PYRR could be found at 3175 cm^{-1} and 3185 cm^{-1} respectively. These bands associated to the titanium complexes and the ν_{N-H} of free PIP and PYRR were absent in these two catalysts. These were very different from the result mentioned. Because the bond of N→Ti was stronger than O→Ti. So these two titanium complexes kept unchanged not like those of EB. This could be further proved by DTA results of the $TiCl_4$2PYRR and $TiCl_4$EB. The thermal decomposition temperature (160 °C, 213°C) of the former was higher than the latter (194°C).

It is worth to note that as shown in table 3. the titanium complexes $TiCl_4$EB and $TiCl_4$2PYRR were inactive for polymerization of propylene. Under the same polymerization condition the milled products of titanium complex with $MgCl_2$ exhibited considerably active even if D/Ti > 1 (D=electron donor) in it. The activity of

catalyst $MgCl_2/TiCl_4 2EB$ was much lower than that of $MgCl_2/TiCl_4 EB$. At the same time it can be seen that the increase of EB content in catalyst could not result in the increase of isotacticity of polymer produced, but on the contrary, result in the decrease of that. This behavior is agreement with the catalyst preparated by milling-soaking method[5].

Table 3. The content of EB and Ti, activity and isotacticity of catalysts

Catalyst	EB(wt.-%)	Ti(wt.-%)	EB/Ti (molar ratio	Activity[a] (g PP/g Ti h)	I.I[b] (%)
$MgCl_2/TiCl_4 EB$	9.7	3.25	0.96	4000	79.9
$MgCl_2/TiCl_4 2EB$	17.7	2.89	2.0	1820	74.8
$TiCl_4 EB$		14.50	1.0	none	
$MgCl_2/PIP/TiCl_4$		3.30		1350	43.0
$MgCl_2/PYRR/TiCl_4$		1.15		2200	55.8
$TiCl_4 2PYRR$		13.90		none	

a) Polymerization of propylene was carried out at 60°C under constant pressure of 581 mm Hg in a glass reactor with 100 ml of n-heptane solvent, Al/Ti=20.

b) I.I. was defined as the fraction insolubel in boiling heptane.

The results as shown in table 4. indicated that EB content of the supported catalyst preparated by milling-soaking method are frequently more than stoichiometric amounts of $TiCl_4 EB$. The activity and stereospecivicity of $MgCl_2/PIP/TiCl_4$ and $MgCl_2/PYRR/TiCl_4$ were lower relatively.

5. Far-IR spectra of catalyst

The far-IR spectra of M-Cl(M=Mg, Ti) in Ti complexes and catalysts were investigated on the basis of previous IR data of related compounds[6]. It probably provided useful information on the proposal structure of the catalysts. The ν_{Mg-Cl} and ν_{Ti-Cl} stretching frequencies in 200-500 cm^{-1} region were observed. It can be

Table 4. The contents of Ti and EB of $MgCl_2$/EB/$TiCl_4$

EXP.NO.	Ti(wt.-%)	EB(wt.-%)	EB/Ti(molar ratio)
1[a)]	2.09	11.9	1.6
2[a)]	2.44	11.0	1.4
3	2.40	9.0	1.2

a) Taken from Ref. 5); the interaction of $MgCl_2$/EB with $TiCl_4$ was at 80°C.

seen that a strong broad band at around 280 cm^{-1} along with a weak band at 370 cm^{-1} appeared in IR patern of $MgCl_2$/EB, $MgCl_2$/EB/$TiCl_4$, $MgCl_2$/$TiCl_4$EB (Figure 5), $MgCl_2$/PIP and $MgCl_2$/PIP/$TiCl_4$ (Figure 6). It can be assigned to the ν_{Mg-Cl}. The strongest band at 393 cm^{-1} for $TiCl_4$EB and at 345 cm^{-1} for $TiCl_4$2PIP can be assigned to the Ti-Cl stretching frequencies. No ν_{Ti-Cl} in the $MgCl_2$/EB/$TiCl_4$ and $MgCl_2$/$TiCl_4$EB was observed. This further confirms that EB is coordinated to $MgCl_2$ as mentioned above. The far-IR spectra of the $MgCl_2$/PIP/$TiCl_4$ were different from that of the above-mentioned catalysts. A broad new band of medium intensity at 356 cm^{-1} is found from Figure 6. This band is close to that of $TiCl_4$2PIP and may presumably be assigned to the ν_{Ti-Cl} vibration, which has been shifted due to coordination of $TiCl_4$/PIP complexe to $MgCl_2$ through chlorine bridge.

The ν_{Ti-Cl} of $TiCl_4$2PYRR was at 365 cm^{-1} and a new band at 374 cm^{-1} was found in $MgCl_2$/PYRR/$TiCl_4$. It could be similarly assigned to ν_{Ti-Cl}.

6. Result of XPS determination

It is known that XPS technique may be used for studying the chemical bands in the coordination compounds according to the fact that the binding energy of the inner-shell electrons depends on the effective charge. The determination of binding energy can provide an information on charge-shift and thus it possesses special function for studying coordination complex and catalyst structure.

The binding energy of N1S, Mg2S, $Ti2P_{3/2}$ and $Cl2P_{3/2}$ of the related elements in milled products, catalysts and titanium complexes

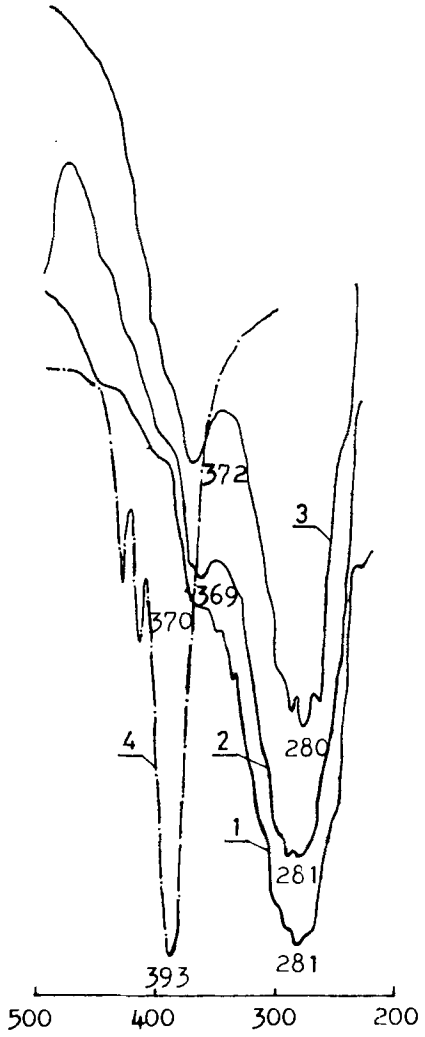

Fig. 5. Far-IR of complexes and catalysts 1-$MgCl_2$/EB, 2-$MgCl_2$/$TiCl_4$EB, 3-$MgCl_2$/EB/$TiCl_4$ and 4-$TiCl_4$EB.

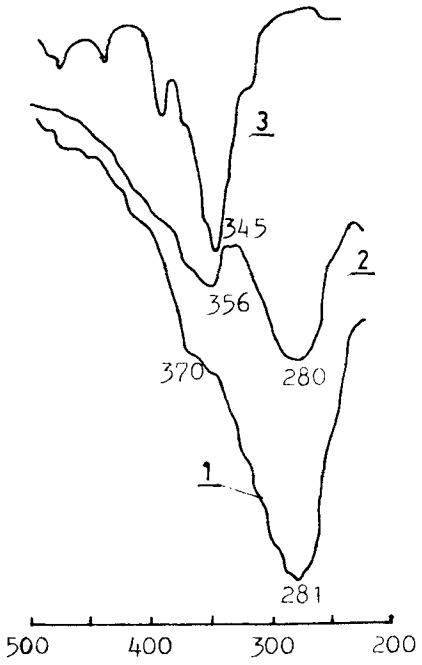

Fig. 6. Far-IR of complexes and catalysts 1-$MgCl_2$/PIP, 2-$MgCl_2$/PIP/$TiCl_4$ and 3-$TiCl_4$2PIP.

were determined. The results obtained are given in table 5.

The binding energy of Mg2S decreased with coground $MgCl_2$ with PIP and PYRR respectively. This exhibited that the charge have been removed from nitrogen atom to Mg atom and the core electron density of Mg atom was increased therefore the binding energy of inner-shell

Table 5. Measured results of binding energy Eb

Compound	Binding energy (ev)			
	N1S	Mg2S	$Ti2P_{3/2}$	$Cl2P_{3/2}$
$MgCl_2$		90.5		199.4
$MgCl_2$/PIP	401.8	90.2		199.3
$MgCl_2$/PIP/$TiCl_4$	401.3	90.0	458.6	199.1
$TiCl_4$2PIP	401.2		458.5	198.2
$MgCl_2$/PYRR	401.4	89.7		199.1
$MgCl_2$/PYRR/$TiCl_4$	400.5	89.7	458.1	198.9
$TiCl_4$2PYRR	400.8		458.3	198.1

was decreased and formed N→Mg coordination bond. It was further demostrated that the surface complex was found when $MgCl_2$ milled with donor. In the comparison of binding energy of N1S of milled products and catalysts with that of their corresponding titanium complexes, it was found that the results of catalysts ($MgCl_2$/PIP/$TiCl_4$, $MgCl_2$/PYRR/$TiCl_4$) were very similar to those of titanium complexes of PIP and PYRR, but were diffent from $MgCl_2$/PIP and $MgCl_2$/PYRR respectively. The difference was 0.5-0.9 ev (see Table 5). The difference of Eb for $Ti2P_{3/2}$ between them was not obvious. So it can be imagined that charge density of titanium complexes and the titanium atom in the catalysts were almost the same as them in titanium complexes. For this reason, it would be seen that the result obtained by XPS was consistent with that of IR. That is, the electron donor reacted with $TiCl_4$ in the supported catalysts.

REFERENCE

1. S.Kvisie, O.Ninisen and E.Rytter, IUPAC Int. Symp. Florence, 1980, Preprints, 2, P.32.
2. Norio KaShiwa. Polymer Journal. Vol.12, No.9, P.603-608 (1980).
3. R. Spitz, I.L, Lacombe., IUPAC Macromol. Symp., 28th, P.257(1982).
4. Guo GuoLin, Xie YouChang and Tang YouQi, SCIENTIA SINICA (Series B) Vol. XXVII No.1 1-11 (1984).

5. Xiao Shijing, Cai Shimian, Liu Huanqin, Zhang Shuqing and Zhou Lirong. Journal of Catalysts Vol.1, No.4, P.291-297 (1980).
6. Xiao Shijing, Cai Shimian, Liu Huanqin and Chen Zengbo. "Spectrossopic Properties of Complexes for Supported Ziegler-Natta Catalyst" Journal of Catalysts (in press).
7. J.C.J.Bart, I.W.Bassi, M.Culaterra, E.Albizzati, U.Giawnini and S.Parodi, Z.Anorg. Allg. Chem. 482, 121-132 (1981).

A NOVEL MULTIFUNCTIONAL CATALYTIC ROUTE FOR BRANCHED POLYETHYLENE SYNTHESIS

YURY V. KISSIN and DAVID L. BEACH
Gulf Research and Development Company, P.O. Drawer 2038, Pittsburgh, Pennsylvania 15230, USA

ABSTRACT

A new concept for the synthesis of linear low density polyethylene from a single feed (ethylene) has been developed. The concept utilities application of a dual functional catalyst for the process. One component of the catalyst dimerizes ethylene to 1-butene and the second catalyst component copolymerizes the 1-butene with ethylene to form branched polyethylene. Evaluation of various catalysts for this purpose allowed identification of several dual functional systems with the least interference between the components. One of the catalysts, including the $AlEt_3$-$Ti(Oi\text{-}Pr)_4$ system as the dimerization component and the $AlEt_3$-$TiCl_4/MgCl_2$/polyethylene system as the polymerization component, has been studied in detail in bench-scale experiments. These kinetic studies were used as a basis for evaluation of the catalyst in a continuous LLDPE synthesis in a pilot plant.

INTRODUCTION

A primary focus of polyethylene research during the past several years has been the development of new technology for the synthesis of branched low density polyethylene at low pressure, with the identification of suitable catalysts a major emphasis. This has been accomplished by using supported organometallic chromium catalysts[1-4] or Ziegler-Natta catalysts[5] to copolymerize ethylene with various alpha olefins, predominantly 1-butene.

Properties of resulting polyethylene have been sufficiently attractive that a number of new commercial processes have been developed[6], one of which (Union Carbide's) has received significant attention[7]. Approximately 10 wt% of 1-butene in a copolymer is

sufficient to decrease polymer density from 0.96 to 0.93-0.92 and its crystallinity from ca. 70 to 35-40%, e.g., the level typical for polyethylene obtained in radical polymerization at high pressure.

An alternative route to the synthesis of branched polyethylene at low pressure is to use a catalytic system capable of simultaneous ethylene dimerization and copolymerization of the in situ formed 1-butene with ethylene.

Such a catalytic system capable of the synthesis of branched polyethylene has a major advantage of needing only a single monomer, ethylene. The catalyst system should contain active centers of two types (dimerization and polymerization centers) which are compatible with each other, i.e., do not interfere chemically and operate under the same reaction conditions of temperature, monomer pressure, solvent, etc.

The activity of the dimerization component of such a catalyst should be sufficient to provide the necessary amount of 1-butene for the formation of polyethylene with desirable and easily controllable chain branching.

We have evaluated several ethylene dimerization catalysts with respect to their compatibility with Ziegler-Natta catalysts for ethylene polymerization, selected several combinations which showed promise as dual functional catalysts. Kinetic behavior of one of the catalysts, $AlEt_3$-$Ti(Oi\text{-}Pr)_4$ - $TiCl_4/MgCl_2$/polyethylene, was studied in conditions simulating continuous polymerization. This catalyst was also tested in a large-scale continuous polymerization unit.

EXPERIMENTAL

Ethylene polymerization and dimerization reactions were studied in a 1 L stainless steel autoclave equipped with a magnetic stirrer. The autoclave had several inlets for vacuum pumping, solvent supply, monomer supply, etc., and several catalyst charge cylinders for the introduction of catalyst suspensions and solutions.

Purified ethylene (after initial gas drying by molecular sieves, O_2 removal with reduced copper catalyst at 100°C, and final gas drying by molecular sieves) was fed into a stainless steel high pressure cylinder (volume 1.20 L) used as an ethylene reservoir in polymerization experiments. After polymerization for some period of time (usually 1-2 h), the polymerization process was stopped by a rapid ethylene discharge from the reactor and by system cooling.

Kinetic analysis of simultaneous dimerization and polymerization of ethylene requires knowledge of concentrations of ethylene and 1-butene at any given time during the process. When ethylene consumption from the reservoir was measured, significant deviation from ideality of the ethylene pressure/gas density relationship was taken into account[8].

Gas phase composition in the ethylene polymerization system was monitored by the GC method every 10-15 min. 2 cc samples were taken from the gas phase of the reactor (through a rubber septum) without disturbing reaction. A Hewlett-Packard 7620A GL Research Chromatograph equipped with a Chromosorb 102 6 ft column and a thermal conductivity detector was used for analysis of the gas phase in the reactor.

The composition of the liquid phase was calculated from the gas phase composition utilizing gas-liquid equilibrium data for the ethylene-1-butene-n-heptane system at reaction temperature and pressure[9].

Copolymerization of ethylene and 1-butene with the $TiCl_4$/$MgCl_2$-$AlEt_3$ catalyst was studied in the same reactor that was used for ethylene polymerization with the dual functional catalyst. In the copolymerization experiments, the solvent, n-heptane, was preliminarily saturated with 1-butene at various pressures at the reaction temperature (which typically took ca. 30 min), ethylene was then dissolved in the system and followed by the introduction of the catalyst components.

The solid supported catalyst for ethylene polymerization was obtained by the reported method[10]. Its weight composition was: Ti - 4.02%, Mg - 1.44%, Cl - 7.17%, Al - 1.96% (residue - polyethylene).

Analysis of polymerization products obtained in the presence of dual functional catalysts was carried out by ^{13}C-NMR, IR, x-ray, and DSC methods[9].

RESULTS

Evaluation of ethylene dimerization catalysts. Several ethylene dimerization catalysts were evaluated for compatibility with typical Ziegler-Natta catalysts for ethylene polymerization. The first prerequisite for the application of dimerization catalysts as components in dual functional catalysts is activity in the temperature range 70-100°C and ethylene pressure range 5-20 atm, typical for catalytic ethylene polymerization.

The obvious candidates for such process are combinations of titanium tetraalkoxides and trialkylaluminum compounds.[11-13] A series of different titanium tetraalkoxides in combination with $AlEt_3$ were tested at 50-70°C and reaction pressure 7.12 atm. Figure 1 shows data on 1-butene formation with these catalysts and the dependence of the effective reaction rate on time. All titanium tetraalkoxides soluble in n-heptane produce fairly active catalytic systems for ethylene dimerization, whereas insoluble compounds make ineffective catalysts. At this temperature, catalytic species formed in the $Ti(OR)_4$-$AlEt_3$ systems are not stable. Initial catalytic activity of the three most active titanium compounds, $Ti(OEt)_4$, $Ti(Oi\text{-}Pr)_4$, and $Ti(OBu)_4$, are similar and deactivation rates are similar as well, which suggests that the active centers in all these systems are similar. The products of this reaction, in addition to 1-butene (>90%) include 2-butenes (cis -~0.5%, trans - ~1%), isomeric hexenes and a small admixture of polyethylene (ca. 2-4%).

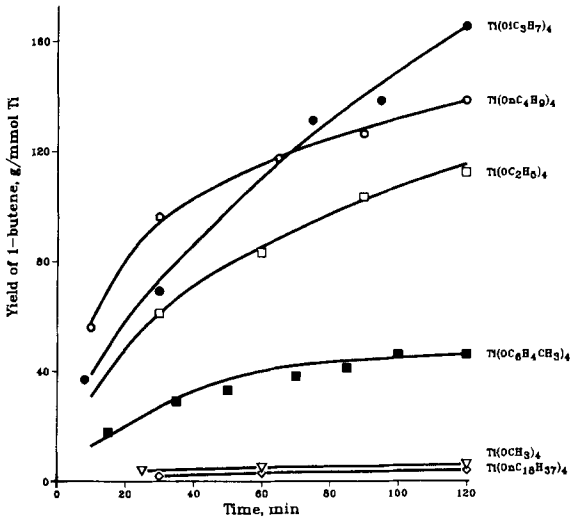

Figure 1. Kinetics of ethylene dimerization with the $Ti(OR)_4$-$AlEt_3$ catalysts at 70°C (heptane, pressure 7.12 atm).

It has been previously demonstrated[14] that the ratio between yields of 1-butene and polyethylene formed in this reaction at 60°C depends on the mixing procedure of catalyst components. If this mixing is carried out in the presence of ethylene, the yield of 1-butene increases and that of polyethylene decreases. We examined

the effect of two monomers, ethylene and 1-butene on the performance of this catalyst at 90°C. Figure 2 shows the kinetics of ethylene consumption by the $Ti(Oi\text{-}Pr)_4$-$AlEt_3$ system mixed in vacuum, in the presence of 1-butene, and in the presence of ethylene. In the first two cases, the catalyst components reacted in n-heptane medium for 30 and 15 min before ethylene admission. It is evident from this figure that olefin presence is essential for high activity of the dimerization catalyst. At 90°C, this catalyst is very unstable in time and its formation in the presence of ethylene provides a method for achieving high 1-butene yield during the lifetime of the system.

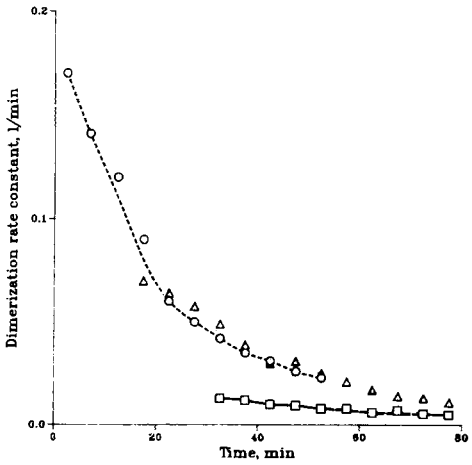

Figure 2. Ethylene consumption by the $Ti(Oi\text{-}Pr)_4$-$AlEt_3$ system formed at 90°C in vacuum (□) and in the presence of 1-butene (Δ) and ethylene (○).

Several other catalytic systems for ethylene dimerization were evaluated under the same conditions as those in previous experiments. These data are collected in Table 1 and show that no other system matches productivity of the $Ti(OR)_4$-$AlEt_3$ system for 1-butene formation at high temperatures.

Table 1. Ethylene oligomerization with various catalysts in the presence of $AlEt_3$

Catalyst	Al : M (mol/mol)	Temp. °C	Time min	1-Butene Yield g/g cat
$Ti(Oi\text{-}Pr)_4$	5.6	90	120	720
$Ti(NMe_2)_4$	2.9	90	120	35
$(acac)TiCl_2$	4.9	90	120	80
$(acac)_2Ti(OEt)_2$	6.1	90	120	38
$Ti(OC_6H_4Me)_4$	3.7	90	120	292
$VO(Oi\text{-}Pr)_3$	3.8	90	160	80
"-"	3.8	90	160	154

Evaluation of ethylene polymerization catalysts. Four ethylene polymerization catalysts were evaluated as components of dual functional catalysts: δ-$TiCl_3 \cdot 0.33AlCl_3$ (Stauffer Chemical Company), a supported catalyt $TiCl_4/MgCl_2$/polyethylene[10], a supported catalyst $TiCl_4/MgCl_2$/ethyl anisate[15,16] (Ti - 1.52%) and $VOCl_3$.

All of the Ti-containing catalysts in combination with $AlEt_3$ are very active catalysts for ethylene homopolymerization and copolymerization with 1-butene at temperatures of 50-100°C. They were evaluated for compatibility with the $Ti(Oi\text{-}Pr)_4$-$AlEt_3$ dimerization system in a series of experiments in which the solids were charged first to a reactor, followed by the dimerization catalyst in the sequence solid component, $AlEt_3$, $Ti(Oi\text{-}Pr)_4$, ethylene. These tests demonstrated that δ-$TiCl_3 \cdot 0.33AlCl_3$ is not compatible with the dimerization catalyst. When 0.05 g of the solid was allowed to react with 0.94 mmole of $AlEt_3$ for 2 min in the absence of ethylene at 90°C, no 1-butene was formed. After subsequent addition of 0.17 mmole of Ti $(Oi\text{-}Pr)_4$ at 90°C and reaction pressure of 7.1 atm for 120 min, 0.5 wt% of 1-butene in the gas phase was found. In the same reaction in the presence of triplicate amounts of $AlEt_3$ and $Ti(Oi\text{-}Pr)_4$, the only reaction product was linear polyethylene. This behavior should be compared with the performance of the unmodified $Ti(Oi\text{-}Pr)_4$-$AlEt_3$ system which produces 37 g of 1-butene in these conditions, corresponding to ca. 40% of 1-butene in the gas phase. A

possible reason for this change is the formation of $AlEt_2Cl$ in the reaction between $TiCl_3 \cdot 0.33AlCl_3$ and $AlEt_3$ at increased temperatures. When an equimolar mixture of $AlEt_3$ and $AlEt_2Cl$ (0.94 mmole each) reacted with 0.17 mmole of $Ti(Oi\text{-}Pr)_4$ at 90°C, no 1-butene was formed in the presence of ethylene, the only product being a small amount of linear polyethylene.

Two tested suuported $TiCl_4$-based catalysts influenced ethylene dimerization with the $Ti(Oi\text{-}Pr)_4$-$AlEt_3$ system to a much lesser degree. For example, when the same testing procedure was used in the $TiCl_4/MgCl_2$/polyethylene catalyst (0.1 g), 1-butene content in the gas phase dropped to ca. 1%; however, in the presence of triplicate amounts of $AlEt_3$ and $Ti(Oi\text{-}Pr)_4$, 1-butene content increased to 32% after 120 min.

Ethylene polymerization with the dual functional catalyst $AlEt_3$ - $Ti(Oi\text{-}Pr)_4$-$TiCl_4/MgCl_2$/polyethylene. Initial polymerization experiments with this dual functional catalyst system were performed at 70°C. The order of charging of catalyst components into the reactor was $AlEt_3$, $Ti(Oi\text{-}Pr)_4$, solid catalyst, with minimal intervals between additions. In all these runs, the amounts of the supported catalyst in the polymerization reactio was 0.1 g (corresponding to 0.08 mmole $TiCl_4$), $AlEt_3$ (4.7 mmole), and $Ti(Oi\text{-}Pr)_4$ varied in the range of 0-0.5 mmole. Polymerization reactions were carried out at a total pressure of 7.1 atm (corresponding to an ethylene partial pressure of 6.7 atm) for 2 h. Polymer yields were 60 to 90 g. The $Ti(Oi\text{-}Pr)_4/MgCl_2$/polyethylene-$AlEt_3$ system, when used in ethylene homopolymerizationn in the 80-90°C range, exhibits very stable kinetic behavior for several hours. Effective polymerization rate constants for the first 2 hours were 1200-1800 g/g Ti·atm·h. All polymers obtained with this dual functional catalyst were branched and the level of branching depended on catalyst composition. Figure 3 shows the dependence of catalyst activity and polyethylene branching as functions of $Ti(Oi\text{-}Pr)_4$ content in the catalyst. Polymerization activity decreased with increasing $Ti(Oi\text{-}Pr)_4$ amounts. Two reasons for this effect are a decrease of polymerization rate due to copolymerization of 1-butene and ethylene and partial poisoning of polymerization centers by reaction products of the $AlEt_3$-$Ti(Oi\text{-}Pr)_4$ system. Polyethylene branching increases with the content of $Ti(Oi\text{-}Pr)_4$ for an obvious reason, an increase of 1-butene amount in the polymerization medium. It can be seen that branching typical for low

density polyethylene (23-30 CH_3/1000C) is easily attainable with this dual functional catalyst.

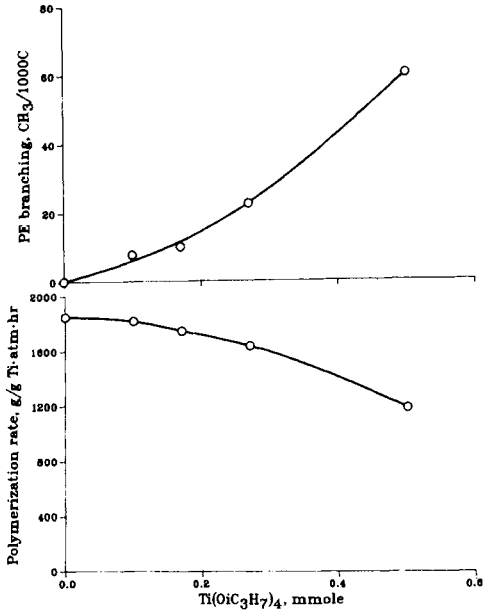

Figure 3. Activity of the dual functional $TiCl_4/MgCl_2$/PE - Ti(Oi-Pr)$_4$-$AlEt_3$ at 70°C and polyethylene branching as functions of Ti(Oi-Pr)$_4$ concentration.

Table 2 contains data on ethylene polymerization with the same catalyst at 90°C. In these experiments, the Ti(Oi-Pr)$_4$-$AlEt_3$ component of the dual functional catalyst was allowed to dimerize ethylene for some period of time (pre-run time in the table) to provide nearly constant concentrations of ethylene and 1-butene in the course of their copolymerization. One example of the kinetic data for such experiments is shown in Figure 4.

Table 2. Ethylene polymerization with the dual functional catalyst $Ti(Oi\text{-}Pr)_4$-$AlEt_3$ - $TiCl_4/MgCl_2$/PE at 90°C, 7.1 atm, 0.0825 mmol Ti

$Ti(Oi\text{-}Pr)_4$ mmol/l	$AlEt_3$ mmol/l	Al:Ti mol/mol	Pre-run time min	Reaction rate g/g Ti·atm·h	PE branching CH_3/1000C
0.134	1.56	11.6	60	1030	3.0
0.134	1.87	13.9	30	680	7.0
0.168	1.87	11.1	30	760	7.5
0.202	1.85	9.3	30	660	18.0
0.269	1.85	7.0	30	500	15.1
0.336	1.87	5.6	15	560	22.5
0.403	1.87	4.6	15	500	24.0
0.470	2.50	5.3	15	440	35.5
0.670	3.12	4.6	18	460	45.0

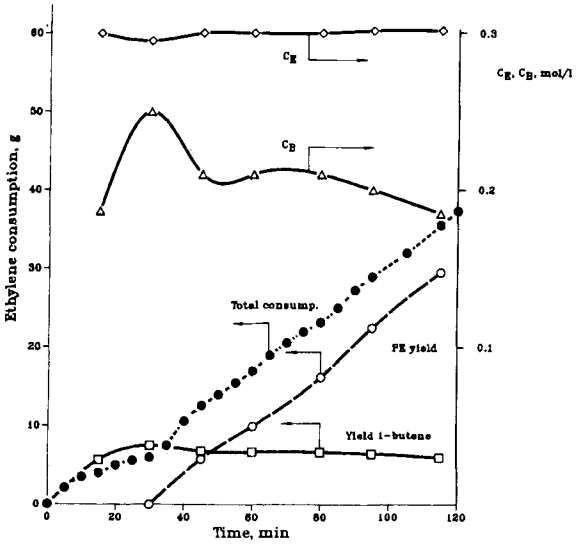

Figure 4. Kinetics of ethylene polymerization with the $TiCl_4/MgCl_2$/PE - $Ti(Oi\text{-}Pr)_4$-$AlEt_3$ system at 90°C.

The solid catalyst was introduced into the reaction medium after 1-butene concentration (measured by the GC method) reached a definite level anticipated from the amount of the dimerization catalyst. As a result, both ethylene and 1-butene concentrations in

these experiments remained approximately constant throughout the runs allowing synthesis of polyethylene with an unchanged level of branching. The rate of polyethylene formation estimated from the total ethylene absorbance and the change of the 1-butene concentration in solution remained nearly constant in these runs (see Figure 4) indicating high stability of the polymerization catalyst.

As can be seen from the data in Table 2, polyethylene branching increases with the amount of the dimerization catalyst, as at 70°C (Figure 3). However, the performance of the dimerization catalyst depends to a significant degre on the Al:Ti molar ratio which explains the absence of a straightforward correlation between branching and the amount of $Ti(Oi\text{-}Pr)_4$ introduced in the system. These data show also that polymerization activity of the dual catalyst depends primarily on two parameters - the concentration of 1-butene in the reaction medium (reflected in polyethylene branching) and the concentration of the dimerization component.

This catalyst is sensitive to hydrogen. When 2.7 atm of H_2 were introduced in the reactor prior to solid catalyst admission, polymer with melt index 1.0 was obtained, instead of a high molecular weight product (melt index less than 0.1) in the absence of hydrogen. Another heterogeneous catalyst component, $TiCl_4/MgCl_2$/ethyl anisate was used instead of $TiCl_4/MgCl_2$/PE with similar results. At $Ti(Oi\text{-}Pr)_4$ and Al concentrations corresponding to 0.3 and 1.87 mmol/l respectively, and an initial ethylene pressure of 6.4 atm at 90°C, polyethylene with branching of 18.6 CH_3/1000C was obtained at the average polymerization rate of 2100 g/g Ti·atm·h.

Kinetics of ethylene dimerization with the $Ti(Oi\text{-}Pr)_4$-$AlEt_3$ system. Ethylene dimerization in the presence of titanium alkoxides in combination with trialkylaluminum compounds has been known for more than 30 years[12]. Many important features of this reaction are known including principal chemical, kinetic, and mechanistic data[17-19]. According to chemical ionization mass spectrometric data[17], interaction of excess $AlMe_3$ with $Ti(Oi\text{-}Pr)_4$ results in the formation of two complexes:

$$Ti(OR)_4 + Al(CH_3)_3 \longrightarrow$$

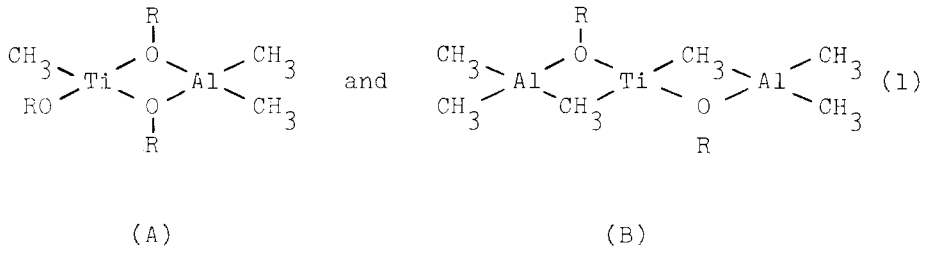

(1)

(A) (B)

with Ti in +3 and +2 oxidation states. These reduced species containing Ti-C bonds are potentially active ethylene dimerization centers. It is known that these centers are unstable and activity of these catalysts in ethylene dimerization rapidly decreases with time[18].

We studied the kinetics of ethylene dimerization with the $Ti(Oi\text{-}Pr)_4$-$AlEt_3$ catalyst in heptane solutions at 90°C using conditions similar to those used for the application of this catalyst as the dimerization component of the dual functional catalyst. Only macrokinetic features of this reaction, essential for the performance of the dual functional catalyst, were investigated.

Figure 5 shows kinetics of ethylene dimerization with the catalyst at 90°C, $Ti(Oi\text{-}Pr)_4$ concentration of 0.336 mM and Al:Ti ratio of 5.6. Results show a rapid accumulation of 1-butene in the system, accompanied by a slight decrease in ethylene concentration (Figure 5-B), due to the fact that the total reaction pressure was kept constant during this reaction. As can be seen from Figure 5-A, the rate of ethylene consumption rapidly decreases with time, indicating high instability of the dimerization centers under the conditions used. Analysis of these data in terms of simple kinetic relationships demonstrated (Figure 5-C,D) that under these conditions, the rate of catalyst deactivation is reasonably described by the first order law:

$$\text{Dimerization rate} = R_{dim} = k_{dim} C_E C^* \qquad (2)$$

$$\text{Rate of catalyst deactivation } C^* = C_o \exp(-k_d t) \qquad (3)$$

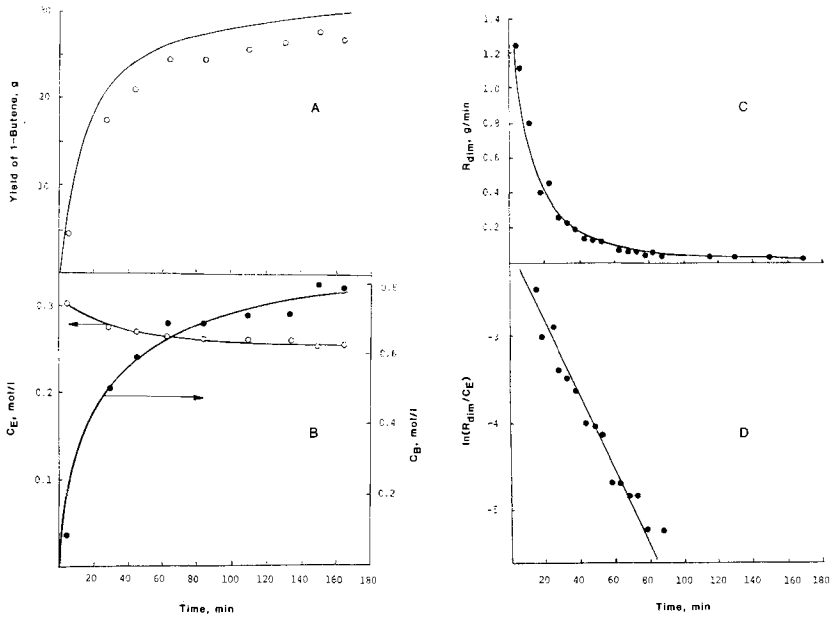

Figure 5. Kinetics of ethylene dimerization with the $Ti(Oi\text{-}Pr)_4$-$AlEt_3$ system in heptane at 90°C. C_{Ti} = 0.34 mmol/l, Al:Ti = 5.6, reaction pressure 7.12 atm. A: solid line - ethylene consumption, o - GC data. B: change of C_E and C_B with time, GC data. C: dimerization rate vs. time from data of Figure 5-A . D: data of Figure 5-C coordinates of Eqn. 3.

where k_{dim} = the rate constant of ethylene dimerization, k_d = the rate constant of catalyst deactivation, C_E = ethylene concentration, C^* = concentration of dimerization centers (C_o = the initial concentration, proportional to the concentration of $Ti(Oi\text{-}Pr)_4$ in the reaction, C_{Ti}). However, similar experiments performed at various Al:Ti ratios demonstrated that with the increase in the ratio, the kinetic order of catalyst deactivation changes from the first (Eqn. 3) to the second one, described by Eqn. 4:

$$1/C^* - 1/C_o = k_d t \qquad (4)$$

Apparently, the catalyst contains several active species, e.g., A and B in Eqn. 1 (with proportions depending on the Al:Ti ratios), some of which decompose in monomolecular reactions and some in bimolecular reactions.

Productivity of the catalyst in the dimerization reaction depends on the Al:Ti ratio. At low ratios (ca. 5-6) the initial activity of the catalyst, $R_{dim}/(C_E \cdot C_{Ti})$, which represent the product $k_{dim}(C_o/C_{Ti})$ is ca. 1.15 l/mmol min and k_d in Eqn. 3 is ca. 0.035 l/mol min. At high Al:Ti ratios, initial activities $R_{dim}/(C_E \cdot C_{Ti})$ in the experiments are in the range 0.7-1.3 l/mmol min and the ratio between k_{dim} and k_d (in Eqn. 4) is in the range of 0.9-2. Thus, the initial activity of the catalyst does not depend on the Al:Ti ratio. However, due to different rates of catalyst deactivation, the total productivity of the dimerization catalyst is higher if it is used at lower Al:Ti ratios. For example, if the reaction is carried out at an ethylene pressure of 6.2 atm, 1-butene formation for 1 h at an Al:Ti ratio of 5-6 is ca. 2.5-3.5 mol/mmol and that at an Al:Ti ratio of 23 is ca. 0.7-1 mol/mmol.

In applications of the dual functional catalyst for the synthesis of low density polyethylene in the continuous mode, the possibility exists that the performance of the dimerization component will be affected by the products of decomposition of the system. Although a detailed evaluation of such effects is not possible to carry out in batch experiments, some of their manifestations were evaluated by carrying out the ethylene dimerization reaction with the $Ti(Oi\text{-}Pr)_4$-$AlEt_3$ system in heptane at 90°C, discharging formed 1-butene from the system, and repeating the experiment in the same liquid medium, now containing products of catalyst deactivation. Results of these experiments showed that the yield of 1-butene for 90 min in the second experiment is only 70% of the yield in the first experiment. However, the rates of catalyst deactivation in both experiments calculated in coordinates of Eqn. 3 were the same, indicating that the initial concentration of active species rather than their deactivation reactions were affected by the products of catalyst deactivation.

Reactivity ratios in ethylene-1-butene copolymerization with the $TiCl_4/MgCl_2$/polyethylene - $AlEt_3$ catalyst and with the dual functional catalyst. If the copolymerization experiments with the $TiCl_4/MgCl_2$/PE-$AlEt_3$ system are carried out at high 1-butene concentrations and low ethylene concentrations, the copolymer products formed are strongly heterogeneous and contain easily separable components of different compositions. The phenomenon of composition inhomogeneity is well known for olefin copolymers obtained with

heterogeneous Ziegler-Natta catalysts[22]. Strong compositional inhomogeneity makes worthless estimations of two reactivity ratios for this catalytic system in a wide range of monomer concentrations. For this reason, the copolymerization experiments were carried out at relatively low 1-butene concentrations in solution, which resulted in the formation of ethylene-1-butene copolymers with low 1-butene content, in the range of 0-7 mol%. Copolymers formed in these conditions are relatively homogeneous in composition.

The general expression for copolymer composition is:

$$f = F(r_1F + 1)/(r_2 + F) \tag{5}$$

where $r_1 = k_{11}/k_{12}$ and $r_2 = k_{22}/k_{21}$ are reactivity ratios (k_{ij} is the propagation rate constant for the addition of monomer M_j to a polymer chain with the last unit M_i), and $f = (C_1/C_2)$cop and $F = (C_1/C_2)$mon are the molar ratios of two monomers, in copolymers (f) and in the reaction system (F). If monomer M_1 is much less reactive than monomer M_2 (as in our case 1-butene is much less reactive than ethylene, $r_1 >> 1$ and, if F values are low, $r_1F << 1$ and $r_2 >> F$. In such a case, Eqn. 5 can be approximated as

$$f = F/r_2 \tag{6}$$

e.g., a linear correlation should exist between f and F values with the slope being $1/r_2$. Analysis of experimental data for ethylene-1-butene copolymerization with the supported catalyst indicated that Eqn. 6 holds for the F range of 0-1.0 (corresponding to the f range of 0-0.05). The $r_2 = k_{EE}/k_{EB}$ value estimated in this way is 20±4.

Most batch experiments on ethylene polymerization with the dual functional catalyst $AlEt_3$-$Ti(Oi\text{-}Pr)_4$ - $TiCl_4/MgCl_2$/polyethylene were performed in such a way (shown in Figure 4) that 1-butene was accumulated in the reaction system for some time prior to the admission of the polymerization component of the catalyst. This procedure allows synthesis of ethylene-1-butene copolymers with nearly constant compositions. Concentrations of ethylene and 1-butene in such experiments were estimated by several independent methods, including direct experimental measurements of the gas phase compositions in the reactor, measurements of 1-butene yields at the ends of prepolymerization periods (30 min in Figure 4), and calculations of gas-

liquid equilibria in the ethylene-1-butene-n-heptane systems. These estimations yielded an r_2 value for ethylene polymerization with the dual functional catalyst of ca. 40±5, i.e., approximately two times higher than for the polymerization component alone. This difference emphasizes again significant mutual effects of the components of the dual functional catalyst (dimerization and polymerization) on each other. The polymerization component can affect the dimerization component by partially poisoning it. Similarly, the dimerization component can influence the polymerization component by modifying (e.g., selectively poisoning) some of the polymerization centers. In the described case, the centers most affected by the dimerization component are apparently the centers exhibiting increased reactivity towards 1-butene in the copolymerization reaction.

Effect of 1-butene on activity of the $TiCl_4/MgCl_2/PE$ - $AlEt_3$ catalyst. Appearance of 1-butene in the reaction system during the course of ethylene polymerization with the dual functional catalyst system studied brings about a change in the activity of the catalyst. Figure 6 presents values of the effective polymerization rate constant with the catalyst as a function of F (the molar 1-butene:ethylene ratio in the reactor). A monotonous decrease of a factor of two in the polymerization activity with an increase in F is apparent. Similarities between the data for the dual functional catalyst and for ethylene-1-butene copolymerization with the $AlEt_3$ - $TiCl_4/MgCl_2/PE$ system obvious from the figure suggest that the

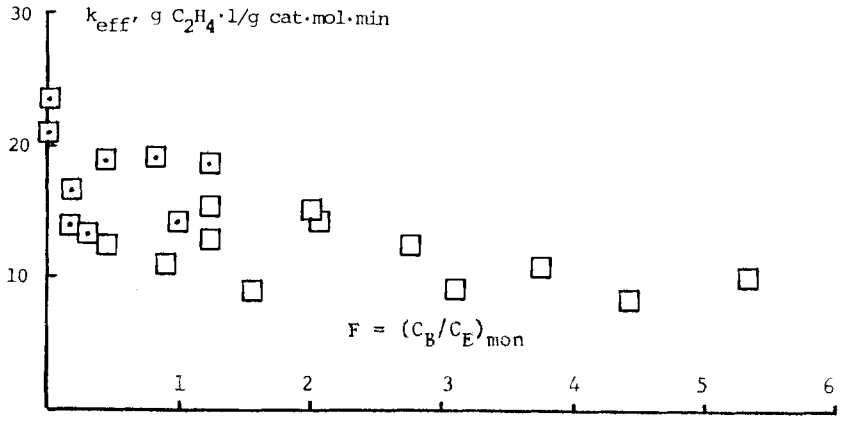

Figure 6. Effect of 1-butene on activity of the $AlEt_3$ - $TiCl_4/MgCl_2$/ polyethylene catalyst at 90°C. ⊡ -ethylene-1-butene copolymerization, ⊡ -ethylene polymerization with the dual functional catalyst.

principal reason for the polymerization activity decrease is the presence of 1-butene in the reaction medium. Such a decrease is a general phenomenon in olefin copolymerization[21]. The principal reason for the decrease is the reduced reactivity of ethylene in addition to polymer chains ending with 1-butene monomer units (k_{12}, see explanations to Eqn. 5) compared with ethylene reactivity in the case of chains ending with ethylene units (characterized by k_{22})[21,22].

Pilot plant evaluation of the dual functional catalyst. Bench-scale testings of the dual functional catalyst $AlEt_3$ - $Ti(Oi\text{-}Pr)_4$-$TiCl_4/MgCl_2$/polyethylene and kinetic analysis of the mutual influence of its components, the dimerization system and the polymerization system, proved feasibility of the utilization of the catalyst for conversion of ethylene intro branched, low density polyethylene in a continuous polymerization process. These studies had culminated in a pilot plant testing of the catalyst. The testing was carried out in a vertical loop reactor of total volume 120 L in isobutane medium. Reaction conditions were: temperature - 85°C, total reaction pressure - ca. 40 atm, catalyst residence time - 2.0-2.5 h. Amounts of the dimerization and polymerization components of the catalyst and hydrogen concentration in the reactor were adjusted to provide synthesis of polymer with desirable properties (density, branching degree, melt index) at a desirable productivity level. Figure 7 shows kinetics of the polyethylene synthesis in the continuous mode during the pilot plant evaluation. Stable supply of the $Ti(Oi\text{-}Pr)_4$ solution (0.3 vol% in isobutane) at the rate shown in the figure allowed maintaining stable concentrations of ethylene and 1-butene in the reactor.

In this 24 h period of evaluation, LLDPE with 0.924 g/cc density and 1.9 melt index was produced. As anticipated from the kinetic study, reactor productivity was ca. 50% of the productivity expected in the synthesis of unbranched HDPE under the same reaction conditions.

Kinetic analysis of the bench scale experiments, the results of the pilot plant testing, and kinetic models of continuous LLDPE production with the dual functional catalyst demonstrated validity of the concept for large scale LLDPE production as a viable alternative to conventional ethylene-1-butene copolymerization.

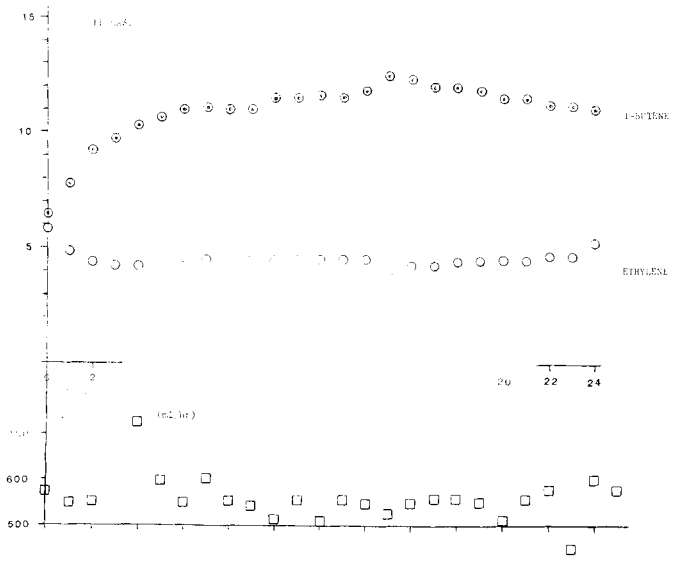

Figure 7. Kinetics of LLDPE synthesis from ethylene with the dual functional catalysts in a continuous pilot plant test.

ACKNOLWEDGEMENTS

Experimental assistance of Mr. W. B. Payne is greated appreciated. Supervision of the pilot plant testings by Mr. T. C. Ho is gratefully acknowledged.

REFERENCES

1. F.J.Karol, W.L.Munn, J.L.Goeke, B.E.Wagner, and N.J.Maraschin, J. Polym. Sci., Polym. Chem. Ed., 16, 771 (1978).
2. F.J.Karol and C.Wu, J. Polym. Sci., Polym. Chem. Ed., 12, 1549 (1974).
3. F.J.Karol, G.L.Brown, and J.M.Davison, J. Polym. Sci., Polym. Chem. Ed., 11, 413 (1973).
4. F.J.Karol, G.L.Karapinka, C.Wu, A.W.Dow, R.N.Johnson, and W.L.Carrick, J. Polym. Sci., Polym. Chem. Ed., 10, 2621 (1971).
5. C.Cipriani and C.A.Trishman, Jr., Chem. Eng., 89, 66 (1982).
6. G.E.Weismantel, Chem. Eng., 88, 47 (1981).
7. Chem. Eng., 86, 80 (1979).
8. Y.V.Kissin and D.L.Beach, J. Appl. Polym. Sci., 29, 1171 (1984).
9. D.L.Beach and Y.V.Kissin, J. Polym. Sci., Polym. Chem. Ed., 22, 3027 (1984).

10. R.K.Kochhar and R.J.Rowatt, US Patent 4,021,599 (1977).
11. T.Tokuzami, Chem. High Pol. (Japan), 25, 721 (1968).
12. K.Ziegler and H. Martin, US Patent 2,943,125 (1960).
13. C.E.H.Bawn and R.Symcox, J. Polym. Sci., 34, 139 (1959).
14. M.Farina and M.Ragazzini, Chim. e'l Ind., 40, 816 (1958).
15. D.L.Beach and A.Zambelli, US Patent 4,366,086 (1982).
16. D.L.Beach and A.Zambelli, US Patent 4,328,123 (1982).
17. C.P.Christenson, J.A.May, and L.E.Freyer, "Transition Metal Catalyzed Polymerizations: Alkenes and Dienes", R.P.Ouirk, ed., Harwood Academic Publ., NY, 1983, p. 763.
18. G.P.Belov, V.I.Smirnov, T.I.Solovjeva, and F.S.Dyachkovsky, Zh. Fis. Khim., 51, 2132 (1977).
19. T.S.Djabiev, Z.M.Djabieva, G.P.Belov, and F.S.Dyachkovsky, Neftekhimia, 16, 706 (1976).
20. Y.V.Kissin, Adv. Polym. Sci., 15, 91 (1974).
21. V.S.Shteinback, V.V.Amerik, F.I.Yakobson, Y.V.Kissin, D.V.Ivanyukov, and B.A.Krentsel, Eur. Polym. J., 11, 457 (1975).
22. Y.V.Kissin, "Transition Metal Catalyzed Polymerizations: Alkenes and Dienes", R.P.Quirk, ed., Harwood Academic Publ., NY, 1983, p. 597.

The stereospecific polymerization of α-olefins: recent developments and some unsolved problems

P.Pino, B. Rotzinger, E. von Achenbach

Swiss Federal Institut of Technology, Institut fuer Polymere.
Universitätsstrasse 6, 8092 Zuerich, Switzerland

Abstract

On the basis of systematic experiments on the polymerization of α-olefins with the catalytic system $TiCl_4/MgCl_2/AlR_3/LB$ (LB=Lewis base) a simple stereochemical model is proposed for the transition states regulating regioselectivity and stereoselectivity in the polyinsertion process.
Some applications of the above model are considered which allow to present a consistent picture of the results obtained in the polymerization of ethylene, propylene 1-butene and racemic α-olefins with heterogeneous and homogeneous catalytic systems. Some unsolved problems including the synthesis and deactivation of the catalytic centers for the polyinsertions are shortly discussed.

1) Introduction

After more than 30 years since the discovery of the synthesis of linear polyethylene (1) by polyinsertion (2) and of linear, stereoregular and stereoirregular, poly-α-olefins (3), polymer chemists are still confronted with a number of unsolved problems such as the control of molecular weight distribution, the synthesis of poly-α-olefins with predetermined degree of tacticity, and the synthesis of copolymers of olefins with polar monomers.
A rational approach to the solution of the above problems requires a better knowledge of the structure of the catalytic centers responsible for the polymerization and of the methods to control the synthesis of the active sites.

No systematic attempts have been made up to now to classify the large number of catalytic systems available today for the polymerization of ethylene and α-olefins to linear polymers. The nature of the catalytic centers being unkown the existence of

monometallic (4) or bimetallic (5) catalytic sites is based mostly on speculations. Therefore only a classification of the catalytic systems on the basis of the number and type of catalyst precursors can be attempted.

Table 1

Attempted Classification of the catalysts for the polymerization of olefins to linear polymers.

Number of catalyst's precursors	Catalytic Systems Nomenclature	Examples
1	Monometallic	$Cp'_2Lu\text{-}CH_3(C_2H_5)_2O$; $(Cp)_2NdH$; $Ti(CH_2\text{-}C_6H_5)_4$;
2	Homobimetallic	$Cp_2TiCl_2/Cp_2Ti(C_6H_5)_2$; $TiCl_4/TiCl_3CH_3$
2	Heterobimetallic	$TiCl_4/AlR_3$; $VCl_4/Al(C_2H_5)Cl_2$; $Cp_2TiCl_2/Al(CH_3)_3$

The proposed classification avoids the confusion existing in the literature concerning the catalysts prepared from two precursors both containing the same metallic element sometimes present in different oxidation states. These catalysts, first discovered in 1958, (6,7) are indicated as a) monometallic catalysts, thus meaning that the catalytic species contains a single metallic element, or b) as bimetallic catalysts thus meaning that two derivatives of the same metal must react to produce the actual catalyst and that two metal atoms are supposed to be present in the catalytic site.

This type of classification does not distinguish, for the heterogeneous systems, between inert supports just increasing the catalyst surface (e.g. polyethylene, polystyrene) or supports which might actively take part into the catalytic processes (e.g. $MgCl_2$). To eliminate this drawback we propose to consider all the supports as "inert" and therefore to classify the catalysts arising e.g. from systems of the type $SiO_2/Al_2O_3/CrO_3$ or $Al_2O_3/Ti(CH_2C_6H_5)_4$ as "monometallic" catalysts.

From the point of view of the nature of the active centers the most investigated catalysts are the heterobimetallic ones which have been shown, by indirect methods, to be chiral racemic as first proposed by Natta and coworkers in 1957 (8). Although generalizations in this field should be avoided, it seems very likely that the polymer chain grows on a transition metal atom even if a main group metal is present in the catalyst, as conclusively shown for the $TiCl_4/AlC_2H_5Cl_2$ catalytic system (9). Despite the large number of theoretical and experimental investigations the detailed structure of these centers and particularly the role of the catalyst precursor(s) has never been understood. Even the actual oxidation number(s) of the transition metals in the catalytic centers of different catalytic systems has not been fully clarified.

Only the general features of the mechanism of the polymerization of α-olefins using organometallic catalysts have been determined already in 1956 (10); the detailed reaction path for the polyinsertion the structure, the synthesis and the deactivation of the catalytic centers have been mostly the subject of speculations and of undue generalizations.

Concerning the detailed reaction path for the polyinsertion, the step whose transition state has the highest energy has not been determined. The possible role of the formation of a π complex between olefin and a metalatom of the catalytic centers, preceeding the insertion of the olefin into the metal to carbon bond, remains uncertain. The discovery of highly active and very reproducible catalytic systems of the type $TiCl_4/MgCl_2/AlR_3$ (11) whose productivity and stereospecificity can be reversibly modified by addition of Lewis bases (12) and, more recently, the discovery of soluble stereospecific catalysts of the type Titanocenedichloride/Methylalumoxanes (II)(13) and Zirconocenedichloride/Methylalumoxanes (III)(14) have offered the possibility to obtain a deeper insight into the structure of these catalytic systems which, broadly speaking, belong to the class of the heterobimetallic catalysts originally proposed by Ziegler (1) for the low pressure polymerization of ethylene. In this review we shall briefly summarize the hints concerning the nature of the active centers we have obtained from the studies of the diastereomeric composition, the microtacticity and in some cases the molecular weight and the molecular weight distribution of the polymers obtained using the catalytic systems (I) and (III)(1-2 bistetrahydroindenylethylene as ligand). The experimental results (15)-(19) have allowed us to formulate a stereochemical model for the transition state, believed to

determine regio- and stereoselectivity,valid at least for the catalytic systems (I), (II) and (III) which accounts for the regio- and stereospecificity observed in the polymerization of the α-olefins, the unexpectedly large number of classes of catalytic centers existing in the catalytic system (I) and for the double role played by the Lewis bases in increasing the stereospecificity of the catalytic system (I)(18). Furthermore it has been shown that particular relationships exist between the structure of the monomers and the structure of the catalytic centers able to polymerize them. Depending on the structure of the monomer, isotactic polymers are mainly produced on different types of catalytic centers.

2) A stereochemical model for the activated complexes responsible for the polymerization of olefins to linear polymers.

It is well known from the classical kinetics that,starting with the structure and composition of the reaction products, only some hints concerning the structure and the relative energy of the transition states controlling the formation of the reaction products can be obtained. From these transition states some hints on the structure of the catalytic centers can then be obtained.
For a polyinsertion reaction we have assumed that regioselectivity and stereoselectivity depend on the relative energy of the transition states corresponding to the olefin insertion into the bond between the carbon atom of the growing chain end and a metal atom of the catalytic centers.

In the case of ethylene we postulate for the transition state of the insertion step, a structure (fig.1a) in which the olefinic double bond is parallel to the metal to carbon bond, the incoming molecule interacting with the growing chain and with at least three other ligands (X, Y and Z) bound to the metal. Only steric interactions between the incoming monomer and catalytic sites are considered; these interactions can be easily represented in a plane ,containing the metal atom as well as the first carbon atom of the growing chain end, which is perpendicular to the direction of approach of ethylene to the metal to carbon bond as shown in Fig.1b. As previously discussed (20)the projection plane is devided in 4 quadrants in which the steric interaction with the olefin substituents (H in the case of ethylene) is different depending on the relative size of CH_2,X,Y and Z.

In the case of α-olefins if the insertion takes place by formation of a Mt-CH_2 bond (1-2 addition) and taking into account only steric interactions between the substi-

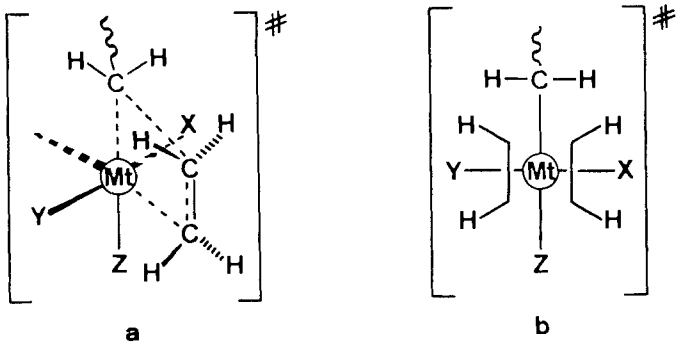

Fig. 1 Simplified representation of the transition state of ethylene insertion into a metal to carbon bond (a) and projection of the above geometrical situation on a plane, containing the Mt-C bond and perpendicular to the direction of approach of ethylene (b).

tuent at the ethylenic double bond and the 4 substituents at the metalatom (CH_2,X, Y,Z) 4 transition states must be considered (fig.2,c,d,e,f) each of which will have a different energy.

If in the insertion step a Mt-CHR bond is formed (2-1 addition) four pairs of transition states must be considered because the carbon atom bound to the metal is asymmetric (fig.2); (g,h,i,j).

Of course as the considered steric interactions occur between a catalytic site and an incoming monomer, the shape of the substituent (R) bound to the ethylenic double bond, which is also present in the growing chain, is expected to be a further important factor in determining the rate, regioselectivity and stereospecificity of the insertion polymerization.

The relationships existing between the extent of interaction of the metal ligands with the incoming monomer and regio- and stereoselectivity (19) have been summarized in Table 2. Possible occasional errors in the type of insertion (1-2 or 2-1) and in the enantioface discrimination have not been considered.

The extent of steric interaction depends on the geometry of the catalytic site and on the preferred direction followed by the monomer in its approach to the reactive metal to carbon bond. Small changes in these two factors can easily produce families

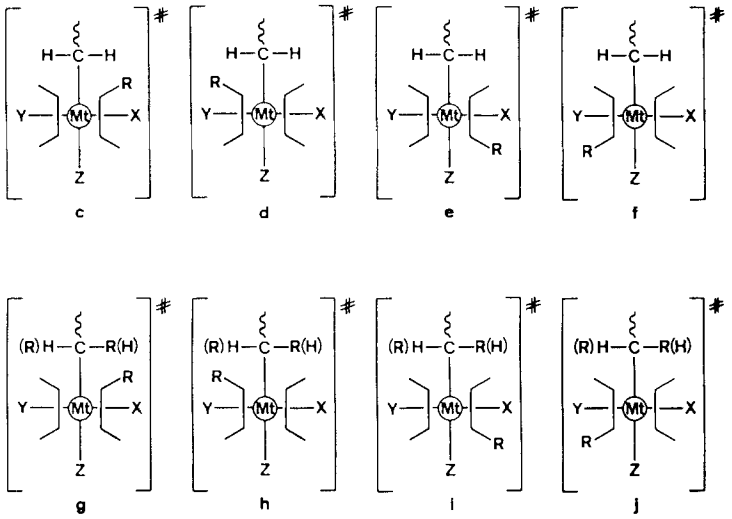

Fig. 2.Planar representation of the transition states for the insertion of an α-olefin into a Me-C bond.

of transition states with slightly different monomer-ligands interactions, and therefore with different energies, leading to polymers with slightly different structural regularity and stereoregularity. Furthermore a slight modification (due to the above geometric factors,) of the relative energy of the transition states leading to monomer insertion and to chain transfer with the monomer respectively (16), can explain the differences in $\overline{M}_v$ observed in macromolecules with similar structure and stereoregularity, and can account for the large molecular weights distribution ($\overline{M}_w/\overline{M}_n > 5$) observed in polyinsertions with heterogeneous catalysts.

According to the model, non stereospecific centers are conceivable which have free coordination sites; such centers can be largely modified by addition of suitable ligands (e.g. Lewis bases) (18) occupying one of the free coordination sites.

Considering monomers with R having very different sizes (e.g. CH_3,CH_2-$CH(CH_3)_2$,C_6H_5, $CH(CH_3)_2$, $C(CH_3)_3$) it is conceivable that they are mainly polymerized on different types of catalytic sites the ones having a bulky substituents being mainly polymerized on catalytic sites in which the ligands exert a lower hindrance to the monomer approach. Therefore centers which, due to the low steric interactions between mono-

Table 2

Possible influence on regio- and stereoselectivity of the steric interactions between incoming α-olefin and substituents (X,Y,Z,CH_2 or CHR) at the Metal Atom (Mt) bearing the growing polymer chain according to fig.2.

Transition state	Extent of Steric interaction [f]					Type of Regioselectivity in the insertion step	Degree of Enantioface Discrimination	Stereoregularity Type expected
	X	Y	Z	$-CHR-CH_2-Mt$	$-CH_2-CHR-Mt$			
1 [a]	ℓ	ℓ	ℓ	s	-	no insertion	-	-
2	ℓ	s	ℓ	s	-	1 - 2	high	isotactic
2'	s	ℓ	ℓ		-			
3 [b]	s	s	ℓ	s	-	1 - 2	lower or none	isotactic or stereoirregular
4 [a]	ℓ	ℓ	s	-	m	no insertion	-	-
5 [c]	ℓ	s	s	-	m	2 - 1	high	isotactic
5'	s	ℓ	s	-				
6 [d]	s	s	s	-	m	2 - 1	medium	syndiotactic
6' [e]	s	s	s	-	m	2 - 1		

Remarks

a) insertion of C_2H_4 possible

b) isotactic at low temperature (13)

c) never hypothesized or observed

d) Configuration (S) for the Mt-CHR-CH_2 group

e) Configuration (R) for the Mt-CHR-CH_2 group

f) ℓ = large, s = small, m = medium.

mer and X and Y ligands, are not able to discriminate between the two enantiofaces in propylene can sufficiently discriminate the enantiofaces in 3-methyl-1-butene or styrene.

The model could also indicate why 1-1 disubstituted ethylenes are in general very slowly polymerized or not polymerized at all with organometallic catalysts. In fact in these cases a very low steric interaction with the substituents of the olefin must exist in two adjacent quadrants in order to allow a sufficiently small distance between incoming monomer and reactive Mt-C- bond in the transition state, a situation which seems to happen very seldom in the heterogeneous catalytic systems considered above.

3) Interpretation of the experimental data obtained with the catalytic system (I) on the basis of the proposed stereochemical model.

a) Polymerization of propylene and 1-butene.

As pointed out by different authors, (12)(21)(15) the addition of a Lewis base to the catalytic system (I), when the ratio Lewis base/AlR_3(r) is larger than 0,1, causes a decrease of the catalyst productivity. A systematic investigation of this effect using propylene and 1-butene as monomers has shown that, in general, the decrease of productivity by increasing (r) is larger for the stereoirregular fraction than for the stereoregular one (Fig.2).

This effect, which is reversible (22), (19) has been interpreted assuming the existence of families of catalytic centers with different steric hindrance to the approach of the monomer to the reactive Mt-C bond. The most important types of centers of the $MgCl_2/TiCl_4/AlR_3$ catalytic systems correspond to the transition states 2,2' and 3 (Table 2) and are indicated with C_ℓ,C_d and C respectively.

A number of experiments (17) (24) have shown the existence of equilibria (1)-(3). The tendency to be reversibly deactivated by the bases is larger for the less stereospecific centers.

$$C + AlR_3.(LB) \rightleftharpoons C.(LB) + AlR_3 \qquad (1)$$

$$C_d + AlR_3\ (LB) \rightleftharpoons C_d(LB) + AlR_3 \qquad (2)$$

$$C_\ell + AlR_3\ (LB) \rightleftharpoons C_\ell(LB) + AlR_3 \qquad (3)$$

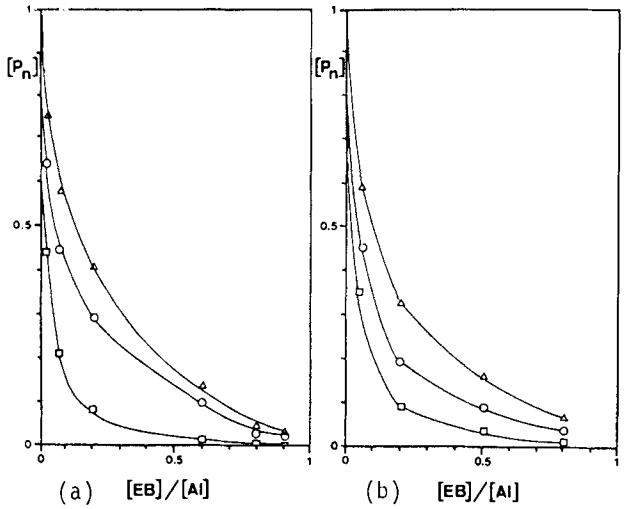

Fig. 3.Normalized productivity (18) in the polymerization of propylene (a) and 1-butene (b) with $MgCl_2/TiCl_4/AlR_3$/LB catalytic system as a function of[LB]/[AlR_3] ratio (r). LB=ethylbenzoate.
(Δ) isotactic fraction (□) stereoirregular fraction (O) total polymer

It has been assumed (24) that the catalytic centers C, C_d and C_ℓ are Lewis acids stronger than AlR_3 and that the deactivation is connected with the formation of catalytically inactive Lewis salts such as C(LB), C_ℓ(LB),C_d(LB). According to this assumption the results reported in fig. 3 should be explained by a larger "Lewis Acidity" for the non stereospecific centers C than for the stereospecific centers C_ℓ and C_d.

The larger Lewis acidity of the centers C with respect to the centers C_ℓ and C_d is in keeping with the smaller steric interactions with the monomers at centers C indicated by the transition state 3 with respect to the corresponding situation in transition states 2 and 2' (Table 2).

Investigation of the influence of Lewis bases at low values of (r) has shown that in general the productivity of the amorphous polymers decreases by increasing (r). On the contrary with some Lewis bases by increasing (r) the productivity of the isotactic polymers increases, reaches a maximum and than decreases (25) (Table 3).

Table 3

Polymerization of propylene with the catalytic system $MgCl_2/TiCl_4/AlR_3/LB$ [a] at low (r) [b].

Lewis Base (LB)	(r) [b]	Normalized productivity (P_N) [c]		
		overall	A [d]	B [e]
Ethyl Benzoate	0,02	0,63	0,42	0,99
	0,08	0,43	0,20	0,83
TMBE [f]	0,02	0,96	0,86	1,09
	0,08	0,80	0,65	0,99
Menthyl Crotonate	0,02	0,90	0,83	1,13
Menthyl Methacrylate	0,02	0,89	0,79	1,07
Triethylamine	0,03	0,85	0,75	1,05

a) Prepared by comilling $TiCl_4$ and $MgCl_2$ (2,8%Ti); polymerization conditions $T=60^oC$; $p_{C_3H_6}=2bar$; $AlR_3=Al(iC_4H_9)_3$; Al/Ti=20; solvent:n.heptane

b) $(r)=[LB]/[\bar{A}lR_3]$

c) P_N= Productivity in the presence of LB/Productivity without LB

d) A = Acetone ins., diethylether soluble fraction

e) B = Heptane insoluble fraction

f) TMBE = trimethylbenzoic-acid-ethyl-ester ;

This interesting phenomenon shown for the first time by Kashiwa (21) has been explained, in keeping with some results obtained in the stereoelective polymerization of 3,7-dimethyl-1-octene (18),assuming the existence of centers which originally possess two unoccupied coordination sites, one of which is saturated by the Lewis base already at very low (r), according to equilibria (4) and (5).

$$C' + AlR_3(LB) \rightleftharpoons C'(LB) + AlR_3 \qquad (4)$$

$$C'(LB) + AlR_3(LB) \rightleftharpoons C'(LB)_2 + AlR_3 \qquad (5)$$

The centers C' and C'(LB) give rise to low energy transition states of the type m, n, p and q (Fig.4) which are very similar to that indicated as 3,2 and 2' in Table 2,

and which finally give rise to stereoirregular or to isotactic polymers respectively.

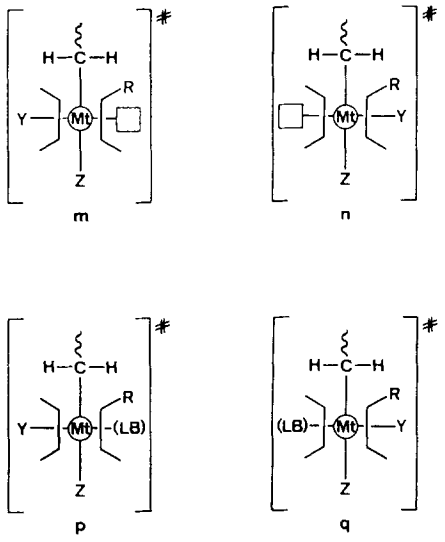

Fig. 4. Transition states involving catalytic centers (C') having free coordination sites (□) (m,n) and centers C'(LB) containing the Lewis base (p and q).

Correspondingly a decrease of non stereospecific centers should occur as experimentally observed. For steric and electronic reasons the Lewis acidity of C' should be higher and the Lewis acidity of the centers C'(LB) should be lower than the average Lewis acidity of the centers C.

The regular change of microtacticity and of viscosimetric average molecular weight ($\bar{M}_v$) of the stereoirregular and isotactic polymers by increasing (r),(22) confirms also in this case that C, C', C'(LB)C_ℓ and C_d correspond actually to families of catalytic centers comprising centers with slightly different properties.

In general the observed result that the ratio mmmm/rrrr in the stereoirregular fractions decreases and $\bar{M}_v$ increases by increasing (r) shows that small changes in the geometry of similar catalytic sites is sufficient to change appreciably the differences between the energy of the diastereometric activated complexes leading to m or r diads or to chain growth- or chain transfer with the monomer,which is the pre-

ferred type of chain termination under the polymerization conditions used.

The existence of families of centers of the same type with different catalytic properties fits well in the frame of the previously discussed stereochemical model; particularly interesting is the lower ratio between chain growth rate and chain transfer rate observed for the stereospecific centers in comparison to the non stereospecific centers and, within each type of centers, the increase of $\overline{M}_v$ with (r). In the frame of the stereochemical model used this observation may indicate that the chain transfer reaction rate is larger in less hindered and in more acidic catalytic centers.

b) The influence of the Lewis bases on the polymerization of ethylene.

Also in the case of ethylene the catalyst's productivity decreases with increasing (r); however in this case not only the productivity decreases but also the change of polymerization rate with time is different (16) and the viscosimetric average molecular weight first increases, reaches a maximum for (r) = 0,2 and than decreases (fig. 5).

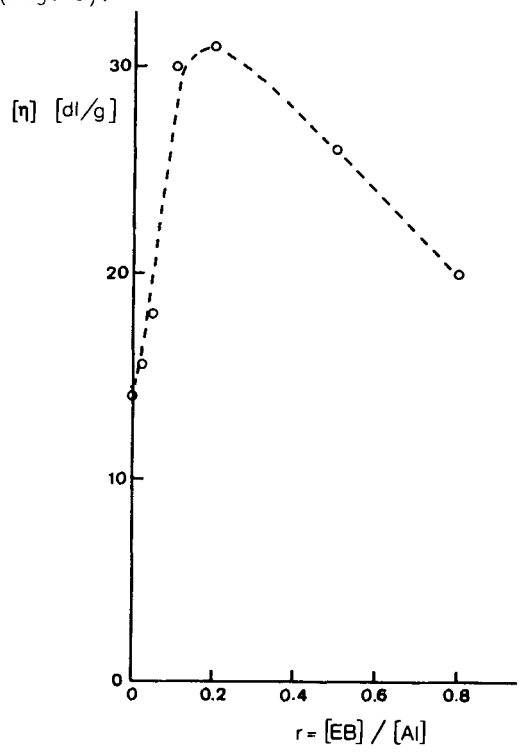

Fig. 5. Intrinsic Viscosity of Ethylene Homopolymers in Tetralin at 135°C as a function of (r)

The following experimental facts must be considered to attempt an interpretation of the above results:

- For low values of (r) the number of catalytic centers polymerizing ethylene is more than 50 times larger than that of the centers polymerizing propylene (26).
- For (r)=0 the polymerization rate increases with time and after 30 minutes it remains constant indicating the existence of centers different from the ones which polymerize propylene.
- Correspondingly at (r)=0 the productivity (mol polymerized monomer/g Ti x moles of dissolved monomer $x\ell^{-1}$) with the same catalytic system is 45 times higher for ethylene than for propylene (22).
- For (r)=0,8 the polymerization rate rapidly increases with time reaching a maximum after few seconds and then decreasing with time as observed for propylene polymerization. The productivity for ethylene is about 70 times lower than in the absence of Lewis base, and is only 17 times higher than the productivity found under the same conditons for polymerization of propylene.

The above results have been explained (16) assuming that in the $MgCl_2/TiCl_4/AlR_3$ catalytic systems, for (r)=0 together with the centers polymerizing propylene a large number of centers (C_E) exists which are active in the polymerization of ethylene but not in the polymerization of α-olefins.On the contrary for (r)=0,8 ethylene and propylene are polymerized on the same catalytic centers (C_ℓ and C_d) the polymerization rate constant being about 17 times higher for ethylene than for propylene.

The existence of the centers C_E fits well in the proposed stereochemical model for the transition state of the insertion step. The transition states corresponding to 1 or 4 of Table 2 imply for the catalytic centers (C_E) very severe steric interactions with the incoming monomer.

The stability of the centers in the first two hours of polymerization and the high growth rate constant to chain transfer rate constant ratio (shown by the high average viscosimetric molecular weight) are in keeping with the prediction from the stereochemical model. The change of [η] with (r) (fig.5) indicates that also the centers C_E polymerising ethylene but not propylene are actually a family of catalytic centers with different Lewis acidity, the centers with higher Lewis acidity yielding polymers with lower viscosymetric molecular weight. The decrease of the average molecular weights for (r) > 0,2 can be explained with the increasing role played by

the centers C_ℓ and C_d which polymerize also propylene and for which k growth/k transfer ratio is smaller than for the centers C_E probably due to geometric factors.

The above results, based on a series of experiments actually suggested by the proposed stereochemical model, indicate an interesting possibility to decrease the fraction of ethylene homopolymers and block copolymers in the ethylene-propylene copolymerization,operating in the presence of Lewis bases (22).

c) Polymerization of propylene and 4-methyl-1-hexene with the catalytic system (III).

One of the most exciting recent finding in the field of α-olefins polymerization to linear polymers is the use of soluble heterobimetallic catalytic systems prepared from methylaluminoxanes and 1,2-ethylene-bis-indenyl- and 1,2-ethylene-bis-tetrahydroindenyl derivatives of titanium or zirconium (13)(14).

Using the racemic 1,2-ethylene-bis-tetrahydroindenyl-zirconiumdichloride, first prepared by Brintzinger and coworkers (27) and polymeric methylaluminoxanes we have repeated the synthesis of isotactic polypropylene first described by Kaminsky (14) and we have attempted the polymerization of racemic 3,7-dimethyl-1-octene and racemic 4-methyl-1-hexene.

Concerning the propylene polymerization our data are in keeping with the data obtained by Kaminsky (14). The NMR ^{13}C spectrum in the region of the bands corresponding to the CH_3 resonances shows, for the diethylether insoluble heptane soluble fraction some interesting features: the syndiotactic pentads, always present in the heptane soluble fractions of polypropylene obtained with the catalytic system (I), are substantially absent and correspondingly the expected 1:2 ratio between the mrrm and mmrr pentads has been found (Table 4). The only other small steric impurity consists of mrmm pentads and might be connected to the presence of small amounts of the meso complex in the racemic zirconium complex; this steric impurity contributes to increase the percent of the mmmr pentads which is slightly higher than that of the mmrr pentads.

This NMR spectrum indicates that the polymer is produced substantially by only one type of catalytic center, the main steric impurities being connected with a relatively low difference in the energy of the activated complexes leading to isotactic or syndiotactic diads respectively.

Concerning the polymerization of the racemic olefins, 3,7-dimethyl-1-octene does not polymerize at all under the conditions used. 4-Methyl-1-hexene polymerizes rapidly to a low molecular weight isotactic poly-4-methyl-1-hexene. The investigation of the ^{13}C NMR spectrum of the diethylether insoluble fraction (Fig.6) shows a close similarity with the spectrum of isotactic poly (S) 4-methyl-1-hexene indicating a stereoselectivity of the polymerization higher than that observed in the polymerization carried out with the most stereospecific heterogeneous catalysts.

Table 4

Microtacticity of the diethylether insoluble heptane soluble fraction of polypropylenes produced with different catalytic systems determined from the ^{13}C NMR spectrum

Pentads	A %	B %	C %	D %	E %
mmmm	51.4	39.7	77.0	84.6	73.8
mmmr	9.8	8.9	9.4	6.7	8.9
rmmr	1.3	1.4	0	0	1.1
mmrr	10.9	10.3	6.4	4.8	7.1
mrmm + rmrr	6.2	9.1	2.1	0.6	2.3
mrmr	1.9	1.6	1.2	0.7	1.3
rrrr	6.0	15.3	0.2	0.2	0.6
rrrm	4.5	8.5	0.9	0.5	1.4
mrrm	7.9	5.6	2.8	1.9	3.5

A: Catalyst: $MgCl_2/TiCl_4/Al(i\text{-}Bu)_3$; Temp: 60°C, $p_{C_3H_6}$: 1 bar, 2 h

B: Catalyst: $MgCl_2/TiCl_4/Al(i\text{-}Bu)_3EB$; Temp. 60°C, $p_{C_3H_6}$: 2 h; EB/$Al(iBu)_3$=0,8 Temp: 25°C; $p_{C_3H_6}$: 1 bar; 2 h.

C: Catalyst:rac-1-2-ethylene-bis(tetrahydroindenyl) $ZrCl_2$/Methylalumoxane, Temp. 25°C; $p_{C_3H_6}$: 1 bar; 2h.

D: Catalyst: rac-1-2-ethylene-bis-(indenyl)$ZrCl_2$/Methylalumoxane, Temp: 25°C; $p_{C_3H_6}$: 1 bar, 2 h;

E: Catalyst: like C,Temp: 25°C; $p_{C_3H_6}$:1 bar; 16 h.

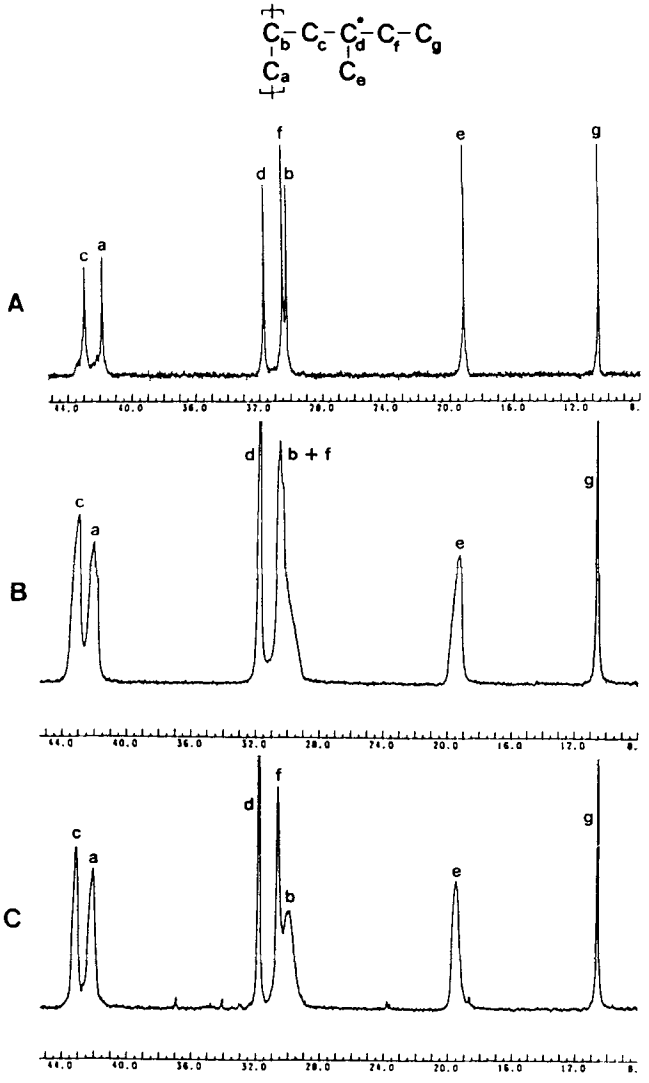

Fig. 6. ^{13}C NMR spectrum of poly-4-methyl-1-hexenes: A: poly(S)-4-methyl-1-hexene; B: poly(R)(S)-4-methyl-1-hexene produced with the catalytic system (I); C: poly(R)(S)-4-methyl-1-hexene produced with the catalytic system (II).

The use of the proposed stereochemical model for the transition state corresponding to the monomer insertion step allows us to relate the data obtained with the heterogeneous and homogeneous catalysts and shows the reliability of the hypotheses made for the active sites of the heterogeneous catalysts.

Although the exact structure of the catalytic sites of the catalytic system (III) is still not known we think that the essential features of the centers are, beside the two bonds between the Zr atom and the cyclopentadienyl groups of the ligand, a bond between the zirconium atom and the alumoxane macromolecule and a bond between the zirconium atom and the last carbon atom of the growing polymer chain. The corresponding structure of the low energy transition state leading to an isotactic diad, and of the transition state with higher energy leading to a syndiotactic diad are represented in Fig. 7 r and s, respectively,

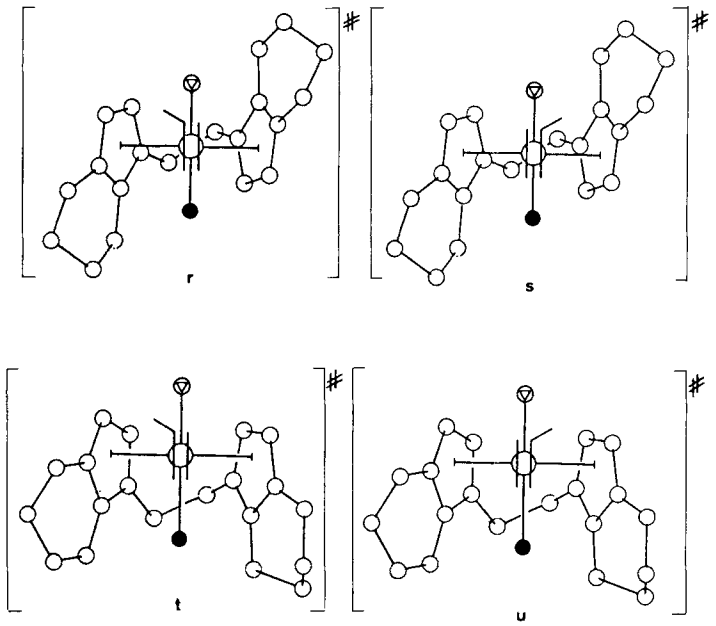

Fig. 7. Possible transition states in the polymerization of propylene with the catalytic systems ethylene bis-(4,5,6,7- tetrahydro-1-indenyl)$TiCl_2$(racemic or meso) and $[-(CH_3)Al-O-]_n$; $\oslash=CH_2\sim\sim\bullet=O-Al(CH_3)(O-Al(CH_3)_n-CH_3$

The cyclohexenyl group of one of the indenylgroups represents a ligand with a large steric hindrance to the incoming monomer (e.g. X in fig. 1b) the two CH groups of the cyclopentadienyl ring of the other indenylgroup represent the substituent with low steric hindrance to the incoming monomer (e.g. Y in fig. 1b), and the aluminoxane macromolecule represents (13) a ligand with a large steric hindrance to the incoming monomer (e.g.Z in fig. 1) which renders the 1-2 insertion favoured over the 2-1 insertion as in all isotactic-specific centers. The above transition state corresponds to the ones indicated with 2 and 2' in Table 2 the centers being of the type of the chiral catalytic sites C_ℓ and C_d. For completness Fig. 7 shows the transition states involving a meso Ti complex leading at room-temperature to actactic polymers (13) and corresponding to the transition state indicated with 3 in Table 2, the centers being of the type C.

As suggested, (18) centers of the type C_ℓ or C_d are not able to polymerize efficiently α-olefins with a methyl branching in the α position with respect to the double bond like 3,7-dimethyl-1-octene, but polymerize 4-methyl-1-hexene. The large stereoselectivity observed with the soluble catalysts (III) shows that the soluble catalytic sites have a better defined geometry more suitable for distinguishing between the two antipodes of the monomer than the heterogeneous catalytic systems (I). The narrow distribution of the molecular weight obtained with the homogeneous well defined catalytic sites (14) is in keeping with the assumption that the large molecular weight distribution observed in the polymers prepared with the heterogeneous catalysts is due to the existence of families of catalytic sites, basically with the same structure but with small differences in their geometry leading to different steric interactions with the incoming monomer and to different chemical reactivity (e.g. different chain growth rate to chain transfer rate ratio).

4) Final remarks

A large amount of data is available at the present on the polyolefins produced by the catalytic systems of the type (I). The use of the very simple stereochemical model for the transition state responsible for the monomer-insertion step presented in this paper allows us to classify most of the above results and to relate them to the results obtained with the soluble catalytic systems (III) having catalytic centers essentially of only one type.

From the different types of centers corresponding to the predicted transition states (Table 2) C_E, C, C'(LB), C_ℓ and C_d have been roughly characterized according to their Lewis acidity chemo- regio- and stereoselectivity. The characterization of the centers which produce syndiotactic polypropylene (C_S) is in progress. Fractions having up to 40% of r pentads have been isolated (28). It appears that the presence of syndiotactic pentads in diethylether soluble and in heptane soluble fractions is due to the presence of macromolecules with syndiotactic structure and not to stereoblock macromolecules. The centers C_S seem to have a very low Lewis acidity as they are still active at r = 0,8.

The resulting picture shows the need of further information particularly on the type of addition (1-2 od 2-1) occurring at the centers C, C'(LB) and C_S and on the chain transfer with the monomer which seems to be the most important mode of termination of the polymer chains.

Of course, due to the roughness of the stereochemical model which gives no information on the chemical nature of the groups X,Y and Z, and does not take into consideration electronic effects which could remarkably affect the rate constants of the growth reaction and of the chain termination reaction, a large number of questions arising from the experimental results are still unanswered.

A contribution to the clarification of the structure of the active centers might arise from the investigation of the relationships between the structure of the Lewis bases and their reactivity with the catalytic sites, as shown in a preceding paper (19).

Information on the structure of the catalytic centers might finally arise from the reactions leading to the formation and to the deactivation of the catalytic centers of the catalytic system (I)(23).

The rate of formation of the catalytic centers seems to be proportional to the AlR_3 concentration and the decrease of the number of the active cencters, as shown by the decrease of the polymerization rate with time, corresponds to a second order reaction with respect to the active centers concentration and to an order 1/2 with respect to AlR_3 concentration (22).

The deactivation involves a decrease in the oxidation number of the Ti atoms present in the centers as shown by the fact that the original productivity can be restored

by addition of Cl_2 or other oxidating agents (29).

Due to the lack of methods for a precise determination of local structure on a solid surface and due to the scarse knowledges existing in the field of surface chemistry, no explanation of the above facts is possible. For the same reasons a rational approach to the synthesis of catalytic systems (I) containing catalytic sites of a single type is, at the present, out of the experimental possibilities. Perhaps the best chances existing today in preparing catalysts containing catalytic sites of a single type are given by the heterogenization of catalytic systems of the type (III) which at the present, despite their stereospecificity and activity are not competitive with the catalytic systems (I) at least for the polymerization of propylene and 1-butene. However this promising approach needs a much better knowledge of the synthesis of the catalytic system (III) and of its precursors.

References

1) K.Ziegler, H.Breil, H.Martin, E.Holzkamp, Ges.Pat. 973626 Filing date 1953
2) G.Natta, P.Pino, G.Mazzanti, U.Giannini, E.Mantica, M.Peraldo, J.Polym.Sci. 26, 120 (1957)
3) G.Natta, P.Pino, P.Corradini, F.Danusso, E.Mantica, G.Mazzanti, G.Moraglio J.Am.Chem.Soc., 77, 1708 (1955)
4) P.Cossee, J.Catal.,3, 80 (1964)
5) P.Pata t H.Sinn, Angew.Chem., 70, 496 (1958)
6) P.Pino, G.Mazzanti, Ital.Pat. 583 219 (1958)
7) C.Beerman, H.Bestian, Angew.Chem.,71,618 (1959)
8) G.Natta, P.Pino, G.Mazzanti, Gazz.Chim.Ital., 87, 528 (1957); G.Natta, J.Inorg.Nucl.Chem. 8, 589 (1958)
9) G.Fink, Habilitationsschrift, Technische Universität München (1976)
10) G.Natta, P.Pino, E.Mantica, F.Danusso, G.Mazzanti, M.Peraldo,Chimica e Industria, 38, 124 (1956)
11) A. Mayr, P.Galli, E.Susa, G.Di Drusco, E.Giachetti, Brit.Pat.,1286867 (1969)
12) U. Giannini A. Cassata, P.Longi, R.Mazzocchi, Belg.Pat., 785 332 (1972)
13) J.A.Ewens, J.Am.Chem.Soc., 106, 6355 (1984)
14) W.Kaminsky, K.Kulper, H.H.Brintzinger,F.R.W.P. Wild, Angew.Chem.Int.Ed Engl.24, 507 (1985)
15) P.Pino, R.Mühlhaupt, Angew.Chem. Int.Ed.Engl. 19, 857 (1980)

16) P.Pino, B.Rotzinger, Makrom.Chem. Suppl. 7, 41, 1984
17) P.Pino, G.Fochi, A. Oschwald, O. Piccolo, R.Mühlhaupt, U.Giannini in Coordiation Polymerization, C.C. Price and E.Vandenberg ed. Plenum Pubbl., Corp. (1983) p 207.
18) P.Pino, G.Guastalla, B.Rotzinger, R.Mühlhaupt, in Transition Metal Catalyzed Polymerization, R.P.Quirk ed., Harwood Academic Publishers (1983) p.435
19) P.Pino, B.Rotzinger, E.von Achenbach, Makrom.Chem.Suppl. 13, 105-122 (1985)
20) G.Consiglio, P.Pino, Top.Curr.Chem., 105, 77 (1982)
21) N.Kashiva in Transition Metal catalyzed Polymerizations, R.P.Quirk ed., Harwood Academic Publishers (1983) p.379
22) B.Rotzinger, Thesis ETH Zürich (1984)
23) T. Keii, E.Suzuki, M.Tamura, M.Murata, Y. Doi Makromol.Chem., 183, 2285 (1982)
24) P.Pino, G.Fochi, O.Piccolo, U.Giannini, J.Am.Chem.Soc., 104, 7381 (1982)
25) P.Pino, B.Rotzinger, R.Mühlhaupt, paper presented at the SPSJ Polymer Symposium commemorating the 30th Anniversary of the SPSJ (1982)p. 16
26) Yu.I.Yermakov in Structural Order in Polymers, F.Ciardelli and P.Giusti ed., Pergamon Press N.Y. (1981) pag. 41
27) F.R.W.P.Wild, L.Zsolnai, G.Huttner, H.H.Brintzinger, J.Organomet.Chem. 232 233 (1982), F.R.W.P.Wild, Thesis Univ. of Konstanz (1983)
28) P.Pino, J.Wei, unpublished results.
29) N.Kashiwa, private communication.

This page intentionally left blank

Index

This page intentionally left blank